THE UNIVERSITY of ADELAIDE

SYNTHESIS AND COORDINATION CHEMISTRY OF POLYPYRIDYL AMIDE LIGANDS

A thesis submitted for the degree of

Doctor of Philosophy

by

Maisara Abdul Kadir

School of Chemistry & Physics

The University of Adelaide

SEPTEMBER 2012

Table of Contents

Abstract

This thesis provides an account of the synthesis and study of fifteen amide-containing polypyridyl ligands, eleven of which are new compounds. These ligands all possess at least one amide moiety, potentially capable of anion binding and one or more pendant pyridyl donor groups as the metal coordinating sites. A further evolution over previously reported compounds is that a majority of the amide compounds incorporate a pre-organised amide component that will constitute the anion binding region. The alkyl and phenyl spacers were utilised to confer flexibility to these compounds and to extend the spacing between the anion binding moiety and the pendant metal complexing groups. The compounds investigated in this work are divided into three categories; (i) unsymmetrical monoamide ligands that possess one amide functional group, one ester protected carboxylate and one external donor pyridyl moiety; (ii) symmetrical flexible amide ligands that possess two or more internal amide groups and two external pyridyl metal coordinating sites, and; (iii) symmetrical amide bridging ligands that incorporate two di-2-pyridylmethylamine chelating motifs.

The coordination chemistry and metallo-supramolecular chemistry of these ligands was investigated with a range of late transition metals including cadmium(II), copper(II), cobalt(II), silver(I), zinc(II) and palladium(II). Palladium(II) precursors, with a selection of monodentate or bidentate chelating ancillary blocking ligands, were utilised to form discrete mono- and dinuclear assemblies with a view to investigating anion complexation in solution. Other transition metal precursors were studied with a focus on the synthesis of coordination polymers that display anion coordinating pockets. Reaction of the monoamide ligands containing a pendant 3-pyridyl group with copper salts led to the formation of five very similar discrete planar and cleft-containing $[Cu_2L_2]$ dinuclear metallo-macrocyclic complexes. The monoamide compounds, lacking a methylene spacer between the amide and the pendant pyridyl ring, form near planar $[Cu_2L_2]$ dinuclear metallo-macrocyclic complexes; meanwhile introduction of a CH_2 spacer, by using a more flexible ligand, results in the formation of cleft-containing complexes. Reaction of the more flexible ligand with copper perchlorate results in a cleft-containing complex whereby encapsulation of a perchlorate anion in the cavity is stabilised by anion-π interactions. The flexible monoamide ligand with a pendant 4-pyridyl group forms 1-D coordination polymers based on a similar dinuclear metallo-macrocycle

building block motif. Reaction of a related ligand with cadmium(II) nitrate and copper(II) acetate led to a formation of two 2-D coordination polymers, both prepared *via* a solvothermal approach. The 2-D coordination polymer obtained with cadmium(II) nitrate has small oval channels with the oxygen atoms of the nitrate anions and ligands lining the channels. This contrasts with the 2-D coordination polymer obtained with copper(II) acetate which is close-packed in the solid-state.

In a similar manner to studies on the monoamide ligands, the symmetrical flexible diamide ligands and tetraamide ligands were used to form discrete complexes and metallo-macrocyclic containing coordination polymers. Two mononuclear Pd(II) supramolecular cages were obtained from the reaction of flexible diamide ligand with pendant 3-pyridyl groups, while a mixture of Pd(II) supramolecular isomers was obtained with the analogue of this ligand. A crystal structure of a mononuclear palladium(II) complex showed specific anion interactions between the pre-organised NH donors and hexafluorophosphate anions in the solid-state. Similar interactions were observed in the majority of the coordination polymers obtained with the flexible diamide and tetraamide ligands. In the crystal structures of three isostructural dinuclear metallo-macrocycle based coordination polymers containing the diamide ligand with pendant 3-pyridyl groups, the pre-organised NH donors are hydrogen bonded to the counterions, including nitrate and perchlorate. In addition to this interaction, the structures were stabilised by π-stacking interactions between the pendant pyridine groups and pyridyl cores. Reaction of the flexible diamide ligand containing pendant 4-pyridyl groups with cadmium(II) and zinc(II) nitrate provided access to two isostructural and isomorphous 1-D coordination polymers, while slow evaporation with cadmium(II) perchlorate gave 2-D coordination polymer. Reaction of the set of flexible tetraamide ligands containing pendant 4-pyridyl groups gave two coordination polymers that adopt semi-helical and close-packed structures in the solid-state. Only one coordination polymer was able to be obtained with the tetraamide ligands with pendant 3-pyridyl groups. The coordination chemistry of the chelating amide ligands with silver(I), cadmium(II) and palladium(II) salts were also studied and these ligands found to act as a bis(bidentate) ditopic bridge to connect two metal ions.

This study has revealed that the monoamide or unsymmetrical amide ligands in combination with copper(II) salts can form discrete anion cages potentially capable of interacting with anions *via* hydrogen bonding and anion-π interactions. The symmetrical and flexible diamide ligands also show potential to interact with anions in the solid-state and may be used for the development of materials suitable for anion separation or sequestration and

also as design elements of anion binding moieties for sensors. Unfortunately, the incorporation of more flexible amide ligands into metallo-supramolecular assemblies was not shown to increase the 'size' of the anion pocket of the assemblies but, due to the additional flexibility, results in the formation of more close-packed structures. It is also shown that self-association may limit the applicability of the tetraamide ligands to bind with either cations or anions in solution. The preliminary anion competition studies have shown that the coordination compounds derived from **L5** and **L6** tend to precipitate salts of either sulfate or, more likely based on the Hofmeister series, perchlorate anions under competitive conditions.

All compounds obtained in this work were characterised by a combination of ^{1}H and ^{13}C NMR spectroscopy, IR spectroscopy, mass spectrometry, elemental analysis and X-ray crystallography. Simultaneous Thermal Analysis (STA) and Powder Diffraction X-ray Diffraction (PXRD) results for selected compounds are also described. In this thesis, crystal structures of seven ligands and twenty nine novel coordination compounds are described.

Declaration

NAME: Maisara Abdul Kadir PROGRAM: Chemistry

This work contains no material which has been accepted for the award of any other degree or diploma in any university or other tertiary institution and, to the best of my knowledge and belief, contains no material previously published or written by another person, except where due reference has been made in the text.

I give consent to this copy of my thesis, when deposited in the University Library, being made available for loan and photocopying, subject to the provisions of the Copyright Act 1968.

I also give permission for the digital version of my thesis to be made available on the web, via the University's digital research repository, the Library catalogue, the Australasian Digital Theses Program (ADTP) and also through web search engines, unless permission has been granted by the university to restrict access for a period of time.

SIGNATURE: …… DATE:…….

Acknowledgement

First and foremost, I would like to offer my sincerest gratitude to my supervisor, Dr Christopher Sumby, for his invaluable assistance and guidance during my PhD years. I thank him so much for giving me the opportunity to carry out this research which has captivated my interest and passion. His patience, wealth of knowledge, constant support and dedicated supervision have made this thesis possible.

I would also like to convey my thanks to Assoc. Prof. Jonathan Morris for his guidance and helpful discussions, especially relating to the organic synthesis. I extend my thanks to Phil Clements for his assistance and guidance in operating the Electrospray Ionisation Mass Spectrometer (ESI-MS) and Nucleus Magnetic Resonance (NMR) spectrometers.

I was privileged to enjoy the company of Sumby group. Special thanks go to Courtney and Rachel that have been working alongside me for these past three years. Not forgetting the former members of Lab 5; Wit, Damien, Nectaria, Lam, Steph and Jenny. Thanks for all the help that I've received here, both directly or indirectly.

I gratefully acknowledge the funding sources that made my Ph.D. work possible. Thanks to the Ministry of Higher Education, Malaysia and Universiti Malaysia Terengganu for providing the financial support for my PhD studies and also to Australian Government through The University of Adelaide for providing laboratory and education facilities.

My special thanks go to my beloved mum, Hajah Raunah Hj Ahmad, my husband, Mohd Azmir Kurish and my kids, Haziq Aiman and Suffiyah Najwa for their understanding and endless love. Their unwavering support during the final stages of this Ph.D. is so much appreciated. To all my friends, thank you so much for the motivation, moral support and good advice.

List of Abbreviations

DMSO	dimethyl sulfoxide
COSY	correlation spectroscopy
NOESY	nuclear Overhauser effect spectroscopy
DOSY	diffusion ordered spectroscopy
ES-MS	electrospray mass spectrometry
FTIR	Fourier transform infrared spectroscopy
DMF	*N*,*N*'-dimethylformamide
bipy	2,2'-bipyridine
en	1,2'-ethylenediamine
Ph	phenyl
Py	pyridine
PXRD	powder X-ray diffraction
TGA	thermal gravimetric analysis
STA	simultaneous thermal analysis
m/z	mass to charge ratio
L	ligand
1-D	one-dimensional
2-D	two-dimensional
3-D	three-dimensional

CHAPTER 1

INTRODUCTION

Chapter 1

1. Introduction

1.1. Supramolecular chemistry

Supramolecular chemistry is often defined as 'the chemistry beyond the molecule'.[1,2] This term was introduced by Jean-Marie Lehn who won the Nobel Prize in Chemistry in 1987, together with Donald J. Cram and Charles J. Pedersen. They received the prize for their contributions to the synthesis of shape-selective and ion-selective receptors, in particular the development of selective 'host-guest' complexes. In broader terms, supramolecular chemistry is defined as self-assembly of small molecular subunits into large aggregates *via* weak intermolecular forces or reversible covalent bonding. The interactions commonly involved in the self-assembly process are hydrogen bonds, π-π interactions (stacking of aromatic rings), van der Waals forces, cation-interactions, and metal-ligand (M-L) interactions. The order of strength for the intermolecular interactions from very weak to very strong is broadly as follows: hydrophobic/hydrophilic interactions, van der Waals forces, H-bonding interactions, electrostatic forces and metal coordination.[3] In general, the intermolecular interactions are individually weak, but by using multiple weak intermolecular forces within the assemblies, robust structures can be generated.

Hydrogen bonding interactions are commonly employed in supramolecular chemistry. Hydrogen bonding occurs between a proton donor attached to an electronegative atom such as O, N, S, F or C (D-H) and an acceptor (A). The donor is partially positive hydrogen while the acceptor is partially negative atom with unshared valence electrons or polarisable π electrons. The strength of hydrogen bonds is typically around 20 $kJmol^{-1}$, but can even be as strong as 163 $kJmol^{-1}$, as has been reported for the $F^{\cdots}HF$ interaction.[4] Figure 1.1 shows the standard way of expressing donor and acceptor atoms, where D is a donor atom and A is an acceptor atom. The bond lengths (D = 3.2-4.0 Å and d = 2.2-3.2 Å) and the bond angles (D-$H^{\cdots}$A = 90-150°) are the parameters used to describe weak hydrogen bonds.

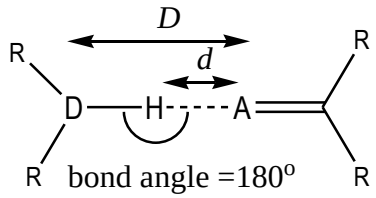

Figure 1.1. A general description of a hydrogen bonding interaction in the context of amides showing the important parameters used to describe hydrogen bonds (distances (Å), *D* = D···A, *d* = H···A; and bond angle (°); D-H···A).

Figure 1.2 shows several other types of hydrogen bonding arrangements. The simplest hydrogen bonding interaction (type (a)) has a bent D-H···A arrangement with an angle close to 180°. Type (b) hydrogen bonding has one hydrogen atom interacting with two acceptor atoms in a three centre arrangement. Less frequently occurring hydrogen bond interactions is type (c) where one acceptor atom interacts with two hydrogen donor atoms. A significant number of variations on this theme exist but are outside the scope of this work.

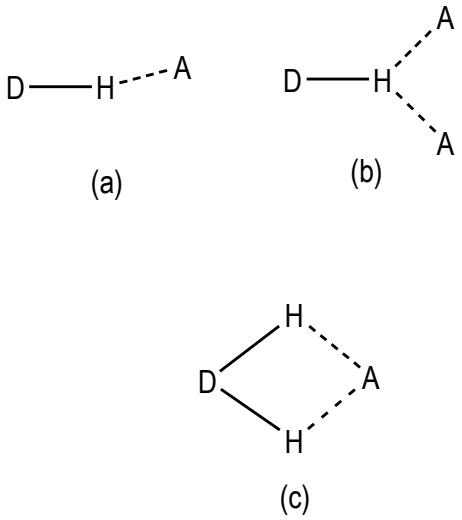

Figure 1.2. Different hydrogen bond arrangements (a) simple, almost linear, (b) donating bifurcated, (c) accepting bifurcated.

Weak interactions involving π-systems such as π-stacking interactions (π···π) are observed in many supramolecular systems.[5,6] A π-stacking interaction occurs between the aromatic rings which are arranged either in a face-to-face arrangement (Figure 1.3(a)) or an edge-to-face arrangement (Figure 1.3(b)) with bonding energies in the range 5-50 kJmol^{-1}. Other weak interactions involving π-systems are C-H···π, cation···π and anion···π interactions. The C-H···π interaction is classified as weak H-bonding and have similar properties to the weak hydrogen bonds. Cation···π interactions occur between metallic or organic cations and π-bonded systems of the molecule. This interaction is relatively weak with bonding energies in the range 5-80 kJmol^{-1}.

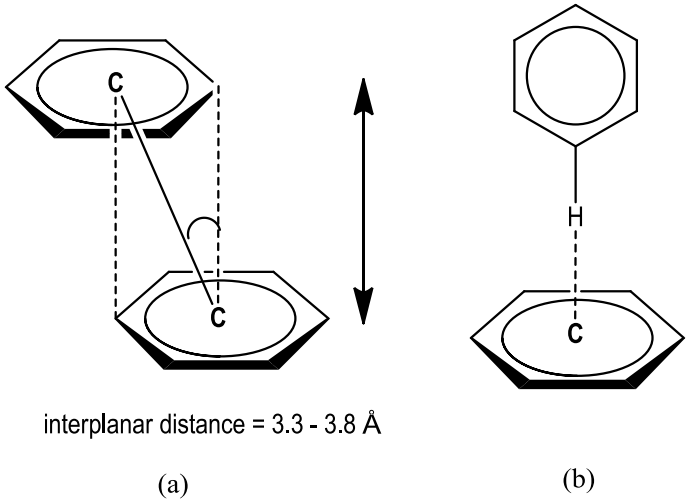

Figure 1.3. The two types of π-stacking interactions observed in supramolecular chemistry. The parameters for these interactions are described in structure (a) which involves interplanar distances of about 3.3 – 3.8 Å and centroid-centroid distances (C-C) of about 3.5-4.6 Å.

Other important weak interactions in supramolecular chemistry are hydrophobic effects and van der Waals forces. The hydrophobic effects arise from the exclusion of non-polar groups from aqueous media, where the water molecules interact preferentially among themselves or with other polar molecules in solution. The van der Waals forces arise from fluctuations of the electron distribution between species that are in close proximity to one another. The bonding energies for van der Waals forces are in the range 2-20 kJmol^{-1}. Other highly utilised reversible

interactions that are commonly described in this study are the metal to ligand bonding. These interactions are important for the synthesis of metallo-supramolecular assemblies (see 1.3). These interactions have a wide range of bonding energies ranging from 80-350 $kJmol^{-1}$ depending on the metal and donor atom combination.

The synthesis of supramolecular species is typically considered straightforward, facile and high yielding, compared to conventional synthetic approaches. The synthetic approach often involves fewer linear steps and is a convergent process culminating in the self-assembly of the most thermodynamically stable product.[7,8] Self-assembly is a process whereby individual molecules form aggregates, involving spontaneous reactions which are under thermodynamic control. During the self-assembly process, defective subunits are rejected and the more thermodynamically stable species are formed. Thus, supramolecular assemblies have become attractive targets due to their facile synthesis. In addition to this, their interesting structures, chemical and physical properties have led to applications in molecular recognition and host-guest chemistry.

In general, the functions of supramolecular assemblies cover three major aspects, molecular recognition, catalysis and transport.[9] Molecular recognition in supramolecules is defined as a process that involves both binding and selection of a substrate by a given receptor molecule. The recognition process 'rests' on the molecular information stored in the interacting species. In a supramolecular approach, the receptors are molecules (hosts) that bind with substrates (e.g. cations, anions) by intermolecular interactions (Figure 1.4) Receptors that bear appropriate reactive functionality in addition to binding sites may function as a supramolecular catalyst. Chemical transformations on the bound substrate may be undertaken in such systems. Finally, supramolecular assemblies that can bind chemical species, protons or electrons could also be used in transport, facilitating transmembrane transport of ions for example.

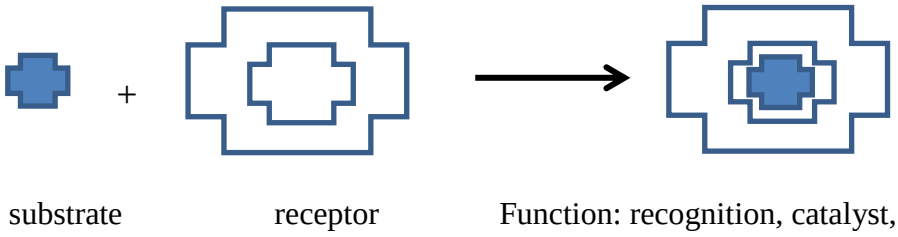

Figure 1.4. The design of a functional supramolecular species.

1.2. Anion coordination chemistry

Anion coordination chemistry or anion recognition is a topical area in supramolecular chemistry.[10-14] This field describes the binding of anions by receptors (hosts) using one or more of the weak intermolecular interactions as described above. The birth of this field is inspired by Nature with inspiration arising from the nature of intermolecular interactions in protein assemblies and DNA.[3,5,15,16] Further impetus is also generated by the impact of anions in the environment and biology. This particularly involves fertiliser run-off (nitrate and phosphate), toxic metallo-anion species and sulfate anion contamination of low-level nuclear waste that demands the production of synthetic anion receptors that could sense, remove or separate various range of anionic species.[17-20]

Amides, thioamides and thioureas all have N-H hydrogen bonding donor groups. Amides have been extensively used for the development of highly selective artificial neutral anion receptors by using the hydrogen bond groups as the donors.[21] Thioamides are weak hydrogen bond acceptors and they have been extensively used in the construction of anion hosts.[22] The synthesis of one of the first examples of a host that can bind or interact with anions (guests) was reported by Park and co-workers.[23] They described the encapsulation of halide anions inside a protonated macrobicyclic diamine receptor. The anions were bound through hydrogen bonding interactions with the receptor. Lehn and co-workers have also reported the synthesis of stable cryptates which exhibit interesting host-guest chemistry. These molecules have potential to encapsulate spherical anions (e.g. chloride, fluoride, bromide) inside their macrotricyclic polyamine cavities.[24] There are many other examples of organic molecules that have the ability to bind anions *via* hydrogen bonding interactions and/or electrostatic interactions. Sessler and co-

workers have reported the potential of macrocyclic (sapphrin) receptors to bind anions using hydrogen bonds and electrostatic interactions.[25] They have also described the interactions between octamethylcalix[4]pyrrole that forms a cone-like conformation with four NH protons bound to halide anions (chloride, fluoride) and dihydrogen phosphate anions.[27,28] The rearrangement of the molecule and the binding with chloride is shown in Figure 1.5. Gale and co-workers have also reported selective binding of calix[4]pyrrole in DMSO.[29,30] The selectivity is affected by the presence of a small positive pocket which can fit small anion like fluoride.

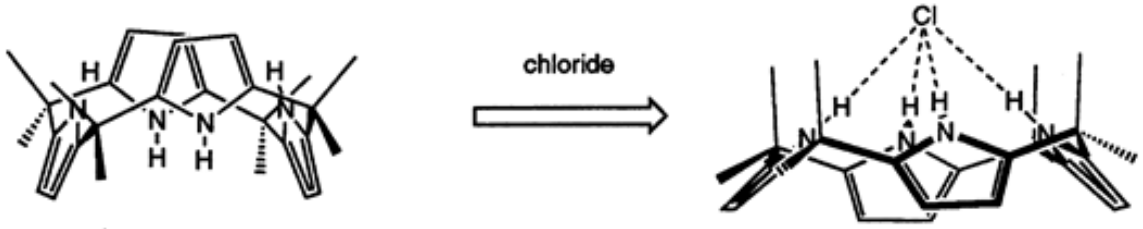

1.1 **1.2**

Figure 1.5. Anion binding interactions in the calix[4]pyrrole **1.2**.

Macrocyclic organic hosts are commonly utilised to complex anions. Polyamine and polyamide receptors, for example, have been widely studied for anion recognition.[31] The most well studied polyamine receptors for anionic species are azacorands (the nitrogen analogues of crown ethers)[32] and azaoxacorands. These molecules are cyclic analogues of biological polyamines such as histamine, spermidine and putrescine. Amide based macrocycles are another common example of organic receptors that have been extensively used for the development of highly selective artificial, neutral, anion receptors by utilising the hydrogen bond groups as donors.[21,33] The rigid macrocyclic tetraamides (**1.3**) reported by Chmielewski and Jurczak[34] (Figure 1.6) have been studied for anion recognition. These molecules contain 2,6-pyridine dicarboxamide groups that are linked by short aliphatic spacers. In these compounds, all amide NH groups are directed inwards toward the macrocyclic cavity by intramolecular hydrogen bonding of the pyridine cores. This leads to a strong and directional hydrogen bonding interaction with anions. Other macrocyclic amides, including the polyamide cryptand (**1.4**) reported by

Bowman-James,[35] are able to encapsulate anions within its molecular cavity. Interestingly, this compound has a high affinity and selectivity for fluoride over other anions.

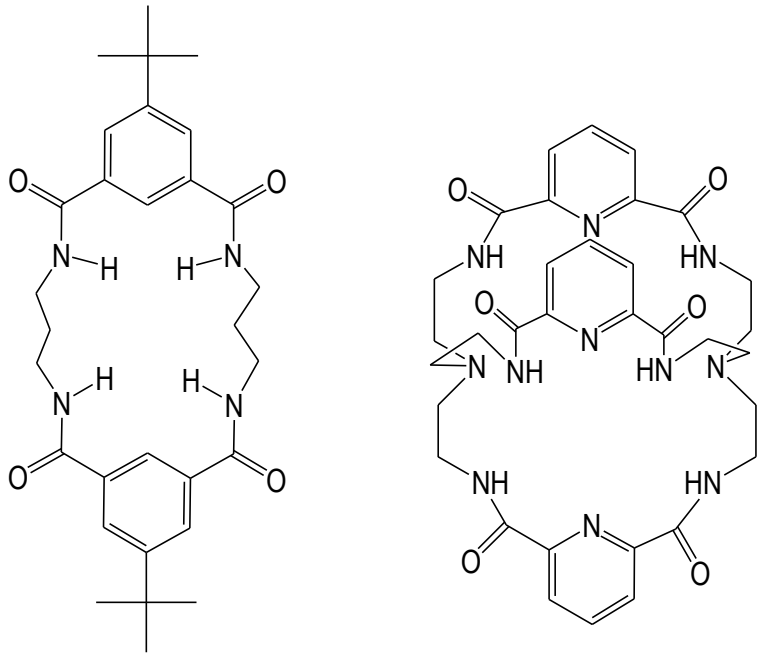

1.3 **1.4**

Figure 1.6. The structures of macrocyclic tetraamides (**1.3**) and cryptand (**1.4**).

One example of a supramolecular assembly capable of anion binding has been reported by Beer.[36] In the structure of this compound, the chloride anion templates the formation of pseudorotaxanes (Figure 1.7). A similar compound prepared from a combination of chloride template and π-π donor-acceptor interaction has also been reported by Beer and co-workers.[37] The anion exchange properties of this supramolecular assembly have been investigated.

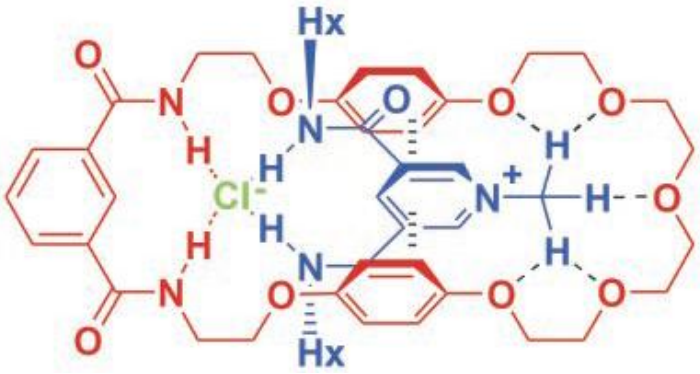

1.5

Figure 1.7. The pseudorotaxane reported by Beer and co-workers (image sourced from [36]).

1.3. Metallo-supramolecular Chemistry

Metallo-supramolecular chemistry involves the use of combinations of metal ions and ligands in the construction of supramolecular assemblies. This term was introduced by Constable in 1994[38] to describe the self-assembly of large molecular aggregates *via* metal to ligand bonding. In the assembly, the metals act as a 'glue' to hold together the assemblies of organic molecules.[39-44] In metallo-supramolecular chemistry the approaches of traditional coordination chemistry are combined with the use of weaker interactions, such as H-bonds and π-π stacking interactions, to form either discrete or polymeric aggregates. Complex supramolecular coordination networks in 1-, 2- or 3-dimensions can also be generated by using bridging ligands that can coordinate to more than one metal centre. The nature of the products obtained is influenced by the choice of metal ion, solvent and counterions and has received much attention. For example, the choice of metal centre defines the coordination number, geometry and stereochemical preference and thus the nature of the assembly obtained. Therefore, by using combinations of suitable components, metallo-supramolecular species with specific or multifunctional properties can be designed and synthesised using the principles of supramolecular chemistry.

1.3.1. Self-assembly

Metallo-supramolecular assemblies are generated *via* a self-assembly processes involving metal ions and organic ligands. The self-assembly process relies on the coordination requirements of

the metal ions and the number and relative positions of the donor atoms in the ligand precursors. The 'encoded' information results in the formation of a discrete assembly or a coordination polymer.[40,41,45-50] Metal-directed self-assembly plays an important role in the formation of a diverse range of discrete coordination arrays, such as ladders, boxes, helicates, triangles, cubes and grids, rotaxanes and catenanes, and or course coordination polymers (section 1.4).

1.3.2. Rigid versus Flexible Components

Target molecules can be designed by using molecular building blocks that can logically self-assemble into a predictable structure. Greater control over the self-assembly process can be achieved by using rigid components. The use of rigid ligands can limit the type of structures that can be obtained and often leads only to a particular, highly symmetrical assembly.[44] Access to a greater variety of structures can be achieved by using flexible ligands. The use of flexible ligands enables different conformations of a compound to be accessed by rotation about the single bonds in the compound. The short alkyl chains such as methyl, ethyl and propyl are examples of common subunits that have been employed as 'spacers' to promote flexibility.[51] By employing conformationally free components, the self-assembly process allows access to a greater number of structures but can lead to the formation of unpredictable products. To counterbalance flexibility in self-assembly, the use of elements of pre-organisation within the components can enable regions of the resulting supramolecular assembly to be controlled during synthesis, i.e. the coordination environment of a metal or a region of the organic ligand.[52] Thus, complete loss of control during the self-assembly process can be prevented and various interesting topologies can be accessed with flexible ligands. Lehn and co-workers for example, have reported a comparison between supramolecular architectures is obtained from the assembly of rigid and flexible bridging ligands. In an early report, they described the formation of a helicate (Figure 1.8) from the reaction of semi-flexible tris(bipyridine) ligand (**1.6**) with silver(I), whereby the chelating moieties of the ligand are constrained but allowed to flex relative to each other. [53]

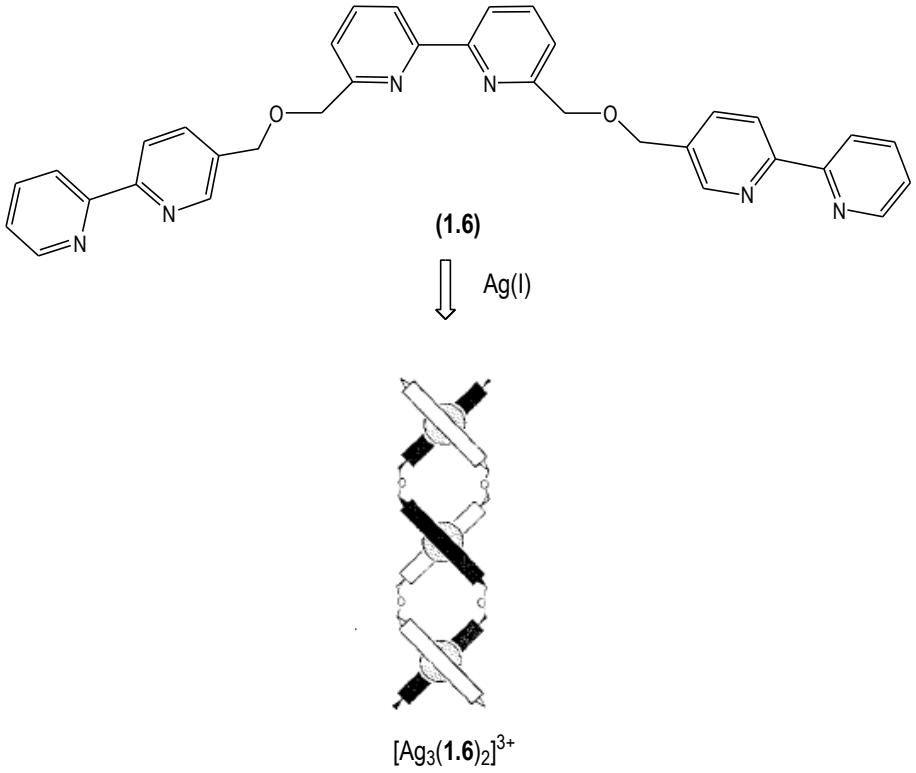

Figure 1.8. A helicate complex obtained from the use of a semi-flexible ligand.

Subsequently, Lehn reported the formation of grid-type complex[54] (Figure 1.9) obtained from the reaction of a rigid pyridazine-derived ligand with silver(I). The removal of the flexible spacer between the pyridazine rings provides the rigidity that leads to the self-assembly of a thermodynamically stable grid-type structure.

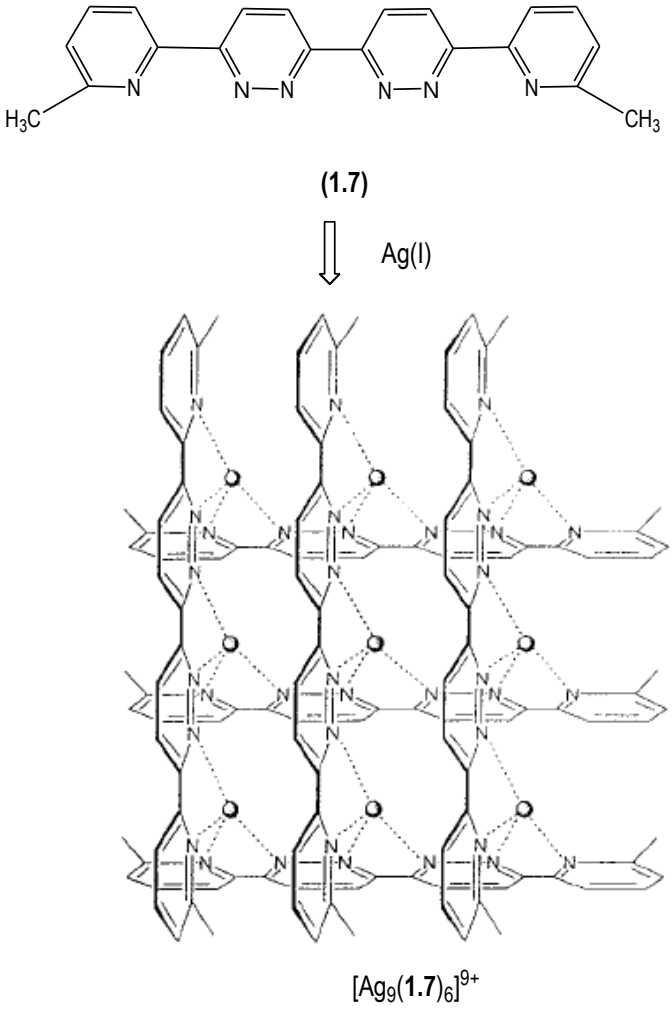

Figure 1.9. The formation of grid-type complex from using rigid ligand.

Kitagawa and co-workers has also investigated the effect of using rigid and flexible linkers in the formation of porous coordination networks.[55] By changing the pillar module of the structure, from the rigid ligand 4,4'-bipyridine (**1.9**) to a flexible ligand 1,4'-bis(4-pyridyl)ethane (**1.10**), two different frameworks can be obtained. The first ligand led to a formation of a stacked 2-D rectangular grid-like structure (**1.11**) while the flexible ligand gave a 2-D bilayer network (**1.12**). In this latter instance, bilayers were interpenetrated to give a 3-D framework (Figure 1.10)

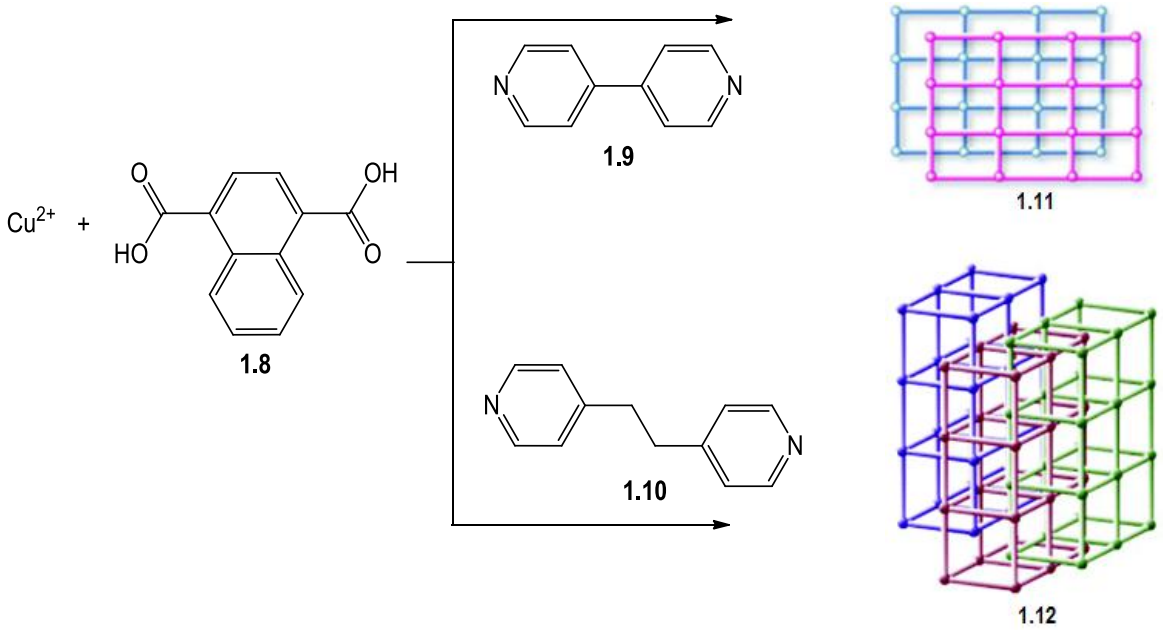

Figure 1.10. The representations of two different topologies incorporating rigid (**1.9**) or flexible (**1.10)** ligand into a PCP (image sourced from [55]).

1.3.3. 2-D assemblies and their host-guest chemistry

As outlined above, highly symmetrical assemblies can be achieved by using rigid ligands.[44] The combination of a linear metal centre and a linear bridging ligand leads to the formation of one-dimensional coordination polymers (Figure 1.11(a)), while the assembly of linear bridging ligands and a *cis*-capped square planar metal centre gives rise to two-dimensional polygons, such as molecular squares (Figure 1.11(b)).

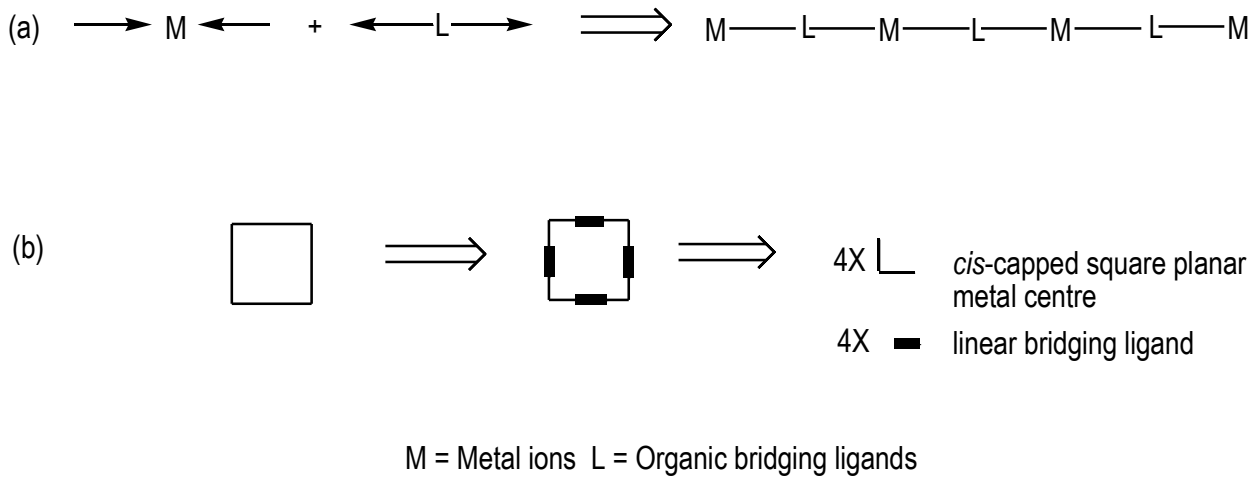

Figure 1.11. The examples of the combination of bridging ligands and metal centres.

One of the first reported molecular squares (**1.14**) was prepared by Fujita[50] from the reaction of a linear bridging ligand, 4,4'-bipyridine (**1.9**) with ethylenediaminedinitropalladium(II) (**1.13**), which adopts a square planar geometry with two exchangable donors in a *cis* arrangement (Scheme 1.1). Other molecular squares prepared by Stang,[56,57]Lehn,[58] Hupp[59] and Hong,[60] for example, have also been reported. The majority of these molecular squares were found to form cavities capable of guest inclusion.

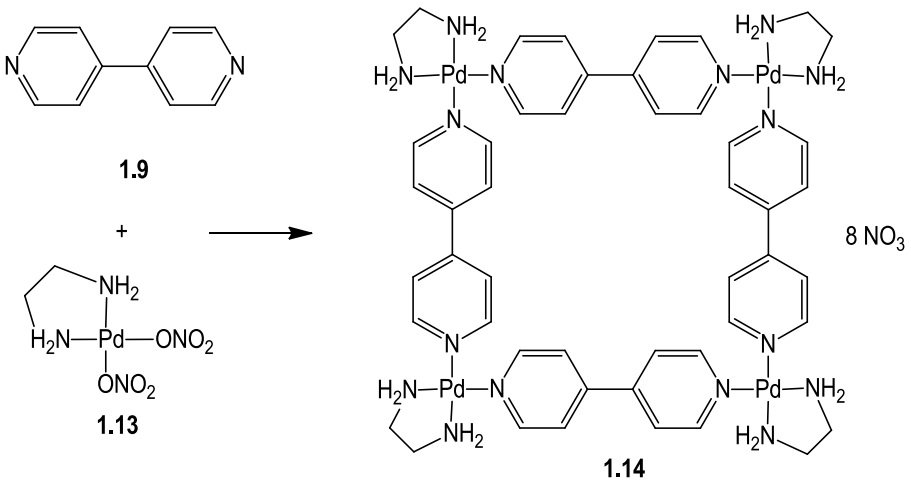

Scheme 1.1. The molecular square reported by Fujita. Platinum containing squares can also be prepared.

The self-assembly of ditopic ligands and metal centres with different angles between their reactive sites can lead to the formation of other two-dimensional polygons such as triangles and hexagons (Figure 1.12). Molecular triangles can be formed by combination of bridging ligands with 60° angles between the reaction sites and linear metal centres or the reverse combination where the metal centre provides the angular component (Figure 1.12(a)). Selected examples are given below. Similarly, metallo-supramoleular hexagons can be prepared with an angular component that has a 120° angle between reactive sites (Figure 1.12(b)).

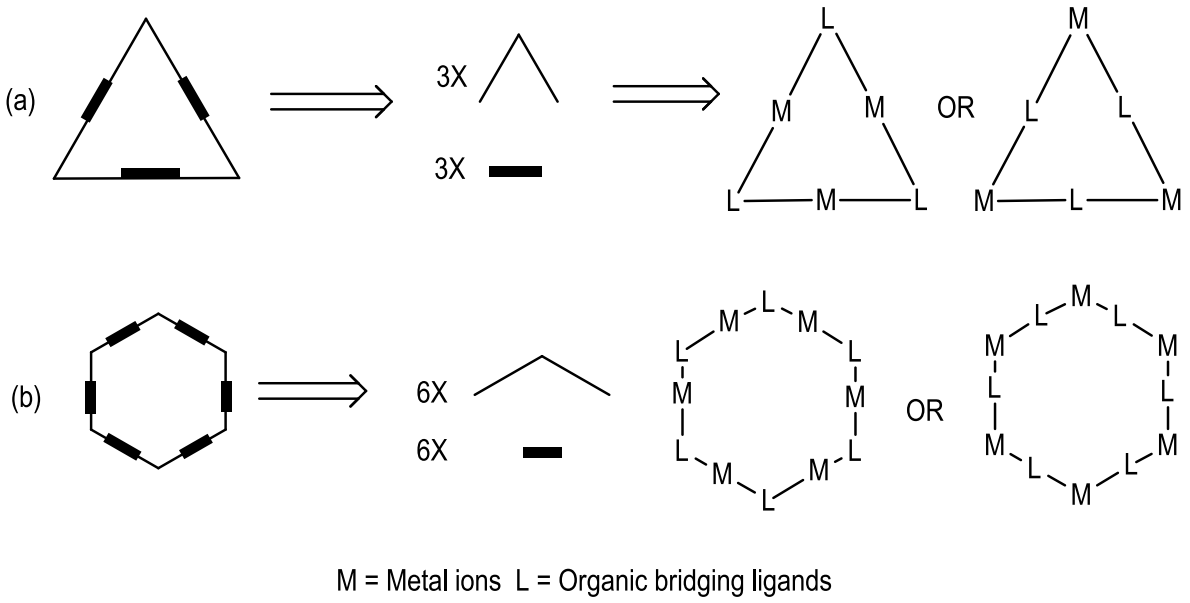

Figure 1.12. The formation of metallo-supramolecular triangles and hexagons.

Mukherjee and co-workers have reported the self-assembly of a heterometallic triangle (**1.17**) from the reaction of 1,1-(bisphosphino)ferrocene palladium(II) ditriflate (**1.15**) with sodium nicotinate (**1.16**) (Scheme 1.2).[61] Other example of triangular assembly has been reported by Lippert and co-workers.[62] The triangle (**1.20**) was prepared from the assembly of palladium (**1.18**) and platinum precursors such as trans-diaminedichloroplatinum(II) (**1.19**) (Scheme 1.3).

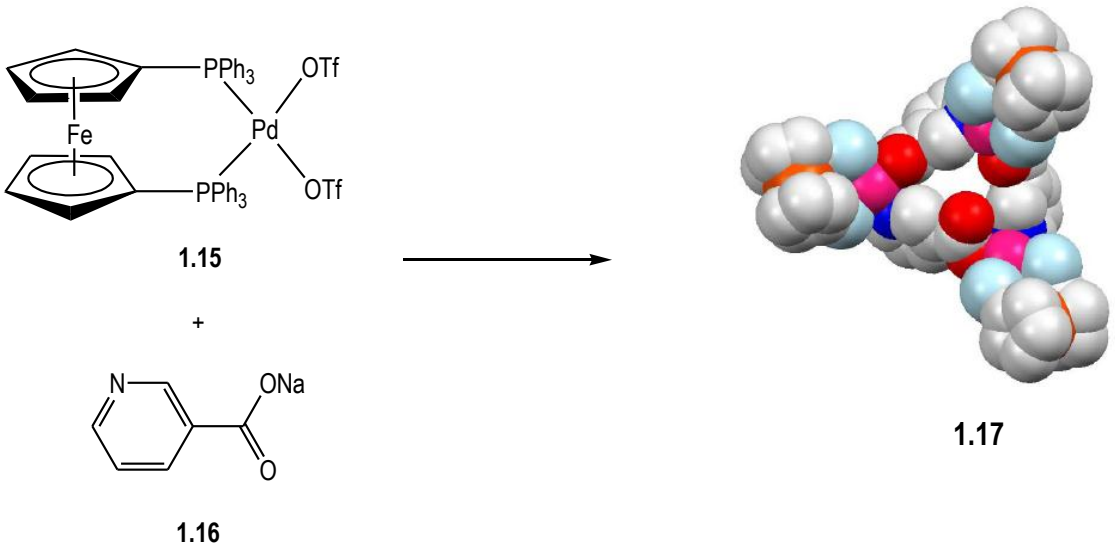

Scheme 1.2. Synthesis of the heterometallic triangle reported by Mukherjee and co-workers.[61]

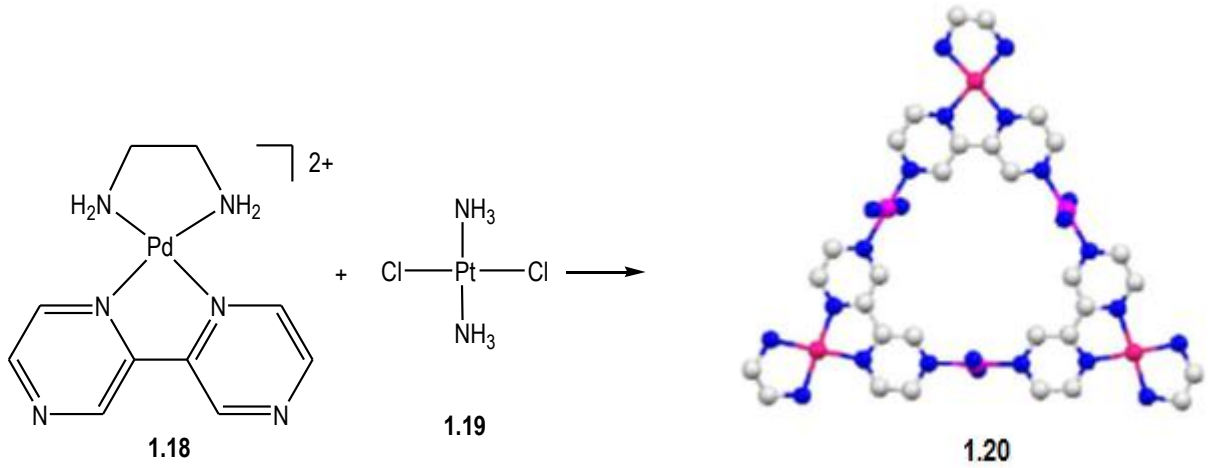

Scheme 1.3. Synthesis of the triangular metallo-supramolecular assembly reported by Lippert and co-workers.[62]

Hunter and co-workers[63] have also reported the structure of an interesting porphyrin-based trimeric assembly (**1.21**) which incorporates more than one pre-organised amide NH moieties (Figure 1.13). Depending upon your viewpoint the structure has a triangular or hexagonal shape.

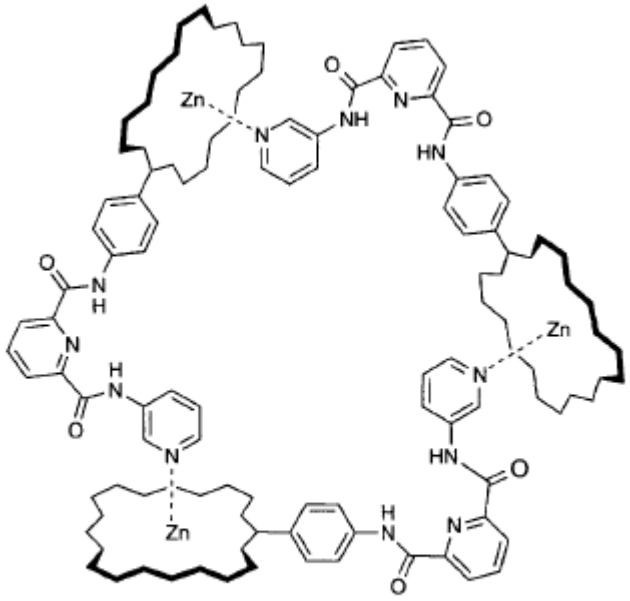

1.21

Figure 1.13. The structure of a porphyrin-based triangular assembly as reported by Hunter and co-workers (the solubilising groups R at the porphyrin meso positions and the porphyrin ring bonds are omitted for clarity).[63]

1.3.4. 3-D assemblies and their host-guest chemistry

Selected examples of 3-D assemblies, with structures relevant to the work conducted in this project or that contain related amide ligands are discussed in the following section. These illustrate the synthesis of metallo-supramolecular assemblies as receptors. By using a directional bonding approach, highly symmetrical supramolecular cages with structures based on the platonic solids (tetrahedra, cube, dodecahedra), or trigonal bipyramidal, adamantoid and trigonal prisms can be obtained. Metallo-supramolecular cubes can be constructed by two different approaches. The first approach involves edged-directed self-assembly (Figure 1.14(a)), while the second approach involved face-directed self-assembly (Figure 1.14(b)). Examples of such structures have been reported by Thomas [64] and Grieco,[65] respectively.

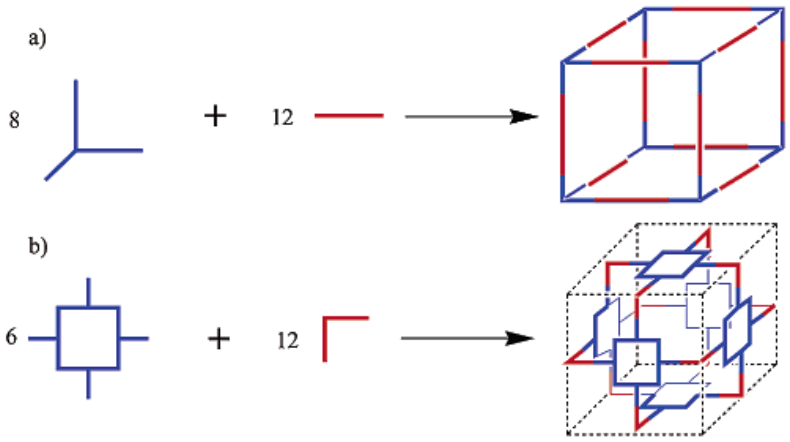

Figure 1.14. Two approaches to metallo-supramolecular cubes (image sourced from [66]).

Work involving the synthesis of tetragonal prismatic cages is also relevant to the work conducted in this thesis. Atwood and co-workers[67] have reported a tetragonal prism (**1.22**) incorporating four bidentate ligands and two copper(II) ions (Figure 1.15). Of particular interest in this instance was the fact that this assembly incorporates an amide containing ligand that was ideally suited to anion interactions although a cluster of water solvate molecules was the primary interest of this work.

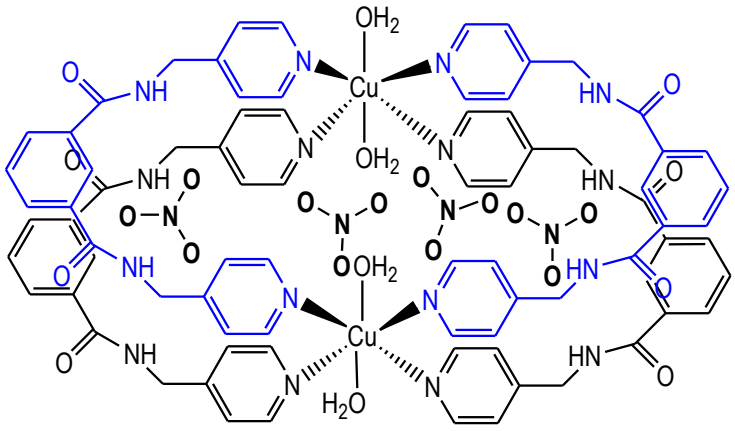

1.22

Figure 1.15. A tetragonal prism incorporating four bidentate diamide ligands and two copper(II) ions.

A more recent contribution by Puddephatt and co-workers described the potential of palladium(II) tetragonal prismatic cage (**1.23**) to encapsulate anions and water molecules in a specific manner within the solid-state structure (Figure 1.16).[68]

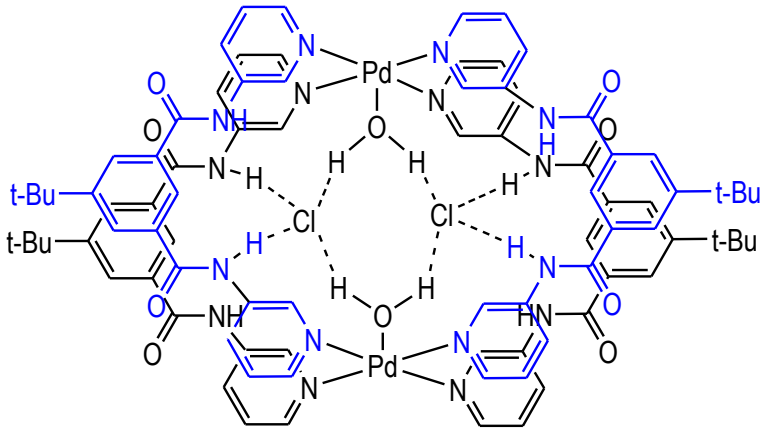

1.23

Figure 1.16. The tetragonal prismatic cage reported by Puddephatt.

Fujita and co-workers have also reported the synthesis of a tetragonal prismatic cage (**1.25**) using a rigid ligand (**1.24**) and palladium(II). Nitrate anions are encapsulated within the cavity of **1.25**.[69] A representation of Fujita's tetragonal prismatic cage is shown in Figure 1.17.

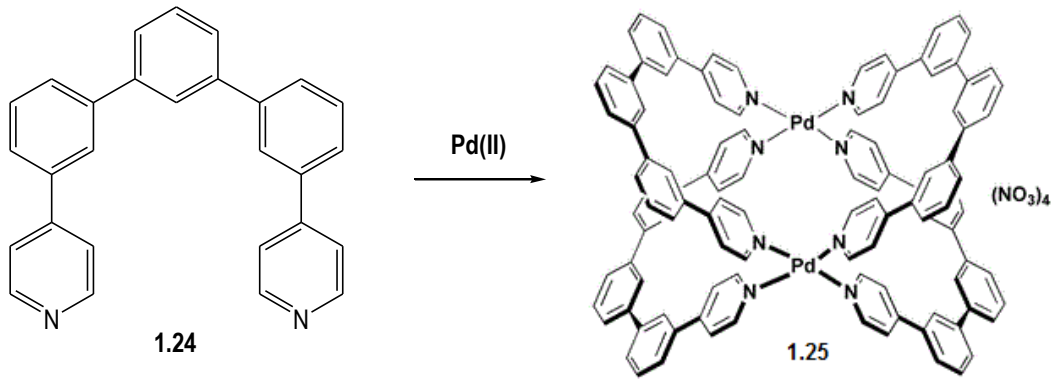

1.24 **1.25**

Figure 1.17. Fujita's tetragonal prismatic cage with nitrate anions omitted.

Another common 3-D structural motif that displays host-guest chemistry of relevance to this work is a helicate. In metallo-supramolecular chemistry helicates are obtained by the metal ions being wrapped in strands of the organic ligands, in a helical fashion. Helicates are commonly obtained using flexible ligands. Flexibility of the ligands enables them to twist and obtain a helical shape. A number of classifications to describe the structures of helicates, although based on the ligands employed, helicates can be classified into two categories, homotopic and heterotopic. If the coordinated ligand strands contain similar binding sites along their length, they will form homotopic helicates. If the ligand strands have different binding sites, the resulting helicates will be categorised as heterotopic helicates (Diagram 1.1).

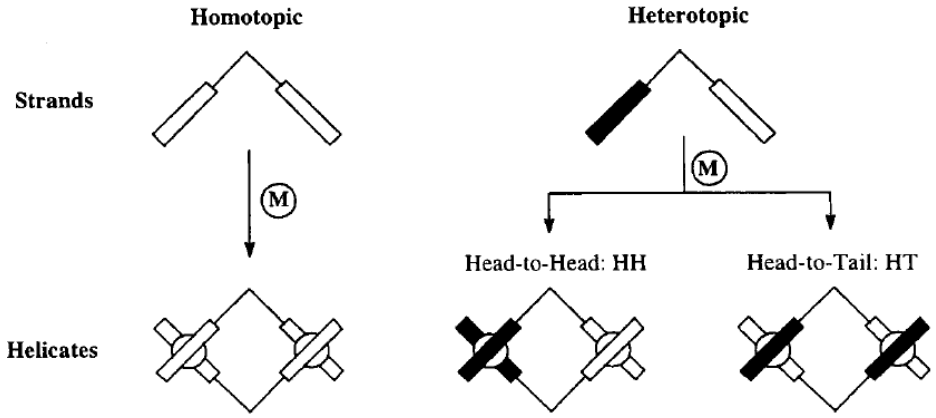

Diagram 1.1. General categories of helicates (image sourced from [70]).

Many helicates have been used as hosts in the binding and recognition of anionic guests. For instance, Rice and co-workers[71] have reported the binding of nitrate anion by a cobalt triple stranded helicates, while Janiak and co-workers[72] in their work described the anion binding potential of mononuclear $[FeL_3]^{2+}$ helicates. Lehn and co-workers have also demonstrated cyclic helicates (**1.26**) which trap templating chloride anions inside their structures (Figure 1.18).

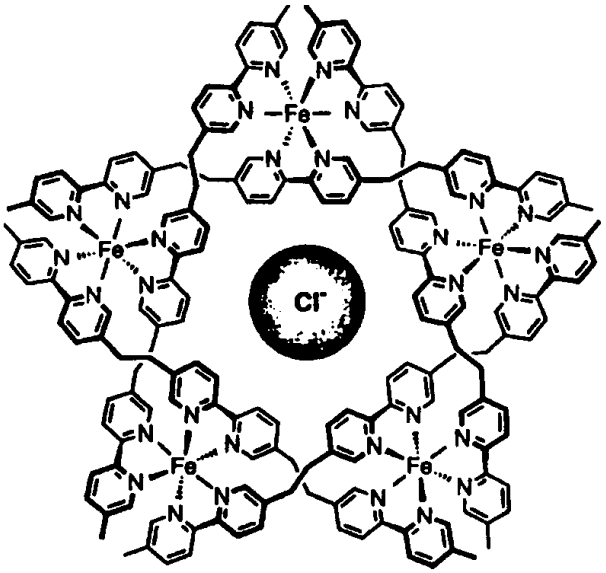

1.26

Figure 1.18. A pentametallic double-stranded helicate reported by Lehn and co-workers (image sourced from [70]).

1.3.5. Applications of discrete metallo-supramolecular species

A large number of the metallo-supramolecular species have been investigated for the development of materials for anion receptors or anion sensing. This includes the investigation of materials which complex anions in organic solvents,[74] materials that complex anions in aqueous solvent mixtures[75] and the use of compounds to bind and sense anions of biological interest *in vivo*.[76] Compounds with potential to detect the concentration of anion pollutants in water have also been developed.[77] The employment of amide hydrogen bond donors to bind anions pendant to or within metallo-supramolecular assemblies has been investigated due to the possibility of forming specific hydrogen bonding interactions with anions[78-83] and guest molecules.[84,85] Beer for instance,[86,87] is one of the pioneers of this area that involves in the investigation of metallo-hosts capable of anion sensing. Watanabe and co-workers have reported the synthesis and properties of a ruthenium complex (**1.27**) that can selectively recognise phosphoesters, where the binding with the anion is observed from the enhancement of the luminescence of the complex (Figure 1.19(a)).[88] Similar observations were reported by Beer, where the binding of anions was found to enhance the emission of the ruthenium-bipyridyl complexes.[89] Recent investigations reported by

Gale and co-workers[17,90] has described the use of square planar platinum(II) centres to pre-organise substituted quinoline ligands for anion binding (Figure 1.19(b)). The molecule (**1.28**) is capable of effectively binding a number of different anions in a competitive solvent such as DMSO.

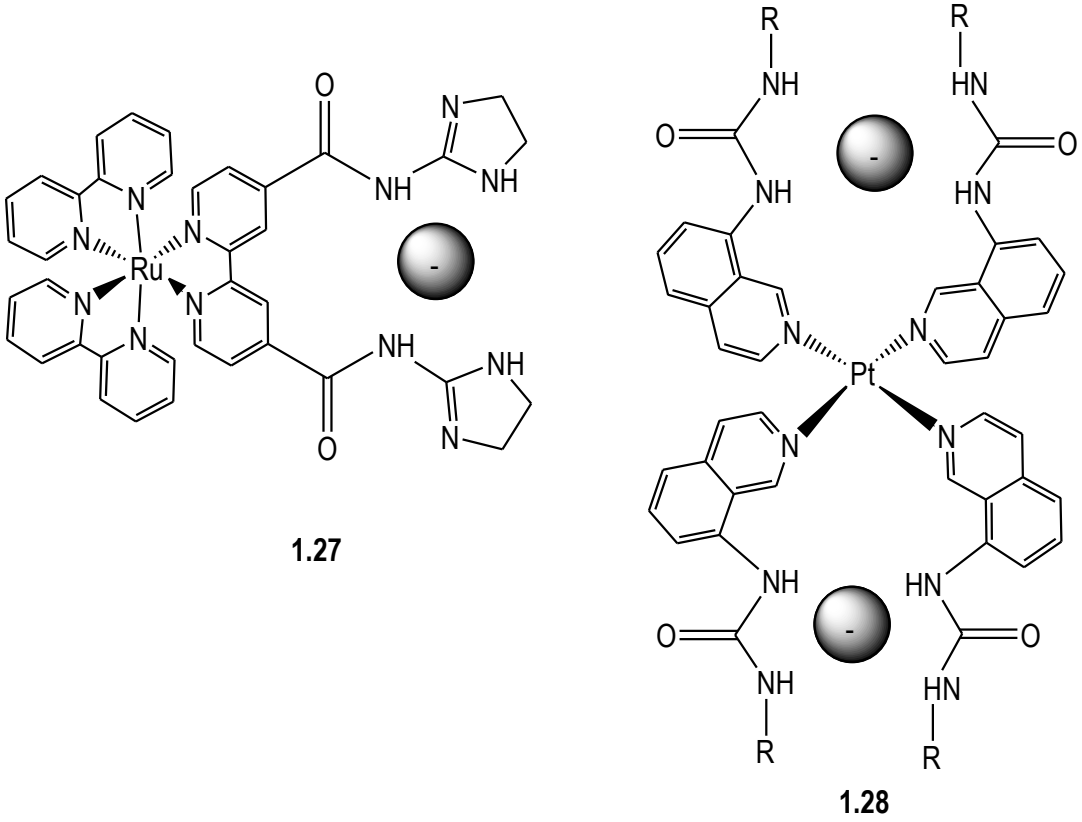

1.27 **1.28**

Figure 1.19. (a) The structure of the ruthenium complex that acts as a sensor for phosphoesters reported by Watanabe and co-workers. (b) A platinum complex that has two urea pockets for complexing anions.

Other examples of interesting metallo-hosts that acts as anionic receptors, particularly for phosphate anions, have been reported by Anslyn and co-workers. In the hosts (**1.29** and **1.30**), the phosphate anions were found to be encapsulated within the cavities formed upon coordination of the metal by the macrocyclic ligand (Figure 1.20).[91]

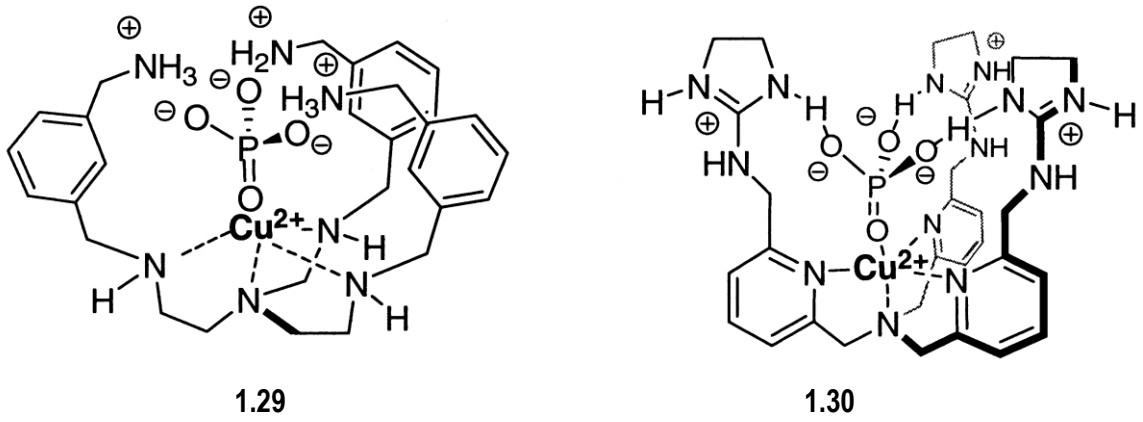

1.29 **1.30**

Figure 1.20. Representations of the hosts **1.29** and **1.30** with phosphate anions located inside the molecular cavity of the host (image sourced from [90]).

1.4. Coordination Polymers (CPs)

Coordination polymers are defined as infinite one-dimensional (1-D), two-dimensional (2-D) and three-dimensional (3-D) networks, assembled by the connection of metal ions or metal clusters through organic bridging ligands. Terms such as metal-organic coordination networks and metal-organic frameworks are also widely used to describe these types of materials. For example, the term metal-organic framework (MOF) is often used to describe highly ordered 2-D and 3-D coordination polymers that are assembled from metal oxides clusters and carboxylate donors (Figure 1.21). The nomenclature and terminology surrounding these materials is receiving considerable attention at present.[92]

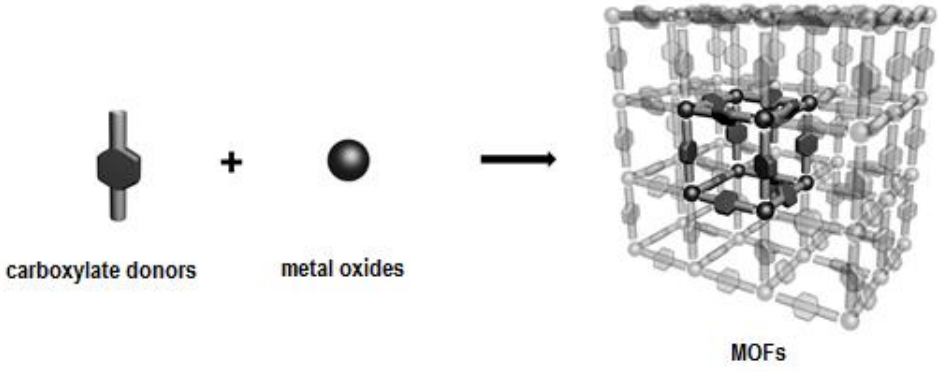

Figure 1.21. The assembly of organic linker with metal oxides to form MOFs.

There are several methods available for the synthesis of coordination polymers[93] such as: saturation/slow evaporation, diffusion, solvo-thermal, microwave and ultrasonic methods. In the saturation method, the crystals are allowed to grow from a concentrated mixture of reagents, while in the diffusion method, two different species are allowed to be slowly brought into contact before crystallisation. The solvothermal method allows the self-assembly of infinite solid-state structures from soluble precursors, and the high temperatures employed, among other things, enable bond making and breaking reaction to occur to give a phase pure product. Typically microwave and ultrasonic methods are used to improve the solubility of the reagents in order to promote reaction of the species involved. In this thesis, a majority of the coordination polymers were prepared by slow evaporation approaches. In this technique, the solution of the ligand was added to a solution of metal salt and the mixture was heated for a few minutes before the solution was left to evaporate at room temperature (Figure 1.22).

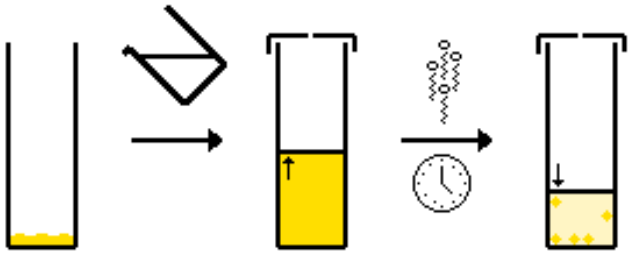

Figure 1.22. A cartoon representation of slow evaporation or saturation process commonly applied in this study.

1.4.1. Types of structures

Just as in the formation of discrete structures, as described above, the assembly of molecular building blocks, metal ion (connector) and organic ligands (linkers), leads to the formation of various 1-D, 2-D and 3-D materials with different structures and properties.[94-101] By utilising different metals, which have different hardness or softness properties, and in particular different coordination numbers and geometries (e.g., octahedral, tetrahedral, square planar *etc.*), structures with different network topologies can be prepared. The counter anions and solvents used are also important building blocks in the construction of coordination polymers. The counter anions are necessarily employed to balance the charge of the metal cation present. In 1-D coordination polymers, the metal is coordinated to two individual ligands with the ligands and the metal ions arranged alternately to form infinite chains (Figure 1.23). Various classes of 1-D coordination

polymers have been described by Leong and Vittal in their review.[102] The incorporation of metal ions that can be coordinated by three or four ligand subunits leads to the formation of 2-D coordination polymers (Figure 1.24). In turn, metal ions with higher coordination numbers provide access to 3-D coordination polymers (Figure 1.25).

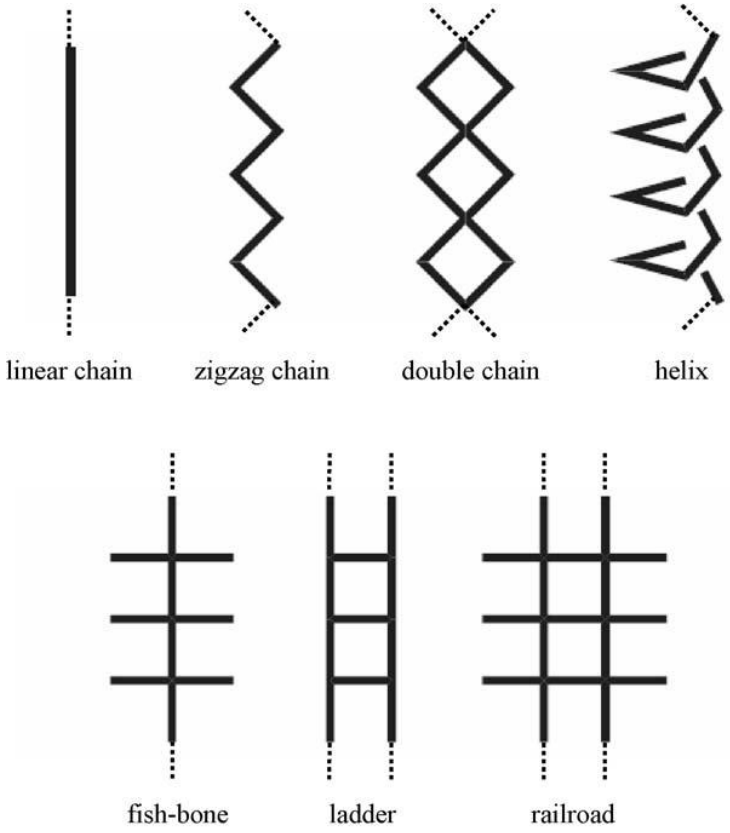

Figure 1.23. Examples of 1-D coordination polymer motifs (image sourced from [93]).

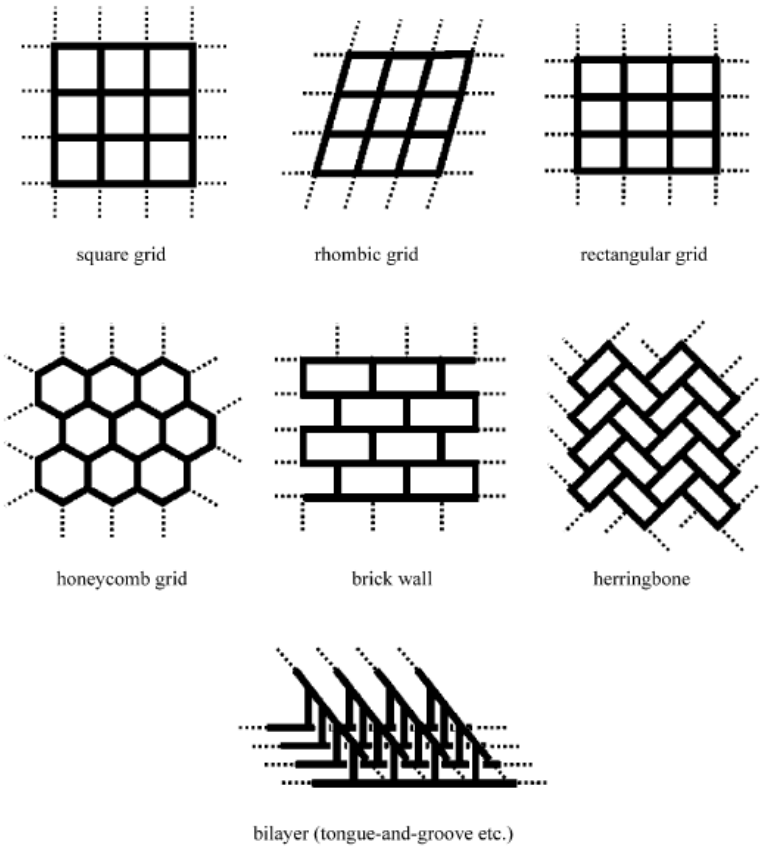

Figure 1.24. Examples of 2-D coordination polymer motifs (image sourced from [93]).

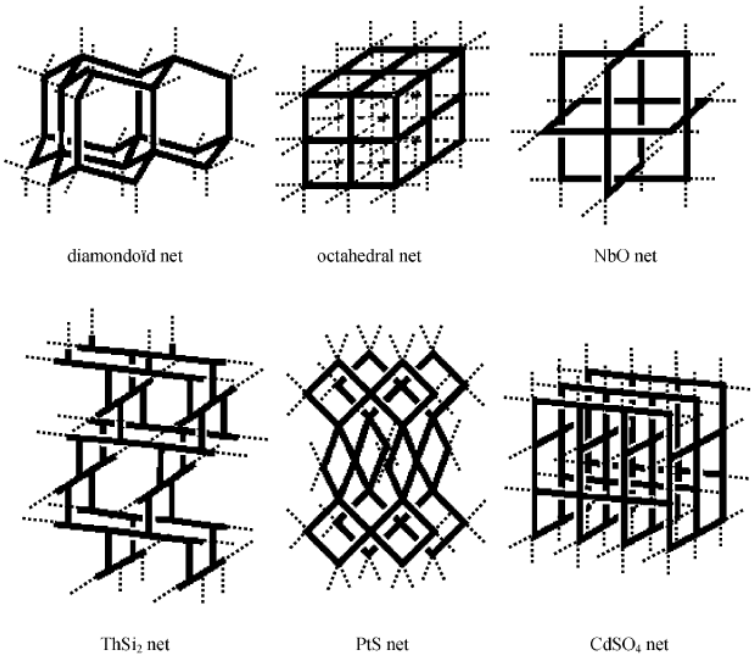

Figure 1.25. Examples of 3-D coordination polymer motifs (image sourced from [93]).

1.4.2. Types of ligands used in coordination polymers

The choice of ligand donor groups, such as carboxylate, nitrogen heterocyclic and nitrile donors dictates the relative strength of metal-ligand interactions and can influence the relative thermal and chemical stability of a framework. Besides the incorporated structural metal ions, the overall network topology is also influenced by the structure of the organic ligands. For instance, flexible aliphatic linkers typically lead to non-porous structures while rigid, conjugated linkers promote more open and robust frameworks.[96,99-101] The length and the shape of the organic ligand can influence the framework topology as well as the fundamental properties of the materials, including crystallinity, porosity and surface area. Furthermore, the number of donor groups on the ligand (bidentate, tridentate etc), will also determine the topology of the framework.

Carboxylate ligands (Figure 1.26) are the most common bridging ligands used to generate porous materials. Combination of these types of ligand with metal ions provides strong metal-ligand bonds about nodes generally comprised of individual metal centres or metal oxide clusters. Due to the nature of the coordination, materials containing such ligands commonly possess high crystallinity, structural stability and large surface areas. The ability of these materials to selectively adsorb and exchange guest species depends on the robustness of the porous material and the functionalisation of the pores by alterations to the ligand structure.

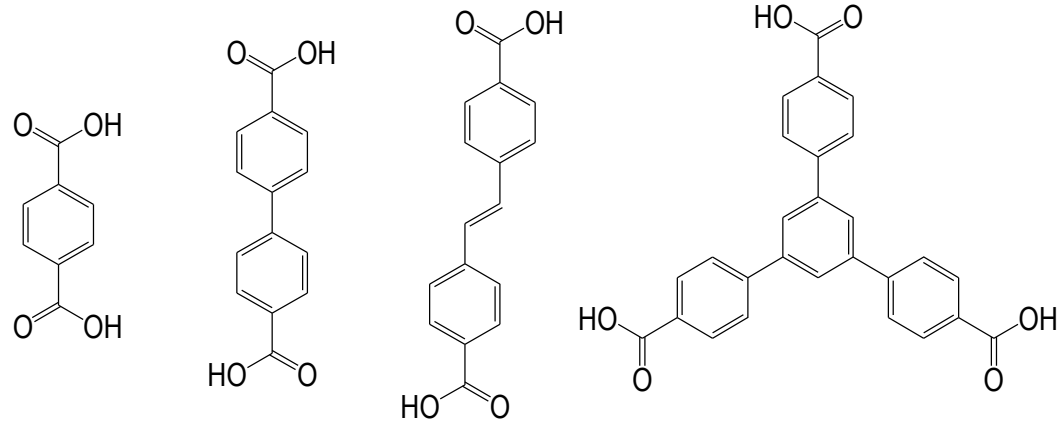

Figure 1.26. Examples of compounds with carboxylate donor groups.

Other typical examples of bridging ligands used as organic linkers contain pyridyl donor groups (Figure 1.27). The use of nitrogen heterocycles such as pyridine as the metal coordinating sites has become a popular approach to generate stable coordination polymers. The azines, such as pyridine, are π-electron deficient heterocycles that form stable complexes due to the metal to ligand back-bonding from metal *d*-orbitals into low lying π*-orbitals on the azine.

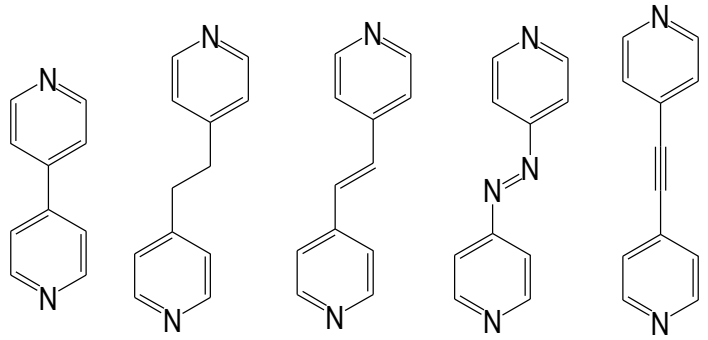

1.35 **1.36** **1.37** **1.38** **1.39**

Figure 1.27. Examples of conjugated heterocyclic compounds with pyridyl donor groups.

Finally, Figure 1.28 shows a few examples of organic bridging ligands incorporating nitrile groups as the donors. These linkers have been commonly used to generate coordination polymers that are capable of anion binding and the selectivity or anion exchange properties of these materials for a range of anions has been investigated.[19,103,104]

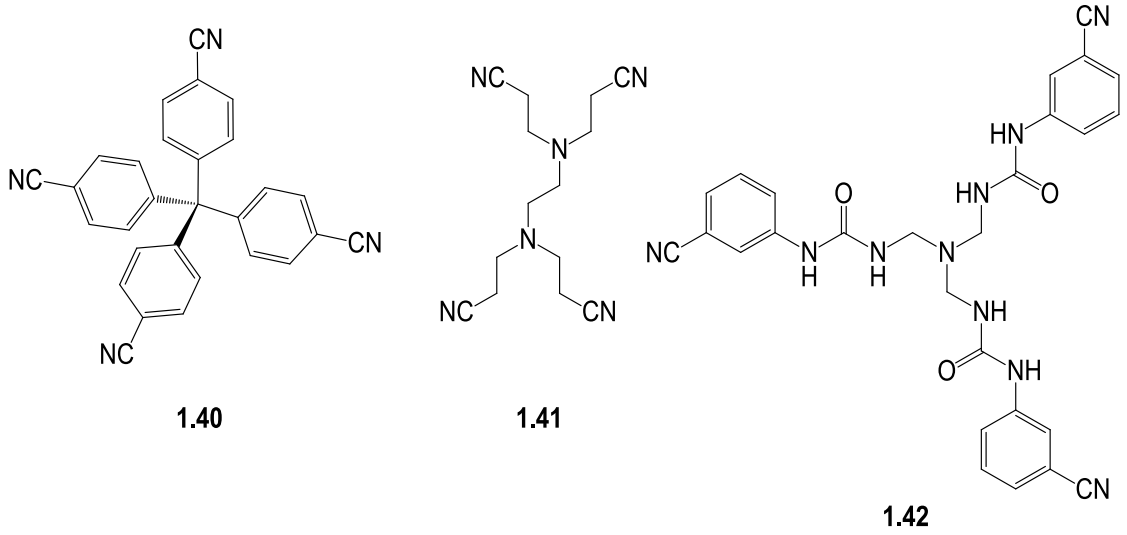

Figure 1.28. Examples of bridging ligands incorporating nitrile donors.

In terms of ligand design and synthesis, previous studies on thiourea, urea and amide derivatives have found that successful anion guest binding in supramolecular assemblies can be achieved. This would indicate that ligands containing these functional groups may act in a similar manner within metallo-supramolecular assemblies and coordination polymers. The development of amide ligands containing the 2,6-pyridinedicarboxamide core are of considerable interest and have been used for the synthesis of metallo-supramolecular assemblies capable of anion binding. Puddephatt and co-workers[105-108] for instance, have studied the use of dipyridylamides as a bridging ligand in the construction of metallo-supramolecular triangles. Several reported pre-organised amide ligands are shown in Figure 1.29.[109] Ligands such as these or closely related to these compounds could be applied to the synthesis of metallo-supramolecular assemblies and coordination polymers. Nevertheless, it is clearly indicated from the literature studies that the use of flexible dipyridylamides in metallo-supramolecular assemblies or coordination polymers is still in its infancy and need to be further explored. The use of flexible ligands could also lead to a dynamic coordination framework that responds to specific guest molecules as these types of ligands could also change their cavity to suit the size or the shape of the guest molecule.[110] Realising the advantages of using flexible ligands and their unique properties, the work described in this thesis has focused on the incorporation of pre-organised amide ligands with limited degrees of freedom into metallo-supramolecular assemblies and coordination polymers, that may generate new anion binding motifs.

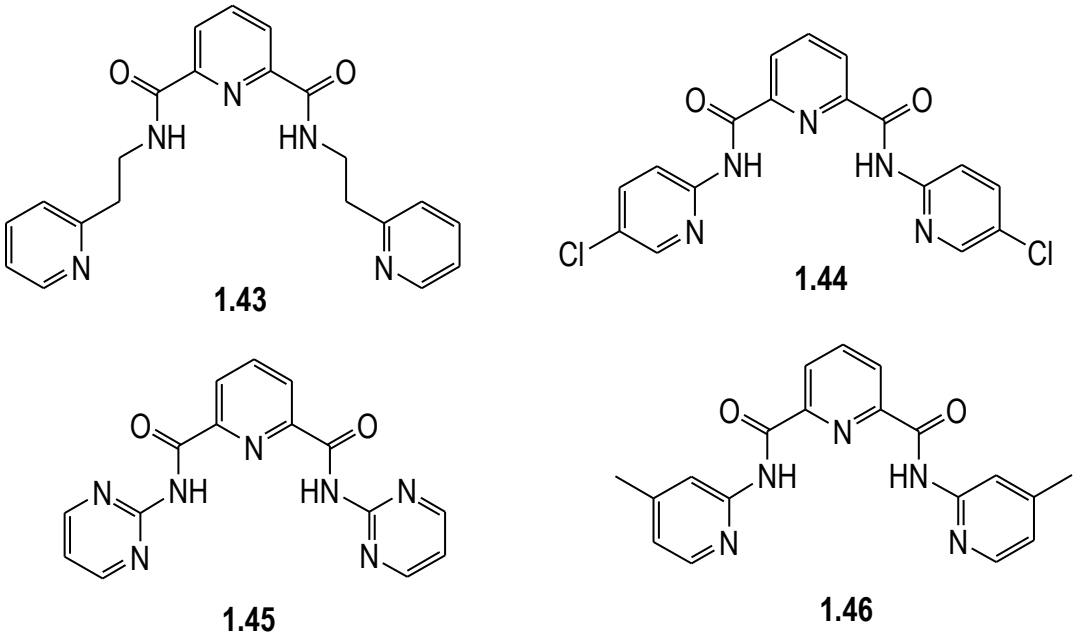

Figure 1.29. Several examples of reported ligands incorporating pre-organised amide moieties.

1.4.3. Applications of coordination polymers

Many of the potential applications of porous coordination polymers are focused in areas that take advantage of the robust and porous nature of these solids, including physisorption, chemisorption, molecular sieving, ion exchange, separation science and catalysis. In addition to being useful in chemical separations, as sensors and as potential catalysts, one proposed applications of porous materials, such as coordination polymers or MOFs is their ability to store gaseous guest species.[111-114] Significant attention has been directed toward MOFs as hydrogen storage materials due to the publication of targets for H_2 uptake by the United States Department of Energy (DOE).[115] Porous materials with the desired properties required for gas storage can be rationally prepared by controlling the type of network and the chemical nature of the pores. The examples of well-known MOF-5 (**1.47**) and MOF-177 (**1.48**) that have been prepared from the reaction of 1,4-benzene-dicarboxylate and Zn^{2+}, and 1,3,5-benzene tricarboxylate and Zn^{2+} are shown below.

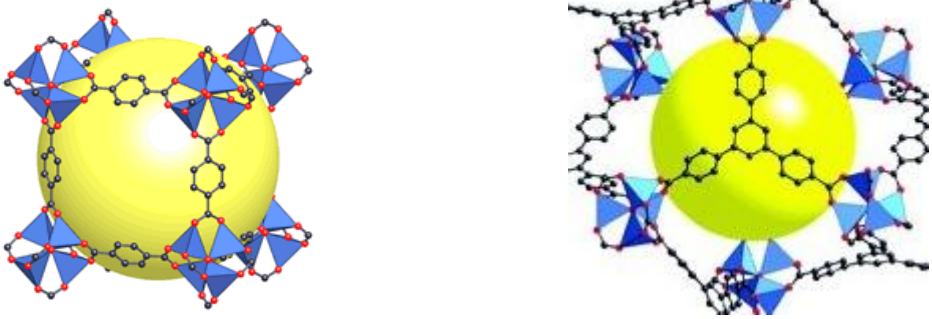

1.47 **1.48**

Figure 1.30. Individual repeating units in the structures of MOF-5 and MOF-177 (image sourced from [96]).

Framework flexibility has been recognised as an advantage for high performance molecular recognition, separation and sensing applications.[116,117] In contrast to rigid porous materials, flexible porous coordination polymers (PCPs) can expand, shrink, or distort their soft coordination networks to fit the target molecules.[117-120] In many cases, flexible organic ligands are chosen as bridging links to build interesting PCPs.[121] Furthermore, these third generation coordination frameworks may act as actuators in molecular recognition and sensors, respectively.[122-125]

A further potential application, and one with direct relevance to the work contained in this thesis, is to utilise these materials as anion receptors. Recently, coordination polymers that can selectively precipitate particular anion salts from solution in the presence of a mixture of charged species have been reported.[126] The principles of anion selectivity and separation has been described in detail by Custelcean and Moyer in their review.[78] There are two stages to the mechanism proposed for anion exchange in coordination polymers, which involves dissolution (Scheme 1.4(a)) and crystallisation (Scheme 1.4(b)). As part of this process, the anion selectivity in coordination polymers or MOFs is also influenced by intermolecular interactions between the anions and the crystalline matrix. The separation of the anion is based on the nature and the strength of the interactions between the anion and the frameworks, where the weakest interactions will follow the Hofmeister anion exchange order ($PO_4^{3-} < CO_3^{2-} < SO_4^{2-} << Cl^- < Br^- < NO_3^- < SCN^- < I^- < ClO_4^-$). Selectivity based on anion size is also important for framework

materials and this may be the origin of anion selectivity in certain cases. There have been a number of recent studies into the use of coordination polymers for anion separation[78,127,128] and some of these are outlined below.

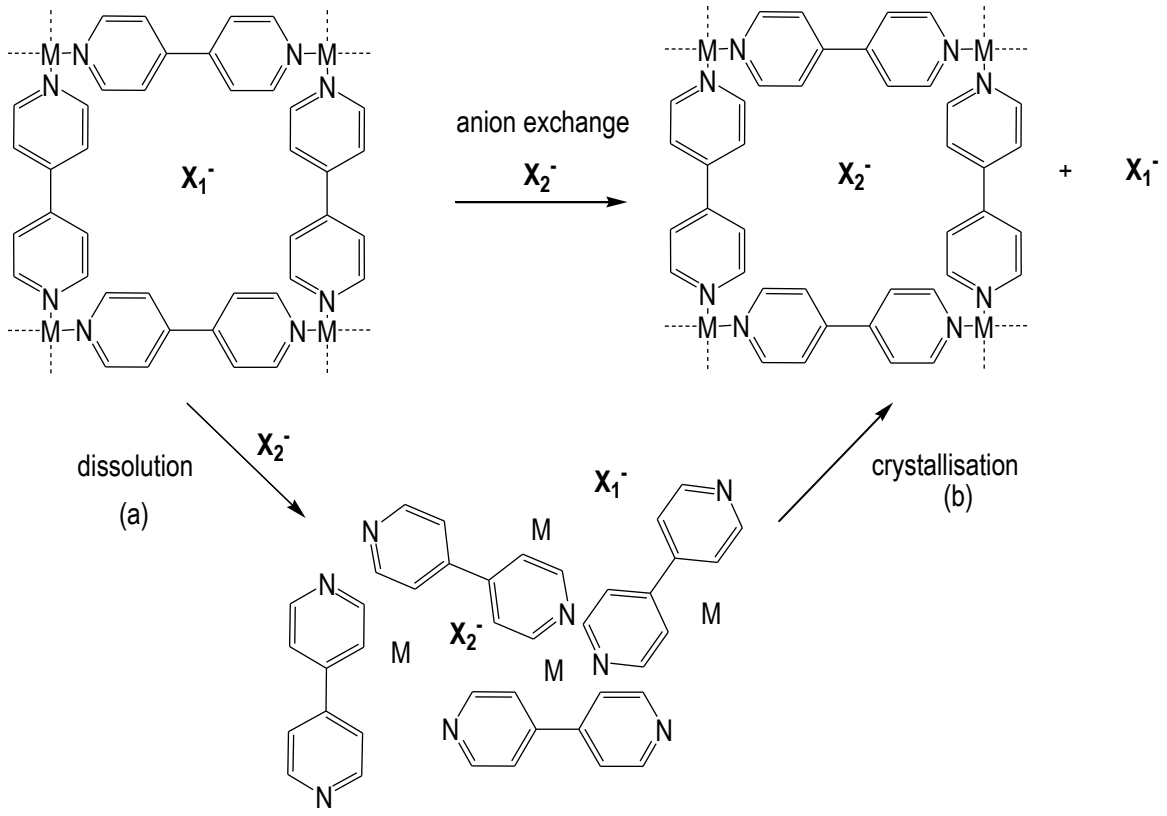

Scheme 1.4. Proposed mechanisms for anion exchange in MOFs.

As noted above, coordination polymers derived from ligands functionalised with hydrogen bond donors are of current interest because of the possibility of forming inter-network hydrogen bonding,[129,130] and their ability to recognise counter anions[78,79,81-83,103,131,132] and various guest molecules *via* hydrogen bonding interactions.[84,85] Such materials, with the ability to form hydrogen bonding interactions with anionic guest molecules, can be represented schematically as shown in Figure 1.31.

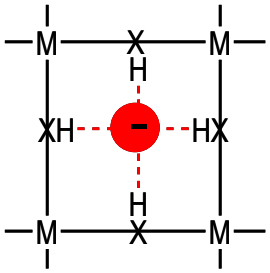

Figure 1.31. A subunit of a coordination polymer and its interactions with anion guests through hydrogen bond donors.

As part of related studies of coordination polymers containing ligands functionalised with hydrogen bond donors, it has been noted (vide infra) that hydrogen bonding groups typically prefer to self-associate to form intramolecular hydrogen bonds within the network. This can potentially diminish their ability to bind anions. To overcome this tendency, molecules with very strong and directional hydrogen bonding groups can be introduced as the domains for the anion guest. By using this approach, Custelcean and co-workers have reported several coordination polymers incorporating hydrogen bonding groups for anion recognition and separation.[133] In particular, they have used urea-anion hydrogen bonds interactions within the coordination frameworks.[78,133]

1.5. Research Aims

In the work described in this thesis, new ligands were targeted that provide access to novel materials (metallo-supramolecular assemblies and coordination polymers) incorporating amide containing cores as the basis of anion coordinating motifs. The targeted ligands contain pre-organised amide moieties intended for anion recognition and two exterior metal coordinating sites that comprises of pendant pyridine donors. In particular, these materials are targeted for their anion binding and sequestration properties, either as discrete complexes and metallo-supramolecular assemblies (Figure 1.32(A)) or coordination polymers (Figure 1.32(B)). By studying the coordination behaviour of these ligands, established either in discrete metal complexes or coordination polymers, an understanding of solid-state chemistry of such materials will be enhanced. It was anticipated that the presence of amide groups may alter the nature of pores within structure, making them suitable for selective anion binding.

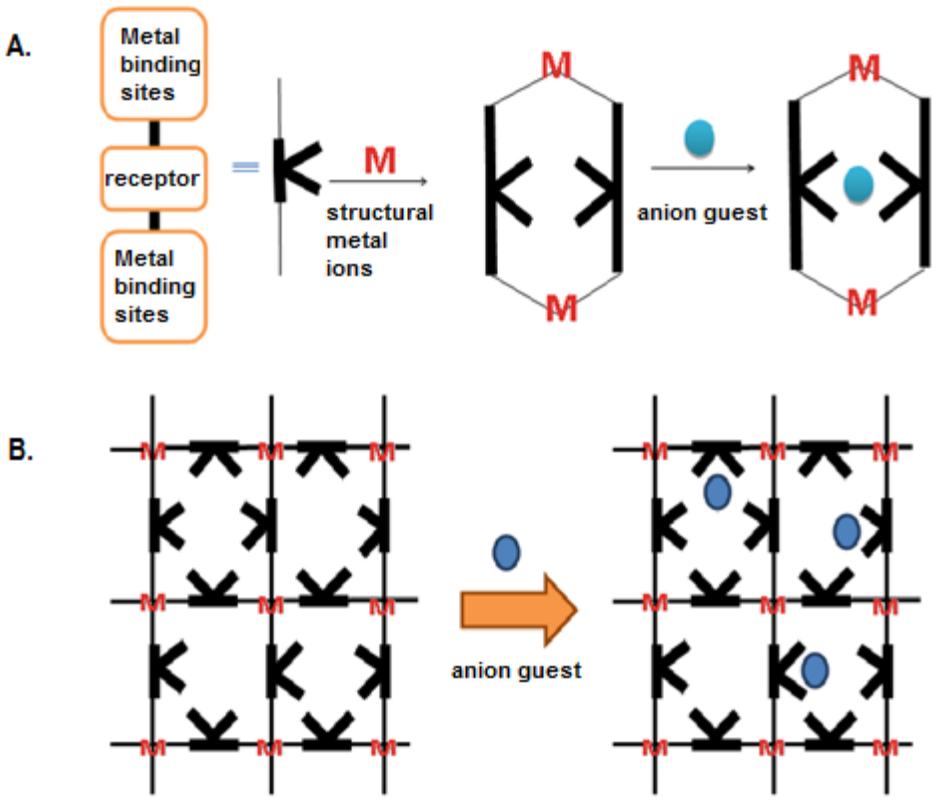

Figure 1.32. The representation of anion binding models incorporating preorganised amide ligands investigated in this study (A) A discrete complex (B) Coordination polymers.

1.6. Thesis coverage

This thesis describes the synthesis and coordination chemistry of amide-containing polypyridyl ligands derived from 2,6-dimethylpyridinedicarboxylate and other related precursors. The details of the synthesis and characterisation of the ligands involved are outlined in Chapter 2. Chapter 3 presents the coordination chemistry of monoamide ligands (**L1**-**L4**). The coordination chemistry of the diamide ligands (**L5**-**L6**) and tetraamide ligands (**L7**-**L12**) is described in Chapter 4, along with the preliminary anion competition experiments for **L5** and **L6**. Chapter 5 presents the synthesis and coordination chemistry of three novel bridging ligands with chelating motifs (**L13**-**L15**). Chapter 6 presents a summary of the thesis and future directions, while the experimental and the instrumental details are outlined in Chapter 7.

CHAPTER 2

LIGAND SYNTHESIS

Chapter 2

2. Ligand synthesis

2.1. Introduction

In this chapter the syntheses of four known amide ligands and eleven new amide ligands are described. The majority of these ligands are derived from 2,6-dimethylpyridine dicarboxylate (**2.1**) and related precursors to provide a pre-organised 2,6-pyridine dicarboxamide central moiety and two pre-arranged amide NH donors. By employing the 2,6-pyridine dicarboxamide moiety, rigid and highly pre-organised systems with internally directed hydrogen bond donors with the potential to bind anions may be generated (Figure 2.1(a)). Figure 2.1(b) provides an example of these hydrogen bonding interactions as observed in one of the complexes prepared in this study.

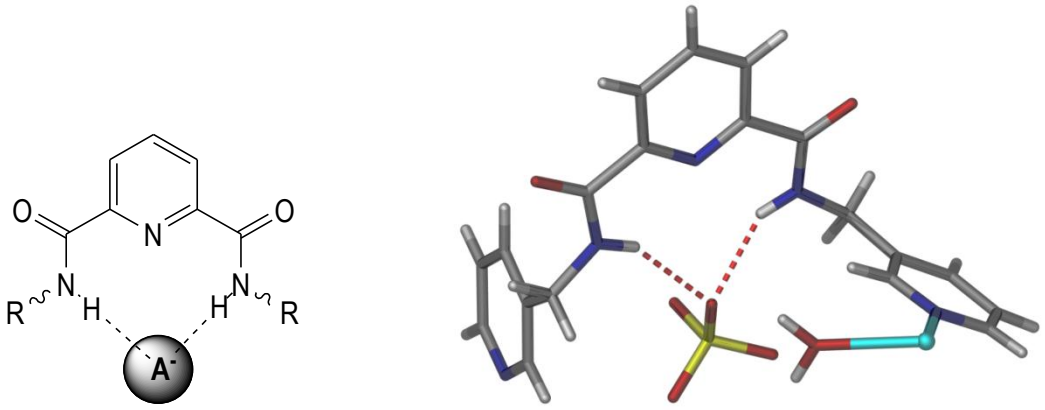

(a) (b)

Figure 2.1. (a) The general structure of 2,6-pyridine dicarboxamide pre-organised NH amide (where the R groups are pyridyl donors, which are capable of metal coordination) and (b) a crystal structure of one of the complexes obtained in this project showing the binding of perchlorate molecules with both amide NH donors.

The mono-, di, and tetraamide ligands discussed in this chapter have either one, two or four pyridyl groups as pendant donors for metal coordination. The four monoamide compounds (**L1**-**L4**), whose coordination behaviour is outlined in Chapter 3, contain only one amide moiety for linking the 2,6-pyridine dicarboxamide to a single pendant pyridyl donor. The bis-pyridyl amide compounds (**L5**-**L12**) contain two or more amide moieties, directed for anion complexation within discrete and infinite metallo-supramolecular structures, and two external pyridyl groups ready for metal coordination. The structures and synthesis of the majority of the pre-organised amide ligands investigated in this study are shown below.

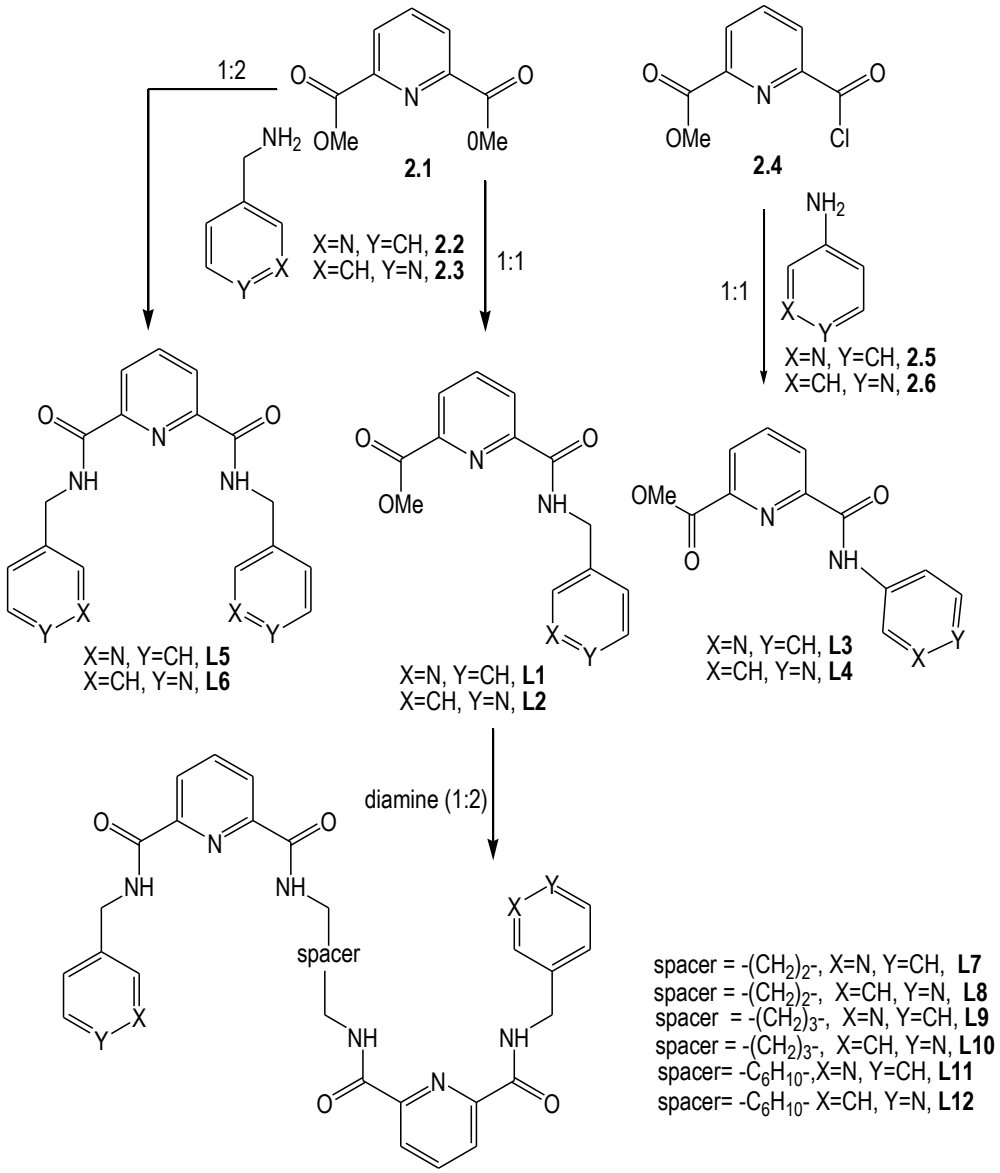

Scheme 2.1. A summary of the synthesis for the majority of the pre-organised amide ligands discussed in this thesis.

The final set of compounds described in this thesis have two chelating metal groups derived from di-2-pyridylketone separated by a pyridine dicarboxylate or related arene core. In nearly all compounds investigated, a methylene group (-CH_2-) was located between the amide and the pyridine ring, which conferred additional flexibility to the compounds obtained.

2.1.1. Pyridine dicarboxamide in supramolecular chemistry

2,6-Pyridine dicarboxamide and its derivatives have been studied in many aspects of chemistry, as molecular receptors,[134,135] for dendrimer synthesis[136] and in asymmetric catalysis.[137,138] Derivatives of 2,6-pyridine dicarboxamide have also been investigated for their anti-inflammatory, antipyretic and analgesic activity,[139] while the derivatives of *N,N'*-dipyridyl-2,6-pyridine dicarboxamides in particular have found use in the treatment of atherosclerosis.[140] Apart from this general interest, amides are frequently used in the design of anion receptors. These molecular receptors are often designed with some degree of pre-organisation which direct the formation of cleft-like structures.[141,142] Isopthalamide or 2,6-pyridine dicarboxamide units are among the most common building blocks used for forming pre-organised hosts.[143,144]

Researchers, including Davis, Gale, and Quesada have reported various types of pre-organised amide receptors that are able to complex a range of anionic guests *via* hydrogen bonding.[145] More interestingly, the potential of isophthalamide derived receptors to transport chloride across the vesicle membranes has been reported by one of these groups.[146] Gale and co-workers have replaced the isophthalamide core with 2,6-pyridine dicarboxamide moiety and as a result, a highly pre-organised receptor that exhibits higher chloride affinity and membrane flux was obtained.[146] The use of 2,6-pyridine dicarboxamide to generate pre-organised receptors arises from the propensity of the 2,6-pyridine dicarboxamide moiety to form a *syn-syn* bis(amide) conformation.[147] This conformation creates convergent H-bonding sites, which is effective for binding anions. Gale and co-workers have also reported the potential of 2,6-pyridine dicarboxamide derived receptors to recognise neutral guests such as ureas, imidazoline and barbiturates from a mixture of solvent.[148] Figure 2.2 shows an example of barbital complex that has been reported by Gale.

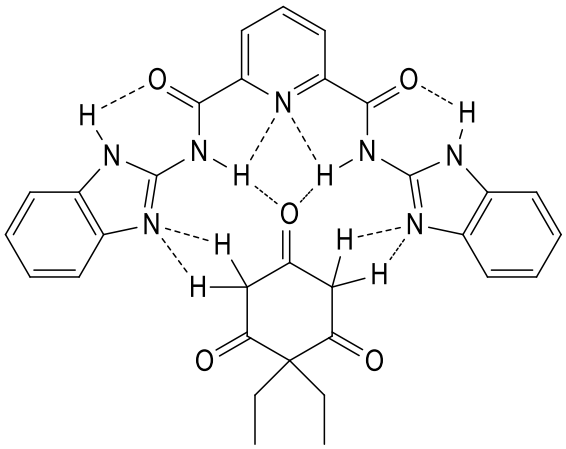

2.6

Figure 2.2. The example of pre-organised amide receptors and it barbital complexes.

Anatoly and co-workers have also reported a number of pre-organised amide receptors suitable for anion recognition.[10] In their study they observed that the 2,6-pyridine dicarboxamide hosts are bound to the anion by the amide NH donors to form anion complexes. For example, compound **2.7** was found to interact with chloride through intramolecular hydrogen bonding interactions from both amides NH and pyridinium CH donors (pendant arms).

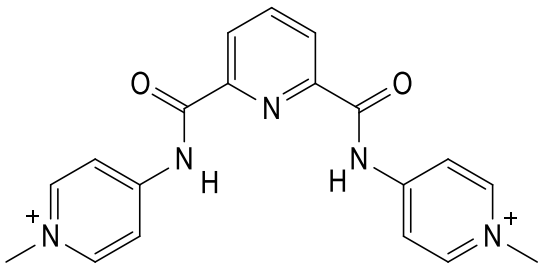

2.7

Figure 2.3. An example of a reported amide receptor incorporating pre-organised 2,6-pyridine dicarboxamide core.

More recently, molecular receptors have been investigated for dual applications such as anion recognition and catalysis.[149-151] Kinsella and co-workers, for example, have investigated the

catalytic properties of some molecular receptors containing amide moieties in the Baylis-Hillman reaction.[149] The study has shown that the bifunctional amide receptors incorporating an *N*-acylsulfonamide moiety (**2.8**) gave the best catalytic profile compared to other bisamide receptors.

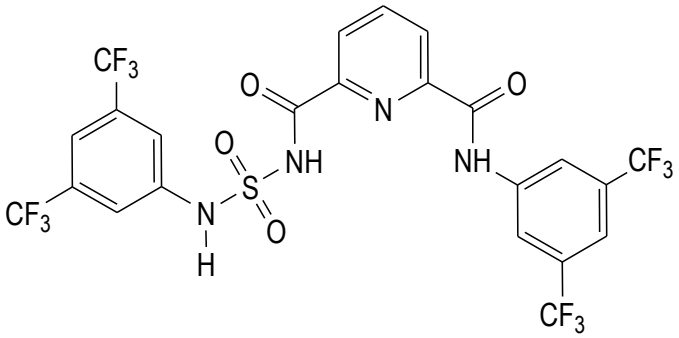

2.8

Figure 2.4. The structure of compound **2.8**.

In summary, the pre-organised amide moiety is a very attractive and important host not only for binding anions, but also to complex neutral guest molecules. The use of substituted 2,6-pyridine dicarboxamides as groups for neutral or anion binding, and more recently as catalysts, has inspired further exploration of this area. Due to these and other developments, the ligands outlined in this chapter were synthesised to further develop aspects of anion coordination within discrete complexes and coordination polymers. All compounds exhibit amide NH hydrogen bonding donor groups that may be useful for anion separation or sequestration. By installing additional flexibility (or degrees of freedom) over previously reported amide ligands of this type, it was proposed that the ligands would allow for the formation of larger metallo-supramolecular assemblies or more open coordination polymers which in turn are capable of accommodating larger sized guest molecules within their molecular cavities or pores. In this study, 2,6-pyridine dicarboxamide is utilised as the binding host for its preorganisation but also because this moiety is more electron deficient and could provide superior anion binding properties compared to isopthalamide moieties.[152,153]

2.1.2. Synthetic approaches to amides

Most commonly, pyridine carboxamide compounds can be prepared from condensation reactions between pyridylamines and acyl carbonyl compounds. This involves the acylation of amines or ammonia by acyl halides, anhydrides, carboxylic acids, carboxylic esters and amides.[154,155] Among of all these approaches, the treatment of acyl halide derivative (**2.9**) with ammonia or, more importantly in the context of this thesis, an amine (**2.10**) is the very general and useful method in the preparation of amides (**2.11**) (Scheme 2.2).

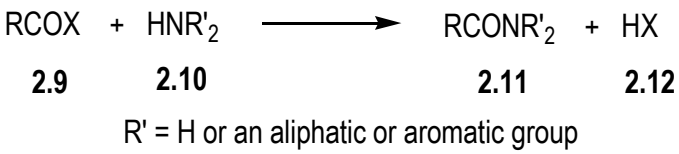

Scheme 2.2. Acylation of ammonia by acyl halides.

Other approaches, such as acylation of amines by carboxylic acids, can be used to produce amides. In this approach, coupling agents such as 1,1'-carbonyldiimidazole, diphenoxyphosphoryl azide or triphenylphosphite are used to promote the reactions.[137,156,157] Acylation of amines by carboxylic esters is also a very useful approach to generate amides. These amide compounds can be prepared by an appropriate choice of the amine. In this work, the majority of the flexible amide ligands are prepared by a one-step nucleophilic substitution of 2,6-dimethylpyridine dicarboxylate with picolylamine, rather than the equivalent acid chloride.[158] This synthetic route was chosen because it is straightforward, using an ester that can be prepared on multi-gram quantities and stored for months without apparent hydrolysis, and high yielding. Under the alkaline conditions, the ester reaction is catalysed by excess amine and thus reactions require a slight excess of amine. In this approach, a proton is being transferred in the rate determining step and two molecules of amine are involved (Scheme 2.3). At the end of this reaction, an alcohol is obtained as the by-product.

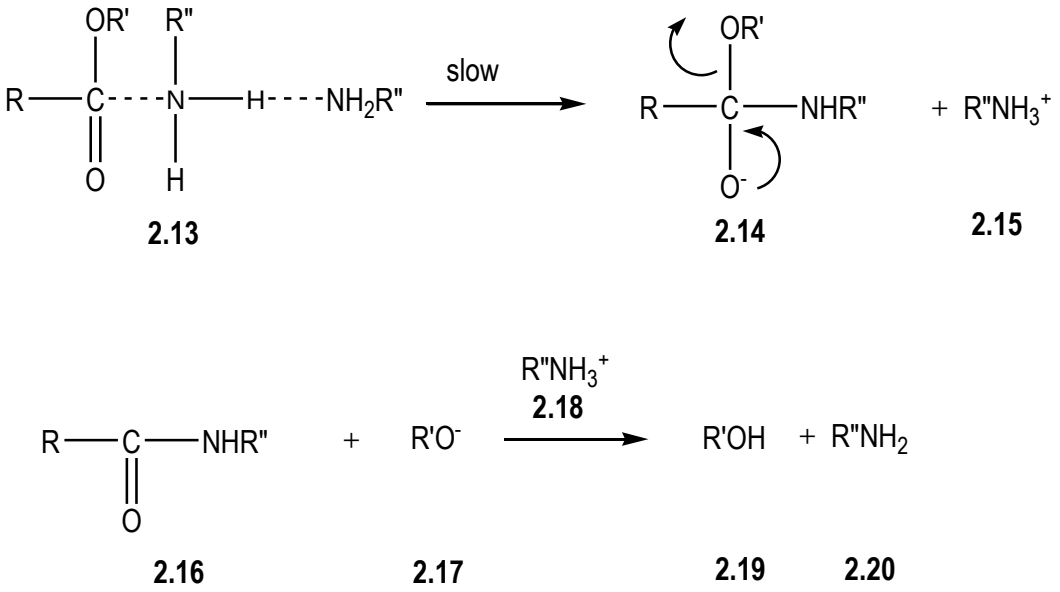

Scheme 2.3. Amide synthesis from an ester under base-catalyzed conditions.

Amide synthesis from an ester can also take place under acidic conditions. Under these conditions the breakdown of **2.14** becomes rate determining (Scheme 2.4). These reactions are equilibria so the reverse reactions result in hydrolysis of the amides to yield an amine and the carboxylic acid. The amide hydrolysis of one monoamide ligand is described in Chapter 3 and observed for at least one compound in Chapter 5.

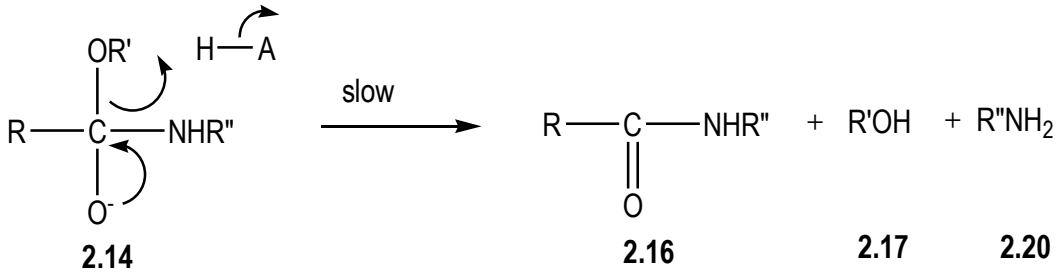

Scheme 2.4. . Amide synthesis from an ester under acid-catalysed conditions.

2.1.3. The use of amide ligands in metallo-supramolecular chemistry

As outlined in Chapter 1, amide ligands have found extensive use in metallo-supramolecular chemistry. The ability of compounds incorporating functional groups such as amide,[78-83] [84,85] sulphonamide[159] and urea[160] to bind anions and various guest molecules *via* hydrogen bonding interactions has been extensively explored. As described in Chapter 1, while rigid linkers generally provide somewhat limited access to higher complexity supramolecular architectures, flexible ligands can be readily used to construct interesting and complex supramolecular structures. Therefore this research has focused on the incorporation of moderate to highly flexible amide ligands into such assemblies. The internal amide may alter the chemical nature of cavities or pores within these assemblies making them suitable for selective binding of wide range of guest molecules.

2.1.4. Related amide ligands

The compounds prepared and investigated in this research constitute three groups. In the first section, the preparation of four monoamide ligands containing a 2,6-diamidopyridine core are described. The compounds *N*-6-[(3-pyridylmethylamino)carbonyl]-pyridine-2-carboxylic acid methyl ester (**L1**) and *N*-6-[(4-pyridylmethylamino)carbonyl]-pyridine-2-carboxylic acid methyl ester (**L2**) have been previously reported, but the coordination chemistry of these compounds was not investigated.[161] These compounds were synthesised by a method based on a procedure previously reported for *N*-6-[(2-pyridylmethylamino)carbonyl]-pyridine-2-carboxylic acid methyl ester (**2.21**),[162,163] where the monoamide derivatives are favoured by the use of a 1:1 stoichiometry in the reaction between the amine and 2,6-dimethylpyridine dicarboxylate. The structures of these three isomeric monoamide compounds are shown below.

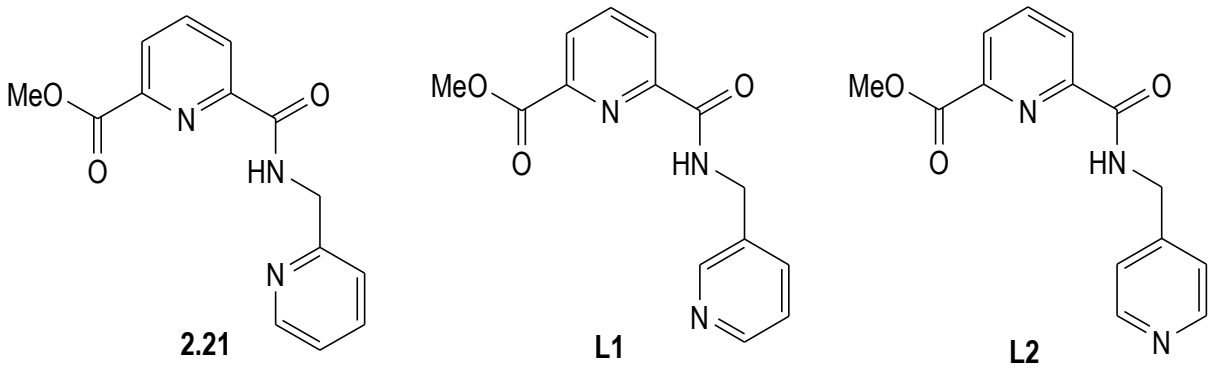

Figure 2.5. Examples of monoamide ligands related to this research.

Two related monoamide compounds, *N*-6-[(3-pyridylamino)carbonyl]-pyridine-2-carboxylic acid methyl ester (**L3**) and *N*-6-[(4-pyridylamino)carbonyl]-pyridine-2-carboxylic acid methyl ester (**L4**) with a more rigid structure were prepared to allow a comparison to the coordination chemistry observed for **L1** and **L2**. In contrast to the flexible amide compounds, the rigid monoamide derivatives were prepared by reaction of 3- or 4-aminopyridine with 6-(methoxycarbonyl)pyridine-2-carboxyl chloride. This is similar to the preparation the isomeric 2-pyridyl analogue of **L3** and **L4,** labelled as **2.22** in Figure 2.6.[163-164]

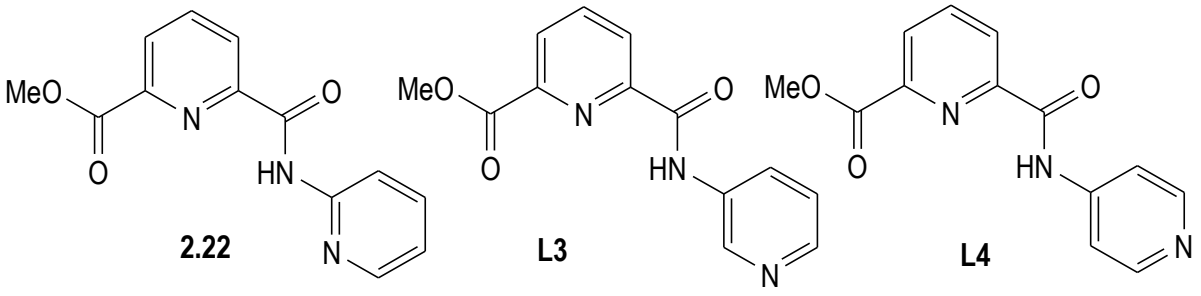

Figure 2.6. The more rigid monoamide ligands **2.22**, **L3** and **L4**. An investigation of the coordination chemistry of **L3** and **L4** is reported in this thesis.

The second section in this chapter describes the preparation of a series of flexible symmetrical amide ligands, derived from 2,6-dimethylpyridine dicarboxylate and picolyl amines,

or the monosubstituted amide derivatives, **L1** and **L2**, and aliphatic diamines. These first two compounds were prepared in a similar manner to that described for **L1** and **L2**, by altering the stoichiometry of the reaction to favour formation of the desired diamide products. The synthesis of the diamide compounds, *N,N'*-2,6-*bis*(3-pyridylmethyl)pyridine dicarboxamide (**L5**) and *N,N'*-2,6-*bis*(4-pyridylmethyl)pyridine dicarboxamide (**L6**) (Figure 2.7), have been previously reported, but very little of their coordination chemistry had been investigated at the commencement of the project.[161] Thus, this thesis will also describe the coordination chemistry observed for the diamide compounds, **L5** and **L6**. The isomeric compound, *N,N'*-2,6-*bis*(2-pyridylmethyl)pyridine dicarboxamide (**2.23**), which is the 2-pyridyl analogue of **L5** and **L6**, has been reported. It was prepared by reaction of pyridine-2,6-dicarbonyl dichloride with 2-aminomethylpyridine, using triethylamine as a base.[164,165] Copper(II) complexes of this compound have also been reported and extensively investigated by Lawrance.[166] However though, aside from this report, very little attention has been paid to these flexible ligands in comparison to their more rigid analogues (**2.24** – **2.26**) that lack the methylene spacer between amide nitrogen and the pyridine donor. In contrast to **L5** and **L6**, **2.25** and **2.26** have been extensively used for the synthesis of metallo-supramolecular cages[105,167] and coordination polymers.[109,167-172]

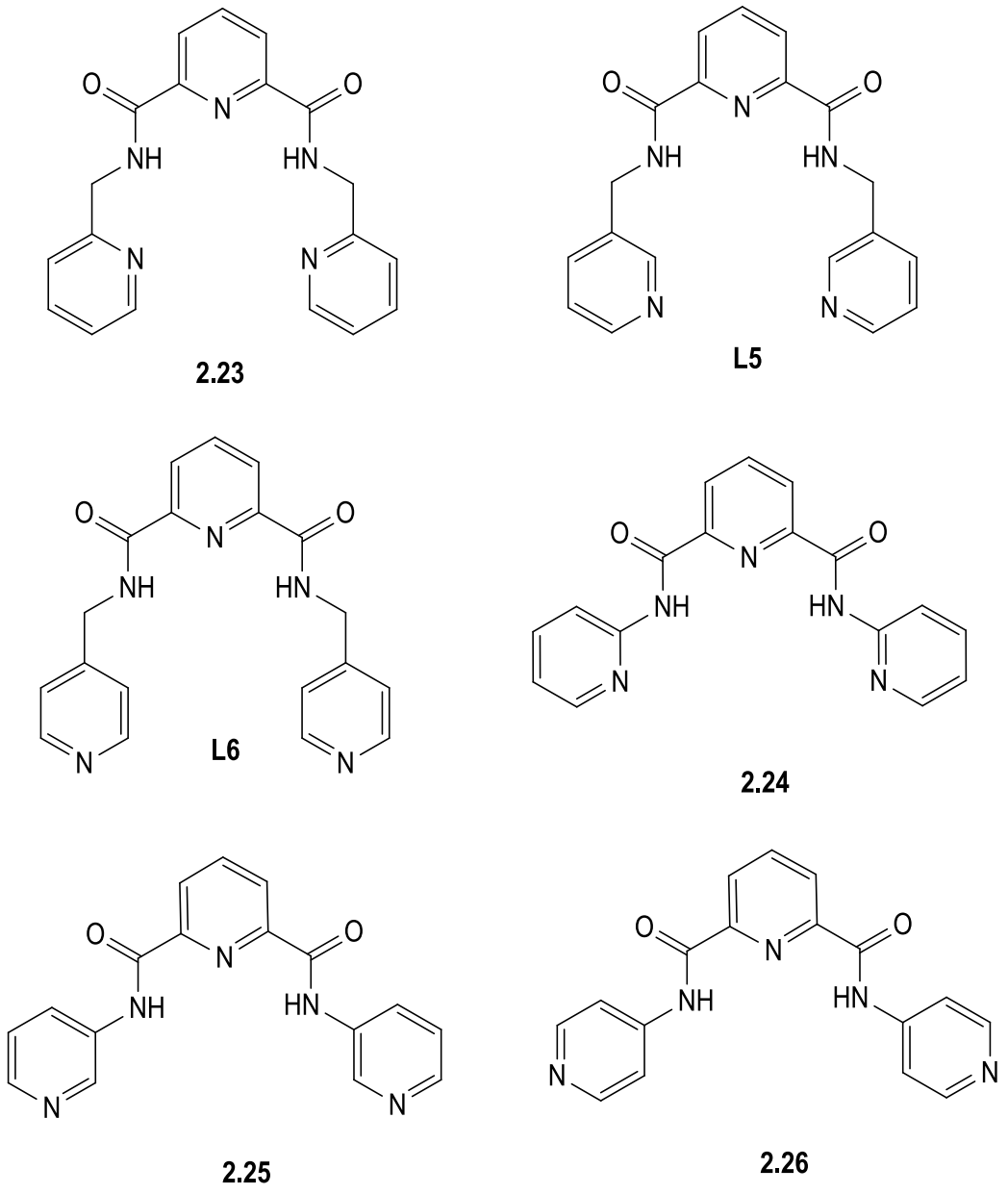

Figure 2.7. The structures of reported diamide ligands and compounds **L5** and **L6**.

The synthesis of four new tetraamide compounds, 1,2-bis[*N,N'*-6-(3-pyridylmethylamido)pyridyl-2-carboxyamido]ethane (**L7**), 1,2-bis[*N,N'*-6-(4-pyridylmethylamido)pyridyl-2-carboxyamido]ethane (**L8**) 1,2-bis[*N,N'*-6-(3-pyridylmethylamido)pyridyl-2-carboxyamido]propane (**L9**) and 1,2-bis[*N,N'*-6-(4-pyridylmethyl amido)pyridyl-2-carboxyamido]propane (**L10**), is also discussed in the same section (Figure 2.8). These flexible ligands possess one 'pocket' for anion binding in one conformation and two in a

second conformation, due to the free rotation at the sp^3 -CH_2-CH_2- central linker. A potentially interesting aspect of these compounds is that each pyridine-2,6- dicarboxamide moiety could act to replace a single (thio)amide or (thio)urea moiety in many of the related compounds reported in the literature. This will provide, as noted above, multiple preorganised anion binding moieties in each compound.

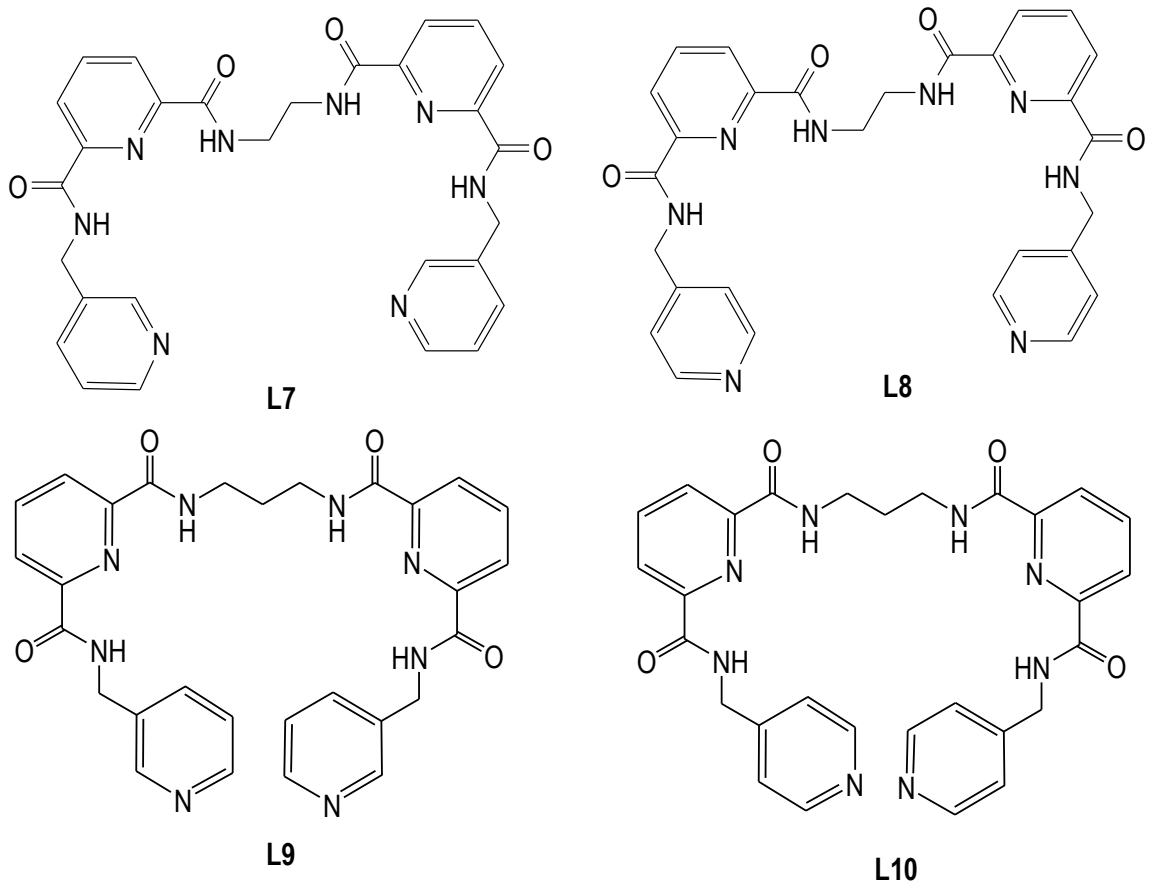

Figure 2.8. The tetraamide ligands investigated in this study with ethyl (**L7** and **L8**) and propyl spacers (**L9** and **L10**) between the pre-organised 2,6-pyridine dicarboxamide subunits.

Instead of using acyclic aliphatic spacers to generate the flexible ligands,[173-178] the use of a cyclohexane spacer has also been reported.[137,138,176,179] In this research, two novel amide compounds containing 1,2-disubstituted cyclohexane spacer were prepared (Figure 2.9). Compounds 1,2-bis[*N,N'*-6-(3-pyridylmethylamido)pyridyl-2-carboxyamido]cyclohexane (**L11**) and 1,2-bis[*N,N'*-6-(3-pyridylmethylamido)pyridyl-2-carboxyamido]cyclohexane (**L12**) were

synthesised from a racemic mixture of *trans*-1,2-diaminocyclohexane in two steps. The incorporation of a cyclohexyl spacer was anticipated to limit the relative arrangements of the two 2,6-pyridine dicarboxamide moieties that are available to **L11** and **L12**.

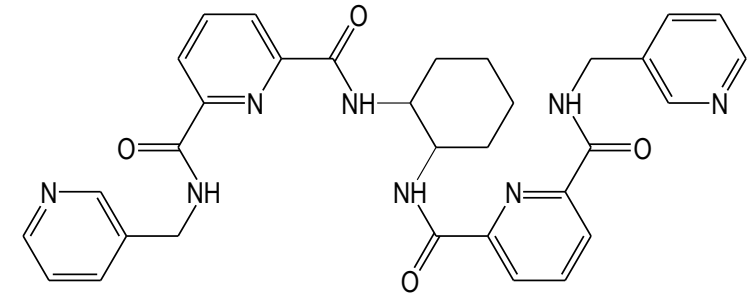

L11

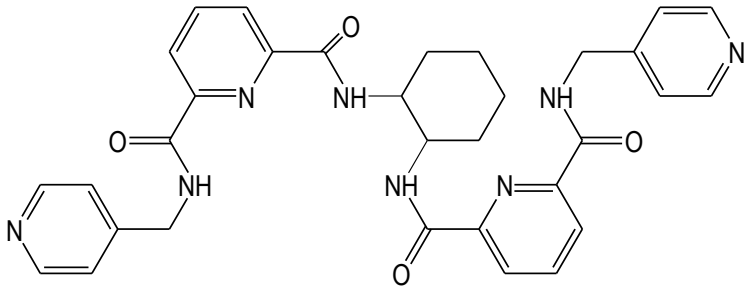

L12

Figure 2.9. Further examples of the tetraamide ligands described in this chapter that incorporate a cyclohexyl spacer.

The third and final group of the compounds investigated in this research were synthesised by reaction of di-2-pyridylmethylamine (**2.37**) with pyridine-2,6-dicarbonyl dichloride, terephthaloyl dichloride or isophthaloyl dichloride. The three new amide ditopic bridging ligands, 2,6-[*N,N'*-bis(di(pyridin-2-yl)methyl)pyridine]-2,6-dicarboxamide (**L13**), 1,3-*N,N'*-[bis(di(pyridin-2-yl)methyl)]isophthalamide (**L14**) and 1,4-*N,N'*-bis[(di(pyridin-2-yl)methyl)]terephthalamide (**L15**) (Figure 2.10) were obtained in one step. The chelating di-2-pyridylmethyl coordination sites[180] in these three compounds were expected to provide access to a wide range of coordination compounds and metallo-supramolecular assemblies. Furthermore,

by employing chelating metal coordinating sites, it was proposed that a more stable discrete coordination compounds or metallo-supramolecular assemblies would be obtained.[178,180]

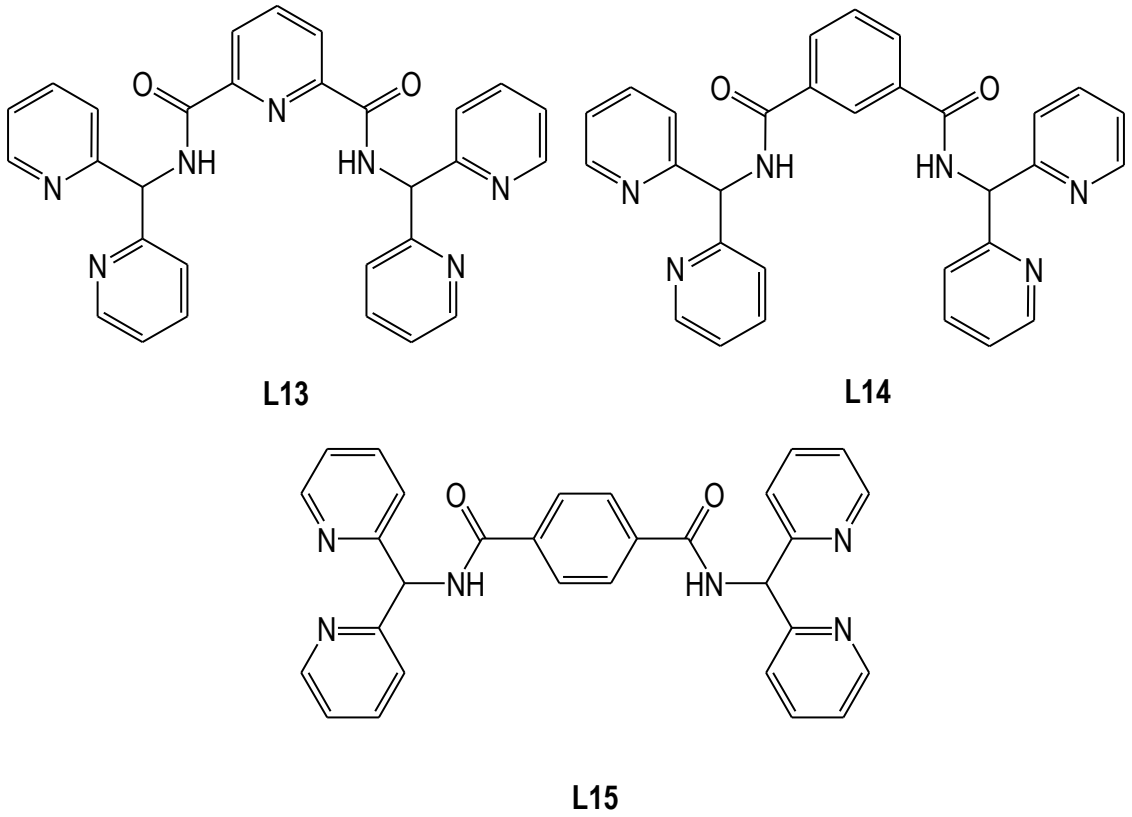

Figure 2.10. The new chelating amide ligands **L13**-**L15**.

This chapter presents a detailed description of the synthesis and characterisation of these compounds by solution NMR spectroscopy, mass spectrometry, IR spectroscopy, and, in certain cases, single crystal X-ray crystallography. Discussion of the synthesis of related amide compounds is discussed herein, but literature, pertinent to the coordination and metallo-supramolecular chemistry of those compounds, is discussed separately in Chapters 3, 4 and 5. The solution behaviour of selected compounds, as investigated by ^{1}H NMR spectroscopy is also described and similar investigations, in the gas phase, by mass spectrometry are discussed.

2.2. Syntheses of the monoamide ligands

All the monoamide ligands investigated in this thesis were liberated from their corresponding esters during the course of reactions undertaken with transition metals. Thus, the syntheses of the esters are reported herein, and discussion of the *in-situ* ester hydrolysis is relegated to Chapter 3. As noted above, the synthesis of the precursor to two flexible amide compounds that can act as tetradentate ligands, *N*-6-[(3-pyridylmethylamino)carbonyl]-pyridine-2-carboxylic acid methyl ester (**L1**) and *N*-6-[(4-pyridylmethylamino)carbonyl]-pyridine-2-carboxylic acid methyl ester (**L2**) was previously described. These compounds have been reported as intermediates in the synthesis of diamide compounds,[161] but not investigated as ligands in their own right. Two closely related compounds, *N*-6-[(3-pyridylamino)carbonyl]-pyridine-2-carboxylic acid methyl ester (**L3**) and *N*-6-[(4-pyridylamino)carbonyl]-pyridine-2-carboxylic acid methyl ester (**L4**), which are also potential precursors to tetradentate ligands, are also reported here. These latter two compounds possess more rigid structures, which were used to further explore the coordination chemistry of such monoamide derivatives but also to provide a comparison for the coordination chemistry observed for **L1** and **L2**.

Two similar synthetic approaches were employed in the synthesis of these compounds; the flexible amide ligands were synthesised by reaction with the requisite picolylamine with the diester, 2,6-dimethylpyridine dicarboxylate, while the rigid amide ligands were prepared from the monoacid chloride. All compounds obtained were characterised by a combination of NMR spectroscopy, combustion analysis, mass spectrometry, IR spectroscopy and in one case single crystal X-ray crystallography. While colourless crystals of **L2** were serendipitously obtained by slow evaporation of a methanol solution containing metal ions, crystals of the precursors of the other three compounds could not be obtained, despite many approaches by various crystallisation methods being attempted.

2.2.1. Syntheses of the flexible monosubstituted amide ligands

N-6-[(3-Pyridylmethylamino)carbonyl]-pyridine-2-carboxylic acid methyl ester (**L1**) and *N*-6-[(4-pyridylmethylamino)carbonyl]-pyridine-2-carboxylic acid methyl ester (**L2**) were synthesised by a method based on reported literature procedures with some modifications.[161,173] Commercially available pyridine-2,6-dicarboxylic acid (**2.27**) was converted into the dimethyl

ester (**2.1**) with methanol in the presence of a catalytic amount of sulfuric acid (Scheme 2.5). As reported, the dimethyl ester, 2,6-dimethylpyridinedicarboxylate (**2.1**) and 3-aminomethylpyridine (**2.2**) or 4-aminomethylpyridine (**2.3**) were suspended in toluene and heated at reflux for approximately 24 hours. The compound obtained was isolated by a simple work-up procedure and further purification was carried out using silica gel flash column chromatography. The synthesis of **L2** required the length of time heating at reflux to be extended from 24 hours to 36 hours to improve the isolated yield. This longer reaction time relates to the reduced nucleophilicity of the amine starting material. Compounds **L1** and **L2** were thus obtained in 65% and 70% yields, respectively.

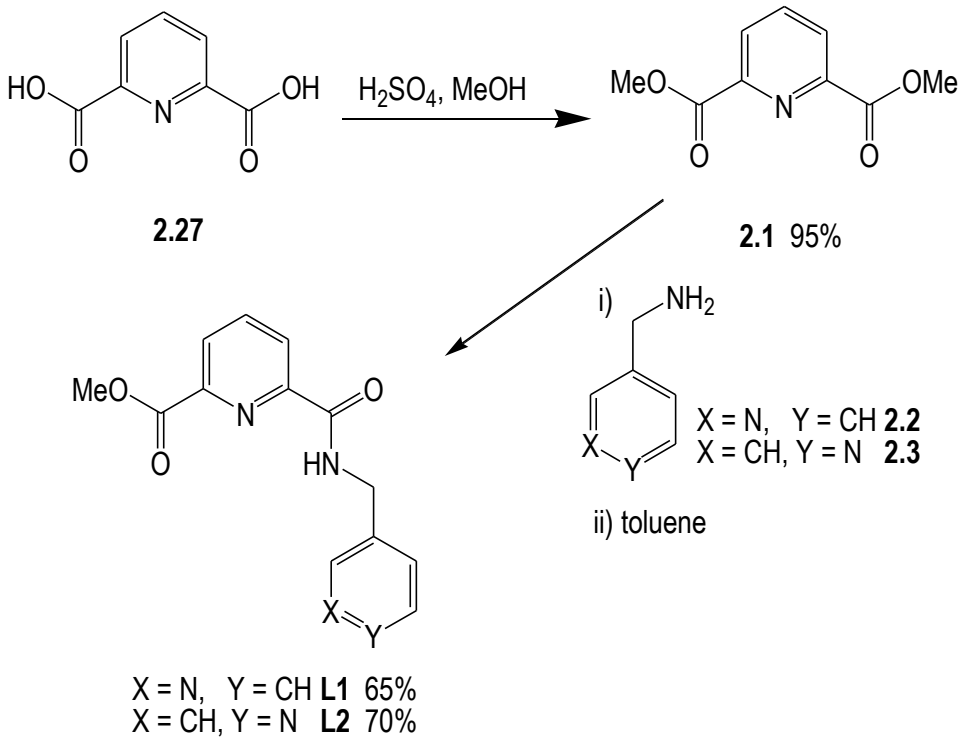

Scheme 2.5. Synthesis of **L1** and **L2**.

The two compounds, **L1** and **L2**, were characterised by a combination of NMR spectroscopy, and IR spectroscopy and the data obtained were compared to that previously reported by Sumby.[161] The ^{1}H and ^{13}C NMR spectra are consistent with the expected monoamide compounds and the previously reported data, and the elemental analysis indicates that the

products are analytically pure. The crystal structures of **L1** and **L2** were not obtained in the original study by Sumby and therefore crystals of **L2**, which were obtained by slow evaporation of a methanol solution of **L2** and cadmium(II) acetate, were analysed by single crystal X-ray crystallography.

Crystal structure of **$(L2)_3 \cdot 9H_2O$**

Crystals of compound **L2** were obtained by slow evaporation of a methanol solution of **L2** and cadmium acetate. No cadmium acetate was present in the structure. Compound **L2** crystallises in the triclinic space group *P*-1, with three molecules of **L2** and nine molecules of water in the asymmetric unit. All three molecules of **L2** in the asymmetric unit have very similar bond lengths and angles, albeit with subtle variations in those parameters. The major difference between the three molecules of **L2** is the conformation of the compounds and/or the nature of the hydrogen bonding interactions that they are involved in. In all three molecules in the crystal structure, the pyridine dicarboxamide moieties and the methyl ester groups are located in the same plane. The pendant pyridine rings are twisted by about 112˚ out of the plane of the pyridine dicarboxamide moiety due to free rotation at the sp^3 methylene linker (for example C19 in Figure 2.11).

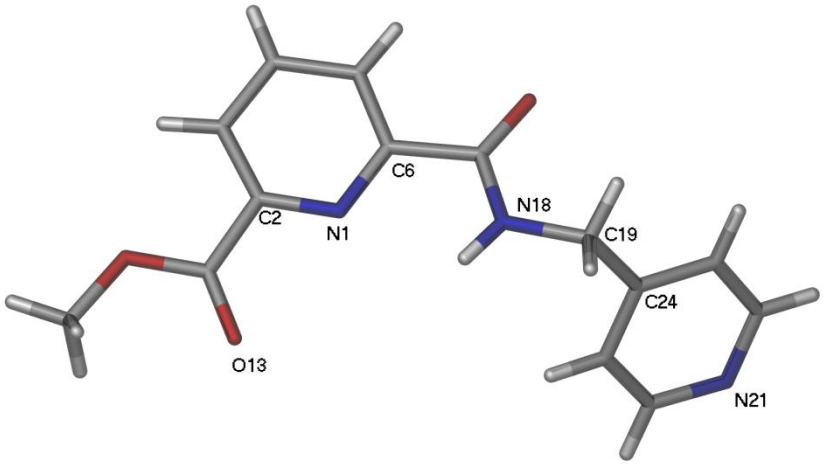

Figure 2.11. A perspective view of compound **L2**. Selected bond lengths (Å) and angles (°) : N(1)-C(2)1.335(3), N(1)-C(6) 1.315(3), C(2)-N(1)-C(6) 116.54(2) and N(18)-C(19)-C(24) 114.40(2).

In the crystal packing, individual molecules of **L2** are arranged along the *b* axis of the unit cell in double tapes as part of an extensive hydrogen bonding network involving the solvate water molecules in the channels that run down the *c* axis. A cluster of three water molecules serve to bridge three molecules of **L2** and contribute to the formation of a single unidirectional tape and also to link two tapes together to produce the double tape shown in Figure 2.12. These water clusters, which act as three connecting nodes, have internal O-H···O hydrogen bonding interactions ($d_{OH\cdots O}$ = 1.803 – 2.046 Å; $D_{O\cdots O}$ = 2.770 – 2.834 Å). Each molecule of **L2** forms three hydrogen bonds with water molecules *via* the amide NH donor (N-H$^{\cdots}$OH$_2$, *d* = 2.126 Å, *D* = 2.969 Å), the carbonyl oxygen (C=O$^{\cdots}$H-OH, *d* = 2.164 Å, *D* = 3.021 Å) and the nitrogen of the pyridyl ring ($N_{py}^{\cdots}$H-OH, *d* = 2.018 Å, *D* = 2.897 Å).

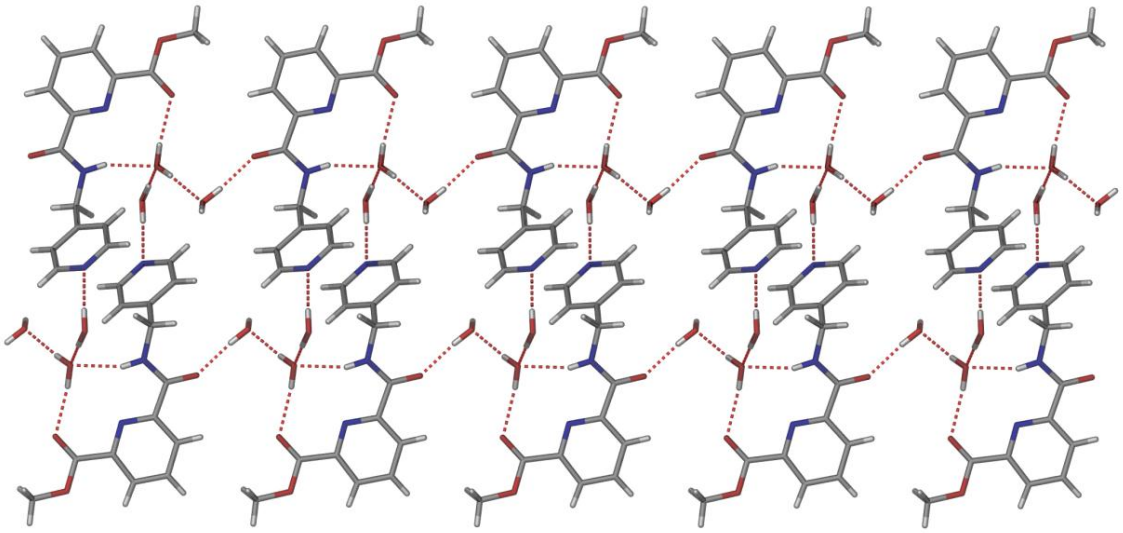

Figure 2.12. A perspective view of the extended structure of **L2** in the *ab* plane showing the 1-D hydrogen bonded double tapes.

Adjacent 1-D double tape motifs are connected together by hydrogen bonding through water solvate molecules to form an extended 2-D hydrogen bonded network, and interdigitated with adjacent sheets when viewed down the *a*-axis (Figure 2.13). Similar hydrogen bond interaction is expected to be occurred in **L1**.

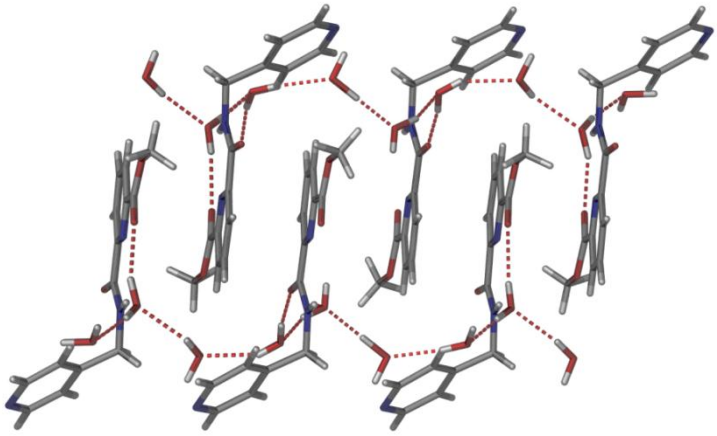

Figure 2.13. A view of the connections between the 1-D tapes in the 2-D hydrogen bonded network present in the crystal structure of **L2** (viewed down the *a*-axis).

2.2.2. Syntheses of the rigid monoamide ligands

In contrast to the flexible nature of compounds **L1** and **L2**, the two other monoamide compounds synthesised in this work possess a more rigid structure with fewer degrees of freedom, which originates from using the amine compounds 3-aminopyridine or 4-aminopyridine as the source of the pendant pyridyl donors. The method used for the synthesis of the flexible amide ligands was not considered appropriate for the synthesis of *N*-6-[(3-pyridylamino)carbonyl]-pyridine-2-carboxylic acid methyl ester (**L3**) and *N*-6-[(4-pyridylamino)carbonyl]-pyridine-2-carboxylic acid methyl ester (**L4**) as the amines are much less effective nucleophiles. Instead, these compounds were prepared by reaction of 3-aminopyridine (**2.5**) or 4-aminopyridine (**2.**6) with 6-(methoxycarbonyl)pyridine-2-carboxyl chloride, **2.4**.

The required mono-carboxylic acid precursor (**2.4**), was prepared from **2.28** by mono-deprotection with potassium hydroxide, using a method described in the literature.[173] The mono-carboxylic acid was suspended in dry dichloromethane, excess thionyl chloride and a catalytic amount of DMF were added, and the reaction heated at reflux for approximately one hour to give the acid chloride (**2.4**) (Scheme 2.6). The resulting acid chloride was then reacted with one equivalent of the appropriate amine to give compounds **L3** and **L4** in 60% and 78% yield, respectively. While these yields were satisfactory, a small amount of unreacted mono-carboxylic

acid made the purification difficult. These compounds were recrystallised from methanol and ethanol several times but impurities still remained. To alleviate this problem, the reaction was repeated using an excess of the amine and the consumption of starting material monitored by TLC. After the reaction was completed, the same work-up procedure was applied. The crude product was washed with saturated sodium bicarbonate solution and dried over magnesium sulfate, before taken to dryness to give brown oils. Compounds **L3** and **L4** were isolated as pale brown solids in reasonable yields of 51% and 75% respectively, after recrystallisation from ethanol.

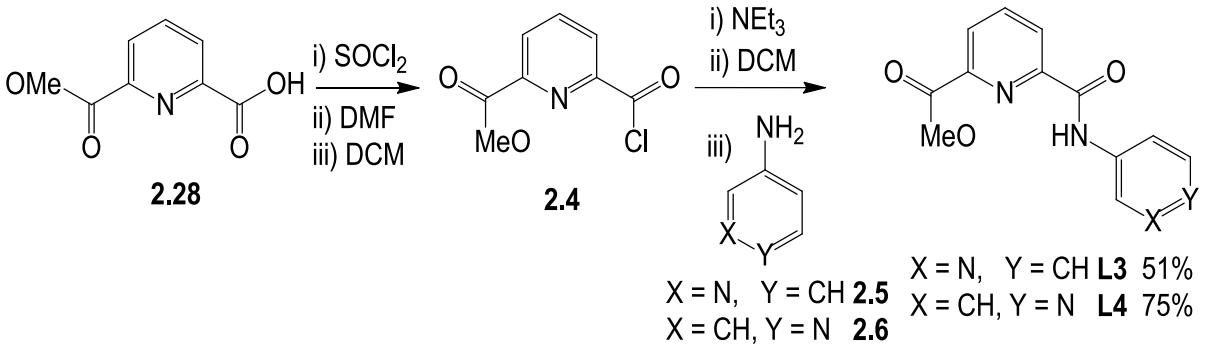

Scheme 2.6. The synthesis of **L3** and **L4**.

Compounds **L3** and **L4** were characterised by a combination of ^{1}H and ^{13}C NMR spectroscopy, IR spectroscopy, mass spectrometry and combustion analysis. Elemental analysis has suggested that compound **L3** was obtained as a pure compound with an excellent agreement between calculated and found C, H and N percentages. Compound **L4** was isolated as a hydrate, with formula **L4**·H_2O, on the basis of the elemental analysis. The IR spectra of compounds **L3** and **L4** have NH stretches in the range 3208-3242 cm^{-1}. The C=O stretch for the amides were observed at approximately 1730 cm^{-1}. The NMR spectra were assigned unambiguously, with the pyridine aromatic signals observed in the region 7.2 to 9.5 ppm. Other expected signals for **L3** and **L4** were observed in their ^{1}H NMR spectra, with the NH signal located reasonably far downfield at 10.12 and 10.31 ppm, compared to the NH signals recorded for **L1** and **L2**, at 8.55 and 8.57 ppm, respectively.[161] This is a consequence of greater deshielding by the pendant pyridine rings in **L3** and **L4**. Electrospray Ionisation Mass Spectrometry (ESI-MS) in methanol

revealed peaks for the parent ions (MH^+) at *m/z* 258.1. Unlike the related diamide ligands,[161] no hydrogen bonded aggregates of either **L3** or **L4** are observed by mass spectrometry under the conditions of the experiment. Several approaches have been utilised in an attempt to crystallise **L3** and **L4** to examine the conformations of these two compounds, but unfortunately, none of these attempts were successful.

2.3. Syntheses of the ditopic amide ligands

In the second section of this chapter, the synthesis of eight ditopic amide ligands are described, along with the characterisation and single crystal X-ray crystallography of those compounds. This latter aspect provides some insight into the possible conformations that were observed for the amide links in a series of discrete and polymeric coordination compounds reported in Chapter 4. Based on the report by Sumby *et al*.[161] compounds **L5** and **L6** were proposed to be suitable ligands for transition metals and ideally placed to also interact with anions due to the pre-organised hydrogen bond donor motif. With these attributes in mind, these compounds were prepared for investigation of their coordination chemistry and metallo-supramolecular chemistry. To investigate the chemistry of other, structurally related flexible amide ligands, compounds **L7-L12** were also prepared. In contrast to **L5** and **L6**, these new compounds have two pre-organised amide moieties capable of anion binding and aliphatic acyclic and cyclic spacers incorporated between the two 2,6-pyridine dicarboxamide moieties to generate longer and more flexible amide ligands. This latter group of compounds were expected to possess either one large anion recognition pocket or two, smaller pockets. Both conformations were expected to be observed in the coordination chemistry of these compounds.

2.3.1. Synthesis of the diamide ligands

The two reported diamide ligands *N,N'*-2,6-*bis*(3-pyridylmethyl)pyridine dicarboxamide (**L5**) and *N,N'*-2,6-*bis*(4-pyridylmethyl)pyridine dicarboxamide (**L6***)* were re-synthesised.[37] As noted, these ligands have symmetrical diamide structures, with two external pyridyl groups for metal coordination sites and preorganised amide moieties capable of anion binding. To synthesise these compounds, the diester precursor **2.1** was reacted with a slightly greater than two-fold excess of the amines, **2.2** and **2.3** in toluene and heated at reflux for 3 days (Scheme 2.7). The resulting disubstituted products, **L5** and **L6**, were isolated in 70% and 80% yields, respectively. These

compounds were characterised by NMR and IR spectroscopy, and mass spectrometry, consistent with the data previously reported.

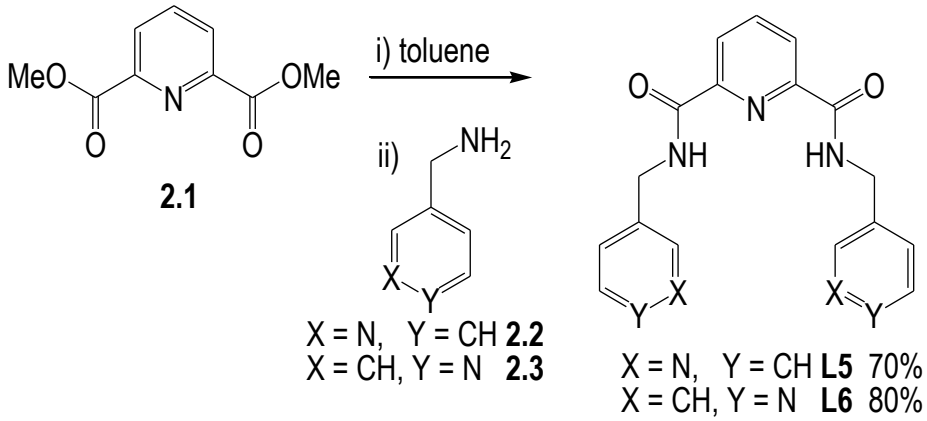

Scheme 2.7. The synthesis of **L5** and **L6**.

2.3.2. Synthesis of the tetraamide ligands

The synthesis of tetraamide ligands is of interest, since two pre-organised amide are incorporated within each compound. A survey of the literature indicated that the macrocyclic tetraamides have been studied for anion recognition,[34] but the investigation on the open chain tetraamide compounds is limited. In the first attempt to generate longer and more flexible tetraamide ligands, commercial and readily available linear aliphatic amines such as 1,2-ethylenediamine, 1,3-propylenediamine and 1,2-cyclohexanediamine were used as spacers. These new symmetrical bridging ligands exhibit far greater flexibility than previously reported macrocyclic tetraamides owing to the greater degree of freedom in the aliphatic chains. The potential for formation of a larger anion pocket created by amide side chains was proposed to be a source of interesting anion encapsulation behaviour.

By implementing a previously reported synthetic approach,[161] compounds **L7**-**L10** were successfully synthesised in moderate yields. Compounds 1,2-bis[*N,N'*-6-(3-pyridylmethylamido)pyridyl-2-carboxyamido]ethane (**L7**) and 1,2-bis[*N,N'*-6-(4-pyridylmethylamido)pyridyl-2-carboxyamido]ethane (**L8**) were synthesised from 1,2-ethylenediamine (**2.29**) and **L1** or **L2**, respectively. Reaction of **L1** and **L2** with 1,3-

propylenediamine (**2.30**) gave 1,2-bis[*N,N'*-6-(3-pyridylmethylamido)pyridyl-2-carboxyamido] propane (**L9**) and 1,2-bis[*N,N'*-6-(4-pyridylmethylamido)pyridyl-2-carboxyamido] propane (**L10**), respectively (Scheme 2.8). Precursors **L1** or **L2** and 1,2-ethylenediamine in 2:1 molar ratio were suspended in toluene and heated at reflux for 36 hours. The solvent was removed and the cream solid was purified by flash column chromatography, where methanol-dichloromethane 1:9 was used as the eluting solvent. This yielded both **L7** and **L8** in *ca* 30% yield. This reaction was initially done on a small scale. A larger scale reaction was performed subsequently and the yield was doubled to *ca* 60% for each product. Elemental analysis is consistent with the isolation of the hydrate of both compounds, **L7**·H_2O and **L8**·H_2O, respectively.

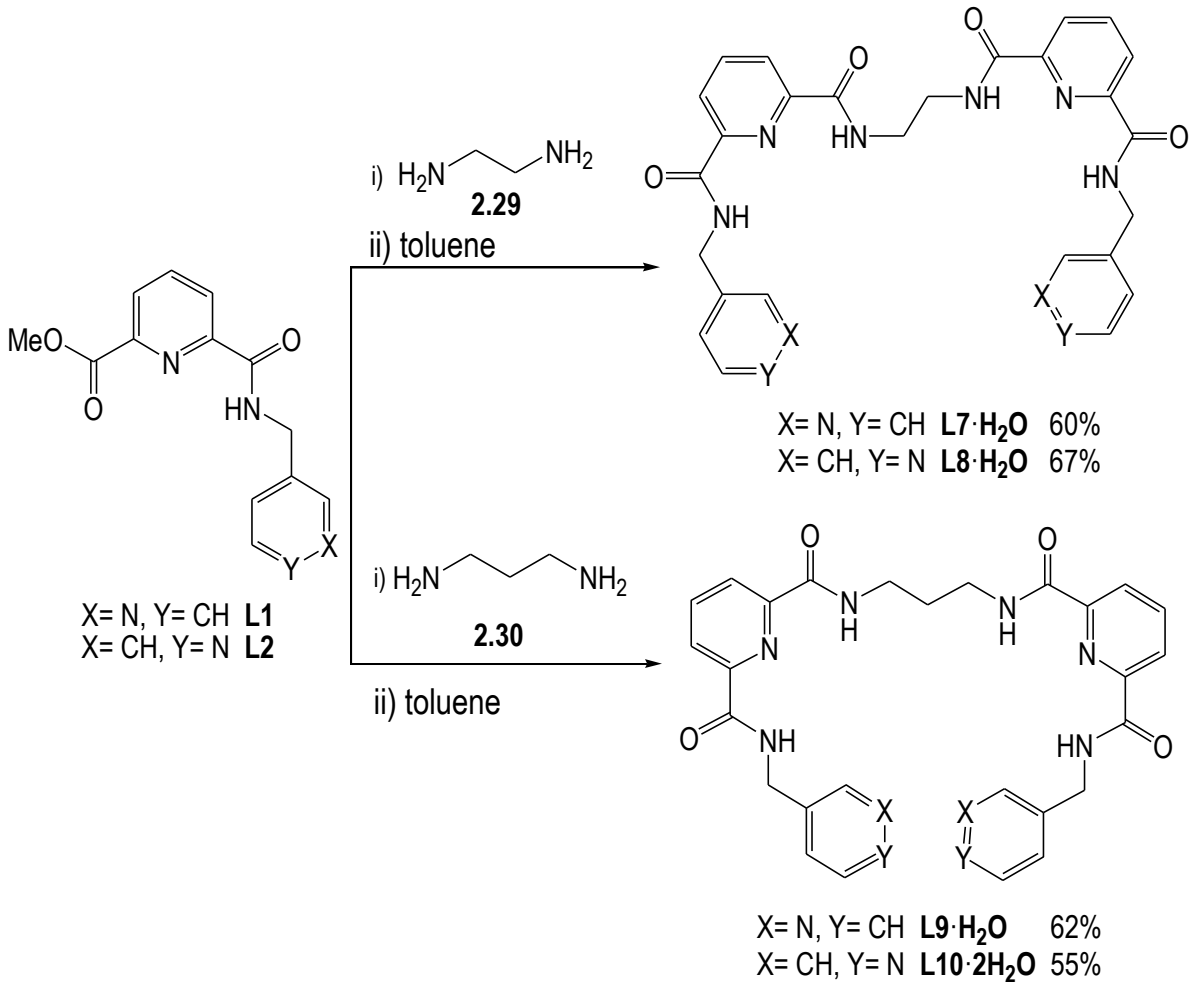

Scheme 2.8. The synthesis of **L7**-**L10** derived from **L1** or **L2**.

These compounds were further characterised by NMR spectroscopy and mass spectrometry. The NH amides of compound **L7**·H_2O in deuterated chloroform are defined by the resonances in the ^{1}H NMR spectrum at 9.14 ppm and 9.07 ppm, respectively. The methylene spacer of ethylenediamine is observed at 3.62 ppm, while the other methylene spacer that links the amide and pendant pyridine is observed at 4.77 ppm. In the ES-MS spectrum measured in methanol, a protonated species $[\mathbf{L7}+H]^+$ was identified at *m/z* 539.2 and $[\mathbf{L7}+Na]^+$ was observed at *m/z* 561.2. The protonated species bound to water, $[\mathbf{L7}\cdot H_2O+H]^+$ (m/z 557.2), was also observed in relatively low abundance and a dimers, $[(\mathbf{L7})_2+H]^+$ and $[(\mathbf{L7})_2+Na]^+$, were observed at *m/z* 1081 and 1145.7, respectively.

The isomeric compound, **L8**, was anticipated to be spectroscopically different, due to the greater symmetry of the 4-substituted pendant pyridine ring. In the ^{1}H NMR spectrum of **L8**·H_2O, the signals corresponding to the amide NH moieties are overlapped to give a multiplet at 9.23 ppm. The 4-pyridine resonances were observed between 7.2 and 8.5 ppm, with methylene protons adjacent to the pyridine ring being observed at 4.76 ppm. The methylene spacer (CH_2-en) is shifted slightly upfield to 3.56 ppm in comparison to **L7**. The ESI-MS for compound **L8**·H_2O in methanol led to the ionisation of two major species, $[\mathbf{L8}+Na]^+$, and $[\mathbf{L8}+H]^+$ observed at 561.3, 100% and *m/z* 539.3, 65%, respectively. Similar to the reported diamide compounds (**L5** and **L6**),[161] and **L7**, hydrogen bonded aggregates were observed by ESI-MS experiments. A protonated dimer $[(\mathbf{L8})_2+H]^+$ and a dimer with a sodium cation $[(\mathbf{L8})_2+Na]^+$ were both observed, at *m/z* 1076.7 and 1098.8, respectively. IR spectroscopy of the extended compounds indicates strong N-H, C=O, C=N and C=C stretches at approximately, 3359 and 1670-1529 cm^{-1}, respectively. Crystals of **L7** and **L8**·H_2O were obtained from solutions containing copper acetate and cobalt acetate, respectively. Colourless rectangular block-shaped crystals were obtained from both solutions after several days standing at room temperature and these crystals were subjected to single crystal X-ray crystallography to provide the solid-state structures of **L7** and **L8**·H_2O.

Crystal structure of **L7**

Compound **L7** crystallises in the monoclinic space group *C*2/*c* from a methanol solution of the compound and copper acetate. The asymmetric unit comprises half a molecule of compound **L7**.

This molecule has intramolecular hydrogen bonding which pre-organises the NH-functionalities of the ligand into a central pocket (N1A···H14A = 2.308; N-H···N angle = 106.88°) and (N1A···H18A = 2.225 Å, N-H···N angle = 109.42°). In the crystal structure, the tetraamide ligand adopts a similar conformation to the two previously reported diamide ligands, **L5** and **L6** with the hydrogen bond amide donors of the central 2,6-pyridine dicarboxamide moieties directed into the cavity of the compound and with both pendant pyridyl donors oriented in the same direction (Figure 2.14). This is typical to the compounds incorporated with the 2,6-pyridine dicarboxamide cores.[10,147,148,181] The formation of intramolecular hydrogen bonding in **L7**, as observed in **L5** and **L6**,[161] pre-organises the amide NH functionalities into a central pocket, which was expected to favour anion interactions in complexes of this compound. The overall effect of this pre-organisation is to generate a wide U-shaped pocket within **L7** in the solid-state.

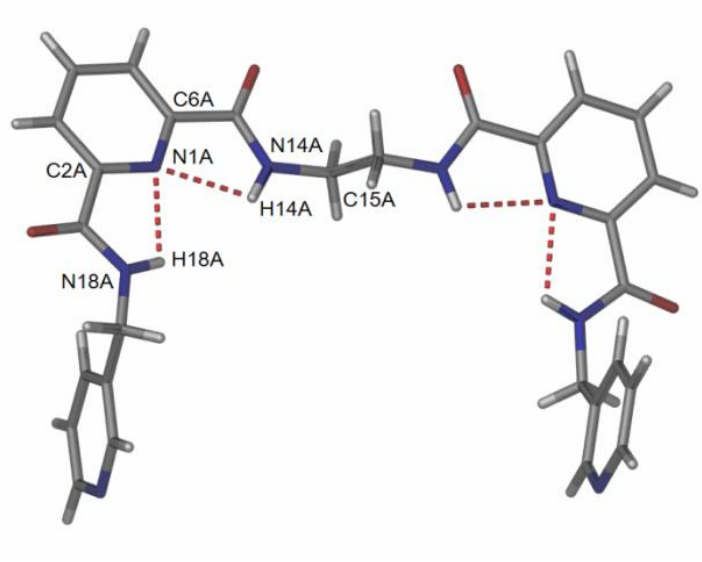

Figure 2.14. A perspective view of the asymmetric unit of compound **L7**, showing the pre-organising intramolecular hydrogen bonding interactions in the amide core. Selected bond lengths (Å) and angles (°) : N(1A)- C(2A) 1.339 N(14A)- C(6A) 1.346 N(1A)-H(14A) 2.308, N(1A)-H(18A) 2.225, C(2A)-N(1A)-C(6A) 117.99 and N(14A)-C(15A)-C(15B) 112.05.

The crystal structure of **L7** revealed that intermolecular hydrogen bonding interactions between the central pre-organised amide hydrogen donors and hydrogen bonded pendant pyridine rings of adjacent molecules gives rise to interdigitated double chains in the crystal packing

(Figure 2.15). The crystal structure contains no solvate molecules and thus no further siginificant hydrogen bonding interactions were observed in the structure.

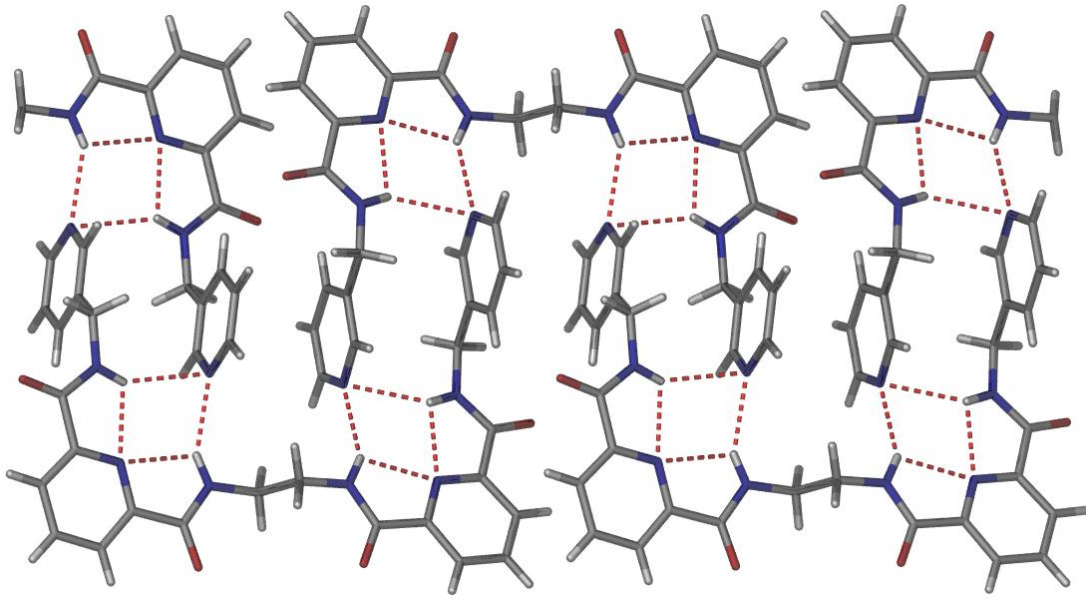

Figure 2.15. A perspective view of the extended structure of **L7** showing the pre-organised amide intramolecular hydrogen bonding and the intermolecular hydrogen bonding from the pyridine ring that gives 1-D double chains in the crystal structure.

Crystal structure of **L8·4H$_2$O·2CH$_3$OH**

In similar manner to **L7**, compound **L8** crystallises in the monoclinic space group *C*2/*c*, but with half a molecule of **L8**, two water molecules and one methanol in the asymmetric unit. There is one solvated water molecule which acts as the hydrogen bond acceptor for the amide N-H donors in **L8** (NH···O, *d* = 2.083 & 2.115 Å). This water molecule is in turn hydrogen bonded to a methanol molecule and to a second water molecule. The second water molecule is in turn also hydrogen bonded to the carbonyl group of **L8** (Figure 2.16).

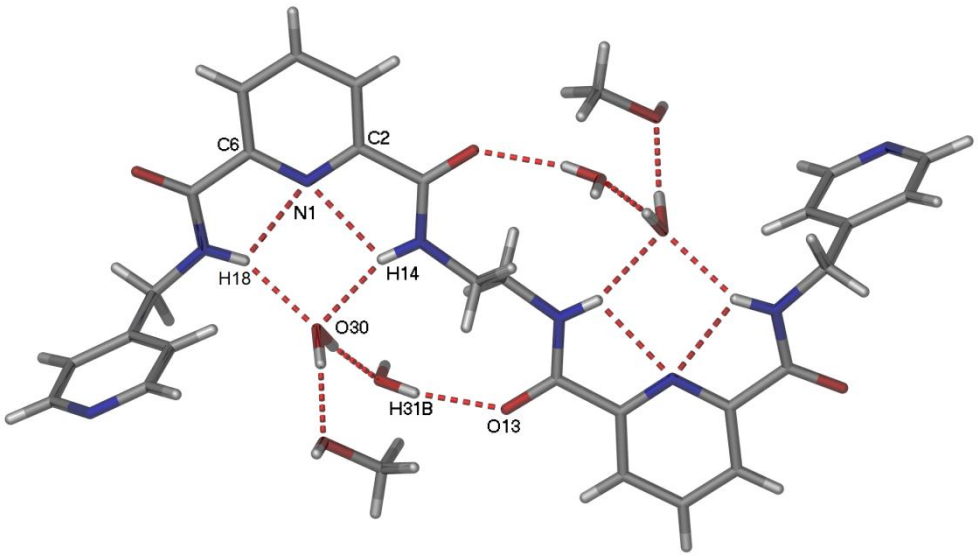

Figure 2.16. (a) A perspective view of molecule **L8** showing the pre-organising intramolecular hydrogen bonding interactions. Selected bond lengths (Å) and angles (°) : N(1)-C(2) 1.332(3), N(1)-C(6) 1.348(3), N(1)-H(14A) 2.276, N(1A)-H(18A) 2.303, O(30)-H(18) 2.083, O(30)-H(14) 2.155, C(6)-N(1)-C(2) 117.6(2) and N(14)-C(15a)-C(15) 111.0(3).

The crystal structure of **L8** reveals that this compound adopts quite a different conformation to **L7** in the solid-state. Due to free rotation provided by the ethylene spacer and the intermolecular hydrogen bonding interactions with solvate molecules (C=O···H-OH), the two pyridine dicarboxamide cores are directed almost opposite one another. Thus as expected, it appears that either one or two anion pockets could be observed for compounds **L7** and **L8** but based on NMR spectroscopy, these conformers are free to interconvert in solution. Figure 2.17 shows the extended structure of compound **L8** in the crystal packing. The intermolecular hydrogen bonding between two molecules of **L8**, mediated predominantly by water and methanol solvate molecules, leads to the formation 1-D extended polymeric hydrogen bonded chains. The packing of the 1-D hydrogen bonded chains of **L8** into 2-D sheets is also mediated by the second water solvate molecule. This facilitates an additional set of O-H···O=C hydrogen bonds that serve to link between two 1-D chains.

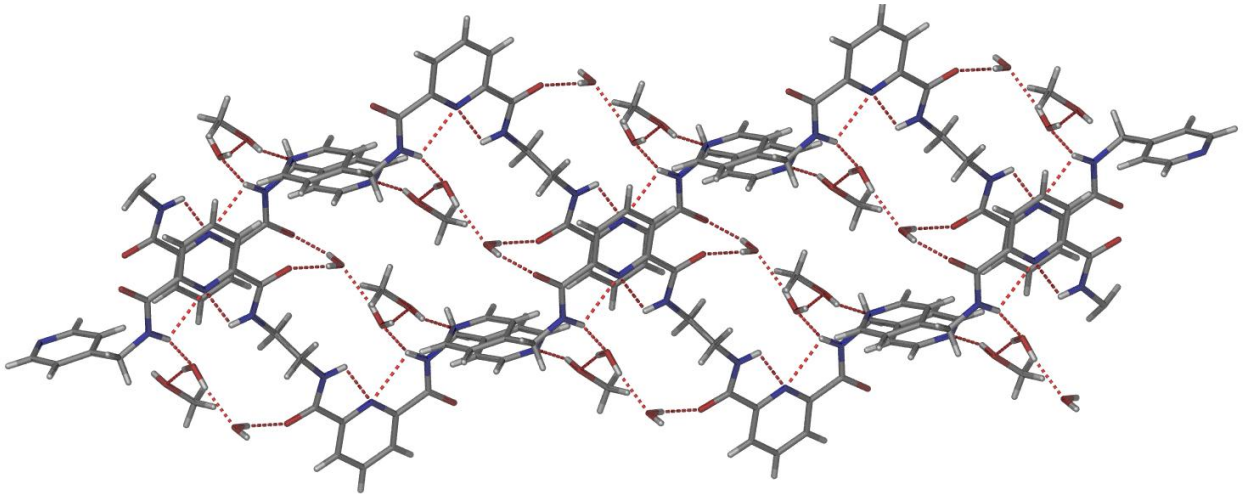

Figure 2.17. A view of the crystal packing of **L8**·4H_2O·2CH_3OH.

As outlined earlier, to synthesise 1,2-bis[*N,N'*-6-(3-pyridylmethylamido)pyridyl-2-carboxyamido] propane (**L9**) and 1,2-bis[*N,N'*-6-(4-pyridylmethylamido)pyridyl-2-carboxyamido] propane (**L10**), required 1,3-propylenediamine to be employed as the linker. These two compounds were synthesised based on the method described for **L7** and **L8**, as shown in Scheme 2.9. The synthesis of **L9** is straightforward with the product being obtained directly from the reaction; a cream solid began to precipitate from the reaction mixture after 36 hours heating at reflux in toluene. This solid was filtered under vacuum, washed with diethyl ether and collected without further purification, to give **L9** in 62% yield. In contrast to the synthesis of **L9**, reaction of **L2** with propylenediamine to form **L10** required considerably longer periods for the reaction to reach completion, typically taking approximately 96 hours heating at reflux. The crude product was purified *via* column chromatography to give **L10** in 55% yield. The formulations of both compounds **L9**·H_2O and **L10**·2H_2O were obtained by elemental analysis.

The syntheses of both compounds were confirmed by the observation of characteristic resonances in the ^{1}H NMR spectra. The N-H amide signals of **L9**·H_2O and **L10**·2H_2O were observed at 9.10 and 8.89, and 9.33 and 9.24 ppm, respectively. While the ^{1}H NMR spectrum displayed readily noticeable differences between the resonances for amide protons in both compounds, only small differences were observed in the resonances for the propylene and methylene linkers. Compound **L9**·H_2O has signals for propylene spacer at 3.49 and 3.97 ppm,

compared to 3.50 and 3.98 ppm in **L10**·$2H_2O$. Similarly, a peak for the methylene linker was observed at 4.68 ppm for **L9** and 4.69 ppm for **L10**. ESI-MS of **L9** conducted in methanol led to observation of peaks for $[\mathbf{L9}+H]^+$ (*m/z* 553.0, 65%) and a dimer $[(\mathbf{L9})_2+H]^+$ (*m/z* 1106.1, 10%). The ESI-MS of compound **L10**, also conducted in methanol, showed peaks for $[\mathbf{L10}+H]^+$ (*m/z* 553.3, 100%), a dimer $[(\mathbf{L10})_2+H]^+$ (*m/z* 1104.7, 10%) and a trimer $[(\mathbf{L10})_3+H]^+$ (*m/z* 1656.8, 5%). The presence of dimeric or trimeric species indicates that these compounds appear to readily form hydrogen bonded aggregates in the gas phase and that the solution chemistry may be affected by such interactions. The IR spectra showed a distinctive C=O stretching vibration at approximately 1624-1654 cm^{-1} for both compounds. Attempts to crystallise compounds **L9** and **L10** with a view to obtaining crystals suitable for structure studies were unsuccessful.

Due to the observation that ligands **L7**-**L10** adopt at least two different conformations and additionally, that the greater flexibility of these compounds may affect the synthesis of coordination polymers with desirable properties, new extended ligands which have more limited flexibility were synthesised. These incorporate 1,2-diaminocyclohexane (**2.31**) as the spacer. **L11** and **L12** were prepared from the diamide **2.32** which could be synthesised from 6-(methoxycarbonyl)pyridine-2-carboxylic acid, **2.28**. To synthesise **2.32**, compound **2.28** was converted into the acyl chloride **2.4** and then reacted with racemic mixture 1,2-diaminocyclohexane to give compound **2.32** in *ca* 90% yield over two steps. To prepare compound **L11**, precursor **2.32** and 3-aminomethylpyridine was suspended in toluene and heated at reflux for approximately 72 hours to give the desired product (Scheme 2.9).

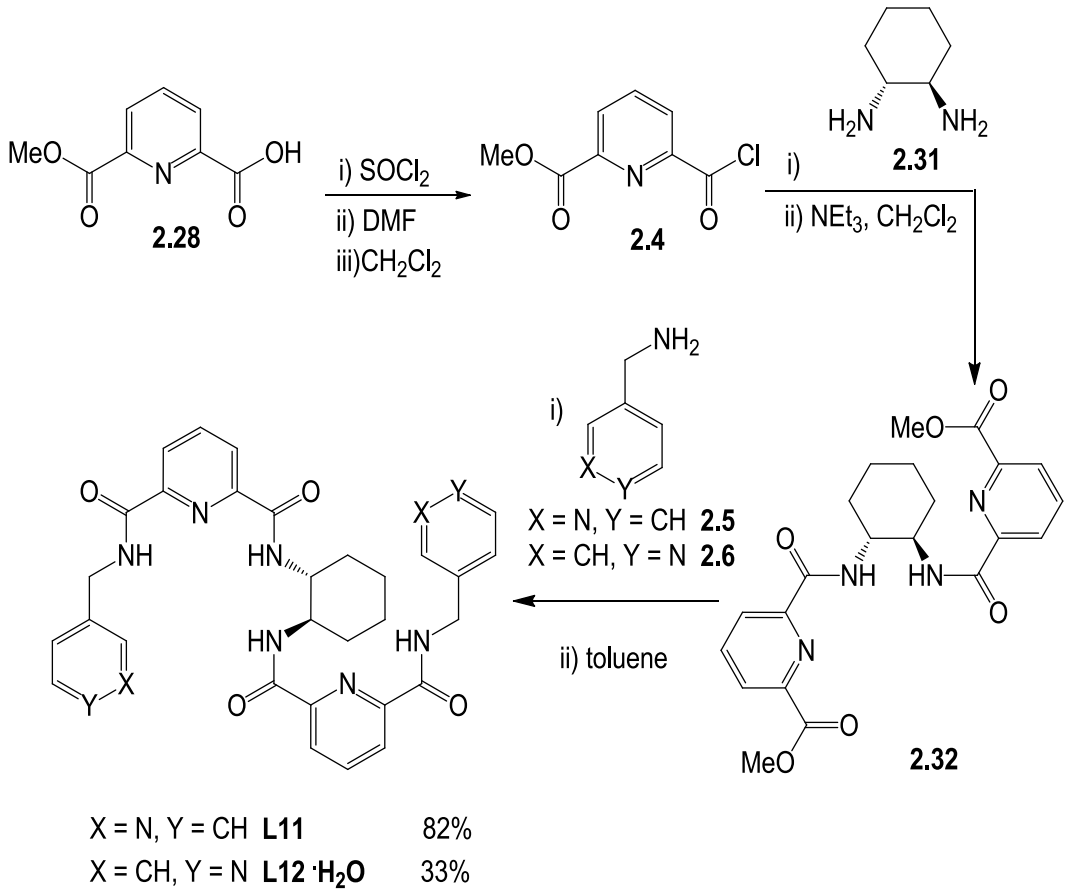

Scheme 2.9. The synthesis of **L11** and **L12**.

The crude product of **L11** was obtained as an off-white solid, after being isolated *via* straight-forward work-up procedures. This was re-dissolved in hot ethanol, insoluble solids removed by filtration, and the filtrate left to evaporate to afford **L11** as a fine white powder in 82% yield. This product was confirmed as **L11** by elemental analysis. The ^{1}H NMR spectra of **L11** was recorded in deuterated chloroform. A signal that appears as a triplet at 9.09 ppm corresponds to the N-H protons of the pyridine core amide. The signals for the cyclohexyl amide and the pendant pyridyl H2' are overlapped to give a broad singlet at 8.65 ppm. Another two signals (H6' at 8.53 and H5'at 8.28 ppm) were assigned to the pendant pyridine protons H6' and H5', while the multiplet near 7.8 ppm corresponds to the overlap between one triplet and doublets from the pyridine carboxamide H4 proton and the H4' of the pendant pyridine ring. The nearby doublet was assigned as the H3 and H5 hydrogen atoms from the pyridine core. The multiplets at 4.77 ppm arise from the CH_2 protons from the methylene linker in adjacent to the

pyridine rings. The cyclohexane protons are doublets which appear upfield at 3.87, 2.17, 1.65 and 1.32 ppm. The ESI-MS obtained on a methanol solution of **L11** revealed peaks for the parent ion $[\mathbf{L11}+H]^+$ at *m/z* 591.2. Meanwhile, a peak at *m/z* 1204.2 correspond to the hydrated dimeric species, $[(\mathbf{L11})_2 \cdot H_2O+H]^+$, while a hydrated trimeric species $[(\mathbf{L11})_3 \cdot H_2O+H]^+$ was observed at *m/z* 1793.2 in low relative abundance. There is also a peak observed for a sodium-containing ion, $[\mathbf{L11}+Na]^+$, at *m/z* 614.5 (25%).

Based on the conditions employed for the synthesis of **L11**, reaction of **2.13** with a greater than two-fold excess of 4-aminomethylpyridine gave **L12.** Similar to the synthesis of **L11**, the reaction was heated at reflux for approximately 72 hours, and the formation of the product monitored by TLC and NMR spectroscopy. Compound **L12** was isolated by flash column chromatography techniques, using the mixture of dichloromethane-methanol (9:1) as the eluting solvent system. Unfortunately, **L12** was isolated in a much lower yield (33%) compared to **L11**. This is a consequence of the reduced nucleophilicity of the amine nitrogen compared to the 3-substituted precursor. Elemental analysis of the product obtained supports the isolation of the hydrate, $\mathbf{L12} \cdot H_2O$.

Another approach to synthesise compounds **L11** and, in particular, **L12** using an acyl chloride precursor was investigated in an attempt to improve the isolated yield of **L12**. In this approach, three additional reactions were required over two steps. Precursor **2.32** was treated with a methanolic solution of potassium hydroxide to form the dicarboxylic acid **2.33**. Using standard conditions, compound **2.33** was reacted with an excess of thionyl chloride to give **2.34**, which was then reacted with 3- or 4-aminomethylpyridine (**2.5** or **2.6)** at the final stage (Scheme 2.10). Unfortunately, this approach was abandoned because the crude product was shown to be a complex mixture of starting materials, intermediates and products. For example, a TLC of the product mixture of the reaction to prepare **L12** showed two small spots and one large spot which have similar polarity and thus were unlikely to be readily separated by column chromatography. Thus, the first approach continued to be used for the synthesis of compound **L12**. In the ^1H NMR spectrum of $\mathbf{L12} \cdot H_2O$, the amide protons were observed downfield compared to **L11**, with a triplet at 9.35 ppm and a doublet at 9.05 ppm. The remaining signals between 7.2-8.5 ppm correspond to the protons from pyridine ring and the pyridine core. The methylene linker has a resonance at 4.72 ppm, while the cyclohexane protons have signals at 3.77, 2.04, 1.73 and 1.43

ppm. The mass spectrometry indicated the presence of a dominant molecular ion corresponding to [**L12**+H]$^+$ at *m/z* 592.3 (100%).

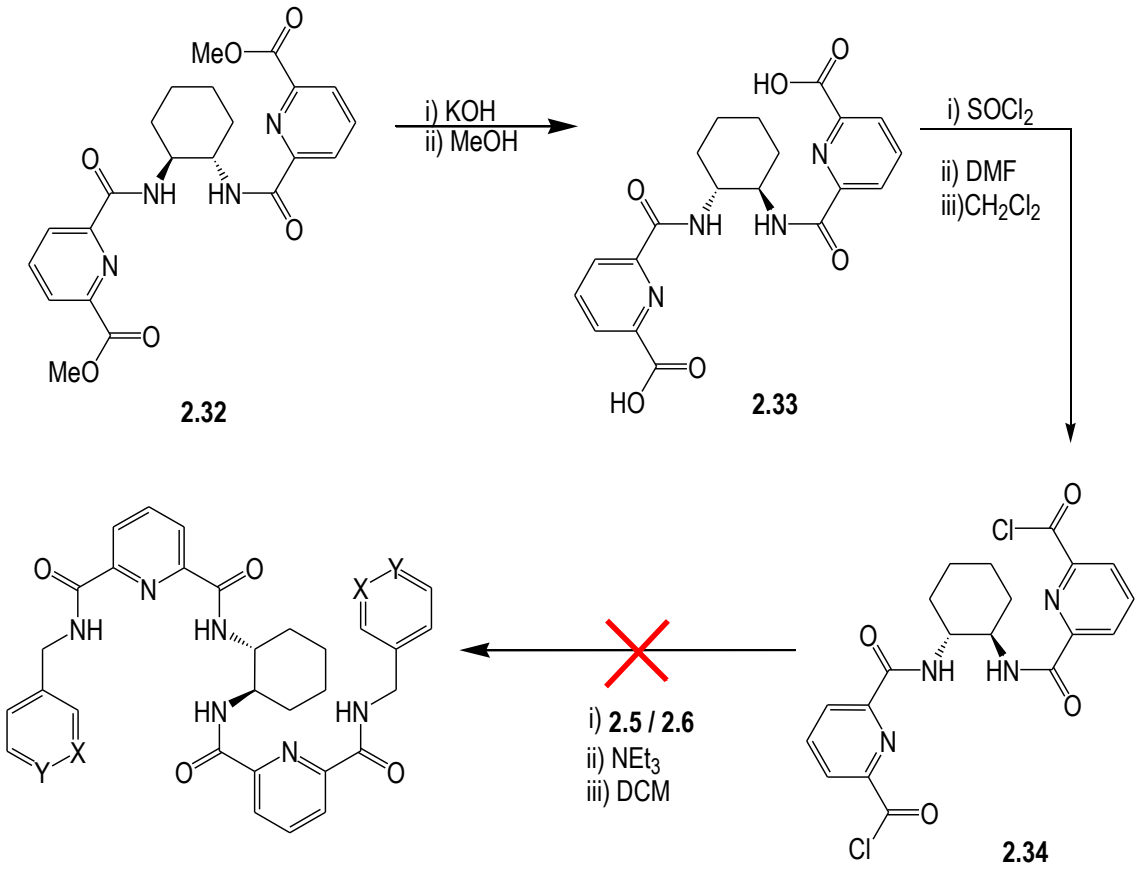

Scheme 2.10. The attempted synthesis of **L11** and **L12** from the acid chloride **2.34**, which failed to give the desired product.

Compounds **L11** and **L12**·H_2O were found to crystallise preferentially from solutions containing metal salts; in fact the insolubility of these two compounds limited the ability to obtain coordination complexes. Rectangular block-shaped colourless crystals of both compounds were obtained from several different reactions and were suitable for X-ray crystallography. Single crystal X-ray structures of **L11** and **L12** were obtained and these are discussed below.

Crystal structure of **L11**

The particular crystals of **L11** studied here were readily obtained from a methanol solution of copper nitrate and **L11**, consistent with the poor solubility of these compounds. Compound **L11** crystallises in the triclinic space group *P*-1 with one molecule of **L11** in the asymmetric unit. The structure reveals that this compound retains the two pre-organised amide hydrogen bond donor regions in the anticipated conformation (Figure 2.18), but as observed in molecule **L8**, these are arranged to form two separate pockets rather than one larger pocket. This is not surprising given the arrangement of the substituents on the cyclohexane ring at the 1 and 2 positions. In the conformation of **L11** observed in the crystal structure, it appears there are intramolecular N-H···O=C and N-H···N hydrogen bonds that stabilise the folded conformation. These hydrogen bonds have the following distances, N15-H15···O14 (*d* = 2.201 Å, *D* = 2.953 Å), N49-H49···O14 (*d* = 2.333 Å, *D* = 3.157 Å), N49-H49···N41 (*d* =2.308 Å, *D* = 2.697 Å) and N15-H15···N41 (*d* = 2.251 Å, *D* = 2.663 Å). The N-H···N angles are 106.78° and 108.41°, respectively.

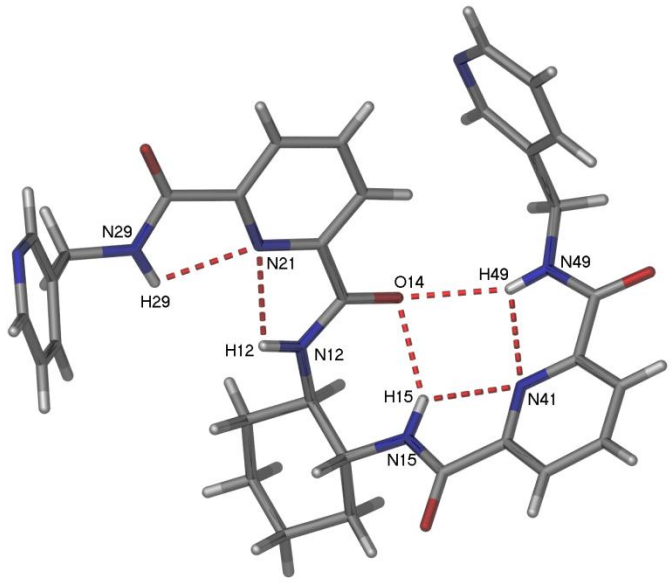

Figure 2.18. The asymmetric unit of compound **L11**. Selected bond lengths (Å) and angles (°) : N(41)-C(42) 1.333(6), N(41)-C(46) 1.344(6), N(21)-C(22) 1.342(6), N(21)-C(26) 1.340(5), C(42)-N(41)-C(46) 117.2(4) and C(22)-N(21)-C(26) 117.4(4).

Figure 2.19 shows that several intermolecular interactions are responsible for the formation of a dimeric arrangement of **L11** in the solid-state. The dimer is stabilised by four N-H···O=C hydrogen bonds between each molecule of **L11** (N12-H12···O17, *d* = 2.158 Å, *D* = 3.000 Å; and N29-H29···O17 *d*= 2.111 Å; *D* = 2.951 Å). The structure is further stabilised by π-π stacking interactions between the pyridine rings. In the dimer, the pendant pyridyl group and the central pyridine core interact in an edge-to face interaction, in which the C-H···π(centroid) distance is 2.912 Å.

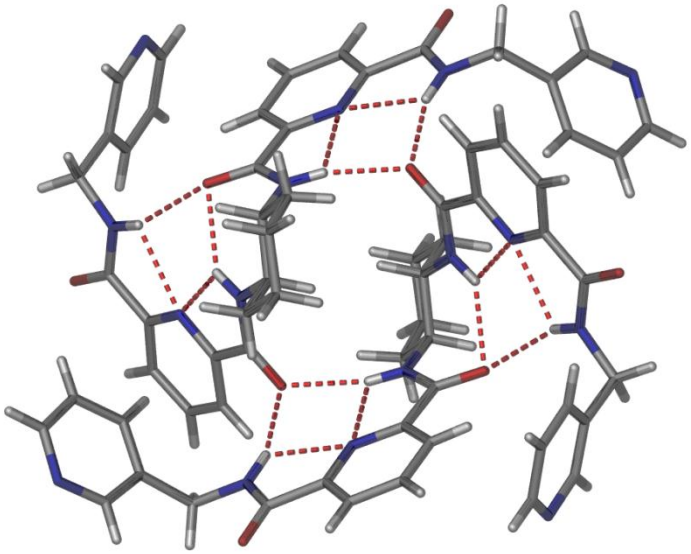

Figure 2.19. A perspective view of a dimer of **L11** showing the weak intramolecular and intermolecular hydrogen bonds responsible for the conformation of **L11** and the formation of the dimeric aggregate. The structure is also stabilised by weak π-π stacking interactions between a pendant pyridine ring and the central 2,6-pyridine dicarboxamide core of both molecules.

Adjacent dimers are then further involved in π-stacking interactions involving one 2,6-pyridine dicarboxamide core of each molecule of **L11** (Figure 2.20). The two pyridine cores form a weak face-to-face π-stacking interaction (centroid-centroid distance 4.20 Å; angle 47.46°; centroid offset 1.32 Å). This ultimately results in 1-D chain like arrangement of the dimers.

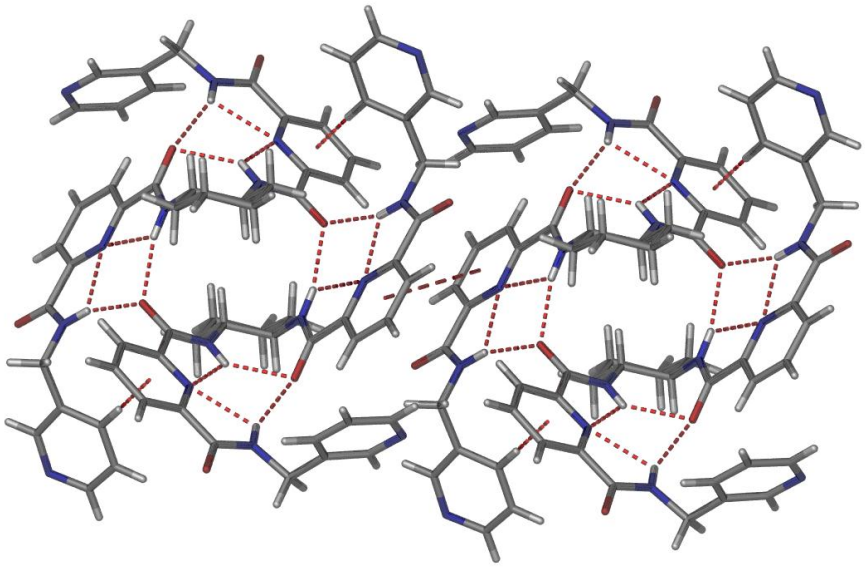

Figure 2.20. A perspective view of the π-π stacking interactions observed between the two pyridine cores of molecules of **L11** that are involved in forming dimers.

Crystal structure of **L12**

Crystals of **L12** were obtained from a methanol solution of copper perchlorate and compound **L12.** Like compound **L11**, compound **L12** also crystallises in the triclinic space group *P*-1 but with two complete molecules of compound **L12** in the asymmetric unit. The two molecules of **L12** have similar conformations, with the major distinction between the two molecules being differences in bond lengths and angles for the two molecules. As observed in compound **L11**, intramolecular hydrogen bonding (*d* = 2.249 -2.445 Å; N-H···N angles = 107.7 and 105.60°) pre-organises the NH functionalities of the compound to provide two anion pockets (Figure 2.21). Like **L11**, one of these pockets is occupied by a carbonyl oxygen of the other 2,6-pyridine dicarboxamide moiety (N-H···O, *d* = 2.380 Å ; *D* = 3.234 Å, *d* = 2.240 Å, *D* = 2.974 Å).

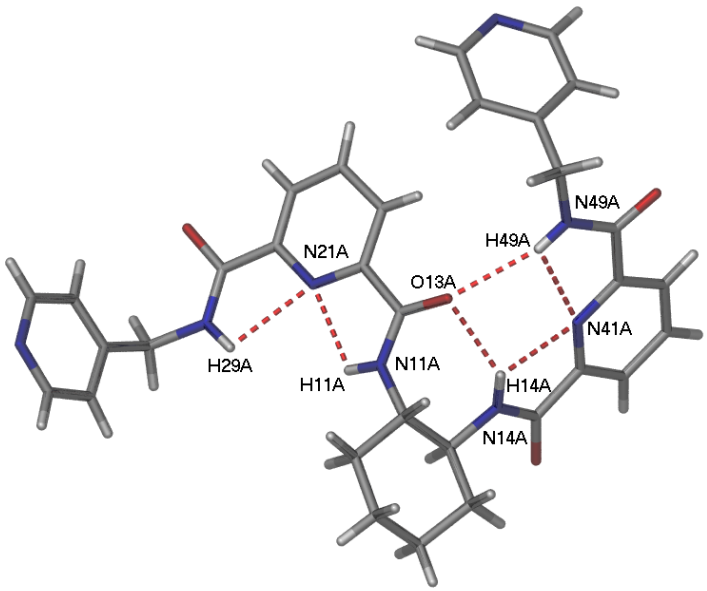

Figure 2.21. A perspective view of one of the molecules of **L12** in the asymmetric unit, showing the pre-organising intramolecular hydrogen bonding interactions. Selected bond lengths (Å) and angles (°): N(21A)-C(22A) 1.377(9), N(21A)-C(26A) 1.336(10), N(41A)-C(42A) 1.348(8), N(41A)-C(46A) 1.314(8), C(22A)-N(21A)-C(26A) 120.6(7) and C(42A)-N(41A)-C(46A) 118.5(6).

Once again, intermolecular hydrogen bonding between the carbonyl oxygen (N-H···O) (*d* = 2.107 Å and *D* = 2.135 Å) and the pre-organised amide, leads to the formation of a dimer in the solid-state (Figure 2.22). Both of the molecules in the asymmetric unit demonstrate the same hydrogen bonding motifs with slightly different hydrogen bond distances. One of the dimers has N-H···O hydrogen bond lengths of *d* = 2.109 - 2.137 Å, while the second dimer has hydrogen bond lengths of 2.106-2.153 Å. As observed in compound **L11**, the structures are also stabilised by intermolecular π-π stacking interactions. In the crystal packing, compound **L12** is stabilised a centroid-centroid π-stacking interaction involving the two pendant pyridine rings (centroid-centroid distance 3.731 Å).

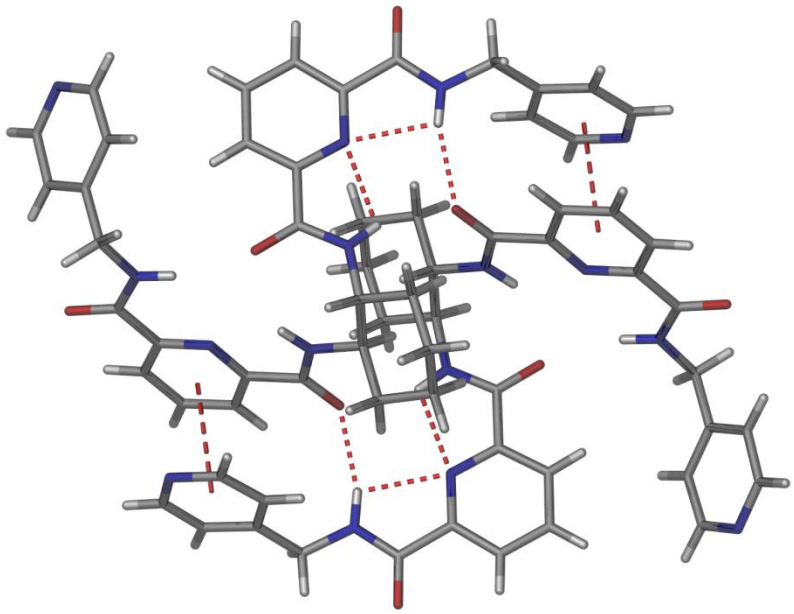

Figure 2.22. A perspective view of one of the dimers of compound **L12**, showing the intramolecular and intermolecular interactions, including the π-stacking interactions.

2.4. ^{1}H NMR studies on the tetraamide compounds, L7-L10

In investigating anion complexation by the amide compounds synthesised in this work, one consideration was the extent with which these compounds self-associate in solution and the solid-state. As has been observed in the previous section, the tetraamide compounds form a number of intramolecular and intermolecular hydrogen bonding interactions in the solid-state. Furthermore, by mass spectroscopy, several ions are observed that are consistent with the formation of dimeric and trimeric aggregates in solution. This self-association may or may not contribute to diminished ability to interact with anions in solution, either as organic receptors or as ligands in a coordination complex observed for other systems. Furthermore, the tetraamide series has a greater possibility of form hydrogen bonded aggregates due to a larger number of amide moieties.

Sumby and co-worker [161] have reported their investigation on the behaviour of **L5** and **L6** in solution by NMR spectroscopy. In the study, compounds **L5** and **L6** were found to self-associate by hydrogen bonding involving the central 2,6-pyridine dicarboxamide moiety and also the external pyridine rings. This was observed from the dramatic changes in the spectra when the

concentration was increased. The results obtained from NMR spectroscopy were consistent with mass spectrometric studies which indicate the formation of dimeric and trimeric aggregates in solution. Thus, concentration dependent ^{1}H NMR spectroscopy was used to examine the behaviour of the tetraamide ligands in solution. This experiment was undertaken based on the methods described in the literature.[161,182] In this analysis, the ^{1}H NMR spectra for **L7** – **L10** were recorded in both DMSO-d_6 and $CDCl_3$. As some of these compounds have limited solubility in these NMR solvents, probably owing to intermolecular hydrogen bonding, for this experiment, the compounds were prepared with starting concentrations of *ca.* 0.03 M. The spectra of these initial solutions were measured and then each solution was diluted in two steps to observe the changes in chemical shifts upon dilution (Diagram 2.1). As a consequence, the nature of and the chemical moieties involved in the association could be measured.

Diagram 2.1. The dilution steps in the preparation of the NMR samples.

It is possible, by using the resonance frequencies of the protons that directly involved in the self-recognition, to determine binding constants for the self-association.[183] Despite this being possible, these experiments were not undertaken. Dilution experiments on all compounds in DMSO-d_6 showed negligible shifts in all resonances for **L7 - L10** as the concentration was decreased. The limited change in the spectra upon dilution indicates that in a competitive polar solvent like DMSO, no hydrogen bonded aggregates are present in solution. This is similar to the observations reported for **L5** and **L6**,[161] and suggests that in appropriate solvents, the formation of hydrogen bonded aggregates will be less of a problem for investigating complexes of these ligands. Figure 2.23 reveals the limited changes in the chemical shifts for **L7** in DMSO-d_6 as the concentration was lowered from *ca*. 0.03 M to 0.0006 M. The negligible shifts were also indicated in the ^{1}H NMR spectra of **L8**, **L9** and **L10** when the concentration was decreased (Appendix 1).

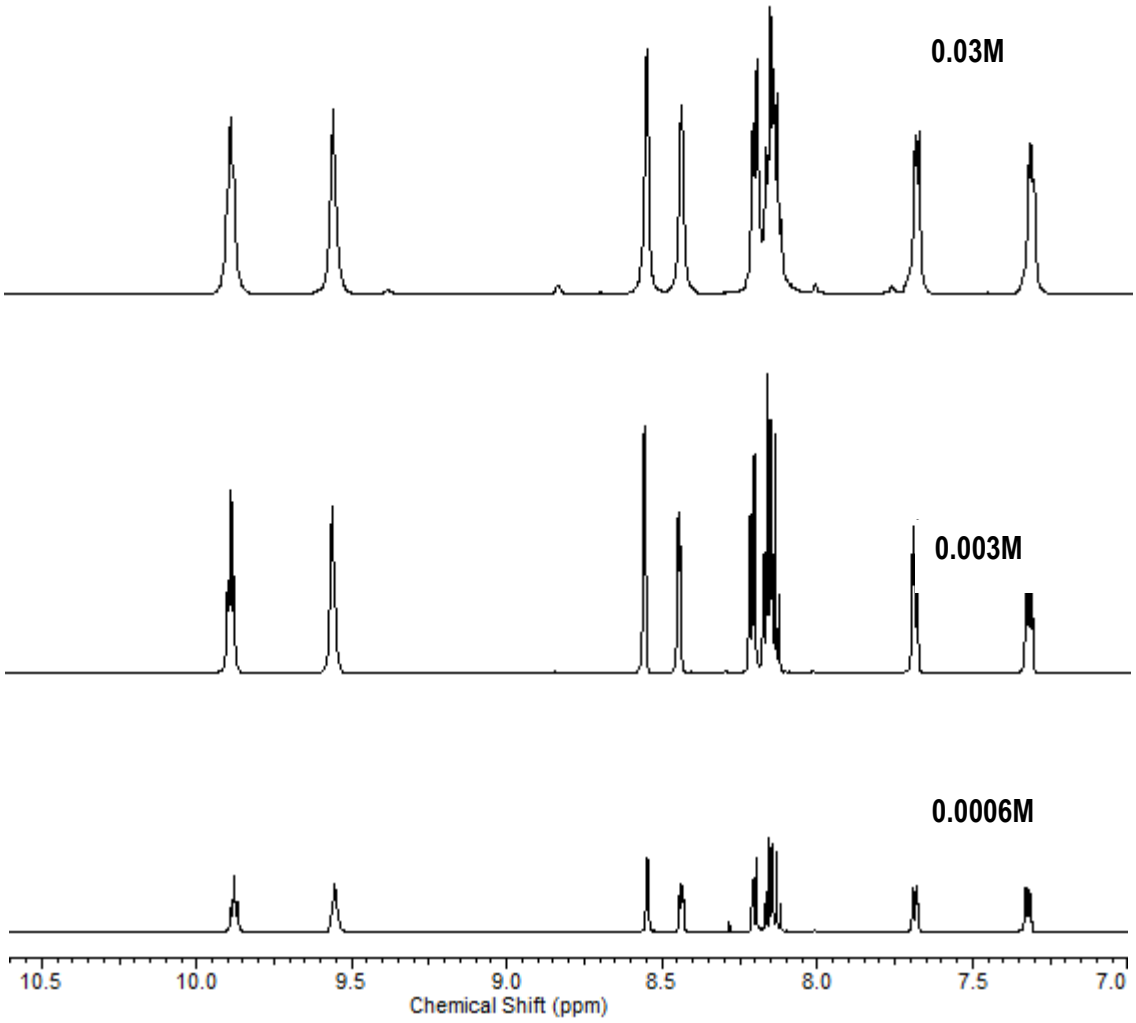

Figure 2.23. The aromatic regions of the ^{1}H NMR spectra of **L7** in DMSO-d_6 recorded at different concentrations.

In contrast to the results obtained in DMSO-d_6, the dilution experiments on these compounds in $CDCl_3$ showed quite significant changes with concentration. Significant upfield shifts for the NH protons were observed for all compounds upon decreasing concentration. This is similar to the changes observed for compounds **L5** and **L6**,[161] and indicates the formation of strong intermolecular NH amide hydrogen bonds in chloroform. This supports the proposal that these compounds self-associate in relatively non-polar solvents and suggests that, in less competitive solvents, self-association and anion complexation will compete. Less dramatic upfield shifts were observed for the signals corresponding to the pyridine core and pendant pyridine protons as the concentration decreased. This is related to the formation of hydrogen

bonded dimers at higher concentration in which the pyridyl protons of **L7** are shielded by adjacent molecules or, potentially, due to the adoption of a more coiled conformation (Figure 2.24).

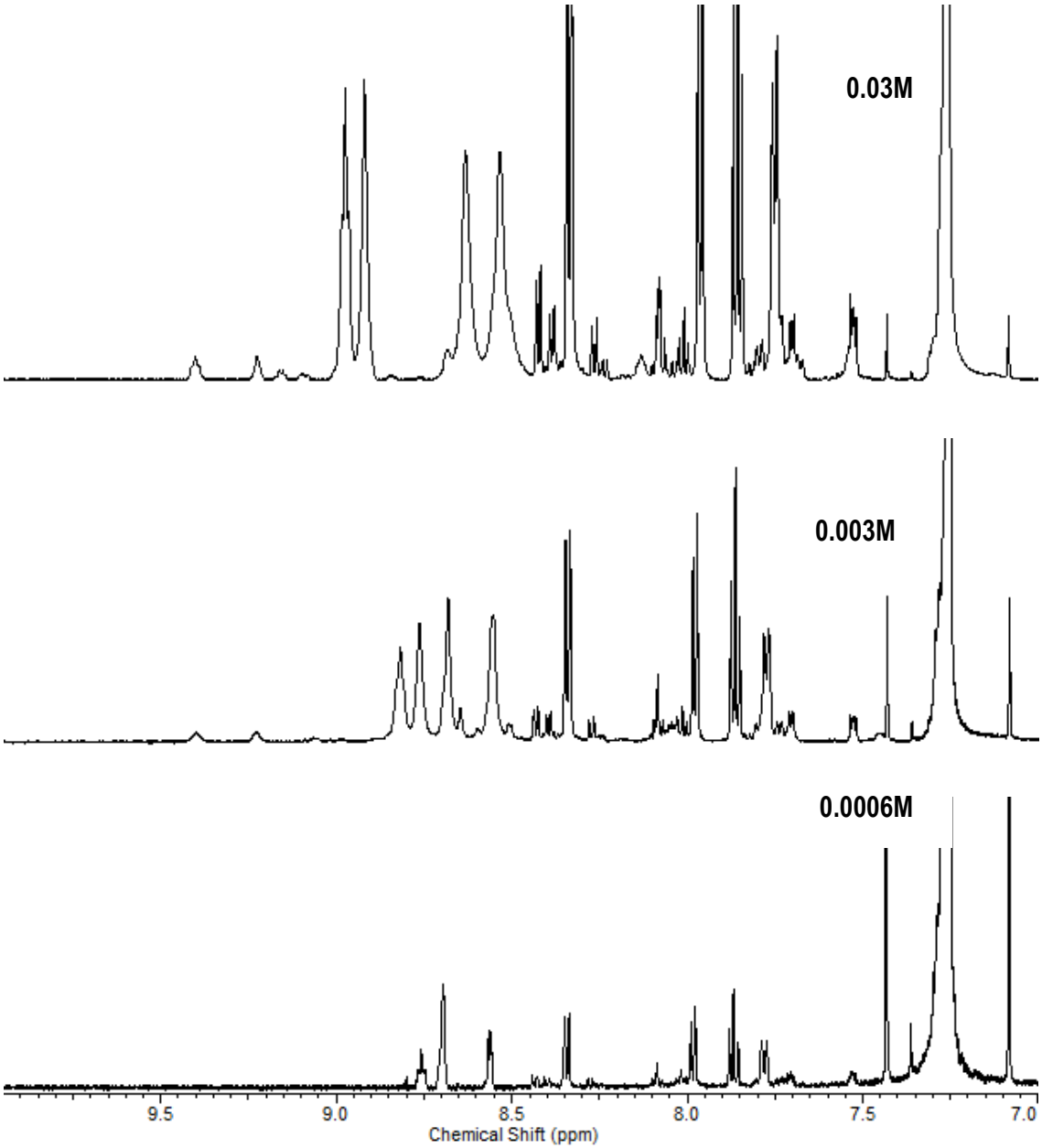

Figure 2.24. The ^{1}H NMR spectra of compound **L7** showing the changes in the chemical shift upon changes in concentration.

The ^{1}H NMR spectra of compound **L8** also indicated the formation of strong intramolecular hydrogen bonds involving the amide moieties. This is evident from significant upfield shifts of NH resonances of the ligand when the concentration is decreased (Figure 2.25).

Significant downfield chemical shifts of the aromatic protons in the more concentrated solutions of **L8** are also observed indicating the presence of hydrogen bonding interactions involving the pyridyl groups as acceptors within the hydrogen bonded dimers. The formations of dimeric species were observed by mass spectrometry for this compound.

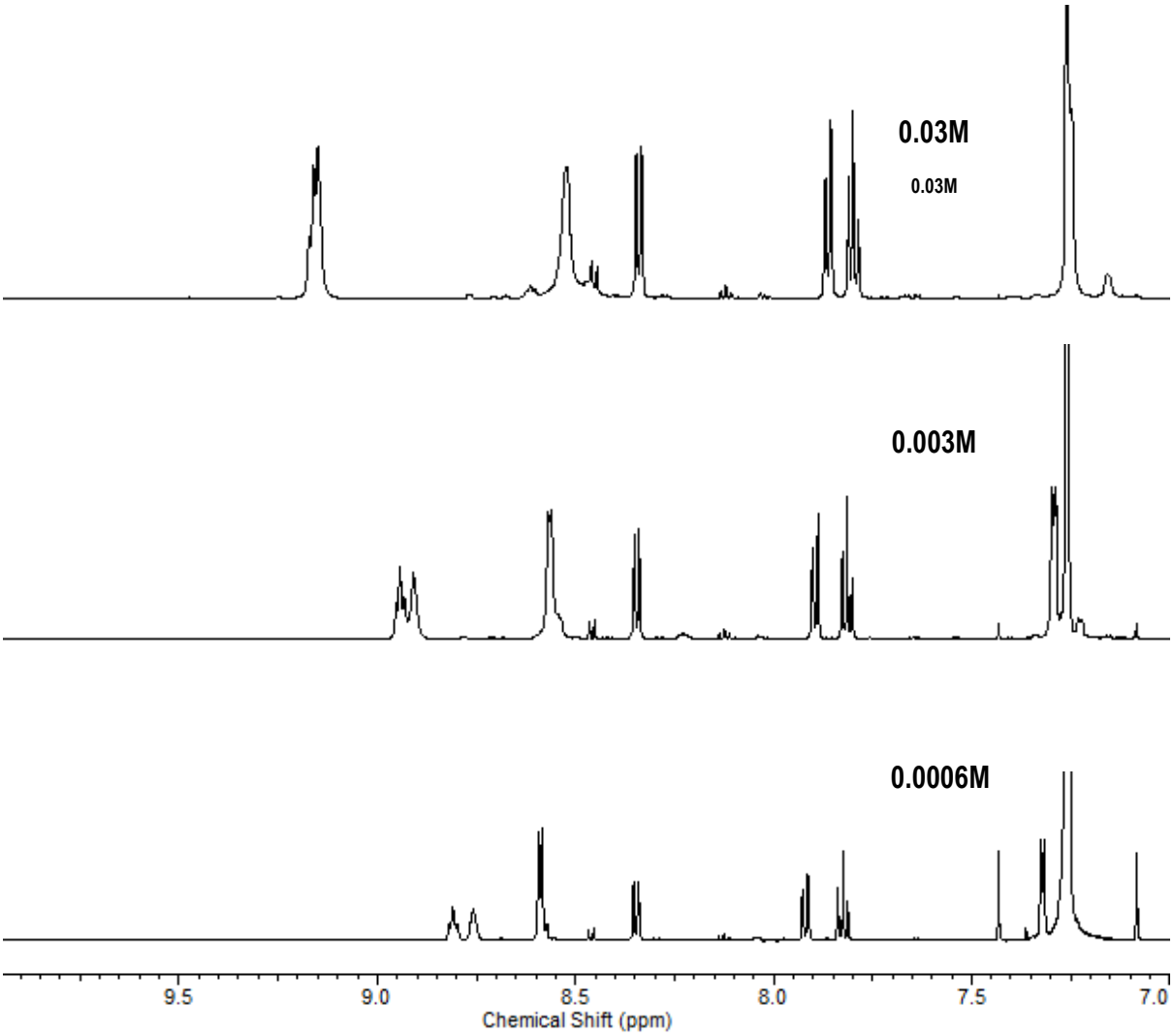

Figure 2.25. Expansions of the aromatic regions of the ^{1}H NMR spectra of compound **L8** in $CDCl_3$.

Compounds **L9** and **L10** also showed significant downfield shifts at NH amide resonances when the concentration is increased (Figure 2.26 and 2.27). In compound **L9**, significant downfield shifts were observed particularly at the pendant pyridine resonances, perhaps indicating the formation of a hydrogen bonded dimer by insertion of the pendant pyridyl ring into the 2,6-pyridine carboxamide pocket of a second molecule. The presence of the dimeric

species was also indicated by mass spectrometry. Figure 2.26 shows the ^{1}H NMR spectra observed upon dilution of compound **L9**. From the ^{1}H NMR spectrum of compound **L10** (Figure 2.27), it is clearly evidenced that compound **L10** behaves in a similar manner to other tetraamide compounds described in this thesis.

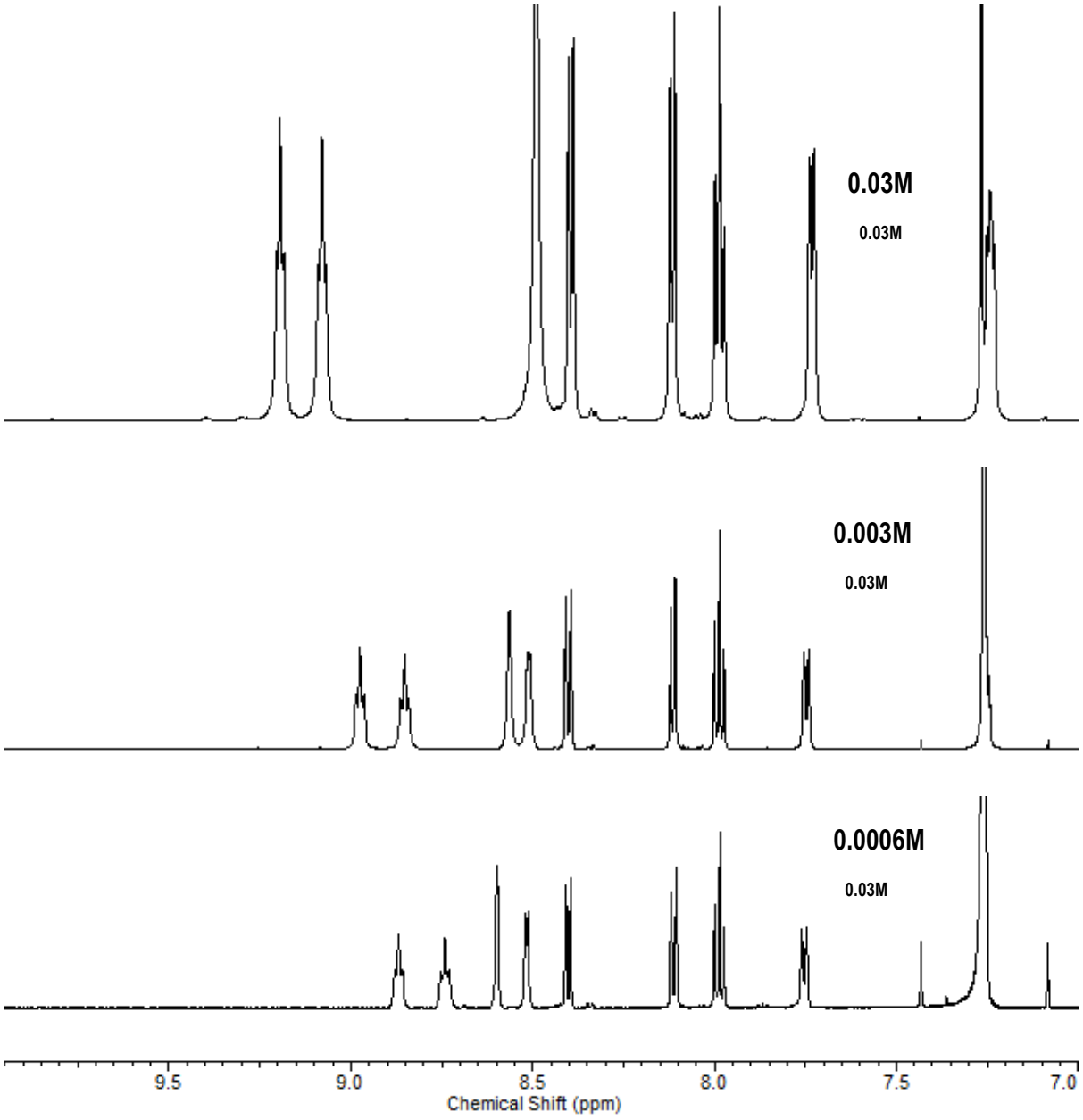

Figure 2.26. Expansions of the aromatic regions of the ^{1}H NMR spectra of compound **L9** in $CDCl_3$.

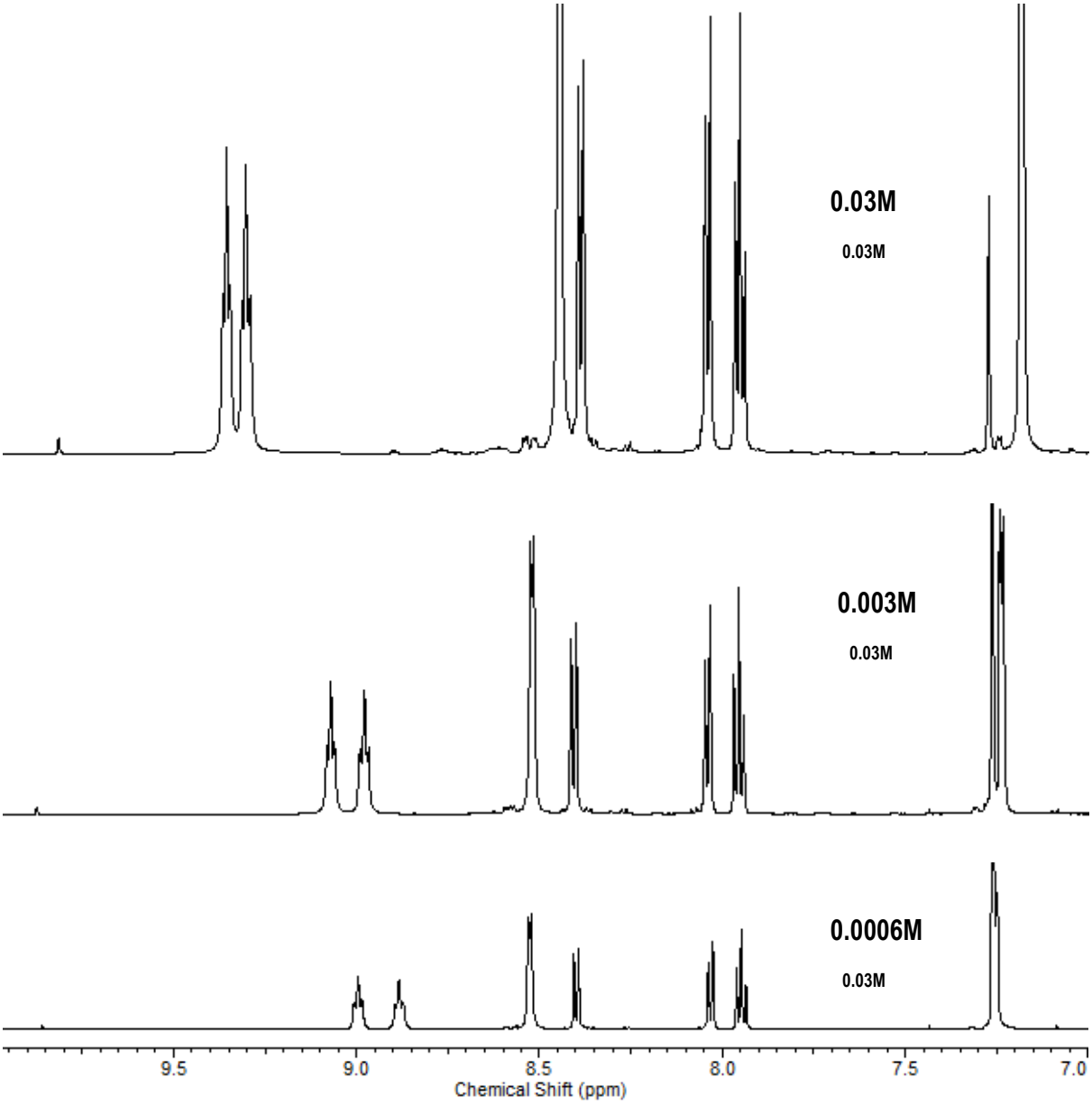

Figure 2.27. Expansions of the aromatic regions of the ^{1}H NMR spectra of compound **L10** in $CDCl_3$.

This series of experiments indicates that the tetraamide compounds do self-associate in less competitive solvents such as $CDCl_3$. In such solvents these compounds would be anticipated to bind anions too but, depending on the concentration, it would be expected that this would occur in competition with self-association. This behaviour is expected to be similar to that proposed for

compounds **L5** and **L6**,[161] indicating that these compounds would also be suitable for complexing with transition metals and binding anions as part of discrete metallo-supramolecular assemblies and coordination polymers. However, the propensity to form hydrogen bonded aggregates in solution and the solid-state could restrict the capability of these compounds to interact with anions in the manner intended.

2.5. Syntheses of the amide chelating ligands

In this final section, the synthesis of three new amide chelating ligands are described where two bidentate chelating groups have been appended to a 2,6-disubstituted pyridine, isophthalamide or terephthalamide core. In all three compounds, di-2-pyridylmethylamine was used to provide the chelating donor groups. The synthesis of di-2-pyridylmethylamine was adapted from Meunier *et al*.[184] involving the reductive amination of di-2-pyridyl ketone oxime with zinc powder. The first amide chelating ligand, compound **L13**, was synthesised from 2,6-pyridinedicarbonyl dichloride to give compound **L13** in a good yield (*ca* 60% yield). By using the same method, two related chelating ligands containing isophthalamide or terephthalamide cores were successfully synthesised. All new compounds were characterised by a combination of IR spectroscopy, combustion analysis, NMR spectroscopy, mass spectrometry and, where possible, suitable crystals were subjected to single crystal X-ray crystallography.

2.5.1. Syntheses of a 2,6-pyridine carboxydiamide based chelating ligand

As noted, di-2-pyridylmethylamine was synthesised in two steps using slightly modified literature procedures.[184-186] In the first step, di-2-pyridyl ketone oxime (**2.36**) was prepared from commercially available di-2-pyridyl ketone **2.35** by the approach shown in Scheme 2.11. A mixture of di-2-pyridyl ketone and hydroxylamine hydrochloride were treated as described to give **2.36** as a pale pink solid in 89% yield. Di-2-pyridylmethylamine (**2.37**) was then prepared by reductive amination of **2.36** in 80% yield, a 71% yield over the two steps.

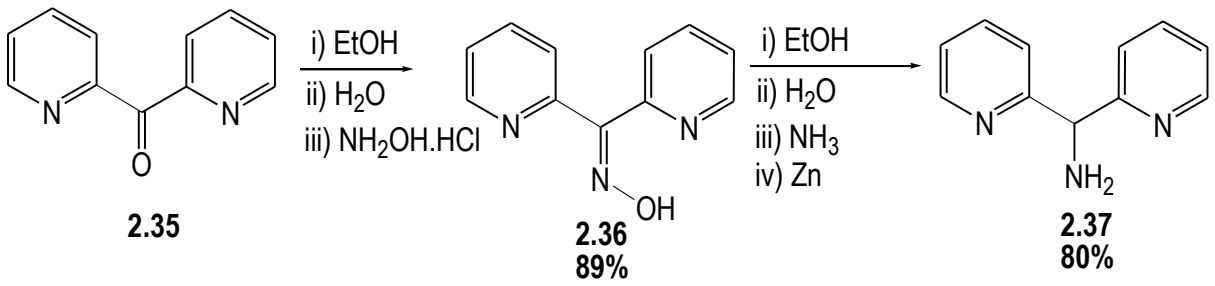

Scheme 2.11. The synthesis of di-(2-dipyridyl)methaneamine (**2.37**).

Compound **2.37** was then reacted with 2,6-dimethylpyridine dichloride (**2.38**), which was prepared immediately prior from dipicolinic acid (**2.27**) using typical conditions for the acid chloride synthesis. Compound **2.18** was isolated by column chromatography (SiO_2) using a solvent system of 5% methanol/dichloromethane to give **L13** as a light brown solid in 64% yield (Scheme 2.12). Elemental analysis suggested that this product was obtained as a hydrate with formula **L13**·H_2O. This compound was characterised by ^{1}H NMR spectroscopy with the expected number of resonances for a di-substituted derivative. The NH signal was observed noticeably downfield at 10.32 ppm. The IR spectra of **L13** exhibits several characteristic strong bands, such as a C=O stretching at approximately 1671 cm^{-1}, a strong band at 3354 cm^{-1} that is attributed to the N-H stretching vibration, and a band at 1503 cm^{-1} that is due to C=N stretches. ESI-MS, conducted in a mixture of methanol-acetonitrile solution, showed the expected positively charged ion of [**L13**+H]$^+$ at *m/z* 501.6 (40%). Furthermore, an ion corresponding [**L13**+Na]$^+$ was observed at *m/z* 523.4 (100%). Compound **L13** was recrystallised by dissolution in hot methanol-acetonitrile and, on standing at room temperature for 5 days, yielded yellowish crystals with a block-shaped morphology which were suitable for structure analysis using single crystal X-ray crystallography.

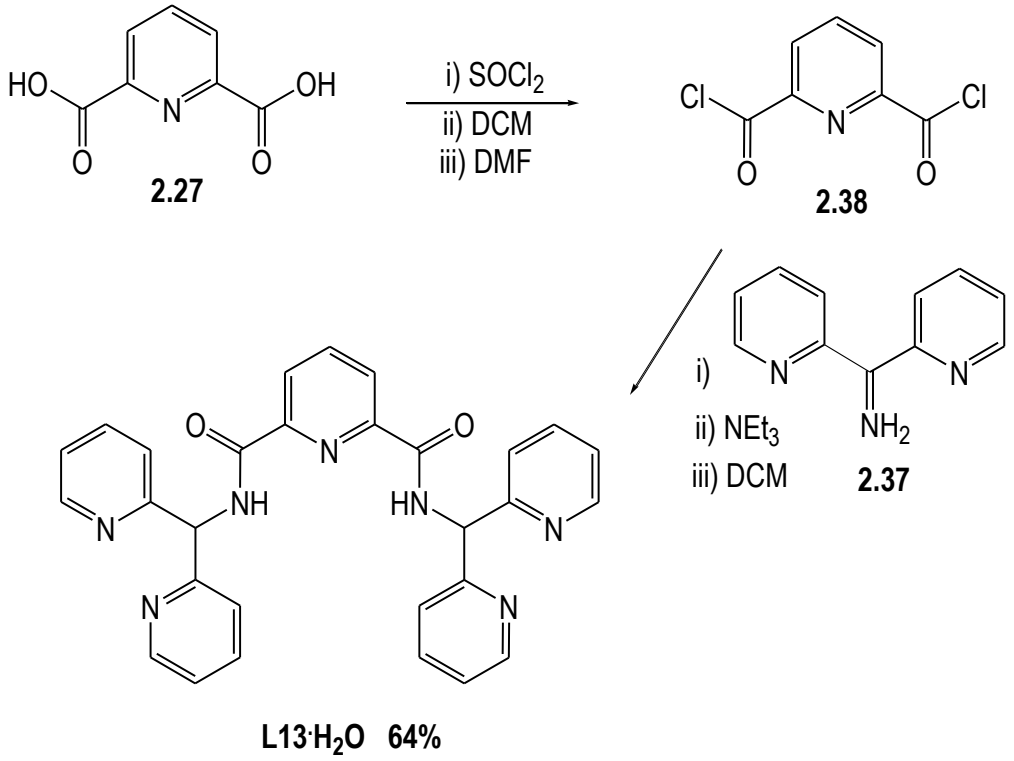

Scheme 2.12. Synthesis of **L13**·H_2O.

Crystal structure of **L13**

Compound **L13** crystallises in the monoclinic space group $P2_1/c$, with one molecule of **L13** in the asymmetric unit. In the crystal structure, the two di-2-pyridylmethyl arms have quite different arrangements; one has the two 2-substituted pyridine rings directed either side of the plane of the 2,6-pyridine dicarboxamide core, while the second arm has one pyridine ring almost in the plane of the 2,6-pyridine dicarboxamide core and the other ring nearly perpendicular to the 2,6-pyridine dicarboxamide core. In case of the second di-2-pyridylmethyl arm, the in plane pyridine ring (N57) is involved in a hydrogen bond (d = 2.220 Å; D = 2.639 Å) with one of the the NH donors of the 2,6-pyridine dicarboxamide core. The flexibility of this ligand might be reduced or further controlled by the presence of the weak nitrogen-hydrogen hydrogen bonding interactions.[187] In a similar manner to the other diamide and tetraamide compounds investigated in this thesis, the structure of compound **L13** demonstrates that the 2,6-pyridine dicarboxamide core preorganises the amide moieties by intramolecular hydrogen bonding interaction N-H···N (d = 2.248 Å and 2.321 Å; D = 2.660 Å and 2.700 Å; N-H···N angles = 109.23 and 106.49°) (Figure 2.28).

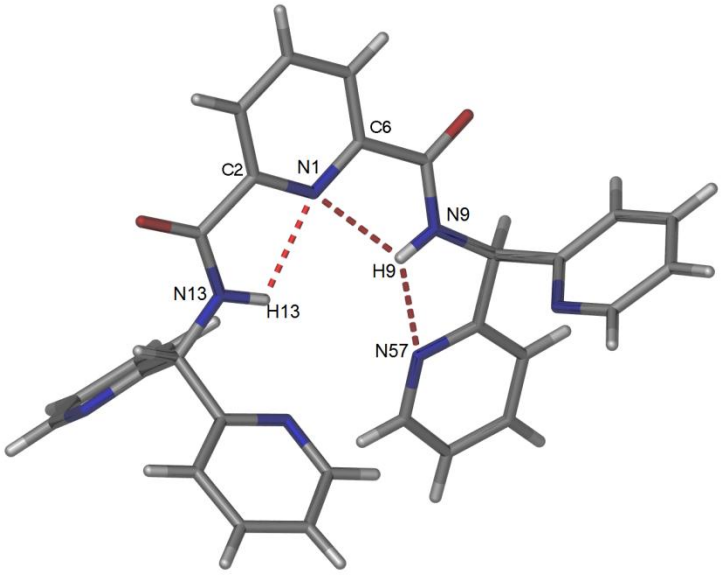

Figure 2.28. A view of the asymmetric unit of compound **L13**. Selected bond lengths (Å) and angles (°) : N(1)-C(2) 1.337, N(1)-C(6) 1.341, C(2)-N(1)-C(6) 117.18, C(2)-N(1)-C(6) 117.71 and N(13)-C(11)-C(2) 113.77.

Aside from the intramolecular hydrogen bonding involving the pre-organised amide moiety and one of the pendant pyridine arms, the packing diagram does not reveal any other significant hydrogen bonding interactions. The association of two molecules of **L13** seems to be driven by overlap of the 2,6-pyridine dicarboxamide cores of adjacent molecules, where the pyridine ring of one molecule lies over the amide functional group of an adjacent molecule (centroid-centroid distance 4.64 Å; angle 66.57°; centroid offset 1.39 Å) (Figure 2.29). This is considerably longer than the distances usually observed for such interactions.[5]

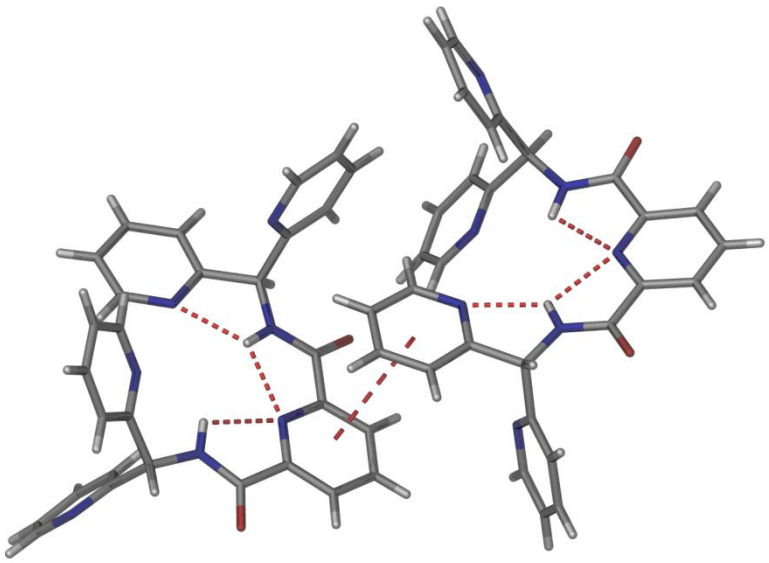

Figure 2.29. A section of the crystal packing of compound **L13**, with the centroid-centroid π-stacking interactions shown as large dashed bonds.

2.5.2. Syntheses of the isophthalamide or terephthalamide chelating ligands

As mentioned previously, di-(2-pyridyl)methylamine was used for the synthesis of this group of chelating ligands. In this section, a description of the synthesis of two compounds which do not have the 2,6-pyridine dicarboxamide core that typifies all other ligands studied, is outlined. These compounds were prepared by reaction of commercial isophthaloyl chloride and terephthaloyl dichloride with di-(2-pyridyl)methylamine. Compound **L14**·H_2O was derived from isophthaloyl chloride by treatment with di-(2-pyridyl)methylamine (**2.37**) in dichloromethane and triethylamine. After heating at reflux for 3 days, the product was obtained as a brown solid after removal of the solvent. The brown solid was recrystallised from ethanol to give compound **L14**·H_2O as a fine brown powder in 75% yield (Scheme 2.13). The ^{1}H NMR spectrum of compound **L14**·H_2O was consistent with the expected 2-fold symmetric disubstituted compound. The NH resonance was observed at 8.87 ppm, located reasonably upfield compared to NH signal observed for **L13**. Peaks at *m/z* 501.1 and 522.4, which correspond to [**L14**+H]$^+$ and [**L14**+Na]$^+$ respectively, were observed in the electrospray mass spectrum of the compound. In the IR spectra, the presence of a strong absorbance band at 1650 cm^{-1} is attributed to the C=O stretching of the amide moiety.

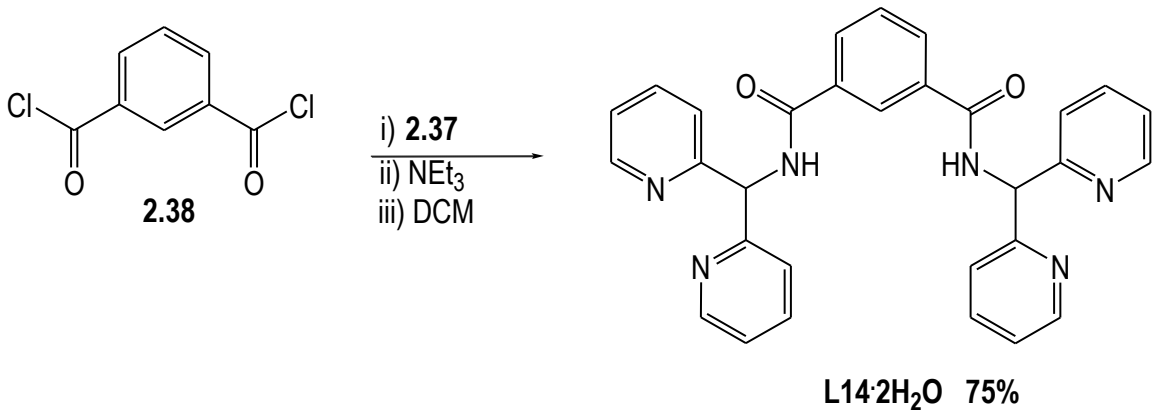

Scheme 2.13. Synthesis of compound **L14**·H_2O

Another potentially ditopic chelating ligand (**L15**), this time incorporating a terephthaloyl core, was prepared using the same procedure described for compound **L14**·H_2O. A mixture of terephthaloyl chloride (**2.39**), di-(2-pyridyl)methylamine (**2.37**) and triethylamine was suspended in dichloromethane, and heated at reflux for approximately 3 days. After this time, a brown solid precipitated out from the reaction mixture. This solid was collected and washed with diethyl ether and recrystallised from methanol to give a pure sample of **L15** (82% yield) as a light brown powder (Scheme 2.14).

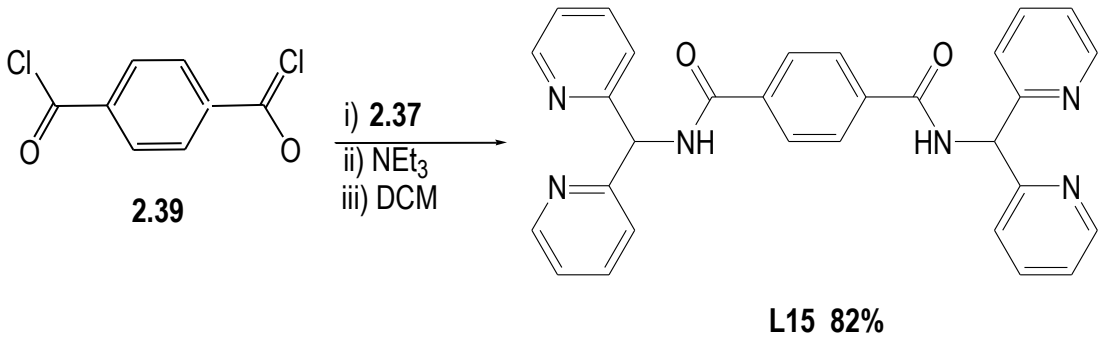

Scheme 2.14. Synthesis of **L15**

^{1}H NMR spectroscopy of **L15** once again gave a spectrum consistent with a symmetric disubstituted compound, with the NH signal at 8.96 ppm. This is reasonably similar to the chemical shift for the NH proton in the isomeric compound **L14**·H_2O but is much further upfield than NH protons of **L13** (10.32 ppm). This difference in chemical shift must be due to the different conformations of the amides about the central pyridine and phenyl cores in **L13** – **L15**. Presumably, the conformation adopted by **L14** and **L15** means the amide NH protons are less deshielded by the adjacent arene rings. The amide C=O and NH stretches were observed at 1642 and 3211 cm^{-1} in the IR spectrum. The ESI-MS showed a peak at *m/z* 501.2 corresponding to $[\mathbf{L15}+H]^+$, while $[\mathbf{L15}+Na]^+$ was observed at *m/z* 523.2 in low relative abundance. Crystals of **L15** were obtained by slow evaporation of a methanol solution of **L15** and cadmium sulfate. The crystals were obtained as colourless rectangular block-shaped crystals which were suitable for X-ray crystallography.

Crystal structure of **L15**

Compound **L15** crystallises in the triclinic space group *P*-1, with one molecule of ligand **L15** in the asymmetric unit. The phenyl core is planar, although the amide groups are twisted slightly out of the plane of the ring (torsion angles 119.60 and 117.05°) when compared to the behaviour of the 2,6-pyridine dicarboxamide. The two di-2-pyridyl units are further twisted relative to the phenyl, as shown in Figure 2.30. In a similar way to compound **L13**, the two pyridyl rings are not co-planar. The rings are arranged in *trans* conformations which brings the nitrogen atoms from the two pyridyl rings closer to the benzene core. This conformation has been observed in a crystal structure of a related chelating ligand, namely 1,2-bis(di-pyridylaminomethyl)benzene.[187]

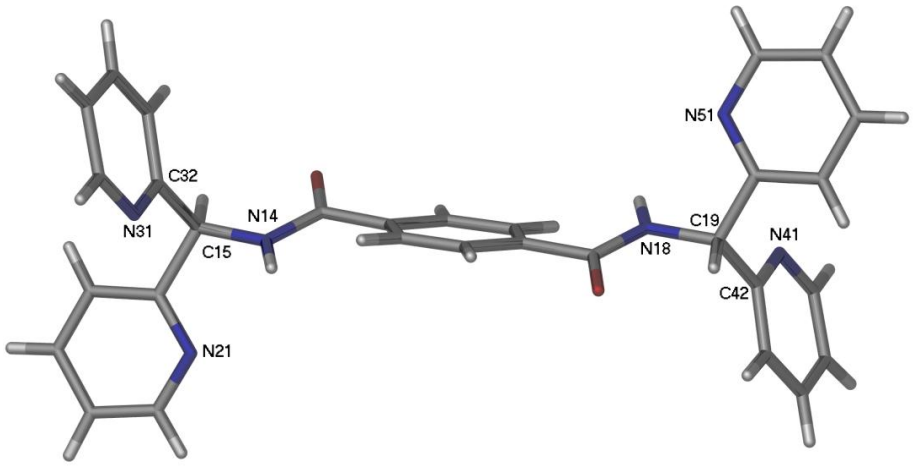

Figure 2.30. The view of the asymmetric unit of **L15**. Selected bond lengths (Å) and angles (°) : N(14)-C(15) 1.443(4), N(18)-C(19) 1.474(4), N(31)- C(32) 1.351(5), N(41)- C(42) 1.328(4), C(32)-C(15)-N(14) 110.0(3) and C(42)-C(19)-N(18) 110.7(3).

The packing of **L15** is stabilised by a C-H···π interaction between the hydrogen atom from the phenyl ring and the pendant pyridine with H-centroid distance of 2.788 Å (Figure 2.31). This distance is close to other edge-on C-H···π interaction distances reported for other compounds.[188]

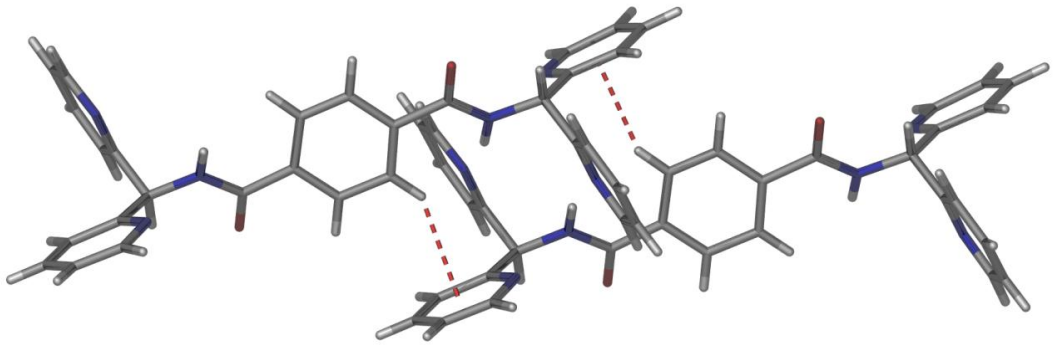

Figure 2.31. A section of the crystal packing of compound **L15**.

2.6. Summary

Fifteen amide compounds have been successfully synthesised in moderate to good yields. The majority of the compounds contain a 2,6-pyridine dicarboxamide moiety, that directs the hydrogen bond donors internally and hopefully enables simultaneous anion binding and metal complexation within discrete complexes and coordination polymers. Included in this are a series of four previously reported pre-organised and flexible amide ligands (**L1**, **L2**, **L5** and **L6**) that were prepared from the reaction of 2,6-dimethylpyridine dicarboxylate and commercially available picolyl amines using 1:1 or 1:2 ratios, respectively. In contrast to the synthesis of the flexible monoamide compounds, more rigid examples (**L3** and **L4**) were synthesised by reaction of 3- or 4-aminopyridine with 6-(methoxycarbonyl)pyridine-2-carboxyl chloride in 1:1 ratio. These products were obtained as pale brown solids by recrystallisation from ethanol.

A series of novel tetraamide ligands (**L7**-**L12**) were also prepared. In approach employed, derivatives of the monoamides **L1** and **L2** were linked by diamines such as 1,2-ethylenediamine, 1,3-propylenediamine and 1,2-diaminocyclohexane to give six novel tetraamide compounds, **L7 – L12**. These diamine compounds were used as a spacer and their incorporation into the bridging ligands was employed to lengthen the distance between the metal coordinating sites and to confer additional flexibility to the compounds. Three different chelating amide ligands (**L13**-**L15**) were also described in this chapter. These doubly bidentate bridging ligands were obtained from the reaction of di-2-pyridylmethylamine and an acid chloride. In these compounds, the di-2-pyridylmethane chelating motifs were utilised as metal chelating sites, while the amide cores derived from 2,6-dimethylpyridine dichloride, isophthaloyl chloride and terephthaloyl chloride were intended as potential anion complexation sites.

All compounds obtained were characterised by a combination of NMR spectroscopy, IR spectroscopy, mass spectrometry and combustion analysis and the crystal structures were determined using X-ray crystallography. The ^{1}H NMR spectra for the flexible ligands showed characteristic N-H proton signals at the range of 9-9.5 ppm. Compared to the flexible ligands (i.e. **L1** and **L2**), a characteristic downfield shift of N-H proton signals was observed for the less flexible monoamide ligands **L3** and **L4**. This is due to the absence of the methylene spacer between the amide NH and the pyridyl rings which brings the protons of the amide NH group

closer to the deshielding region of the pendant pyridine rings. In the ^{1}H NMR spectra of the amide chelating ligands **L13**, **L14** and **L15**, compound **L13** that incorporates a central pyridine core has N-H proton signals at 10.32 ppm, while the ligands containing isophthalamide and terephthalamide cores have N-H proton signals at 8.87 and 8.96 ppm, respectively. This difference in chemical shift is due to the quite different conformations expected for these compounds in solution; **L13** has the pre-organised pocket but **L14** and **L15** are expected to have the amide groups twisted out of the plane to reduce steric clash between the amide N-H and the ortho hydrogen atoms of the arene rings. The proton signals for the pendant pyridyl rings were typical.

The behaviour of the tetraamide ligands in solution was further investigated by the NMR spectroscopy. The results showed that the tetraamide compounds tend to self-associate at higher concentrations in non-competitive solvents such as $CDCl_3$, while in DMSO-d_6 no significant changes in chemical shift were observed indicating that individual species are well solvated. These compounds would be anticipated to bind anions too but, depending on the concentration, it would be anticipated that this may occur in competition with self-association. This observation might limit the ability of these ligands to simultaneously bind anions and cations in solution. The presence of dimeric and trimeric aggregates of these compounds with solvate molecules were also observed in the electrospray mass spectrum, and also in the crystal packing in the solid-state. In the crystal structures of the flexible amide ligands, the amide N-H hydrogen atoms are nearly always involved in intramolecular hydrogen bonding interactions. These interactions are important to stabilise the structures of the molecules as well as to pre-organises the amide moieties into a pocket. In the crystal structure of **L8** for example, the pre-organised N-H hydrogen atoms are not only involved in intramolecular interactions, but also forming intermolecular interacts with the solvate molecules. It was also observed in the crystal structures of the majority of these compounds that their crystal packing was stabilised by π-π stacking interactions between the pyridyl cores or between the pyridyl cores and the pendant pyridyl arms.

In summary, the synthesis and characterisation of fifteen ligands, four reported and eleven new, have been successfully delineated. Investigation into the speciation of the compounds in solution has been investigated and discussed. Significant hydrogen bonding interactions were observed through ^{1}H NMR spectra, electrospray mass spectrometry and X-ray crystallographic

analysis. Further investigation on the coordination chemistry of the ligands prepared in this chapter will be described in the next three chapters.

CHAPTER 3

COORDINATION CHEMISTRY OF THE MONOAMIDE LIGANDS

Chapter 3

3. Coordination chemistry of the monoamide ligands

3.1. Introduction

As noted in Chapter 1, the area of chemistry concerned with the synthesis and properties of coordination polymers has undergone extraordinary development[93,102,189-193] due to the potential applications of such materials in gas storage,[114,194-196] separation[194] and catalysis.[194,197] These materials have often been formed from heterocyclic ligands or carboxylate ligands, or a combination of the two.[102,198,199] The well-known material, MOF-5,[200] for example, has been prepared from one of the simplest symmetrical dicarboxylate linker, 1,4-benzenedicarboxylic acid (**3.1**) and $Zn(NO_3)_2$ (Scheme 3.1). Incorporation of 4,4'-bipyridine (**3.2**) and its derivatives with different structure metrics into coordination polymers has also been investigated.[201]

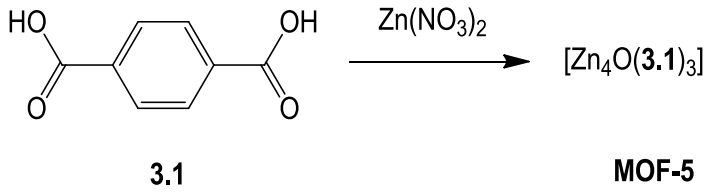

Scheme 3.1. The general synthesis of MOF-5.

Another common approach in the synthesis of porous materials is to incorporate different organic ligands within the same frameworks.[202-207] Common examples of coordination polymers being prepared from this approach are the 3-D primitive cubic-type (α-Po) structures.[207] In the structures of these coordination polymers the 2D layers, which contain paddle wheel cluster units $[M_2(O_2CR)_4]$ (where M = Cu^{2+}, Zn^{2+} and Co^{2+}) and the dicarboxylate linkers (**L**), are connected by pillars (**P**) to form 3D coordination polymers. Figure 3.1 shows examples of pillaring methods involving **3.1** linkers and pillaring compounds **3.2** and **3.3** (Figure 3.1). Typically, and as in the cases highlighted, the use of symmetrical ligands is preferred because crystallisation is often easier.

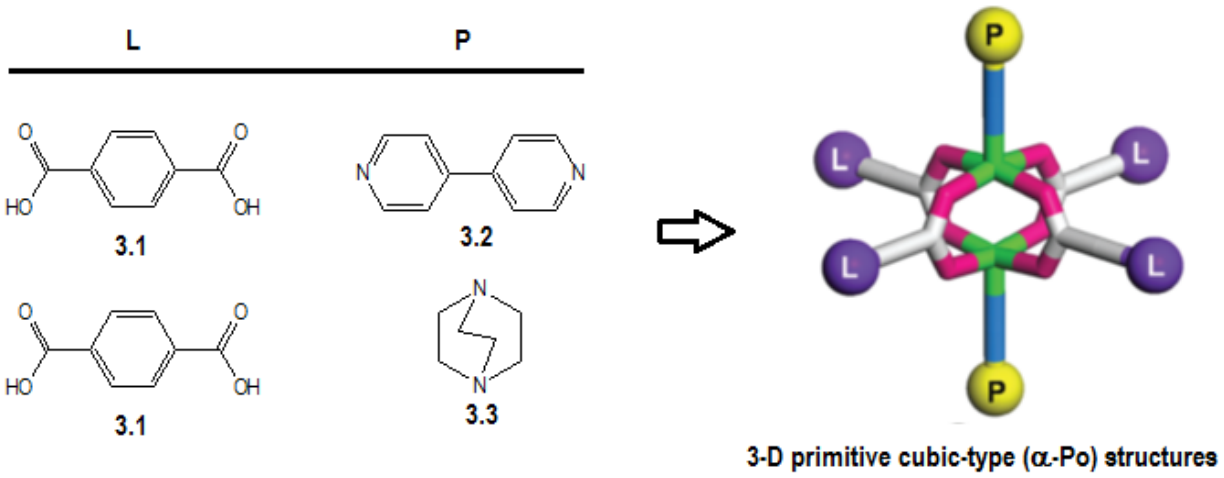

Figure 3.1. The ligands (3.1 – 3.3) and the secondary building unit formed in the synthesis of 3-D primitive cubic-type (α-Po) structures.

Unsymmetrical organic ligands such as biphenyl-3,4,5-tricarboxylic acid (**3.4**) can also form highly symmetric and porous structures with metal ions such as Cu^{2+} [208] and Mg^{2+}.[209] The gas adsorption studies on these materials have shown that they are permanently porous and structurally robust. The copper complex for example has shown relatively high excess gravimetric and volumetric H_2 uptake.[208]

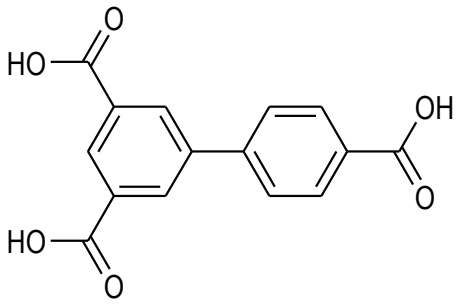

3.4

Figure 3.2. Unsymmetrical carboxylate linker, namely biphenyl-3,4,5-tricarboxylic acid.

While coordination polymers can be formed from mixed ligand systems (i.e. a combination of two or more ligands), materials that are formed from lesser numbers of

sturucturally complex linkers can be desirable.[210,211] These reduce the complexity of the self-assembly step and arguably provide improved control over the assembly. Furthermore, the use of unsymmetrical ligands can lead to a broader range of coordination polymers and provide access to novel topologies and architectures. This arises because unsymmetrical ligands have different coordinating functional groups with different donor ability, and therefore these ligands can be arranged in diverse arrangements around the metal centres. Examples of unsymmetrical linkers with two different functional groups, such as pyridine and carboxylic acid are shown in Figure 3.3. These ligands have been investigated for the synthesis of porous MOFs. [212,213]

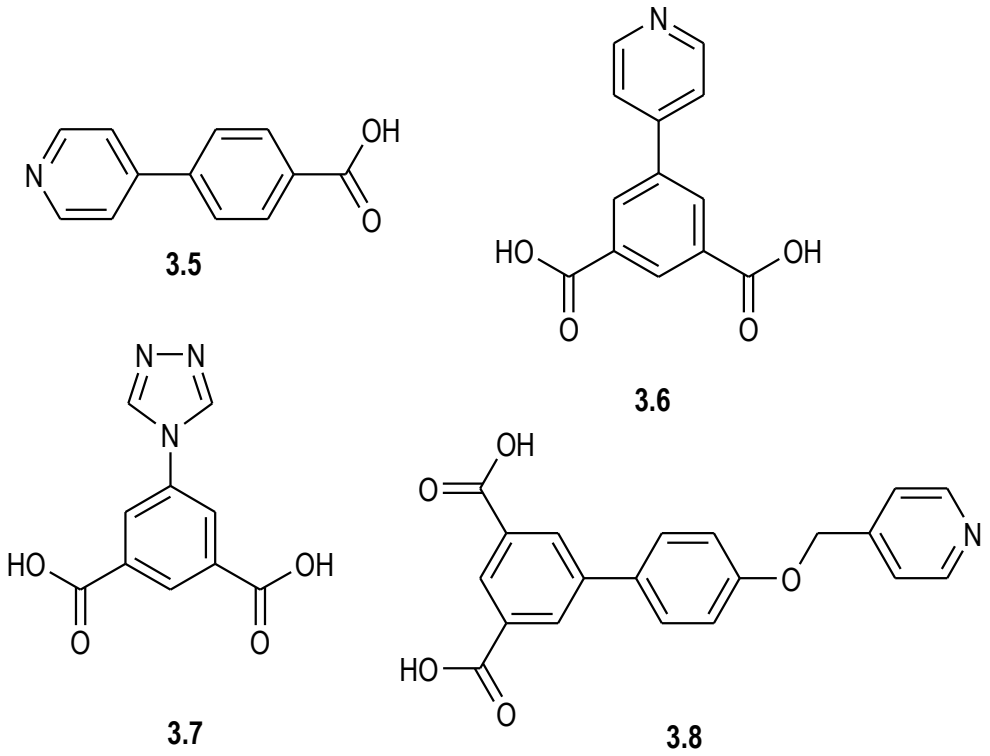

Figure 3.3. Examples of unsymmetrical ligands with two different functional groups.

Within the field of coordination polymer chemistry, interest in the synthesis and properties of materials suitable for anion sensing, exchange and sequestration has also received a significant level of attention. In this approach, linkers containing heterocyclic amide and urea ligands have been widely used to generate the coordination polymers and discrete supramolecular

assemblies.[214,215] The employment of linkers containing thio(amide), thio(urea) and imidazolium moieties has been investigated in an attempt to develop materials that are amenable to such applications.

As noted earlier (Chapter 1), the use of carboxylate donors has been well established in metal-organic framework chemistry, but it is worth noting that the use of carboxylate donors to synthesise coordination polymers for anion inclusion and exchange is more limited. Kitagawa and co-workers,[216] for instance, have designed a MOF that could stabilise the anionic guests or intermediates in a catalytic reaction through hydrogen bonding interactions. This MOF is derived from N^1,N^3,N^5-tri(pyridin-4-yl)benzene-1,3,5-tricarboxamide ligand.

With this in mind, the research in this chapter was focused on the incorporation of simple unsymmetrical heterocyclic amide ligands, *N*-6-[(3-pyridylmethylamino)carbonyl]-pyridine-2-carboxylic acid methyl ester (**L1**),[161] *N*-6-[(4-pyridylmethylamino)carbonyl]-pyridine-2-carboxylic acid methyl ester (**L2**),[161] *N*-6-[(3-pyridylamino)carbonyl]-pyridine-2-carboxylic acid methyl ester (**L3**) and *N*-6-[(4-pyridylamino)carbonyl]-pyridine-2-carboxylic acid methyl ester (**L4**) into metallo-supramolecular assemblies and coordination polymers. The flexible and preorganised amide ligands, **L1** and **L2**[161] were studied with regard to their potential to bind anionic guests in metallo-supramolecular assemblies and coordination polymers. The related, more rigid analogues (with respect to the absence of methylene linker adjacent to the 'pendant' pyridyl ring), **L3** and **L4** were investigated for the same reasons. These compounds are unsymmetrical bridging ligands in the sense that the pendant donor is a monodentate pyridyl group, as shown in Figure 3.4(a), while the ligand is capable, after *in situ* hydrolysis of the methyl ester, of also coordinating a second metal in a O, N, O tridentate fashion through the 2,6-pyridine dicarboxylate moiety. Compounds closely related to **L1** and **L2** have been previously studied. The unsymmetrical compounds, *N*-6-[(2-pyridylmethylamino)carbonyl]-pyridine-2-carboxylic acid methyl ester (**3.9**) and *N*-6-[(2-pyridylmethylamino)carbonyl]-pyridine-2-carboxylic acid (**3.10**) were studied by Lawrance and co-workers.[166] The studies have shown that these ligands act as a N, N, N tridentate ligand (R = Me) and a tetradentate ligand (R = H) upon reaction with cobalt, (Figure 3.4(b)), while reaction with copper(II) led to a formation of a neutral dinuclear copper complex, with formula $[Cu_2(\mathbf{3.10}\text{-}2H^+)_2(OH_2)_2]$.

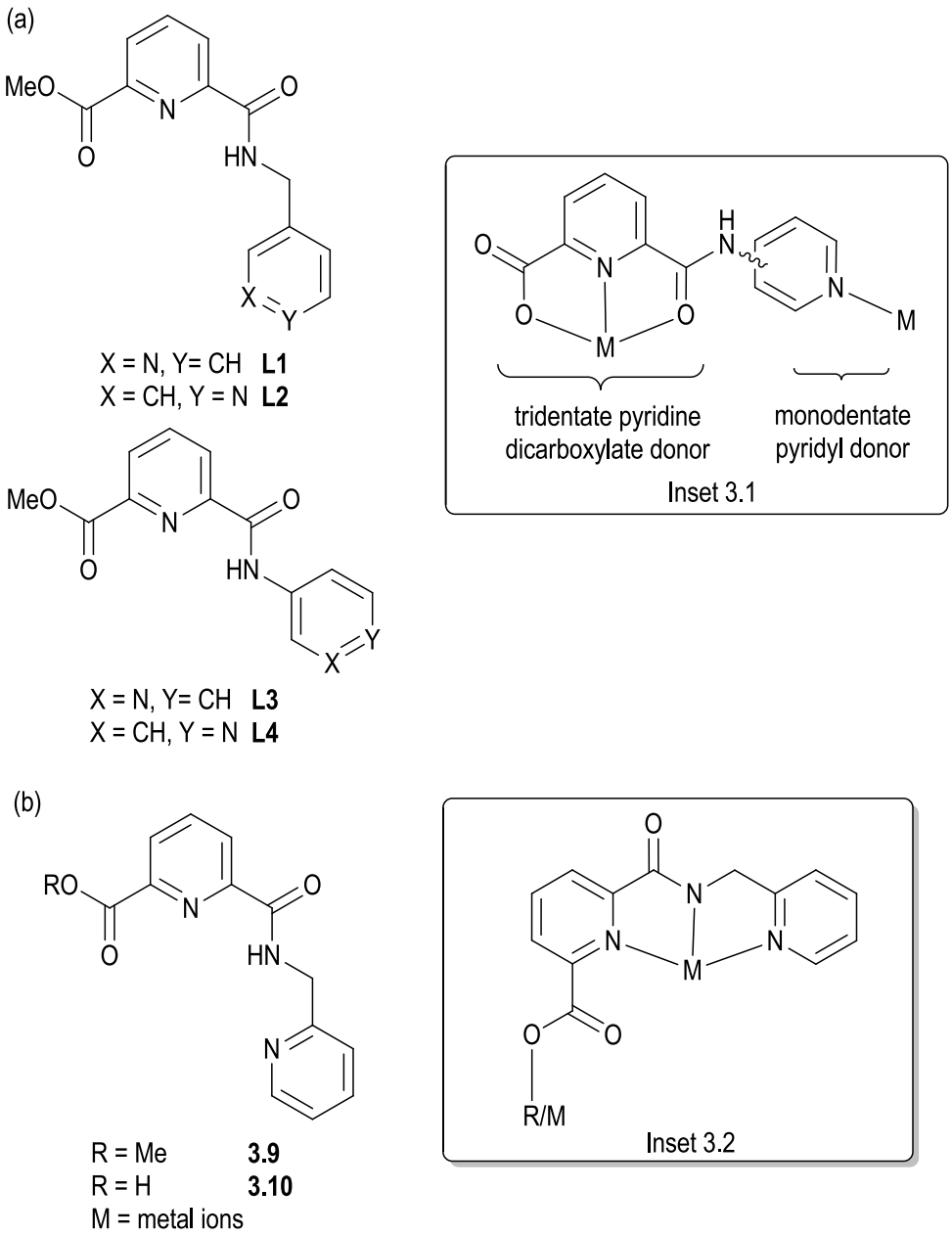

Figure 3.4 (a) The ligands investigated in this study (**L1**-**L4**), along with the coordination mode most commonly encountered in this study (Inset 3.1). (b) The related compounds, *N*-6-[(2-pyridylmethylamino)carbonyl]-pyridine-2-carboxylic acid methyl ester (**3.9**) and *N*-6-[(2-pyridylmethylamino)carbonyl]-pyridine-2-carboxylic acid (**3.10**) studied by Lawrence, and their coordination mode encountered in $[Cu_2(\mathbf{3.10}\text{-}2H^+)_2(OH)_2]$ (Inset 3.2).

Interestingly, pyridine dicarboxylate compounds with this coordination motif (ONO) (Figure 3.5(a)) are quite rare[166,217] compared to examples of pyridine dicarboxamide compounds that can coordinate in an N, N, N chelating fashion (Figure 3.5(b)).[218-220] The N, N, N chelating modes are commonly obtained from the deprotonation of the NH amide from symmetrical pyridine dicarboxamide moieties upon reaction with metal salts.

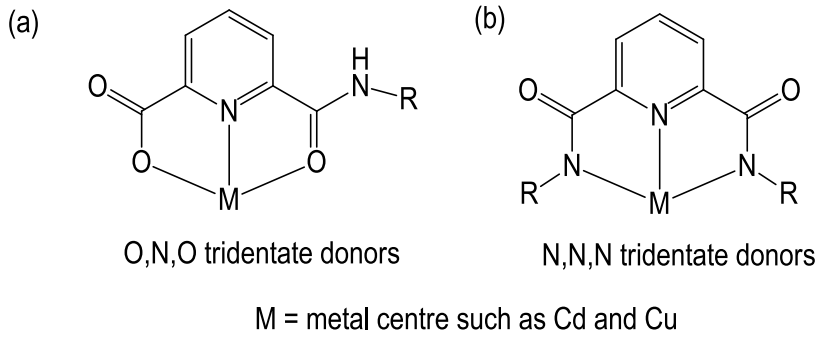

Figure 3.5. The chelating fashion through 2.6-pyridine dicarboxylate moiety.

The monoesters investigated in this project, **L1**-**L4**, can be hydrolysed to their corresponding carboxylic acids by treatment with aqueous potassium hydroxide or ammonium hydroxide but the isolation and purification procedure is somewhat tedious. In the work at hand it was shown that the methyl esters could be utilised as starting materials in the formation of discrete metallo-macrocyclic complexes and coordination polymers, whereby hydrolysis of the ester occurs *in situ* to provide access to the desired carboxylate complexes. The hydrolysis of the esters is also promoted by the coordination of metals to the ligand. Thus, heating **L1** – **L4** in methanol in the presence of a transition metal yields the free carboxylic acids and a tridentate O, N, O chelating site, Scheme 3.2. This approach to carboxylate compounds has been employed elsewhere.[221-224]

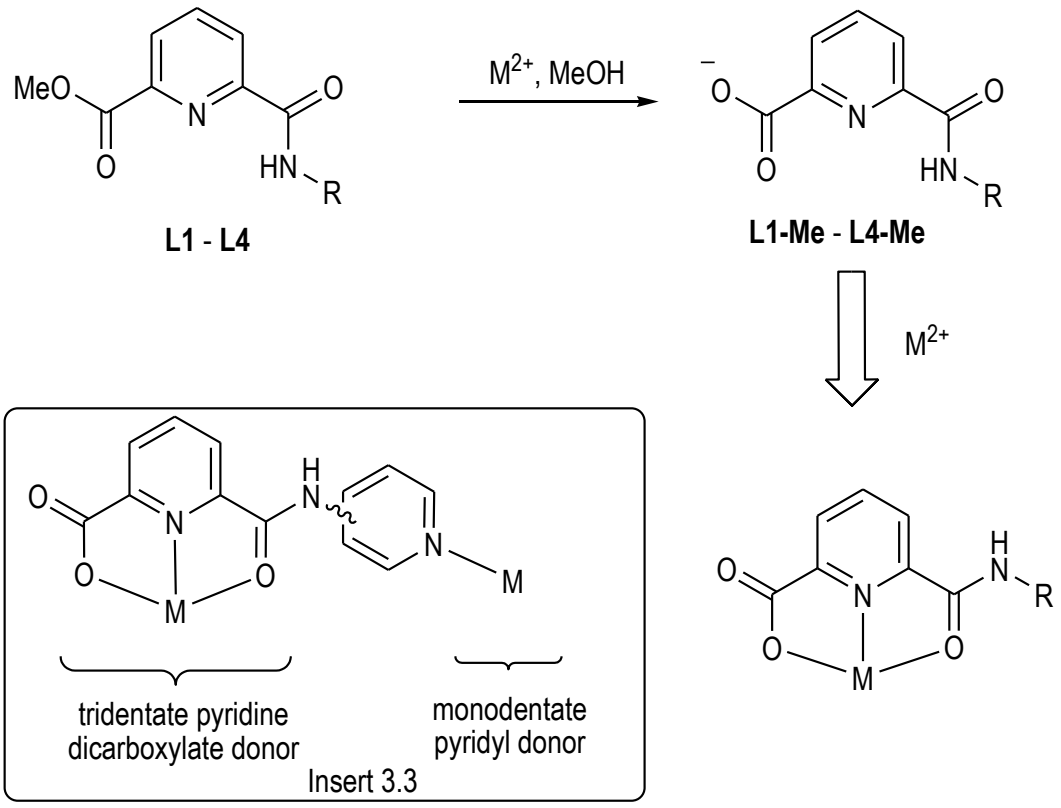

Scheme 3.2. Transition metal (M) catalysed hydrolysis of the methyl esters **L1** – **L4** and generation of the O, N, O chelating site (Inset 3.3).

This chapter reports the coordination chemistry and metallo-supramolecular chemistry of the hydrolysed derivatives of **L1**-**L4**. Upon reaction with transition metals, particularly copper(II) and cadmium(II), the ester is readily hydrolysed to unmask the tridentate, 2,6-pyridine dicarboxylate moiety. The convergent ligand **L1,** containing a pendant 3-pyridyl group, self-assembles with copper(II) to form three discrete dinuclear ($[M_2L_2]$) metallo-macrocyclic complexes with cleft-shaped structures, while cadmium(II) nitrate gives a 1D coordination polymer. In contrast to **L1**, **L3** gave planar macrocyles which may be useful building blocks for the synthesis of coordination polymers. Lindoy and co-workers have described the alternative approach to form porous frameworks using hierarchical self-assembly strategy.[225,226] This involves the combination of discrete void-containing metallo-macrocyclic components possessing unsaturated metal centres with bridging ligands and has been utilised to form permanently porous coordination polymers.[227-229] In the work of Lindoy, the metallo-macrocyclic

precursors were formed from β-di-ketonate ligands.[227-229] Results obtained for **L2** showed the propensity of this compound to form coordination polymers based on self-assembled dinuclear metallo-macrocyclic building blocks. Although not isolated independently, the $[M_2L_2]$ motif arises in the coordination polymers, indicating the usefulness of such materials for the coordination polymers synthesis.

In this chapter, the synthesis and structures of eleven novel discrete metallo-macrocycle complexes and metallo-macrocycle based coordination polymers are described. Results obtained from Powder X-ray Diffraction (PXRD) and Thermal Gravimetric Analysis (TGA) for the bulk samples of selected 2-D coordination polymers are also discussed.

3.2. Coordination chemistry and metallo-supramolecular chemistry of L1-L4

The four monoamide ligands investigated in this work possess a relatively unusual combination and disposition of the donor set. In an effort to establish the coordination modes that are accessible for these compounds, the methyl ester forms of these ligands were reacted with a selection of first and second row transition metal salts, incorporating both coordinating and non-coordinating anions. In the main, initial complexes were formed by gently heating a mixture of the ester precursor and hydrated metal salts, presumably to form a mixture of complexes of **L1** – **L4**. As described in more detail below, mass spectrometry studies of the solutions obtained at this stage did not indicate that discrete complexes of the hydrolysed ligand were present. Over time, typically days to weeks, crystals of complexes containing the hydrolysed form of the ligands were obtained by slow evaporation techniques. Invariably these reactions were carried out in 1:2 metal-ligand stoichiometries to give the products described below, as other stoichiometries, namely 1:1, were tried but under these conditions the products took considerably longer to form. This indicates that the ester hydrolysis is probably the rate limiting step; such slow hydrolysis is known to be beneficial for the formation of crystalline coordination polymers, where addition of the carboxylic acid form of the ligand often leads to an immediate precipitation of an insoluble product.

3.2.1. Coordination chemistry of L4

Reactions of **L4** with a range of copper(II) and cadmium(II) salts (MX_2, where M= Cu, Cd and X = Cl, NO_3, OAc; $CuSO_4$) failed to give isolable complexes, and invariably resulted in products that were oils (Scheme 3.3). Reaction of **L4** and zinc perchlorate in methanol yielded yellow crystals. X-ray crystallography revealed the formation of zinc chloride complex (**3.11**) with **L4**, with the coordinated chloride anions presumably originate from initial samples of **L4** being isolated as its hydrochloride salt. Unexpectedly, compound **L4,** and not **L4**-CH_3, was the form of the ligand coordinated to the zinc(II) centre. As described below, in all cases involving **L1**, **L2** and **L3** described in this thesis the ester is hydrolysed and thus this represents an isolated result.

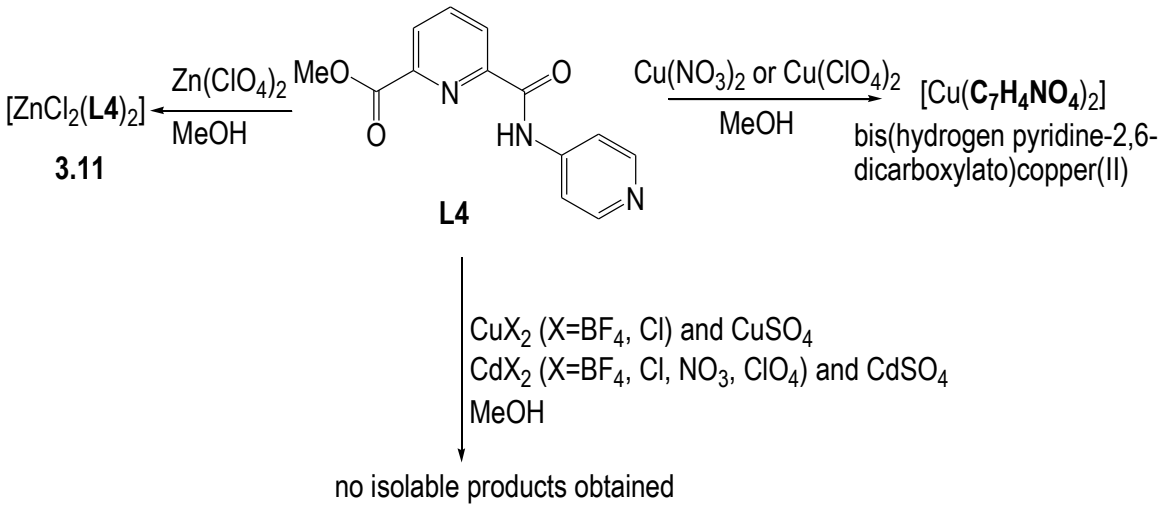

Scheme 3.3. The attempted reactions of **L4** with several metal salts with only **3.11** isolated as yellow crystals.

X-ray crystallography revealed that the zinc chloride complex crystallises in the monoclinic space group, *P*2*/c* with one zinc(II) centre, a molecule of **L4**, one coordinated chloride and one methanol molecule in the asymmetric unit (Figure 3.6(a)). The extended structure of **3.11** is shown in Figure 3.6(b) with two molecules of **L4** coordinated to the Zn atom. In the crystal structure, the zinc atom adopts a highly distorted tetrahedral geometry, with the angles between the donors in the range 103.62(11) – 122.74(8)°. The methanol molecule is hydrogen bonded to the amide moiety with the bond lengths O-H30···O12 and N-H17···O30 of

1.988 and 2.078 Å, respectively. Unfortunately, the product was difficult to isolate and only obtained in a very low yield. As such, this has prevented further analysis of this compound.

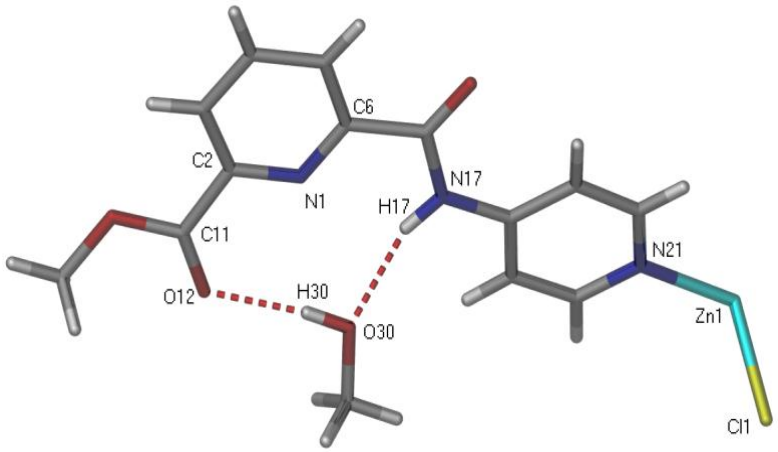

(a)

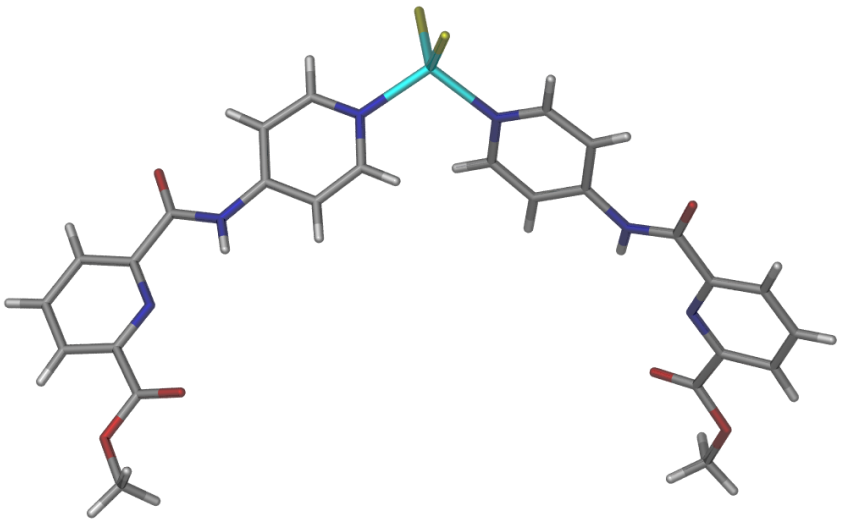

(b)

Figure 3.6. A perspective view of (a) the asymmetric unit of complex $[ZnCl_2(\mathbf{L4})_2]$ (**3.11**). (b) The extended structure of **3.11**. Selected bond lengths (Å) and angles (°) around the zinc atom : Zn(1)-Cl(1) 2.2309(13), Zn(1)-N(21) 2.049(4), N(21)-Zn(1)-Cl(1) 103.62(11) and N(21)-Zn(1)-Cl(1A) 103.62(11) 122.74(8)°.

In two cases, for example with two copper salts (CuX_2, where X = BF_4, ClO_4), which were reacted with **L4** in 1:2 metal-to-ligand ratio, isolatable and crystalline products were obtained. However, these materials were a mixture of products, including single crystals of bis(hydrogen pyridine-2,6-dicarboxylato)copper(II)[230] (Figure 3.7(a)) and in the case of copper perchlorate, crystals of bis(hydrogen pyridine-2,6-dicarboxylato)copper(II) and hydroperchlorate salt of **L4** (Figure 3.7(b)).

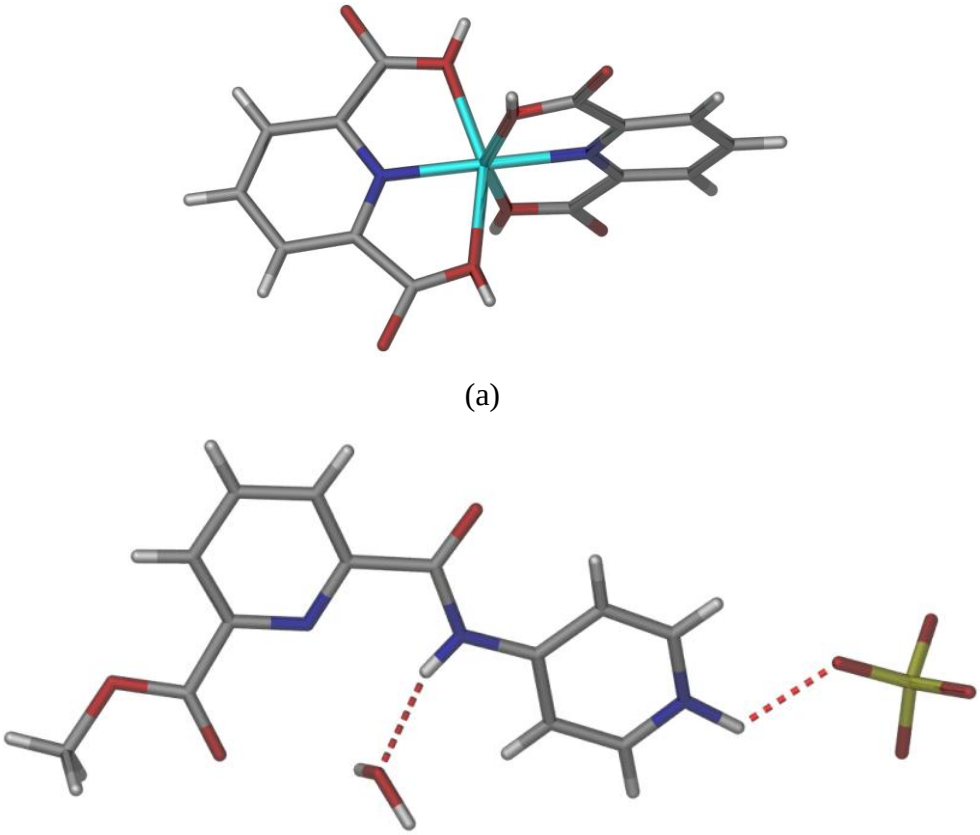

(a)

(b)

Figure 3.7. Crystal structure of (a) bis(hydrogen pyridine-2,6-dicarboxylato)copper(II)[47] and (b) hydroperchlorate salt of **L4** obtained from this study.

The inability to isolate single products from reactions of **L4** with metal salts was attributed to the relative ease with which this compound appears to undergo hydrolysis (despite in two cases intact **L4** being observed in the products) in the presence of metal salts. Decomposition of related amide ligands has been observed in other work[231,232] and thus, in this

study, it was proposed that amide hydrolysis was responsible for the difficulties involved in obtaining (pure) complexes of either **L4** or **L4**-CH_3. Therefore, the coordination chemistry of **L4** was not pursued further.

3.3. Syntheses of dinuclear metallo-macrocycles of L1 and L3.

Reaction of methyl esters **L1** and **L3** with copper(II) metal salts, where the anion was chloride, nitrate, and perchlorate, gave five isolatable discrete $[M_2L_2]$ metallo-macrocycles. Complexes of **L1**-CH_3 are cleft-shaped and hinged at the methyl spacer, while complexes of **L3**-CH_3 give planar macrocycles. As mentioned earlier, these materials may be useful building blocks for coordination polymers. For this reason, further investigation was carried out to explore the syntheses and structures of complexes of this type. Details on the synthesis and structures of the five complexes are delineated in the following section.

3.3.1 Synthesis of dinuclear metallo-macrocycles of L1

Reaction of copper salts, CuX_2 (X = NO_3, ClO_4, Cl) with **L1** in 1:2 metal to ligand ratio instantly gave rise to intensely blue coloured solutions which were left to evaporate for a period of several days to weeks to yield blue crystals of the complexes $[Cu_2(NO_3)_2(\mathbf{L1\text{-}CH_3})_2]$ (**3.12**), $[Cu_2Cl_2(\mathbf{L1\text{-}CH_3})_2(H_2O)]\cdot{}^1/_2CH_3OH\cdot 3^1/_2(H_2O)$ (**3.13**), and $[Cu_2(\mathbf{L1\text{-}CH_3})_2(CH_3OH)_2](ClO_4)_2\cdot H_2O\cdot ½CH_3OH$ (**3.14**) in good yield. These crystals were suitable for single crystal X-ray crystallography. X-ray crystallography revealed the formation of three closely related dinuclear metallo-macrocyclic copper complexes having 1:1 metal-to-ligand ratio. The same complexes could be prepared from reactions undertaken with an initial 1:1 metal-to-ligand stoichiometry; however, the desired products take considerably longer to form under these conditions. Complexes **3.12**, **3.13** and **3.14** have similar cleft-shaped structures which are hinged at the flexible sp^3-spacer. These products differ only in the type of ligands in the axial coordination sites of the copper atoms (Scheme 3.4). The formulation of the dinuclear metallo-macrocycles obtained with ligand **L1**, $[Cu_2(NO_3)_2(\mathbf{L1\text{-}CH_3})_2]$ (**3.12**), $[Cu_2Cl_2(\mathbf{L1\text{-}CH_3})_2(H_2O)]\cdot{}^1/_2CH_3OH\cdot 3^1/_2(H_2O)$ (**3.13**), and $[Cu_2(\mathbf{L1\text{-}CH_3})_2(CH_3OH)_2](ClO_4)_2\cdot H_2O\cdot ½CH_3OH$ (**3.14**), were all confirmed by elemental analysis, IR spectroscopy, and studied in solution by electrospray ionisation mass spectrometry (ES-MS).

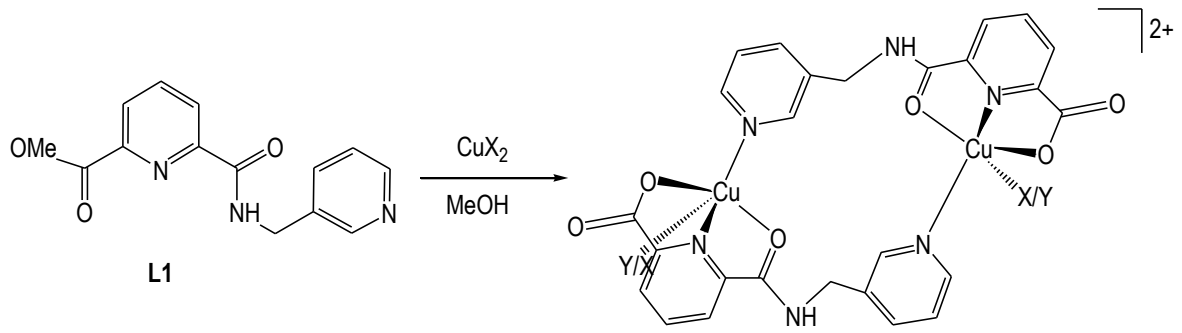

$[Cu_2(NO_3)_2(\mathbf{L1\text{-}CH_3})_2]$, X = NO_3 (**3.12**)
$[Cu_2Cl_2(\mathbf{L1\text{-}CH_3})_2(H_2O)]\cdot½CH_3OH\cdot3½(H_2O)$, X = Cl (**3.13**)
$[Cu_2(\mathbf{L1\text{-}CH_3})_2(CH_3OH)_2](ClO_4)_2\cdot H_2O\cdot ½CH_3OH$, Y = CH_3OH (**3.14**)

Scheme 3.4. The synthesis of cleft-like metallo-macrocyclic complexes derived from **L1**.

An investigation into the formation of these metallo-macrocyclic complexes in solution by ES-MS was attempted. The crystals of complexes **3.12**, **3.13** and **3.14** were dissolved in the minimum amount of DMSO solution (typically about 100 μL), diluted in methanol and analysed using ES-MS. During this investigation, peaks at *m*/*z* 699.8, 701.8 and 703.8, which correspond to the species $[Cu_2(NO_3)(\mathbf{L1\text{-}CH_3})_2]^+$ ($[M\text{-}(NO_3)]^+$) were identified. Similar peaks were not observed for complex **3.14**, although a peak corresponding to the **3.14** with an additional water ligand was identified. No peaks consistent with the formation of **3.13** could be observed, possibly linked with the inability to easily ionise this compound, which would require displacement of a chloride ligand. To further investigate the behaviour of these metallo-macrocycles in solution, the reaction mixture was analysed shortly after mixing the metal salt and ligand. Freshly prepared methanol solutions of the reaction mixture were analysed by ES-MS and electron impact mass spectrometry (EI-MS) analysis for comparison. Both techniques failed to give evidence for the metallo-macrocycles in freshly prepared solutions and still revealed the presence of non-hydrolysed ester, i.e. **L1**.

The IR spectra of these discrete complexes showed several characteristic strong stretching bands, such as a C=O stretch at approximately 1650 cm^{-1} and and O-H stretch in the range 3300-3100 cm^{-1}. The strong stretching bands for all three complexes in the range 1418 -1436 cm^{-1} correspond to the C=N stretch. In the case of complexes **3.12** and **3.14**, distinctive infrared stretches were observed for the N-O stretch in the nitrate anion at 1383 cm^{-1} and Cl-O stretch of the perchlorate anion at 1086 cm^{-1}.

Crystal structures of **3.12**, **3.13** and **3.14**

Crystal structures of **3.12** to **3.14** revealed the dinuclear metallo-macrocycles to have closely related structures, which are chiral in the solid-state. This chirality arises due to the bowl-shaped structures of these compounds whereby the unsymmetrical nature of the ligand means these species can either be arranged in a clockwise (Figure 3.8(a)) or anticlockwise manner (Figure 3.8(b)). Thus, while individual metallo-macrocycles are chiral, the bulk sample is a racemic mixture and it is likely that in solution the complexes are able to interconvert by inversion of the bowl or dissociation.

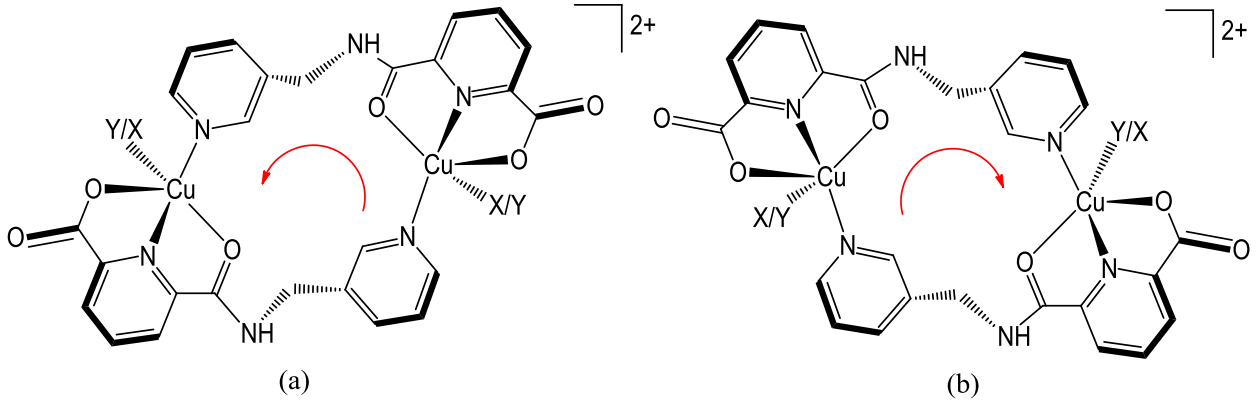

Figure 3.8. The (a) anticlockwise and (b) clockwise arrangement of the ligand **L1** in the metallo-macrocyclic structures **3.12** – **3.14**.

The three dinuclear metallo-macrocycles that were crystallised are structurally similar in the solid-state with the only major distinguishing features being the type of the ligand in the axial coordination sites of the copper centre and the conformation of the metallo-macrocycle. This conformation varies from the pinched cleft in **3.14** to a more open cavity in **3.12**. The axial ligands are bridging μ_2-nitrate anions in **3.12**, chloride anions in **3.13** (and a single water ligand) and methanol ligands in **3.14**. Related supramolecular clefts or clips[233-236] or shallow bowl-like structures[237-242] are well known in the literature whereby assembly of flexible ligands or metals with malleable coordination geometries (i.e. with silver(I), copper(I)) leads to the self-assembly of cleft- or bowl-like structures. Organic molecules, like CTV[243,244] and related metallo-supramolecular derivatives,[187,229,243-246] also have cleft and bowl-shaped structures that can act as hosts for neutral and anionic guests.

Crystal structure of **3.12**

$[Cu_2(NO_3)_2(L1\text{-}CH_3)_2]$. As outlined above, slow addition of $Cu(NO_3)_2 \cdot 2½H_2O$ to a solution of **L1** in methanol resulted in the immediate development of a deep blue colour indicating the formation of a Cu(II) complex. Crystals were obtained in 34% yield by slow evaporation of a methanol solution of the complex. The complex $[Cu_2(NO_3)_2(\mathbf{L1\text{-}CH_3})_2]$ crystallises in the orthorhombic space group *Pbcn*, with the bowl-shaped structure outlined earlier. Both enantiomers of the metallo-macrocycle are present in this particular structure. The asymmetric unit of this bowl-shaped dimer comprises one hydrolysed carboxylate form of **L1** (referred to as **L1-CH$_3$**), one copper atom, and one coordinated nitrate (Figure 3.9).

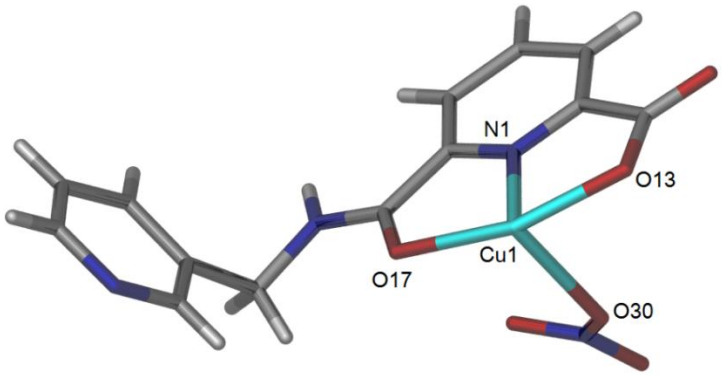

Figure 3.9. A perspective view of the asymmetric unit of complex **3.12.** Selected bond lengths (Å) and angles (°) : Cu(1)-N(1) 1.898(2), Cu(1)-O(13) 2.019(1), Cu(1)-O(17) 2.087(1), Cu(1)-O(30) 2.386(2), N(1)-Cu(1)-O(17) 79.37(7), N(1)-Cu(1)-O(13) 81.50 (7) and O(13)-Cu(1)-O(30) 81.66(6).

Compound **L1-CH$_3$** is coordinated to the Cu(II) centre via three donor atoms, the nitrogen from the 2,6-pyridine core (Cu1-N1 1.898(2) Å), the carboxylate oxygen (Cu1-O13 2.019(1) Å), and the carbonyl oxygen of the amide (Cu1-O17 2.087(1) Å). The Cu1-N1 distance is short, a feature commonly observed for this chelating motif due to the necessity to complex the carboxylate and carbonyl oxygen atoms. Common Cu-N distance reported for the related compounds is in the range of 1.90 – 2.10 Å.[109] The bowl-shaped dimer is formed by coordination of the copper to the nitrogen of a pyridyl ring of a second ligand (Figure 3.10(a)). To complete

the coordination environment a nitrate anion binds to one axial coordination site, located on the outer face of the cleft structure (Figure 3.10(b)) and within the crystal structure, a second nitrate anion from another metallomacrocycle coordinates the other axial site. The Cu-ONO_2 bond length is 2.553(2) Å. The -CH_2- linker of **L1** acts as a hinge to allow the dimeric macrocycles to flex and generate the cleft-like structure. The cleft is relatively open with a Cu-Cu distance of 7.094 Å but within the crystal this is filled by anions from two nearby metallomacrocycles. In the crystal packing, other bowl-shaped macrocycles stack face-to-face within the cavity of an adjacent bowl structure limiting the access of other guests (solvent, anions) to the cavity.

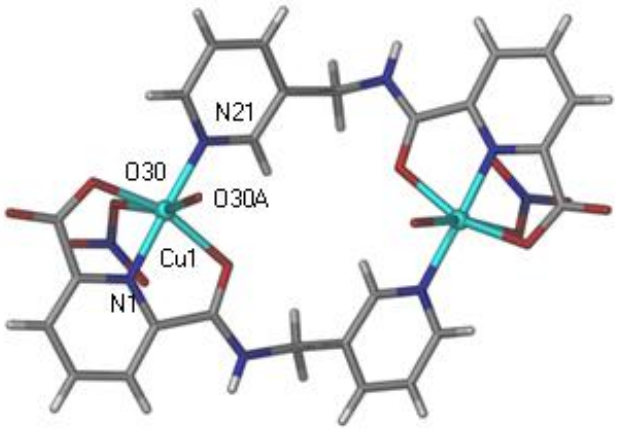

(a)

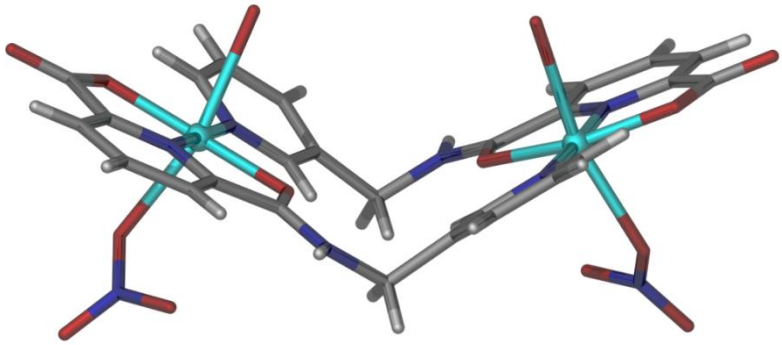

(b)

Figure 3.10. A perspective view of the cleft-shaped structure of complex [$Cu_2(NO_3)_2$(**L1-CH_3**)$_2$], (**3.12**) from (a) the top and (b) the side, with the oxygen atoms of the bridging nitrate anions from two adjacent metallo-macrocycles shown in the cleft.

In the crystal packing of **3.12** the cleft-shaped macrocycles are connected by bridging nitrate anions to form a 2-D sheet in the *ab* plane (Figure 3.11(a)). Adjacent sheets are packed with the interior of the cleft in the opposing direction and interdigitated with face-to-face π-stacking interactions between the sheets such that each macrocycle within a sheet overlaps with macrocycles in two other layers (Figure 3.11(b)). The offset face-to-face packing places two macrocycles within the cavity of each dinuclear structure and thus precludes the inclusion of any guest molecules (aside from the bridging anions) into the cleft in this particular solid-state structure.

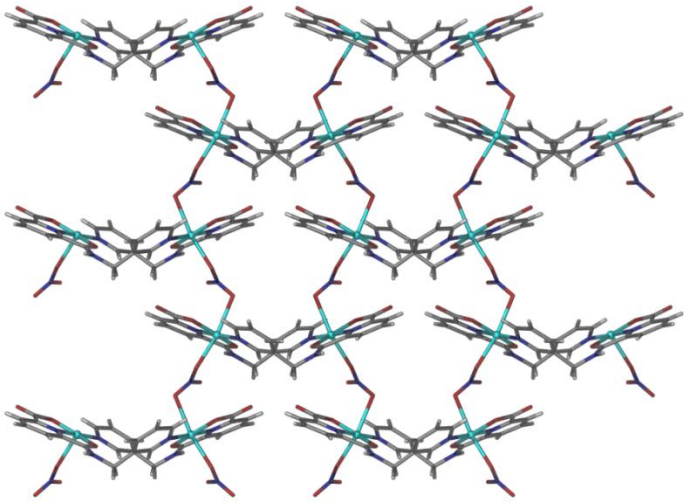

(a)

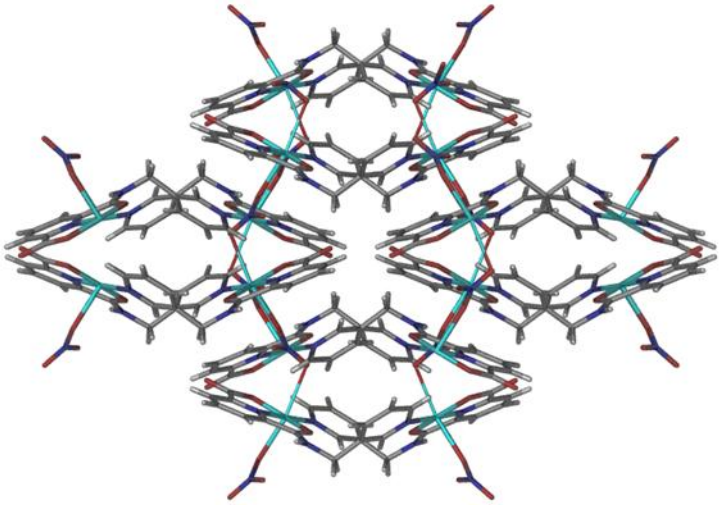

(b)

Figure 3.11. A perspective view of (a) the extended structure of complex **3.12**. (b) The face-to-face packing arrangement between adjacent 2-D sheets of molecules of **3.12** viewed along *a* axis.

Crystal structure of **3.13**

$[Cu_2Cl_2(L1\text{-}CH_3)_2(H_2O)]\cdot{}^1/_2CH_3OH\cdot3^1/_2(H_2O)$. In much the same manner as reported for **3.12**, reaction of ligand **L1** with $CuCl_2\cdot2H_2O$ resulted in the formation of sky-blue diamond-shaped crystals of $[Cu_2Cl_2(\mathbf{L1\text{-}CH_3})_2(H_2O)]\cdot{}^1/_2CH_3OH\cdot3^1/_2(H_2O)$. Complex **3.13** crystallises in the chiral monoclinic space group $P2_1$ to reveal a very similar type of cleft-like complex. The asymmetric unit of this structure comprises two copper atoms, two molecules of the carboxylate form of **L1**, two coordinated chlorine atoms, one coordinated water molecule, and a partially occupied non-coordinated methanol (or water solvate) (Figure 3.12).

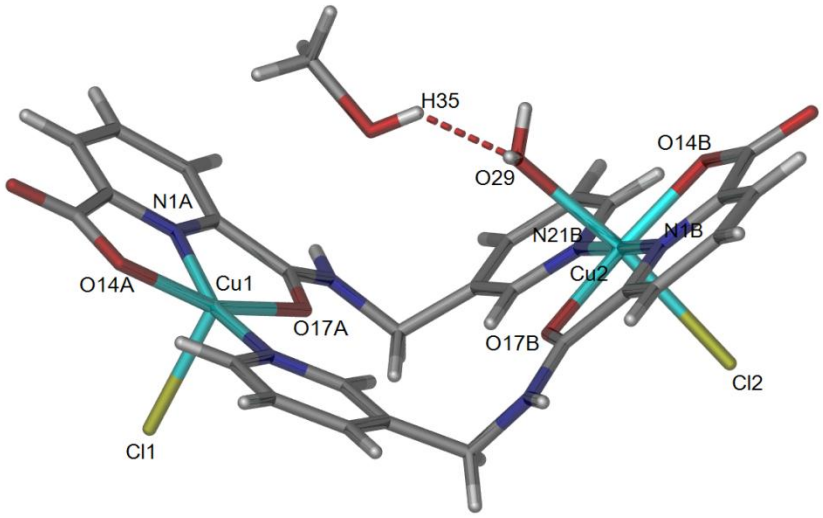

Figure 3.12. A perspective view of the asymmetric unit of complex **3.13** with the methanol solvate molecule. Selected bond lengths (Å) and angles (°) : Cu(1)-N(1A) 1.959(2), Cu(2)-N(1B) 1.917(2), Cu(1)-N(21A) 1.948(2), Cu(2)-N(21B) 1.965(2), Cu(1)-O(17A) 2.058(1), Cu(1)-O(14A) 2.014(2), Cu(2)-O(17B) 2.097(1), Cu(2)-O(14B) 2.038(2),Cu(1)-Cl(1) 2.4717(7), Cu(2)-Cl(2) 2.702(7), N(1A)-Cu(1)-O(17A) 79.59(8), N(1A)-Cu(1)-O(14A) 80.66 (7), N(1B)-Cu(2)-O(17B) 79.09(7) and N1B(1)-Cu(2)-O(14B) 80.81(6).

This complex adopts an almost identical conformation about the -CH_2- hinge to complex **3.12** (Cu-Cu distance of 6.912 Å, compared to 7.094 Å), but the coordination environment of the one of the copper(II) centres is different to the previous copper nitrate structure. A water molecule is coordinated to one of the copper atoms in an axial coordination site and as a consequence, the copper atoms have two different coordination environments – square pyramidal (τ = 0.07)[247] and octahedral. As a consequence, the cavity of this complex is occupied by a coordinated water molecule and a non-coordinated methanol solvate, which is hydrogen bonded to the water molecule in the solid-state. Two oxygen atoms, from carboxylate and carbonyl amide groups, coordinate to the copper atom with bond lengths of 2.014(2) Å and 2.097(1) Å respectively. A slightly different arrangement of the metallomacrocycles observed in the packing of **3.13**. The molecular packing showed that this complex is arranged down the *ac* diagonal with the methanol and water molecules included in the channels. To accommodate the non-coordinated methanol and water solvate molecules, and the coordinated water ligand in **3.13** there is slightly less overlap between the face-to-face packed metallo-macrocycles.(Figure 3.13).

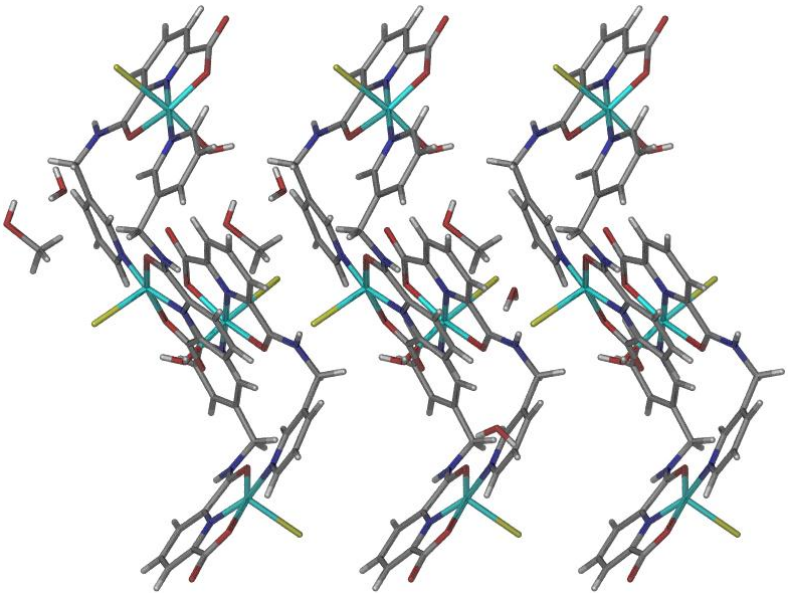

Figure 3.13. Crystal packing of **3.13** when viewed from the *ab* plane.

Crystal structure of **3.14**

$[Cu_2(L1\text{-}CH_3)_2(CH_3OH)_2](ClO_4)_2 \cdot H_2O \cdot ½CH_3OH$. Slow evaporation of a methanol solution of **L1** and $Cu(ClO_4)_2 \cdot 6H_2O$ led to the isolation of blue crystals of another bowl-shaped complex. This complex crystallises in monoclinic space group *C*2. There are two subtly different types of metallo-macrocycle in the structure; consequently the asymmetric unit contains two independent half molecules of **3.14**. The asymmetric unit contains two independent copper positions, two molecules of the hydrolysed carboxylate form of **L1**, and each copper(II) centre is coordinated by a methanol molecules (Figure 3.14). There are also three independent non-coordinated perchlorate positions in each asymmetric unit, two with 50% occupancy. The encapsulated perchlorate anions appear to have a slightly flattened tetrahedral geometry (O-Cl-O angles in the range 101.57(14) – 106.81(18)°) due to a poor fit within the cavity and slight disorder.

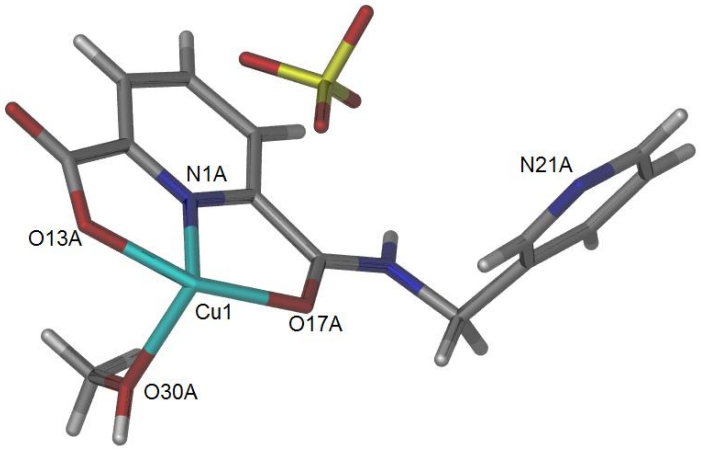

Figure 3.14. A perspective view of one of the half molecules in the asymmetric unit of complex **3.14**. Selected bond lengths (Å) and angles (°): Cu(1)-N(1A) 1.917(6), Cu(1)-O(13A) 2.010(5), Cu(1)-O(17A) 2.034(5), N(1A)-Cu(1)-O(17A) 80.30(2), N(1A)-Cu(1)-O(13A) 80.52(2) and N(1A)-Cu(1)-O(30A) 98.6 (2). The other molecule has bond lengths (Å) and angles (°): Cu(2)-N(1B) 1.908(2), Cu(2)-O(13B) 2.020(6), Cu(2)-O(17B) 2.027(5), N(1B)-Cu(2)-O(17B) 80.00(2), N(1B)-Cu(2)-O(13B) 81.10(3) and N(1B)-Cu(2)-O(30B) 98.4 (3).

In the crystal structure each metallo-macrocycle has very subtle differences in the bond lengths and angles about the copper centres. In one structure the two oxygen atoms from carboxylate and carbonyl amide groups coordinate to the copper atom with bond lengths of 2.010(5) and 2.038(5) Å, respectively. This compares with 2.010(5) and 2.034(5) Å in the other metallo-macrocycle. The Cu1-N1 distance of these complexes are 1.908(2) and 1.917(6) Å, which are slightly longer compared to the Cu-N distance (Cu1-N1 = 1.898(2) Å) in complex **3.12**. However, this distance is slightly shorter compared to the Cu-N distance (Cu1-N1 = 1.959(2) Å) of complex **3.13**. The major distinction between the two dinuclear species appears to be Cu-Cu separation; in one complex the distance is 6.444 Å while in the second the distance is 6.586 Å indicating that these clefts can be enlarged and contracted. This is more evident when one compares these values for the Cu-Cu separation to those obtained for **3.12** and **3.14** (7.094 and 6.912 Å, respectively). This is in spite of each copper centre being displaced from the mean plane of the four donors in the square plane (bond angles of *ca*. 162°) to facilitate the closing of the cleft.

In contrast to the 'empty' cleft in **3.12** and the solvent included cleft in complex **3.13**, the cleft of compound **3.14** is occupied by a non-coordinated perchlorate anion located in the cavity of the bowl-shaped structure (Figure 3.15). Additionally, the cleft is compressed to produce a tighter fit about the anion; as noted the Cu-Cu distances are *ca*. 0.5 Å shorter than those in complexes **3.12** and **3.13**. Despite the shorter distance the copper does not appear to be coordinated by the perchlorate. The shortest Cu-O contact is 3.55 Å and 3.66 Å longer than the combined van der Waals radii of Cu and O. However, it appears that the cleft pinches to allow anion-π contacts with the electron deficient 2,6-disubstituted pyridine ring of **L1-CH$_3$**.The shortest contact, between the C2 of the central pyridine ring is 3.03 Å from the oxygen of the encapsulated perchlorate anion in one structure and 2.95 Å in the second structure, within the van der Waals radii of C and O of 3.22 Å. These distances are comparable to such interactions previously reported in the literature.[248,249] The presence of perchlorate anion with the cleft of **3.14** hints at potentially interesting anion binding ability for these bowl-shaped structures.

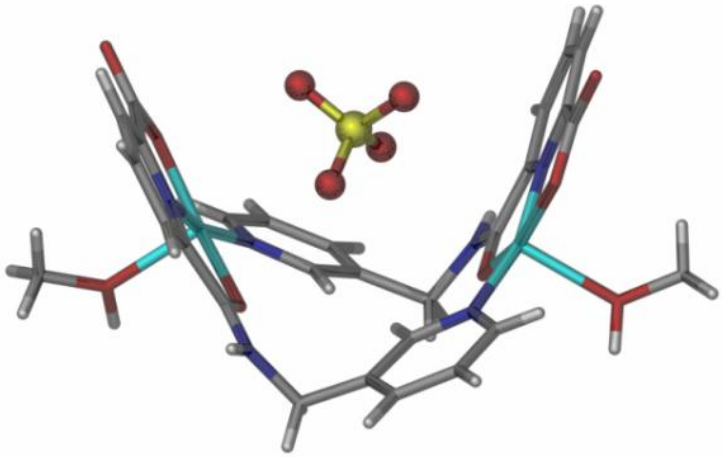

Figure 3.15. A perspective view of the more sharply folded bowl-shaped structure of complex **3.14** with perchlorate anions in the bowl cavity.

As there are no bridging anions, or solvent molecules within the structures, the discrete metallomacrocycles are simply interdigitated in a face-to-face manner. In **3.13** there is overlap between metallo-macrocycles in the crystal packing but in **3.14** this is limited due to a more tightly folded cavity which envelopes the perchlorate anion guest (Figure 3.16).

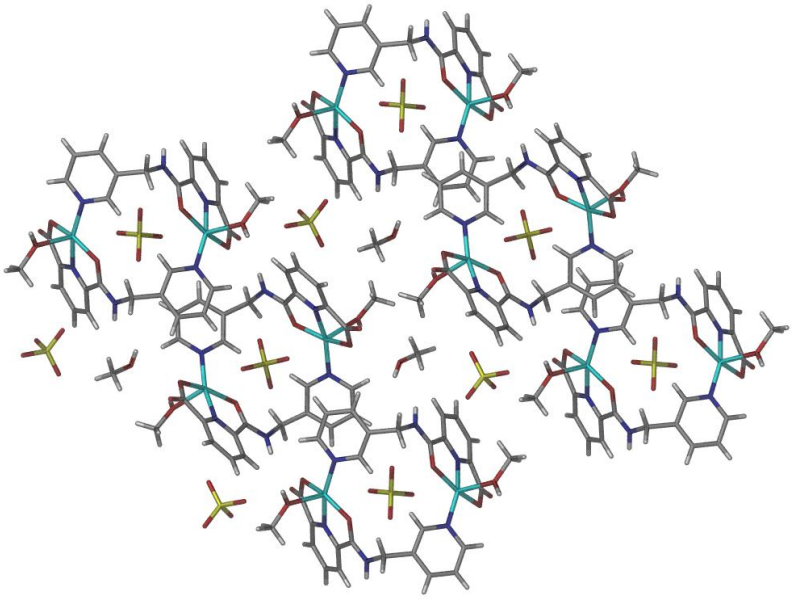

Figure 3.16. Crystal packing of complex **3.14** when viewed along *ac* axis.

3.3.2. Synthesis of dinuclear metallo-macrocycles of L3

The less flexible analogue of **L1**, compound **L3**, also forms dinuclear metallo-macrocycles and the synthesis and structure of these compounds are discussed here. In the rigid ligands, the methyl spacer adjacent to the amide nitrogen has been removed; therefore a planar or more open metallo-macrocycle could be expected. As a consequence of the planarity in the structure, these metallo-macrocycles are not chiral. In a similar manner to studies on **L1**, CuX_2 metal salts (X = NO_3, ClO_4) were reacted with **L3** in 1:2 metal-to-ligand ratio in methanol to give light green/blue solutions. Once again, these solutions were heated for approximately 45 minutes and kept at room temperature for crystallisation. Crystals of two further dinuclear metallo-macrocycles were obtained, that crystallise as a trimeric aggregate $[Cu_6(NO_3)_2(\mathbf{L3\text{-}CH_3})_6(H_2O)_6](NO_3)_4{\cdot}2CH_3OH$ (**3.15t**) and a discrete complex $[Cu_2(\mathbf{L3\text{-}CH_3})_2(ClO_4)_2(H_2O)_2]_2$ (**3.16**) with two crystallographically independent molecules in the unit cell, respectively (Scheme 3.5). Other reactions with other copper(II) salts and cadmium(II) salts gave oils which could not be isolated as solids, crystalline or otherwise, despite several attempts and a multitude of different conditions, such as variation in the stoichiometry, solvent and crystallisation technique.

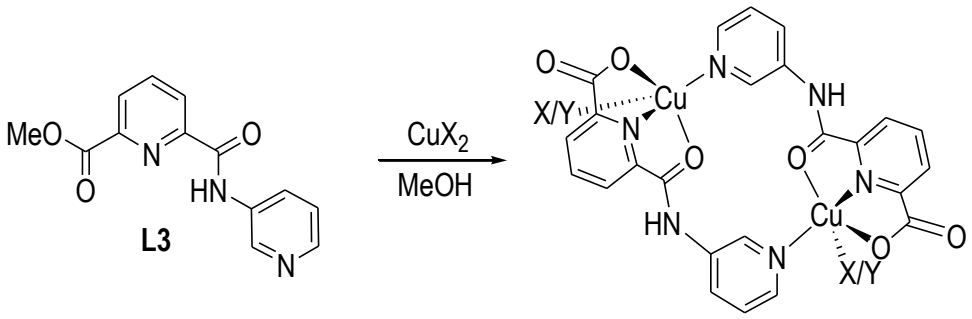

$[Cu_2(NO_3)_2(\mathbf{L3\text{-}CH_3})_2(H_2O)_2](NO_3)$ X=NO_3 and Y = H_2O (**3.15**)
$[Cu_2(\mathbf{L3\text{-}CH_3})_2(ClO_4)_2(H_2O)_2]_2$ X=ClO_4 and Y = H_2O (**3.16**)

Scheme 3.5. The synthesis of planar metallo-macrocyclic complexes derived from **L3**.

While these reactions reproducibly provide the dinuclear metallo-macrocycles and the structures are supported by elemental analysis, mass spectrometry, and distinctive stretching bands in the infrared (N-O, 1383 cm^{-1} and Cl-O, 1122 cm^{-1}), the bulk material sometimes appears to be contaminated with byproducts. These are anticipated to arise from complete decomposition of the ligand, namely amide hydrolysis (in addition to the ester hydrolysis required to form the complexes). This is not unknown for amide ligands of this type and there are several examples of amide ligands that do not form complexes of the intact amide due to hydrolysis. In the case of **L3**, these contaminants are occasionally visible in the bulk sample and observed as inconsistent elemental analyses. Attempts to pick mainly crystalline material does improve the fit of calculated and found elemental analysis data but the reaction byproducts could never be completely removed from the isolated product. The formation of complexes **3.15** and **3.16** was again studied by ES-MS. Crystals of complexes **3.15** and **3.16** were dissolved in minimum amount of DMSO, diluted in acetonitrile and analysed using ES-MS. For complex **3.6**, ions at m/z 672.9, 674.9 and 676.8 were observed, which correspond to the species $[(Cu_2(NO_3)(\mathbf{L3\text{-}CH_3})_2]^+$. Similarly, for complex **3.16**, ions corresponding to $[(Cu_2(ClO_4)(\mathbf{L3\text{-}CH_3})_2]^+$ were observed. In the case of the perchlorate salts of complex **3.16**, and owing to the ease with which the amide is deprotonated and the anion lost, a series of ions corresponding to $[(Cu(\mathbf{L3\text{-}CH_3}(-H))(\mathbf{L3\text{-}CH_3})]^+$ were also observed in the mass spectrum.

Crystal structure of **3.15t**

$[Cu_6(NO_3)_2(L3\text{-}CH_3)_6(H_2O)_6](NO_3)_4 \cdot 2CH_3OH$. Complex **3.15** crystallises in the monoclinic crystal system with space group $P2_1/c$ as a trimeric aggregate of the expected dinuclear metallo-macrocycle. The asymmetric unit of **3.15t** consists of three copper centres, three anionic forms of **L3-CH$_3$**, three coordinated water molecules, three non-coordinated nitrate anions and one molecule of non-coordinated methanol (Figure 3.17).

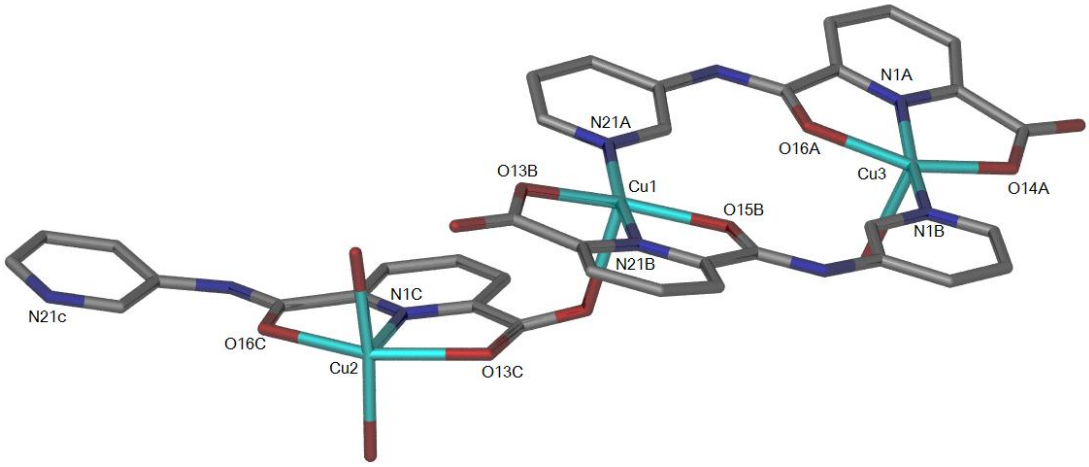

Figure 3.17. A perspective view of the asymmetric unit of complex **3.15t**, with hydrogen atoms, methanol and nitrate molecules omitted for clarity. Selected bond lengths (Å) and angles (°) : Cu(1)-N(21A) 1.967(3), Cu(1)-N(21B) 1.917(2), Cu(3)-N(1A) 1.911(3), Cu(3)-N(1B) 1.957(5), Cu(2)-N(1C) 1.991(3), Cu(1)-O(13B) 2.007(3), Cu(1)-O(15B) 2.086(2), Cu(3)-O(16A) 2.097(3), Cu(3)-O(14A) 1.993(5), Cu(2)-O(13C) 2.257, Cu(2)-O(16C) 2.372(3), N(21A)-Cu(1)-O(13B) 81.63 (2), N(21A)-Cu(1)-O(15B) 78.88 (2), N(1A)-Cu(3)-O(14A) 81.82(2), N(1A)-Cu(3)-O(16A) 78.51(2), N(1C)-Cu(2)-O(13C) 78.64(2), N(1C)-Cu(2)-O(16C) 73.86(2), O(13B)-Cu(1)-O(15B) 160.27 (2), O(16A)-Cu(3)-O(14A) 158.56(2), and O(16C)-Cu(2)-O(13C) 152.46 (3).

In contrast to the complexes described for **L1**, this metallo-macrocycle crystallised as a M_6L_6 aggregate (Figure 3.18). Within this aggregate all three metallomacrocycles are close to planar; the -CH_2- spacer that provides the 'hinge' in structures of **L1-CH$_3$** is absent and thus the macrocycles are locked into a near planar arrangement. The three copper atoms of the asymmetric unit have slightly different coordination environments. The copper centre on the end of the trimeric aggregate (Cu3) is five coordinate with a square-pyramidal geometry (τ = 0.17),

while the other two copper centres have a Jahn-Teller distorted octahedral coordination geometry. In the central macrocycle (Cu1), the octahedral environment is completed by the coordination of three donor atoms provided by the carboxamide moieties (with elongated bonds to the two O atoms of the ONO chelating motif), the N-pyridyl donor from other neighboring planar ligand and two water molecules. The third copper centre (Cu2) has the same four donors provide by the ligand to form the metallo-macrocycle but is coordinated in the axial positions by a carboxylate oxygen from the central metallo-macrocycle and a nitrate anion. The bond lengths between these donors and the three copper ions are in the range 1.910(3) to 2.467(3) Å.

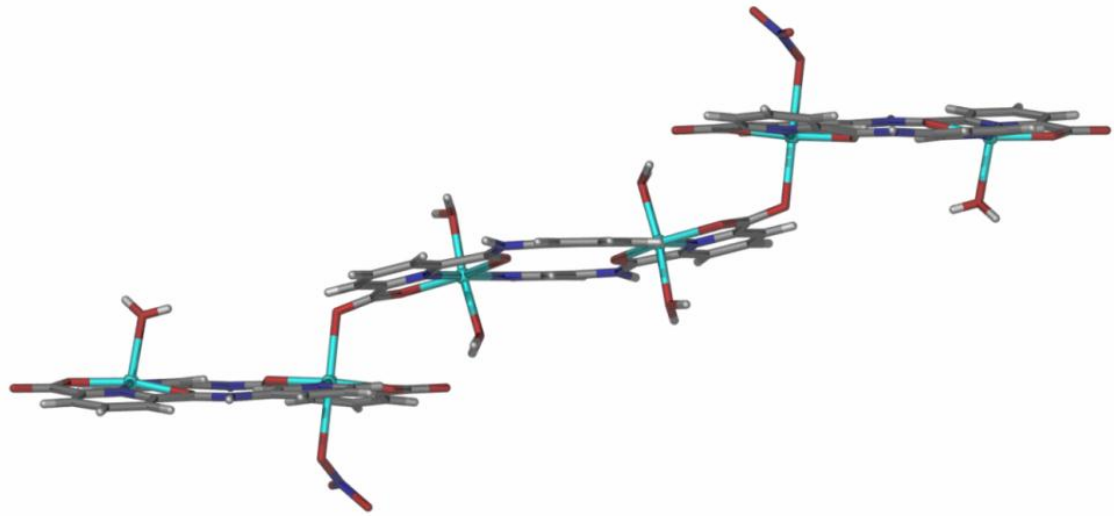

Figure 3.18. A perspective view of the hexameric aggregate in the crystal structure of complex **3.15**.

In crystal packing of this complex, each layer of the complex is connected by hydrogen bonding interactions from the coordinated water molecules and the carbonyl oxygen atoms from the amide moieties (O-H···O=C, d = 1.876 Å and D = 2.702 Å). The extensive hydrogen bonding interactions were mediated by nitrate anions which leads to the formation of a 3-D hydrogen bonded network within the crystal (Figure 3.19). These types of extended intermolecular hydrogen bonding interactions are not observed in the cleft-structures of complexes **3.12** to **3.14**.

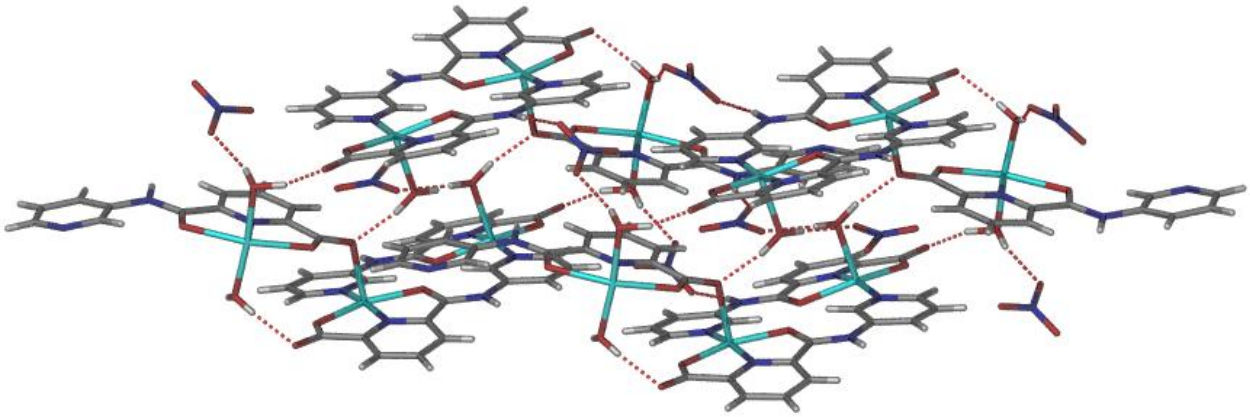

Figure 3.19. A perspective view of the intermolecular hydrogen bonding interactions of complex **3.15**.

Crystal structure of **3.16**

$[Cu_2(L3\text{-}CH_3)_2(ClO_4)_2(H_2O)_2]_2$. Complex **3.16** also crystallises in the monoclinic space group $P2_1/c$ but with two copper atoms, two anionic ligands (**L3-CH$_3$**), two coordinated water molecules and two weakly coordinated perchlorate molecules from two different dinuclear metallo-macrocycle in the asymmetric unit (Figure 3.20). The two independent half molecules are located on independent inversion centres. Once again the metallo-macrocycle is close to planar with a slight puckering of the structure to allow coordination. In the crystal structure each metallo-macrocycle has very subtle differences in the bond lengths and angles about the copper centres.

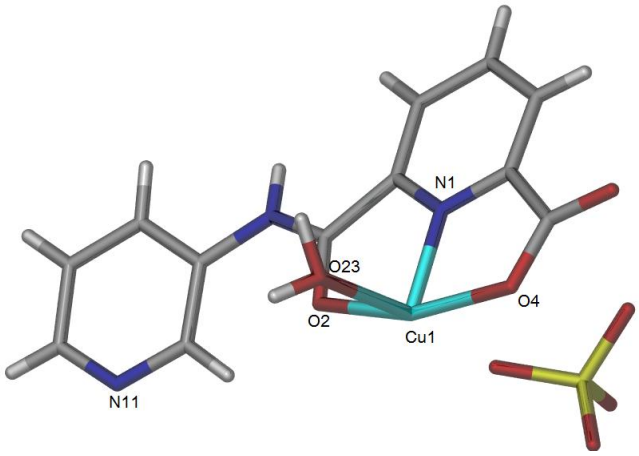

Figure 3.20. A view of asymmetric unit of complex **3.16** with only one structure of the molecules shown for clarity. Selected bond lengths (Å) and angles (°): Cu(1)-N(1A), 1.913(2), Cu(1)-O(4)

1.996(3), Cu(1)-O(23) 2.305(2), Cu(1)-O(2) 2.102(3), N(1)-Cu(1)-O(4) 76.33 (2), N(1)-Cu(1)-O(2) 83.58 (2) and N(1)-Cu(1)-O(4) 76.33(3). The other molecule has bond lengths (Å) and angles (°): Cu(2)-N(1B) 1.905(2), Cu(2)-O(13B) 2.004(2) Cu(2)-O(17B) 2.038(6), (2), N(1B)-Cu(2)-O(13B) 76.80(2) and N(1B)-Cu(2)-O(17B) 82.47(3).

The copper atoms in **3.16** adopt Jahn-Teller distorted octahedral geometries with all of three donors (O, N, O,) from one molecule of **L3-CH$_3$** and the pyridine nitrogen donor of another in the equatorial positions, and a water molecule and the weakly coordinated perchlorate anion in the axial sites (Figure 3.21(a) and Figure 3.21(b)). Compound **3.16** appears ideally placed as a tecton for self-assembly into higher order structures by exchange of the axially bound water ligand and perchlorate anion. There are no further interactions indicated in the crystal packing of **3.16** instead of a very weak hydrogen bonding interaction between the perchlorate anions and one of the hydrogen atoms from the water molecules.

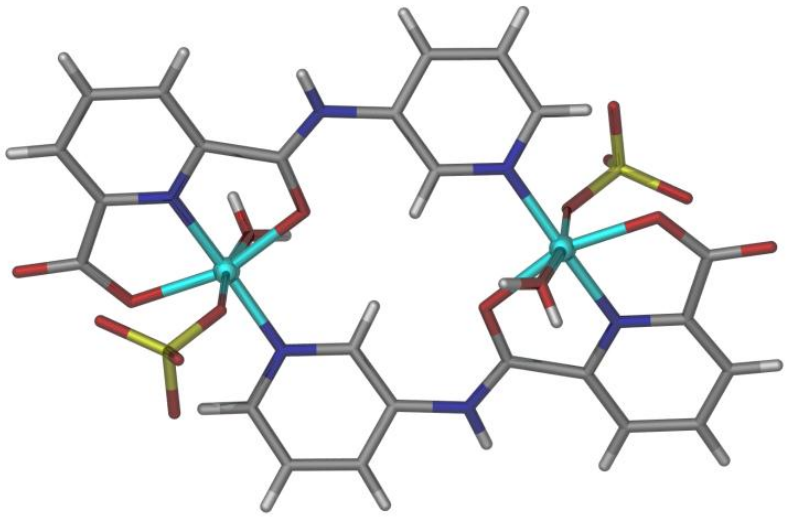

(a)

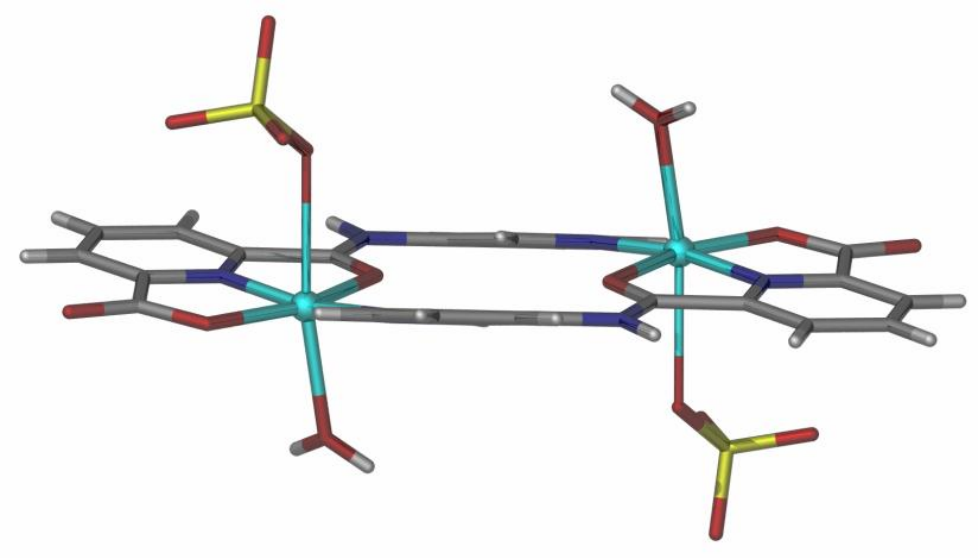

(b)

Figure 3.21. Perspective views of one of the dimetallomacrocycles formed from copper perchlorate and **L3-CH$_3$**. (a) A top view of the structure of **3.16** and (b) a view along the plane of the pendant pyridyl rings that reveals the slight twisting or puckering of the structure.

The crystal structure of each metallo-macrocycle (**3.12** – **3.16)** have very subtle differences in the bond lengths and angles about the copper centres. The bond lengths and angles indicated for complexes **3.12** – **3.14** are compared with the literature compounds, [Co(**3.9**)$_2$] and [Cu$_2$(**3.10**)$_2$(OH$_2$)$_2$] reported by Lawrance[166] (Table 3.1). The copper atom in the literature compound has a distorted square pyramidal geometry coordinated by ligand *N*-6-[(2-pyridylmethylamino)carbonyl]-pyridine-2-carboxylic acid (**L**) *via* its N, N, N tridentate motif. The fourth oxygen donor is coordinated to the other copper atom to form a dinuclear metallo-macrocyclic complex similar to those observed in this work.

Conversely, the copper ions in complexes **3.12** – **3.16** adopt distorted octahedral geometries coordinated by three donors (O, N, O,) from one molecule of the convergent ligands and the pyridine nitrogen donor of another in the equatorial positions. The axial positions of these molecules are coordinated by solvent or anion molecules to complete the octahedral environment. The major differences between these metallo-macrocycles are the Cu-Cu separation and the cleft structures of the compounds. Compounds **3.12** and **3.13** have wider cavities compared to **3.14**, with Cu-Cu distances 7.094 and 6.912 Å. This is *ca*. 0.5 Å longer than those in complex **3.14**

(Cu-Cu distances = 6.444 and 6.578 Å). These compare with the Cu-Cu distances in $[Cu_2(\mathbf{3.10})_2(OH_2)_2]$, reported by Lawrance,[166] which is noticeably shorter at 5.2739(7) Å. However, in the compound reported by Lawrance, the bond distance to the copper is longer for N1 (by *ca.* 0.13 Å) compared to the dinuclear complexes described in this study. It is also noted that cobalt complex has Co-N distances which are slightly longer compared to the Cu-N distances in complexes **3.12, 3.13** and **3.14.**

Table 3.1. Distances [Å] and angles [◦] around the metal ions in complexes with the flexible ligands. The structures of the literature compounds $[Co(\mathbf{3.9})_2]$ and $[Cu_2(\mathbf{3.10})_2(OH_2)_2]$ are shown in Figure 3.4.

Bonds and angles[a]	$[Co(\mathbf{3.9})_2]$ (N, N, N)	$[Cu_2(\mathbf{3.10})_2(OH_2)_2]$ (N, N, N)	**3.12** (O,N,O)	**3.13** (O,N,O)	**3.14** (O,N,O)
Cu-Cu		5.2739(7)	7.094	6.912	6.444 6.586
M-N_1	1.985(6)	2.0568(16)	1.898(2)	1.959(2) 1.948(2)	1.917(6) 1.908(2)
M-N_2	1.867(7)	1.9202(17)			
M-N_3	1.985(6)	2.0174(17)			
Cu-O_1		2.2591(16)	2.019(1)	2.058(1) 2.097(1)	2.010(5) 2.020(6)
Cu-O_2			2.087(1)	2.014(2) 2.038(2)	2.034(5) 2.027(5)
O_1-Cu-N_1			79.09	79.59(8)	80.52(2)
N_1-Cu-O_2			81.50	80.66 (7) 79.09(7)	80.34(2) 80.00(2)
N_1-M-N_2	82.0(3)	81.87(7)			
N_2-M-N_3	84.6(3)	81.94(7)			

[a] Guide to numbering used in Table 3.1.

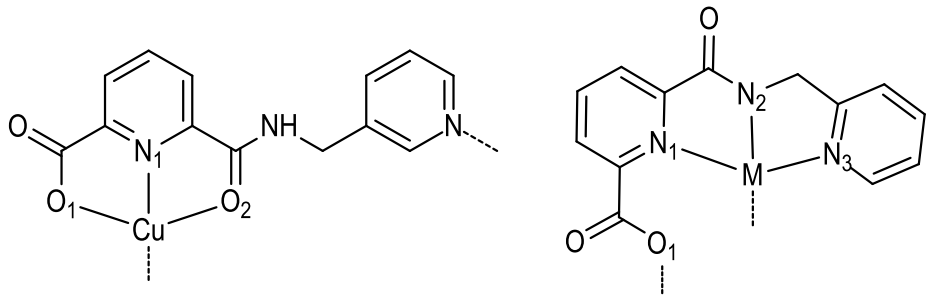

Unlike **3.12**, **3.13** and the literature compound **3.10**, the cleft of compound **3.14** is occupied by a non-coordinated perchlorate anion located in the cavity of the bowl-shaped structure. This anion inclusion is stabilised by anion-π interactions from the 2,6-disubstituted pyridine ring of **L1-CH$_3$** and may be able to be exploited for selective anion binding. In contrast to the metallo-macrocycles derived from **L1,** the metallo-macrocycles derived from **L3** are near planar due to the absence of the -CH_2- spacer that provides the 'hinge' in structures of **L1-CH$_3$**. X-ray crystallography reveals that these macrocycles have planar arrangement in the solid-state. Complex **3.15** was obtained as a trimeric aggregate while complex **3.16** was obtained as a discrete metallo-macrocycle. The axial positions of these complexes are bound by weak ligands, which may enable these molecules to be used as a tecton for self-assembly into higher order structures.

3.4. Synthesis of coordination polymers of L1 and L2

A unique feature of the coordination chemistry of the flexible monoamide ligands **L1** and **L2** is their ability to form a dinuclear metallo-macrocyclic structural motif [M_2L_2] that is observed in both discrete complexes and in coordination polymers. The formations of dinuclear and trinuclear metal clusters linked by these metallo-macrocyclic structural motifs results in 1-D and 2-D coordination polymers, respectively. In this section of the thesis, the propensity of compound **L2** to form various coordination polymers based on the dinuclear metallo-macrocylic building blocks will be discussed. The two 2-D coordination polymers obtained with **L2** were prepared from solvothermal approaches.

3.4.1. Synthesis of coordination polymers of L1

The only coordination polymer of **L1** isolated in this work was obtained from the reaction of **L1** with cadmium nitrate. This reaction yielded colourless crystals of a 1-D coordination polymer $\{[Cd(\mathbf{L1\text{-}CH_3})(H_2O)(\mu_2\text{-}H_2O)](NO_3)\cdot{}^1/_4H_2O\}_n$ (**3.17**). This structure, determined by single crystal X-ray crystallography, differs markedly from other complexes described in this chapter by showing no coordination by the pendant pyridyl group. A strong characteristic N-O stretch was found at 1377 cm^{-1} in the IR spectrum of this complex, confirming the presence of the nitrate anion.

Crystal structure of **3.17**

$\{[Cd(L1\text{-}CH_3)(H_2O)(\mu_2\text{-}H_2O)](NO_3)\cdot{}^1/_4H_2O\}_n$. Complex **3.17** crystallises in the triclinic space group *P*-1, with an asymmetric unit that comprises one molecule of carboxylate form of **L1**, one cadmium atom, one non-coordinated nitrate and two coordinated water molecules (Figure 3.22). The Cd1-N1 bond distance is 2.352(2) Å, which is in the range for typical Cd-N bonds reported in the literature (*vide infra*).[347]

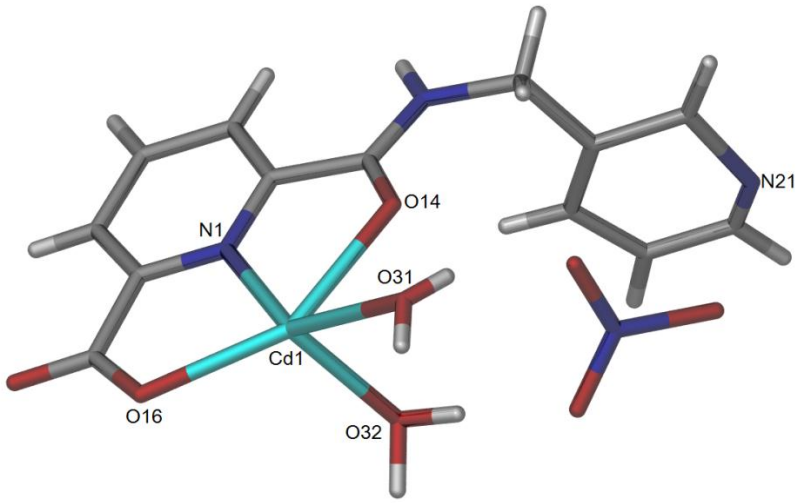

Figure 3.22. A perspective view of the asymmetric unit of complex **3.17**. Selected bond lengths (Å) and angles (°) : Cd(1)-N(1) 2.352(2), Cd(1)-O(14) 2.425(3), Cd(1)-O(16) 2.390(3), Cd(1)-O(31) 2.361(2), N(1)-Cd(1)-O(14) 67.11(2) and N(1)-Cd(1)-O(16) 68.55(3).

Unlike the structures described in the following section, compound **3.17** is a coordination polymer constructed from Cd_2L_2 dimers that are only bridged by μ_2-H_2O ligand; none of the molecules of **L1** utilise their pendant pyridyl group to bridge metal centres or clusters (Figure 3.23). As is observed throughout this work, the ester has been hydrolysed during the synthesis and the ligand chelates using the O, N, O chelating motif of the pyridine carboxamide moiety. The carboxylate oxygen bridges to a second cadmium centre to form a dimer and these dimers are then assembled into 1-D chains that extend down the *a*-axis by two μ_2-H_2O ligands. A water ligand completes the coordination sphere of each cadmium(II) centre. The non-coordinated pendant pyridine is disordered over two positions with approximately 50% occupancy of each site (only one position is shown in Figure 3.23).

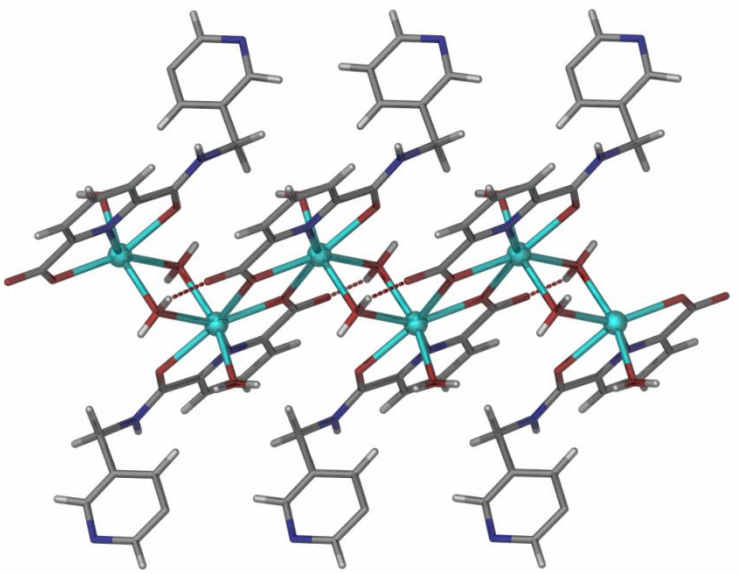

Figure 3.23. An image of the 1-D coordination polymer formed from Cd(II) and **L1-CH$_3$**. The anions, water solvate molecules and the disorder of the non-coordinated pendant pyridine ring are not shown for clarity.

The 1-D coordination polymers in **3.17** are packed within the crystal in an intricate 3-D hydrogen bonding network involving the non-coordinated water solvate molecule, the non-coordinated anion, and the pendant pyridine, amide NH, and coordinated water ligands of the polymer (Figure 3.24). Along the *b*-axis the 1-D polymers are hydrogen bonded to adjacent

polymers through the non-coordinated nitrate anion and water molecules, while packing along the *c*-axis is mediated by a water molecule. The hydrogen bonding interactions involving the carbonyl oxygen donor and coordinated water molecule have d = 1.902 Å and D = 2.048 Å, while the hydrogen bond distances between the nitrate anions and the coordinated water molecule are typical for moderately strong hydrogen bonds, $d_{O\text{-}H\cdots O}$ = 1.725 and 1.831 Å, respectively.

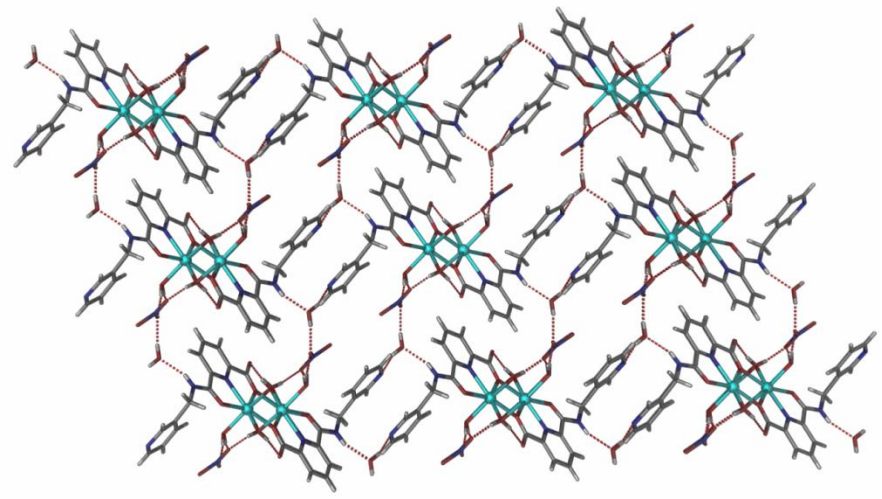

Figure 3.24. A view of the 3-D hydrogen bonding network in **3.17** viewed down the *a*-axis.

3.4.2. Synthesis of coordination polymers of L2

L2 was also reacted with a series of metal ions. In a similar manner to studies on **L1**, copper(II) (CuX_2, where X = Cl, NO_3, OAc, ClO_4, BF_4; and $CuSO_4$), zinc(II) (ZnX_2, where X = OAc, ClO_4), and cadmium(II) (CdX_2, where X = NO_3, and $CdSO_4$) metal salts were reacted with **L2** in 1:2 metal-to-ligand ratio in methanol. In the case of copper(II) perchlorate, blue crystals of a material with the formula $\{[Cu_3(\mathbf{L2\text{-}CH_3})_3(\mathbf{L2})_2(H_2O)_2(CH_3OH)](ClO_4)_3\}_n$ (**3.18**) were obtained from slow evaporation approaches. A solvothermal approach, using DMF reaction was also used successfully for reactions of **L2** with copper acetate and cadmium nitrate. X-ray crystallography revealed that the reaction of **L2** with copper(II) perchlorate had yielded in a 1-D coordination polymer but the reaction failed to reliably reproduce this material and an analytically pure sample could not be obtained for further analysis. This could be related to the presence of a mixture of hydrolysed and intact **L2** in the product which requires crystallisation to be linked to hydrolysis rates. The IR spectra of this complex showed a strong Cl-O stretch at 1121 cm^{-1}. To further

explore the coordination chemistry of **L2** it was reacted with cadmium nitrate and cadmium sulfate in methanol. This provided crystals of two closely related metallo-macrocycle based 1-D coordination polymers $\{[Cd(\mathbf{L2\text{-}CH_3})(CH_3OH)(H_2O)](NO_3)\cdot 2CH_3OH\}_n$ (**3.19**) and $\{[Cd(\mathbf{L2\text{-}CH_3})(SO_4)(H_2O)]\}_n$ (**3.20**), respectively (Scheme 3.6).

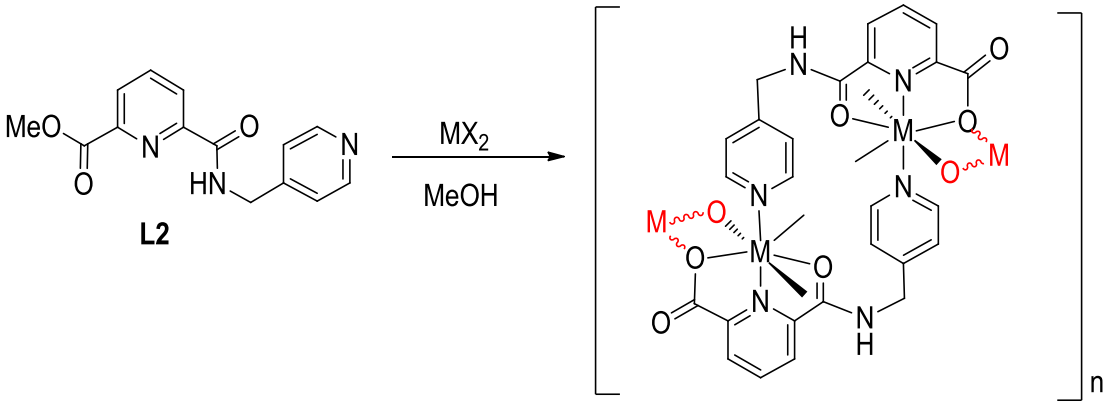

Scheme 3.6. The metallo-macrocycle based motif observed in most of the coordination polymers described in this chapter (M = Cd). The red atoms are contributed by the next metallo-macrocyclic building blocks in the polymeric structure.

Undertaking the reaction of cadmium nitrate with **L2** under solvothermal conditions in DMF provided quite a different material, $\{[Cd_3(\mathbf{L2\text{-}CH_3})_3(NO_3)(\mathbf{L2})(CH_3OH)](NO_3)_2\cdot ½H_2O\}_n$ (**3.21**). Colourless crystals of **3.21** were obtained from the reaction mixture by allowing a DMF-methanol solution, obtained by vapour diffusion of methanol into the DMF reaction mixture, to slowly evaporate (Scheme 3.7). In contrast to **3.19**, which is also formed by reacting of **L2** and cadmium(II) nitrate, compound **3.21** is a 2-D coordination polymer constructed from very similar dimetallo-macrocyclic units that connect trinuclear, as opposed to dinuclear, cadmium(II) clusters (Scheme 3.7). The N-O stretch of the nitrate anions was observed at 1383 and 1371 cm^{-1} for complexes **3.19** and **3.21**, respectively.

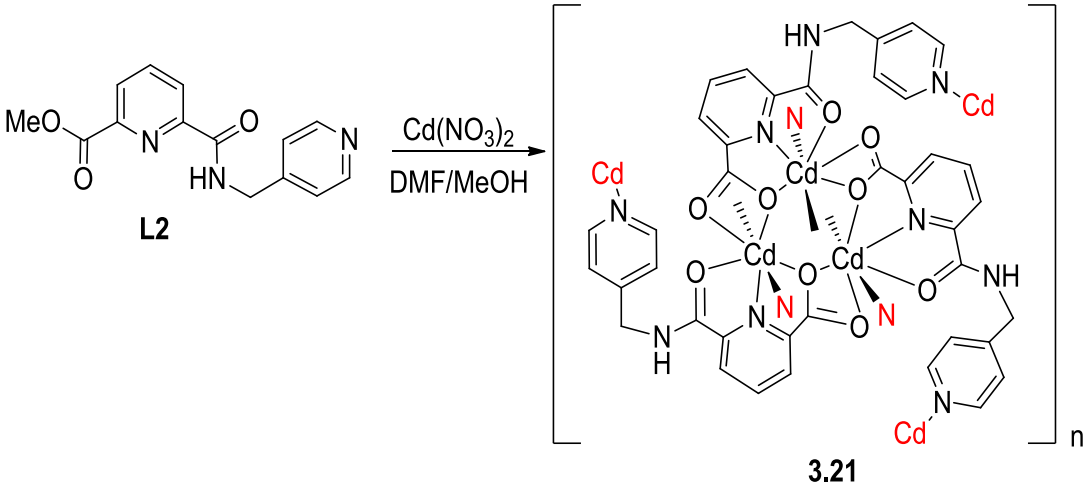

Scheme 3.7. The 2-D coordination polymer (**3.21)** containing trinuclear cluster units.

Employing a solvothermal approach, reaction of **L2** with copper acetate was found to generate an isolable crystalline solid {[Cu(**L2(-H)-CH$_3$**)]}$_n$ (**3.22**), from which suitable crystals for a synchrotron data collection were obtained. The structure of **3.22** is a 2-D coordination polymer formed from quite different dimetallo-macrocyclic units. Schematic summary of the five coordination polymers obtained from **L2** is shown below.

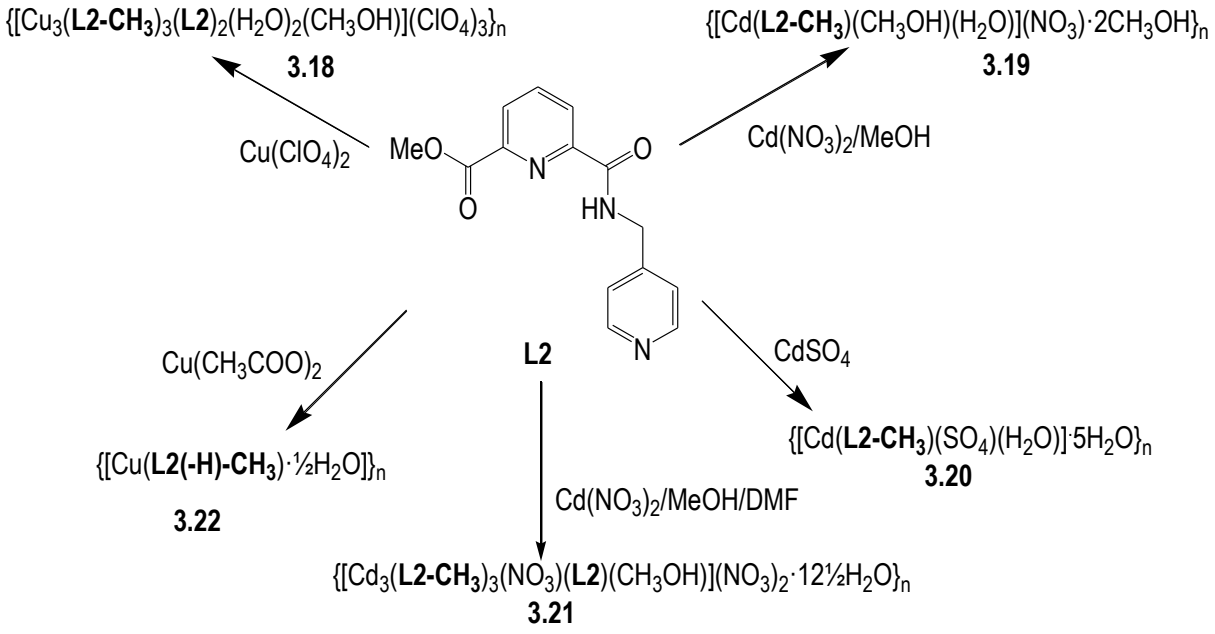

Scheme 3.6. The synthesis of coordination polymers derived from the convergent ligand **L2**.

Crystal structure of **3.18**

{[Cu_3(L2-CH_3)$_3$(L2)$_2$(H_2O)$_2$(CH_3OH)](ClO_4)$_3$}$_n$. Blue crystals in irregular shape were grown from the reaction solutions of ligand **L2** with copper perchlorate in methanol upon slow evaporation. The crystals obtained were subjected to X-ray crystallography analysis where crystals of complex {[Cu_3(**L2-CH_3**)$_3$(**L2**)$_2$(H_2O)$_2$(CH_3OH)](ClO_4)$_3$}$_n$ were solved in the monoclinic space group *C2/c*. The asymmetric unit contains a repeating unit of the coordination polymer, with three copper atoms, three anionic carboxylate forms of the ligand **L2,** two neutral forms of ligand **L2** and four partially-occupied non-coordinated perchlorate anions. An extended view of this structure reveals that it is a 1-D coordination polymer in which M_2L_2 units are linked by the carboxylate donors (Figure 3.25). Attempts to reproduce better quality crystals for X-ray crystallography were not successful and, therefore, this compound was not further investigated. A possible reason for this may lie in the fact that the materials contain a mixture of hydrolysed and non-hydrolysed forms of **L2**.

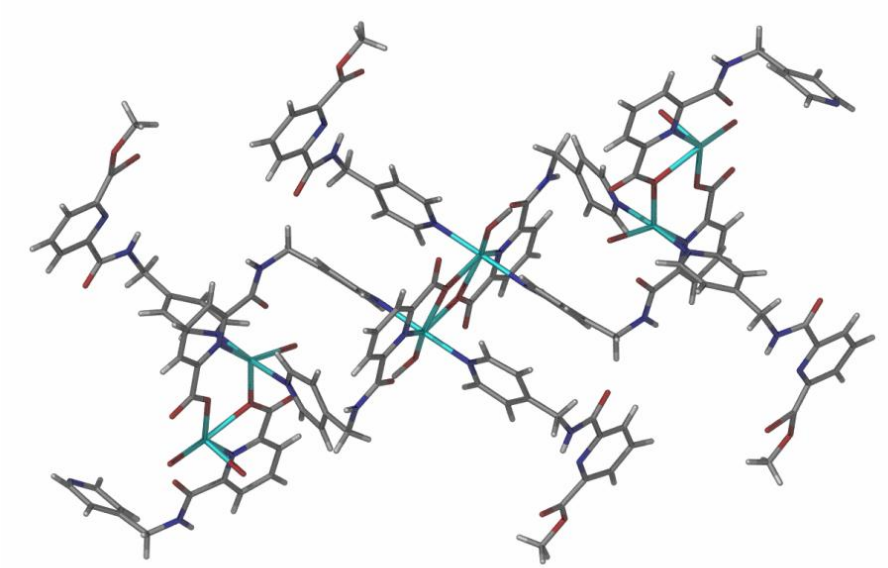

Figure 3.25. A view of the 1-D coordination polymer of complex **3.18**.

Crystal structure of **3.19**

{[Cd(L2-CH_3)(CH_3OH)(H_2O)](NO_3)·2CH_3OH}$_n$. A 1-D coordination polymer was obtained from the reaction of ligand **L2** with $Cd(NO_3)_2$. This complex was obtained colourless crystals in moderate yield by slow evaporation techniques. Compound **3.19** crystallises in the triclinic space

group *P*-1 with an asymmetric unit that comprises one cadmium atom, one molecule of hydrolysed form of **L2** (which is **L2-CH$_3$**) one coordinated water, one coordinated methanol, one non-coordinated nitrate anion and two non-coordinated methanol molecules (Figure 3.26).

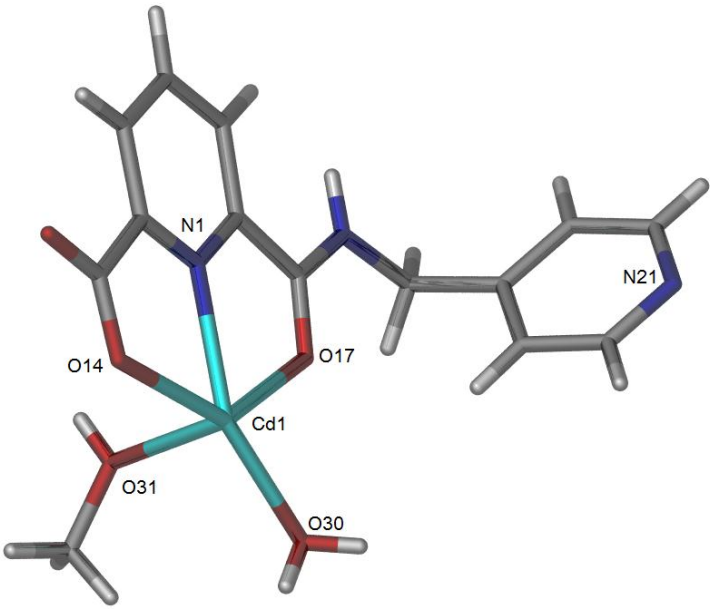

Figure 3.26. A perspective view of the asymmetric unit of complex **3.19** with two non-coordinated methanol and one non-coordinated nitrate omitted for clarity. Selected bond lengths (Å) and angles (°) : Cd(1)-N(1) 2.360(2), Cd(1)-O(14) 2.461(3), Cd(1)-O(17) 2.452(3), Cd(1)-O(31) 2.346(3), Cd(1)-O(30) 2.289(3), N(1)-Cd(1)-O(14) 68.59(2), N(1)-Cd(1)-O(17) 66.55(3), N(1)-Cd(1)-O(30) 139.18(3) and N(1)-Cd(1)-O(31) 92.16(3).

The cadmium atom is seven coordinate with a pentagonal bipyramidal geometry, chelated by the O, N, O chelate motif of **L2-CH$_3$**. The pyridyl ring from the neighbouring ligand molecule occupies the axial position to form the dimetallo-macrocyclic motif commonly encountered throughout the work described in this chapter. The dimetallic units are linked by μ_2-carboxylate oxygen atoms of the ligand to form the 1-D coordination polymer with the closest cadmium to cadmium distance being 3.966 Å (Figure 3.27(a)). Related coordination polymers constructed from Cd_2O_2 clusters have been described elsewhere.[250] A methanol solvate occupies the other axial coordination site and a water ligand completes the coordination sphere.

The crystal packing in this structure is completed by weak hydrogen bonding interactions between the N-H amide donors to the non-coordinated nitrate anion (d = 2.025 Å) which in turn are hydrogen bonded by the coordinated methanol molecules of an adjacent 1-D coordination polymer (d = 1.931 Å) (Figure 3.27(b)). Thus, adjacent 1-D coordination polymers are packed into 2-D hydrogen bond networks through hydrogen bond interactions mediated by the non-coordinated nitrate anions.

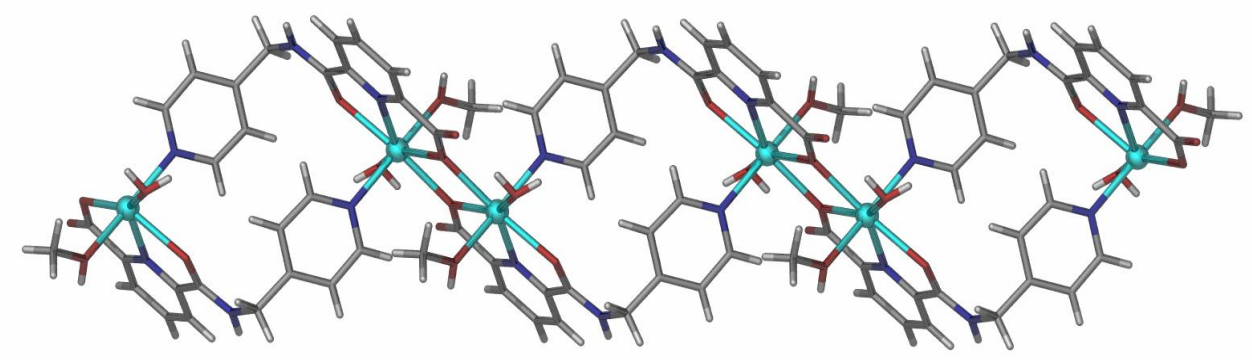

(a)

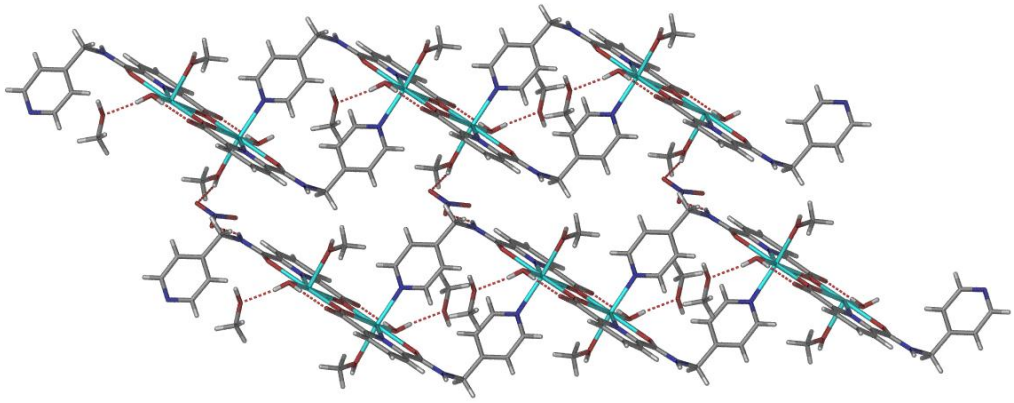

(b)

Figure 3.27. (a) A view of the 1-D coordination polymer **3.19**. Non-coordinated solvate molecules and nitrate anions are omitted for clarity. (b) A perspective view of the crystal packing of complex **3.19**, along with the hydrogen bonding in the crystal packing to generate the 2-D networks.

Crystal structure of **3.20**

{[Cd_2(L2-CH_3)$_2$(SO_4)(H_2O)$_2$]·5H_2O}$_n$. Complex **3.20** was also obtained as rod-shaped colourless crystals from the evaporation of a methanol-water solution containing cadmium sulfate and **L2**. This complex crystallises in the monoclinic space group *C*2/*c*. The asymmetric unit of this complex comprises one hydrolysed form of ligand **L2**, one coordinated sulfate and one coordinated water molecule (Figure 3.28). The sulfate anion is disordered over two positions with an 80:20 occupancy.

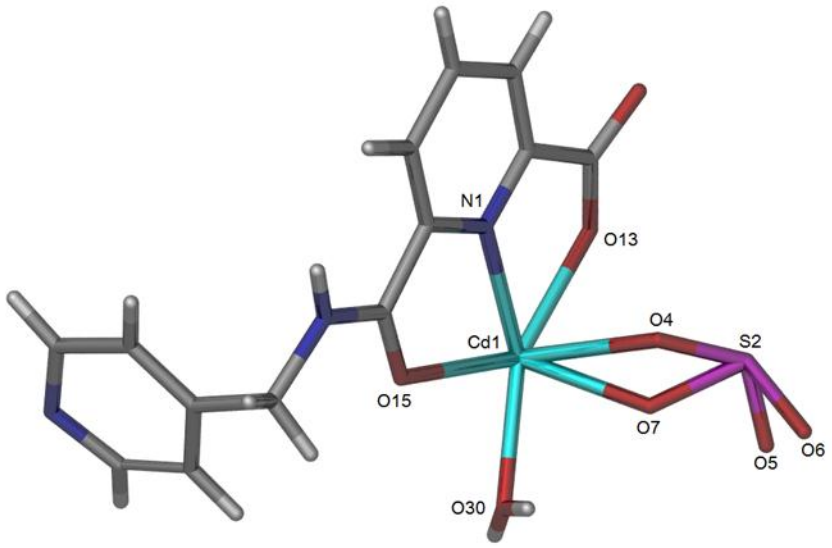

Figure 3.28. A perspective view of the asymmetric unit of complex **3.20**. Selected bond lengths (Å) and angles (°) : Cd(1)-N(1) 2.352(3), Cd(1)-O(13) 2.417(2), Cd(1)-O(15) 2.471(1), Cd(1)-O(30) 2.295(1), Cd(1)-O(4) 2.295(1), Cd(1)-O(7) 2.300(1), S(1)-O(5) 1.545(2), S(1)-O(6) 1.325(3), N(1)-Cd(1)-O(13) 66.43(2), N(1)-Cd(1)-O(15) 66.76(2),), N(1)-Cd(1)-O(4) 103.72(2) and N(1)-Cd(1)-O(30) 136.05(2).

The repeating unit in the structure of **3.20** is also based around similar seven-coordinate bimetallic cadmium centres, bridged by the carboxylate oxygen atom of **L2-CH_3**, as seen in **3.19**. In this structure the sulfate anion also acts as a μ_2-bridging ligand. The cadmium atom has a similar pentagonal bipyramidal geometry to that observed in compound **3.10**, with coordination by the O, N, O chelate motif of one **L2-CH_3** molecule, a monodentate water molecule, a bridging sulfate anion and the pyridyl nitrogen donor of a second equivalent of **L2-CH_3**. The Cd-N and Cd-O bond lengths of this compound are similar to the bond lengths reported for compound **3.19**.

Both compounds have Cd-N and Cd-O have bond lengths about 2.3Å and 2.4Å, respectively. Whereas in compound **3.19** both pyridyl nitrogen donors that are coordinated to opposite faces of the dinuclear cadmium(II) moieties (an anti-arrangement), in **3.20** these donors coordinate to the same face of the dinuclear cadmium(II) unit (a *syn* arrangement). This has important consequences for the 1-D polymeric structure, which instead of having a step-like structure adopts an undulating arrangement (Figure 3.29). The 1-D polymers extend down the *ac* diagonal with small, presumably solvent-filled, channels (along the *ab* diagonal) separating the polymers. Unlike other 1-D coordination polymers described in this chapter, no significant hydrogen bond interactions were observed in the crystal packing of this molecule.

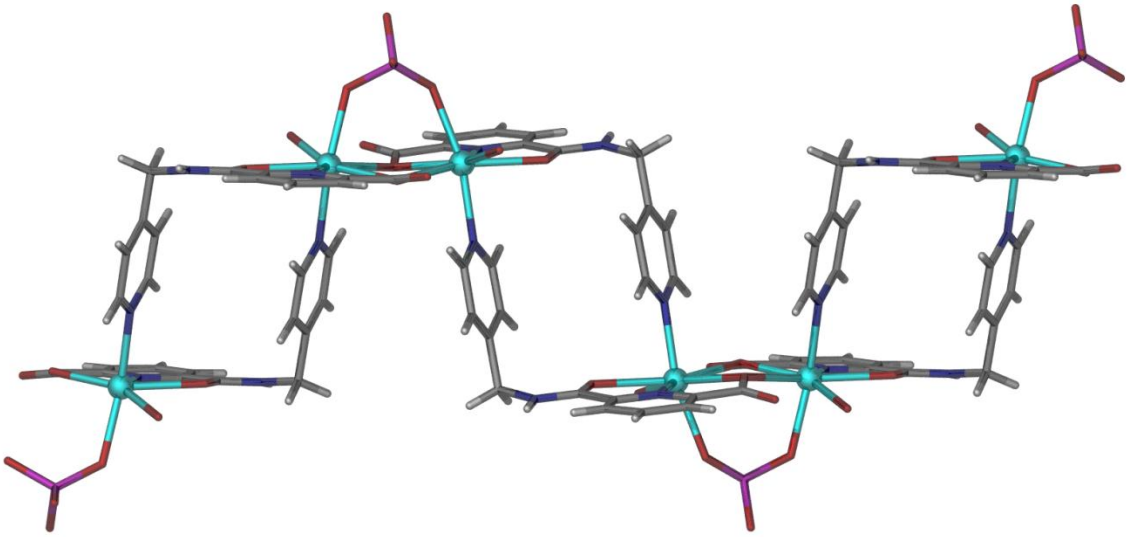

Figure 3.29. A view of the 1-D coordination polymer **3.20** showing the undulating structure. The disorder of the sulfate anions and pendant pyridyl rings is omitted for clarity.

Crystal structure of **3.21**

{[Cd_3(L2-CH_3)$_3$(NO_3)(L2)(CH_3OH)](NO_3)$_2$·12½H_2O}$_n$. Crystals of complex **3.21** were obtained as rod-shaped colourless crystals by slow evaporation of a DMF solution diffused with methanol. The complex crystallises in the monoclinic space group, $P2_1/n$. The asymmetric unit of compound **3.21** contains one trinuclear cluster, composed of three cadmium(II) centres and three hydrolysed ligand molecules, a molecule of **L2**, three nitrate anions, a water solvate molecule, and a coordinated methanol molecule. The trinuclear cluster has a triangular arrangement whereby the three cadmium(II) centres have very similar seven-coordinate coordination

environments, albeit with different axial donors (**L2**, methanol and nitrate). The hydrolysed ligand **L2-CH$_3$** coordinates to a cadmium using the O, N, O tridentate chelating site observed throughout this work and in turn the carboxylate oxygen is then coordinated to an adjacent cadmium centre to produce the trinuclear motif (Figure 3.30(a) and 3.30(b)). The cadmium centres have Cd-O bond lengths of 2.294(5) – 2.540(4) Å and Cd-N bond lengths in the range 2.298(5) – 2.389(5) Å.

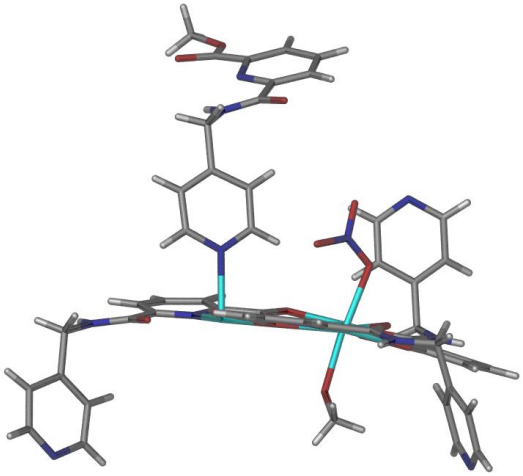

(a)

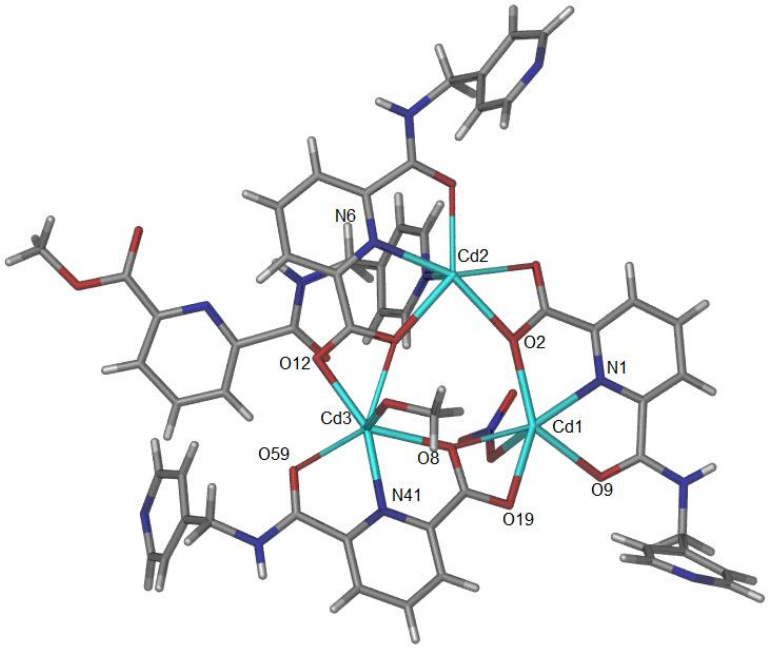

(b)

Figure 3.30. Perspective views of the M$_3$(**L2-CH$_3$**)$_3$ cluster showing (a) the coordination by the co-ligands and (b) the trinuclear cluster of **3.21** from above, showing the M$_3$(**L2-CH$_3$**)$_3$ cluster

and the coordinated nitrate anion, **L2** ligand and methanol ligands in the axial coordination sites of the three cadmium centres. The remaining three axial coordination sites are coordinated by pyridyl nitrogen donors from three other clusters. Selected bond lengths (Å) and angles (°) : Cd(1)-N(1) 2.346(3), Cd(1)-O(2) 2.377(2), Cd(1)-O(8) 2.444(1), Cd(1)-O(19) 2.389(1), Cd(2)-N(6) 2.360(3), Cd(2)-O(2) 2.401(2), Cd(2)-O(7) 2.401(1), Cd(2)-O(4) 2.393(1), Cd(3)-N(41) 2.333(3), Cd(3)-O(12) 2.309(2), Cd(3)-O(8) 2.364(1), Cd(3)-O(59) 2.460(1), N(1)-Cd(1)-O(2) 54.60(2), N(6)-Cd(2)-O(4) 69.10(2) and N(41)-Cd(3)-O(8) 69.30(2).

The trimeric cluster is then connected to three other clusters *via* the dimetallo-macrocycle motif commonly encountered for these ligands to give the 2-D 6,3-connected coordination polymer (the ligands are considered topologically trivial) (Figure 3.31). The 2-D coordination polymers lie in the *bc* plane of the structure but are not planar and undulate up and down at the connection of each hexagonal ring (Figure 3.32). The channels within the structure lie down the *a*-axis (within the hexagonal ring) and are lined by oxygen atoms from nitrate anions, water solvate molecules and the ester carbonyl oxygen of the only intact **L2** molecule. In the crystal structure no significant electron density is located in these channels which are not particularly large; the shortest O-O separation is 7.22(1) Å and the longest 8.22(1) Å. Based on the elemental analysis results, these channels are filled with disordered water molecules that are presumably involved in hydrogen bonding with the oxygen atoms lining the channels.

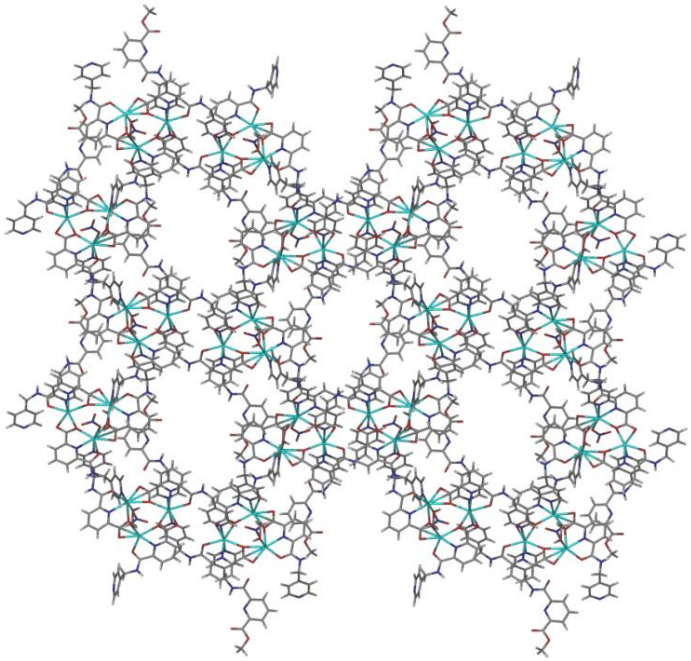

Figure 3.31. A perspective view of the 6,3-connected 2-D coordination polymer in compound **3.21**.

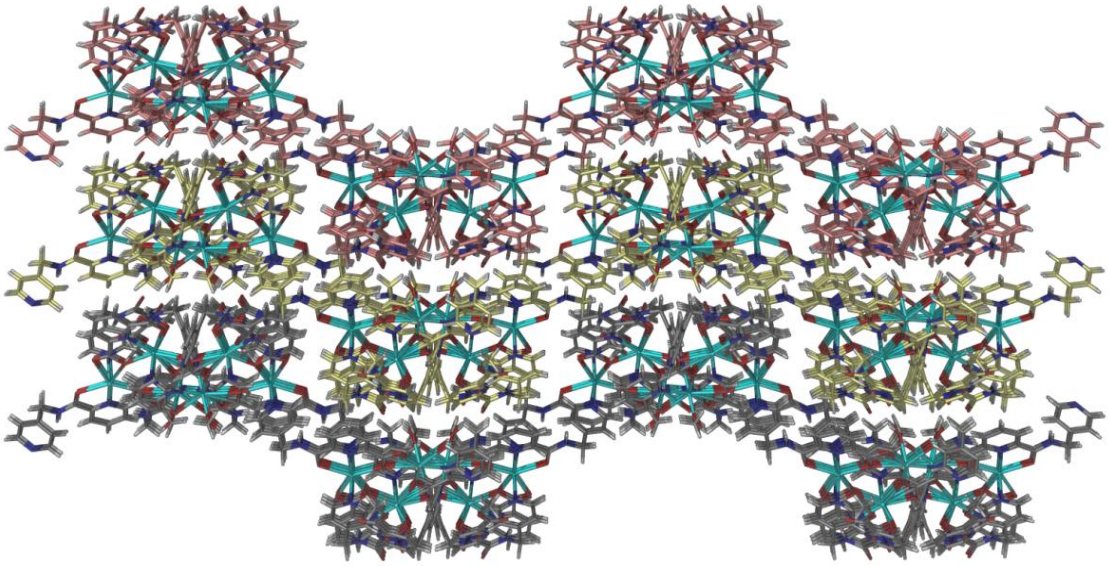

Figure 3.32. Layering of the 6,3-connected 2-D coordination polymers in the crystal packing of compound **3.21**.

In a similar manner to the synthesis of **3.21**, a 2-D coordination polymer, **3.22** has been successfully obtained from reaction of **L2** with copper acetate. In the structure of **3.22**, the ligand **L2** has not only undergone hydrolysis but the amide NH has been deprotonated to form **L2(-H)-CH$_3$** which acts as a dianionic bridging ligand. In this form the ligand coordinates to the copper centre *via* a tridentate O, N, N chelating motif and also to a second copper through the pendant monodentate pyridyl donor. This is in contrast to the coordination mode of complexes **3.19**, **3.20** and **3.21** that adopt a common O, N, O chelating motif through the 2,6-pyridinedicarboxylate donors. The details on the crystal structure of complex **3.22** are discussed in the following section. Table 3.2 showed the comparison between the bond lengths and angles around the metal centres in the two modes; O, N, O and O, N, N. It is indicated from Table 3.2 that the O, N, N chelating motifs has larger angles compared to ones with the O, N, O chelate rings.

Table 3.2. Distances [Å] and angles [°] subtended around the metal ion in complexes.

Bonds and angles	**3.19**	**3.21**	**3.22**
M-N_1	2.360(2)	2.346(3)	1.926(3)
M-O_1	2.461(3)	2.377(2)	2.063(2),
M-O_2	2.452(3)	2.444(1)	
M-N_2			1.994(1)
N_1-M-O_1	68.59(2)	69.10(2)	78.94(3)
N_1-M-O_2	66.55(3)	66.88(2)	
N_1-M-N_2			80.83(4)

[a] M = Cd(II) or Cu(II)

[b] Guide to numbering used in Table 3.1.

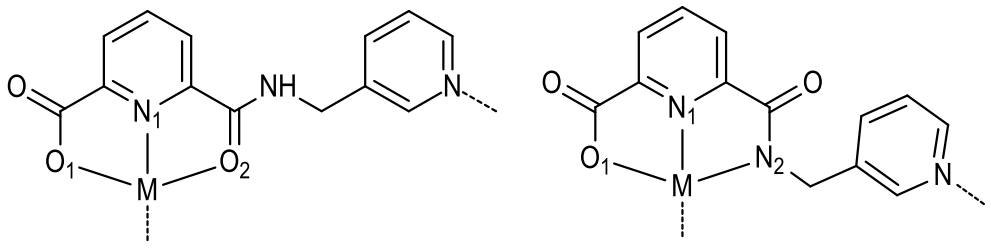

Crystal structure of **3.22**

{[Cu(L2(-H)-CH$_3$)]·½H$_2$O}$_n$. Compound **3.22** crystallises in the orthorhombic space group *Pbca* with one dianionic form of ligand **L2** and one copper centre in the asymmetric unit. In this structure, the ligand chelates in a tridentate manner to the copper centre using a O, N, N chelating motif (Figure 3.33) rather than the O, N, O chelating motif observed in other complexes. The bond lengths of **3.22** are in the normal range, but the bond angles of O, N, N chelating motifs are larger than those in structures with O, N, O chelate rings.

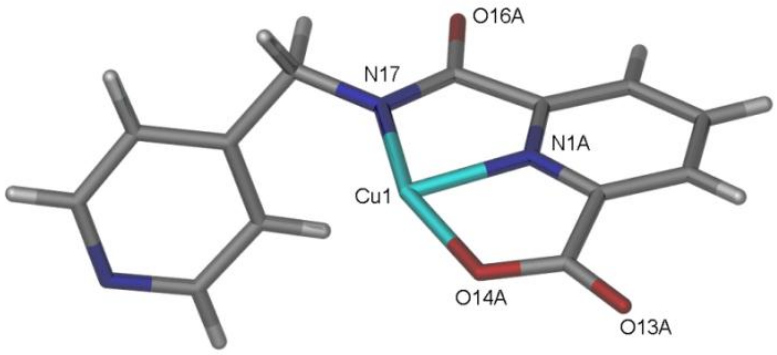

Figure 3.33. A perspective view of the asymmetric unit of **3.22**. Selected bond lengths (Å) and angles (°): Cu(1)-N(1A) 1.926(3), Cu(1)-O(14A) 2.063(2), Cu(1)-N(17) 1.994(1), N(1A)-Cu(1)-N(17) 80.83(4), N(1A)-Cu(1)-O(14A) 78.94(3).

Despite this change in coordination by the ligand a dinuclear metallo-macrocycle is still present but in this case the macrocycle has no cleft when compared to the other complexes obtained with **L1** or **L2** (Figure 3.34). Within the dinuclear metallo-macrocycle the pendant pyridine rings of **L2(-H)-CH$_3$** are involved in a close face-to-face π-stacking interaction (centroid-centroid distance 3.40 Å; angle 114.5°; centroid offset 1.19 Å). The Cu-O and Cu-N bond lengths are in the range 1.926(2) – 2.212(2) Å and typical of compounds studied in this work and the copper centre has a distorted square pyramidal geometry ($\tau = 0.25$).[166]

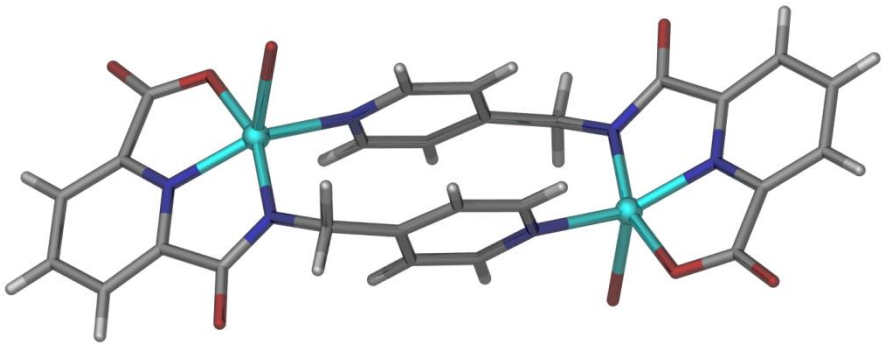

Figure 3.34. The dimetallo-macrocycle building block of **3.22**. These units form the repeating structure of the 2-D coordination polymer.

Within **3.22** each dinuclear metallo-macrocycle acts as a 4-connecting node. Both copper centres are coordinated by the carboxylate oxygen atom of two other dimetallo-macrocycles and in turn the carboxylate oxygen atom of each ligand coordinates two other metallo-macrocycles to give a 4,4-connected 2-D coordination polymer (Figure 3.35). The layers are then interdigitated with adjacent 4,4-connected 2D coordination polymers to complete the crystal packing along the *a*-axis. Compound **3.22** is close packed in the solid-state with no solvent molecules identified in the crystal structure.

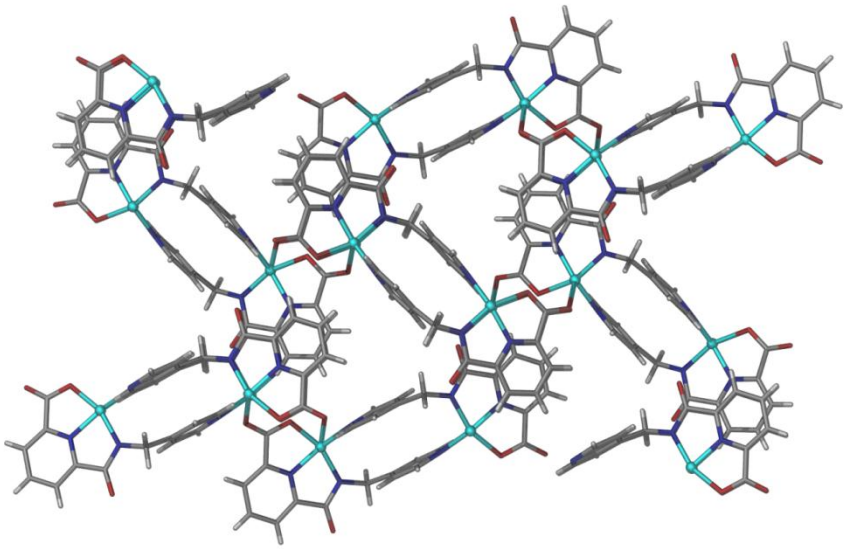

Figure 3.35. A view of the 4,4-connected 2-D coordination in the *bc* plane.

3.5. PXRD and TGA analysis

PXRD and TGA were used to further analyse the properties of the 2-D coordination polymers obtained from ligand **L2-CH$_3$**. This distinction was made as during the majority of the research only limited access to PXRD was available and these materials were deemed to be of lower priority and interest in the context of studying other properties such as gas adsorption PXRD was used primarily to analyse the phase purity of bulk samples by comparison of experimental data to the calculated pattern generated from single crystal data of the same sample. Figure 3.36 shows the comparison between the experimental PXRD pattern and a pattern simulated from the single crystal data. From the close match of the experimental and simulated PXRD patterns it is clear that the bulk material has the same structure as that obtained for the single crystal. PXRD of complex **3.21** also confirmed crystallinity was maintained upon removal from solvent.

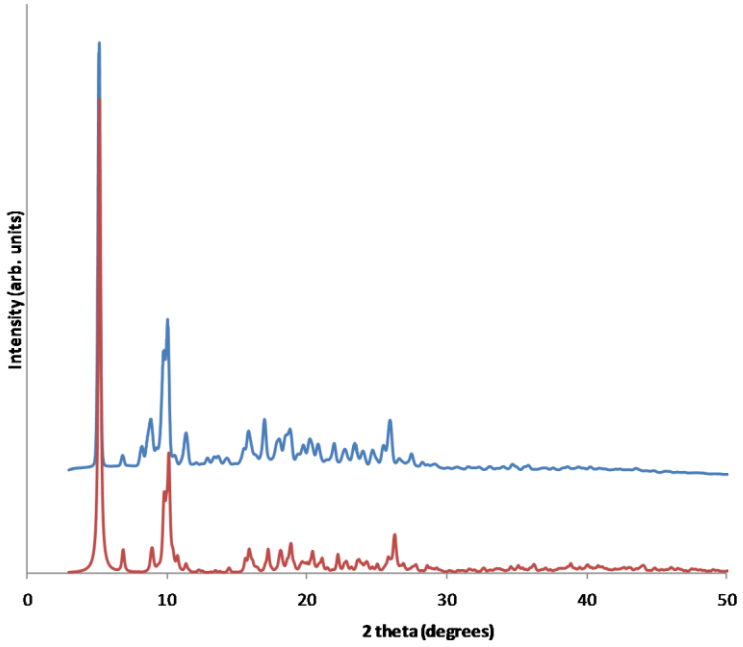

Figure 3.36. PXRD of complex **3.21** (where blue = experimental, red = pattern simulated from the single crystal X-ray structure).

The PXRD shows not only that the bulk sample is consistent with the formulation identified by other analyses and it appears, due to its relatively low porosity structure, that complex **3.21** is stable to desolvation. The potential surface area of this material was calculated at 228 m^2/g using the Materials Studio software package. While this value is low in the context of

surface areas both predicted and measured for other reported materials, if the self-assembling metallomacrocycles of this type can be pillared by linkers then these materials may form the basis of interesting porous materials. [225-227] Figure 3.37 showed the perspective view of the van der Waals surface for the structure. Unfortunately, compound **3.21** could only be obtained from reactions carried out on a small scale and any attempts to scale-up the synthesis for further investigation did not produce the desired materials.

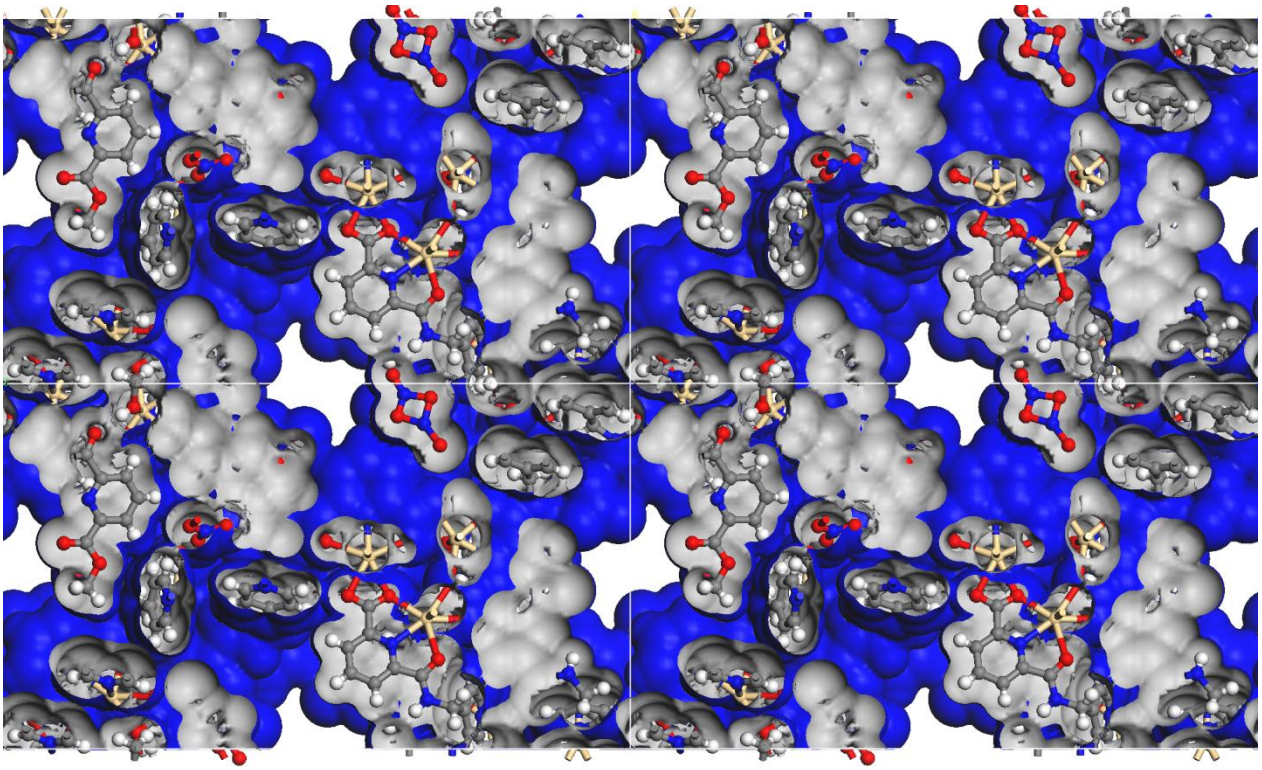

Figure 3.37. A perspective view on the van der Waals surface for **3.21** (with solvent removed).

TGA was used to examine the stability and to track the changes in the weight of a sample of **3.21** over a temperature range 30-600˚C. TGA for complex **3.21** indicates that the compound is stable to around 150 °C. The analysis shows a gradual two-stage solvent loss (stage 1 up to 150°: found 5.7%; *calc.* 5.9%, $6H_2O$; stage 2 from 150-500 °C; found 49.5%) and then decomposition at approximately 500°C.

Figure 3.38 showed the comparison between the experimental PXRD pattern and a pattern simulated from the single crystal data for compound **3.22**. Again, from the close match of the experimental and simulated PXRD patterns it is clear that the bulk material has the same structure as that obtained by single crystal X-ray crystallography. PXRD of complex **3.22** also confirmed crystallinity was maintained upon removal from solvent. This is undoubtedly due to its close-packed nature.

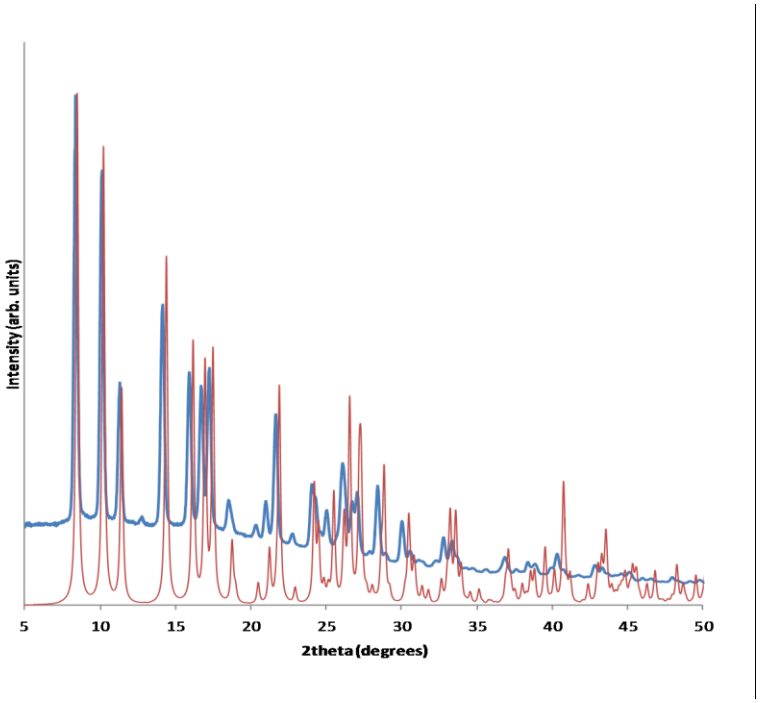

Figure 3.38. PXRD of complex **3.22** (where blue = experimental, red = pattern simulated from the single crystal X-ray structure).

TGA was also used to examine the stability and to track the changes in the weight of a sample of **3.22** over a temperature range 30-600˚C. The elemental analysis indicates a partial water solvate molecule and this is supported by TGA (Figure 3.39) for complex **3.22** which shows minimal weight loss (*found* 1.9%; *calc*. 2.7%, $^{1}/_{2}H_2O$) up to *ca.* 240°C at which time the ligand decomposes to give residual CuO (incomplete by the maximum accessible temperature).

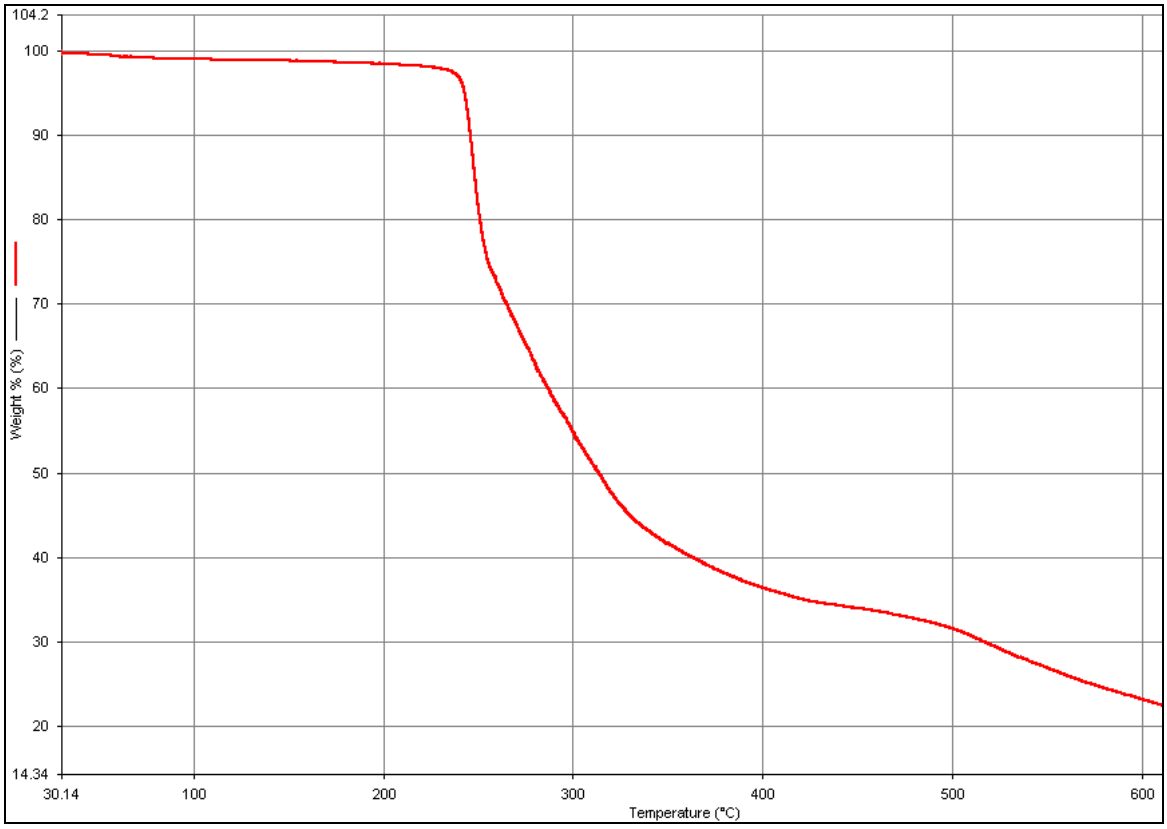

Figure 3.39. TGA results for complex **3.22**.

3.6. Summary

From these studies, four heterocyclic ligands containing a 6-carbonyl-pyridine-2-carboxylate chelating moiety have been incorporated into a range of discrete dinuclear metallo-macrocyclic complexes and metallo-macrocyclic based coordination polymers. As described in chapter 2, these ligands were successfully prepared in concise one or two step synthetic routes from commercially available starting materials. All four bridging ligand precursors (**L1** – **L4**) are flexible linkers with a potentially tridentate chelating site and pendant monodentate donor functionality. The more flexible of these compounds *N*-6-[(3-pyridylmethylamino)carbonyl]-pyridine-2-carboxylate (**L1-CH$_3$**) and *N*-6-[(4-pyridylmethylamino)carbonyl]-pyridine-2-carboxylate (**L2-CH$_3$**) gave a greater array of compounds incorporating the self-assembled dinuclear metallo-macrocyclic species. Unfortunately, trying to instil greater control during the self-assembly process by using the more rigid links *N*-6-[(3-pyridylamino)carbonyl]-pyridine-2-carboxylate (**L3-CH$_3$**) and *N*-6-[(4-pyridylamino)carbonyl]-pyridine-2-carboxylic acid methyl

ester (**L4**) was unsuccessful as these compounds are less stable and shown to more readily hydrolyse.

In all but one case, self-assembled dinuclear metallo-macrocyclic units form the basis of the structures to give discrete and polymeric materials. With **L1-CH$_3$** and **L3-CH$_3$** discrete dinuclear metallo-macrocyclic complexes are formed, whereby complexes **3.12** – **3.14**, containing link **L1-CH$_3$**, are cleft shaped with a hinge at the methylene spacer, which allows the cleft to widen and contract to accommodate different packing modes in the solid-state, while the rigid link in **L3-CH$_3$** gives near planar metallo-macrocyclic structures. The cavities in complexes **3.12** – **3.14** can act as a solid-state host and complex **3.14** displays anion-π interactions that support the inclusion of an anionic guest. Complexes **3.15** and **3.16** could potentially be used as tectons for self-assembly into higher order structures using hierarchical approaches as described in the literature.

The dinuclear metallo-macrocyclic motif is also present in coordination polymers of ligand **L2-CH$_3$** whereby discrete metal centres (**3.18**) and dinuclear (**3.19** and **3.20**) or trinuclear (**3.21**) clusters are linked by these macrocycles to give 1-D and 2-D coordination polymers. Compounds **3.21** and **3.22** are 2-D are coordination polymers with **3.22** is close-packed in the solid-state. In the case of reactions of **L2** with cadmium(II) nitrate a 1-D coordination polymer (**3.10**) is formed in a reaction carried out under ambient conditions; when the same reaction is conducted under solvothermal conditions a 2-D structure (**3.21**) is formed. Compound **3.21** has small oval channels lined by the oxygen atoms of the nitrate counterions down the *a*-axis of the unit cell. Compound **3.22** is the only coordination polymer obtained with O, N, N chelating motifs. This compound has larger bond angles about the tridentate chelate and longer metal-metal separations compared to coordination polymers with the O, N, O chelate rings.

The 2-D coordination polymers were further investigated. PXRD indicated close match of the experimental and simulated patterns which means that the bulk material has the same structure as that obtained for the single crystal. PXRD of complex **3.21** and **3.22** also confirmed crystallinity of both compounds was maintained upon removal from solvent. The stability of the 2-D coordination polymers, **3.21** and **3.22** were investigated by TGA and they were found to be stable to around 150°C and 240°C, respectively. Compound **3.21** is the most interesting structure

and could be useful for further study. However, the synthesis of this material is challenging. As mentioned in the discussion, this material could only be obtained in a small scale and attempts to prepare in a large scale gave undesired side products.

CHAPTER 4

COORDINATION CHEMISTRY OF THE SYMMETRICAL AMIDE LIGANDS

Chapter 4

4. Coordination chemistry of the symmetrical amide ligands

4.1. Introduction

As noted earlier, identifying new motifs capable of anion binding is a topical area in supramolecular chemistry,[11-13,251-255] due to the importance of anions in biology, medicine, catalysis, and the environment.[251,255-257] Considerable effort has been focused in the synthesis of anion receptors[14,258-262] for different applications, such as fluorescent and chromogenic anion sensors[263-266] ion selective electrodes,[267,268] phase-transfer catalysis,[269] or as templates for supramolecular synthesis.[270,271] A continuing focus is on the development of moieties that can selectively complex anions. This often involves the use of hydrogen bonding donor groups such as amide,[272-279] thiourea[12,21,158,255,280,281] urea[17,282-288] and pyrrole groups (calixpyrroles),[28,30,287,289-296] as the anion binding sites. The use of pre-organised organic hosts with cleft structures, such as calixarene[297-302] functionalised with hydrogen bond donors and cyclic amides[74,143] is also of interest due to their efficient binding and advantageous recognition properties.

Self-assembly by anion templation has been reported for a significant number of metallo-supramolecular assemblies.[80,303-305] This includes discrete circular helicates,[306] coordination nanotubes,[307] and various polygonal[308-312] or polyhedral assemblies.[40,45,46,313] In the context of identifying new motifs for anion binding, such self-assembling species are attractive since the structural and functional properties of metal centres can be combined with the recognition properties of the organic hosts to obtain the target host systems.[80,297,314,315] This approach has been commonly used for the preparation of supramolecular cages containing palladium and platinum centres and bispyridyl ligands. The rigid ligands, *N,N'*-bis(4-pyridyl)pyridine-2,6-dicarboxamide (**4.1**) and *N,N'*-bis(4-pyridyl)isophthalamide (**4.2**),[167] containing a moieties within the organic component capable of anion binding are employed in these reactions. Reactions of **4.1** and **4.2** with [Pd(dppm)(CF_3SO_3)$_2$] led to a formation of discrete metallo-supramolecular metallocyles (**4.3** and **4.4**) with encapsulation of two triflate anions (Scheme 4.1). [105,167] The

triflate anions are bound to **4.3** through hydrogen bonding interactions with the central hydrogen bond donor regions.

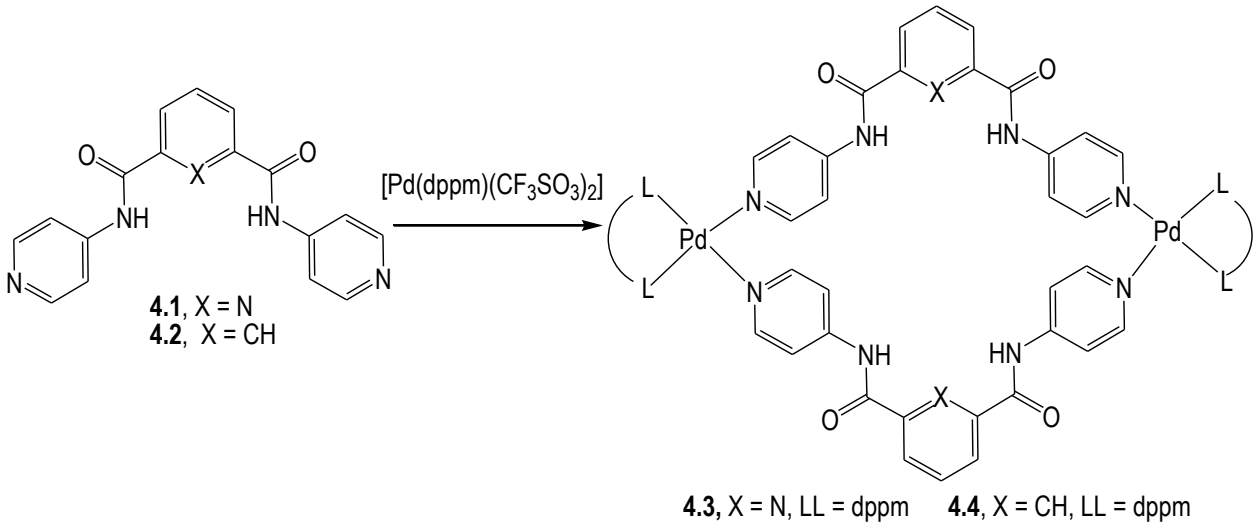

Scheme 4.1. The synthesis of palladium(II) supramolecular cages derived from the rigid bis-pyridyl diamide ligands **4.1** and **4.2**.

Vilar and co-workers[316] have also prepared a series of Pd(II) supramolecular cages using a self-assembly approach. In contrast to the complexes described above, these complexes were prepared from palladium(II) precursors and flexible bis-pyridyl ligands containing amide hydrogen bond donors. By using flexible ligands such as *N,N'*-bis(3-pyridylmethyl)benzene-1,3-dicarboxamide (**4.5**) and *N,N'*-bis(4-pyridylmethyl)benzene-1,3-dicarboxamide (**4.6**) (Figure 4.1(a)), bowl-shaped palladium(II) metallo-macrocyles were obtained.[316] In the crystal structure of the [2+2] metallo-supramolecular macrocycle derived from **4.6**, a triflate anion was found localised inside the cavity of the bowl-like metallo-macrocyclic assemblies and interacting with the macrocycle *via* weak hydrogen bonds and anion-π interactions (Figure 4.1(b)). Of note is the fact that the lack of preorganisation does not lead to interactions between the amide hydrogen bond donors and the encapsulated anion.

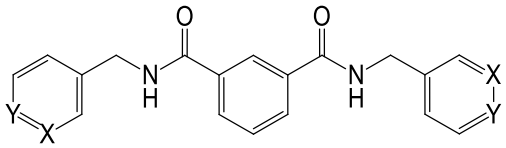

X = N, Y = CH **4.5**
X = CH, Y = N **4.6**

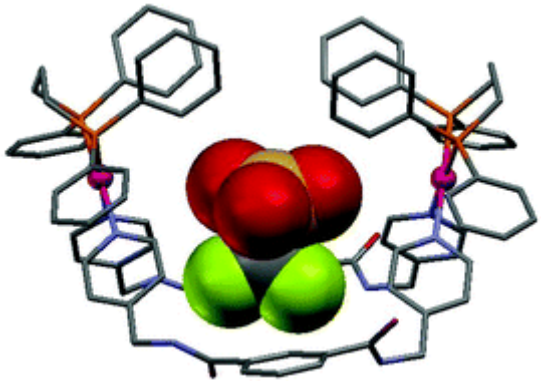

(a) (b)

Figure 4.1. (a) The structure of the angular ligands **4.5** and **4.6**, and (b) encapsulation of anion inside the cavity of the discrete metallo-macrocyclic derived from **4.6** (image sourced from [316]).

In a similar manner to the research described above, the incorporation of coordination polymers with ligand-based hydrogen bonds has also been a strategy of first choice to generate coordination frameworks capable of interaction with anions.[80,317-320] The synthesis and properties of coordination polymers containing N-H hydrogen bonds donor groups as the anion binding host have been described in a number of independent studies.[17,79,130,168,214,321-327] Custelcean and co-workers have successfully synthesised three 1-D zinc coordination polymers with urea moieties. These compounds form weak hydrogen bonding interactions with the anions through the urea moieties.[133] The presence of the Zn-anion coordination bonds and the hydrogen bonding interactions within the three coordination polymers is shown in Figure 4.2. In more recent work, Custelcean and co-workers have concentrated on the coordination and separation of anions by selective crystallisation of coordination polymers containing urea based ligands.[20,133,328]

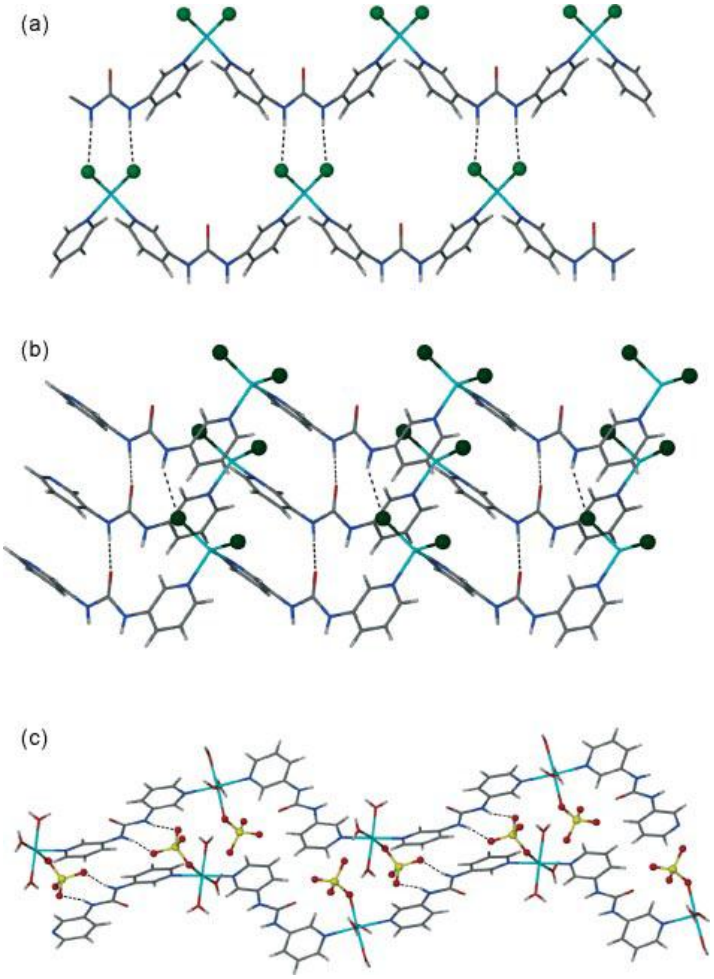

Figure 4.2. Crystal structures of zinc complexes containing showing the cooperative binding of the anions to the Zn centres and urea groups. The anions involved are (a) Cl^- (b) Br^- (c) SO_4^-.

Related work has been reported by a number of other groups. The anion binding studies of monopyridyl urea ligands complexed with Ag(I) have been described by Steed's group[329-333] Dastidar, in a large proportion of his work, has focused on the preparation of coordination polymers of ligands with hydrogen bond donors, such as urea.[85,127,327,334-336] The anion coordination chemistry of the pyridyl urea ligands has also been investigated by Janiak and co-workers,[337] while coordination networks incorporating pyridyl amide ligands have been extensively reported by Biradha's group.[167,177,338,339] Most recently, Nangia and co-workers have reported silver complexes containing urea moieties.[327] In the crystal structure of one of the reported discrete complexes $[Ag(\mathbf{L})_2](MeCN)(NO_3)$, where **L** = *N*-4–chlorophenyl-*N'*-4-pyridyl urea), nitrate anions were hydrogen bonded to the NH donors from the urea moiety and

incorporated into the crystal lattice. The hydrogen bonding interactions, as part of a 1-D hydrogen bonded chain, between the NH urea donors and the nitrate anions are shown in Figure 4.3.

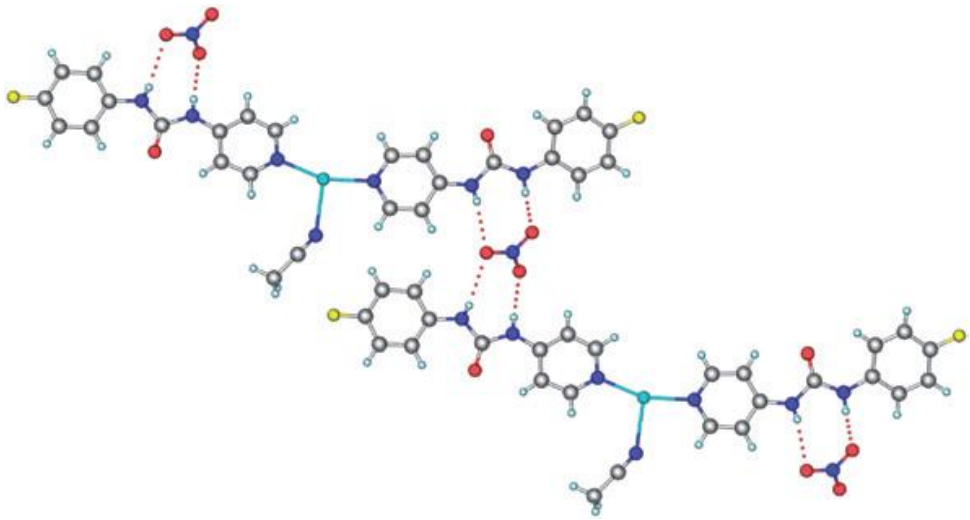

Figure 4.3. A perspective view of the hydrogen bonding interactions between nitrate anions and the urea ligands in the crystal packing of $[Ag(\mathbf{L})_2](MeCN)(NO_3)$.

Some examples of flexible amide ligands that have potential to bind anions in metallo-supramolecular assemblies are outlined in Figure 4.4.[161] As described above, compounds **4.5** and **4.6** have been used to prepare two metallo-supramolecular cages and **4.6** has been previously used in coordination chemistry. The coordination chemistry of the isomeric compounds, *N,N'*-bis(3-pyridylmethyl)benzene-1,4-dicarboxamide (**4.7**) and *N,N'*-bis(4-pyridylmethyl)benzene-1,4-dicarboxamide (**4.8**) has also been studied. In contrast, limited aspects of the chemistry of *N*,*N*′-[1,3-phenylenebis(methylene)]bis-3-pyridinecarboxamide (**4.9**), *N*,*N*′-[1,3-phenylenebis(methylene)]bis-4-pyridinecarboxamide (**4.10**) has been investigated, and nor has the coordination chemistry of the isomers *N*,*N*′-[1,4-phenylenebis(methylene)]bis-3-pyridinecarboxamide (**4.11**) and *N*,*N*′-[1,4-phenylenebis(methylene)]bis-4-pyridinecarboxamide (**4.12**) been investigated. Meanwhile, preliminary investigations of the coordination chemistry of compounds **L5** and **L6** with silver(I) salts has been undertaken also, but the results have not been published.[340] In all, at the outset of this work there was considerable scope for investigating the

use of such ligands to investigate the formation of anion binding motifs within discrete self-assembled metallo-macrocyclic structures and also coordination polymers. This chapter will present some of these results for compounds **L5** and **L6**.

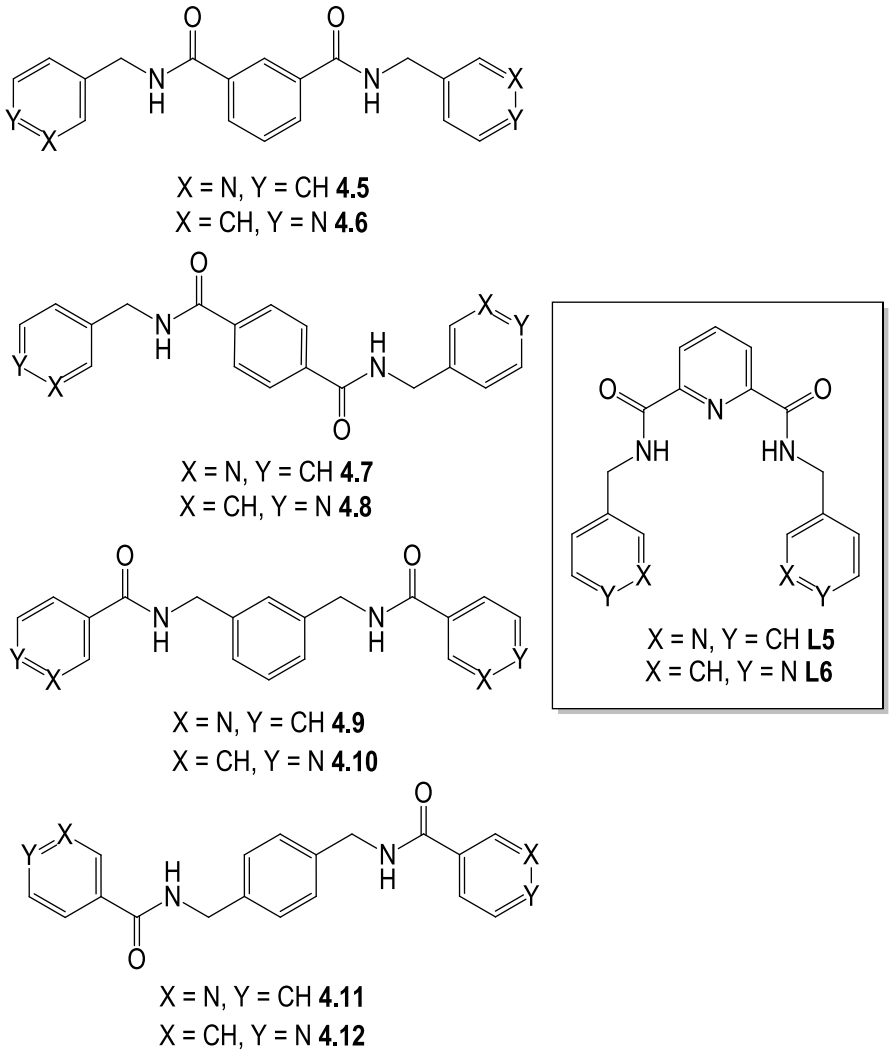

Figure 4.4. Several examples of isomeric flexible bisamide compounds described in the literature.[161]

In addition to studying the coordination chemistry and metallo-supramolecular chemistry of the two reported diamide ligands (**L5** and **L6**), this chapter will also present an investigation into the coordination chemistry of six novel tetraamide ligands (**L7**-**L12**) prepared in this research. Ligands **L5** and **L6** are pre-organised amide ligands with U-shaped conformations in

the solid-state, with the amide N-H directed internally into a pocket with potential for anion binding. Extension of the structures of **L5** and **L6** gave ligands **L7-L12**, which are also pre-organised ligands, but could potentially contain more than one pocket for binding anions. By using combinations of these organic linkers and the transition metal ions, new discrete or metallo-supramolecular assemblies can be prepared. Furthermore, the self-assembly process may be able to be modulated by the choice of anion (Figure 4.5).

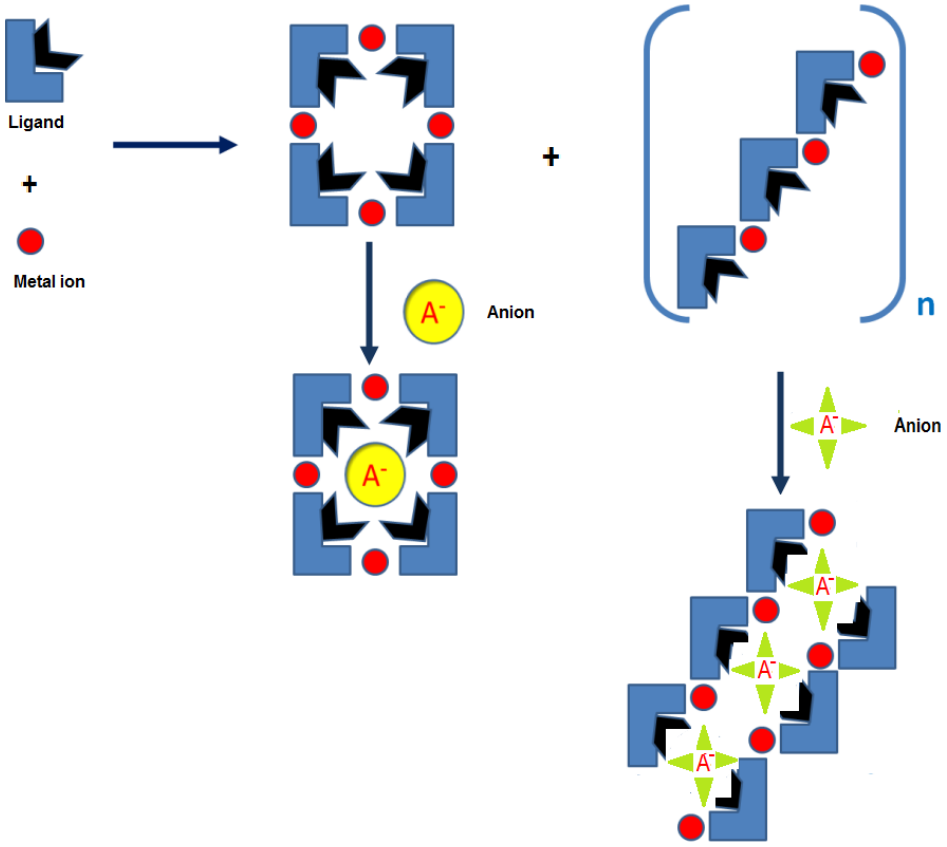

Figure 4.5. The preparation of metallo-supramolecular species and the modulation of the self-assembly process by the choice of anion

4.2. Coordination chemistry and metallo-supramolecular chemistry of L5-L12

In this chapter the coordination chemistry of two previously reported flexible diamide ligands, *N,N'*-2,6-bis(3-pyridylmethyl)pyridine dicarboxamide (**L5**)[161] and *N,N'*-2,6-bis(3-pyridylmethyl)pyridine dicarboxamide (**L6**)[161] and six novel tetraamide ligands, 1,2-bis[*N,N'*-6-

(3-pyridylmethylamido)pyridyl-2-carboxyamido]ethane (**L7**), 1,2-bis[*N*,*N*'-6-(4-pyridylmethylamido)pyridyl-2-carboxyamido]ethane (**L8**), 1,2-bis[*N*,*N*'-6-(3-pyridylmethylamido)pyridyl-2-carboxyamido]propane (**L9**), 1,2-bis[*N,N'*-6-(4-pyridylmethylamido)pyridyl-2-carboxyamido]propane (**L10**), 1,2-bis[*N,N'*-6-(3-pyridylmethylamido)pyridyl-2-carboxyamido]cyclohexane (**L11**) and 1,2-bis[*N,N'*-6-(4-pyridylmethylamido)pyridyl-2-carboxyamido]cyclohexane (**L12**) were investigated. This was done with a range of transition metals including cadmium, copper, cobalt and zinc and a mix of coordinating and non-coordinating anions. In an attempt to generate discrete supramolecular assemblies, the diamide ligands were reacted with selected pre-organised palladium(II) complexes, dichloropalladium(II) 2,2'-bipyridine [$PdCl_2$(2,2'-bipy)], dichloropalladium(II) ethylenediamine [$PdCl_2$(en)] and dichloropalladium(II) triphenylphosphine [$PdCl_2(PPh_3)_2$]. As appropriate, all complexes obtained were characterised by a combination of NMR spectroscopy, IR spectroscopy, mass spectrometry and combustion analysis, and where possible, suitable crystals were characterised by X-ray crystallography. In this chapter, preliminary anion binding studies are also described.

4.2.1. Synthesis of the discrete complexes and metallo-supramolecular assemblies of L5 and L6

4.2.1.1. Discrete complexes of L5

Two rather different results were obtained for the reaction of **L5** with cadmium bromide and zinc perchlorate. In both cases the reactions led to the formation of discrete complexes, with formulations given by elemental analysis as $[CdBr_2(\mathbf{L5})_2]\cdot 6½H_2O$ (**4.14**) and $[Zn(\mathbf{L5})_4(H_2O)_2](\mathbf{L5})(ClO_4)_2\cdot 8H_2O$ (**4.15**), respectively. However, in the former case **L5** acts as a bidentate chelating ligand while, in the second instance **L5** is a monodentate donor. Complex **4.14** was obtained as clumps of colourless crystals in 65% yield from the slow evaporation of a methanol-water solution of cadmium(II) bromide and **L5**. The zinc complex, **4.15** was obtained as colourless block-shaped crystals in 54% yield from slow evaporation of a methanol solution of these components. A distictive peak at 1074 cm^{-1} was observed in the IR spectra of complex **4.15** which corresponds to the Cl-O stretch of the perchlorate anion. The synthesis of these complexes are summarised below.

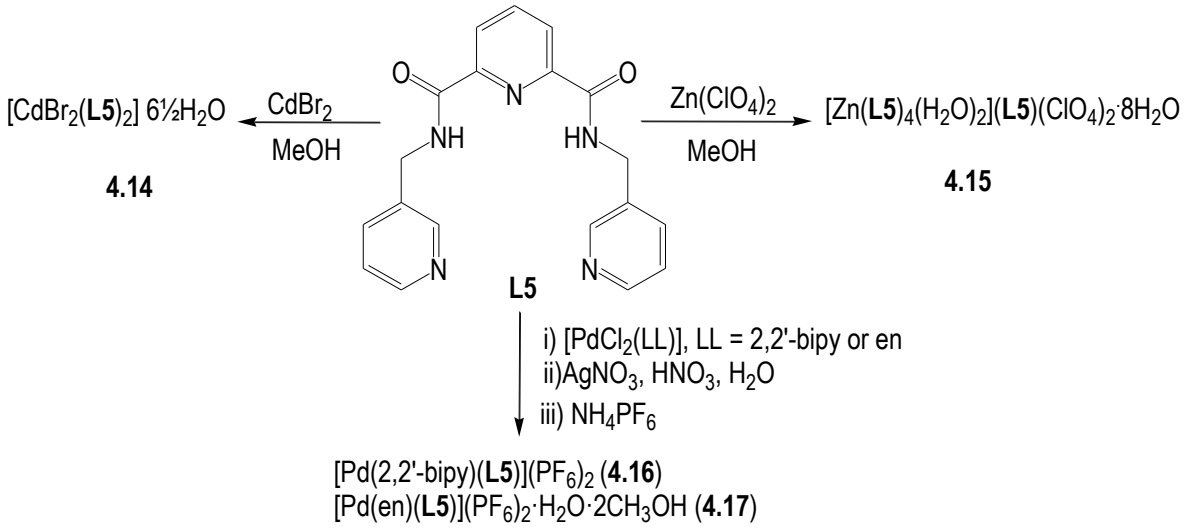

Scheme 4.2. The synthesis of the discrete complexes derived from **L5**.

Reactions of ligand **L5** with $[PdCl_2(2,2'\text{-bipy})]$ and $[PdCl_2(en)]$ gave two mononuclear metallomacrocylic complexes, $[Pd(2,2'\text{-bipy})(\mathbf{L5})](PF_6)_2$ (**4.16**) and $[Pd(en)(\mathbf{L5})](PF_6)_2 \cdot H_2O \cdot 2CH_3OH$ (**4.17**) in good yields. The palladium complexes were prepared based on the methods described in the literature. [105,308,341] The preparations of other discrete metal complexes were attempted under slow evaporation conditions with 1:2 metal-to-ligand ratios. Other approaches using different stoichiometries, such as 1:1, were also tried but under the conditions tried no isolatable products were obtained. The discussion on the crystal structures of complexes **4.14**, **4.15** and **4.16** are described in the following section.

Crystal structure of **4.14**

$[CdBr_2(L5)_2]\cdot 6½H_2O$. Complex **4.14** was obtained as colourless block-shaped crystals in 69% yield. The complex crystallises in the triclinic space group *P*-1 with one cadmium atom (on a centre of inversion), one molecule of **L5** and one coordinated bromide in the asymmetric unit. This molecule has intramolecular hydrogen bonding which pre-organises the NH amide moieties of the ligand into a central pocket (N1···H13 = 2.186 Å; N-H···N angle = 109.61°) and (N1···H17A = 2.294 Å; N-H···N angle = 106.51°) (Figure 4.6). The U-shaped conformation observed for the ligand crystallised as a pure compound is still observed structure of **4.14**. The two pendant 3-pyridyl rings twist out of the plane of the core of the ligand to coordinate to the

cadmium atom and adopt a bowl-like conformation as shown in the figure below (torsion angles for CO-NH-CH_2-C_{aryl} of 109.42 and 118.30°).

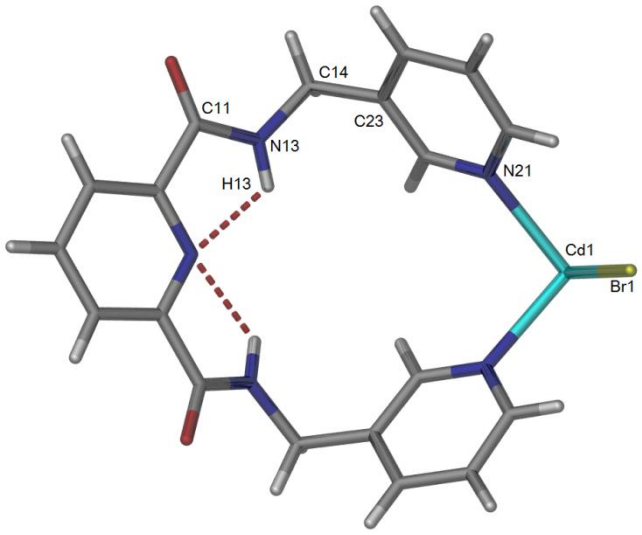

Figure 4.6. A perspective view of the asymmetric unit of **4.14** with the solvate molecules omitted for clarity. Selected bond lengths (Å) and angles (°) : Cd(1)-N(21) 2.410(10), Cd(1)-N(31) 2.391(10), Cd(1)-Br(1) 2.598(3), N(21)-Cd(1)-N(31) 96.00 (3), N(21)-Cd(1)-Br(1) 92.15(3), N(31)-Cd(1)-Br(1) 92.91(3).

The complete structure of complex **4.14** is shown in Figure 4.8. In this complex, the Cd(II) ion adopts an octahedral coordination environment with the bond lengths and angles typical for cadmium(II).[347] The Cd(II) ion is coordinated to four nitrogen atoms from two molecules of **L5** and two bromide anions (Figure 4.7(a)). The two molecules of **L5** occupy the equatorial positions of the cadmium centre while the two bromide anions occupy the axial sites. As noted the ligand forms a 16-atom chelate ring with a bowl-shaped arrangement (Figure 4.7(b)). These bowl structure point in opposite directions due to the inversion centre. Such large chelate rings are not very common but are still observed in a number of large ligand systems with convergent donors.[342] The pre-organising nature of the of the 2,6-pyridine dicarboxamide core favours chelation by providing greater rigidity to **L5**.

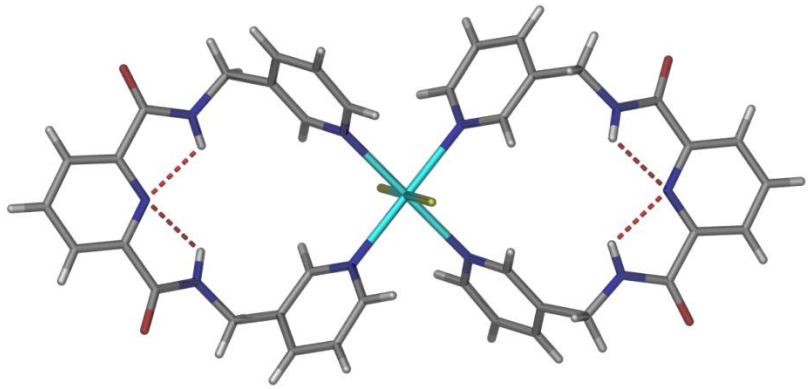

(a)

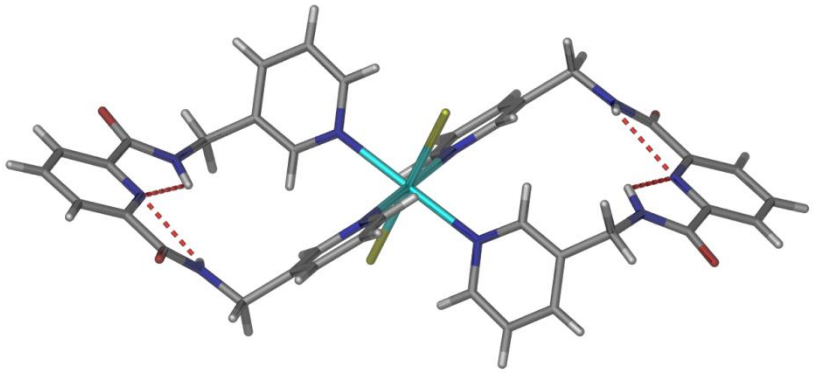

(b)

Figure 4.7. Two perspective views of the extended structure of complex **4.14**.

A consideration of the crystal packing in **4.14** showed that this complex is arranged into 1-D tapes that are stabilised by intermolecular interactions between the amide NH donors and the coordinated bromide anions of an adjacent complex (N-H···Br: *d* = 2.503 Å; *D* = 3.311 Å; *d* = 2.632 Å; *D* = 3.336 Å). The H···Br distance is comparable but slightly shorter than normal H···Br distance of 2.66 Å reported in the literature.[343] These hydrogen-bonded chains of discrete complexes are then interdigitated with adjacent chains. This packing motif is stabilised by centroid-centroid π-π stacking interaction between two central 2,6-pyridine dicarboxamide cores (centroid-centroid distance 3.707 Å) (Figure 4.8).

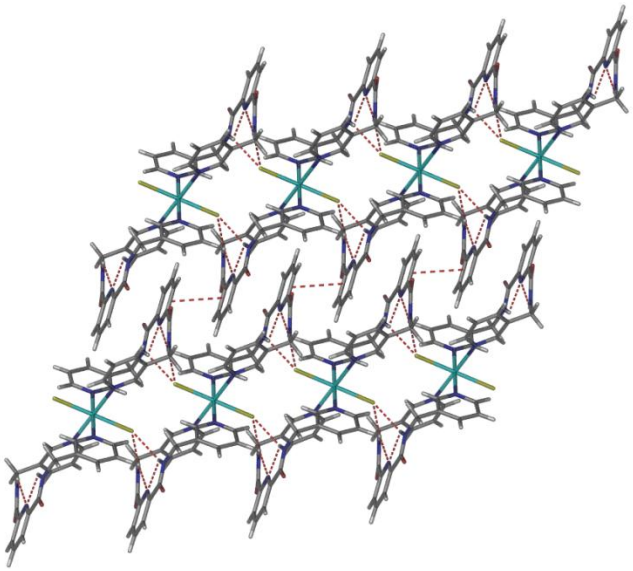

Figure 4.8. A perspective view of the crystal packing **4.14** showing the weak intramolecular and intermolecular hydrogen bonding interactions within the crystal structure. A π-stacking interaction is also observed between the two central 2,6-pyridine dicarboxamide cores of **L5** from adjacent hydrogen-bonded chains.

Crystal structure of **4.15**

$[Zn(L5)_4(H_2O)_2](L5)_2(ClO_4)_2 \cdot 8H_2O$. Ligand **L5** was reacted with $Zn(ClO_4)_2$ in methanol to yield colourless needle-shaped crystals in 54%. X-ray crystallography revealed that compound **4.15** has a significantly different coordination mode compared to all other complexes obtained with **L5**. In particular, the formation of complex **4.15** only involves coordination from one of the pendant pyridyl nitrogen donor of **L5**, while the second pendant nitrogen donor is not coordinated. Single crystal X-ray diffraction also revealed that this coordination compound crystallises in the triclinic space group *P*-1 with the zinc atom lying on the centre of inversion. The asymmetric unit consists of one Zn atom (on a centre of inversion), two coordinating ligands, one coordinated water molecule, one non-coordinated molecule of **L5**, three water solvate molecules and one non-coordinated perchlorate anion. Growing out the asymmetric unit reveals that the zinc atom is coordinated by four molecules of ligand **L5** and two coordinated water molecules to give octahedral environment about the zinc atom (Figure 4.9(a)). The 2,6-pyridine dicarboxamide moieties of the discrete complex make a number of hydrogen bonding interactions

with the non-coordinated perchlorate anions, water solvate molecules and non-coordinated ligand molecules (Figure 4.9(b)) as part of a rather complicated hydrogen bonding network.

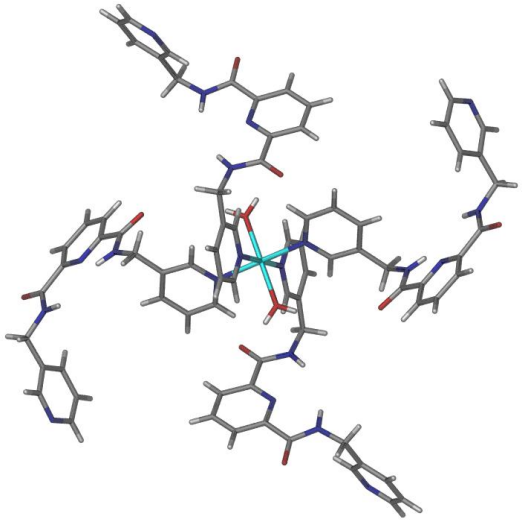

(a)

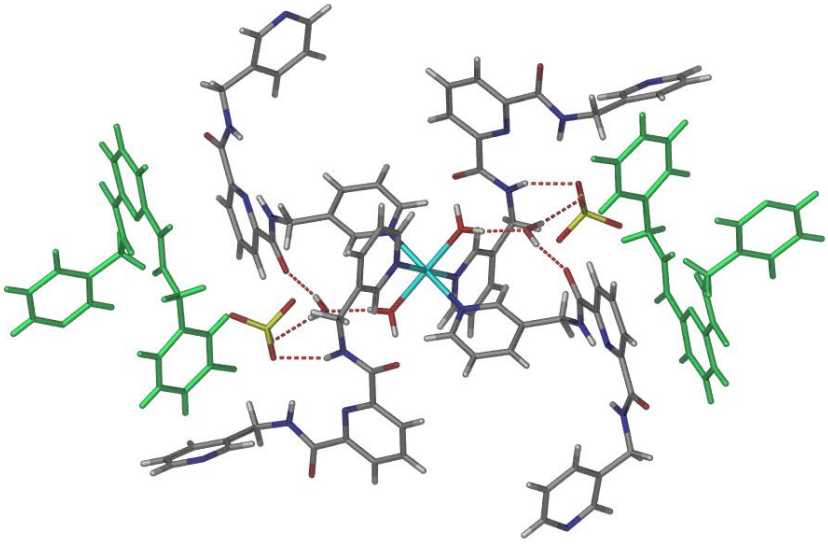

(b)

Figure 4.9. Two perspective views of the structure of complex **4.15**. The non-coordinated molecule of **L5** is shown in green.

As noted, there is extensive hydrogen bonding present in **4.15**. In particular, there are intermolecular hydrogen bonding interactions between the pre-organised NH amide donors of a coordinated ligand molecule and a water solvate molecule (d = 2.155, 2.156 Å and D = 2.984,

2.911 Å). There are also weak hydrogen bonds involving the pre-organised NH amide donors of the second coordinated molecule of **L5** and a perchlorate anion with an H···O hydrogen bond distance of 2.177 Å. An additional water molecule in the crystal lattice, hydrogen bonded to the carbonyl oxygen donors of a coordinated ligand (OH···O=C; *d* =1.978 Å, *D* = 2.841), also hydrogen bonds with the perchlorate anions. Extension of these interactions leads to the formation of 1-D hydrogen bonded network within the crystal (Figure 4.10).

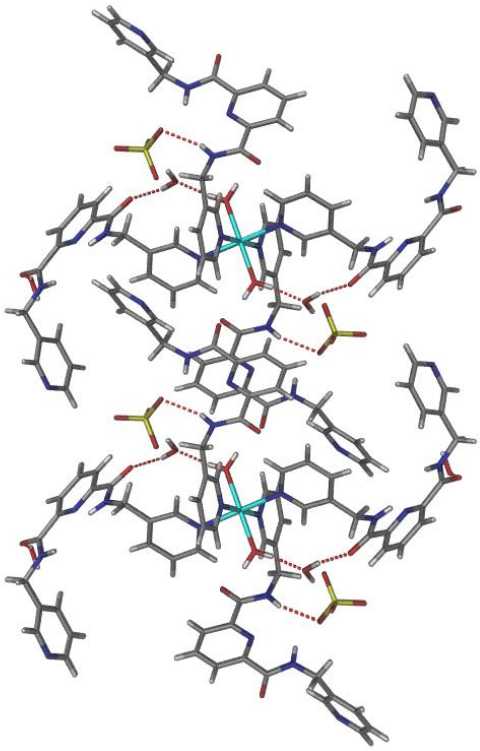

Figure 4.10. A perspective view of the crystal packing of complex **4.15** from the *a* axis. In this figure, the free ligand **L5** and also the solvate water molecules omitted for clarity.

Reactions of **L5** with cadmium(II) bromide and zinc(II) perchlorate had unexpectedly provided two discrete complexes. To deliberately generate such complexes, reactions with palladium metal salts that have two exchangeable coordination sites in a *cis* arrangement have been attempted. It was anticipated that two products could be obtained from each of these reactions, specifically a mononuclear complex [Pd(**L5**)] or a dinuclear [Pd_2(**L5**)$_2$] species (Figure 4.11).

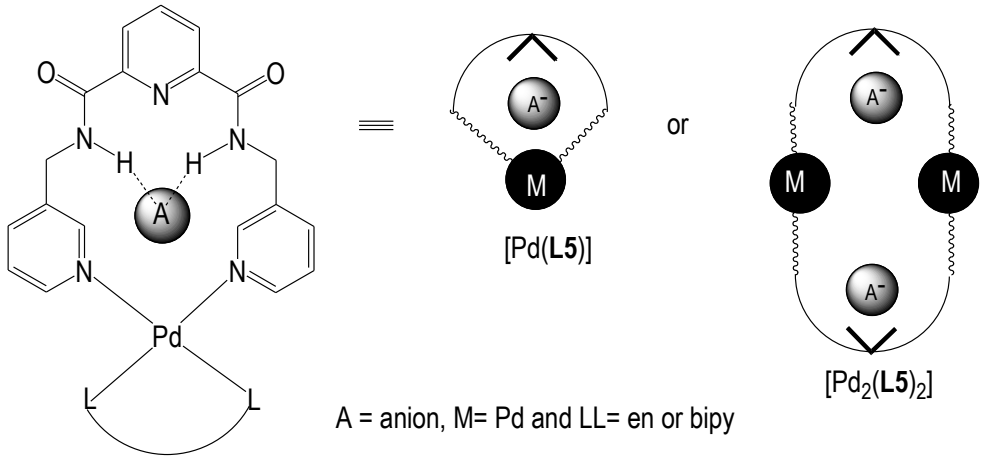

Figure 4.11. A diagram representing the structures of simple mononuclear or dinuclear metallo-supramolecular macrocycles proposed for reactions of **L5** with $[PdCl_2(2,2'\text{-bipy})]$ and $[PdCl_2(en)]$.

Such species might provide useful anion binding regions due to the pre-organised hydrogen bond donor pockets of the molecules of **L5** and an electrostatic contribution to anion binding provided by the palladium(II) centre. As mentioned earlier, reaction of **L5** with $[PdCl_2(2,2'\text{-bipy})]$ and $[PdCl_2(en)]$ gave rise to two mononuclear metallo-macrocylic complexes, $[Pd(2,2'\text{-bipy})(\mathbf{L5})](PF_6)_2$ (**4.16**) and $[Pd(en)(\mathbf{L5})](PF_6)_2{\cdot}H_2O{\cdot}2CH_3OH$ (**4.17**), respectively. Vilar,[80] has similarly studied the formation of related complexes with a bridging diamide ligand but a different chelating co-ligands (1,2-bis(diphenylphosphino)ethane) on the palladium centre. The palladium(II) complexes reported here were prepared based on literature procedures described for the formation of related palladium(II) supramolecular assemblies.[105,308,341] Ligand **L5** was reacted with $[PdCl_2(2,2'\text{-bipy})]$, which has been pre-treated with silver nitrate to remove the chloride anions, in a 1:1 ligand to metal ratio. After stirring for 15 minutes the resulting complex was treated with ammonium hexafluorophosphate and left to stir overnight at room temperature to give a white powder of $[Pd(2,2'\text{-bipy})(\mathbf{L5})](PF_6)_2$ (**4.16**) in 77% yield. In a similar manner, reaction of ligand **L5** with pre-treated $[PdCl_2(en)]$ gave complex $[Pd(en)(\mathbf{L5})](PF_6)_2{\cdot}H_2O{\cdot}2CH_3OH$ (**4.17**) which was also obtained as a white solid in 42% yield. A reaction of **L5** with dichloropalladium(II) bis(triphenylphosphine) $[PdCl_2(PPh_3)_2]$ was

attempted but, unfortunately, no isolable product was obtained despite exploring a number of conditions. This result may be a consequence of the apparent preference **L5** has for forming mononuclear [Pd(**L5**)] complexes; in the product of the reaction of **L5** with $[PdCl_2(PPh_3)_2]$ the triphenylphosphine co-ligands were expected to be arranged *trans* and this would make it difficult for the pyridyl donors of **L5** to chelate the palladium centre (Figure 4.12). In contrast, the formation of a dinuclear $[Pd_2(\mathbf{L5})_2]$ would be favoured by such a metal but the convergent arrangement of the pyridyl donor might disfavour such a species.

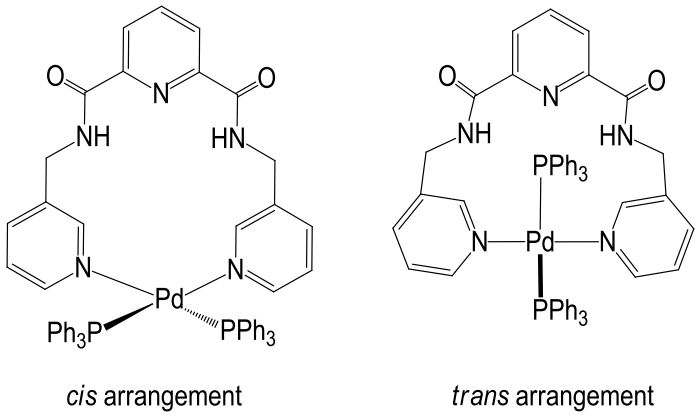

Figure 4.12. A representation of the possible conformations of $[Pd(\mathbf{L5})(PPh_3)_2]$ with the triphenylphosphine (PPh_3) co-ligands in a *cis* or *trans* arrangement.

Electrospray ionisation mass spectrometry (ESI-MS) confirmed the formation of 1:1 discrete metallo-macrocycle complexes in solution for both **4.16** and **4.17**. The ESI-MS conducted in acetonitrile-methanol indicates a low abundance peak at *m/z* 755.3 corresponding to the $[Pd(2,2'\text{-bipy})(\mathbf{L5})]^+$ species. A peak at *m/z* 513.2 was observed for the $[Pd(en)(\mathbf{L5})]^+$ species, also in a relatively low abundance. In the IR spectra, several characteristic strong bands of **L5** were found at 3385, 1667 and 1537 cm^{-1} for complex **4.16** and 3231, 1671 and 1541 cm^{-1} for complex **4.17**. The N-H and C=N stretches of the ligand were shifted to the higher frequency due to the chelation of the ligand to the palladium centre. The ^1H NMR spectra of complex **4.16** and **4.17** were consistent with a symmetrical compound, and consistent with the formula suggested by elemental analysis. In complex $[Pd(2,2'\text{-bipy})(\mathbf{L5})](PF_6)_2$ (**4.16**), the resonance at 9.89 ppm was assigned to the NH peak and the 2,2'-bipyridine protons have signals between 7.25-7.83 ppm. A peak at 4.36 which appears as the expected doublet was assigned to the methylene protons. In the

NMR spectrum of **4.17**, the resonance for NH amide appears slightly further upfield at 9.76 ppm, compared to complex **4.16**. The pendant pyridine and pyridine core protons have signals between 7.64-8.89 ppm, while the methylene group has appears as a doublet at 4.77 ppm. A signal at 5.26 ppm corresponds to the methylene group (-CH_2-) and 5.26 ppm corresponds to (NH_2) from ethylenediamine spacer. The aromatic regions of the ^{1}H NMR spectra of complexes [Pd(2,2'-bipy)(**L5**)]$(PF_6)_2$ (**4.16**), [Pd(en)(**L5**)]$(PF_6)_2 \cdot H_2O \cdot 2CH_3OH$ (**4.17**) and ligand **L5** are shown in Figure 4.13.

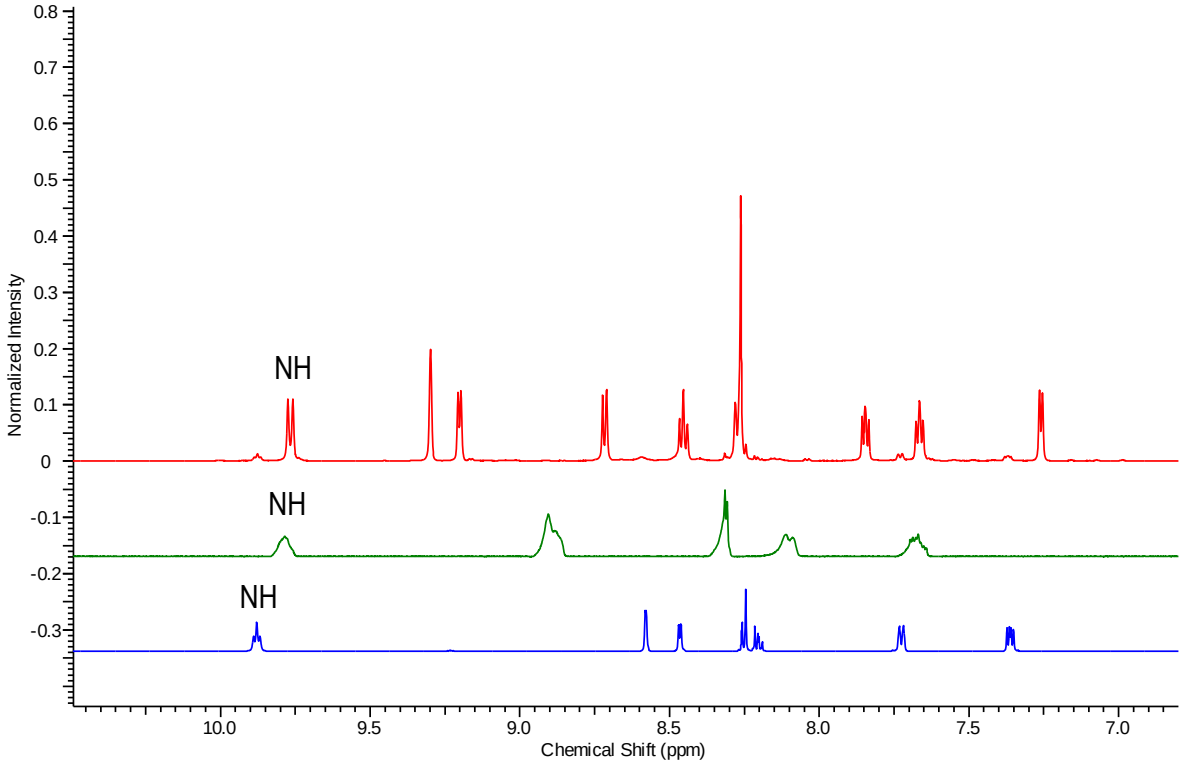

Figure 4.13. The aromatic region of the ^{1}H NMR spectrum of complex **4.16** (red), **4.17** (green) and ligand **L5** (blue) recorded in DMSO-d_6.

A comparison of the ^{1}H NMR spectra for **4.16** and **4.17** and the coordination induced shifts (CIS) calculated for **4.16** and **4.17** are shown in Table 4.1. There are significant changes in the chemical shifts for the H2'/H6' of the pendant pyridine of **L5** in both complexes, although these are significantly more pronounced for **4.16** possessing the 2,2'-bipyridine ancillary ligand.

An aspect of the shifts of these protons is due to the coordination of the pyridyl nitrogen atom to the palladium centre, but as demonstrated by more dramatic changes for **4.16**, also due to the coordination bringing the pendant pyridyl ring into the deshielding region of the 2,2'-bipyridine ancillary ligand.

Table 4.1. ^{1}H NMR chemical shift values for the pyridine pendant rings of ligand **L5** and the complexes **4.16** and **4.17** recorded in DMSO-d_6, with the CIS values shown in italics.

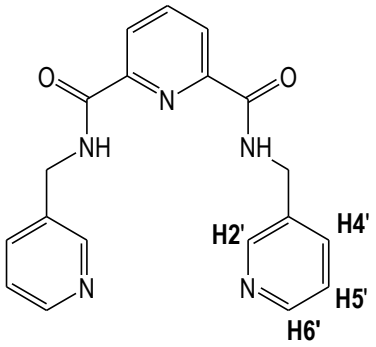

Compounds	NH	CH_2	H2'	H6'	H4'	H5'
L5	9.88	4.63	8.58	8.47	7.72	7.36
4.16	9.89	4.36	9.76	9.28	8.44	8.27
CIS	*0.01*	*-0.27*	*1.18*	*0.81*	*0.72*	*0.91*
4.17	9.76	4.77	8.89	8.85	8.08	7.64
CIS	*-0.12*	*0.14*	*0.31*	*0.38*	*0.36*	*0.28*

To further examine the structure of these complexes in solution and to confirm the ^{1}H NMR spectral assignments, complexes **4.16** and **4.17** were analysed by ^{1}H^{1}H COSY and 2D NOESY techniques, in DMSO-d_6. The ^{1}H^{1}H COSY showed, as expected, a correlation between the protons at the methylene linker -CH_2- and the amide NH protons. The downfield peaks were assigned to the individual pyridyl rings from correlations in the COSY spectrum. More importantly, a through space interaction was observed between the H6' protons of the pendant pyridyl ring of **L5** and the H6' protons of the 2,2'-bipyridine co-ligand in complex **4.16**. The same through space interaction was also observed in complex **4.17**, between the H6' protons of the pendant pyridyl ring of **L5** and the NH_2 protons of the ethylenediamine spacer (Figure 4.14).

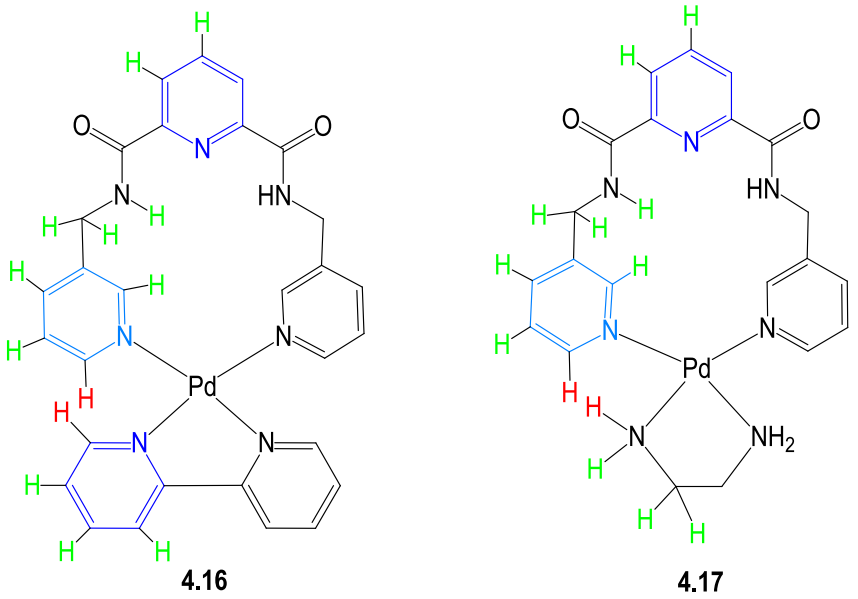

Figure 4.14. The protons correlations indicated by the $^{1}H^{1}H$ COSY experiments are marked in green, the COSY correlations to aromatic region are marked in blue while the through space interactions indicated by 2D NOESY experiments are marked in red.

Diffusion-ordered spectroscopy (DOSY) was used to further investigate the behaviour of these complexes in solution. DOSY NMR is commonly used to identify different compounds in a mixture based on the differing translational diffusion coefficients. This technique is useful to estimate the relative size of a molecule from a comparison of the diffusion rates.[344] DOSY revealed that complex **4.16** has a diffusion coefficient of 0.60 ± 0.01 x 10^{10} m^2/s. The diffusion coefficient of **4.17** under the same condition was 0.62 ± 0.02 x 10^{10} m^2/s. The original ligand (**L5**) has a diffusion coefficient of 0.98 ± 0.02 x 10^{10} m^2/s and the calculated ratio $D_{\mathbf{4.16}}/D_{\mathbf{L5}}$ and $D_{\mathbf{4.17}}/D_{\mathbf{L5}}$ for both mononuclear complexes are 0.60 and 0.63, respectively. Surprisingly, this value is lower from the theoretical ratio of 0.72 – 0.75 expected for a dimeric species of hard spheres[345,346] and within the range of large species such as trimer of hard spheres.[345] This surprisingly slow diffusion rate may be a factor of the vastly different hydrodynamic radii of the unreacted ligand and the bowl-shaped mononuclear palladium complexes. Furthermore, complexation of the anions might increase the hydrodynamic radii of the complex, hence slowing its diffusion rate further. Nonetheless, the results showed that the relative sizes of complexes **4.16** and **4.17** are almost similar. As an attempt to provide further understanding of the structure of

these compounds, **4.16** and **4.17** were dissolved in a mixture of acetonitrile-methanol and left to evaporate at room temperature. After several weeks, complex **4.17** crystallised as plate-like colourless crystals which were suitable for X-ray crystallography. Unfortunately, crystals of **4.16** were not obtained by any recrystallisation approaches.

Crystal structure of **4.17**

[Pd(en)(L5)](PF$_6$)$_2$·H$_2$O·2CH$_3$OH. Complex **4.17** crystallises in the monoclinic space group $P2_1/n$ with one complete molecule of **L5** chelating the palladium(II) ethylenediamine centre, two hexafluorophosphate anions and two methanol molecules and one water in the asymmetric unit. The palladium atom adopts a distorted square planar geometry with typical Pd-N bond lengths (2.024(6) – 2.045(6) Å) and angles (84.51(2) – 92.94(3)°).[347] Similar distances and angles are observed in related mononuclear complexes with palladium.[167,93] The palladium atom is coordinated by two nitrogen donors from the pyridyl groups and two nitrogen atoms from the ethylenediamine ancillary chelating ligand. In this complex, ligand **L5** maintains the U-shape conformation with the amide hydrogen bond donors (N1···H4 = 2.239 Å; N-H···N angle = 107.82°) and (N1···H31 = 2.268 Å; N-H···N angle = 108.13°) controlling the conformation of **L5** (Figure 4.15) and favouring a chelating as opposed to bridging coordination mode in this instance.

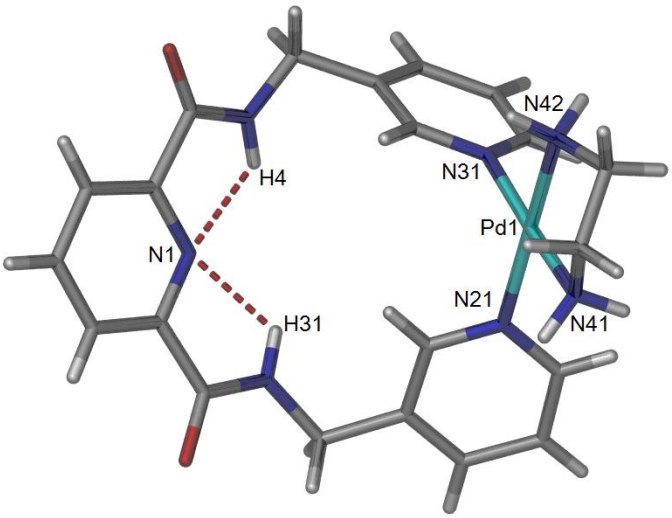

Figure 4.15. A perspective view of the asymmetric unit of complex **4.17** with hexafluorophosphate anions, methanol and water solvate molecules omitted for clarity. Selected

bond lengths (Å): N(21)-Pd(1) 2.024(6), N(31)-Pd(1) 2.028(6), N(41)-Pd(1) 2.017(3) ,N(42)-Pd(1) 2.046(5), N(31)-Pd(1)-N(21) 90.42(2), N(31)-Pd(1)-N(40) 92.94(2), N(41)-Pd(1)-N(42) 84.51(2) and N(21)-Pd(1)-N(41) 91.93(2).

In this complex, twisting of the ligand enables the macrocycle to form a bowl-like structure with one hexafluorophosphate anion encapsulated at the centre of the macrocycle (Figure 4.16). The 3-pyridyl rings twist out of the plane of the core of **L5**, and coordinate the palladium centre to form the metallo-macrocycles (torsion angles for C11-N13-C14-C23 are 110.42 – 112.17°). In similar manner to complex **4.14**, and other bowl-shaped copper metallo-macrocycles described in Chapter 3, the -CH_2- spacer in **L5** provides a hinge in the structure to enable formation of a bowl or cleft-like structure. It is well known that the use of flexible ligands provide access to supramolecular clefts or clips[233,235,236] or shallow bowl-like structures.[237-242] The structure of this complex is also similar to other palladium(II) complexes obtained with angular bispyridyl amide ligands.[316]

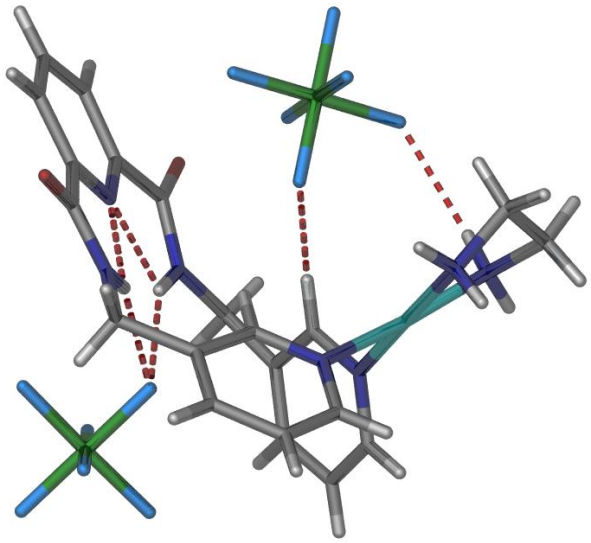

Figure 4.16. A perspective view of complex **4.17** showing one PF_6^- located inside the cavity of the macrocycle and bound through hydrogen bonding interactions with the en NH and $C_{py}H$ donors and anion-π interactions. A second, extra-cavity PF_6^- anion is hydrogen bonded by the 2,6-pyridine dicarboxamide groups. Weak intramolecular and intermolecular hydrogen bonding interactions between the pre-organised amide NH and the PF_6^- anions are shown.

The encapsulation of one hexafluorophosphate (PF_6) anion within the cavity of **4.17** is stabilised by weak C-H···F hydrogen bonding with ligand **L5**; the C···F distance is 3.297 Å, while the F···H distance is 2.501 Å. This is shorter than the sum of van der Waals radii of 2.67Å. The hexafluorophosphate anions also form hydrogen bonds with the co-ligand, ethylenediamine (N-H···F, d = 2.379, D = 3.113 Å). Finally, the encapsulation is stabilised by anion-π contacts between the anion and the central pyridine ring. The shortest contact between the centroid of the pyridine ring is 3.197 Å. This is comparable to such anion-π interactions previously reported in the literature for solid-state structures.[248,249] The second hexafluorophosphate anion is also hydrogen bonded to the complex and forms two intermolecular hydrogen bonding interactions involving the pre-organised NH amide donors (d = 2.342 and 2.324 Å), although this anion is located on the outside of the metallo-supramolecular bowl.

4.2.1.2. Discrete complexes of L6

While reaction of **L5** provided only discrete mononuclear metallo-macrocyclic complexes, reaction of ligand **L6** with pre-treated [$PdCl_2$(2,2'-bipy)] and [$PdCl_2$(en)] led to two different outcomes. Under the conditions used for reactions involving **L5**, the reaction of **L6** with [$PdCl_2$(2,2'-bipy)] led to the formation of a mixture of supramolecular isomers, proposed to be [Pd(2,2'-bipy)(**L6**)]$(PF_6)_2$ (**4.18a**) and [{Pd(2,2'-bipy)}$_2$(**L6**)$_2$]$(PF_6)_4$ (**4.18b**), while reaction of **L6** with [$PdCl_2$(en)] gave a single entity, [{Pd(en)}$_2$(**L6**)$_2$]$(PF_6)_4$ (**4.19**) (Scheme 4.3). [Pd(2,2'-bipy)(**L6**)][PF_6]$_2$ (**4.18a**) and [{Pd(2,2'-bipy)}$_2$(**L6**)$_2$]$(PF_6)_4$ (**4.18b**) were obtained as a mixture in approximately a 1:1 ratio based on ^{1}H NMR spectroscopy from reactions conducted under similar condition described for **L5**. The formation of supramolecular isomers was also supported by elemental analysis consistent with either mononuclear [1+1] and dinuclear [2+2] species in the bulk samples. Despite several attempts, the mixtures of **4.18a** and **4.18b** could not be separated, nor could a sample obtaining only one species be obtained by altering the reaction conditions. The ^{1}H NMR spectrum recorded in DMSO-d_6 shows that both compounds are in equilibrium. The IR spectrum of the mixture revealed characteristic strong bands for the ligand with C=O and C-N stretches at 1642 and 1448 cm^{-1}, respectively.

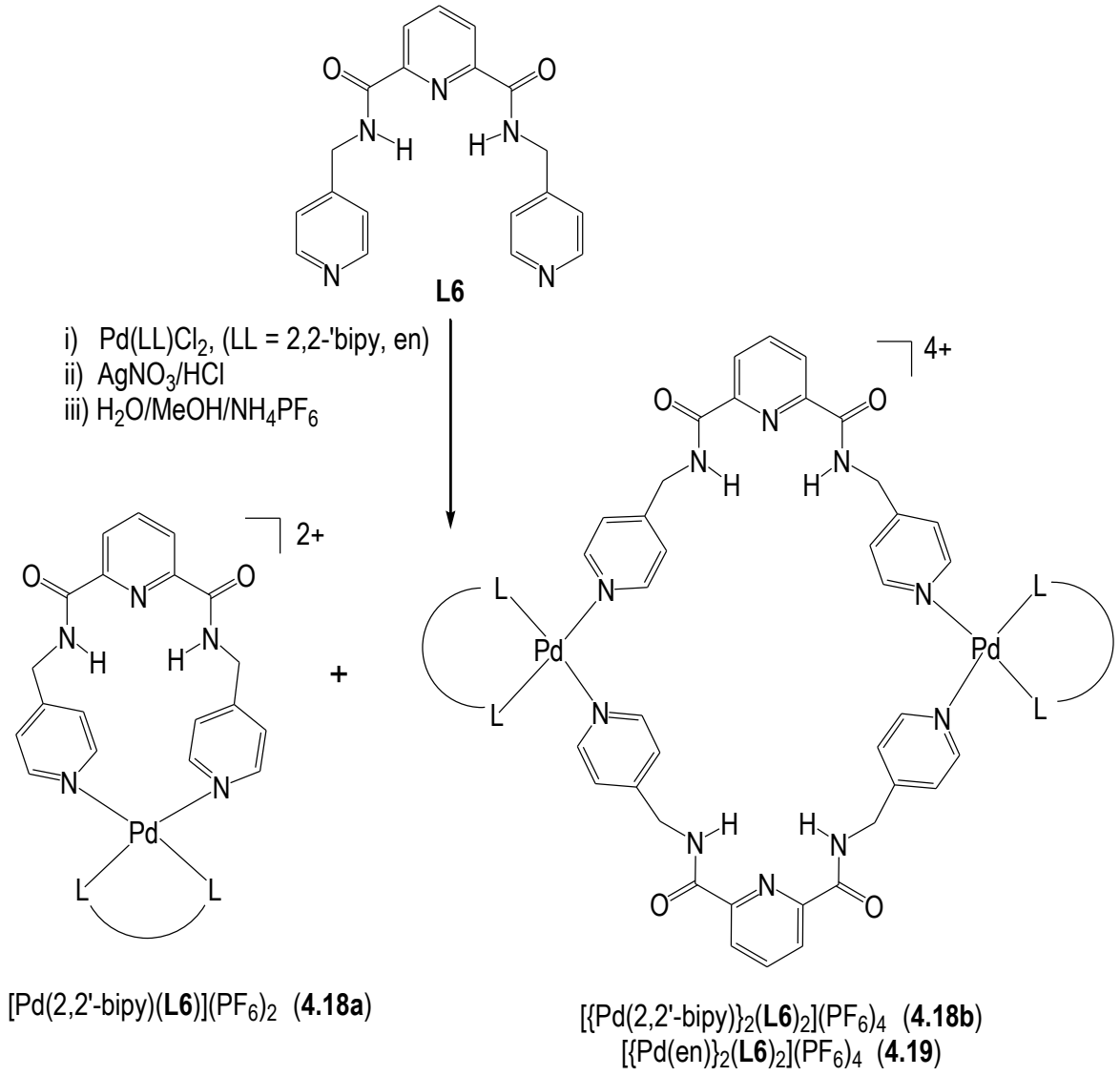

Scheme 4.3. The synthesis of metallo-supramolecular cages incorporating **L6**.

DOSY NMR was employed to identify and distinguish the combined species based on their differing diffusion coefficients. DOSY spectrum of complexes **4.18a** and **4.18b** showed, three major groups of peaks corresponding to the dinuclear and mononuclear complexes, and ligand **L6** (Figure 4.17). The assignment of the species was undertaken by examining the mixture at different concentrations which altered the relative amounts of the two complexes. The diffusion coefficients of these two species **4.18a** and **4.18b** are $0.50 \pm 0.01 \times 10^{10}$ m^2/s and $0.42 \pm 0.01 \times 10^{10}$ m^2/s, while the calculated ratio $D_{\mathbf{4.18a}}/D_{\mathbf{L6}}$ and $D_{\mathbf{4.18b}}/D_{\mathbf{L6}}$ (where diffusion coefficient for **L6** is $0.87 \pm 0.02 \times 10^{10}$ m^2/s) are 0.57 and 0.48, respectively.

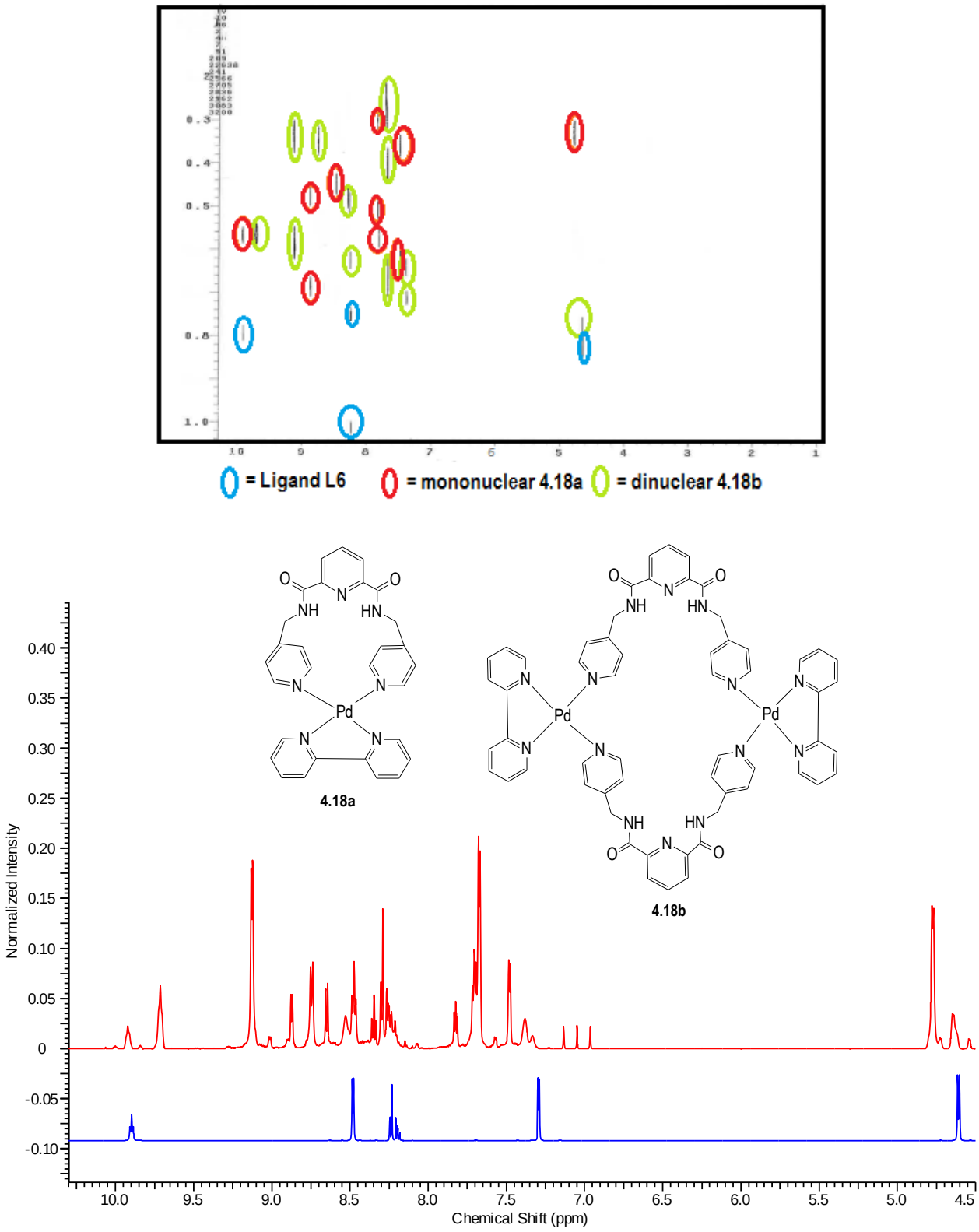

Figure 4.17. The DOSY NMR spectrum for compounds [Pd(2,2'-bipy)(**L6**)]$(PF_6)_2$ (**4.18a**) and [{Pd(2,2'-bipy)}$_2$(**L6**)$_2$]$(PF_6)_4$ (**4.18b**) and the ^{1}H NMR spectrum of the mixture (red) and ligand **L5** (blue) recorded in DMSO-d_6 from region 4.5 – 10.6 ppm.

Under the same conditions, reaction of **L6** with pre-treated $[PdCl_2(en)]$ gave only one product, proposed to be $[\{Pd(en)\}_2(\mathbf{L6})_2](PF_6)_4$ (**4.19**). In some attempts the presence of residual **L6** was also observed but at low concentrations. In the mid-IR spectra, distinctive ligand N-H, C=O and C=N stretches were observed at 3189, 1528 and 1431 cm^{-1}, respectively. This time the ESI-MS, conducted in acetonitrile-methanol for **4.19**, revealed peaks at *m/z* 511.9, 1172.6 and 1316.8 corresponding to a dinuclear species and fragmentation of such a species. DOSY analysis was used to assist in the identification of the product based on its diffusion rate. DOSY indicated that the diffusion coefficients for **4.19** to be 0.48 ± 0.02 x 10^{10} m^2/s and the calculated ratio of diffusion coefficients $D_{\mathbf{4.19}}/D_{\mathbf{L6}}$ to be 0.55 (Figure 4.18).

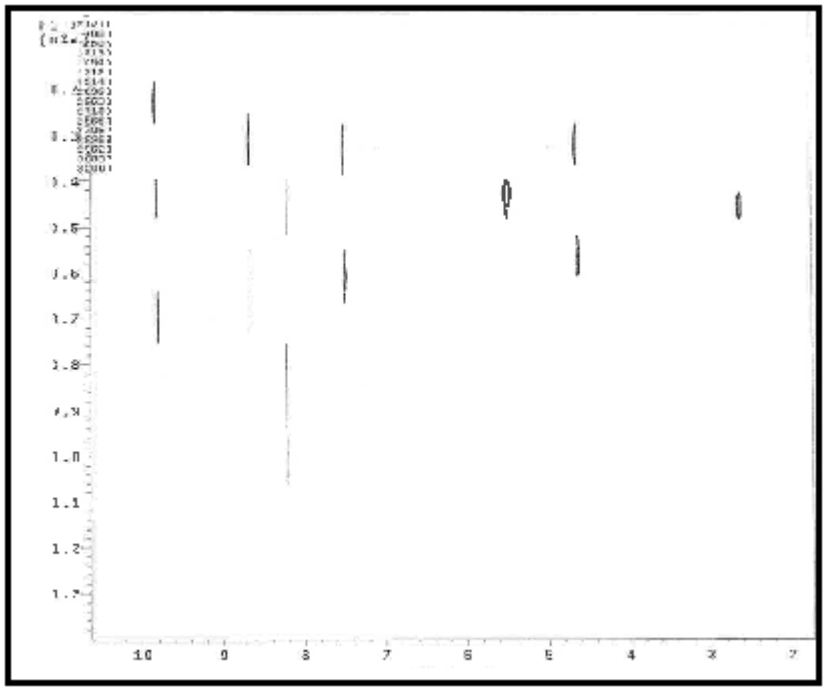

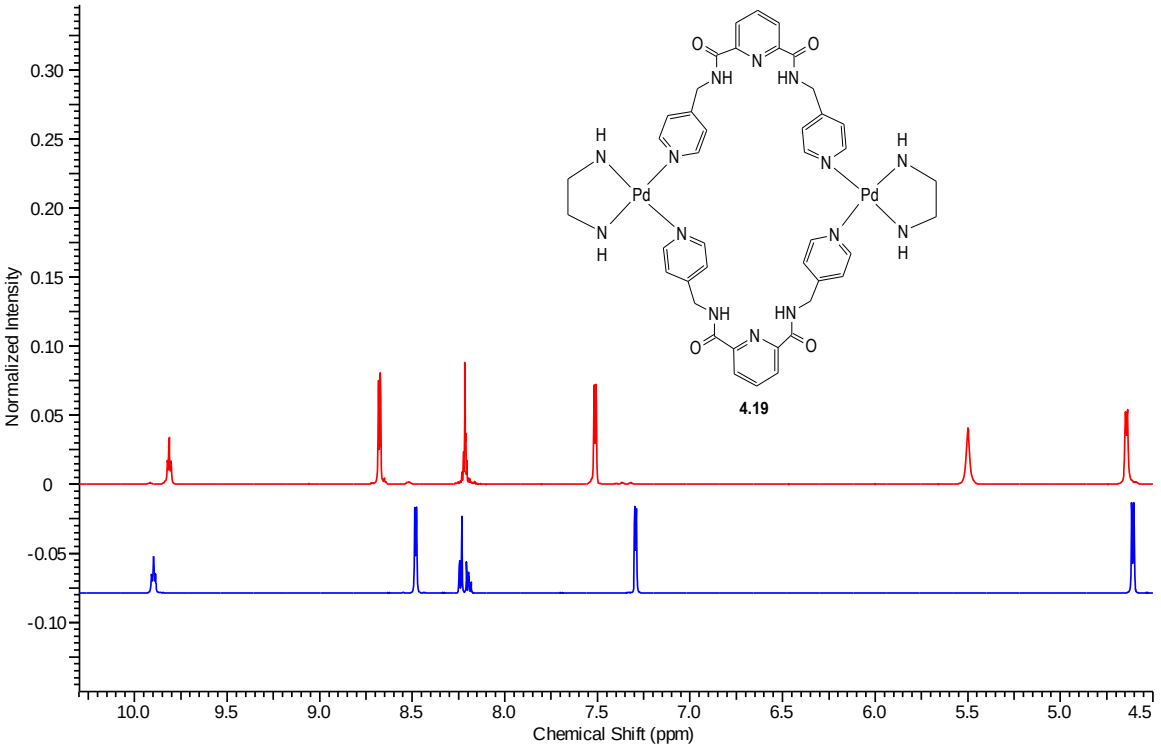

Figure 4.18. The DOSY NMR spectrum of $[\{Pd(en)\}_2(\mathbf{L6})_2](PF_6)_4$ (**4.19**) and the ^1H NMR spectra of **4.19** (red) and **L6** (blue) recorded in DMSO-d_6.

A comparison of the ^{1}H NMR spectra for **4.19** and the coordination induced shifts (CIS) calculated for **4.19** are shown in Table 4.1. There are minor changes in the chemical shifts for the protons from the NH and H2' of the pendant pyridine of **L6**.

Table 4.2. ^{1}H NMR chemical shift values for the pyridine pendant rings of ligand **L6** and the complexes **4.19** recorded in DMSO-d_6, with the CIS values shown in italics.

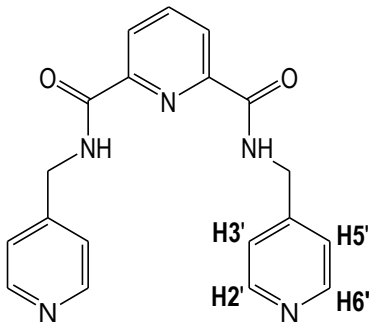

Compounds	NH	CH_2	H2'	H6'	H3'	H5'
L6	9.90	4.60	8.49	8.24	8.20	7.30
4.19	9.82	4.66	8.69	8.23	8.22	7.53
CIS	*-0.08*	*0.06*	*0.20*	*-0.01*	*0.02*	*0.23*

Two different outcomes occur for reaction of *cis*-capped palladium(II) species with **L5** and **L6**. For **L5** the more convergent arrangement of the pendant pyridyl donors contribute to the mononuclear palladium species being favoured in these reactions. In reactions of **L6** the expected dinuclear metallomacrocycle is obtained for reactions with [$PdCl_2$(en)]; very similar dipalladium metallo-macrocyles were reported in the work of Vilar.[316] The situation with [$PdCl_2$(2,2'-bipy)] was more complicated; the expected dinuclear species obtained from the assembly of [$PdCl_2$(2,2'-bipy)] with **L6** is shown in Figure 4.19. The additional steric bulk of the 2,2'-bipyridine capping group must favour the formation of mononuclear palladium complexes, while the divergent nature of the donors in **L6** preferences the assembly of dinuclear species. These effects appear to act in competition to produce a mixture.

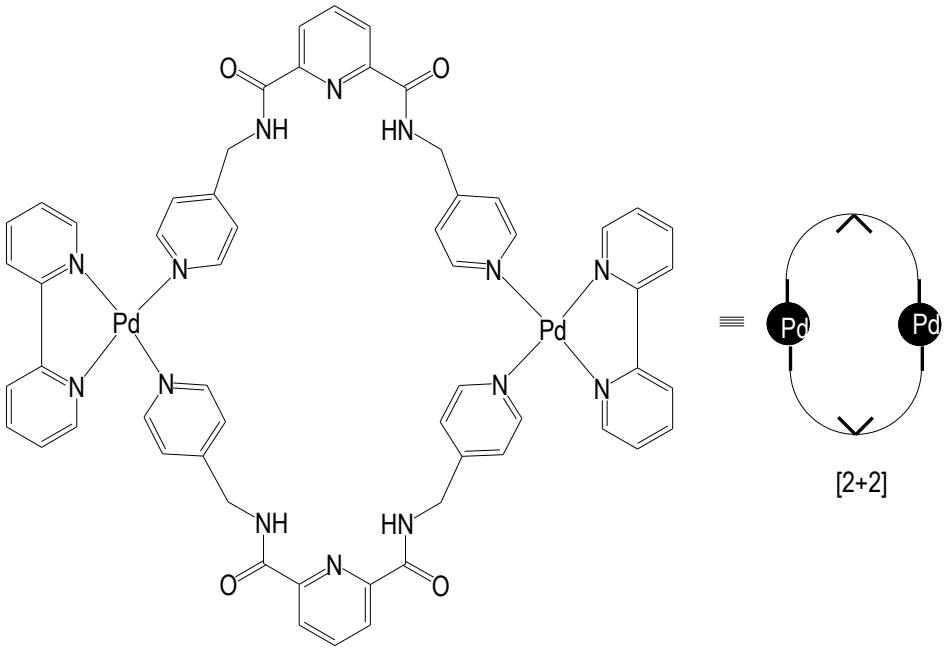

Figure 4.19. The assembly of dinuclear species with **L6**.

As described earlier, reaction of **L5** with $[PdCl_2(PPh_3)_2]$ failed to provide isolatable products. However, reaction of **L6** with $[PdCl_2(PPh_3)_2]$ provided a novel discrete dinuclear species $[\{Pd(PPh_3)_2\}(\mathbf{L6})_2](PF_6)_4 \cdot 2CH_3OH$ (**4.20**). This compound was synthesised based on the literature procedure described by Steel and co-worker.[308] To synthesis this complex, $[PdCl_2(PPh_3)_2]$ was reacted with silver triflate in dichloromethane and acetonitrile to form the intermediate $[Pd(OTf)_2(PPh_3)_2]$. This compound was isolated as pale yellow oil after removal of the solvent on the rotary evaporator. The oil was re-dissolved in dichloromethane and combined with **L6** and ammonium hexafluorophosphate. This mixture was stirred for three days, the solvent removed to give dark yellow oil that was triturated in chloroform/diethyl ether to give a pale yellow solid. The solid was collected and recrystallised from methanol to give a fine cream solid of complex **4.20** in 55% yield (Scheme 4.4). Elemental analysis supported the formula for mononuclear species as a trihydrate. The ES-MS indicated a peak at *m/z* 1122.4 which corresponds to the fragmentation of the dinuclear species.

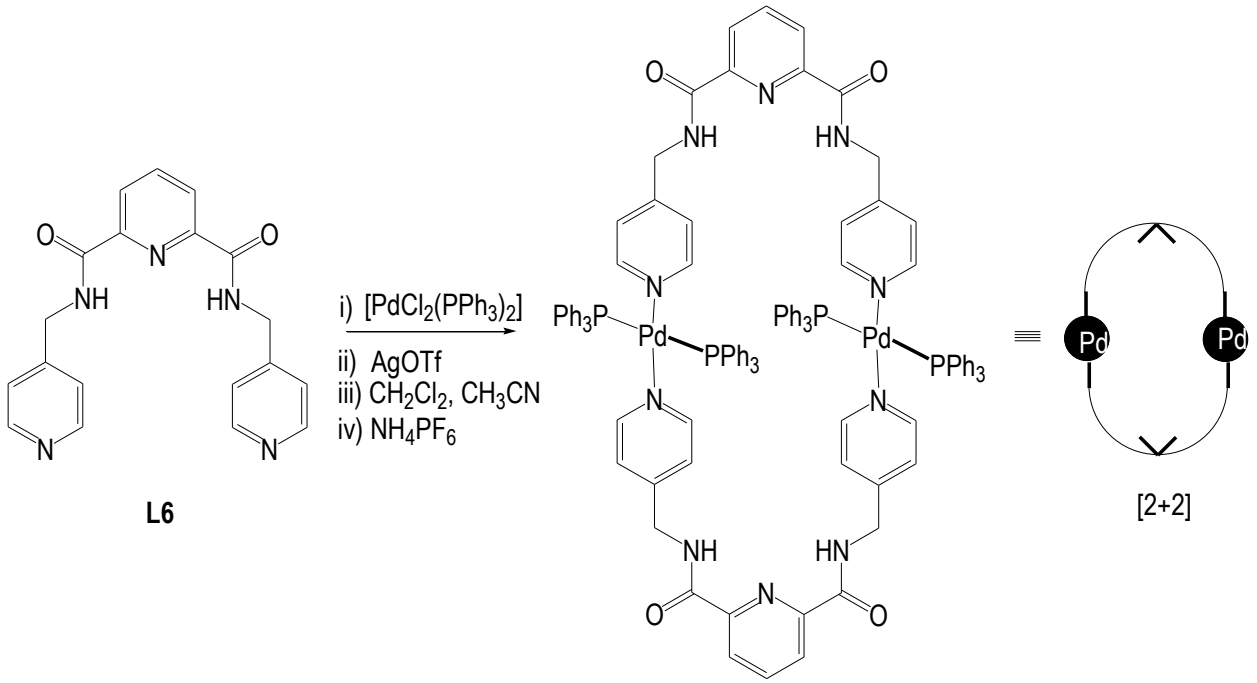

Scheme 4.4. The synthesis of dinuclear $[\{Pd(PPh_3)_2\}(\mathbf{L6})_2](PF_6)_4 \cdot 2CH_3OH$.

The ^{1}H NMR spectrum of complex **4.20** recorded in DMSO-d_6 indicated the presence of a single symmetrical product with a minor impurity. Analysis of the ^{1}H NMR spectrum found that the signals could be unambiguously assigned to **4.20**. A singlet signal at 9.91 ppm corresponds to the amide NH protons. The combination of two signals from H2' and H6' gave a broad peak at 8.70 - 8.5 ppm. The signals of H3 and H5 from the pyridine were found at 8.31 and 8.24 ppm. The proton, from the centre of the pyridine core, H4, was combined with H3'/H5' signals and triphenylphosphine protons signals to give a broad peak at approximately 7.65 ppm to 7.23 ppm. The multiplet peak at 4.63 ppm corresponds to the CH_2 protons from the methylene linker adjacent to the pyridine. Table 4.2 shows comparison of the ^{1}H NMR spectra for **4.20** and the ligand, as well as the coordination induced shift (CIS) for **4.20**. There are noticeable upfield chemical shifts for H2'/H6' of the pendant pyridyl ring due to the coordination by the palladium centre.

Table 4.3. ^{1}H NMR chemical shift values for the pyridine pendant rings of ligand **L6** and complex **4.20** recorded in DMSO-d_6, with the CIS values shown in italics.

Compounds	NH	CH_2	H2'	H6'	H3'	H5'
L6	9.88	4.63	8.58	8.47	7.72	7.36
4.20	9.14	4.36	8.48	8.27	8.15	7.93
CIS	*-0.74*	*-0.14*	*-0.1*	*-0.20*	*0.43*	*0.37*

4.3. Synthesis of coordination polymers of L5 and L6

As outlined earlier, these studies have been in part targeted toward the incorporation of flexible amide ligands into coordination polymers capable of generating novel binding sites for anions (Figure 4.5). Thus, the flexible diamides **L5** and **L6** were reacted with a range of transition metal salts containing both coordinating and non-coordinating anions.

4.3.1. Synthesis of coordination polymers of L5

As discussed in the previous section, reactions of **L5** with cadmium(II) bromide and zinc(II) perchlorate had provided two discrete complexes, **4.12** and **4.13** with two different coordination modes. Further reactions of **L5** with cadmium(II) nitrate, cadmium(II) perchlorate and cobalt(II) nitrate led to the formation of three isomorphous dinuclear M_2L_2 metallo-macrocyclic based coordination polymers, $\{[Cd(\mathbf{L5})_2(H_2O)_2](NO_3)_2{\cdot}H_2O\}_n$ (**4.21**), $\{[Cd(\mathbf{L5})_2(H_2O)_2](ClO_4)_2\}_n$ (**4.22**) and $\{[Co(\mathbf{L5})_2(H_2O)_2](NO_3)_2{\cdot}3H_2O\}_n$ (**4.23**), respectively. Reaction of **L5** with copper acetate also provided a 1-D coordination polymer, $\{[Cu_3(\mathbf{L5}\text{-}2H)_2(CH_3COO)_2(H_2O)_2(CH_3OH)_2]{\cdot}5(CH_3OH)\}_n$ (**4.24**) in which the diamide moiety has been deprotonated. A summary of the synthesis of the 1-D coordination polymers is shown in Scheme 4.5.

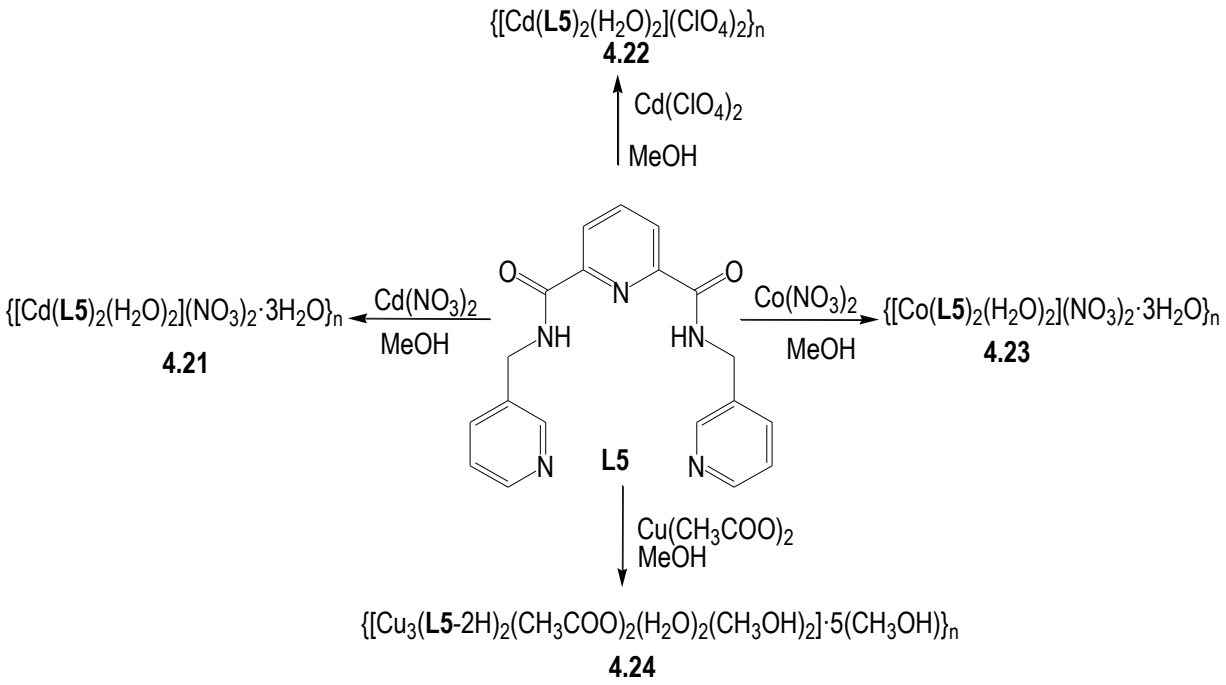

Scheme 4.5. Synthesis of coordination polymers of **L5**.

X-ray crystallography revealed that compounds $\{[Cd(\mathbf{L5})_2(H_2O)_2](NO_3)_2\cdot H_2O\}_n$ (**4.21**), $\{[Cd(\mathbf{L5})_2(H_2O)_2](ClO_4)_2\}_n$ (**4.22**) and $\{[Co(\mathbf{L5})_2(H_2O)_2](NO_3)_2\cdot 3H_2O\}_n$ (**4.23**) are three isomorphous coordination polymers. These compounds display necklace-like motifs with the ligands being connected through metal nodes to form a macrocyclic repeating structure.[102] Like the coordination polymers described in Chapter 3, these coordination polymers are formed from dinuclear metallo-macrocyclic $[M_2L_2]$ species, although the metal centres are points of intersection and thus the metallo-macrocycles cannot exist independently. These compounds are isomorphous in the solid-state with the only differences being subtle differences in bond lengths and angles. Complexes **4.21, 4.22** and **4.23** were all prepared *via* a slow evaporation approach. This typically required heating solutions of the metal salts and ligand in 1:2 metal-to-ligand ratios for approximately 45 minutes and then leaving them to evaporate for a period of days to weeks to yield the crystalline products. In the IR spectra of **4.21** and **4.23**, an N-O stretch was observed at approximately 1384 cm^{-1}, while in the case of compound **4.22**, a distinctive Cl-O stretch was observed at 1070 cm^{-1}. The N-H and C=N stretches of the ligands were also shifted to the higher frequency due to the chelation of the ligand to the metal centre. The formulations of all coordination polymers $\{[Cd(\mathbf{L5})_2(H_2O)_2](NO_3)_2\cdot H_2O\}_n$ (**4.21**), $\{[Cd(\mathbf{L5})_2(H_2O)_2](ClO_4)_2\}_n$ (**4.22**) and $\{[Co(\mathbf{L5})_2(H_2O)_2](NO_3)_2\cdot 3H_2O\}_n$ (**4.23**) were all confirmed by elemental analysis. The

formulation for $\{[Cu_3(L5\text{-}2H)_2(CH_3COO)_2(H_2O)_2\ (CH_3OH)_2]\cdot 5(CH_3OH)\}_n$ (**4.24**) was also confirmed by elemental analysis. In complex **4.24,** the IR spectrum showed several significant shifts of the absorption bands for **L5** (1576 and 1430 vs. 1532 and 1402 cm^{-1}).

Crystal structures of 4.21, 4.22 and 4.23

X-ray crystallography indicates that complexes **4.21**, **4.22** and **4.23** crystallise in the triclinic space group *P*-1 with the asymmetric unit comprising of one ligand molecule, one half occupied metal atom, one coordinated water molecule and one non-coordinated anion. The extended structure of the 1-D coordination polymers shows inclusion of the non-coordinated anions within the anion binding moiety of **L5** (Scheme 4.6). In all cases this involves hydrogen bonding of the anion by the amide N-H donor moieties and the coordinated water molecules. The structures of these compounds are closely related to a 1-D zinc coordination polymer described by Custelcean.[133] Further discussion on the crystal structures of the coordination polymers **4.21**, **4.22** and **4.23** is provided below.

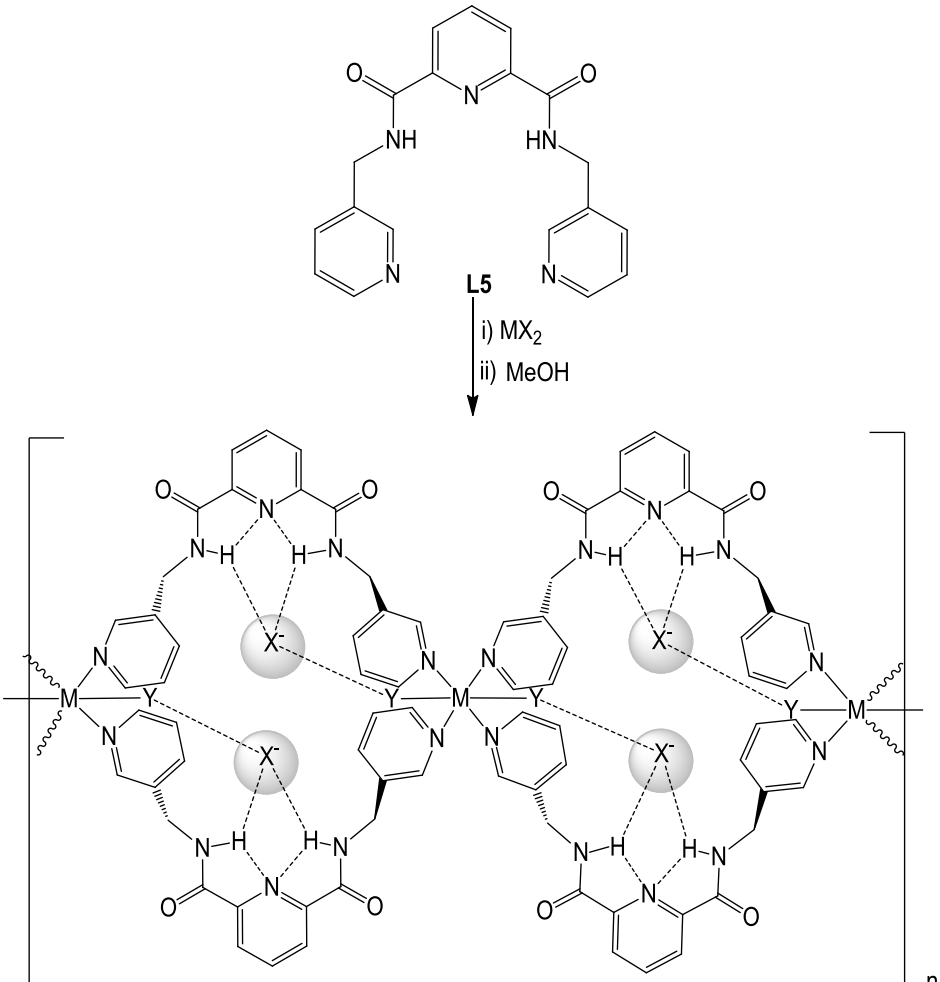

M= Cd, X^- = NO_3 ,Y = H_2O {[Cd(**L5**)$_2$(H_2O)$_2$](NO_3)$_2$.H_2O}$_n$ (**4.21**)

M= Cd, X^- = ClO_4 ,Y = H_2O {[Cd(**L5**)$_2$(H_2O)$_2$](ClO_4)$_2$}$_n$ (**4.22**)

M= Co, X^- = NO_3, Y = H_2O {[Co(**L5**)$_2$(H_2O)$_2$](NO_3)$_2$·3H_2O}$_n$ (**4.23**)

Scheme 4.6. The synthesis of the three isomorphous coordination polymers derived from **L5**.

Crystal structure of **4.21**

{[Cd(L5)$_2$(H_2O)$_2$](NO_3)$_2$·H_2O}$_n$. The asymmetric unit of compound **4.21** comprises one half occupied metal atom (lying on a centre of inversion), one ligand molecule, one coordinated water and one non-coordinated nitrate anion (Figure 4.20). The cadmium centre has an octahedral coordination environment with coordination by the pyridyl donors from four molecules of **L5** and two water molecules. The Cd-N bond lengths of the pyridyl donors are 2.428(3) and 2.315(3) Å with the angles at the cadmium atom environments ranging from 90.37(10) – 94.57(10)°. The bond lengths and angles are fairly typical for such coordination environments.[128] In the coordination polymer, **L5** still maintains the U-shaped conformation that is observed for the

compound in the solid-state alone and this leads to a situation where the amide hydrogen bond donors are oriented to the cavity of the necklace polymer. The Cd-Cd distance in **4.21** is 11.063 Å.

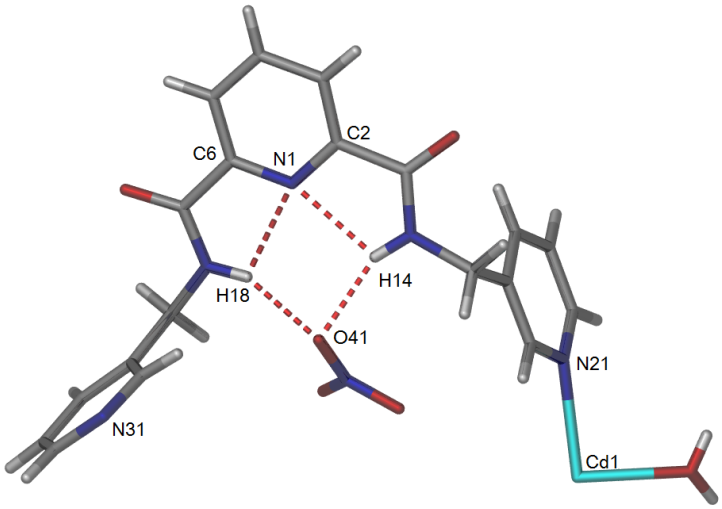

Figure 4.20. A perspective view of the asymmetric unit of complex **4.21**. Selected bond lengths (Å) and angles (°) : Cd(1)-N(21) 2.428(3), Cd(1)-N(31) 2.315(3), Cd(1)-O(45) 2.309(3), N(21)-Cd(1)-N(31) 87.16(10), N(21)-Cd(1)-O(45) 94.57(10) and N(31)-Cd(1)-O(45) 90.37(10).

Weak intramolecular hydrogen bonding (*d* = 2.250, 2.283 Å; *D* = 2.652, 2.675 Å; N-H···N angles = 107.57, 106.88°) pre-organises the NH donors of **L5** into a central pocket. Within the extended structure the compound **4.21** forms four N-H···O-N hydrogen bonds (*d* = 2.062 – 2.078 Å and *D* = 2.882 – 2.902 Å) with the oxygen atoms of the nitrate anions (Figure 4.21). These distances are fairly typical for moderately strong hydrogen bonds interactions[348] and set up an environment ideally suited for encapsulating anions. As a consequence of the U-shaped conformation for **L5**, all the amide C=O groups are directed outward from the coordination polymer which allows for moderately strong hydrogen bonds between the carbonyl oxygen in one molecule and the oxygen atoms from the coordinated water molecules of adjacent 1-D coordination polymers (OH…O=C; *d* = 1.862 Å; *D* = 2.968Å) (Figure 4.21).

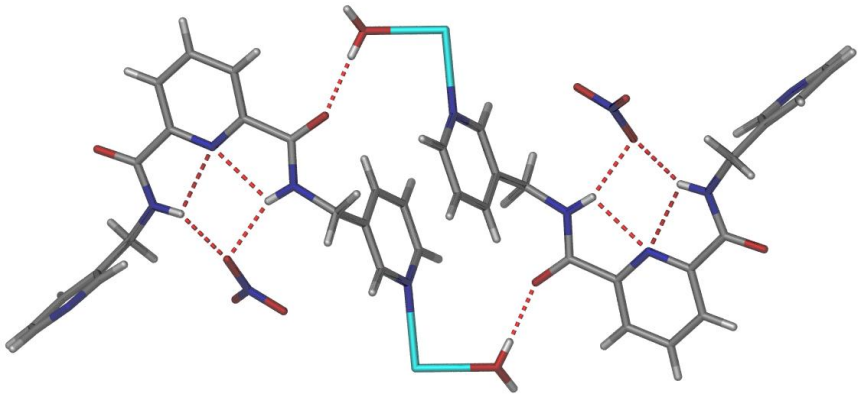

Figure 4.21. The intermolecular hydrogen bonds between the carbonyl oxygen from the ligand and the oxygen atoms from the coordinated water molecules of adjacent 1-D coordination polymers.

In the extended structure of **4.21** (Figure 4.22), the 3-pyridyl rings of each ligand are twisted backward and forward relative to the core of the ligand, and bond the cadmium atom to form an undulating arrangement for the coordination polymer when viewed along the plane of the central 2,6-pyridine dicarboxamide core. The packing within the crystal structure is also stabilised by face-to-face π-stacking interactions between two pendant pyridyl rings (centroid-centroid distance 3.60 Å; angle 106.6°; centroid offset 1.38 Å) of adjacent 1-D coordination polymers.

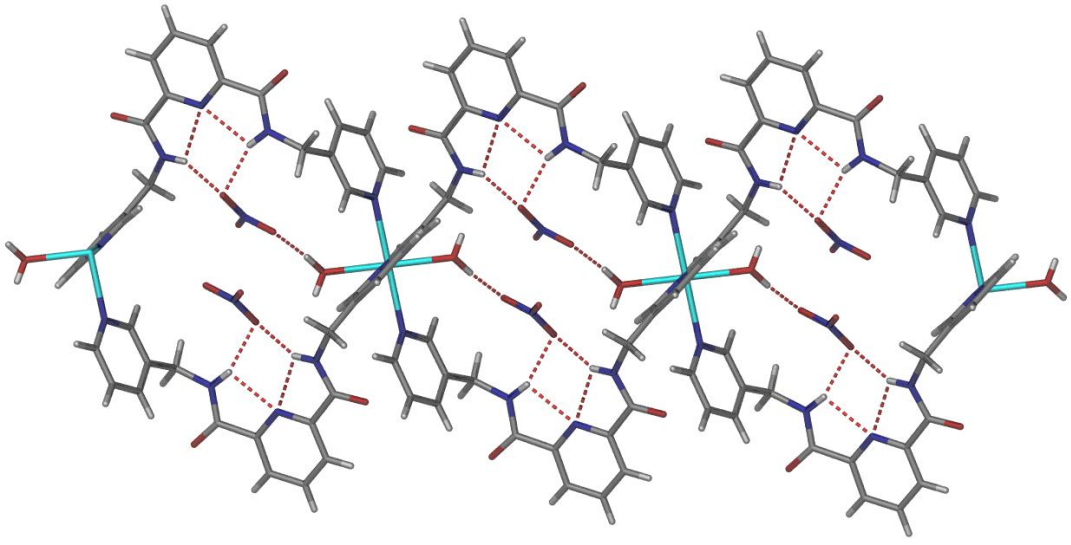

Figure 4.22. A perspective view of the extended structure of complex **4.21**.

Crystal structure of **4.22**

{[Cd(L5)$_2$(H$_2$O)$_2$](ClO$_4$)$_2$}$_n$. As mentioned above, **4.22** also crystallises in the triclinic space group *P*-1 with the asymmetric unit comprising of one half occupied cadmium atom (on a centre of inversion), one ligand molecule, one coordinated water and one non-coordinated perchlorate anion (Figure 4.23). As **4.22** is isomorphous with **4.21**, the cadmium atom adopts a very similar octahedral coordination sphere with coordination by the nitrogen donors from four molecules of ligand **L5** lying in the equatorial positions of the cadmium and two water molecules in the axial sites. The Cd-N bond lengths are 2.238(5) and 2.328(4) Å and the bond angles range from 86.13(15) – 90.17(16)°. These distances and angles are slightly shorter and more acute, respectively, than the Cd-N bond lengths and angles in complex **4.21**, perhaps due to the inclusion of a larger tetrahedral perchlorate anion within the cavity of the necklace-like coordination polymer. The Cd-Cd distance is *ca*. 11.303 Å, which is only 0.24 Å longer than the distance observed in complexes **4.21**. This suggests that the cavity of this coordination polymer can be altered slightly to accommodate different size of polyatomic anions by distortions around the metal centre but that the overall metal-metal distance does not change.

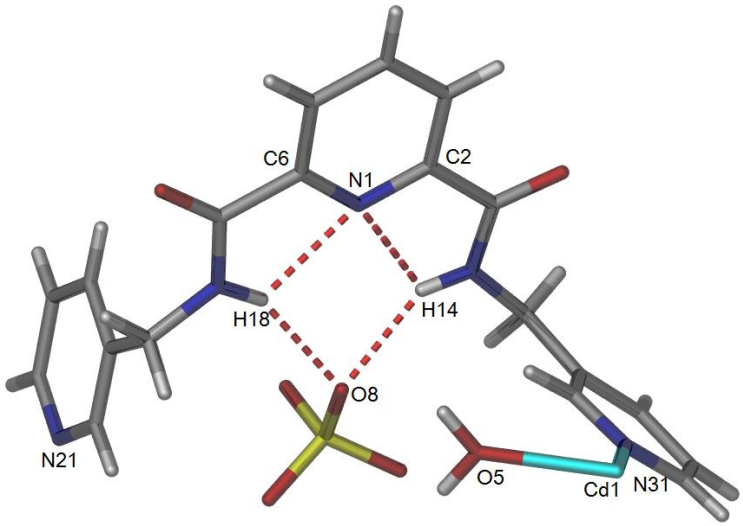

Figure 4.23. A perspective view of the asymmetric unit of complex **4.22** showing the hydrogen bonding around the 2,6-pyridine dicarboxamide moiety. Selected bond lengths (Å) and angles (°): Cd(1)-N(31) 2.328(5), Cd(1)-N(21) 2.424(4), Cd(1)-O(5) 2.299(4), N(21)-Cd(1)-N(31) 86.13(15), N(31)-Cd(1)-O(5) 89.30(18) and N(21)-Cd(1)-O(5) 90.17(16).

Once again, the 3-pyridyl rings of each ligand are twisted relative to the core of the ligand, and bond the cadmium atom to form an undulating arrangement for the coordination polymer (Figure 4.24). The same weak intramolecular hydrogen bonding interactions (*d* = 2.257, 2.279 Å; *D* = 2.666, 2.680 Å; N-H···N angles = 108.19, 107.64°) pre-organise the NH donors of the ligand into a central pocket. The perchlorate anions are hydrogen bonded by the NH amides donors of **L5** and to the water molecules bound to the cadmium atom with the N-H···O distances (*d* = 2.112 – 2.154 Å and *D* = 2.906 – 2.952 Å). In a similar manner to complex **4.21**, a strong hydrogen bond (OH···O=C; *d* = 1.775 Å; *D* = 2.826Å) was observed between the carbonyl oxygen and the water molecules of an adjacent coordination polymer. The crystal packing showed that compound **4.22** displays identical hydrogen bonding arrangements to those observed in complex **4.21**. In addition to these interactions, this molecule is also stabilised by face-to-face π stacking interaction between the two pyridyl rings (centroid-centroid distance 3.60 Å; angle 106.11°; centroid offset 1.38 Å).

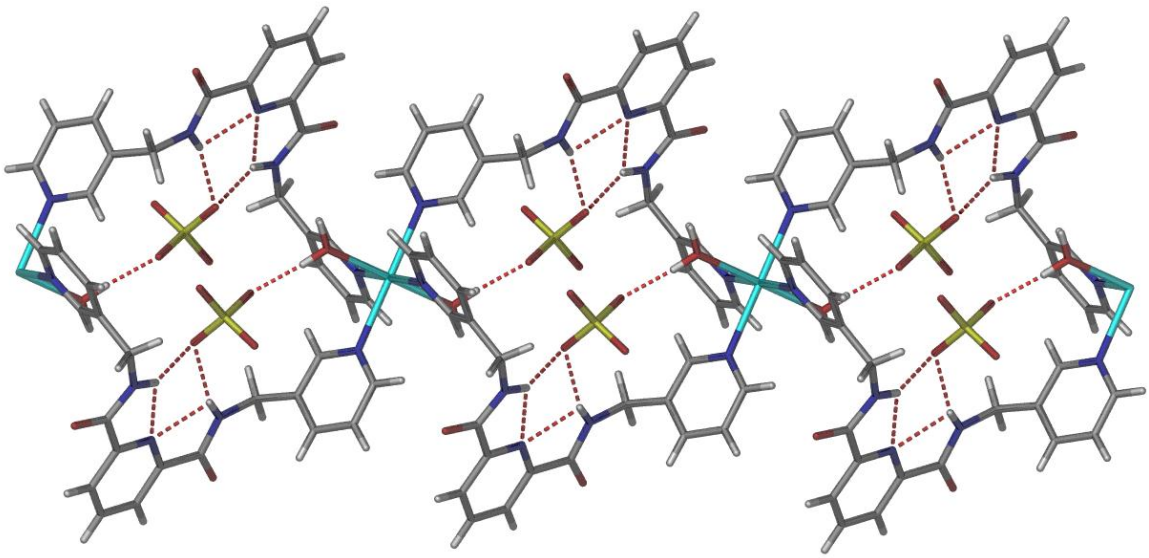

Figure 4.24. A perspective view of the extended structure of complex **4.22**.

Crystal structure of **4.23**

$\{[Co(L5)_2(H_2O)_2](NO_3)_2 \cdot 3H_2O\}_n$. Slow evaporation of a methanol solution containing cobalt(II) nitrate and ligand **L5**, afforded pink crystals of a coordination polymer isomorphous with **4.22**. Naturally this compound crystallises in the triclinic space group *P*-1, with an asymmetric unit

comprising one half occupied cobalt atom (on a centre of inversion), one ligand molecule, one coordinated water and one non-coordinated nitrate anion (Figure 4.25). The cobalt atom is in an octahedral coordination environment with bond lengths and angles in the range of 2.158(2) – 2.269(2) Å and 89.94(8) – 93.81(6)°, respectively. The Co-N distances of this compound are shorter than the M-N distances observed in **4.21** and **4.22**, but slightly longer than the Co-N distances commonly reported in the literature.[335] Interestingly, the ranges of angles around the Co centre are almost identical to the angle range for **4.21**, pointing a close fit within the 'rings of each necklace' for the included anion guests. Similarly, the Co-Co distance is 11.053 Å and identical to the metal-metal distance observed for compound **4.21**, which also has nitrate anions inside the cavity of the anion pocket. Again, weak intramolecular hydrogen bonding (*d* = 2.286, 2.246 Å; *D* = 2.678, 2.649 Å; N-H···N angles = 106.9, 107.64°) pre-organises the NH donors of the ligand into a central pocket.

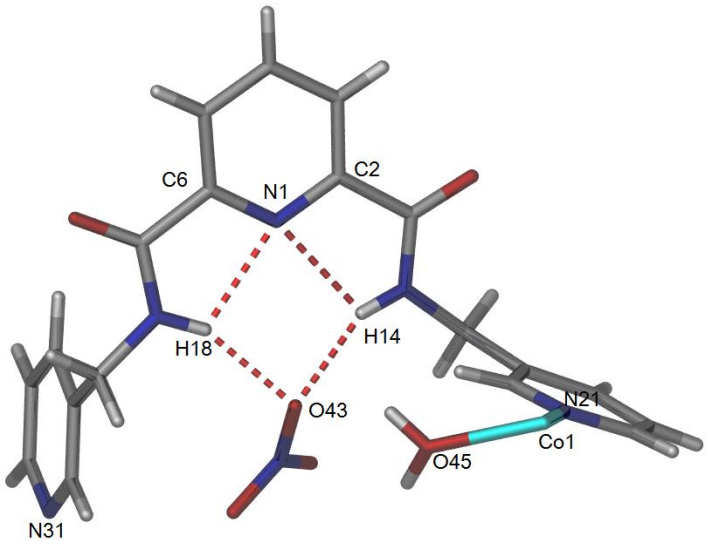

Figure 4.25. A view of asymmetric unit of complex **4.23**. Selected bond lengths (Å) and angles (°): Co(1)-N(21) 2.158(2), Co(1)-N(31) 2.269(2), Co(1)-O(45) 2.067(2), N(21)-Co(1)-N(31) 93.00(8), O(45)-Co(1)-N(21) 89.91(8) and O(45)-Co(1)-N(31) 93.88(8).

Much the same as the previous compounds, compound **4.23** is also constructed from dinuclear metallo-macrocycles leading to the formation of a necklace type coordination polymer (Figure 4.26). The cavity of this necklace type coordination polymer is occupied by nitrate

molecules. Within the structure, the nitrate anions are hydrogen bonded by the NH amide donors (N-H···O: *d* = 2.054 – 2.059 Å and *D* = 2.880 – 2.879 Å) and by a water molecule coordinated to the cobalt atom. As with compounds **4.21** and **4.22**, moderately strong OH···O=C intermolecular hydrogen bonds (*d* = 1.775 Å; D= 2.917 Å) are observed between the adjacent coordination polymers. There is also a face-to face π stacking interaction between the pyridine cores and the two pyridyl rings (centroid-centroid distance 3.61 Å; angle 85.41°; centroid offset 1.34 Å).

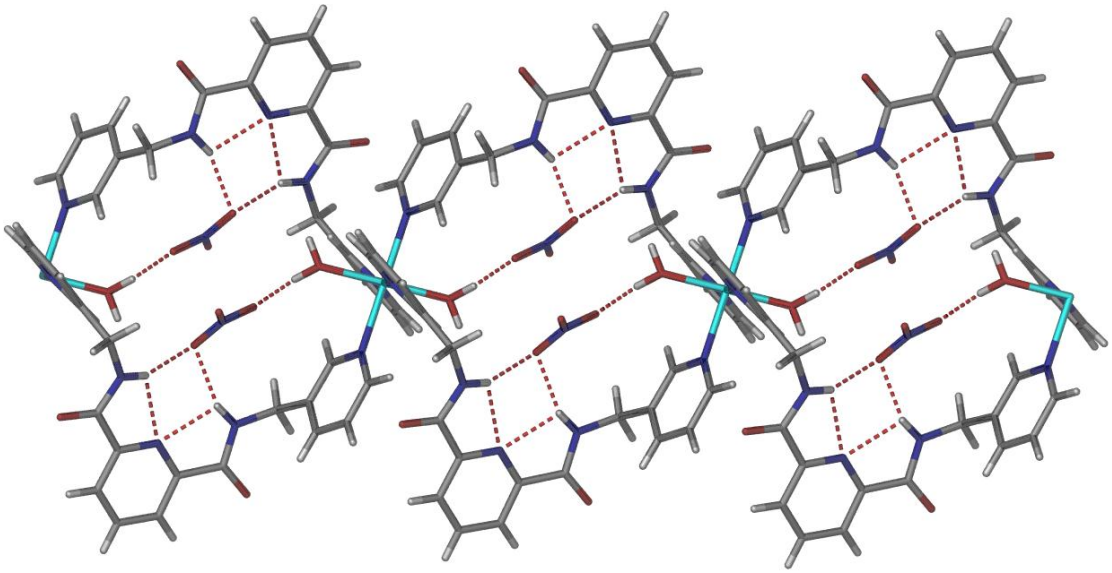

Figure 4.26. A perspective view of the extended structure of complex **4.23**.

While crystal-to-crystal anion exchange was not attempted on the samples **4.21** – **4.23**, it is possible that these materials might be amenable to this process. Consideration of the crystal structures (Figure 4.27, compound **4.21**) reveals that the necklace like arrangement of the 1-D polymers and the resulting crystal packing leads to large anion-filled channels running along the *a*-axis of the unit cell. As a space-filling representation for **4.21** shows, these channels are filled with the anions but they have relatively small apertures (*ca.* 11.105 by 11.063 Å) which may prevent exchange into and out of the material (Figure 4.27(b)).

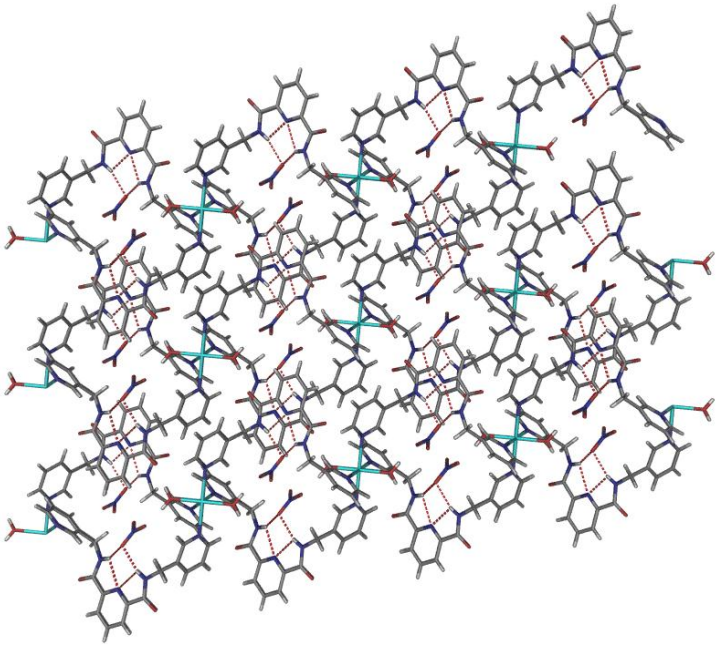

(a)

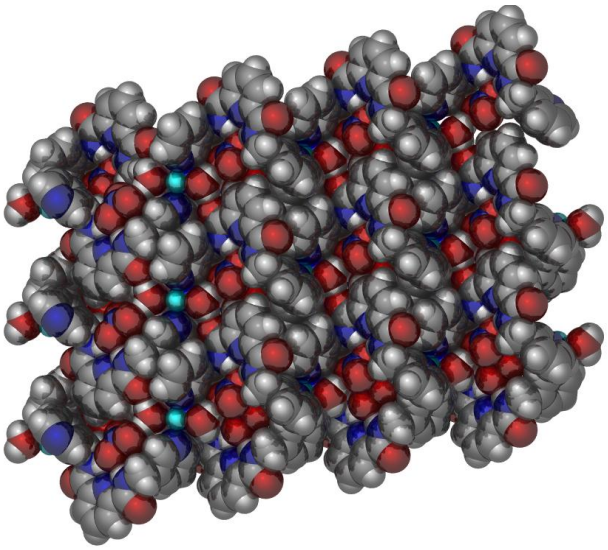

(b)

Figure 4.27. Two representations, (a) rod and (b) space-filling, of the crystal packing of **4.21** viewed down the *a*-axis showing the anion filled channels within the necklace polymers. As structures **4.22** and **4.23** are isomorphous with **4.21** further details of their crystal packing are not shown.

Crystal structure of **4.24**

$\{[Cu_3(L5\text{-}2H)_2(CH_3COO)_2(H_2O)_2(CH_3OH)_2]\cdot 5(CH_3OH)\}_n$. Reaction of **L5** with copper acetate in methanol gave rise to intensely blue coloured solution from which was obtained dark blue crystals of a zig-zag 1-D coordination polymer $\{[Cu_3(\mathbf{L5}\text{-}2H)_2(CH_3COO)_2(H_2O)_2(CH_3OH)_2]\cdot 5(CH_3OH)\}_n$ (**4.24**) in 59% yield. The crystal structure of compound **4.24** was solved in the triclinic space group *P*-1. The crystal structure revealed that **4.24** differs markedly from other discrete complexes and coordination polymers discussed in this chapter by showing a distinctly different coordination mode for **L5**. In addition to coordination by the pendant (external) pyridyl donors, as previously observed, **L5** also coordinates to the copper atom through the central pyridine ring and the deprotonated amide nitrogen atoms. This is known for the isomeric *N,N'*-2,6-*bis*(2-pyridylmethyl)pyridine dicarboxamide ligand as reported by Lawrance *et al.*[163] This deprotonation may have been caused by the presence of acetate ions, which is a stronger base than other anions previously employed. The asymmetric unit of this structure comprises two copper atoms, one molecule of **L5**(-2H), one coordinated acetate anion, one coordinated methanol, four non-coordinated methanol solvate molecules and one coordinated water molecule. Figure 4.28 showed the asymmetric unit of this compound without the non-coordinated methanol molecules.

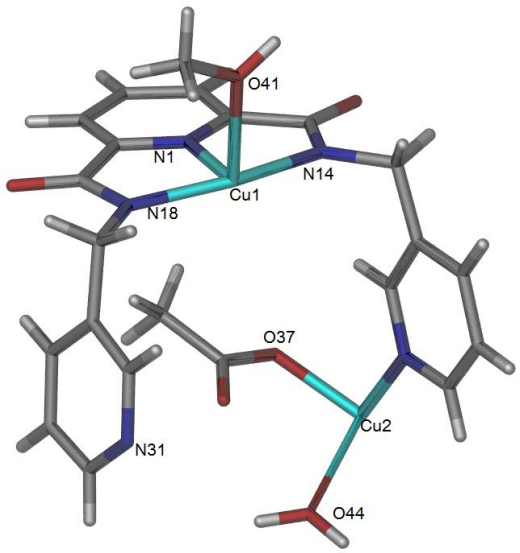

Figure 4.28. A perspective view of the asymmetric unit of compound **4.24** with the non-coordinated solvent omitted for clarity. Selected bond lengths (Å) and angles (°) : Cu(1)-N(1) 1.939(3), Cu(1)-N(14) 2.028(3), Cu(1)-N(18) 2.022 (4), Cu(1)-N(31) 1.990(3), Cu(2)-N(21)

2.019(4), Cu(2)-O(37) 1.960(4), N(1)-Cu(1)-N(18) 80.22(15), N(1)-Cu(1)-N(14) 79.74(14), N(21)-Cu(2)-O44 92.75(15) and N(21)-Cu(2)-O(37) 91.54(17).

The extended structure of compound **4.24**, an undulating 1-D coordination polymer constructed from a combination of dimeric macrocycle M_2L_2, is shown in Figure 4.29. The dimeric building block for this 1-D coordination polymer consists of two deprotonated molecules of **L5** and two copper ions. This unit is very similar to the metallo-macrocyclic structure obtained from reaction of **L2** with $Cu(OAc)_2$ (see chapter 3, compound **3.22**). In that compound the ligand chelates the metal with an N, N, O mode, while here the ligand is coordinated to the metal centre with a tridentate N, N, N chelating mode, which involves one nitrogen donor from the central pyridine ring and two nitrogen atoms from the amide groups. The coordination of a pendant 3-pyridyl group to the copper(II) centre of another entity forms the dimer. The copper-copper distance within this macrocycle is 5.943 Å, which is slightly longer than the distance reported in a literature compound with *N*-6-[(2-pyridylmethylamino)carbonyl]-pyridine-2-carboxylic acid (**3.10**) as a ligand (5.273 Å)[166] and shorter than the corresponding distance in **3.22** (7.262 Å). The dimeric units are linked by the other pendant 3-pyridyl ring of **L5** to a second copper centre to form the 1-D coordination polymer. In this compound, the copper atoms adopt two different geometries. Cu(1) adopts a distorted square pyramidal geometry, with coordination by four nitrogen donors (as described above) and one methanol molecule. The bond lengths of the Cu-N are typical for Cu(II), in the range 1.939(3) – 2.028(3) Å.[347] Meanwhile, Cu(2) adopts an Jahn Teller distorted octahedral coordination environment with the bond lengths (Cu-N = 2.019(4), Cu-O_{OAc} = 1.960(4) and Cu-OH_2 2.684(5) Å) and angles (91.54(5) – 92.75(15)°). This copper atom is coordinated by two nitrogen atoms from the 3-pyridyl rings, two oxygen atoms from the acetate anions and two water molecules. Within the 1-D coordination polymer a π stacking interaction between the two pendant pyridyl rings of the dimeric building block, with the centroid-centroid distance 3.67 Å (angle 97.20°; centroid offset 1.39 Å), stabilises the packing.

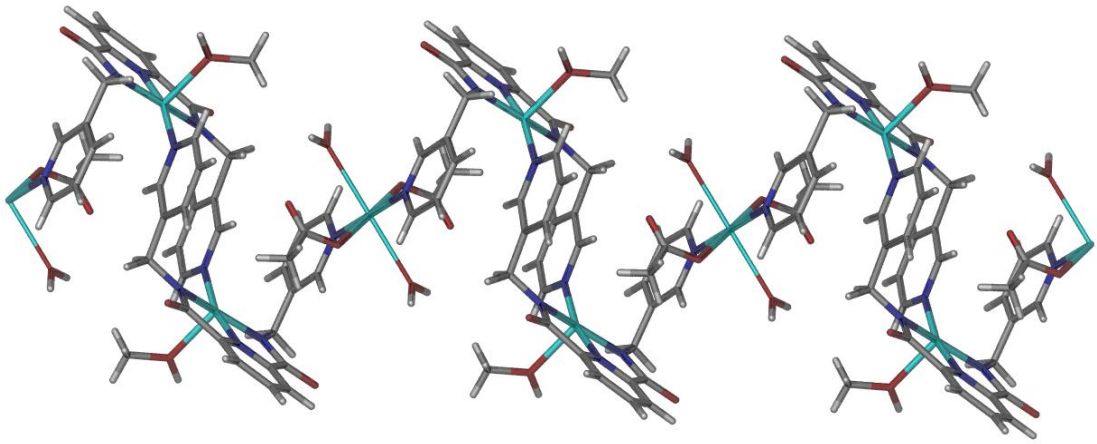

Figure 4.29. A perspective view of the extended structure of 1-D coordination polymer **4.24**.

The packing of the 1-D polymers within the crystal does not involve any significant interactions. A view down the *b*-axis shows the individual polymer chains are simply close packed with the methanol solvate molecules form hydrogen bond interactions to individual polymer chains (Figure 4.30).

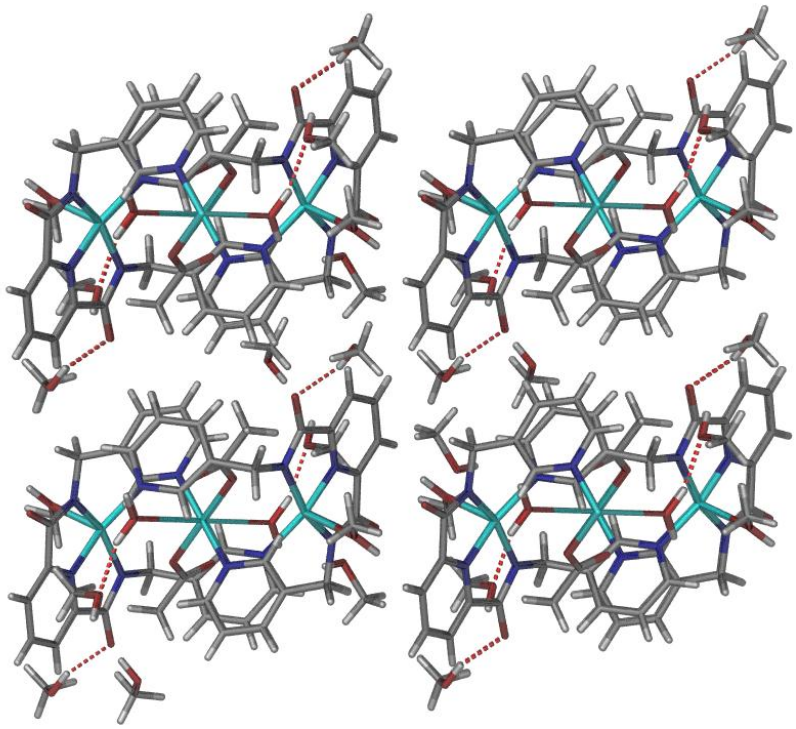

Figure 4.30. A perspective view of the crystal packing of compound **4.24** down the *b*-axis.

4.3.2. Synthesis of coordination polymers of L6

In this study, ligand **L6** was also reacted with a series of metal ion salts to explore its coordination chemistry. Using similar reaction conditions to the studies on **L5**, copper(II) (CuX_2, where X = Cl, NO_3, OAc, ClO_4), cadmium(II) (CdX_2, where X = NO_3, Br_2, ClO_4) and zinc(II) (ZnX_2 where X = NO_3) metal salts were reacted with **L6** in 1:2 metal-to-ligand ratio in methanol. These reactions were also carried out with 1:1 metal-ligand stoichiometries but under these conditions often no products were obtained. Reaction of **L6** with copper(II) metal salts produced oils or oily solids that could not be readily characterised or crystallised. Fortunately, reaction of **L6** with cadmium(II) nitrate also lead to a formation of dinuclear M_2L_2 metallo-macrocyclic based 1-D coordination polymer, $\{[Cd(\mathbf{L6})_2(H_2O)_2](NO_3)_2\cdot 6H_2O\}_n$ (**4.25**). Interestingly, reaction of **L6** with zinc(II) nitrate provided an isomorphous and isostructural 1-D coordination polymer to complex **4.25**, $\{[Zn(\mathbf{L6})_2(H_2O)_2](NO_3)_2\cdot 4H_2O\}_n$ (**4.26**). In contrast to the 1-D coordination polymers isolated with **L5**, the coordination polymers obtained with **L6** have a different arrangement, best described as an undulating (Scheme 4.7). It is worth noting however that the connectivity is the same. Based on elemental analysis, the formula for compounds **4.25** and **4.26** is two ligands to one metal, in support of the crystal structures of these two compounds. The IR spectra for **4.25** and **4.26** confirmed the presence of nitrate with the observation of an N-O stretch at approximately 1313 cm^{-1}.

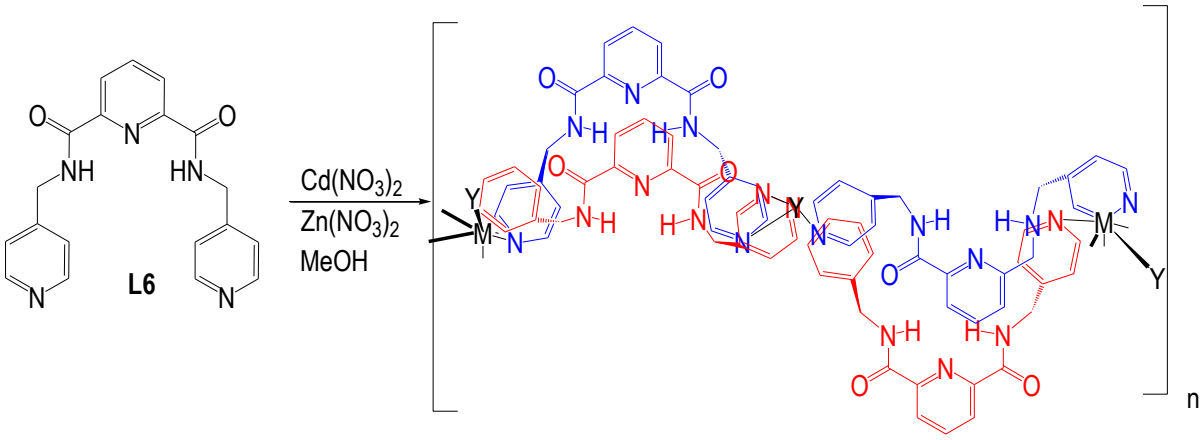

M= Cd, Y = H_2O $\{[Cd(\mathbf{L6})_2(H_2O)_2](NO_3)_2\cdot 6H_2O\}_n$ (**4.25**)
M= Zn, Y= H_2O $\{[Zn(\mathbf{L6})_2(H_2O)_2](NO_3)_2\cdot 4H_2O\}_n$ (**4.26**)

Scheme 4.7. The synthesis of **4.25** and **4.26** and a representation of the undulating structures of **4.25** and **4.26**.

While reactions of **L6** with cadmium nitrate and zinc nitrate gave to two isostructural 1-D coordination polymers, a zig-zag 1-D coordination polymer, $\{[CdBr_2(\mathbf{L6})(CH_3OH)]\cdot CH_3OH\}_n$ (**4.27**) was obtained from the reaction of **L6** with cadmium(II) bromide. Meanwhile, reaction of **L6** with cadmium(II) perchlorate led to the formation of a 2-D coordination polymer, $\{[Cd(\mathbf{L6})_2(H_2O)_2](ClO_4)_2\cdot 3½H_2O\cdot CH_3OH\}_n$ (**4.28**). A strong Cl-O stretch was observed at 1061 cm^{-1} in the FT-IR spectrum for **4.28**. In contrast to the 2-D coordination polymers described in Chapter 3, which were prepared via solvothermal approach, complex **4.28** was obtained *via* slow evaporation. All crystalline products were characterised by combustion analysis, infrared spectroscopy and X-ray crystallography. The synthesis of four coordination polymers obtained with **L6** is summarised in Scheme 4.8.

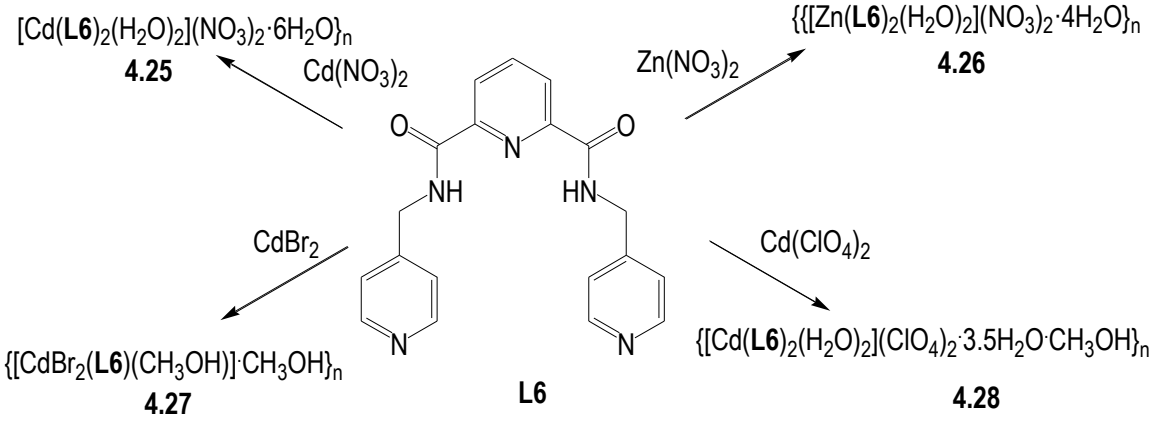

Scheme 4.8. The synthesis of the coordination polymers obtained with **L6**.

Crystal structures of **4.25** and **4.26.**

As mentioned earlier, reactions of **L6** with cadmium nitrate and zinc nitrate provided two isostructural dinuclear metallo-macrocyclic containing 1-D coordination polymers $\{[Cd(\mathbf{L6})_2(H_2O)_2](NO_3)_2\cdot 6H_2O\}_n$ (**4.25**) and $\{[Zn(\mathbf{L6})_2(H_2O)_2](NO_3)_2\cdot 4H_2O\}_n$ (**4.26**). Both compounds crystallise in the monoclinic space group $P2_1/c$ with identical cell dimensions and 1-D undulating polymeric structures. Therefore both compounds are isomorphous and isostructural in the solid-state with the only differences being subtle discrepancies in bond lengths and angles. These structures are closely related to Ag(I) coordination polymers obtained with **L6** in other work undertaken in the laboratory.[349] As a point of note, both the coordination polymers reported here and the closely related Ag(I) structures obtained with **L6** do not refine well. For this reason,

while the structural parameters are described below, all bond lengths and angles must be considered in the context of the relatively high standard deviations on those parameters.

Crystal structure of **4.25**

$\{[Cd(L6)_2(H_2O)_2](NO_3)_2 \cdot 6H_2O\}_n$. Reaction of cadmium(II) nitrate with ligand **L6** in methanol, followed by slow evaporation of the solvent, yielded colourless block-shaped crystals in 51% yield. The asymmetric unit of the structure consists of one cadmium atom, two molecules **L6**, two coordinated water molecules, two non-coordinated nitrate anions and six non-coordinated water solvate molecules (the hydrogen atoms could not be located on these water molecules). The cadmium centre has a slightly distorted octahedral geometry environment with the angles between the donor atoms and the metal ions ranging from 83.6(4) – 93.9(4)°. The cadmium is coordinated by four pendant pyridyl groups and two water molecules. The bond lengths for the Cd-N bonds are in the range 2.318(14) – 2.345(12) Å, while the Cd-O bond lengths are 2.332(11) and 2.360(12) Å. Once again there are weak intramolecular hydrogen bonding interactions (d = 2.250, 2.308 Å; D = 2.644, 2.695 Å; N-H···N angles = 106.96, 106.59°; d = 2.255, 2.306 Å; D = 2.659, 2.656 Å; N-H···N angles = 107.81, 103.69°) that pre-organise the NH donors of the ligand molecules into a central pocket. Figure 4.31 showed a perspective view of the asymmetric unit of **4.25** with water solvate molecules omitted for clarity.

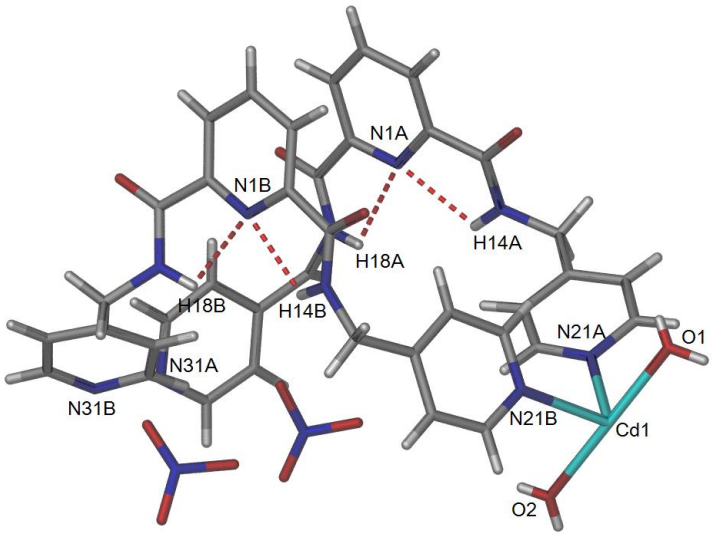

Figure 4.31. A perspective view of the asymmetric unit of **4.25** (non-coordinated water solvate molecules are omitted). Selected bond lengths (Å) and angles (°): Cd(1)-N(21A) 2.318(14),

Cd(1)-N(21B) 2.345(12), Cd(1)-N(31A) 2.328(14), Cd(1)-O(1) 2.332(11), Cd(1)-O(2) 2.360(12), N(21A)-Cd(1)-N(31B) 92.0(5) N(21B)-Cd(1)-N(31A) 93.9(4), O(1)-Cd(1)-N(31A) 85.6(5) and O(1)-Cd(1)-N(21A) 83.6(4).

In similar manner to structures containing **L5**, the U-shape conformation of ligand **L6** is also maintained in coordination polymers of this compound. In this case the pendant 4-pyridyl rings are directed on the same face relative to the core of the ligand, and coordinate the cadmium atom to form a 1-D coordination polymer. Aside from the obvious differences in conformation, the coordination polymers of **L5** and **L6** have identical connectivities. In both cases (i.e. coordination polymers **4.21** – **4.23** and **4.25/4.26**) the metal centres are coordinated by four nitrogen donors and two water ligands. Compound **4.25** has a longer Cd-Cd distances (13.374 Å) than the M-M distances in **4.21** – **4.23** (11.053 – 11.303 Å).

Once again, two are nitrate anions located in each pocket of the coordination polymer (Figure 4.32). In contrast to other structures in this thesis, the nitrate anions are interact with the coordination polymer *via* hydrogen bonding mediated by coordinated and non-coordinated solvent and anion-π interactions directly with the ligand. There are very long hydrogen bonding interactions between the nitrate anion and the methylene proton of the ligand (C-H···O, d = 2.787, D = 3.694 Å) and also an anion-π interaction between the pendant 4-pyridyl ring of **L6** and the nitrate anion with the closest contact of 3.183 Å. In place of the direct amide NH hydrogen bonds to the anion that are typical for compounds in this thesis, a series of hydrogen bonding interactions involving the non-coordinated water molecules that are the primary guests of these pockets stabilise the packing of the anions in the structure.

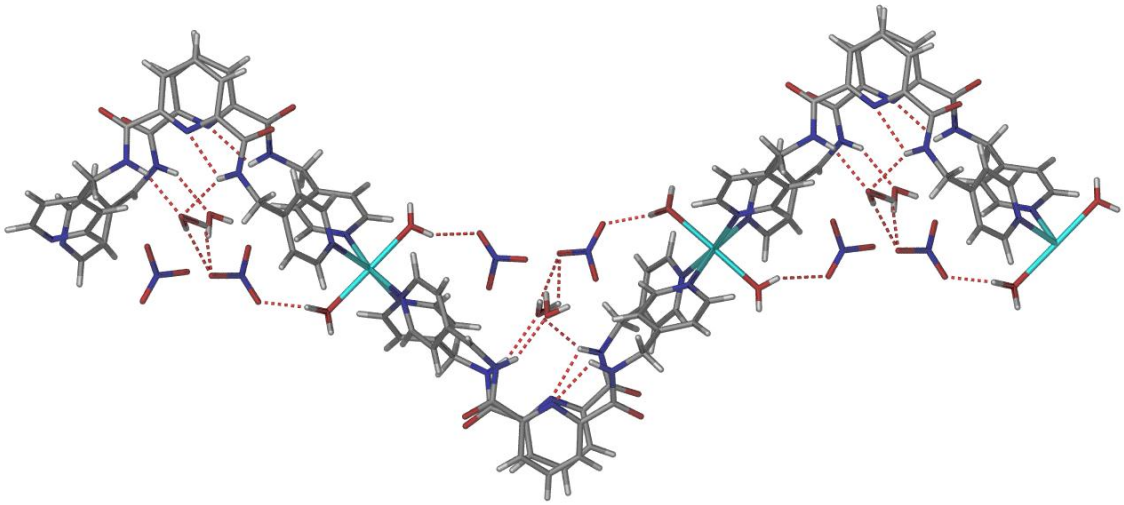

Figure 4.32. A perspective view of the extended structure of **4.25** showing the hydrogen bonding interactions between the anions and the 1-D coordination polymer.

Figure 4.33 shows two perspective views of the crystal packing of **4.25** viewed down the *c* axis. Interestingly, this compound has two different types of large channels. One of the channels, lined with the 2,6-pyridine dicarboxamide moieties of the ligands hosts the hydrogen bonded water molecules and nitrate anions discussed above, while the second (shown empty) accommodates the water solvate molecules.

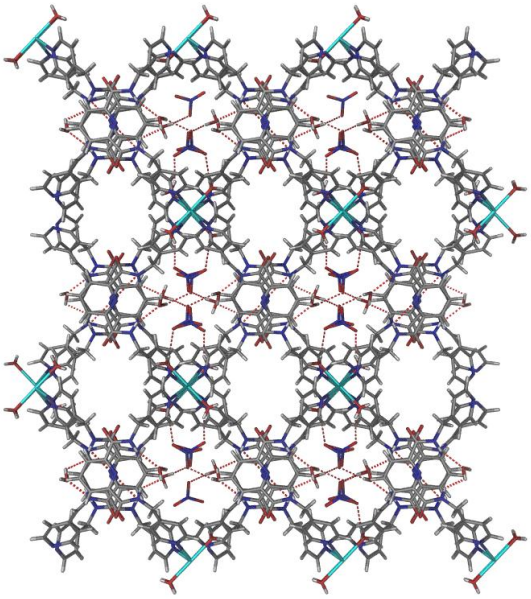

(a)

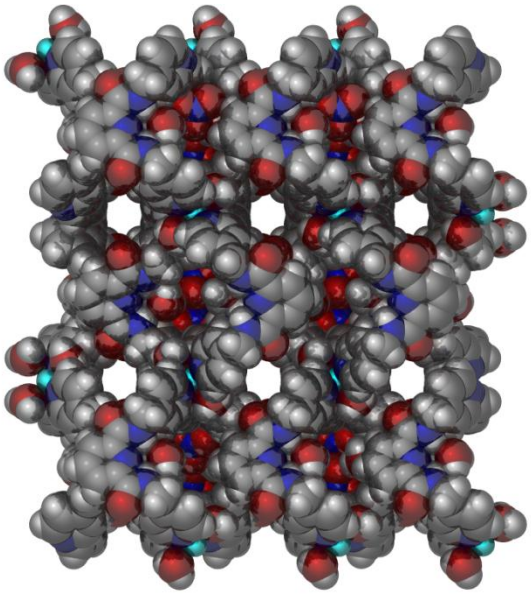

(b)

Figure 4.33. Two perspective views of the crystal packing of **4.25** viewed from the *c*-axis, showing the channels filled with nitrate anions and water molecules or the channels only containing solvate molecules.

Crystal structure of **4.26**

$\{[Zn(L6)_2(H_2O)_2](NO_3)_2 \cdot 4H_2O\}_n$. Slow evaporation of a methanol solution of zinc(II) nitrate and ligand **L6** led to the crystallisation of colourless crystals of compound **4.26** in 45% yield. As it is isomorphous with **4.25** the asymmetric unit contains one zinc atom, two molecules **L6,** two coordinated water molecules, two non-coordinated nitrate anions and four non-coordinated water solvate molecules. A perspective view of complex **4.26** is shown in Figure 4.34 with water molecules omitted for clarity. In **4.26** the zinc atoms occupy distorted octahedral environments with coordination by four pendant pyridyl groups and two water molecules and bond angles ranging from 85.9(2)-91.1(2)°. The bond lengths for the Zn-N bonds are in the range 2.158(6)-2.198(6) Å. These are slightly longer than comparable Zn-N distances reported in the literature which range from 2.0-2.05 Å.[350] Once again the presence of weak intramolecular hydrogen bonding interactions pre-organise the NH donors of the ligands into a central pocket as indicated

in Figure 4.34 (d = 2.219, 2.315 Å; D = 2.612, 2.60 Å; N-H···N angle = 106.68, 103.75°); (d = 2.382, 2.189 Å; D = 2.679, 2.601 Å; N-H···N angles = 100.00, 108.11°).

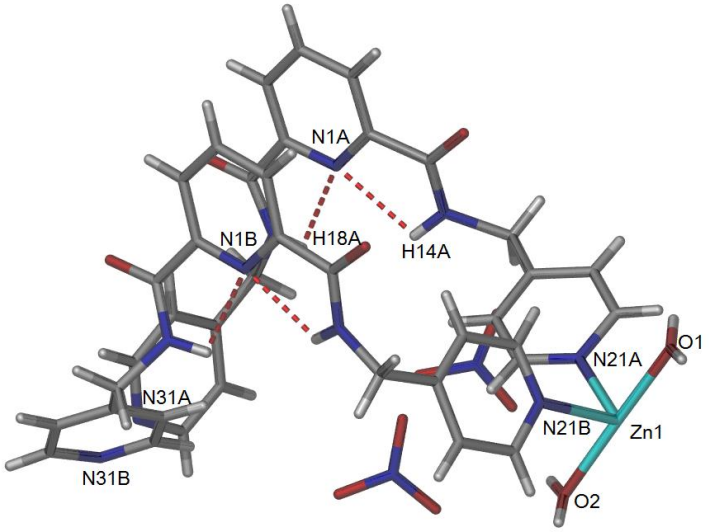

Figure 4.34. A perspective view of complex **4.26** with non-coordinated water solvate molecules omitted for clarity. Selected bond lengths (Å) and angles (°) : N(21A)-Zn(1) 2.158(6), N(21B)-Zn(1) 2.198(6), N(31A)-Zn(1) 2.197(7), N(31B)-Zn(1) 2.179(6), Zn(1)-O1 2.111(6), Zn(1)-O2 2.163(6), N(21A)-Zn(1)-N(21B) 90.3(2), O(1)-Zn(1)-N(21A) 90.9(2), N(21A)-Zn(1)-N(31B) 86.5(2), O(1)-Zn(1)-N(31A) 91.1(2) and O(2)-Zn(1)-N(21B) 85.9(2).

Again, **L6** acts as a bridge to link the two zinc atoms and forming a 1-D coordination polymer (Figure 4.35). The distance between the two Zn atoms is 12.849 Å, which is slightly shorter than the Cd-Cd distance in complex **4.25**. In a similar way to compound **4.25**, the nitrate anions in this compound are bound to the coordination polymer *via* weak hydrogen bonding interactions with the ligand (C-H···O, d = 2.665, D = 3.635 Å) and the between the 4-pyridine ring and the nitrate (C-H···O, d = 2.222 Å, D = 3.101 Å). As with **4.25**, in place of the direct amide NH hydrogen bonds to the anion that are typical for these compounds, a series of hydrogen bonding interactions involving the non-coordinated water molecules that occupy these pockets stabilise the packing of the anions in the structure.

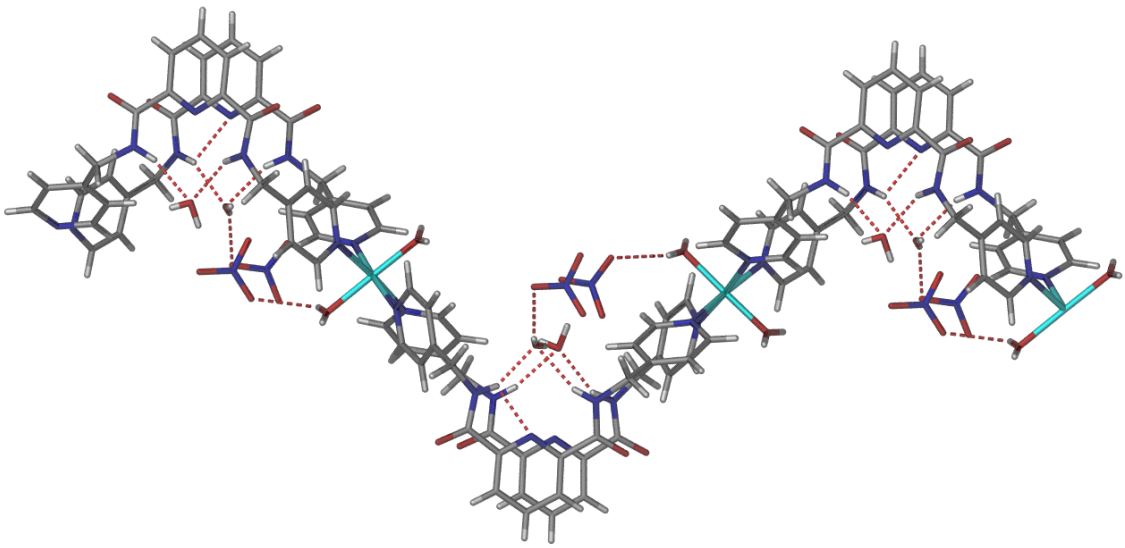

Figure 4.35. A perspective view of the 1-D coordination polymer, **4.25**.

Figure 4.36 shows perspective views of the crystal packing of **4.26** viewed down the *c* axis. Again, the compound has two different types of large channels. One of the channels, lined with the 2,6-pyridine dicarboxamide moieties of the ligands hosts the hydrogen bonded water molecules and nitrate anions as discussed above, while the second (shown empty) accommodates the water solvate molecules.

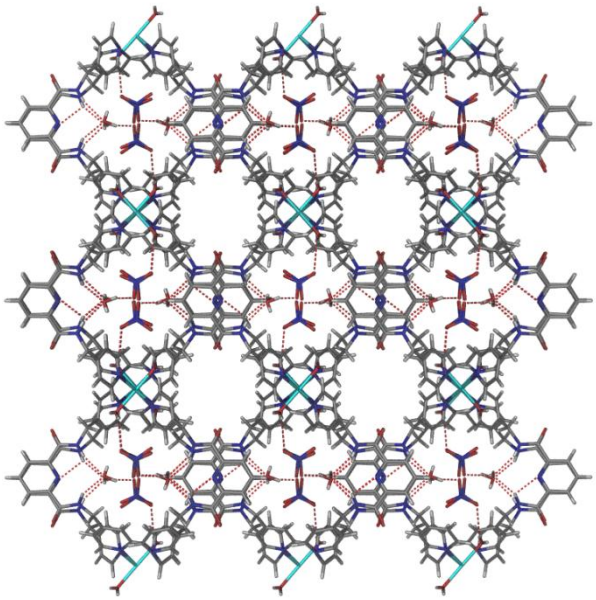

(a)

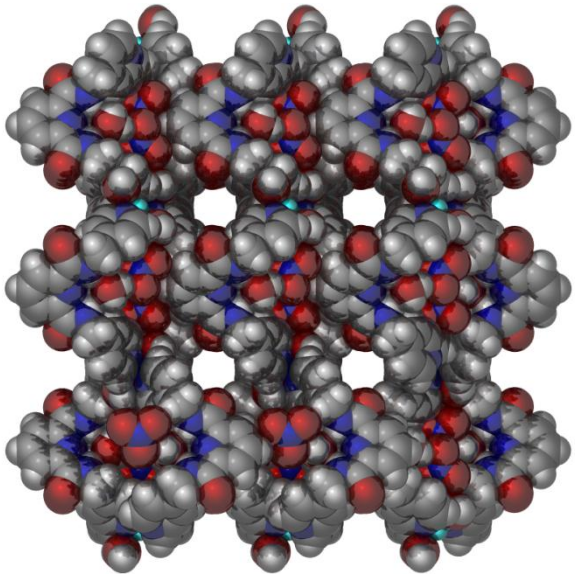

(b)

Figure 4.36. Two perspective views of the crystal packing of compound **4.26**.

The reactions of the two flexible diamide ligands, **L5** and **L6** with late transitions metals as described above has given five closely related 1-D coordination polymers, namely compounds **4.21, 4.22 4.23**, **4.25** and **4.26**. All 1-D coordination polymers are constructed from metallo-macrocyclic-type repeating units but with quite different conformations of the repeating unit. Figure 4.37 shows representations of the coordination polymers obtained. Due to the different substitution of the pendant pyridyl rings, coordination polymers **4.21, 4.22** and **4.23** are arranged in a flatter necklace-like motif, while coordination polymers **4.25** and **4.26** are arranged in an undulating or wave-like motif.

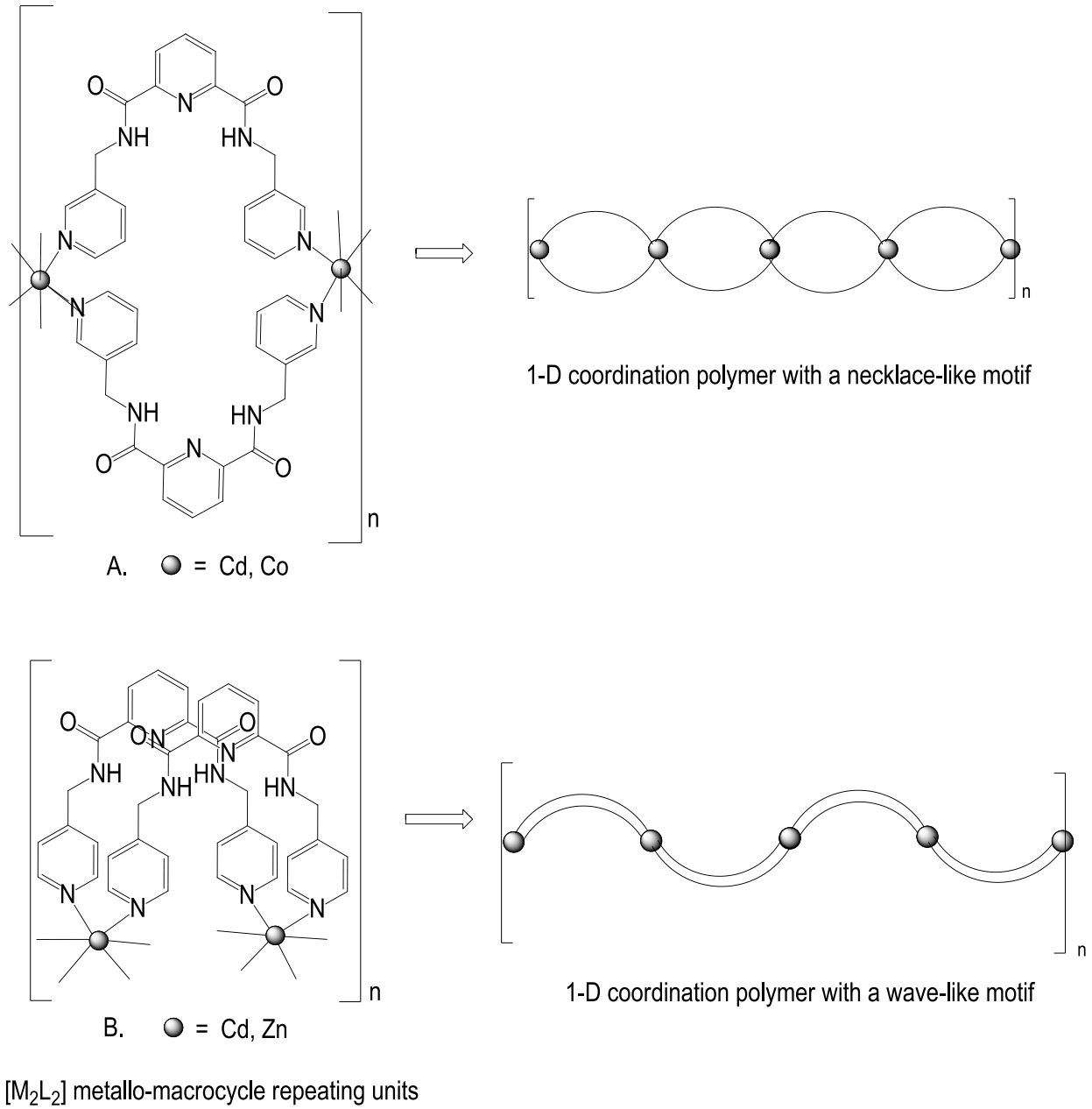

Figure 4.37. Cartoon representations of the 1-D coordination polymers obtained from **L5** and **L6**.

There are further contrasting aspects of the coordination polymers obtained with **L5** and **L6**. In the structures of **4.21, 4.22** and **4.23,** the anions were bound, as expected, directly to the pre-organised amide moieties through hydrogen bonding interactions. It was also observed that the size of the cavity within these coordination polymers could be slightly expanded and contracted to accommodate different sizes of polyatomic anions within this pocket, i.e. the Cd-Cd

distances of compound **4.22** is slightly longer than the Cd-Cd distance in **4.21** in order to accommodate the larger perchlorate anion. In compounds **4.25** and **4.26**, the anion were not directly hydrogen bonded to the pre-organised amide moieties, but interact with **L6** through hydrogen bonding mediated by water solvate molecules and also through weak CH···X hydrogen bonds involving the methylene spacers or the pendant pyridyl rings. In the case of **4.25** the nitrate anions also form anion-π interactions with the pendant pyridyl rings. Compounds **4.25** and **4.26** have two different types of channels running down the *c*-axis of these structures, while **4.21** – **4.23** have only one type of channel that is filled by the anions. In compounds **4.25** and **4.26** the channels are oval in structure with diameters in the range 6.2 – 9.8 Å. The metal-metal distances in the two sets of structures are quite similar and in the range 12.053 – 13.374 Å (Table 4.4).

Table 4.4. A comparison of the metal-metal distances for the 1-D coordination polymers

Compounds	**4.21**	**4.22**	**4.23**	**4.25**	**4.26**
M-M	Cd-Cd	Cd-Cd	Co-Co	Cd-Cd	Zn-Zn
Bond lengths (Å)	11.063	11.303	11.053	13.374	12.894

The 1-D coordination polymers derived from **L5** and **L6** have potentially interesting structures that could be investigated for anion exchange. Studies on the ability of the porous frameworks to reversibly exchange anions within the channels of such materials have been demonstrated.[351,352] Kitagawa[130] has categorised flexible porous networks of this type as 3rd generation materials with regards to their ability to shrink or expand their structure in order to accommodate differently sized of the guest molecules. Kitagawa and co-workers[353] have reported the anion selectivity of coordination polymers derived from a bipyridine ligand and demonstrated that two different anions (perchlorate and hexafluorophosphate) were found to be selectively accommodated in the channels of these structures (Figure 4.38). Of the materials reported in this thesis, compounds **4.25** and **4.26** are perhaps the most suitable candidates for exchange and selectivity studies involving anions. This could be achieved by using competitive crystallisation techniques or solid-state anion exchange experiments. A general description of the anion exchange mechanism by a competitive crystallisation approach was discussed in Chapter 1.

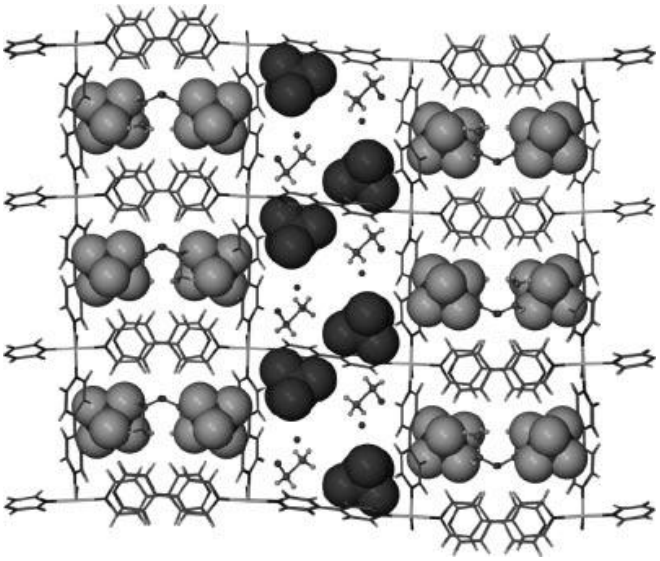

Figure 4.38. The crystal packing of the copper(II) coordination polymer derived from 4,4'-bipyridine showing the segregation of two different anions in alternating channels. (Image sourced from ref [353])

Crystal structure of **4.27**

{[$CdBr_2$(L6)(CH_3OH)]·CH_3OH}$_n$. A 1:2 metal-ligand mixture of cadmium bromide and **L6** was dissolved in methanol-water to give a colourless solution which was then allowed to slowly evaporate. This yielded colourless crystals of complex {[$CdBr_2$(**L6**)(CH_3OH)]·CH_3OH}$_n$ in 36% yield. The compound crystallises in the monoclinic space group *C*2/*c* with one molecule of **L6**, one cadmium atom, one coordinated methanol, one non-coordinated methanol molecule and two coordinated bromide anions in the asymmetric unit (Figure 4.39). The cadmium atom adopts trigonal bipyramidal geometry with Cd-N bond lengths of 2.329(7)-2.371(9) Å and angles of 79.8-120.81(5)°. As usual, there are two intramolecular hydrogen bonding interactions which pre-organise the NH donors of the ligand into a central pocket (*d* = 2.311, 2.286 Å; *D* = 2.702, 2.687 Å; N-H···N angles = 107.01, 107.68°). The N-H···N angles are typical for the 2,6-pyridine dicarboxamide moiety.

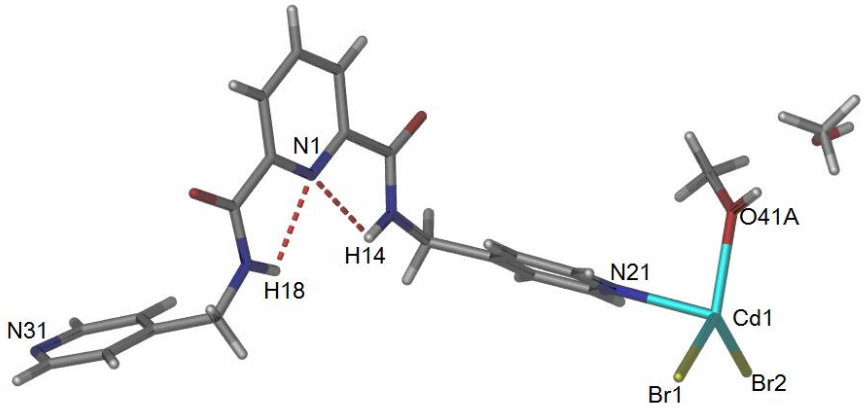

Figure 4.39. A perspective view of the asymmetric unit of complex **4.27**. Selected bond lengths (Å) and angles (°) : N(21)-Cd(1) 2.329(7), N(31)-Cd(1) 2.371(9), Cd(1)-Br(1) 2.5741(11), Cd(1)-Br(2) 2.5967(12), Cd(1)-O(45A) 2.379(9), N(21)-Cd(1)-O(45A) 89.46(10), N(21)-Cd(1)-O(45A) 79.8(3), and Br(1)-Cd(1)-Br(2) 120.81(5).

Figure 4.40 shows the extended structure of complex **4.27**. The cadmium atom is bridged by the ligand, which adopts a conformation common for these diamide compounds, to form a 1-D coordination polymer. The pendant pyridyl rings twist backward and forward relative to the central 2,6-pyridine dicarboxamide core with torsion angles (C12-N14-C15-C24) of 113.09 and 115.13°. The 1-D coordination polymer extends along the *ac* diagonal (Figure 4.40). As a consequence of the cadmium centres having two coordinated anions and a five coordinated geometry, and, as the cadmium centres are bridged by only one diamide ligand, the structure of compound **4.27** is quite a different to other coordination polymers obtained with **L5** and **L6**. In comparison, the majority of the 1-D coordination polymers reported in this chapter have an ML_2 stoichiometry and involve coordination of the metal by four nitrogen atoms from the pendant pyridyl rings of **L5** and **L6**. The coordination polymer motif observed for **4.27** has been reported for many 1-D coordination polymers described in the literature.[354,355]

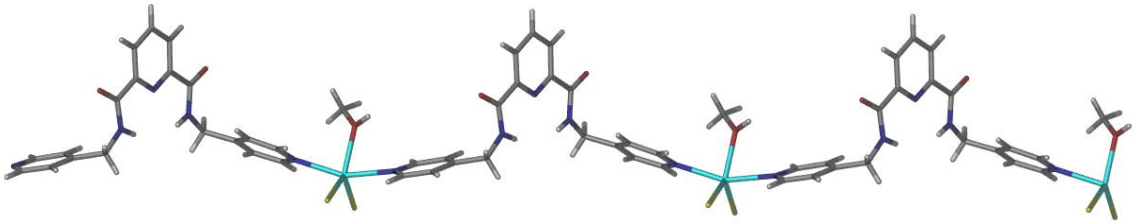

Figure 4.40. A perspective view of the extended structure of complex **4.27**.

The crystal packing of this simple 1-D coordination polymer is relatively complicated. The coordinated bromide anions are involved in inter-chain hydrogen bonding interactions (*d* = 2.090, 2.094 Å, *D* = 2.938, 2.946 Å, bond angle = 121.30°) (Figure 4.41) to generate a double chain structure (Figure 4.41(b)). The molecule is stabilised by face-to-face π stacking interaction between the two pyridyl rings (centroid-centroid distance 3.96 Å; angle 102.36°; centroid offset 1.32 Å).

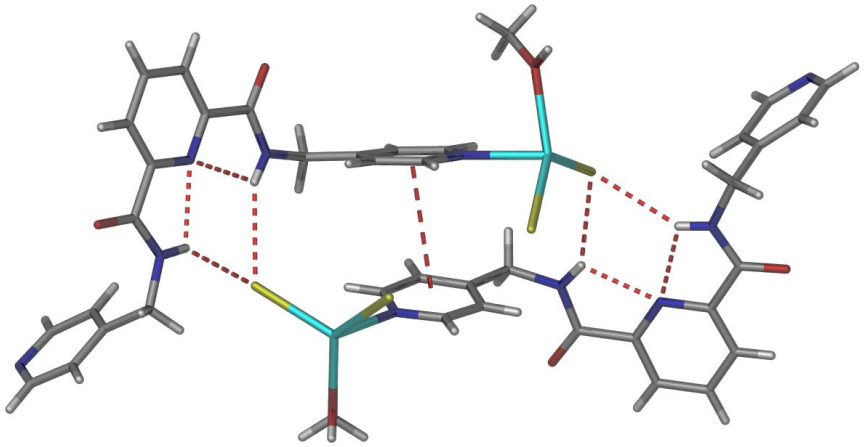

(a)

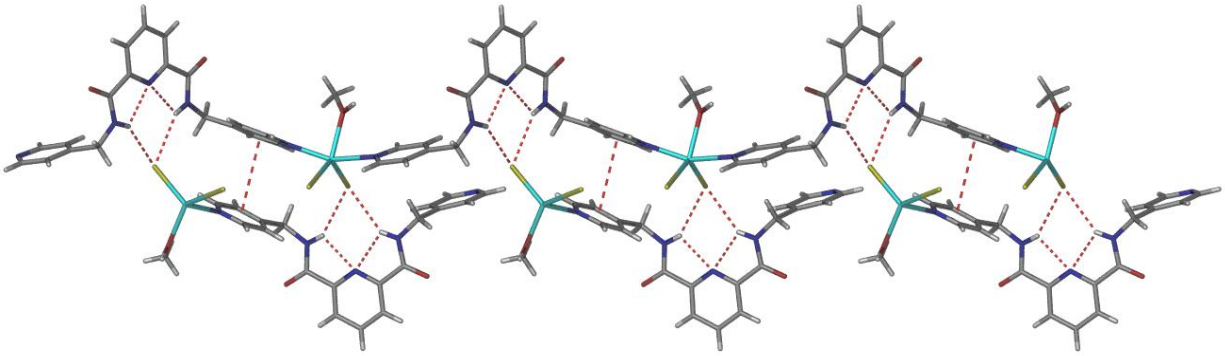

(b)

Figure 4.41. (a) A perspective view of the N-H···Br hydrogen bonds that give rise to the 2-D double chains of 1-D coordination polymers. (b) A view of the 2-D double chains of 1-D coordination polymers.

In the crystal packing, moderately strong hydrogen bonding interactions were also observed between the coordinated and non-coordinated methanol molecules and the carbonyl oxygen atoms of adjacent coordination polymers. The coordinated methanol molecule of one coordination polymer is hydrogen bonded (O-H···O hydrogen bonds) to a non-coordinated methanol molecule with d = 1.994 Å and D = 2.774 Å. The non-coordinated methanol molecules are in turn further hydrogen bonded to a carbonyl group of **L6** in an adjacent coordination polymer by an O-H···O hydrogen bond (d = 1.876 Å and D = 2.692 Å) (Figure 4.42). The combination of interactions that form the double chains (Figure 4.41) and then those that link those double chains (Figure 4.42) results in a 2D hydrogen bonded network of coordination polymers (Figure 4.43).

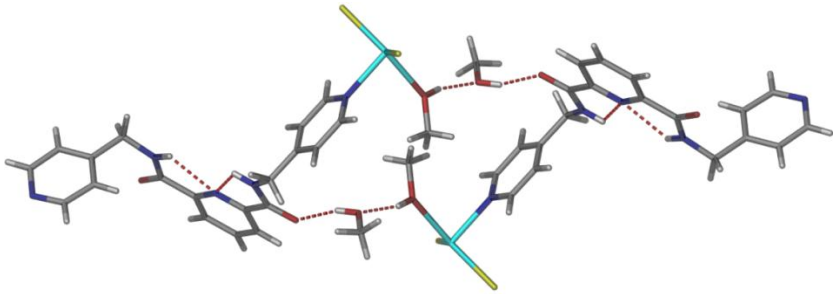

Figure 4.42. The methanol-mediated inter-chain hydrogen bonds in the crystal packing of **4.27**.

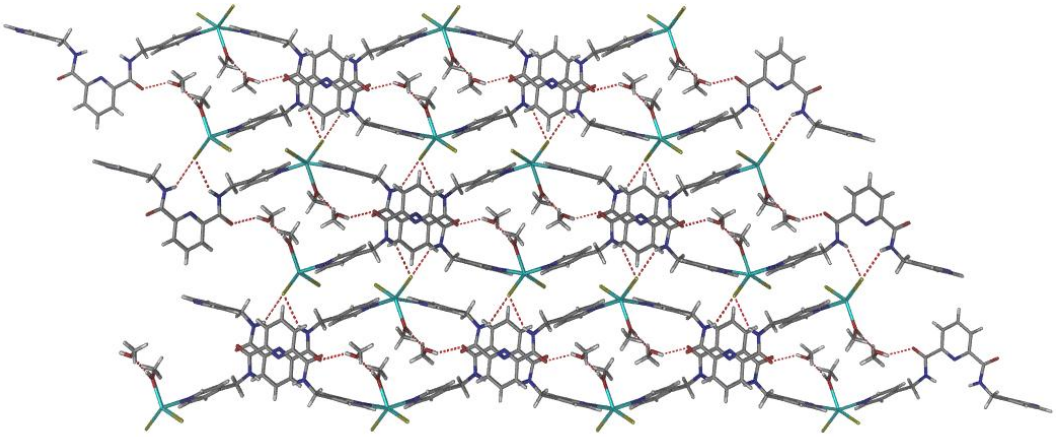

Figure 4.43. The crystal packing of compound **4.27**.

As mentioned earlier, reaction of **L6** with cadmium perchlorate in methanol provided access to a 2-D coordination polymer. Unlike the 2-D structures reported in Chapter 3, compound **4.28** was prepared by slow evaporation and not from solvothermal methods. The structure is a 4-connected 2-D coordination polymer, with $[M_4L_4]$ metallo-macrocycle repeating units in the structure. Each cadmium centre acts as a 4-connecting node in the structure as described below.

Crystal structure of **4.28**

$\{[Cd(L6)_2(H_2O)_2](ClO_4)_2 \cdot 3½H_2O.CH_3OH\}_n$. Slow evaporation of a methanol solution of cadmium perchlorate and ligand **L6** afforded white crystals of a 2-D coordination polymer in 38% yield. Compound **4.28** crystallises in monoclinic space group *C*2/*c*. The contents of the asymmetric unit include one cadmium atom, one molecule of **L6**, one coordinated water

molecule, one non-coordinated perchlorate (disordered over two sites) and one non-coordinated methanol (Figure 4.44). Like other compounds in this thesis, weak intramolecular hydrogen bonding interactions which pre-organise the NH donors of the ligand into a central pocket are observed in this structure (*d* = 2.254, 2.370 Å; *D* = 2.669, 2.718 Å; N-H···N angles = 106.68, 103.87°).

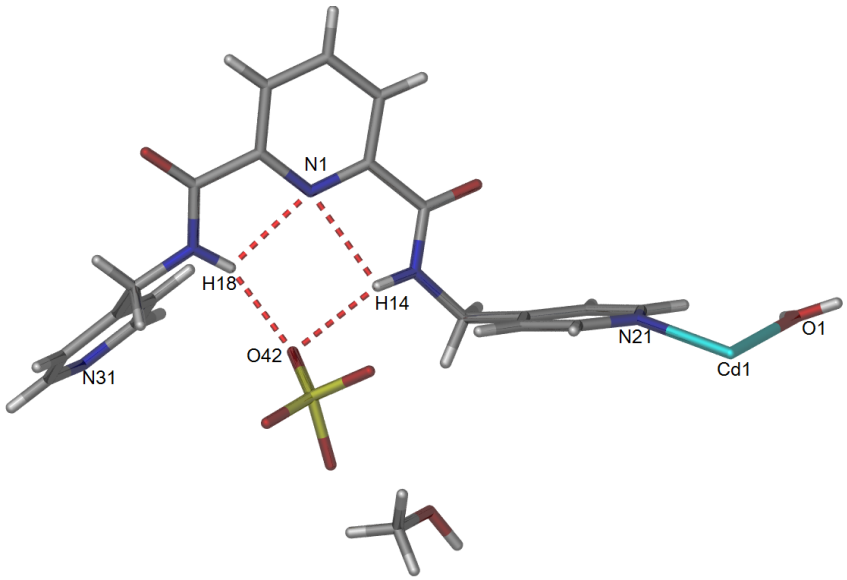

Figure 4.44. A perspective view of the asymmetric unit of complex **4.28**. Selected bond lengths (Å) and angles (°): N(21)-Cd(1) 2.380(3), N(31)-Cd(1) 2.357(3), Cd(1)-O(1) 2.300(3), N(21)-Cd(1)-O(1) 90.53(10), N(21)-Cd(1)-N(31) 93.26(9) and N(31)-Cd(1)-O(1) 90.70(11).

Figure 4.45 shows a section of the extended structure of compound **4.28**. The cadmium adopts octahedral environment with coordination by two coordinated water molecules and four nitrogen atoms from the pendant pyridine rings of ligand **L6**. The cadmium centres have Cd-O bond lengths of 2.300(3) Å and Cd-N bond lengths in the range 2.357(3)- 2.380(3) Å. Considering the cadmium centres as 4-connecting nodes leads to the identification of a metallo-macrocyclic $[M_4L_4]$ subunit arising from the connection of four cadmium centres linked by four molecules of **L6** as shown below. Thus, the coordination polymer is best described as a 4-connected 2-D coordination polymer. In the crystal structure, the perchlorate anions are located inside the cavity of these metallo-macrocycles which are particularly large, with the shortest Cd-Cd distance of 15.210 Å and the longest of 28.785 Å (Figure 4.46(a) and (b)). A similar motif

has been observed in a 2-D copper coordination polymer reported by Biradha.[339] Moderately strong intermolecular hydrogen bonding interactions between the NH amide donors and the perchlorate anions, N-H···O (*d*= 2.183 *D*=2.942 Å) are observed in the crystal packing (Figure 4.47).

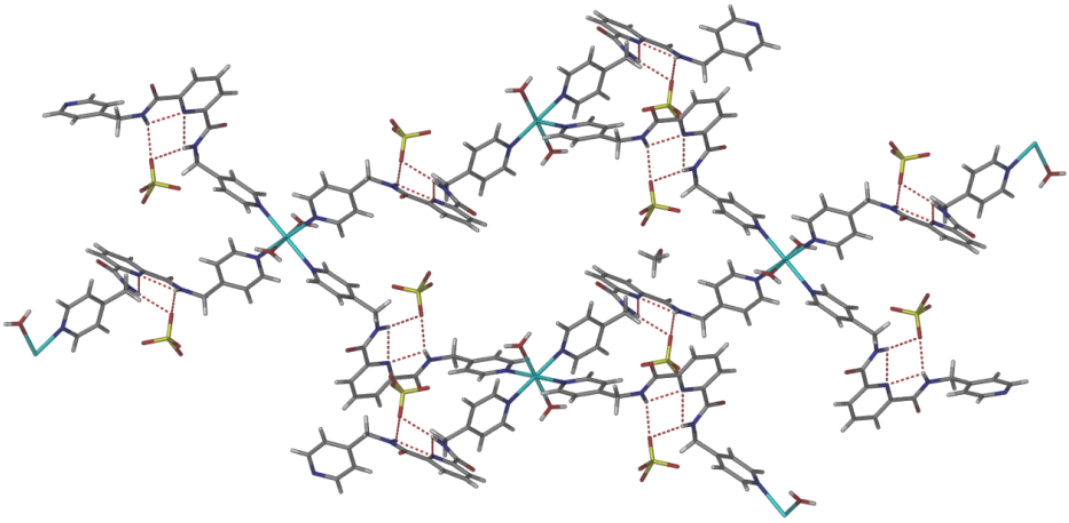

Figure 4.45. A perspective view of the $[M_4L_4]$ metallo-macrocyclic units in **4.28**.

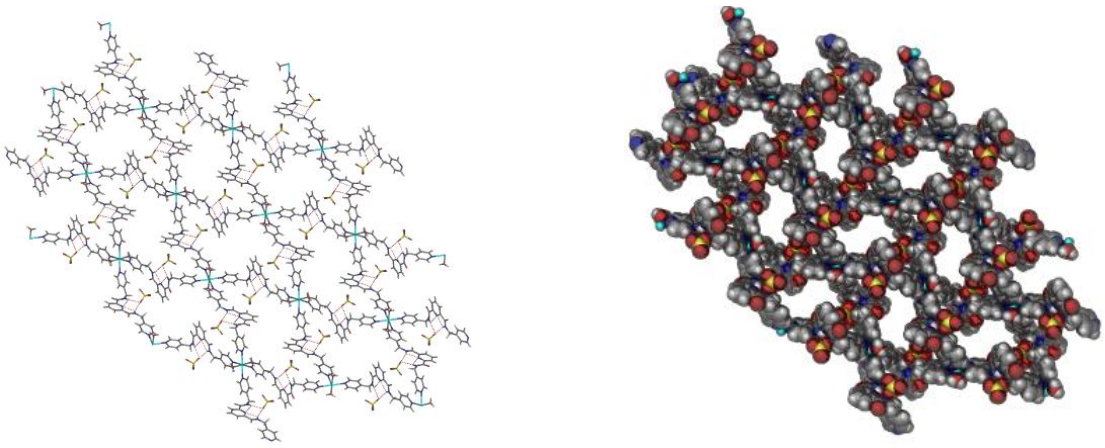

(a) (b)

Figure 4.46. Two perspective views of the extended 4-connected 2-D coordination polymer **4.28** looking down the *b*-axis.

Each 4-connected 2-D coordination polymer is 2-fold interpenetrated (Figure 4.47(a)) and, within the crystal, adjacent 2-D layers (of 2-fold interpenetrated 2-D coordination polymers) are offset to produce zig-zag shaped channels that are occupied by a combination of perchlorate anions and methanol solvate molecules (when viewed down the *b*-axis). The packing between 2-D layers is stabilised by an edge-to-face π stacking interaction between the two pendant pyridyl rings from ligands in adjacent layers (Figure 4.47(b)), with the closest contact of 2.701 Å (95.99°, centroid offset = 1.34 Å). This is fairly typical for an edge-to-face π interaction.[5]

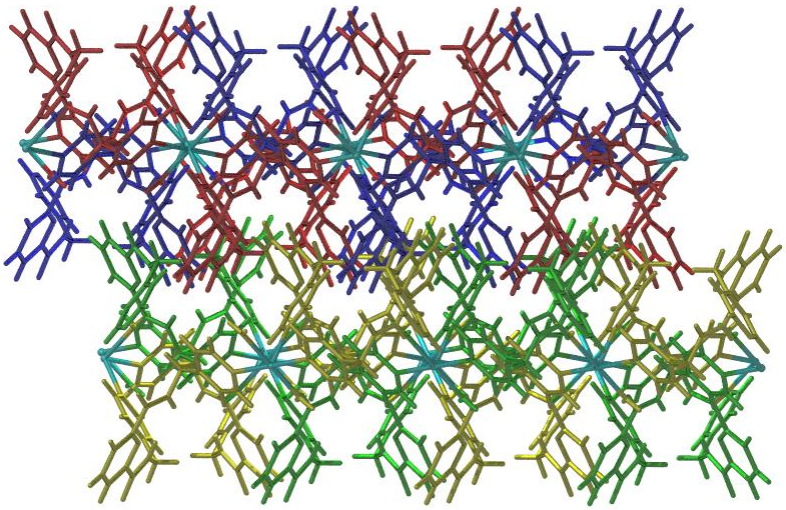

(a)

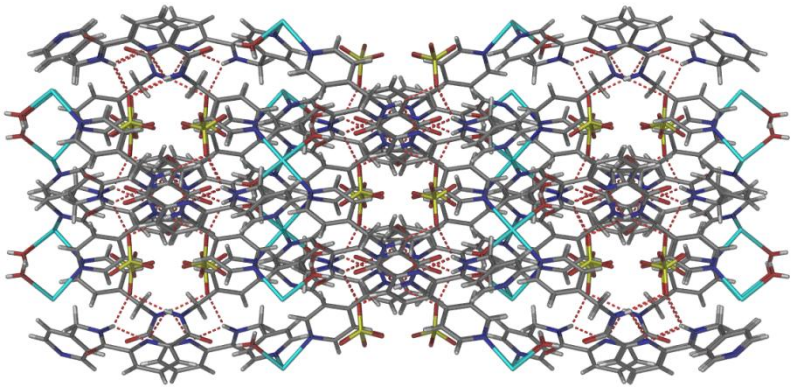

(b)

Figure 4.47. Two perspective views of the crystal packing of **4.28**. (a) A view of the two-fold interpenetration within a layer (blue and red or yellow and green) and then the packing of the

interpenetrated layers. (b) A view of the packing down the *b* axis showing the zig-zag shaped channels that are occupied by a combination of perchlorate anions and methanol solvate molecules.

Further analysis on the bulk sample of **4.28** was undertaken using PXRD. As shown in Figure 4.48, the measured PXRD pattern confirmed the purity of the bulk sample as all peak positions and intensities closely match those for the calculated pattern. Among the crystals, there were white powders that contaminated the sample. This has affected the crystallinity phase of the materials and led to the present of several additional peaks in the experimental patterns.

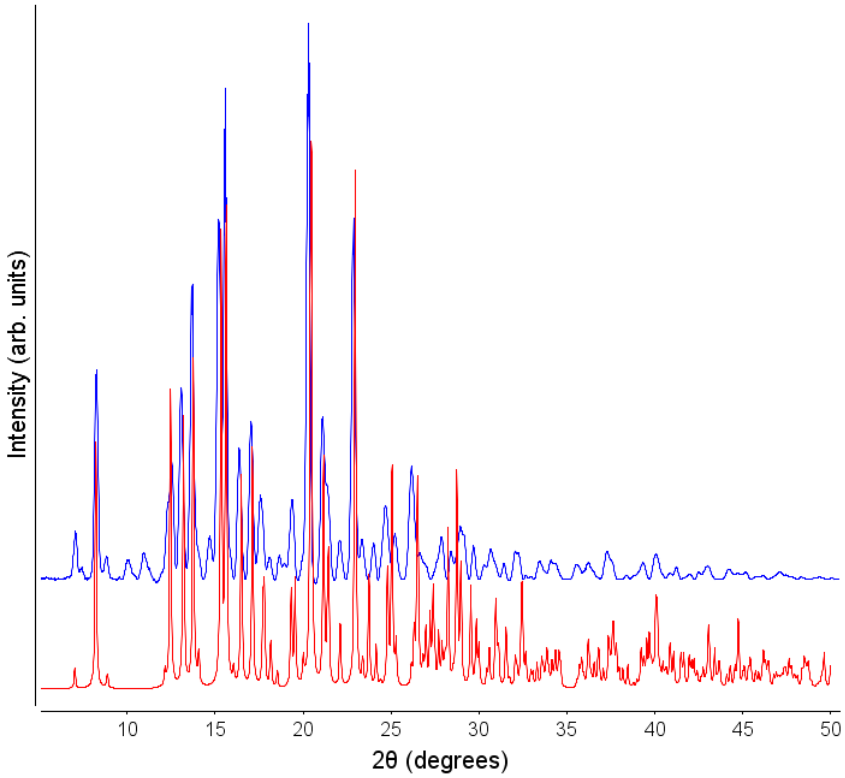

Figure 4.48. PXRD patterns for compound **4.28** (where red = simulated and blue = experimental).

4.3.3. Preliminary Anion Competition Studies

As outlined earlier, methods to assess the anion binding properties of the coordination polymers under competitive conditions have been reported.[39,128,215,356] Given the level of understanding generated from individual investigations of the coordination chemistry of **L5** and **L6** it was decided to explore the anion precipitation properties of these compounds under competitive conditions. To accomplish this, the effect of the diamide compounds **L5** and **L6** on a Cd(II) salt solution having a mixture of oxoanions (sulfate, perchlorate, nitrate) and spherical anions (bromide and chloride) was studied. This approach has been used to investigate the ability of the coordination polymers in separating anions such as sulfate, perchlorate and nitrate.[39,128,350]

In this study, the anion-separation experiment was conducted based on the procedures described in the literature.[128] The preliminary experiment was performed under two different conditions. Under condition I, the amide ligands (**L5** and **L6**) were reacted with a mixture of cadmium salts, including $CdSO_4$, $Cd(NO_3)_2$, $Cd(ClO_4)_2$, $CdBr_2$ and $CdCl_2$ in a metal-to-ligand ratio of 1:2 for each metal salt (Scheme 4.9). This was achieved by combining all cadmium(II) salts (0.05 mmol) in water and then adding a solution of the ligand (0.1 mmol) in methanol. This mixture was heated for approximately 30 minutes and left to stand at room temperature. After 24 hours cream solids were obtained.

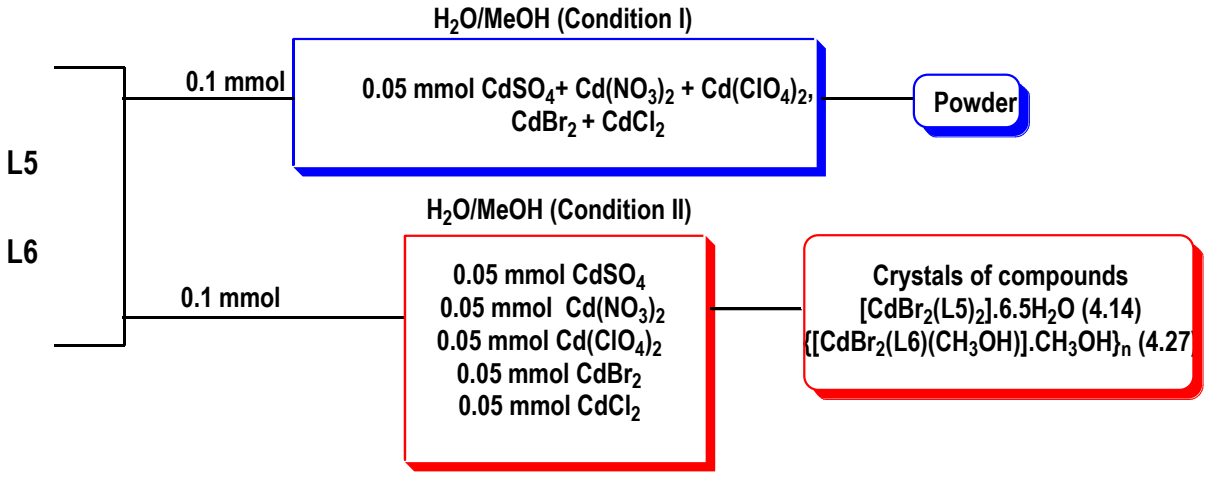

Scheme 4.9. A summary of the preliminary anion-separation experiments undertaken by the *in situ* crystallisation method.

Experiments under non-competitive conditions (condition II) were prepared in a similar manner to the synthesis of individual coordination compounds investigated in this thesis. However, to provide a direct comparison to the competition experiments, all individual coordination polymers were prepared in a mixture of water and methanol. While condition I gave powders as the main product, condition II gave crystals of two 1-D coordination polymers containing bromide anions (already described as **4.14** and **4.27**). The powder and crystals were characterised by a combination of combustion analysis and FT-IR spectroscopy.

FT-IR spectra of the two powder samples prepared under competitive indicate that the ligands may precipitate the same anions or mixture of anions (Figure 4.49). In the FT-IR spectra broad but strong bands are observed in the range 1050 – 1080 cm^{-1}. These correspond to the stretching frequencies for either Cl-O (ClO_4^-) or S-O (SO_4^{2-}). Weaker bands in the range 800-650 cm^{-1} corresponding to either perchlorate (O-Cl-O) and sulfate (O-S-O) were also observed. Thus, the FTIR spectroscopy seems to point toward the precipitation of coordination compounds containing perchlorate and sulfate anions. Given the greater lipophilicity of perchlorate anions it is likely that the species being precipitated is a perchlorate salt. Elemental analysis (Table 5.5) also supported the formation of compounds having either sulfate and perchlorate anions to balance the charge, although in all cases the metal-to-ligand ratio proposed was much higher (1.5:1 – 3.5:1) than was anticipated based on the structural studies described in section 4.3. For **L5** three isostructural coordination polymers with M:L ratios of 1:2 had been observed, including a $Cd(ClO_4)_2$ structure (**4.22**), while for **L6**, $Cd(NO_3)_2$ (**4.25**) and $Cd(ClO_4)_2$ (**4.28**) coordination polymers with M:L ratios of 1:2 were obtained. Thus it appears that none of the structures obtained above are involved in precipitating anions from these competitive conditions.

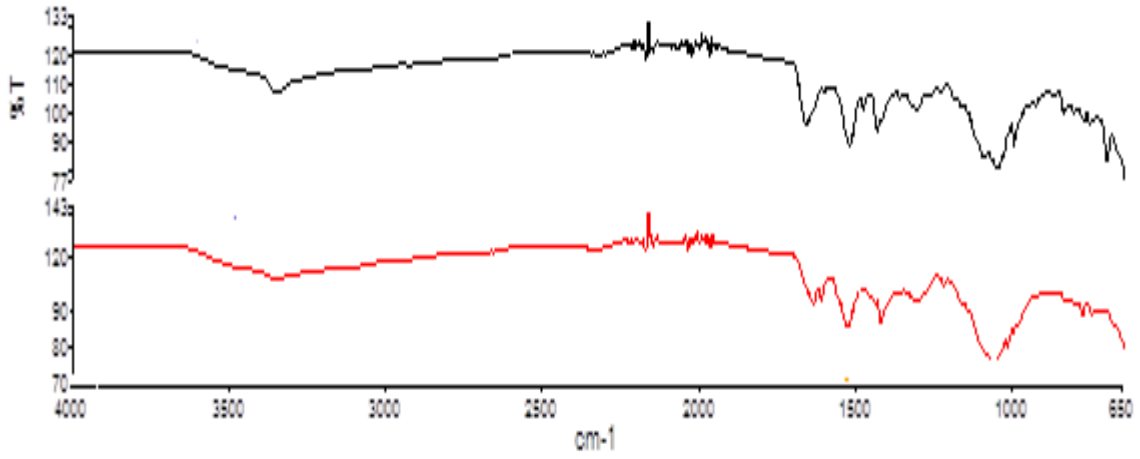

Figure 4.49. The FT-IR spectra of the solids obtained from competitive crystallisation (Condition I). Black = **L5** + CdX_n (**4.29**); red = **L6** + CdX_n (**4.30**).

Table 4.5. Possible formulations of the powders obtained from the competition experiments for **L5** and **L6**.

Sample	Found	Possible calculated formulae	Calculated percentages
4.29	C, 26.43; H, 2.61; N, 8.29%	$[Cd_{1.5}(ClO_4)_3(\mathbf{L5})(H_2O)_3]$	C, 26.28; H, 2.67; N, 8.07%
		$[Cd_2(SO_4)_2(\mathbf{L5})(H_2O)_5]$	C, 26.71; H, 3.19; N, 8.20%
4.30	C, 20.17; H, 2.08; N, 6.49%	$[Cd_{2.5}(ClO_4)_5(\mathbf{L6})(H_2O)]$	C, 19.95; H, 1.68; N, 6.12%
		$[Cd_{3.5}(SO_4)_{3.5}(\mathbf{L6})(H_2O)_2]$	C, 20.50; H, 1.91; N, 6.29%

This preliminary study has established that under competitive conditions, the coordination compounds derived from **L5** and **L6** tend to precipitate salts of either sulfate or, more likely, perchlorate anions. As noted in the literature[128,357,358] perchlorate is one of the more lipophilic anions (sitting high in the Hofmeister series between organic anions and iodide) and thus these experiments are consistent with previous observations and data. The *in situ* competitive crystallisation of coordination compounds from a mixture of complex anions has been previously described for the separation anions by Custelcean[78,126,133,322,328,359] and other researchers[214,321,357]

but considerable further work is required in the examples here to identify the nature of the precipitated product. In contrast to condition I, which demonstrated the ability of **L5** and **L6** to selectively precipitate sulfate or perchlorate salts, the non-competitive experiments (condition II) led to the formation of $CdBr_2$ compounds of **L5** and **L6** (**4.14** and **4.27**, respectively). The details on the crystal structures of these structures were described in the previous sections. Thus these preliminary experiments have revealed that the amide ligands appear to selectivity precipitate coordination compounds containing one type of anion under competitive crystallisation conditions.

4.4. Synthesis of coordination polymers of the tetraamide ligands L7-L12

As an initial approach to generate coordination polymers with potentially larger anion pockets, highly flexible ligands such as **L7** – **L12** were employed. Ligands **L7**-**L12** are potentially longer than **L5** and **L6** but considerably more flexible. To investigate the coordination chemistry of the tetraamide ligands, the six compounds were reacted with an array of first and second row transition metals. These complexes were prepared using conditions that had been successful for obtaining complexes of the structurally similar diamide ligands, **L5** and **L6**. The tetraamide ligands, **L7** - **L12** were reacted with MX_n (where M = Cu, Cd, Co, Zn, Ag; X = ClO_4, NO_3, CH_3COO, Cl, Br; n = 1 or 2) metal salts in 1:2 metal-to-ligand ratio in methanol. The extended amide ligands incorporating 4-pyridyl donors (**L8** and **L10**) showed a propensity to form 1-D coordination polymers when reacted with cadmium(II) salts (CdX_2 where X = NO_3, X_2=SO_4). This is similar to the coordination chemistry observed for structurally-related but simpler monoamide ligand **L2** and the diamide compound **L6**. Reaction of **L7** with the metal salts in methanol solution gave clear solutions, which then evaporated to give oils that could not be characterised. The oils obtained from these reactions were triturated with warm ethanol or diethyl ether but all attempts failed to provide reasonable quantities of any solid. Reaction of **L9** also incorporating 3-pyridyl donors as the metal coordinating sites, also failed to give isolable (crystalline, microcrystalline or amorphous solid) compounds, and resulted in products that were oils. Repeated attempts to optimise the reaction conditions (different solvents, crystallisation conditions) and also to repeat the reaction with different metal-ligand ratios were not successful in producing analytically pure solids (Scheme 4.10).

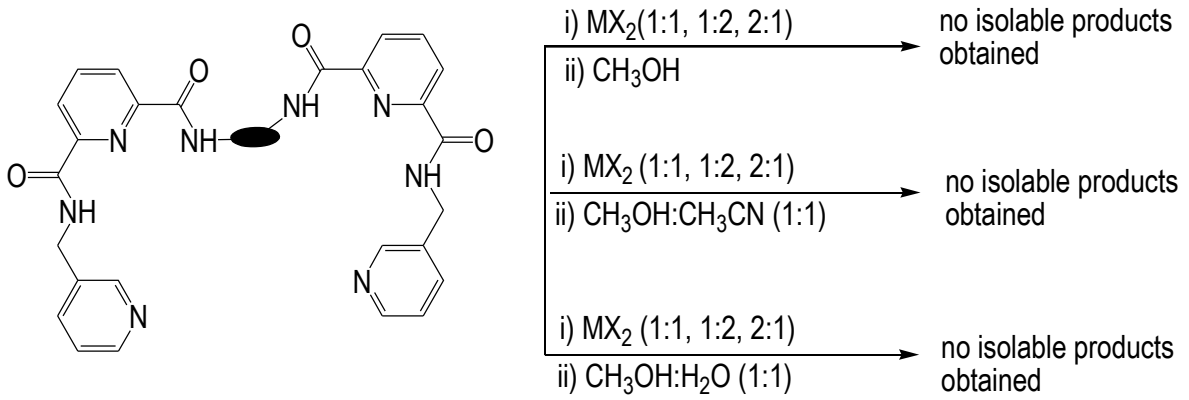

L7 = ⬬ = $-CH_2CH_2-$ **L9=** ⬬ = $-CH_2CH_2CH_2-$

$MX_2 = CuX_2/CdX_n/CoX_2/ZnX_2/AgX$, X= ClO_4^-, NO_3^-, CH_3COO^-,Cl^-, Br^-

Scheme 4.10. A summary of the reactions attempted with the tetraamide ligands incorporating aliphatic spacers and pendant 3-pyridyl donors.

In contrast, reaction of the tetraamide ligands, incorporating pendant 4-pyridyl donors as the metal coordinating sites (**L8** and **L10**), with cadmium salts gave colourless solutions from which were obtained two new coordination polymers, $\{[Cd_{1.5}(\mathbf{L8})_2(H_2O)_4](NO_3)_3\cdot CH_3OH\}_n$ (**4.31**) and $\{[Cd(SO_4)(\mathbf{L10})(H_2O)_2]\cdot 4H_2O\cdot CH_3OH\}_n$ (**4.32**) (Scheme 4.11). Fortunately, a 1-D coordination polymer with formula suggested by elemental analysis, $\{[CdBr_2(\mathbf{L11})_2]\cdot 4H_2O\}_n$ (**4.33**) was obtained with ligand **L11**.

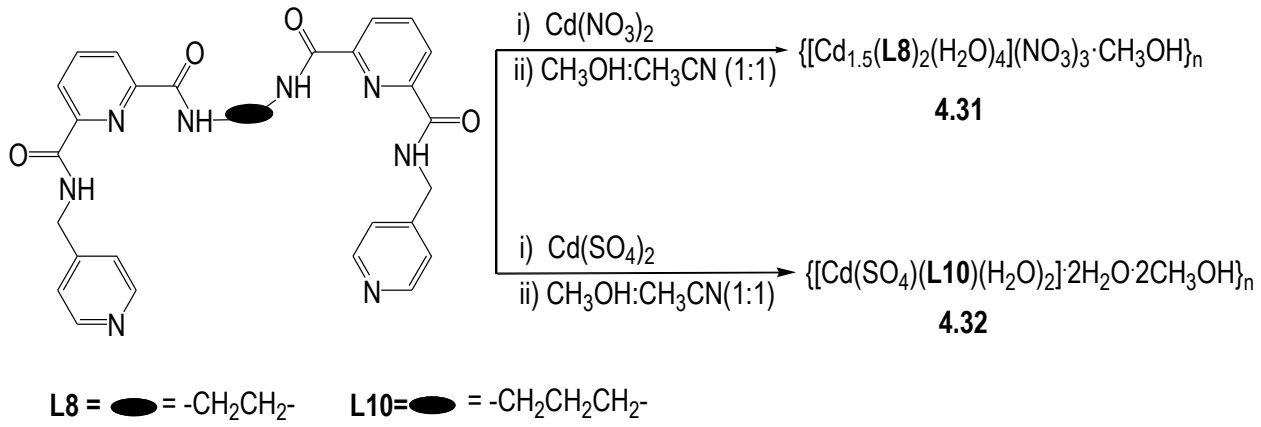

Scheme 4.11. Synthesis of the coordination polymers obtained with the tetraamide ligands incorporating pendant 4-pyridyl donors .

In compounds $\{[Cd_{1.5}(\mathbf{L8})_2(H_2O)_4](NO_3)_3\cdot CH_3OH\}_n$ (**4.31**) and $\{[Cd(SO_4)(\mathbf{L10})(H_2O)_2]\cdot 2H_2O\cdot 2CH_3OH\}_n$ (**4.32**), distinctive infrared stretches were observed in their IR spectra, an N-O stretch at 1315 cm^{-1} and two S-O stretches at 1022 and 670 cm^{-1}, respectively. Complexes **4.31**, **4.32** and $\{[CdBr_2(\mathbf{L11})_2]\cdot 4H_2O\}_n$ (**4.33**) were characterised by elemental analysis which supported the structures observed by X-ray crystallography. X-ray crystallography revealed that these three compounds crystallise in the tricilinic space group *P*-1 but with different structures and crystal packing.

Crystal structure of **4.31**

$\{[Cd_{1.5}(L8)_2(H_2O)_4](NO_3)_3\cdot CH_3OH\}_n$. Reaction of **L8** with cadmium(II) nitrate in methanol, followed by slow evaporation of the solvent yielded colourless rectangular block-shaped crystals of **4.31** in 36% yield. The complex crystallises in the triclinic space group *P*-1. The structure of **4.31** is a 1-D coordination polymer, with the asymmetric unit containing two molecules of ligand **L8**, two cadmium positions (one on a centre of inversion), four coordinated water molecules, one non-coordinated methanol (disordered) and three non-coordinated nitrate anions (two of which are disordered over two positions). Despite the lack of coordination by nitrate anions, both cadmium centres have octahedral geometries but different coordination environments. One cadmium (Cd1) atom is coordinated by two coordinated water molecules and four pyridyl groups from four different molecules of **L8**, while the second cadmium atom (Cd2) was coordinated by

four water molecules and two nitrogen donors from pyridyl units of ligand **L8**. The cadmium centres have Cd-O bond lengths of 2.269(9) – 2.305(7) Å and Cd-N bond lengths in the range 2.295(9) – 2.410(8) Å which is typical.[347] The distances between the Cd-Cd atoms are in the range of 10.605- 19.914 Å.

The presence of weak intramolecular hydrogen bonding interactions which pre-organise the NH donors of the ligand into a central pocket are indicated (*d* = 2.233 – 2.384 Å; *D* = 2.642 – 2.733 Å; N-H···N angles = 104.33 – 108.88°). In one ligand the ethylene spacer (-N-CH_2-CH_2-N- torsion angle = 69.4°) of **L8** acts as a hinge to allow the second part of the ligand to interact with the second cadmium atom and form a metallo-macrocyclic structure. As a consequence of the flexibility provided by the ethylene spacer, the two pre-organised 2,6-pyridine dicarboxamide moieties form independent pockets, but one is occupied by the carbonyl oxygen of the other amide moiety (N-H··O=C, *d* = 2.137, 2.204 Å, *D* = 3.188, 2.731 Å). These distances are fairly typical of moderately strong hydrogen bonds.[348] The second molecule of **L8** adopts the single pocket conformation with both spacers in a syn arrangement that was observed in the structure of **L7**. Figure 4.50 shows the perspective view of the asymmetric unit of complex **4.31** with non-coordinated methanol molecules and nitrate anions omitted for clarity.

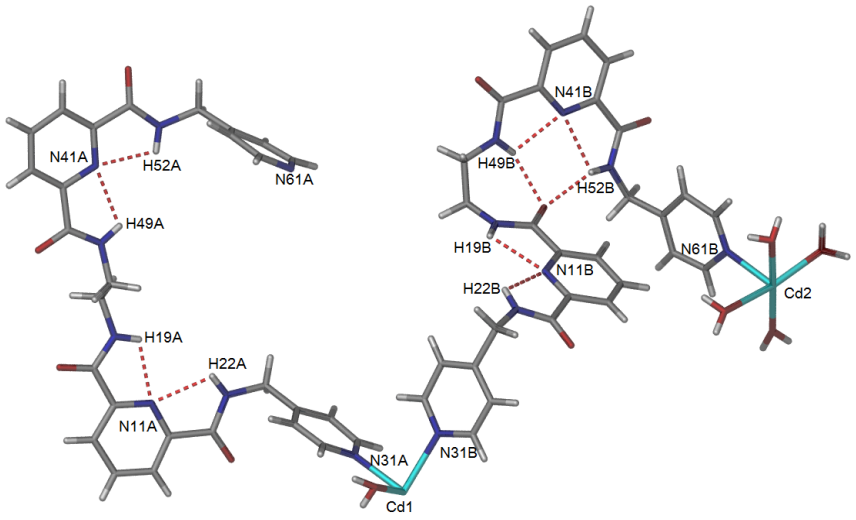

Figure 4.50. A perspective of the asymmetric unit of complex **4.31**. Selected bond lengths (Å) and angles (°) : Cd(1)- N(31A) 2.409(8), Cd(1)-N(31B) 2.410(8), Cd(2)-N(61A) 2.295(9), Cd(2)-N(61B) 2.295(8), Cd(2)-O(4) 2.269(9), Cd(2)-O(3) 2.305(7), Cd(2)-O(69) 2.298(5), O(1)-Cd(1)-N(31B) 90.71(43), N(61A)-Cd(2)-O(69) 89.0(3) and N(31A)-Cd(1)-N(31B) 89.78(3).

The extended structure of compound **4.31** is shown in Figure 4.51(a) with $[M_4L_4]$ metallo-macrocyclic repeating units are arranged into 1-D coordination polymers. Taking the CdN_4O_2 centres as the axis of the 1-D coordination polymer, adjacent CdN_4O_2 nodes in the structure are connected by two loops, each formed from two molecules of **L8** and a CdN_2O_4 centre. These are related by a centre of inversion at the centroid between two CdN_4O_2 centres. Like nearly all the structures in this thesis, the NH amide moieties of the 2,6-pyridine dicarboxamide units are directed inwards facing the core of the 1-D coordination polymers and the C=O groups directed outward. There are moderately strong hydrogen bonds interactions between the amide hydrogen bond donors with the nitrate anions (*d* = 2.029, 2.146 Å, *D* = 2.861, 2.959 Å, see Figure 4.51(b)). The arrangement of the 1-D coordination polymers in the crystal packing is shown in Figure 4.52 with hydrogen atoms omitted for clarity.

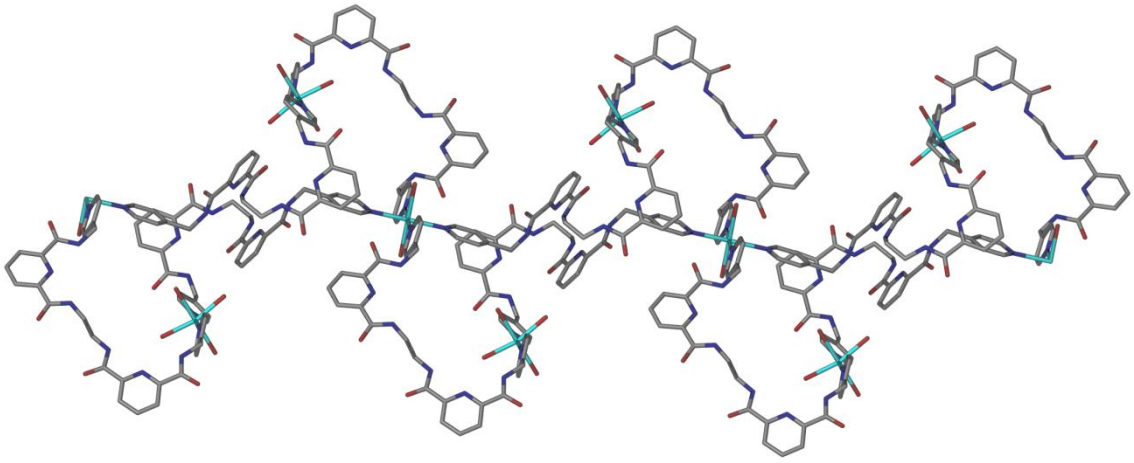

(a)

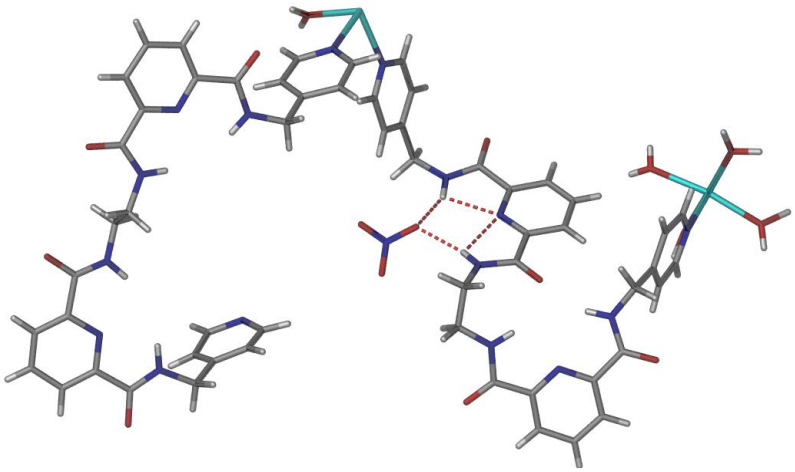

(b)

Figure 4.51. A perspective view of the (a) extended structure of **4.31** (hydrogen atoms omitted for clarity) and (b) hydrogen bonding interactions between the amide NH and a nitrate anion.

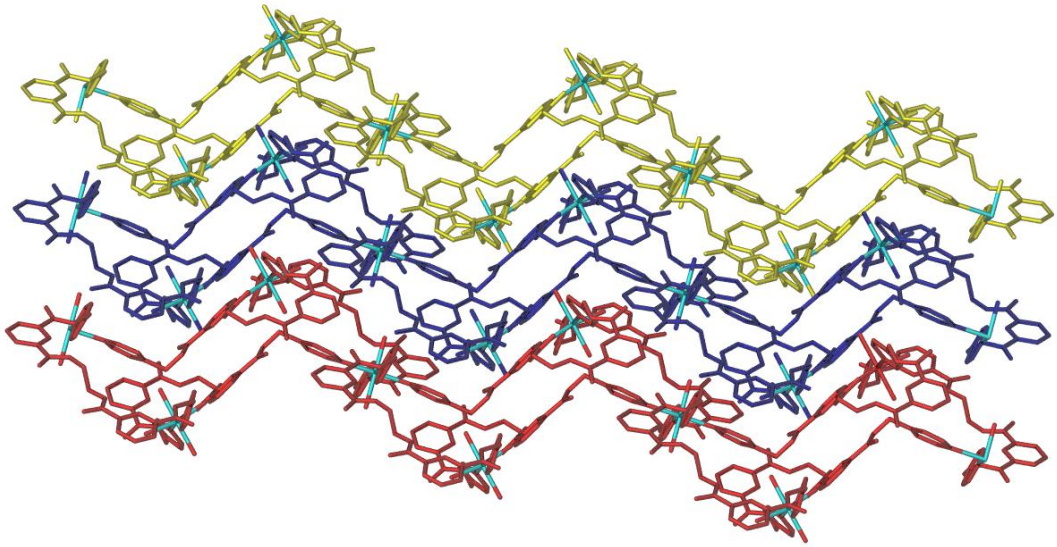

Figure 4.52. A perspective view of the crystal packing of **4.31** with hydrogen atoms, solvate methanol molecules and nitrate anions omitted for clarity.

Crystal structure of **4.32**

$\{[Cd(SO_4)(L10)(H_2O)_2]\cdot 2H_2O\cdot 2CH_3OH\}_n$. Reaction of **L10** with cadmium sulfate yielded rectangular block-shaped crystals in 32% yield. Like **4.31**, this complex also crystallised in the

triclinic space group *P*-1 but with quite a different structure. The asymmetric unit consists of one molecule of ligand **L10**, one cadmium atom, two methanol molecules, one coordinated sulfate, two coordinated water molecules and one non-coordinated water solvate (Figure 4.53). The cadmium atom in this complex adopts an octahedral geometry, coordinated by two μ_2-oxygen atoms from two bridging sulfate anions, two water molecules and two pyridyl donors from two separate molecules of **L10**. The Cd-N and Cd-O distances are in the range of 2.262(6) – 2.284(6) Å.

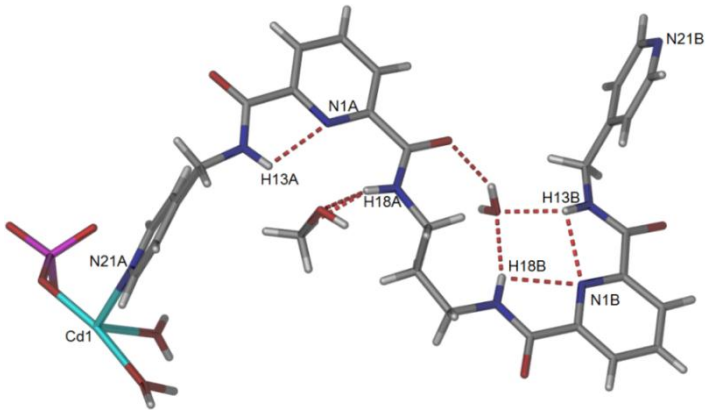

Figure 4.53. A perspective view of the asymmetric unit of complex **4.32** with selected solvate molecules omitted. Selected bond lengths (Å) and angles (°): Cd(1)- N(21A) 2.284(3), Cd(1)-N(21B) 2.262(4), Cd(1)-O(70) 2.329(6), Cd(1)-O(83) 2.553(8), O(70)-Cd(1)-N(21B) 89.03(18) and O(70)-Cd(1)-N(21A) 85.52(19).

An extended view of compound **4.32** is shown in Figure 4.54. The repeating unit in this 1-D coordination polymer is a $[M_4L_2]$ metallo-macrocyclic building block, where two cadmium atoms are bridged by two sulfate oxygen donors. These di-cadmium units are then coordinated by the nitrogen donors of four ligands to form the 1-D necklace-type coordination polymer. The distance between the bridged Cd-Cd subunit is 3.697 Å and the distance between two separated cadmium atoms is 19.685 Å. The adjacent polymer chains of compound **4.32** are arranged with all NH amide units directed inwards facing the cavity of the coordination polymer and the C=O groups directed outward.

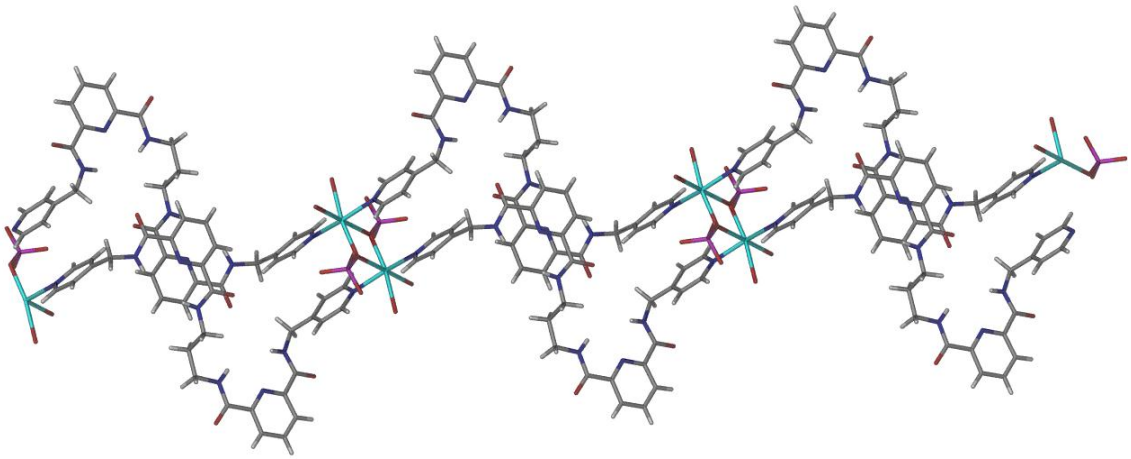

(a)

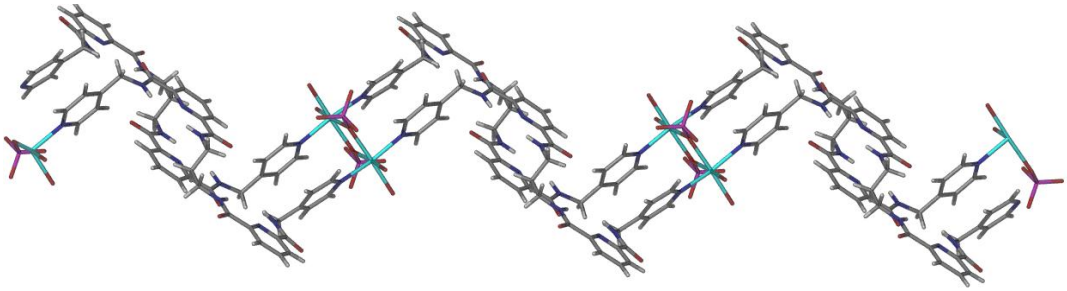

(b)

Figure 4.54. Two perspective views of the extended structure of complex **4.32** with hydrogen at coordinated water molecules omitted for clarity.

This structure is stabilised by intramolecular hydrogen bonding interactions between the pre-organised amide NH donors with water and methanol solvate molecules (Figure 4.55). There are two intermolecular hydrogen bonding interactions between water molecules to carbonyl groups (O-H···C=O, d = 2.003, D = 2.913 Å and d = 2.006, D = 2.874 Å). As noted, the anions are involved in bridging the dicadmium units and not hydrogen bonded to the 2,6-pyridine dicarboxamide moiety.

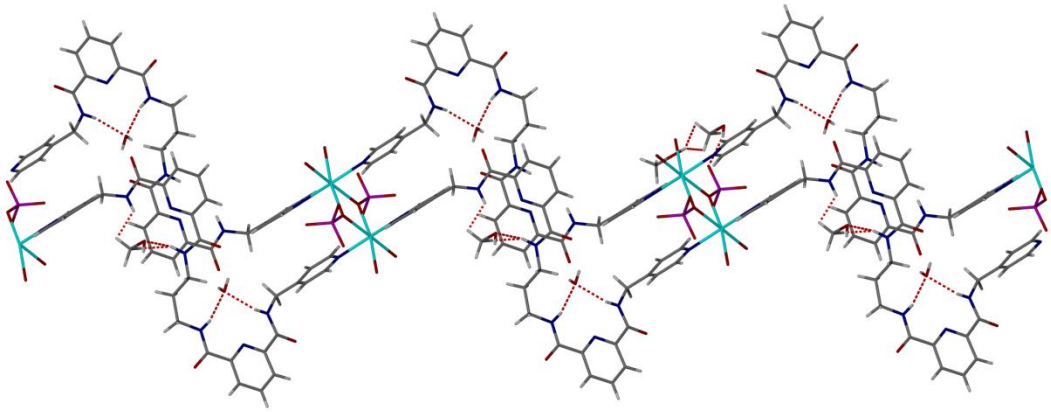

Figure 4.55. A perspective view of the weak interactions involved in the extended structure of **4.32**.

The packing of the coordination polymers are stabilised by face-to-face π-stacking interactions between the pyridyl cores (centroid-centroid distance 3.60 Å; angle 78.02°, centroid offset 1.38 Å) and the two pendant pyridines (centroid-centroid distance 3.80 Å; angle 81.95°, centroid offset 1.39 Å) (Figure 4.56).

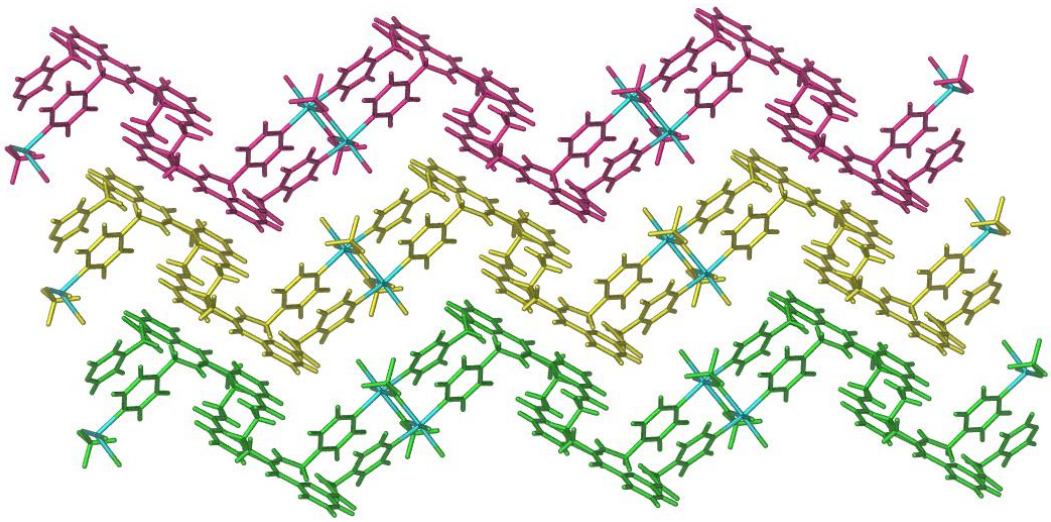

Figure 4.56. A representation of the packing of 1-D coordination polymers in the structure of **4.32**.

Crystal structure of **4.33**

{[$CdBr_2$(L11)$_2$]·4H_2O}$_n$. Crystals of {[$CdBr_2$(**L11**)$_2$]·4H_2O}$_n$ were obtained from a methanol-water solution of **L12** and cadmium bromide upon slow evaporation in 24% yield. Complex {[$CdBr_2$(**L11**)$_2$]·4H_2O}$_n$ crystallised in the triclinic space group *P*-1 with one ligand **L11**, one cadmium atom (on a centre of inversion), two water molecules and one bromide in the asymmetric unit (Figure 4.57). The cadmium atom adopts an octahedral coordination environment, with two bromide atoms in the axial positions and the equatorial positions occupied by four pyridyl donors from four separate molecules of **L11**. The Cd-N bond length is 2.453(4) Å and the Cd-Br bond length is 2.6805(5) Å. The Cd-Br bond distance is approximately 0.08-0.1 Å longer than the Cd-Br distance in compound **4.27**, while the Cd-Cd distance in this compound is 16.765 Å.

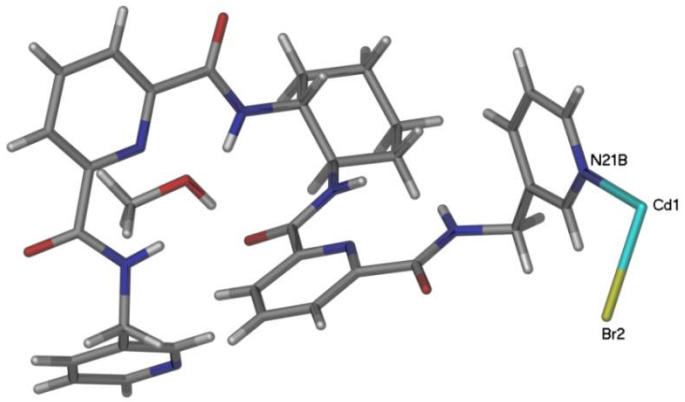

Figure 4.57. A perspective view of the asymmetric unit of compound **4.33**. Selected bond lengths (Å) and angle (°): N(21B)-Cd(1) 2.453(4), Cd(1)-Br(2) 2.6805(5) and N(21B)-Cd(1)-Br(2) 87.45(9).

The extended structure of compound **4.33** is shown in Figure 4.58. Within the ligand the pendant 4-pyridyl rings twist backward and forward relative to the 1,2-cyclohexane core with an -N-CH_2-CH_2-N- torsion angle of 56.3(2)°. This enables the ligand to coordinate to two different cadmium centres which are also linked by a second molecule of **L11**. Each cadmium is coordinated by four molecules of the ligand to generate a necklace-type 1-D coordination polymer. Like other compounds in this thesis, this coordination polymer is also constructed from a dinuclear metallo-macrocylic repeating unit.

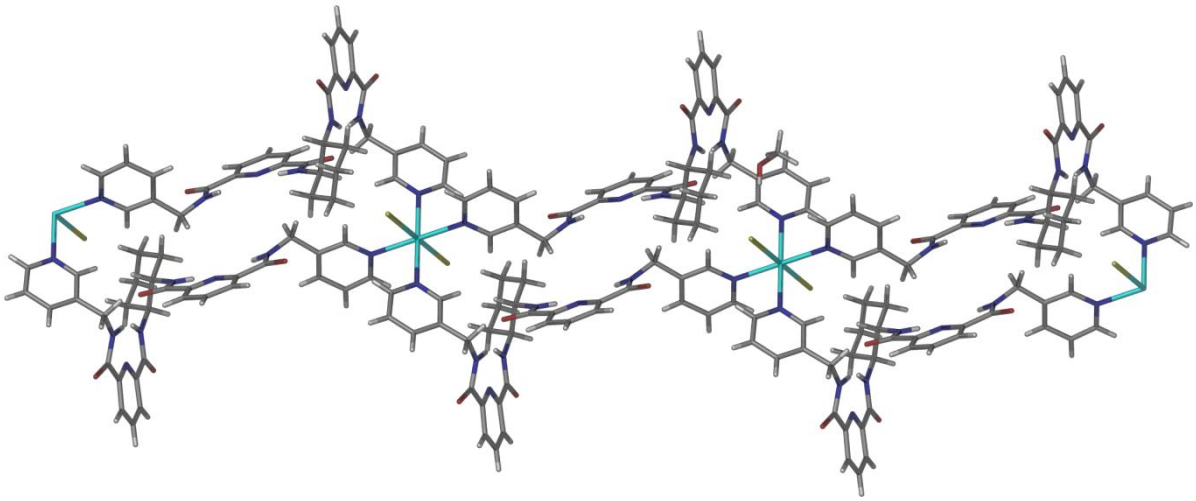

Figure 4.58. A perspective view of the extended structure of complex **4.33**.

Two types of ligand derived hydrogen bonding interactions are responsible for the internal conformation of the coordination polymers and the packing of adjacent 1-D coordination polymers in the solid state. In the inter-polymer packing there are two intermolecular hydrogen bonding interactions (N-H···O=C, *d* = 2.094 Å, *D* = 2.946 Å and *d* = 2.090 Å, *D* = 2.938 Å, N-H···O angle = 161.52°) formed between the pre-organised NH amide donors of a molecule of **L11** in one coordination polymer and the amide carbonyl group of a molecule of **L11** in an adjacent polymer (Figure 4.59(a)). The intermolecular hydrogen bonding leads to the formation of 2-D hydrogen bonded sheets of the 1-D coordination polymers that extend in the *ac* diagonal (Figure 4.59(b)) Internally, each ligand within the coordination polymer adopts a conformation whereby the amide C=O forms a moderately strong N-H···O=C intramolecular hydrogen bonding interaction (*d* = 1.862 Å, *D*= 2.911 Å). This blocks one of the anion binding pockets of the ligand (Figure 4.59 (a)).

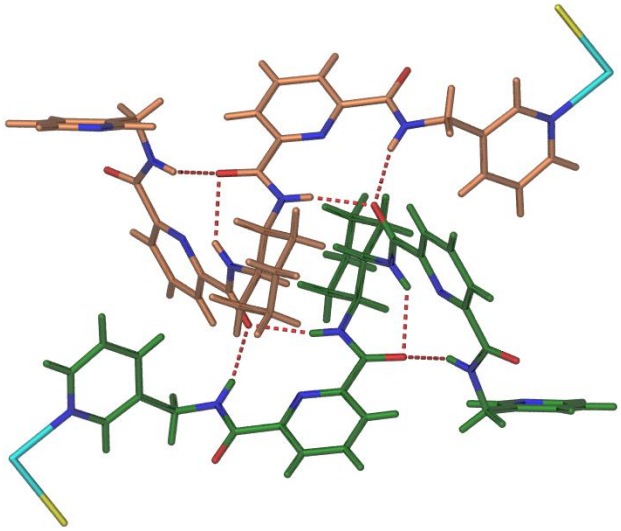

(a)

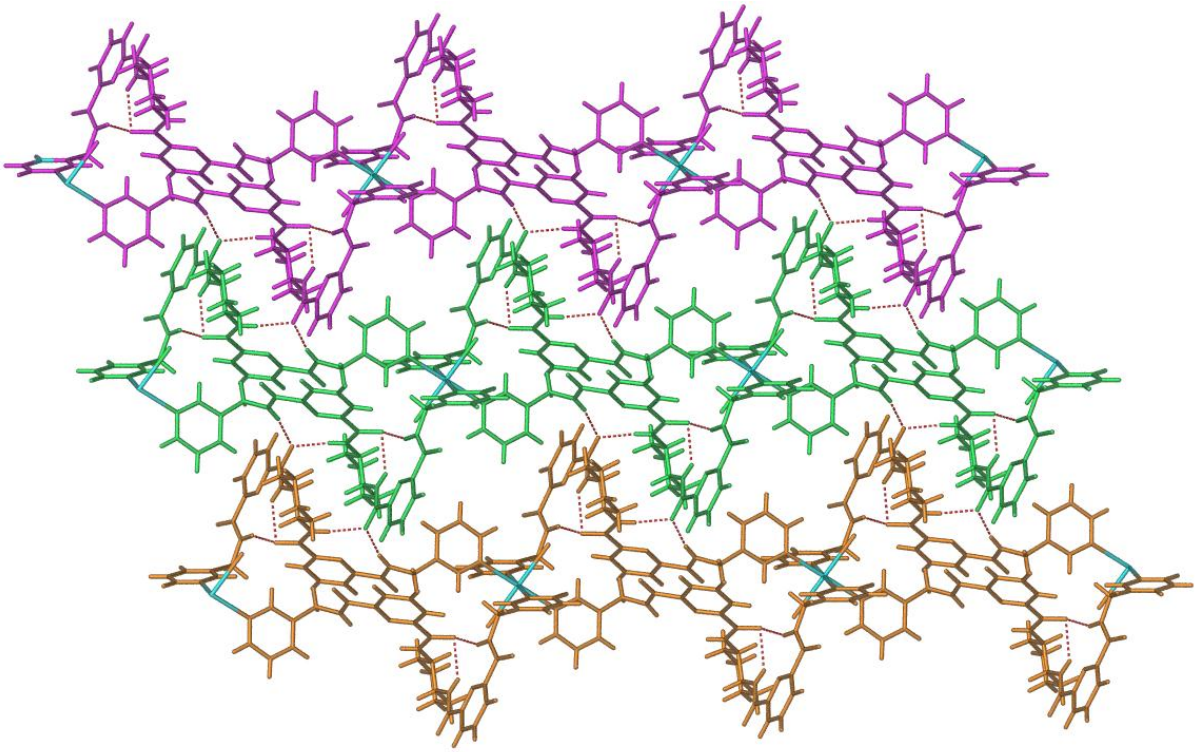

(b)

Figure 4.59. (a) A perspective view of intra- and intermolecular hydrogen bonding involving **L11** in the coordination polymer **4.33**. (b) The packing of 1-D coordination polymers into 2-D hydrogen bonded sheets.

In the 2-D crystal packing, the 1-D coordination polymers in each 2-D layer form C-H···π stacking interactions with 1-D coordination polymers in adjacent layers . These interactions occur between the pendant pyridyl rings of molecules of **L11** in the adjacent layers (C-H-centroid distance 2.73 Å; angle 95.30°, centroid offset 1.39 Å). The view of the crystal packing of **4.33** is shown in the figure below.

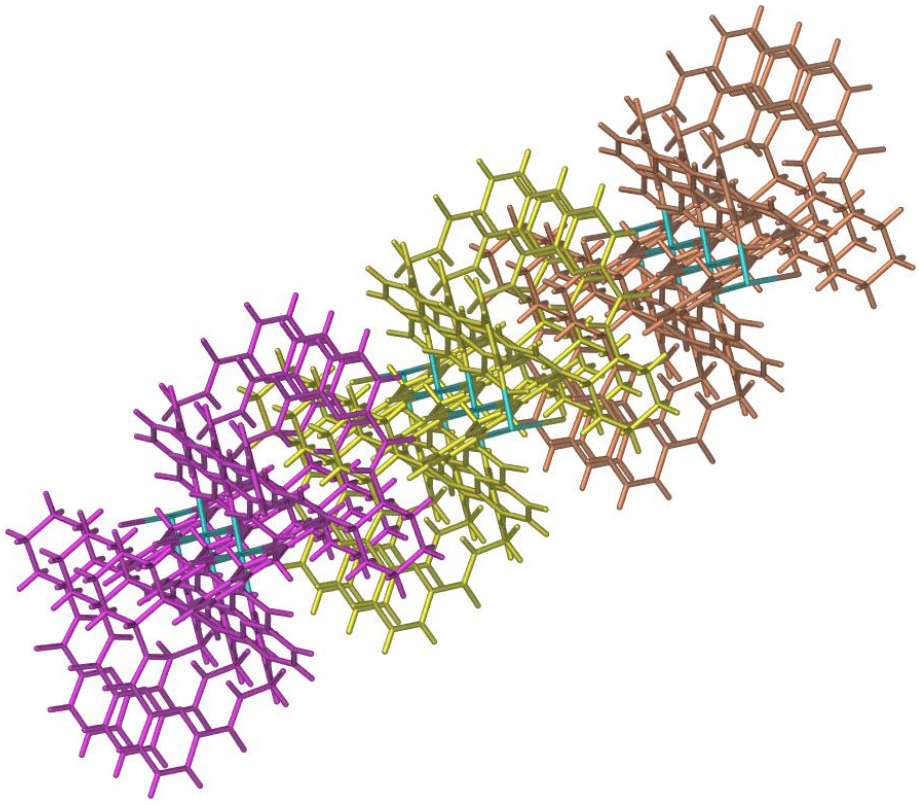

Figure 4.60. A perspective view of the crystal packing of compound **4.33**.

The results described in this section of the thesis have shown that by using tetraamide ligands **L8**, **L10** and **L11**, which are more flexible than **L5** and **L6**, 1-D coordination polymers with interesting supramolecular motifs could be obtained. Nearly all of the compounds fold up on themselves to block the pocket from encapsulating anions or solvent molecules. This is particularly demonstrated by structures **4.31** and **4.32** which contain ligands **L8** and **L10**. Free rotation at the ethylene and propylene spacer leads less control over the conformations of the flexible ligands and thus the compounds obtained are closed-packed in the solid-state.

4.5. Summary

This chapter has described the synthesis of discrete metallo-supramolecular assemblies and coordination polymers of symmetrical pre-organised diamide ligands (**L5** and **L6**) and 1-d coordination polymers of the more flexible tetraamide ligands (**L7** to **L12**). The reactions of the two diamide ligands, **L5** and **L6** gave eight 1-D coordination polymers and one 2-D coordination polymer with a number of these constructed from metallo-macrocyclic-type repeating units. Two distinct conformations of the repeating unit were observed for ML_2 1-D coordination polymers. Most interestingly, a majority of these coordination polymers demonstrate encapsulation of the anion within the amide cavity. In two cases it appears that the cavity of the coordination polymers can be expanded to accommodate different sized polyatomic anions by distortions around the metal centre. In contrast to **L5** and **L6**, incorporation of more flexible ligands such as **L8** and **L10** gave three closed packed coordination polymers. These ligands tend to fold upon themselves to block the anion pocket from encapsulating anions or solvent molecules.

Reaction of compounds **L5** and **L6** with Pd(II) led to the formation of three mononuclear and three dinuclear complexes (in one case a mixture of products was obtained for **L6**). Palladium complexes obtained from reactions with **L5** gave a single mononuclear product, while reactions with **L6** gave either a discrete dinuclear product or a mixture of discrete mononuclear and dinuclear complexes. In the latter case this mixture could not be separated despite several attempts and the mixture was studied by mass spectroscopy and NMR spectroscopy analysis. DOSY NMR was used to identify the components of the mixture based on their differing diffusion coefficients. DOSY NMR was also used to estimate the relative size of the mononuclear and dinuclear complexes based on a comparison of diffusion ratios of the product and the ligand. The results obtained appear consistent within the set of compounds reported in the chapter but are not directly comparable to values of equivalent compounds reported in the literature. Crystals of one of these complexes, a mononuclear palladium(II) complex, $[Pd(en)(\mathbf{L5})](PF_6)_2 \cdot H_2O \cdot 2CH_3OH$ were also isolated. This complex has a bowl-shaped structure with encapsulation of one of the hexafluorophosphate anions inside the bowl and a second on the lower face of the structure. Specific anion-π interactions were observed between the pyridyl rings and the hexafluorophosphate anions inside the bowl, while there are intermolecular hydrogen bonds between the pre-organised NH donors and the hexafluorophosphate anion on the lower face of the structure.

Reactions of the diamide ligands, **L5** and **L6** with a range of transition metals such as cadmium(II), cobalt(II) and zinc(II) provided access to both discrete complexes and metallo-macrocyclic based coordination polymers. Reaction of **L5** with cadmium nitrate, cadmium perchlorate and cobalt nitrate led to formation of three isostructural necklace-like 1-D coordination polymers. In the crystal packing of these molecules, the nitrate or perchlorate anions were found to be incorporated inside the channels of the structure. The ability of these compounds to expand their cavity to accommodate different sized anions was also observed. Reaction of **L6** with cadmium nitrate and zinc nitrate led to formation of two isostructural undulating 1-D coordination polymers. These compounds have potentially porous structures due to the presence of two types of channels in the packing of these structures. One set of channels are filled with a mixture of solvent and nitrate anions while the second group contain only disordered solvent. These isomorphous structures hinted at potentially interesting anion binding and exchange properties for these compounds. Some preliminary investigations were undertaken.

Reaction of **L6** with cadmium perchlorate by slow evaporation approach gave a 2-D coordination polymer. This compound is built from the assembly of $[M_4L_4]$ metallo-macrocycle repeating units into a 4-connected 2-D coordination polymer. Finally, three 1-D coordination polymers were obtained with the tetraamide ligands containing pendant 4-pyridyl donors. In these structures the ligands were found to pack in a collapsed form to block the 2,6-pyridine dicarboxamide core from encapsulating anions or solvent molecules. These results have shown that the incorporation of more flexible tetraamide ligands into coordination polymers led to close-packed structures and not structures containing one large or two closely related 2,6-pyridine dicarboxamide pockets for selective anion encapsulation.

CHAPTER 5

COORDINATION CHEMISTRY OF AMIDE BRIDGING LIGANDS WITH DPM CHELATING MOTIFS

Chapter 5

5. Coordination chemistry of amide bridging ligands with di-2-pyridylmethane (dpm) chelating motifs

5.1. Introduction

Research into the synthesis and properties of bridging ligands containing di-2-pyridyl moieties has received considerable attention.[180] These compounds have been widely employed in the construction of multinuclear metallo-supramolecular assemblies[38,360,361] or coordination polymers. [93,102,180,187,193,240,362-370] In particular, bridging ligands containing di-2-pyridylamine (dpa) and di-2-pyridylmethane (dpm) chelating motifs have received attention in recent years.[180,187,362-365] Derivatives of these compounds have been investigated for their electronic and magnetic properties, supramolecular chemistry (anion-π interactions), as anion receptors and as structural and functional enzyme active site models.[180,187,362-365] Di-2-pyridylamine (dpa) and di-2-pyridylmethane (dpm) contain a single atom spacer in between the two pyridine rings. This means that dpa and dpm form six-membered chelate rings upon coordination (Figure 5.1). The atom spacer in between the pyridine rings acts to insulate the two rings from one another, thus removing the conjugation between the two heterocyclic rings. In contrast to dpa and dpm, the archetypal bidentate ligand 2,2-bipyridine (bpy),[42,371,372] which lacks the atom spacer in between the two pyridine rings, forms five-membered .

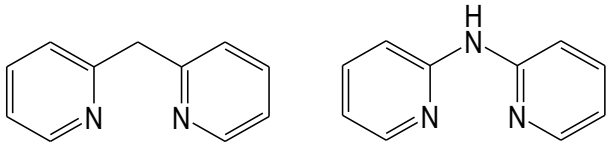

dpm **dpa**

Figure 5.1. Examples of six-membered chelating motifs incorporated into bridging ligands.

The use of bridging ligands that have the capacity to chelate each metal centre bridged by the ligand is important to improve the stability of multinuclear complexes or enhance metal–metal interactions in such species.[180,187,363,373] Steel and co-workers have reported many complexes derived from the bridging ligands containing di-2-pyridyl chelating

motifs.[178,187,363,364,373] This includes the coordination chemistry of di-2-pyridylamine (dpa) based bridging heterocyclic ligands with silver(I), copper(II) and palladium(II).[187,363,364,373] On reaction with silver salts, the ligands act as divergent bridging unit, with only two of the four pyridine rings involved in the coordination to form 1-D coordination polymers. Conversely, on reaction with copper(II) and palladium(II), the ligand uses all four nitrogen donors to coordinate with the metal centres and form stable discrete dinuclear complexes.[364] Several mononuclear and dinuclear ruthenium complexes containing dpa subunit have also been described with such ligands (Figure 5.2).[363] Platinum(II) and palladium(II) complexes containing dpa moieties have also been reported. These materials have structural similarity to cis-Platin and their biological activity has been investigated.[374-377]

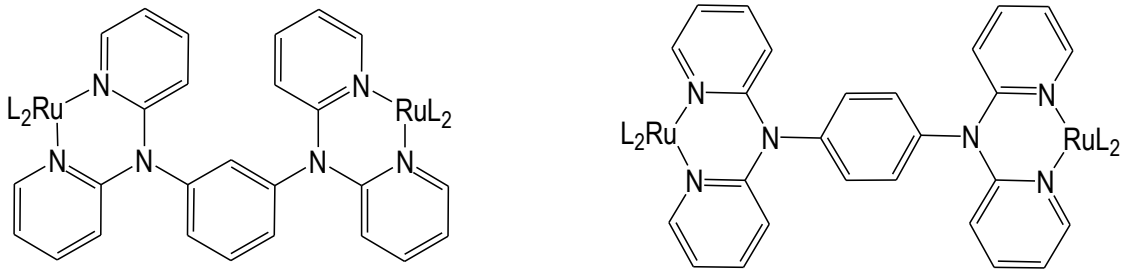

Figure 5.2. Examples of ruthenium complexes incorporating 1,3- and 1,4-bis(di-2-pyridylamino)benzene ligands .

The study of flexible bridging ligands with dpa subunits appended to a xylene core have also been explored.[187,373] Examples of these compounds are shown in Figure 5.3. In these compounds a methylene group separates each dpa fragment from the aromatic core. Complexes of these compounds with silver(I), copper(II) and palladium(II) have been investigated by Antonioli and co-workers.[187,373] By using flexible bridging ligands a diverse range of complexes and crystal packing for these complexes was obtained.

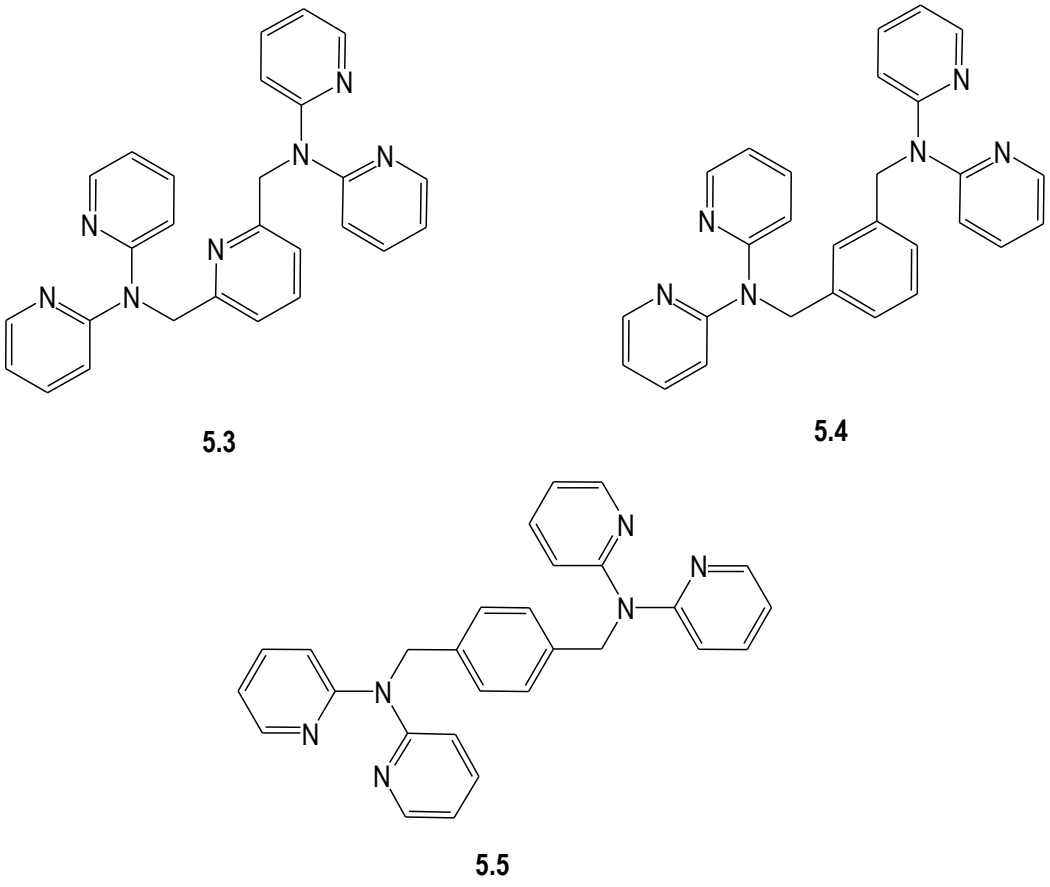

Figure 5.3. Three examples xylenyl bridged dpa ligands.

The coordination chemistry of the parent compound, di-2-pyridylmethane (dpm), and its derivatives have also been explored. Canty and Minchin[378] were the first to describe palladium complexes of a simple bridging ligand, 1,1,2,2-tetra(2-pyridyl)ethane (**5.6**) (Figure 5.4). Dinuclear complexes of copper(II) and zinc(II) with this ligand have been reported by Steel and co-workers.[178] On reaction with silver(I) nitrate, the ligand acts as a tetradentate bridge leading to the formation of a 1-D coordination polymer.

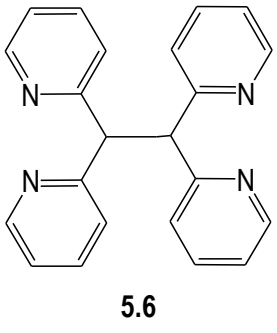

Figure 5.4. A structure of 1,1,2,2-tetra(2-pyridyl)ethane (**5.6**).

In contrast to dpa and dpm, the chelating moiety di-2-pyridylmethaneamine (dipa) has been much less studied, particularly as a component of bridging ligands. In a similar manner to dpm and dpa, this molecule forms six-membered chelating rings upon coordination. Dipa containing bridging ligands will be flexible due to the presence of a methylene spacer between the di-2-pyridyl rings and amine. Only a handful of complexes have been reported for dipa itself, including ruthenium(II) complexes reported by Chang and co-workers,[379] and the synthesis of palladium(II) complexes for investigation of their catalytic activity.[184,380-384] Dipa has been used as a precursor in the preparation of a simple bridging ligand, bis[di(2-pyridyl)methyl]amine (BDPMA) (Figure 5.5).[184] In the work described in this Chapter, dipa was used as a precursor to prepare three novel potentially doubly bidentate bridging ligands, 2,6-[*N,N'*-bis(di(pyridin-2-yl)methyl)pyridine]-2,6-dicarboxamide (**L13**), 1,3-*N,N'*-[bis(di(pyridin-2-yl)methyl)]isophthalamide (**L14**) and 1,4-*N,N'*-bis[(di(pyridin-2-yl)methyl)]terephthalamide (**L15**), investigated in this study.

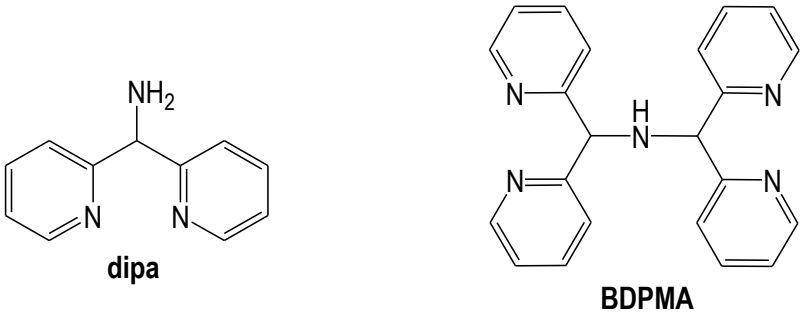

Figure 5.5. The structure of dipa and BDPMA.

To expand the repertoire of di-2-pyridyl-containing bridging ligands available for study, a development, as explored here, would be to incorporate amide moieties into these compounds. Such ligands would maintain the secondary interactions available to amide ligands described earlier in this thesis, but also provide complexes with potentially improved stability due to the incorporation of chelating sites for each coordinated metal centre. This approach has not been extensively explored and a limited number of related compounds have been investigated. Two examples of amide bridging ligands which are related to the compounds investigated in this study are *N,N'*-bis(2,2'-dipyridyl)isophthaloylamide (**5.7**) and

N,N'-2,6-bis(2,2'-dipyridyl)pyridylamide (**5.8**) (Figure 5.6) reported by Guo[231] and Vogtle,[232] respectively.

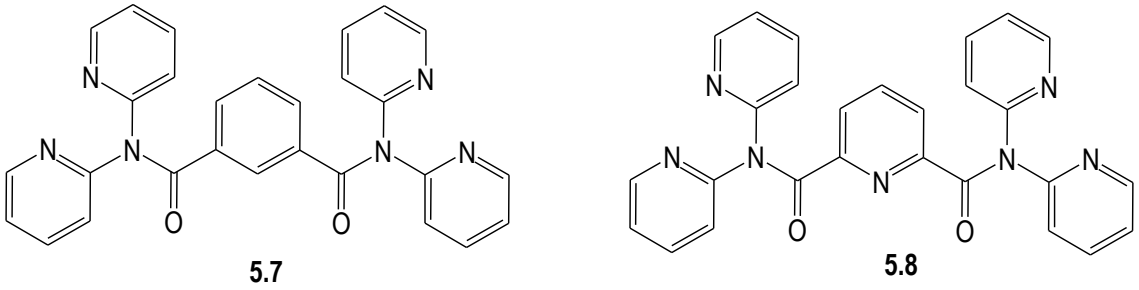

Figure 5.6. Two reported amide bridging ligands incorporating di-2-pyridylamine (dpa) as chelating units.

The coordination chemistry of compounds **5.7** and **5.8** has been investigated, but both compounds were found not to give complexes containing the intact ligand. For example, reaction of 5**.7** with copper(II) gave a complex of di-2-pyridylamine (dpa), $[Cu(dpa)_2](ClO_4)_2$, indicating that *in situ* hydrolysis of the ligand takes place (Scheme 5.1).[231] In the case of **5.8**, no complexes were obtained, but it is not clear from the original paper whether this was due to hydrolysis of the ligand in the presence of metal ions. In both examples, di-2-pyridylamine makes a very good leaving group and the compounds appear prone to hydrolysis.

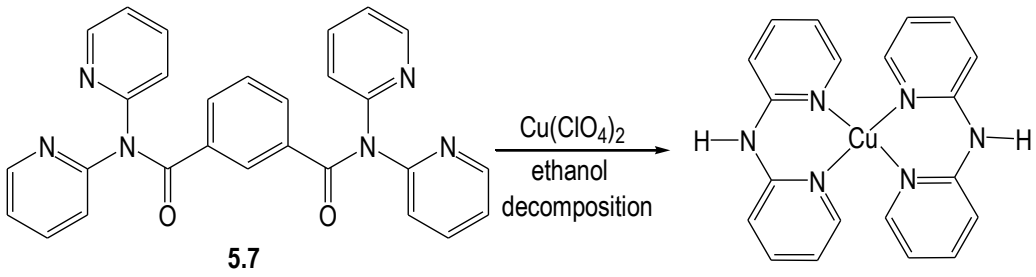

Scheme 5.1. The synthesis of a reported decomposition product of compound **5.7**.

In this chapter, a study of the coordination chemistry of amide bridging ligands derived from di-2-pyridylmethaneamine (dipa) is described. Ligands **L13**, **L14** and **L15** comprise a heteroaryl or aryl core that is connected to two di-2-pyridylmethane (dpm) chelating subunits through amide moieties (Figure 5.7).

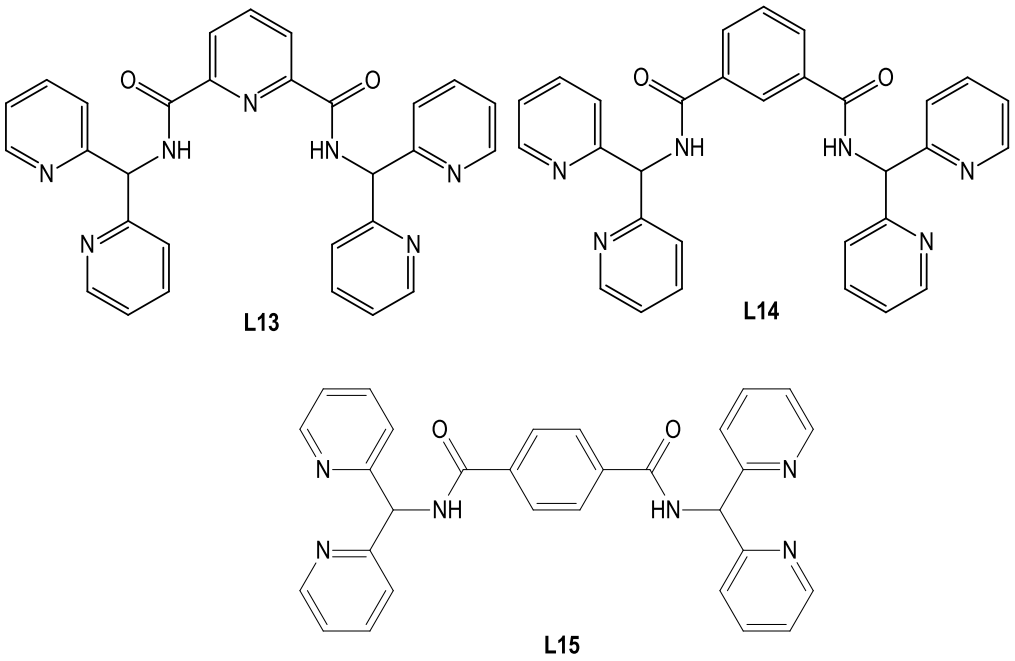

Figure 5.7. The structures of the three novel amide bridging ligands incorporating di-2-pyridylmethane chelating motifs.

In a similar manner to the majority of the amide ligands investigated in this thesis, the ligands described in this chapter were prepared to study the formation of coordination polymers or metallo-supramolecular assemblies potentially capable of anion binding. Ligands **L13**, **L14** and **L15** are expected to act primarily as a bridging ligand but will also be capable of generating pockets capable of binding anions. These new ligands have a methyl spacer between the di-2-pyridyl units to confer flexibility and to minimise the potential for hydrolysis that plagues other related compounds described in the literature.[187,373] The di-2-pyridylmethane unit can coordinate to metal centres through three coordination modes, chelating, monodentate or bridging (Figure 5.8(a)). The predominant coordination mode of the di-2-pyridyl motif is to chelate to particular metal centre. Several coordination modes that can be envisaged for ligands **L13**-**L15** are shown in Figure 5.8(b).

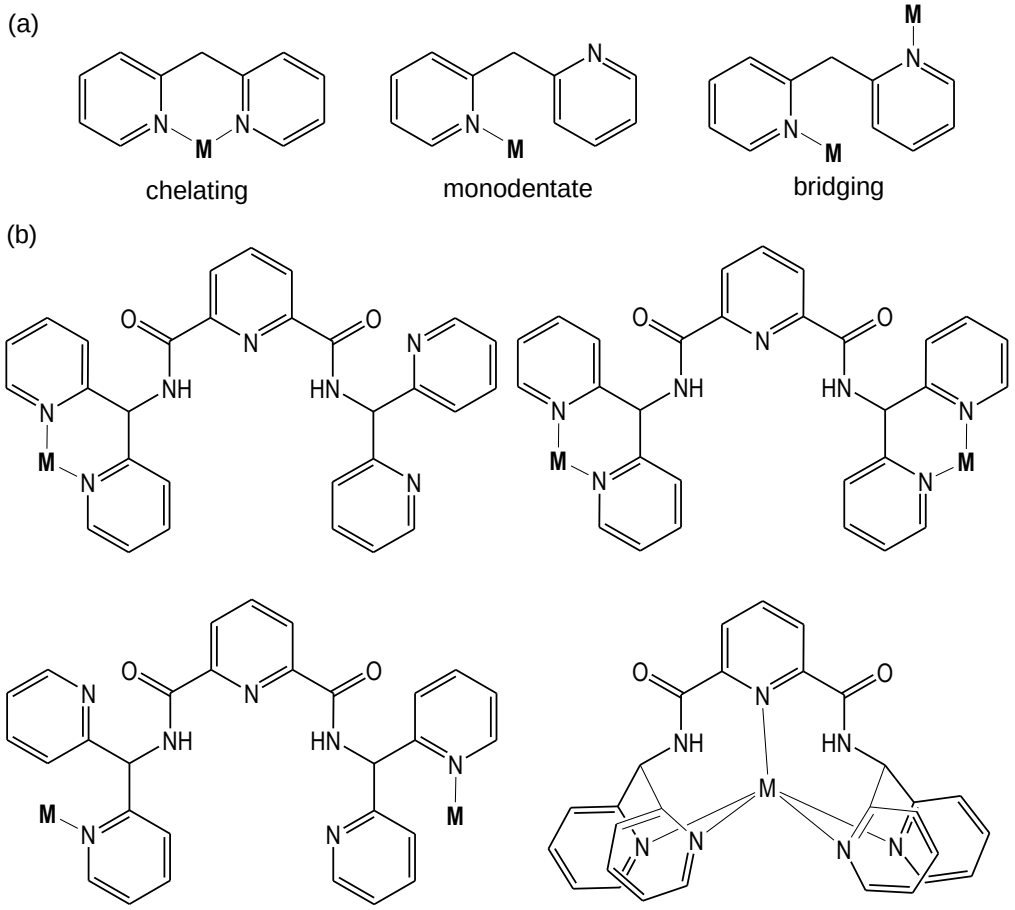

Figure 5.8. (a) The coordination modes available for a dpm chelating subunit. (b) Examples of coordination modes that may be encountered for coordination complexes of the ligands investigated in this thesis (illustrated for **L13**).

5.2. Coordination chemistry and metallo-supramolecular chemistry of L13-L15.

Compounds **L13** – **L15** are all ditopic ligands that, under appropriate conditions, would be expected to form discrete metallo-macrocyclic structures and coordination polymers capable of encapsulating anions in the cavity formed within the macrocyclic structure. To understand the types of structures that can be obtained with **L13** – **L15**, these ligands were reacted with a range of metal salts to provide variety geometries and coordination numbers for the metal component. This includes cadmium(II), copper(II), cobalt(II), silver(I), zinc(II) and palladium(II) with both coordinating and non-coordinating anions. The complexes obtained were characterised by a combination of NMR spectroscopy, FTIR spectroscopy, mass spectrometry, combustion analysis and X-ray crystallography.

5.2.1. Complexes of L13

As mentioned in the discussion above, the ligands prepared in this section are expected to act primarily as bridging ligands that have potential to bind anions *via* hydrogen bonding interactions. In contrast to **L14** and **L15**, ligand **L13** has pre-organised 2,6-pyridine dicarboxamide moieties and therefore could act as a pentadentate ligand with coordination from the five nitrogen donors (or a heptadentate ligand upon amide deprotonation). An example of a reported Fe(II) complex (**5.9**) with a related pentadentate ligand, 2,6-(bis-(di-2-pyridyl)methoxymethyl)pyridine (**5.8**), is shown in Scheme 5.2.[385] In contrast to the work described from this study, **L13** was found to act as tetradentate ligand with coordination from the pendant pyridyl rings only. This is probably related to the size of the chelate ring required if the central pyridine donor of **L13** was coordinated (8-membered vs 6-membered in **5.9**).

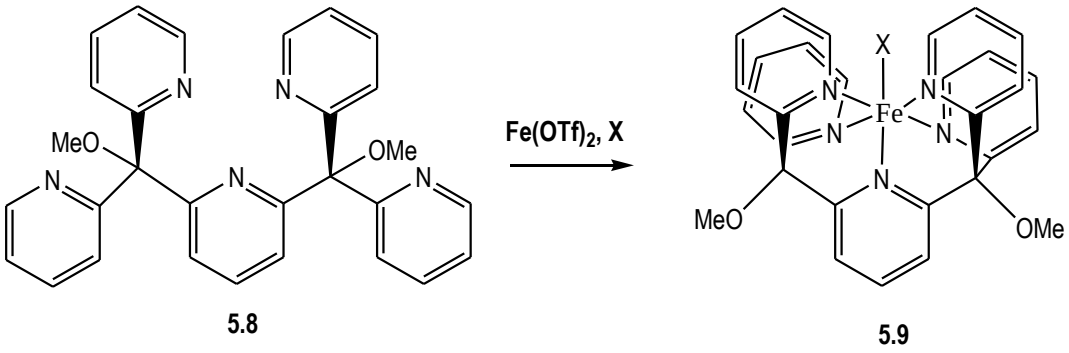

5.8 **5.9**

Scheme 5.2. The synthesis of an Fe(II) complex of 2,6-(bis-(di-2-pyridyl)methoxymethyl)pyridine.

In general, the first attempts at reactions of copper(II) (CuX_2, where X = Cl, NO_3, OAc, ClO_4), cadmium(II) (CdX_2, where X = NO_3, Br, ClO_4) and zinc(II) (ZnX_2, where X = NO_3) metal salts with **L13** in 2:1 metal-to-ligand ratio in methanol-acetonitrile produced only oils or oily solids that were not further characterised or could not be crystallised. Further attempts at these reactions using different ratios (1:1 and 1:2 metal-to-ligand ratios) and different solvent mixtures generally failed to give cleanly isolatable products. However, repeating reactions of **L13** with silver perchlorate and silver nitrate provided single crystals, suitable for X-ray crystallography. Silver nitrate was reacted with **L13** in a 2:1 ratio to give complex **5.10** with composition $[Ag_2(\mathbf{L13})_2](NO_3)_2{\cdot}2H_2O{\cdot}2CH_3OH$ as shown by elemental analysis. This result is supported by a structure determined by X-ray crystallography. In the case with silver perchlorate, the ligand was hydrolysed upon reaction. The silver complex

obtained from this decomposition reaction (**5.11**) was analysed by X-ray crystallography for structure determination. To further investigate the coordination chemistry of **L13**, it was also reacted with palladium chloride in a 2:1 metal-to-ligand ratio. Complex **5.12** was obtained as bright yellow solid by combining a solution of palladium chloride in 2M hydrochloric acid with a solution of **L13** in methanol. Elemental analysis suggested that complex **5.12** has a [$(PdCl_2)_2$(**L13**)] composition which is consistent with a dinuclear palladium complex. The complex is expected to have square planar geometry at each palladium centre. Unfortunately, the yellow solid of complex **5.12** was insoluble in common NMR solvents and could not be examined by NMR spectroscopy. The insolubility of this complex has also prevented the recrystallisation of this product for X-ray crystallography and further analysis in solution. All complexes obtained from **L13** are shown in Scheme 5.3.

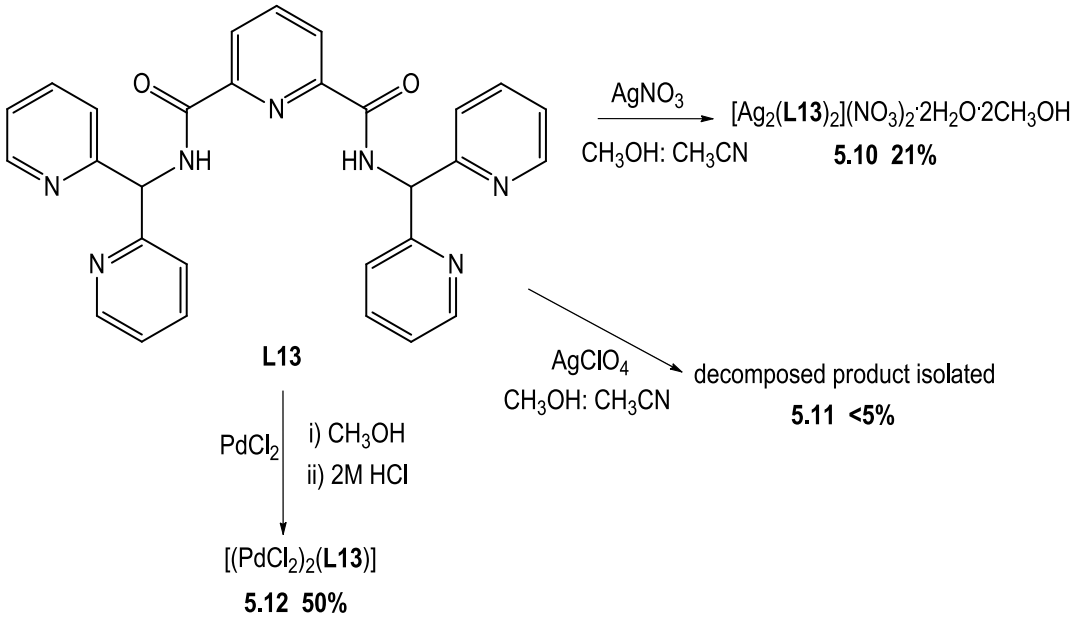

Scheme 5.3. The synthesis of coordination compounds obtained from **L13**.

Complex **5.10** was obtained as colourless rod-like crystals in 21% yield by slow evaporation methanol-acetonitrile reaction medium. The procedure required heating a solution of silver nitrate and ligand in 2:1 metal-ligand ratio for approximately 45 minutes, before the solution was left to evaporate for a period of one week to yield crystalline products. The behaviour of the complex in solution was investigated using ES-MS, ^{1}H NMR spectroscopy

and diffusion ordered spectroscopy (DOSY). In the ES-MS spectrum of compound **5.10** dissolved in dimethylsulfoxide and methanol, a series of positively charged species were observed. Peaks at *m/z* 608.1 and 610.1 correspond to a mononuclear species $[(Ag(\mathbf{L13})]^+$, while a peak at *m/z* 713.9, 715.9, 717.9, 1214.6, 1216.8, 1218.8 correspond to the metallomacrocycle species $([^{107}Ag_2(\mathbf{L13}\text{-H})]^+$, $([^{107}Ag^{109}Ag(\mathbf{L13}\text{-H})]^+$, $([^{109}Ag_2(\mathbf{L13}\text{-H})]^+$, $([^{107}Ag_2(\mathbf{L13})(\mathbf{L13}\text{-H})]^+$, $([^{107}Ag^{109}Ag(\mathbf{L13})(\mathbf{L13}\text{-H})]^+$ and $([^{109}Ag_2(\mathbf{L13})(\mathbf{L13}\text{-H})]^+$, respectively. The IR spectrum of compound **5.10** has a very strong N-O stretch at 1382 cm^{-1}. The ^1H NMR spectrum of compound **5.10** recorded in DMSO-d_6 revealed that the complex remained intact in solution, with small coordination induced chemical shifts (CIS) indicating that the pendant pyridyl donors are involved in coordination (Figure 5.9).

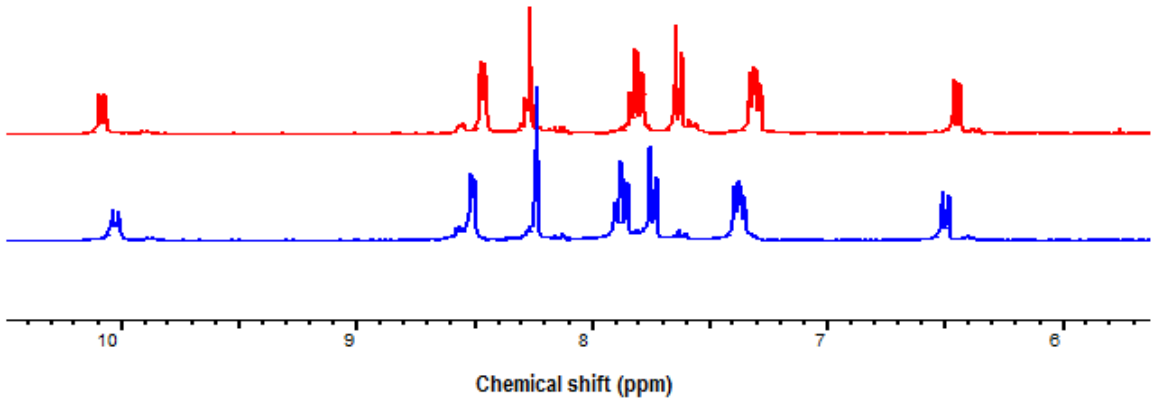

Figure 5.9. Comparison between the ^1H NMR spectrum of metallo-macrocyclic complex **5.10** (blue) and **L13** (red).

Despite the minimal CIS observed for **5.10**, DOSY was employed to examine the behaviour of the complex in solution. The analysis provided diffusion coefficients of 0.63 ± 0.01 × 10^{-10} m^2/s for **5.10** and a diffusion coefficient for **L13,** under the same conditions, of 0.75 ± 0.03 × 10^{-10} m^2/s. Typically, the ratio of diffusion coefficients for a dimer of hard spheres is 0.72 – 0.75.[187,345] The ratio of diffusion coefficients, $D_{\mathbf{5.8}}/D_{\mathbf{L13}}$, calculated here was 0.84 and similar to other related complexes investigated in this work.[386] The tightly packed nature of **5.10** (Figure 5.11(b)) means that the diffusion rate for this species may be faster than expected due to its smaller hydrodynamic volume and thus the $D_{\mathbf{5.8}}/D_{\mathbf{L13}}$ ratio is correspondingly higher.

Crystal structure of **5.10**

$[Ag_2(L13)_2](NO_3)_2 \cdot 2CH_3OH \cdot 2H_2O$. X-ray crystallography revealed that complex **5.10** is obtained as a discrete [2+2] dimetallo-macrocyclic [Ag_2**L13**$_2$] complex with the ligand acting as a tetradentate bridge that connects the two metal atoms to form a dinuclear complex. This complex was obtained as rod-shaped crystals in 21% yield from a mixture of methanol-acetonitrile solution. Compound **5.10** crystallises in the orthorhombic space group *Pbca* with an asymmetric unit comprising one molecule of ligand **L13**, half of a silver atom, one-non coordinated nitrate, and non-coordinated water and methanol solvate molecules (Figure 5.10).

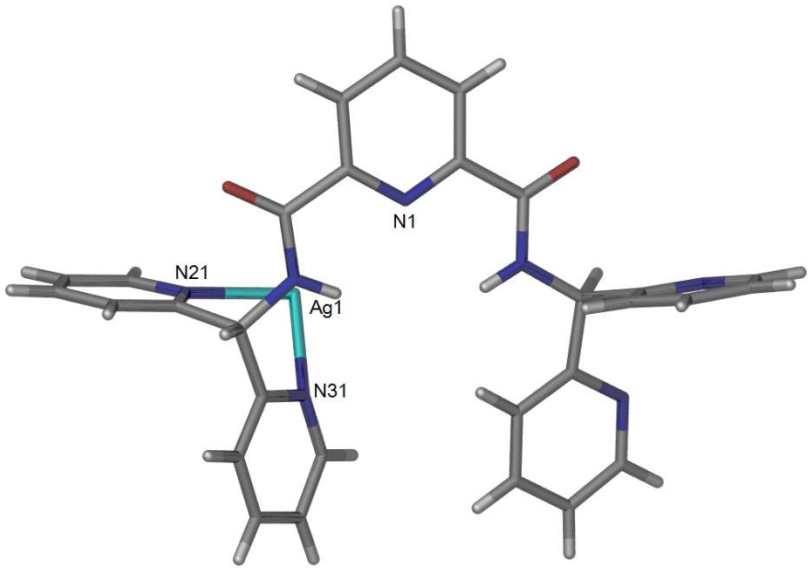

Figure 5.10. A perspective view of the asymmetric unit of complex **5.10** with nitrate and solvent molecules omitted for clarity. Selected bond lengths (Å) and angles (°): Ag(1)-N(21) 2.315(2), Ag(1)-N(31) 2.423(2), N(21)-Ag(1)-N(31) 82.20(8), N(21)-Ag(1)-N(31) 82.11(9), N(21)-Ag(1)-N(31) 82.11(9), N(21)-Ag(1)-N(31) 82.11(9).

A complete view of the [2+2] metallo-macrocyclic structure **5.10** is shown in Figure 5.11(a) with the silver atoms in the structure bridged by two equivalents of ligand **L13**. This provides a silver-silver distance of 8.170 Å. Each Ag atom is bound to two ligand entities through the chelating pyridine donors, which results in a distorted tetrahedral geometry at each silver centre (bond angles in the range 82.20(8) – 140.29(8)°). The Ag-N bond lengths, in the range 2.315(2) – 2.423(2) Å, are typical for tetrahedral silver(I) with four nitrogen heterocyclic donors.[178] Complex **5.10** has a similar structure to a reported discrete [2+2] metallo-macrocyclic silver complex incorporating 1,2-bis(di-2-pyridylaminomethyl)benzene

as a bridging ligand.[187] Thus it seems that the amide moieties do not play a significant role in favouring the formation of such entropically driven [2+2] assemblies. However it is worth noting that the previously reported complex has a more open metallo-macrocyclic structure compared to complex **5.10** and is stabilised by silver-π interactions. No such interactions are observed in this complex as the pyridyl donors saturate the coordination requirements of the metal centres.

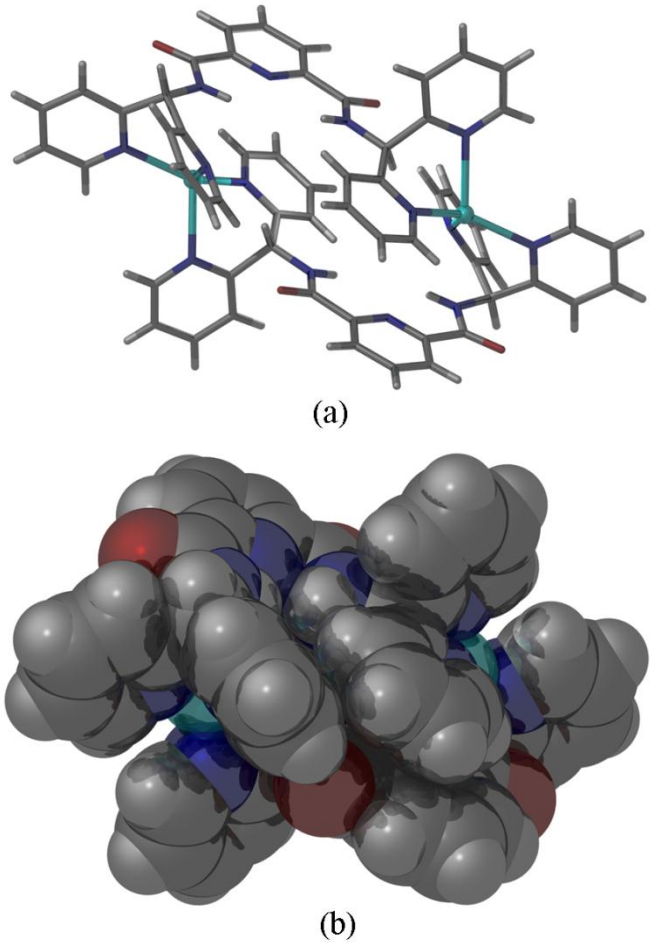

Figure 5.11. Two perspective views of the discrete metallo-macrocycle complex **5.10**.

While the amide NH donors point into the centre of the complex, the resulting cavity is too small for guest inclusion and, due to the steric bulk of the ligand, not accessible (Figure 5.11(b)). Due to this internalisation of the hydrogen bond donors in the crystal packing, no significant hydrogen bond interactions between the complex with the solvents or anion were identified. Sumby and co-workers,[386] in recent work, have prepared a similar dinuclear metallo-macrocycle complex with a flexible diamide ligand, *N,N'*-2,6-bis(3-

pyridylmethyl)pyridine dicarboxamide (**L5**) (Figure 5.12(a)). The hydrogen bond donors in both ligands, **L13** and **L5** are pre-organised to reduce the ability of the diamide compounds to form self-assembled hydrogen bonded tapes.[161] Figure 5.12(b) shows the structure of this previously reported metallo-macrocycle $[Ag_2(NO_2)_2(\mathbf{L5})_2]$, which is far from planar; one 2,6-pyridine dicarboxamide unit is inclined up and the second down. The silver-silver separation in $[Ag_2(NO_2)_2(\mathbf{L5})_2]$ is 13.36 Å, which is 5.192 Å longer than the Ag-Ag distance observed for complex **5.10**. Despite being pinched in the centre, $[Ag_2(NO_2)_2(\mathbf{L5})_2]$ is far more open than the structure of **5.10** and acts as a host for two coordinated nitrite anions of two adjacent molecules of the compound.

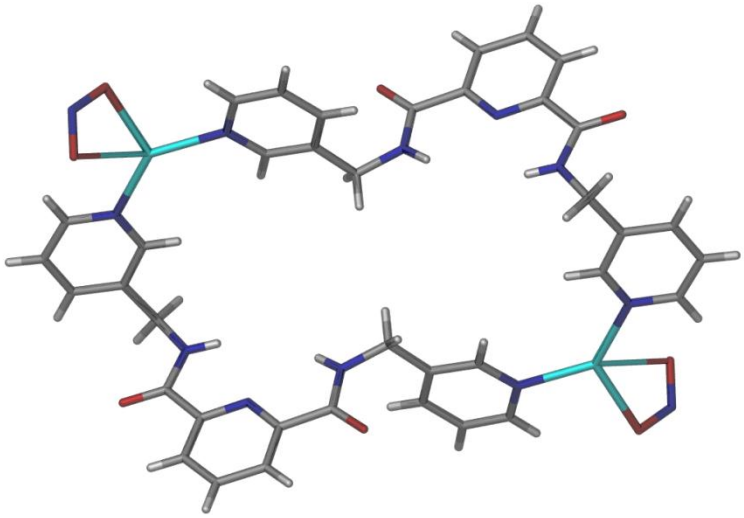

(a)

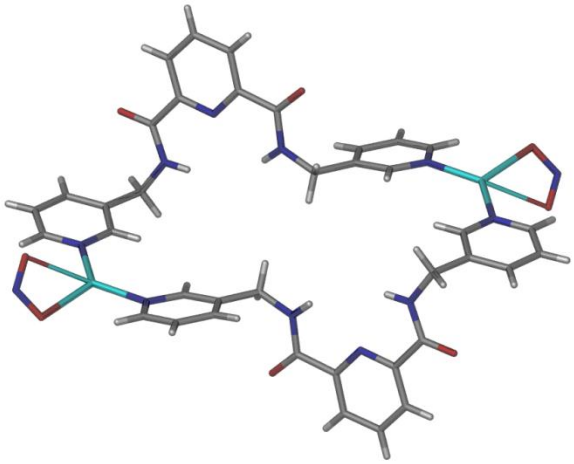

(b)

Figure 5.12. Two perspective views of a Ag(I) metallo-macrocycle reported by Sumby and co-workers.[386]

In stark contrast to the result obtained for complex **5.10**, X-ray crystallography revealed a rather unexpected result for complex **5.11**. The structure of complex **5.11** comprises a silver atom coordinated by two molecules of di-2-pyridylmethanediol, the di-2-pyridylmethanediol presumably resulting from hydrolysis of **L13**. A proposal, based on related work,[387] for the decomposition of **L13** to form di-2-pyridylmethanediol is shown in Scheme 5.4. Unfortunately, this result shows that ligand **L13** can undergo hydrolysis during reaction with metal salts. The methyl spacer between the amide nitrogen atom and the pyridine rings does not, as originally proposed, prevent hydrolysis of **L13**, and this compound can be decomposed as reported in the literature for related compounds.[231,232]

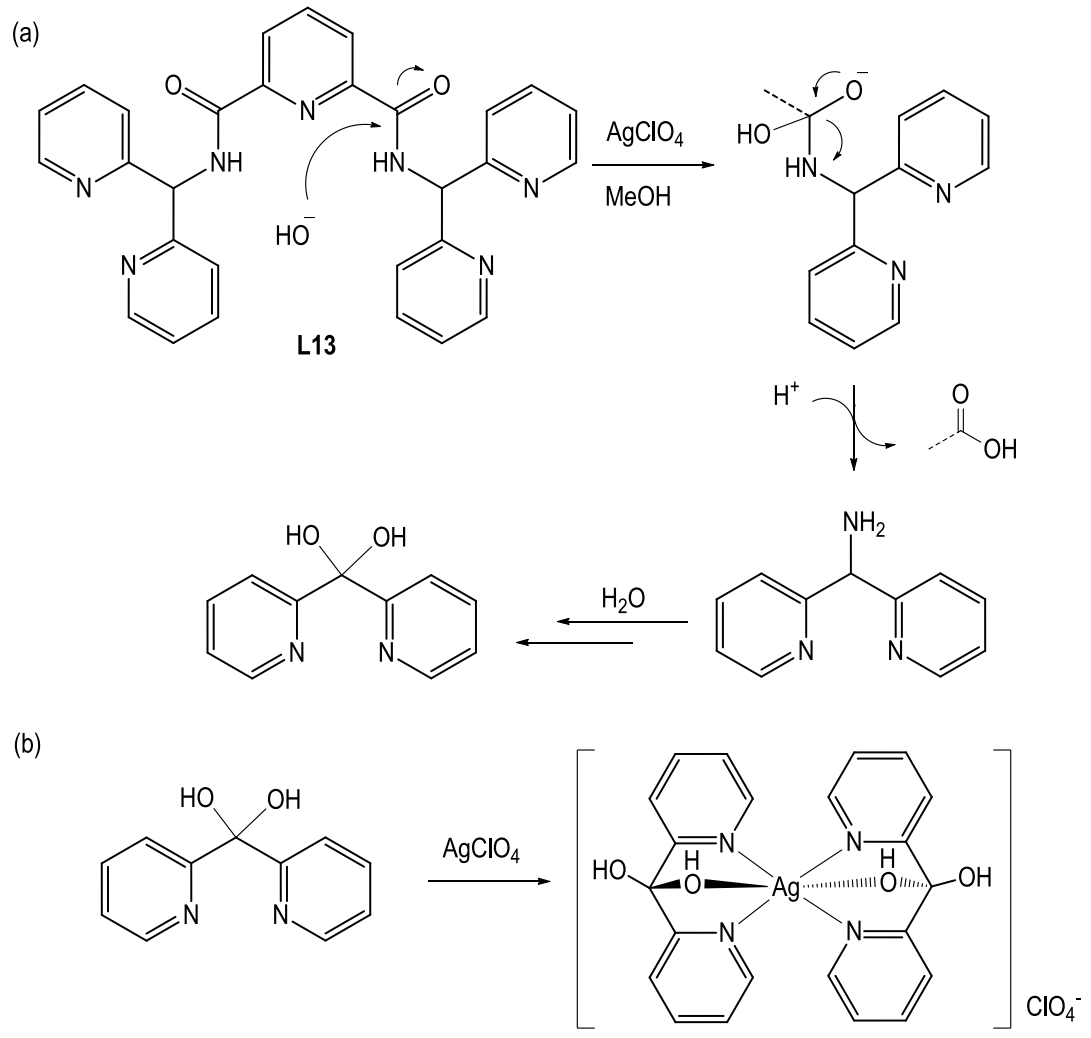

Scheme 5.4. (a) The metal mediated decomposition of **L13**. (b) The synthesis of complex **5.11** from di-2-pyridylmethanediol, a decomposition product of **L13**.

As noted, complex **5.11** was obtained from the reaction of **L13** with silver perchlorate by slow evaporation of the acetonitrile-methanol reaction medium. This complex crystallises in a triclinic space group *P*-1 with an asymmetric unit comprising of one silver atom, two di-2-pyridylmethanediol ligands, three water molecules and one disordered perchlorate anion. A perspective view of complex **5.11** is shown in Figure 5.13 with non-coordinated molecules omitted for clarity. The silver atom adopts distorted octahedral geometry environment coordinated by four pyridyl nitrogen donors and two bridging oxygen atoms. The bond lengths of the silver to nitrogen (Ag-N1 =1.968 Å and Ag-N21= 1.949 Å) are fairly short compared to other silver complexes in this thesis, while the Ag-O1 bond length is 1.855(5) Å. As this complex was formed in a relatively poor yield, and not as a homogeneous sample, further analysis on this product was not pursued.

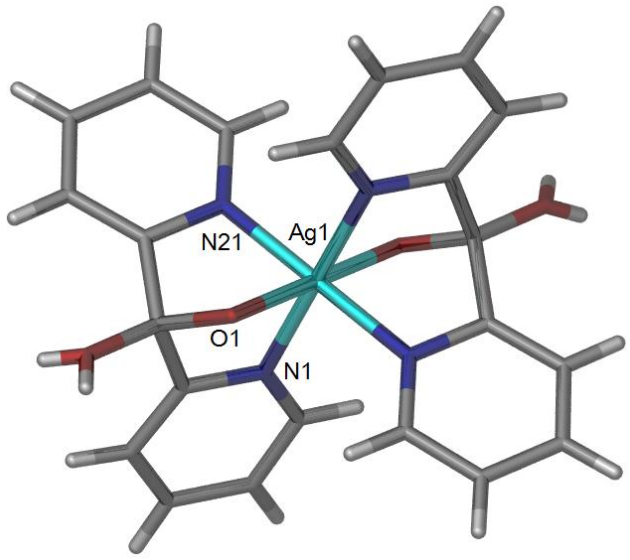

Figure 5.13. Crystal structure of complex **5.11** obtained from the reaction of **L13** with silver perchlorate. The water and perchlorate molecules are omitted for clarity. Selected bond lengths (Å) and angles (°): Ag(1)-N(1) 1.968(4), Ag(1)-N(21) 1.949(5), Ag(1)-O(1) 1.841(5), N(1)-Ag(1)-O(1) 83.84(5), N(21)-Ag(1)-O(1) 81.96(4) and N(21)-Ag(1)-N(1) 86.71(5).

5.2.2. Complexes of L14

Reacting of **L14** with silver nitrate, silver perchlorate and silver chloride in methanol-acetonitrile, under the same condition for the preparation of complex **5.10**, did not provide

any complexes. Fortunately, reaction of cadmium chloride with **L14** gave colourless crystals of a complex **5.13**. These were isolated in 16% yield, analysed as [{$CdCl_2(CH_3OH)$(**L14**)$CdCl_2$}$_2$] and the structure determined by X-ray crystallography. When ligand **L14** was reacted with palladium chloride in a 1:2 ligand-metal stoichiometry, the complex that was isolated, **5.14**, was found to be sparingly soluble in DMSO. A ^{1}H NMR spectrum indicated that the solid was obtained as a complex mixture of products, probably containing starting materials, mononuclear and dinuclear complexes. This mixture could not be readily separated due to the insolubility of the product mixture in many common solvents. The synthesis of the complexes obtained from **L14** is outlined in Scheme 5.5.

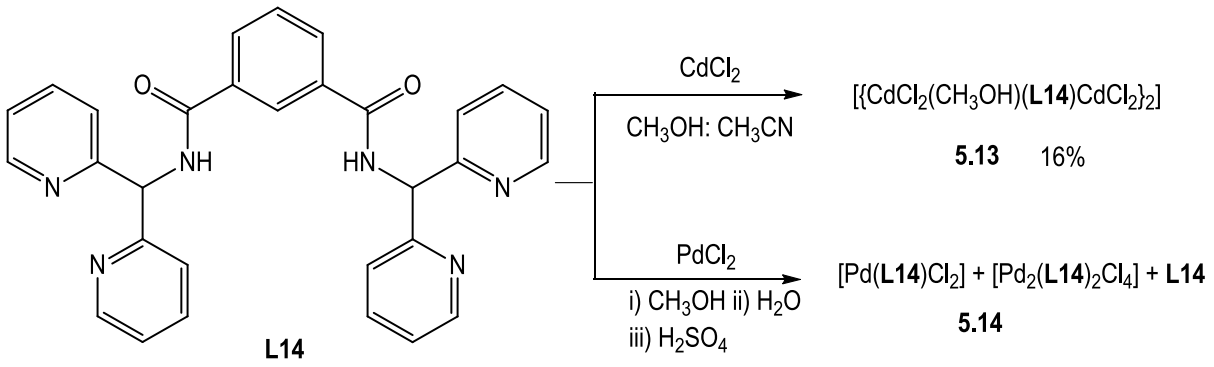

Scheme 5.5. The synthesis of complexes **5.13** and **5.14** obtained from **L14**.

Crystal structure of **5.13**

[{$CdCl_2(CH_3OH)$(L14)$CdCl_2$}$_2$]. Complex [{$CdCl_2(CH_3OH)$(**L14**)$CdCl_2$}$_2$] crystallises in the triclinic space group *P*-1, with one molecule of **L14**, two cadmium atoms, four coordinated chloride anions and one coordinated methanol molecule in the asymmetric unit (Figure 5.14). The Cd-N bond lengths are in the range 2.318(5) - 2.371(5) Å, which are similar to the majority of other cadmium complexes prepared in this study. Complex **5.13** has two cadmium atoms with trigonal bipyramidal geometries, although the cadmium atoms have quite different donor sets. Cd(1) is coordinated by two nitrogen atoms from the pendant pyridyl rings of **L14**, two chloride atoms (one bridging and one monodentate), while the second cadmium atom Cd(2) is coordinated by two nitrogen atoms from the pyridyl rings of **L14**, two chloride atoms and one methanol molecule.

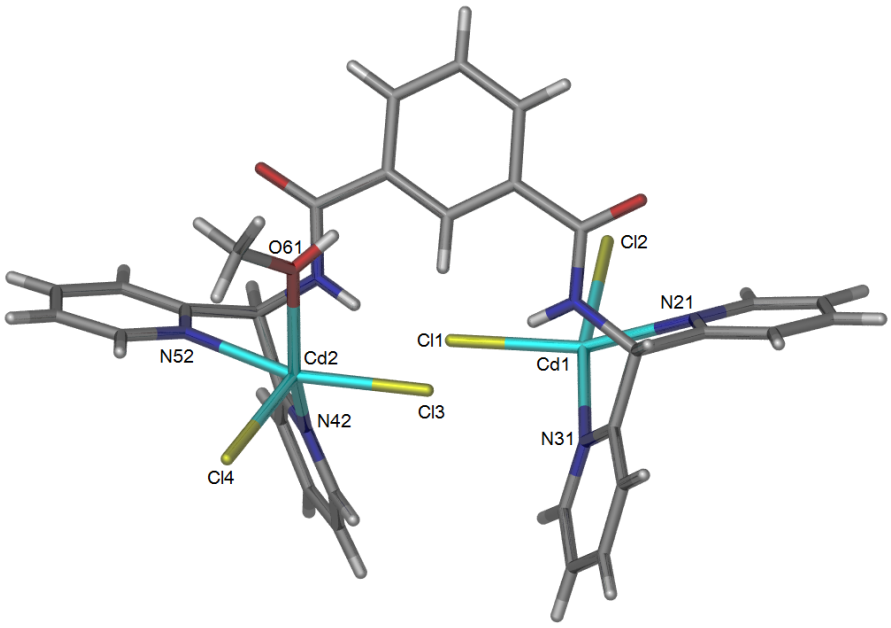

Figure 5.14. A perspective view of the asymmetric unit of complex **5.13**. Selected bond lengths (Å) and angles (°) : Cd(1)-N(21) 2.318(5), Cd(1)-N(31) 2.371(5), Cd(1)-Cl(1) 2.4441(16), Cd(1)-Cl(2) 2.5985(16), Cd(2)-N(41) 2.353(5), Cd(2)-N(51) 2.370(6), Cd(2)-O(61) 2.366(5), Cd(2)-Cl(3) 2.4754(15), Cd(2)-Cl(4) 2.4821(16), N(21)-Cd(1)-N(31) 81.93(18), N(31)-Cd(1)-Cl(1) 97.20(14), Cl(1)-Cd(1)-Cl(2) 98.61(5), N(21)-Cd(1)-Cl(2) 106.49(13), Cl(4)-Cd(2)-Cl(3) 108.95(5), Cl(3)-Cd(2)-O(61) 90.66(14), Cl(4)-Cd(2)-O(61) 98.20(15).

The extended view of complex **5.13** showed that a bridging chloride on Cd2 connects the two dinuclear units to form a dimer (Figure 5.15). The distance between Cd1-Cd2 is 6.40 Å, while the distance between the two cadmium atoms bridged by the chloride anions is much shorter at 3.68 Å. In similar manner to ligand **L13**, and other related ligands,[364] ligand **L14** uses all four nitrogen donors to coordinate with the cadmium atoms.

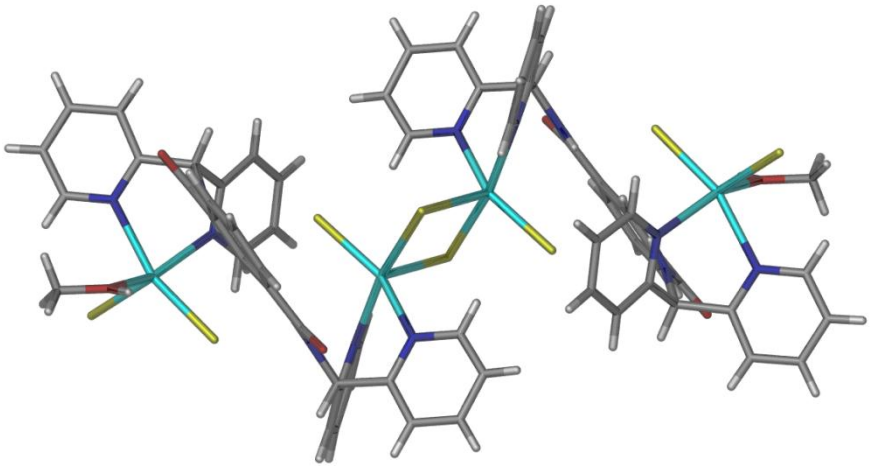

Figure 5.15. A perspective view of the tetranuclear structure of complex **5.13**.

The coordination mode of **L14** in complex **5.11** is quite different to complexes incorporating a related ligand based on a 1,3-phenyl core, 1,3-bis(di-2-pyridylaminomethyl)benzene (**5.4**).[187] In previous work, reaction of **5.4** with silver nitrate gave a discrete [1+1] metallo-macrocycle complex, while reaction with silver perchlorate and silver hexafluorophosphate gave 1-D coordination polymers. The previous study revealed that ligand **5.4** acted as a divergent bridging unit, with only two of the four pyridine rings involved in the coordination to form the complexes. Rather that exhibiting the tetradentate coordination observed for **L14**, complexes of **5.4** are stabilised by silver-π interactions between the non-coordinated pyridine rings and the silver ions. Such interactions are not observed in the any of the complexes described in this chapter.

5.2.3. Complexes of L15

Reaction of **L15** dissolved in acetonitrile with cadmium bromide dissolved in methanol gave complex **5.15**, as colourless crystals in 75% yield that had the composition $[(CdBr_2)_2(\mathbf{L15})(CH_3OH)_2]$ as provided by elemental analysis. A dinuclear palladium complex was also prepared in a similar manner to previously described palladium chloride complexes, to give complex **5.16** as a yellow solid in 25% yield. This composition was confirmed by elemental analysis as $[(PdCl_2)_2(\mathbf{L15})]$. The complex was soluble in DMSO and a ^{1}H NMR spectrum was obtained that was consistent with the expected dinuclear complex. The ^{1}H NMR spectrum, recorded in DMSO-d_6, reveals resonances that are assignable to **5.16**. The signals for all the protons in the dinuclear complex shifted further downfield upon

coordination to palladium. This is typical for such complexes.[388] The coordination induced shifts (CIS) for complex **5.16** are shown in Table 5.1.

Table 5.1.[1]H NMR chemical shift values for the pyridine rings of ligand **L15** and the dinuclear complex **5.16** recorded in DMSO-d_6. Coordination induced shifts (CIS), $\delta_{complex}$ - δ_{ligand}, are also given.

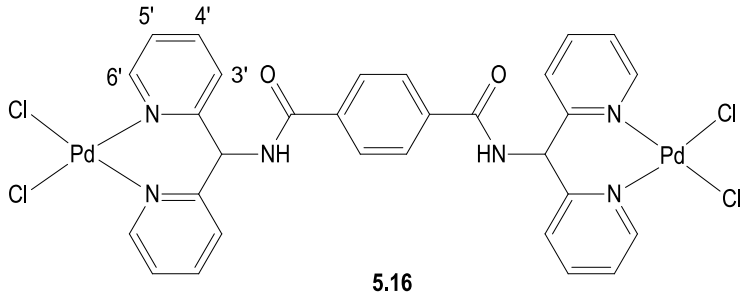

5.16

Compounds	NH	H6’	H5’	H4’	H3’
5.16	10.35	8.85	7.55	7.85	8.10
L15	9.02	8.82	7.34	7.68	7.75
CIS	1.33	0.03	0.21	0.17	0.35

ES-MS analysis conducted in acetonitrile-DMSO indicated the presence of the dinuclear complex with a peak corresponding to $[Pd_2Cl_3(\mathbf{L15})]^+$ at *m/z* 823.1. In the FT-IR spectrum, the Pd-Cl stretch was observed at 350 cm^{-1} which is consistent with the values observed for palladium complexes reported in the literature.[389] Despite repeated attempts, this palladium complex could not be crystallised to provide crystals suitable for X-ray crystallography. The preparation of complexes **5.15** and **5.16** is shown below in Scheme 5.6.

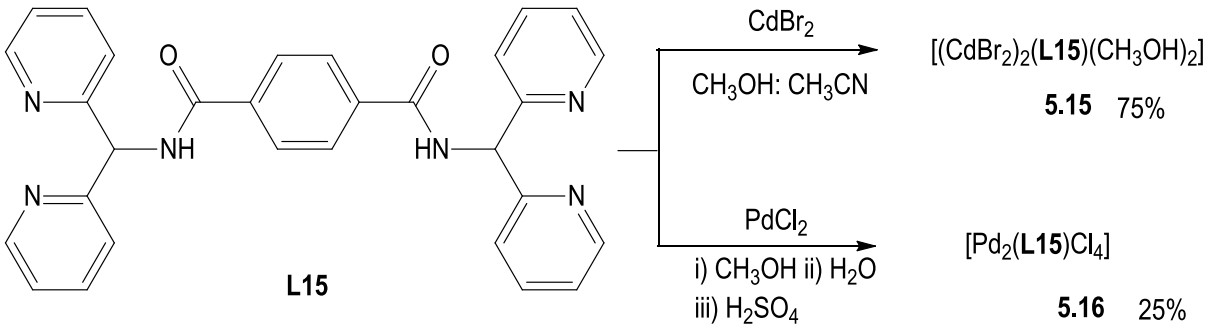

Scheme 5.6. The synthesis of complexes **5.15** and **5.16** from **L15.**

Crystal structure of **5.15**

[(CdBr$_2$)$_2$(L15)(CH$_3$OH)$_2$]. Complex [(CdBr$_2$)$_2$(**L15**)(CH$_3$OH)$_2$] (**5.15**) was obtained in 75% yield by slow evaporation of a methanol-acetonitrile solution containing **L15** and cadmium bromide. Single, rectangular, block-shaped crystals of [(CdBr$_2$)$_2$(**L15**)(CH$_3$OH)$_2$] were separated from the clump and subjected to single crystal X-ray crystallography. The structure obtained by X-ray crystallography reveals the formation of a dinuclear complex, [(CdBr$_2$)$_2$(**L15**)(CH$_3$OH)$_2$] (**5.15**). The compound crystallises in the monoclinic space group, $P2_1/c$ with half a molecule of **L15,** one cadmium atom, two coordinated bromide anions and one coordinated methanol in the asymmetric unit. The structure of compound **5.15** is shown in Figure 5.16. On difference between complexes **5.10**, **5.13** and **5.15** is the relative orientation of the di-2-pyridylmethyl arms. Compounds **5.10** and **5.13** have a syn arrangement of the chelating motifs, while complex **5.15** has anti arrangement. This type of anti arrangement has been commonly reported for several mononuclear and dinuclear ruthenium complexes derived from the di-2-pyridylamine containing ligands.[363]

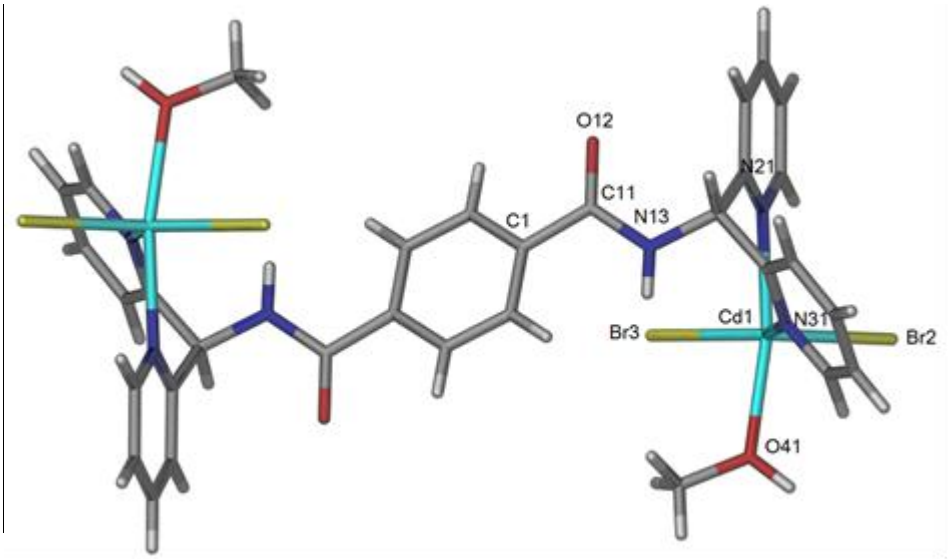

Figure 5.6. A perspective view of complex **5.15**. Selected bond lengths (Å) and angles (°) : Cd(1) -N(21) 2.365(9), Cd(1)-N(31) 2.3119(19), Cd(1)-Br(2) 2.5628(3), Cd(1)-Br(3) 2.5729(3) Cd(1)-O(41) 2.3818(14), O(41)-Cd(1)-Br(3) 88.91(4), O(41)-Cd(1)-Br(2) 99.76(4), N(21)-Cd(1)-Br(2) 95.58(2), N(21)-Cd(1)-Br(3) 90.80(2).

In this structure, the ligand acts as a tetradentate bridge to link two cadmium atoms and form a discrete dinuclear complex with a 2:1 metal to ligand ratio. The cadmium atom has a distorted trigonal bipyramid geometry with one of the chelating pyridyl and one coordinated methanol donor occupying the axial positions. The monodentate pyridine donors twist back towards the core of the ligands in the similar manner to that observed in the dinuclear complexes described earlier. By contrast to complexes **5.10** and **5.13**, the chelating rings in complex **5.15** is twisted by *ca.* 63.3° from the plane of the central phenyl core, which is approximately three times greater than the torsion angles observed in the previous complexes. Due to the *para* substitution of the central arene core, **5.15** has a considerably longer Cd-Cd distance (12.261 Å) than that observed in complex **5.13**.

In the crystal, the discrete complexes were connected to each other by intermolecular hydrogen bonding interactions between the oxygen of the carbonyl group and the coordinated methanol solvent (d = 1.903Å) to form 1-D hydrogen bond chains (Figure 5.17).

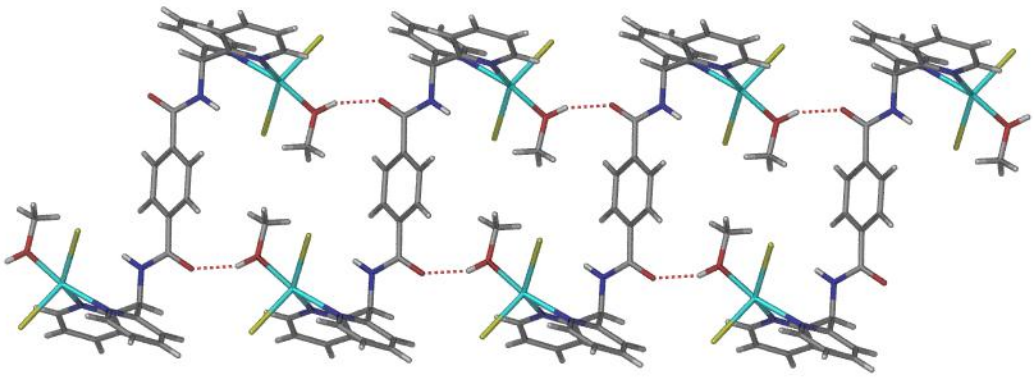

Figure 5.16. A perspective view of the 1-D hydrogen bonded chains in compound **5.15**.

5.3. Summary

In this study, the synthesis and coordination chemistry of three novel diamide chelating ligands, **L13** – **L15** was investigated. These ligands show a propensity to form discrete dinuclear complexes with silver, cadmium and palladium and no coordination polymers were obtained. Despite predicting that decomposition in these compounds would be minimised by incorporation of a methyl spacer between the amide nitrogen and the pendant pyridyl rings, a large number of the attempted reactions with metal salts led to the formation of oils that were linked to decomposition. The ligands, particularly **L13** tends to hydrolyse and decompose in the presence of metal ions. Indeed, in this study, a crystal of a decomposition product of **L13** was isolated and its structure determined by X-ray crystallography.

In one case **L13**, which possesses a pre-organising central 2,6-pyridine dicarboxamide core and two chelating di-2-pyridylmethyl donor groups, was shown to form a dinuclear metallo-macrocycle with silver nitrate. The structure of the silver(I) complex, $[Ag_2(\mathbf{L5})_2](NO_3)_2{\cdot}2H_2O{\cdot}2CH_3OH$ (**5.10**), was confirmed by ES-MS and DOSY NMR spectroscopy in solution and X-ray crystallography in the solid-state. The cavity of this compound is too small for guest inclusion and, due to the steric bulk of the ligand, does not appear to be accessible in this particular compound. A discrete dinuclear complex palladium(II) chloride $[(PdCl_2)_2(\mathbf{L13})]$ (**5.12**) was also obtained with **L13** and the structure confirmed by elemental analysis and mass spectrometry. Ligands **L14** and **L15**, which lack the pre-organising effect of a central 2,6-pyridine dicarboxamide core, form dinuclear complexes or dimers of dinuclear complexes with cadmium(II) and palladium(II).

Reaction of **L14** with palladium chloride gave a mixture of products that could not be separated by any approach; therefore further analysis on this product was not pursued. By contrast, reaction of **L15** with palladium chloride gave a discrete dinuclear palladium complex [Pd_2(**L15**)Cl_4] (**5.16**). The structure of **5.16** was confirmed by NMR spectroscopy, elemental analysis and mass spectrometry. The strong Pd-Cl stretching at 350 cm^{-1} was also observed by FT-IR spectroscopy. In contrast to the silver complex obtained with **L13**, the cadmium complexes of **L14**, [{$CdCl_2$(CH_3OH)(**L14**)$CdCl_2$}$_2$] (**5.13**), and **L15,** [($CdBr_2$)$_2$(**L15**)(CH_3OH)$_2$] (**5.15**), have non metallo-macrocyclic structures due to the coordinating anions and the quite different ligand conformations.

This study has demonstrated that the doubly bidentate bridging amide ligands **L13** – **L15** form discrete complexes with silver, cadmium, and palladium metal ions. Attempts to obtain complexes with other metal salts were not successful due to the possibility of hydrolysis. The coordination chemistry of these ligands may be able to be expanded if the stability of these ligands in solution is further investigated and understood.

CHAPTER 6

CONCLUSIONS AND FUTURE DIRECTIONS

Chapter 6

6. Conclusions and future directions

This thesis has described the synthesis and characterisation of fifteen bridging amide-containing polypyridyl ligands and fourty-one metal complexes of such ligands. All the compounds possess at least one amide moiety as a component of a potential anion binding region and pendant pyridyl groups as the metal coordinating sites. These are the grouped on the basis of the number of amide groups, including four monoamide ligands (**L1** – **L4**), two diamide ligands **(L5** and **L6)** and six tetraamide ligands (**L7** – **L12**). As part of a strategy to combine chelating metal coordinating sites with a pre-organised 2,6-pyridine dicarboxamide moiety, three further amide ligands with di-2-pyridylmethane chelating subunits (**L13** – **L15**) were prepared. The coordination chemistry of all ligands has been investigated with a wide range of late transition metals. A particular goal in the work described in this thesis was to synthesise discrete metallo-supramolecular assemblies or coordination polymers that display anion binding pockets generated upon coordination. All compounds were characterised by a combination of ^{1}H and ^{13}C NMR spectroscopy, diffusion ordered spectroscopy (DOSY), IR spectroscopy, mass spectrometry, elemental analysis and X-ray crystallography. Other techniques such as Simultaneous Thermal Analysis (STA, incorporating thermogravimetric analysis and differential scanning calorimetry) and Powder Diffraction X-ray Diffraction (PXRD) were used to further examine the properties of selected coordination polymers. The nature of anion binding for compounds in the solid-state was probed by X-ray-crystallography.

The synthesis and characterisation of four reported amide ligands (**L1**, **L2**, **L5** and **L6**) and eleven novel compounds were described in Chapter 2. The previously reported compounds were prepared in one step reactions from commercially available precursors as described in the literature. Compounds **L7** – **L12** were prepared by very similar methods to those described in the literature for related compounds but with some minor modifications. In contrast, the rigid ligand precursors **L3** and **L4** were prepared in a different approach that required the synthesis of 6-(methoxycarbonyl)pyridine-2-carboxyl chloride and subsequent reaction with either 3- or 4-pyridylmethylamine. The resulting potentially bidentate chelating ligands, **L13** – **L15,** were also prepared under similar conditions from 2,6-dimethylpyridine dichloride and di-2-pyridylmethylamine. All compounds were obtained in moderate to good

yields. From the work undertaken for this chapter the crystal structures of seven ligands, one of which is a reported compound (**L2**), have been described. These structures reveal useful information about the structures and conformations of these compounds in the solid-state. In the crystal structures of the tetraamide ligands, the presence of intramolecular hydrogen bonding interactions which pre-organise the amide NH groups of the ligand into one central pocket or two smaller pockets were observed. Nonetheless, like **L5** and **L6**, compounds **L7** – **L12** still maintain the pre-organisation of the 2,6-pyridine dicarboxamide but that these either dimerise or have intramolecular hydrogen bonds that block the amide pockets. It was notable that the crystals of a number of the amide compounds were obtained from solutions containing transition metal salts, and demonstrated a preference these compounds have for forming hydrogen bonded networks over metal complexes under the conditions employed. Investigation by NMR solution studies revealed that the tetraamide compounds form hydrogen bonded complexes in solution which may interfere with the ability of these compounds to bind anions. In contrast, for compounds **L5** and **L6** there is a clear mismatch of hydrogen bond donor and acceptor regions preventing ready involvement of the amide NH groups in hydrogen bonded complex formation. This in part explains why ligands **L5** and **L6** may be more suitable compounds for binding both anions and cations as part of discrete metallo-supramolecular assemblies or coordination polymers. This is significant as a larger number of the metallo-supramolecular assemblies and coordination polymers with the potential to selectively bind anions were formed from **L5** and **L6** in this work.

The coordination chemistry of the flexible monoamide ligands, **L1** and **L2**, and the more rigid compounds **L3** and **L4** was investigated with a range of late transition metals such as cadmium(II), copper(II), cobalt(II), silver(I), zinc(II) and palladium(II). The investigation of these compounds has shown that upon reaction with transition metals the methyl ester of **L1**, **L2** and **L3** were hydrolysed and **L1**-CH_3, **L2**-CH_3 and **L3**-CH_3 could coordinate to a metal in a O, N, O tridentate fashion. This led to the formation of three discrete cleft-shaped [Cu_2L_2] dinuclear metallo-macrocyclic complexes of **L1** (complexes **3.12** – **3.14**) and two near planar [Cu_2L_2] dinuclear metallo-macrocyclic complexes of **L3** (complexes **3.15 – 3.16**) in a good yield. The cavities in complexes **3.12** – **3.14** show interesting solid-state host-guest chemistry. In particular, compound **3.14** includes an anion within the hinged cavity and displays anion-π interactions that support the inclusion of an anionic guest. The planar [Cu_2L_2] dinuclear metallo-macrocycles **3.15** and **3.16** are also of interest for further study. These compounds could be used as a tecton for the self-assembly of porous extended

materials as described in the literature.[232] This may involve the use of simple bridging ligand such as pyrazine, DABCO, and 4,4'-bipyridine as linkers to connect these metallo-macrocycles together and form 1-D, 2-D and 3-D porous structures. Several coordination polymers were obtained with **L2**, with the majority displaying a dinuclear $[M_2L_2]$ structural motif related to the macrocyclic structures obtained with **L1** and **L3**. One particularly interesting compound that was obtained from reaction of **L2** and cadmium nitrate is **3.21**, a 2-D 6,3-connected coordination polymer. This compound has a potentially porous structure with channels lined by oxygen atoms from nitrate anions, water solvate molecules and the ester carbonyl oxygen of the only intact non-hydrolysed molecule of **L2**. Unfortunately, this material could only be prepared in a small scale, and attempts to synthesise this compound in a larger scale always gave undesired by-products as significant impurities. Therefore, before further investigation of this compound can be undertaken an improved method for its synthesis is required. Nonetheless, the success in obtaining materials like **3.21** point to considerable potential for this class of ligands. Moderately flexible compounds such as **L1** and **L2** might enable dynamic behaviour within solid-state materials and, when coupled with other rigid bridging ligands in a material may generate porous and dynamic materials utilising these metallo-macrocyclic materials. The work presented in chapter has shown that a simple set of monoamide ligands possessing distinct donor sets at either end has generated a complex range of materials based around a set of robust $[M_2L_2]$ metallo-macrocyclic building blocks.

The coordination chemistry of symmetrical di- or tetra-amide ligands and a range of late transition metals was described in Chapter 4. Several discrete complexes and coordination polymers with novel structures have been prepared from these ligands. In the crystal structures of the resulting compounds the conformations of the precursor amides, as observed in the solid-state structures of these compounds alone, were maintained. This derives from the pre-organisation imparted by the 2,6-pyridine dicarboxamide core, which despite the overall flexibility of many of these compounds, still plays a major role in the conformation of the compound alone and in its resulting complex or coordination polymer. Reaction of **L5** with *cis*-protected palladium(II) precursors gave two mononuclear Pd(II) metallo-macrocycles with the general formula $[Pd(L)(\mathbf{L5})](PF_6)_2$ (L = 2,2,'-bipy or en, **4.16** and **4.17**). Meanwhile, the situation observed with **L6** was more complicated. For $[PdCl_2(en)]$ a dinuclear metallo-macrocyclic structure, $[\{Pd(en)\}_2(\mathbf{L6})_2](PF_6)_4$ was obtained, yet for $[PdCl_2(2,2,'\text{-bipy})]$ a mixture of mononuclear and dinuclear palladium complexes were observed. This difference in behaviour between the complexes with 2,2'-bipy and en

ancillary ligands suggests that steric effects, due to a greater reduction in size of bite angle available at the Pd centre for an incoming ligand, may be having a role in the formation of a mixture when [$PdCl_2$(2,2,'-bipy)] was reacted with **L6**. X-ray crystallography revealed that the mononuclear complex **4.17** has a bowl-like structure with one of the hexafluorophosphate anions located inside the cavity of the complex and the anion interacting with the complex through hydrogen bonding and anion-π interactions, as expected. A second anion lies at the base of the bowl and is hydrogen bonded by the 2,6-pyridine dicarboxamide core. This result provided structural proof that discrete metallo-supramolecular species possessing these ligands can bind anions *via* the NH amide donors and other interactions. This paves the way for anion binding of such complexes to be investigated by NMR spectroscopic titration techniques.

Reactions of **L5** with cadmium nitrate, cadmium perchlorate and cobalt nitrate led to the formation of three 1-D coordination polymers (**4.21** – **4.23**) with a necklace-type of structure. These compounds are packed in the solid-state in such a manner that the anions are located in specific sites surrounded by a range of hydrogen bond donors from the ligand **L5** and coordinated water ligands on the metal centres. These interactions are similar for the three compounds. The packing also generates channels which offer the tantalising possibility that these anions could be selectively exchanged. Two isomorphous 1-D coordination polymers with potentially similar anion exchange properties were obtained with **L6** (**4.25** and **4.26**). In the crystal packing of these compounds two distinct channels were observed, one containing the nitrate anions and a second that contains only solvate. A single 2-D coordination polymer was obtained with **L6**. This compound (**4.28**), which has a 4-connected 2-D structure has channels that are also filled with anions like **4.25** and **4.26**. Thus, in the solid-state structures of complexes and coordination polymers, the diamide ligands have shown a range of anion coordination structures that illustrate their potential in species for anion inclusion and/or separation. Unfortunately, this was not observed for compounds obtained with the tetraamide ligands. In the work presented in this thesis, the tetraamide ligands form 1-D coordination polymers in which the ligands fold upon themselves and the resulting materials are close-packed in the solid-state. This is directly counter to the original aim of this study to utilise these ligands to generate metallo-supramolecular assemblies and coordination polymers with larger pockets for anion inclusion. Obviously the greater flexibility of these compounds has contributed to this result and the resulting close-packed structures are stabilised by intra-molecular hydrogen bonding. One approach to overcoming this may be to reduce the

flexibility of these compounds by replacing the alkyl spacers with rigid aromatic spacers such as phenyl or biphenyl. This will provide the possibility of obtaining metallo-supramolecular assemblies and coordination polymers with larger internal pores lined with anion binding groups.

The coordination chemistry of diamide bridging ligands with chelating motifs has been described in Chapter 5. The initial studies have shown that despite initial consideration in the design of such ligands (i.e. to insert a CH spacer between the amide nitrogen and the pyridine rings) these compounds still appear to decompose upon reaction with metal salts. Nonetheless, this is an improvement over ligands of this type that lack the CH spacer, i.e. where the chelating moiety is di-2-pyridylamine. To this end, only five complexes were obtained with these three ligands, one contained a mixture that could not be separated (**L14** with palladium chloride) while the rest of the reactions failed to give cleanly isolatable products. A discrete [2+2] metallo-macrocyclic complex (**5.10**) was prepared from reaction of **L13** with silver nitrate. This compound, which possesses a small cavity within its macrocyclic structure, may also be interesting for anion binding due to the presence of four amide NH donors being directed into the macrocyclic cavity. A space-filling representation indicated that only very small anions might fit inside this structure, with the nitrate anions preferring to sit on the external grooves of the structure. A ^{1}H NMR spectrum of this compound recorded in DMSO-d_6 indicated that the complex remained intact in solution. Two discrete dinuclear complexes of cadmium(II) were obtained with **L14** and **L15**. In these complexes the metals are bridged by a single molecule of either **L14** or **L15** and they do not display the types of metallo-macrocyclic structures seen commonly in other compounds reported in this thesis or as shown by **5.10**. Like other ligands incorporating two di-2-pyridylmethyl chelating motifs, **L13** – **L15** readily bridge two metals with bidentate chelation at each metal centre. The work described in this chapter could be further expanded by finding conditions to limit hydrolysis of the ligands upon reaction with metal salts.

In summary, this thesis has described the synthesis of fifteen amide-containing polypyridyl ligands, all of which have the potential to interact with anions through an amide binding region of different size and complexity. The reaction of these ligands with metal ions has resulted in the formation of several novel coordination polymers and discrete metallo-supramolecular assemblies with the potential to accommodate anions within the channels or cavities in these structures. The simple monoamide ligands (**L1** – **L3**) and the diamide ligands

(**L5** and **L6)** have been proven to be the most successful in terms of new materials identified and isolated, but also show the most promise in regard to exploiting these systems for anion binding and separation. In contrast, the tetraamide ligands with their more flexible structures failed to generate materials with anions pockets with coordination polymers and instead formed close-packed structures in the solid-state. The outcomes of this research may provide lessons for the development of materials capable of anion separation and sequestration, or the design of selective anion sensors.

CHAPTER 7

EXPERIMENTAL SECTION

Chapter 7

7. Experimental section

7.1. General Experimental

Melting points were measured on a Gallenkamp melting point apparatus and are uncorrected. Elemental analyses were performed by the Campbell Microanalytical Laboratory at the University of Otago, Dunedin, New Zealand. Infrared spectra were collected on a Perkin Elmer Spectrum BX Infrared spectrometer as KBr disks, or a Perkin Elmer Spectrum 100 using a Universal Attenuated Total Reflectance (UATR) sampling accessory. Thermogravimetic analyses (TGA) were carried out on a Perkin Elmer STA 6000 Simultaneous Thermal Analyzer using aluminium sample pans in platinum crucibles. All TGA experiments were conducted under a nitrogen atmosphere.

NMR spectra were recorded on Varian Gemini 300 MHz NMR spectrometer or a Varian Inova 600 MHz NMR spectrometer at 23 ºC using a 5mm probe. ^{1}H NMR spectra recorded in $CDCl_3$ were referenced relative to the internal standard Me_4Si; ^{1}H NMR spectra recorded in DMSO-d_6 were referenced to the solvent peak: 2.6 ppm. ^{13}C NMR spectra were all referenced to their solvent peaks: $CDCl_3$, 77.0 ppm and DMSO, 39.6 ppm. When required, 1-D NOESY, 1-D TOCSY, 2-D DOSY experiments were performed using standard pulse sequences. Unless otherwise stated, the values given for chemical shifts are to the centre of a multiplet. Electrospray (ES) mass spectra were recorded using a Finnigan LCQ mass spectrometer by preparing serial dilutions of a 1 mg/mL solution of the compound.

7.2. X-ray Diffraction Data Collection and Structure Refinement

7.2.1. Single Crystal X-ray Crystallography

Crystals were mounted under paratone-N oil on a plastic loop. X-ray diffraction datasets were collected with Mo-Kα radiation (λ = 0.71073 Å) using (a) a Bruker-AXS Single Crystal Diffraction System fitted with an Apex II CCD detector at 110(2) K (b) a Rigaku Saturn Kappa System at 93(2) K, and; (c) Oxford Diffraction X-calibur single crystal X-ray diffractometer at

150(2) K. Datasets on small or weakly diffracting samples were collected using synchrotron radiation (λ = 0.7107 Å) at 150(2) K on the Protein Micro-crystal and Small Molecule X-ray Diffraction beam lines (MX1 and 2) at the Australian Synchrotron.

All datasets were corrected for absorption using a multi-scan method, and structures were solved by direct methods using SHELXS-97[390] and refined by full-matrix least squares on F^2 by SHELXL-97,[391] interfaced through the program X-Seed.[392] In general, all non-hydrogen atoms were refined anisotropically and hydrogen atoms were included as invariants at geometrically estimated positions, unless specified otherwise in additional details in appendix X. Figures were produced using the program POV-Ray,[393] interfaced through the program X-Seed. Publication materials were prepared using CIFTAB.[394] Details of data collections and structure refinements are attached in Appendix 2.

7.2.2. Powder X-ray Diffraction

Powder X-ray diffraction data was collected on a Rigaku Hiflux Homelab system using Cu-Kα radiation with an R-Axis IV++ image plate detector. Samples were mounted on plastic loops by coating a droplet of paratone-N in samples. Data were collected by scanning 90° in phi for 180-300 second exposures. The data was converted to an xye format using the program DataSqueeze.

7.3. Synthesis of Precursor Compounds

Unless otherwise stated, all chemicals were obtained from commercial sources and used as received. Dichloromethane was dried by standard literature procedures and distilled fresh from calcium hydride as required. 2,6-Pyridinedicarboxylic acid monomethyl ester (**2.6**),[173] *N*-6-[(3-pyridylmethylamino)carbonyl]-pyridine-2-carboxylic acid methyl ester (**L1**),[161] *N*-6-[(4-pyridylmethylamino)carbonyl]-pyridine-2-carboxylic acid methyl ester (**L2**),[161] *N,N'*-2,6-bis(3-pyridylmethyl)pyridine dicarboxamide (**L5**),[161] and *N,N'*-2,6-bis(4-pyridylmethyl)pyridine dicarboxamide (**L6**) [161] were prepared according to methods described in the literature. The palladium precursors with ancillary blocking ligands, dichloropalladium(II) ethylenediamine [$PdCl_2$(en)],[395] dichloropalladium(II) 2,2'-bipyridine [$PdCl_2$(bipy)],[395] dichloropalladium(II) bis(triphenylphosphine) [$PdCl_2(PPh_3)_2$][396] and ditriflatopalladium(II) bis(triphenylphosphine) [$Pd(OTf)_2(PPh_3)_2$][308] were also prepared based on the literature procedures.

7.3.1. Ligand Syntheses

_N_-6-[(3-pyridylamino)carbonyl]-pyridine-2-carboxylic acid methyl ester L3·¼H_2O

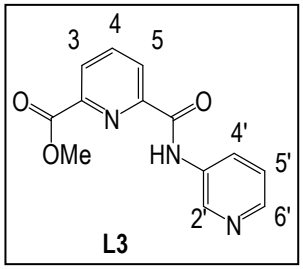

L3

2,6-Pyridinedicarboxylic acid monomethyl ester (**2.6**) (1.06 g, 5.85 mmol) was suspended in dichloromethane (20 mL). Freshly distilled thionyl chloride (5 mL) and dry DMF (100 μL) were added, and the reaction mixture was heated at reflux for 1 hr. After cooling, the solvent was removed *in vacuo* to give a white solid of the crude acid chloride which was dried under high vacuum for 30 mins. The acid chloride was dissolved in dichloromethane (40 mL), 3-aminopyridine (0.58 g, 6.2 mmol) and triethylamine (0.81 mL, 5.9 mmol) were added, and the solution was heated at reflux for 24 hrs. The solvent was removed *in vacuo* to give a brown solid, the residue was dissolved in dichloromethane (100 mL), washed with saturated aqueous sodium bicarbonate solution (2 x 100 mL), and dried over magnesium sulfate. The chlorinated solvent was removed to give a brown solid that was washed with diethyl ether, dried, and recrystallised from ethanol to give **L3**·¼H_2O as a tan solid (0.78 g, 51%). Mp 150-153°C. Anal. found: C, 59.59; H, 4.33; N, 15.69. $C_{13}H_{11.5}N_3O_{3.25}$ requires C, 59.64; H, 4.44; N, 16.06%; ^{1}H NMR (300 MHz; $CDCl_3$; Me_4Si) δ = 4.05 (3H, CH_3), 7.36 (2H, d, *J* = 4.77 Hz pyH5', pyH4'), 8.28 (1H, t, *J* = 7.78 Hz, pyH4), 8.30 (1H, d, *J* = 1.14 Hz, pyH3), 8.36 (1H, m, pyH5), 8.50 (1H, d, *J* = 5.39 Hz, pyH6'), 8.93 (1H, s, pyH2') and 10.24 (1H, s, NH). ^{13}C NMR (75.1 MHz; $CDCl_3$; Me_4Si) δ = 165.00, 162.05, 149.86, 146.60, 145.53, 141.85, 139.19, 134.69, 127.96, 127.48, 125.96, 123.87, 53.30. *m/z* (ES-MS) 258 (MH^+, 40%). Selected IR bands (KBr disk, cm^{-1}): 3449 (m), 3242 (m), 1724 (s), 1684 (s), 1583 (s), 1529 (s), 1417 (s), 1301 (s), 1234 (s), 1161 (m), and 738 (s).

_N_-6-[(4-pyridylamino)carbonyl]-pyridine-2-carboxylic acid methyl ester hydrate L4·H_2O

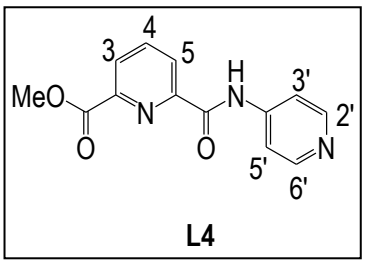

L4

In a similar manner to that described for **L3**, 2,6-pyridinedicarboxylic acid monomethyl ester (**2.6**) (1.02 g, 5.63 mmol) was treated to give the acid chloride as a white solid. Reaction with 4-aminopyridine (0.55 g, 5.8 mmol) and work-up using the method for **L3,** gave an oily brown solid of crude **L4**. The crude product was washed with diethyl ether, dried and recrystallised from ethanol to give **L4**·H_2O as a tan powder (1.07 g, 75%). Mp 113-114°C. Anal. found: C, 56.40; H, 4.76; N, 15.07.

$C_{13}H_{13}N_3O_4$ requires C, 56.71; H, 4.77; N 15.27%. ^{1}H NMR (300 MHz; $CDCl_3$; Me_4Si) δ = 4.06 (3H, s, CH_3), 7.76 (2H, m, pyH3', pyH5'), 8.13 (1H, t, *J* = 7.95 Hz, pyH4), 8.31 (1H, m, pyH3), 8.47 (1H, d, *J* = 4.09 Hz, pyH5), 8.50 (2H, m, pyH2', pyH6') and 10.30 (1H, s, NH). ^{13}C NMR (75.1 MHz; $CDCl_3$; Me_4Si) δ = 164.89, 162.26, 150.72, 149.59, 146.50, 144.80, 139.23, 128.10, 126.10, 114.20, 53.29. *m/z* (ES-MS) 258 (MH^+, 55%). Selected IR bands (KBr disk, cm^{-1}): 3505 (s), 3208 (m), 1728 (s), 1695 (m), 1581 (s), 1303 (s), 1249 (s), 1000 (m), and 826 (m).

1,2-Bis[*N,N'*-6-(3-pyridylmethylamido)pyridyl-2-carboxyamido]ethane hydrate L7·H_2O

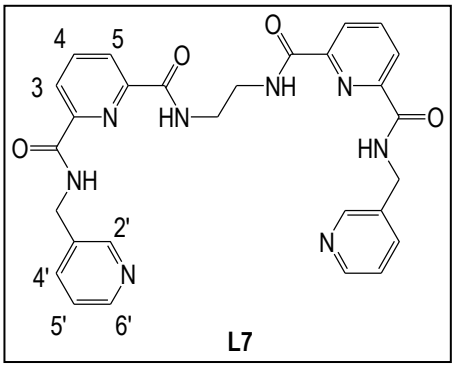

L7

Under a nitrogen atmosphere, a suspension of *N*-6-[(3-pyridylmethylamino)carbonyl]-pyridine-2-carboxylic acid methyl ester (**L1**) (0.50 g, 1.8 mmol) and ethylenediamine (0.062 mL, 0.92 mmol) in toluene (40 mL) was heated at reflux for 36 hrs. The solvent was removed *in vacuo* to give a cream coloured solid. The solid was purified by flash column chromatography on silica gel, eluting with 1:9 methanol–CH_2Cl_2, to give **L7**·H_2O as a cream solid (0.21 g, 41%). Mp 260- 261°C. Anal. found: C, 60.95; H, 4.80; N 20.07. $C_{28}H_{28}N_8O_5$ requires C, 60.41; H, 5.08; N 20.14%. ^{1}H NMR (300 MHz; $CDCl_3$; Me_4Si) δ = 3.57 (4H, m, CH_2NH), 4.77 (4H, d, *J* = 6.52 Hz, pyCH_2NH), 7.35 (2H, m, pyH5'), 7.72 (2H, m, pyH4'), 8.22 (6H, m, pyH3, pyH5, pyH4), 8.46 (2H, m, pyH6'), 8.57 (2H, m, pyH2'), 9.07 (2H, m, CH_2NH) and 9.14 (2H, m, pyCH_2NH). ^{13}C NMR (75.1 MHz; $CDCl_3$; Me_4Si) δ = 165.8, 164.90, 164.19, 160.39, 148.93, 148.69, 148.11, 139.36, 136.48, 132.65, 126.22, 125.56, 124.51, 41.19., *m/z* (ES-MS) 539.2 (MH^+, 100%), 561.2. Selected IR bands (KBr disk, cm^{-1}): 3359 (m), 1670 (s), 1524 (s), 1444 (m), 1419 (m) and 708 (m). Crystals were obtained by slow evaporation of a methanol solution of **L7** and copper acetate.

1,2-Bis[*N,N'*-6-(4-pyridylmethylamido)pyridyl-2-carboxyamido]ethane hydrate L8·H_2OA suspension of *N*-6-[(4-pyridylmethylamino)carbonyl]-pyridine-2-carboxylic acid methyl ester (**L2**) (0.50 g, 1.8 mmol) and a slight excess of ethylenediamine (0.065 mL, 0.96 mmol) in toluene (40 mL) was heated at reflux for 36 hrs under nitrogen. The solvent was removed *in vacuo* to give a brown solid. The solid was purified by flash column chromatography on silica gel, eluting

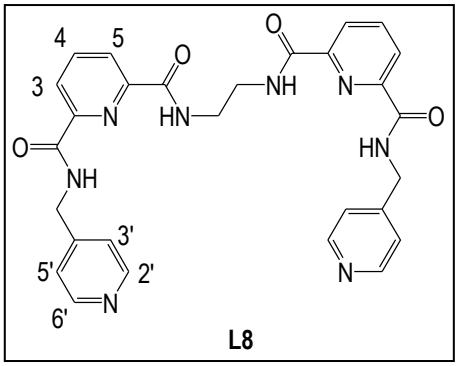

with 1:9 methanol–CH_2Cl_2, to give **L8**·H_2O as a cream solid (0.19 g, 35%). Mp 262-264°C. Anal. found: C, 60.78; H, 4.79; N 20.15. $C_{28}H_{28}N_8O_5$ requires C, 60.41; H, 5.08; N 20.14%. ^{1}H NMR (300 MHz; $CDCl_3$; Me_4Si) δ = 3.56 (4H, m, *CH*$_2$NH), 4.76 (4H, d, *J* = 6.45 Hz, py*CH*$_2$NH), 7.24 (4H, m, pyH3', pyH5'), 7.84 (2H, m, pyH5), 8.36 (2H, m, pyH4), 8.53 (4H, m, pyH2', pyH6') and 9.23 (2H, m, NH). ^{13}C NMR (75.1 MHz; $CDCl_3$; Me_4Si) δ = 165.79, 164.34, 150.27, 148.85, 148.10, 148.00, 139.44, 125.77, 125.75, 124.62, 42.64, 40.71. *m/z* (ES-MS) 539.30 (MH^+, 65%), 561.3, (MNa^+, 100%), 1076.7 (M_2H^+, 5%), 1098.8 (M_2Na^+, 15%), Selected IR bands (KBr disk, cm^{-1}): 3266 (m), 3354 (s), 1648 (s), 1529 (s), 1418 (m), 1307 (w), 1001 (m) and 846 (m). Crystals were obtained by slow evaporation of a methanol solution of **L8** and cobalt acetate.

1,2-Bis[*N,N'*-6-(3-pyridylmethylamido)pyridyl-2-carboxyamido]propane hydrate L9·H_2O

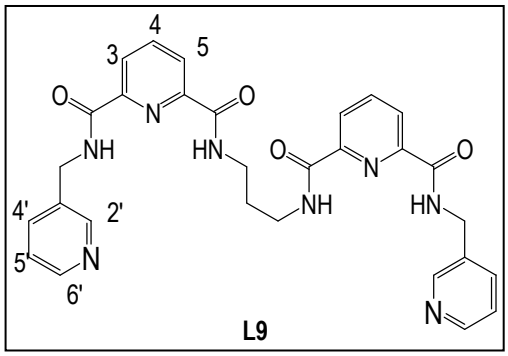

Under a nitrogen atmosphere, a suspension of *N*-6-[(3-pyridylmethylamino)carbonyl]-pyridine-2-carboxylic acid methyl ester (**L1**) (1.24 g, 4.57 mmol) and propylenediamine (0.19 mL, 2.3 mmol) in toluene (40 mL) was heated at reflux for 96 hrs. The solvent was removed *in vacuo* to give a pale brown oil which was dried under high vacuum to give **L9**·H_2O as a cream solid (0.89 g, 68%). Mp 171-172°C. Anal. found: C, 61.80; H, 5.00; N 19.64. $C_{28}H_{30}N_8O_5$ requires C, 61.03; H, 5.31; N 19.64%. ^{1}H NMR (300 MHz; $CDCl_3$; Me_4Si) δ = ^{1}H (300 MHz; $CDCl_3$; Me_4Si) δ = 3.49 (2H, m, *CH*$_2$CH$_2$NH), 3.97 (2H, m, CH$_2$*CH*$_2$NH), 4.68 (4H, d, *J* = 6.45 Hz, py*CH*$_2$NH), 7.26 (4H, m, pyH3', pyH5'), 7.75 (2H, 2d, *J* = 7.87, 4.80 Hz, pyH3), 8.06 (2H, m, pyH5), 8.23 (2H, m, pyH4), 8.40 (2H, m, pyH6'), 8.45 (2H, m, pyH2') and 8.89 (2H, m, NH). ^{13}C NMR (75.1 MHz; $CDCl_3$; Me_4Si) δ = 165.04, 163.91, 149.99, 149.43, 149.03, 146.69, 138.87, 135.86, 134.02, 127.68, 125.78, 123.76, 53.14, 41.12. *m/z* (ES-MS) 553.0, (MH^+, 65%), 1106.1 (M_2H^+, 10%). Selected IR bands (KBr disk, cm^{-1}): 3298 (m), 1654 (s), 1523 (s), 1414 (m), 1309 (m), 1069 (m), 1001 (m) and 743 (s).

1,2-Bis[*N*,*N'*-6-(4-pyridylmethylamido)pyridyl-2-carboxyamido]propane dihydrate L10·2H$_2$O

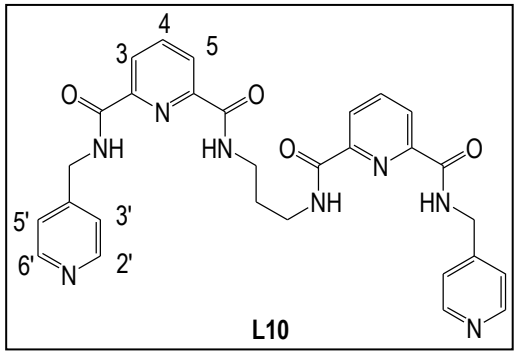

L10

Under an atmosphere of nitrogen, a suspension of *N*-6-[(4-pyridylmethylamino)carbonyl]-pyridine-2-carboxylic acid methyl ester (**L2**) (1.86 g, 6.85 mmol) and propylenediamine (0.292 mL, 3.42 mmol) in toluene (40 mL) was heated at reflux for 96 hrs. The solvent was removed *in vacuo* to give a brown oil which solidified on standing. This solid was further purified by flash column chromatography on silica gel, eluting with 1:9 methanol–CH_2Cl_2, to give **L10**·2H$_2$O as a cream solid (0.65 g, 32%). Mp 145 – 46°C. Anal. found: C, 59.28; H, 5.12; N 19.21. ($C_{29}H_{32}N_8O_6$) requires C, 59.16; H, 5.49; N 19.04%. ^{1}H (300 MHz; $CDCl_3$; Me_4Si) δ = 3.50 (2H, m, *CH$_2$*CH$_2$NH), 3.98 (2H, m, CH$_2$*CH$_2$*NH), 4.69 (4H, m, py*CH$_2$*NH), 7.34 (4H, m, pyH3', pyH5'), 7.99 (2H, m, pyH3), 8.01 (2H, m, pyH5), 8.09 (2H, m, pyH4), 8.44 (4H, m, pyH2', pyH6') and 9.24 (2H, m, NH). ^{13}C (75.1 MHz; $CDCl_3$; Me_4Si) δ = 164.47, 164.31, 149.93, 149.76, 148.59, 148.17, 139.38, 125.45, 124.87, 122.51, 42.42, 34.94. *m/z* (ES-MS) 553 (MH^+, 100%). Selected IR bands (KBr disk, cm^{-1}): 3387 (m), 3316 (m), 1624 (s), 1520 (s), 1429 (m), 1237 (m), and 844 (m).

1,2-*Bis*[6-methoxycarbonyl)pyridyl-2-carboxyamido]cyclohexane 2.13

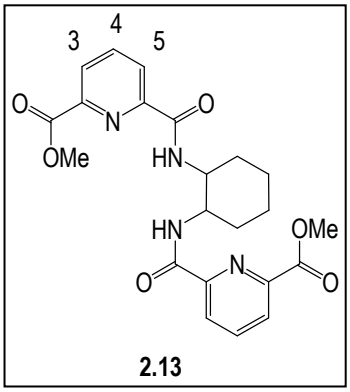

2.13

2,6-Pyridinedicarboxylic acid monomethyl ester (**2.6**) (0.97 g, 5.0 mmol) was suspended in dichloromethane (20 mL). Freshly distilled thionyl chloride (5 mL) and dry DMF (100 μL) were added and the reaction mixture was heated at reflux for 1 hr. After cooling the reaction mixture to room temperature, the solvent was removed *in vacuo* to give a white solid which was dried under high vacuum for 30 mins. The solid was re-dissolved in dichloromethane (40 mL), *trans*-1,2-diaminocyclohexane (0.299 mL, 2.48 mmol) and triethylamine (0.5 mL, 4.97 mmol) were added, and the solution was heated at reflux for 24 hrs. The solvent was removed *in vacuo* to give a sticky brown solid, the residue

was reconstituted with dichloromethane (100 mL), washed with saturated aqueous sodium bicarbonate solution (2 x 100 mL), and the chlorinated layer dried over magnesium sulfate. The solvent was removed *in vacuo* to give a brown solid. The solid was washed with diethyl ether, dried and recrystallised from methanol to give **2.13** as brown crystals (0.75 g, 68%). Mp 121-122 °C. ^{1}H (300 MHz; $CDCl_3$; Me_4Si) δ = 1.46 (3H, m, CH_3), 1.83 (2H, m, cy), 4.02 (2H, m, cy), 4.16 (1H, s, NH*CH*), 7.26 (1H, t, pyH4), 7.88 (1H, m, pyH3), 8.12 (1H, m, pyH5) and 8.22 (1H, s, NH). ^{13}C (75.1 MHz; $CDCl_3$; Me_4Si) δ = 168.74, 161.30, 150.71, 146.69, 140.45, 130.38, 128.80, 53.50, 51.72, 29.23, 23.45. *m/z* (ES-MS) 440 (MH^+, 100%).

1,2-Bis[*N,N'*-6-(3-pyridylmethylamido)pyridyl-2-carboxyamido]cyclohexane L11

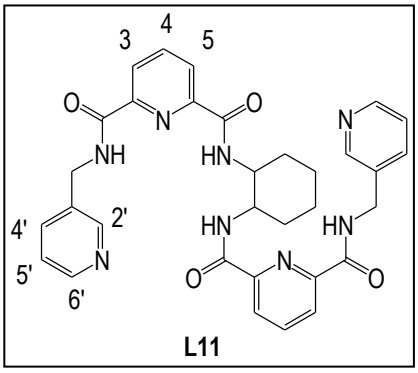

L11

1,2-*Bis*[6-methoxycarbonyl)pyridyl-2-carboxyamido]cyclohexane (**2.13**) (0.50 g, 1.1 mmol) and 3-aminomethylpyridine (0.22 mL, 2.3 mmol) were suspended in toluene (20 mL). The reaction mixture was heated at reflux for 72 hrs, during which time a white solid precipitated. After cooling to room temperature, the solvent was removed *in vacuo*, the residue re-dissolved in dichloromethane (40 mL), washed with saturated aqueous sodium bicarbonate solution (2 x 100 mL) and the chlorinated extract dried over magnesium sulfate. The solvent was removed *in vacuo* to give sticky off-white solid. The solid was washed with diethyl ether, dried and recrystallised from ethanol to give **L11** as a white solid (0.55 g, 82%). Mp 250-252 °C. Anal. found: C, 64.19; H, 5.52; N 18.70. ($C_{32}H_{32}N_8O_4$) requires C, 64.84; H, 5.45; N 18.90%. ^{1}H (300 MHz; $CDCl_3$; Me_4Si) δ = 1.32 (2H, m, CH_2), 1.65 (1H, m, CH_2), 2.17 (1H, m, CH_2), 3.87 (1H, s, CH), 4.15 (2H, d, *J* = 11.43 Hz, CH_2), 7.23 (1H, m, pyH5), 7.82 (2H, m, pyH3, pyH4', pyH4), 8.28 (2H, m, pyH5'), 8.54 (2H, d, *J* = 4.81 Hz, pyH6'), 8.65 (2H, m, NH, pyH2') and 9.07 (1H, d, *J* = 8.38 Hz, NH). ^{13}C (75.1 MHz; $CDCl_3$; Me_4Si) δ = 23.1, 28.3, 45.1, 54.6, 123.9, 125.7, 125.9, 134.8, 136.7, 139.2, 148.1, 149.5, 149.9, 150.8, 161.1, 162.4. *m/z* (ES-MS) 592.2 (MH^+, 100), 593.6 (MH^+, 50%), 614.5 (MNa^+, 65%), 1204.2 ($M.H_2O+H)^+$, 30%). Selected IR bands (KBr disk, cm^{-1}): 3368 (m), 3267 (m), 1627 (m), 1650 (s), 1527 (s), 1424 (m), 1306 (s). Crystals were obtained by slow evaporation of a methanol solution of **L11** and copper nitrate.

1,2-Bis[*N*,*N'*-6-(4-pyridylmethylamido)pyridyl-2-carboxyamido]cyclohexane hydrate L12·H_2O

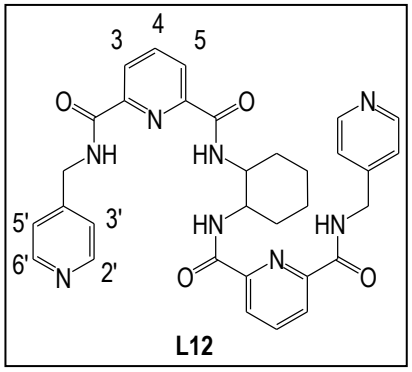

L12

1,2-*Bis*[6-methoxycarbonyl)pyridyl-2-carboxyamido]cyclohexane (**2.13**) (0.52 g, 1.2 mmol) and 4-aminomethylpyridine (0.24 mL, 2.4 mmol) were dissolved in hot toluene (20 mL) and heated at reflux for 72 hrs. During the course of the reaction a yellow solid precipitated. The solvent was removed *in vacuo* to give a yellow solid. The solid was re-dissolved in dichloromethane (40 mL), washed with saturated sodium bicarbonate solution (2 x 100 mL) and the chlorinated layer dried over magnesium sulfate. The solvent was removed *in vacuo* to give yellow oil which was triturated with hot ethyl acetate (5 mL) to give a brown solid. This solid was purified by column chromatography, eluting with 1:9 methanol–CH_2Cl_2 to give **L12**·H_2O as a brown solid (0.24 g, 33%). Mp 220 – 225 °C. Anal. Found: C, 64.67; H, 5.89; N 18.90. ($C_{32}H_{34}N_8O_5$) requires C, 64.84; H, 5.45; N 18.91%. ^{1}H (300 MHz; $CDCl_3$; Me_4Si) δ = 1.43 (2H, m, CH_2), 1.93 (2H, d, *J* = 6.73 Hz, CH_2), 2.14 (2H, d, *J* = 13.29 Hz, CH_2), 3.77 (1H, s, CH), 4.72 (2H, m, CH_2), 7.25 (2H, m, pyH3', pyH5'), 7.74 (2H, m, pyH3, pyH5), 8.32 (1H, m, pyH4), 8.54 (2H, d, *J* = 5.70 Hz, pyH2', pyH6'), 9.15 (1H, d, *J* = 6.25 Hz, NH) and 9.75 (1H, t, *J* = 6.40 Hz, NH). ^{13}C (75.1 MHz; $CDCl_3$; Me_4Si) δ = 22.5, 28.9, 45.6, 54.0, 124.3, 125.6, 125.9, 139.8, 147.3, 148.9, 149.2, 149.9, 160.5, 161.8. *m/z* (ES-MS) 592.3 (MH^+, 100%), 593.1 (MH^+, 75%). Selected IR bands (KBr disk, cm^{-1}): 3282 (m), 2923 (s), 1652 (s), 1671 (s), 1529 (s), 1444 (m), 1414 (m), 672 (s). Crystals were obtained by slow evaporation of a methanol solution of **L12** and copper perchlorate.

Di-(2-pyridyl) ketone oxime (2.36)

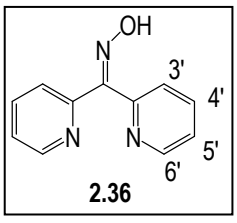

2.36

Di-2-pyridyl ketone oxime (2.48 g, 0.135mmol) and hydroxylamine hydrochloride (1.3 g, 0.0202 mmol) were dissolved in ethanol (18 mL). Sodum hydroxide (2.67 g, 0.03 mmol) was slowly added to the solutionwith strirring over a period of 90 mins, during which time the solution turned dark orange and a white precipitate form. The solution was heated at reflux for 10 mins and cooled to room temperature. The reaction mixture was treated with with water (10 mL) and

concentrated HCl (2.5 mL). The ethanol was removed by rotary evaporation to yield a dark red solution. The pink product was precipitated by addition of saturated aqueous sodium bicarbonate (10 mL). The solid was filtered, washed with water and dried in vacuo at room temperature to yield 12.79 g of hydrated product. (12.79 g, 98%). Mp 101-102 °C . Anal found. C, 66.30; H, 4.70; N 21.80. ($C_{29}H_{25}N_7O$) requires C, 66.32; H, 4.55; N 21.09%. ^{1}H (300 MHz; $CDCl_3$; Me_4Si) δ = 7.35 (2H, td, *J* = 5.5, 2.5 Hz, pyH5'), 7.45 (2H, td, *J* = 6.1, 1.7 Hz, pyH3'), 7.85 (2H, m, pyH4'), 8.65 (2H, d, *J* = 8.1 Hz, pyH6') and 16.0 (1H, s, OH). ^{13}C (75.1 MHz; $CDCl_3$; Me_4Si) δ = 123.90, 126.2, 136.1, 149.2, 152.5, 164.6. *m/z* (ES-MS) 200.08, (MH^+, 75%).

Di-(2-pyridyl)methaneamine (2.37)

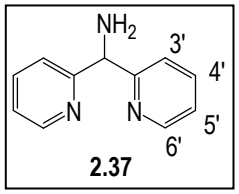

2.37

In a mixture of ethanol (85 mL), water (50 mL) and aqueous NH_3 solution (75 mL), di-2-pyridylketone oxime (5.01 g, 25 mmol) and ammonium acetate (3.32 g, 42.9 mmol) were dissolved and heated to 80°C. Over a period of 30 mins, Zn dust (7.36 g, 113 mmol) was added. The mixture was heated at reflux for 4.5h, and the solid obtained was removed by filtration. The filtrate was concentrated at the rotaevaporator. The resulting aqueous solution (ca. 10 mL) was basified with 10N NaOH solution and extracted with dichloromethane (5 x 15 mL). The combined organic phase were washed with 10 mL brine and dried with $MgSO_4$. After evaporation of the solvent, the compound was obtained as a colourless oil (4.20 g, 91%). ^{1}H (300 MHz; $CDCl_3$; Me_4Si) δ = 2.40 (2H, s, NH_2) , 5.32 (1H, s, C*H*), 7.12(2H, 3d, *J* = 0.8, 4.7, 7.4 Hz, pyH5'), 7.35 (2H, dt, *J* = 7.8, 1.1 Hz, pyH4'), 7.59 (2H, dt, *J* = 1.3, 7.5 Hz, pyH3') and 8.53 (2H, 3d, *J* = 0.9, 1.7, 4.8 Hz, pyH6'). ^{13}C (75.1 MHz; $CDCl_3$; Me_4Si) δ = 62.2, 121.8, 122.5, 136.9, 149.7, 162.9. *m/z* (ES-MS) 186.18, (MH^+, 60%).

2,6-[*N,N'*-bis(di-(pyridin-2-yl)methyl)pyridine]-2,6-dicarboxamide hydrate L13·H_2O

2,6-Pyridinedicarboxylic acid (**2.19**) (1.06 g, 5. 85 mmol) was suspended in dichloromethane (20 mL). Freshly distilled thionyl chloride (5 mL) and dry DMF (100 μL) were added and the reaction mixture was heated at reflux for 1 hr. After cooling to

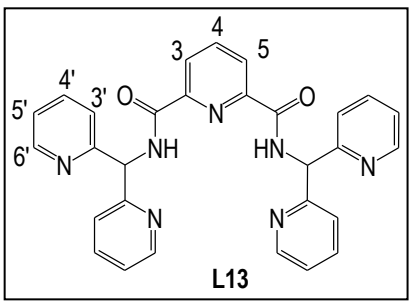

L13

room temperature, the solvent was removed *in vacuo* to give **2.20** as a white solid. The solid was dried under high vacuum for 30 mins. The solid was re-dissolved in dichloromethane (40 mL), di-(2-pyridyl)methylamine (0.58 g, 6.2 mmol) and triethylamine (0.81 mL, 5.9 mmol) were added, and the solution was heated at reflux for 24 hrs. The solvent was removed *in vacuo* to give a brown oil, the residue was redissolved with dichloromethane (100 mL), washed with saturated sodium bicarbonate solution (2 x 100 mL) and dichloromethane layer dried over magnesium sulfate. The chlorinated solvent was removed *in vacuo* to give a brown solid which was isolated from column chromatography in methanol: dichloromethane (1:9) solvent separation system to give **L13**·H_2O as an off-white solid (1.70 g, 51%). Mp 180-183 °C. Anal found. C, 67.30; H, 4.70; N 18.80. ($C_{29}H_{25}N_7O$) requires C, 67.00; H, 4.90; N 18.88%. ^{1}H (300 MHz; $CDCl_3$; Me_4Si) δ = 6.54 (2H, d, *J* = 7.17 Hz, CH_2), 7.14 (4H, m, pyH5'), 7.60 (8H, m , pyH3, pyH4'), 8.02 (1H, t, *J* = 7.78 Hz, pyH4), 8.37 (2H, d, *J* = 7.71 Hz, pyH3'), 8.52 (4H, 2d, *J*=4.81 Hz, pyH6') and 10.32 (1H, d, *J* = 7.02 Hz, NH). ^{13}C (75.1 MHz; $CDCl_3$; Me_4Si) δ = 177.98, 149.57, 141.11, 137.19, 122.74, 122.31, 120.23, 103.87, 59.82. *m/z* (ES-MS) 501.6, (MH^+, 15%), 523.4, (MNa^+, 40%). Selected IR bands (KBr disk, cm^{-1}): 3378 (s), 3354 (s), 1724 (m), 1671 (s), 1587 (m), 1503 (s), 1436 (s) and 997 (s). Crystals were obtained by slow evaporation of a mixture of methanol-acetonitrile solution of **L13**.

1,3-*N,N'*-[bis(di-(pyridin-2-yl)methyl)]isophthalamide hydrate L14·H_2O

Isophthaloyl chloride (0.55 g, 2.8 mmol) was dissolved in dichloromethane (40 mL) and di-(2-pyridyl)methylamine (1.01 g, 5.5 mmol) and triethylamine (0.76 mL, 5.5 mmol) were added. The solution was heated at reflux for 72 hrs. The solvent was removed *in vacuo* to give a brown solid which was collected, washed with diethyl ether, dried and recrystallised from ethanol to give **L14**·H_2O as a light brown solid (0.90 g, 63%). Mp 170-173 °C. Anal. Found: C, 69.13; H, 4.98; N 15.63. ($C_{30}H_{25}N_6O_3$) requires C, 69.61; H, 4.88; N 16.24%. ^{1}H (300 MHz; $CDCl_3$; Me_4Si) δ = 6.42 (1H, CH), 7.18 (2H, m, pyH5), 7.50 (1H, d , *J* = 6.64 Hz, pyH4'), 7.65 (1H, d, 7.65 *J* = 6.56 Hz, pyH3), 8.06 (d, *J* = 4.12 Hz, pyH3'), 8.57 (1H, s, pyH6') and 8.87 (1H, s, NH). ^{13}C (75.1 MHz; $CDCl_3$; Me_4Si) δ = 166.01, 158.95, 149.41, 137.19, 134.77, 130.68, 129.03, 126.23, 122.81, 122.33, 59.74. *m/z* (ES-MS) 501.1 (MH^+,100%), 522.4 (MNa^+, 60%).

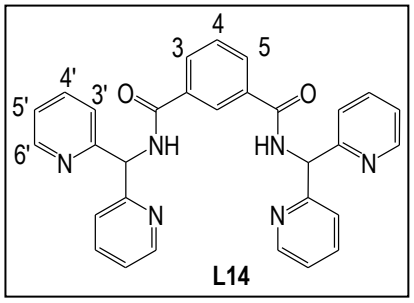

L14

Selected IR bands (KBr disk, cm^{-1}): 3329 (s), 1650 (s), 1569 (s), 1522 (m), 1475 (s), 1257 (m), 997 (m) and 751 (s).

1,4-*N,N'*-bis[(di(pyridin-2-yl)methyl)]terephthalamide L15

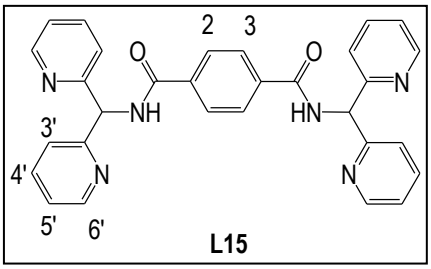

Terephthaloyl chloride (0.30 g, 1.5 mmol) was dissolved in dichloromethane (40 mL), and di-(2-pyridyl)methylamine (0.55 g, 3.0 mmol) and triethylamine (0.41 mL, 3.0 mmol) were added. The solution was heated at reflux for 72h. The solvent was removed *in vacuo* to give a brown solid of **L15**. The solid was washed with diethyl ether, dried and recrystallised from ethanol to give **L15** as a fine brown solid (0.43 g, 57%). Mp 288-289 °C. Anal. Found: C, 71.96; H, 4.89; N 16.94. ($C_{30}H_{24}N_6O_2$) requires C, 71.97; H, 4.84; N 16.79%. ^{1}H (300 MHz; $CDCl_3$; Me_4Si) δ = 6.40 (1H, m, CH), 7.21 (1H, m, pyH5'), 7.54 (1H, m, pyH4'), 7.69 (1H, m, pyH3'), 8.11 (2H, 2m, ph-H3,H5), 8.65 (2H, m, pyH6'), and 8.96 (1H, s, NH). ^{13}C (75.1 MHz; $CDCl_3$; Me_4Si) δ = 165.89, 158.89, 149.47, 137.16, 127.76, 122.83, 122.61, 122.43, 59.60. *m/z* (ES-MS) 500.2, (M^+, 100%), 501.2 (MH^+, 35%), 523.2 (MNa^+, 5%). Selected IR bands (KBr disk, cm^{-1}): 3211 (m), 1642 (s), 1589 (s), 1528 (m), 1437 (s), 1431 (s) and 1291 (m). Crystals were obtained by slow evaporation of a methanol solution of **L15** and cadmium sulphate.

7.4. Synthesis of coordination polymers and discrete complexes

**Caution! Whilst no problems were encountered in the course of this work, perchlorate salts are strong oxidising agents and are potentially explosive and should be handled on a small scale with appropriate care.*

$[ZnCl_2(L4)_2]$ (3.11). $Zn(ClO_4)_2$ (0.013 g, 0.049 mmol) was dissolved in methanol (2 mL). This solution was heated for a few mins before being added dropwise to a solution of **L1** (0.026 g, 0.98 mmol) dissolved in hot methanol (15 mL). A clear solution was obtained rapidly after the addition. The mixture was heated for 45 mins and left to evaporate at room temperature. After a month, the solution afforded **3.11** as white crystals (<5 %). Selected IR bands (KBr disk, cm^{-1}): 3425 (s), 1632 (m), 1620 (s) and 1416 (m). (note : No further characterisation was pursued

because the compound was obtained in a very low yield and was not able to be reproduced).

$[Cu_2(NO_3)_2(L1\text{-}CH_3)_2]$ (3.12). $Cu(NO_3)_2 \cdot xH_2O$ (0.014 g, 0.058 mmol) was dissolved in methanol (2 mL). This solution was heated for a few mins before being added dropwise to a solution of **L1** (0.031 g, 0.12 mmol) dissolved in hot methanol (15 mL). A deep blue solution was obtained rapidly after the addition. The mixture was heated for 45 mins and left to evaporate at room temperature. After a month, the solution afforded **3.12** as blue prismatic crystals (0.013 g, 59%). Mp 245-248°C. Anal. found: C, 40.90; H, 2.96; N 14.35. $C_{26}H_{20}N_8O_{12}Cu_2$ requires C, 40.89; H, 2.65; N 14.68%. Selected IR bands (KBr disk, cm^{-1}): 3445 (s), 1652 (m), 1627 (s), 1418 (m), 1383 (s, N-O stretch). *m/z* (ES-MS) 636.9 ($[^{63}Cu(NO_3)(\mathbf{L1\text{-}CH_3})(\mathbf{L1\text{-}CH_3})H]^+$, 96%), 638.9 ($[^{65}Cu(NO_3)(\mathbf{L1\text{-}CH_3})(\mathbf{L1\text{-}CH_3})H]^+$, 100%), 699.8 ($[^{63}Cu_2(NO_3)(\mathbf{L1\text{-}CH_3})_2]^+$, 68%), 701.8 ($[^{63}Cu^{65}Cu(NO_3)(\mathbf{L1\text{-}CH_3})_2]^+$, 48%), 703.8 ($[^{65}Cu_2(NO_3)(\mathbf{L1\text{-}CH_3})_2]^+$, 14%).

$[Cu_2Cl_2(L1\text{-}CH_3)_2(H_2O)]\cdot{}^1/_2CH_3OH\cdot 3^1/_2H_2O$ (3.13). $CuCl_2 \cdot 2H_2O$ (0.013 g, 0.11 mmol) was dissolved in methanol (5 mL). This solution was heated for a few mins and added dropwise to a solution of **L1** (0.059 g, 0.22 mmol) in hot methanol (15 mL). The addition gave a light blue solution, which was heated for another 45 mins and left to evaporate at room temperature. After 3 weeks, the solution afforded **3.13** as blue diamond-shaped crystals (0.027 g, 60%). Mp 215-216 °C. Anal. found: C, 39.66; H, 3.50; N 10.56. $C_{26}H_{28}N_6O_{10}Cl_2Cu_2$ requires C, 39.90; H, 3.61; N 10.74%. Selected IR bands (KBr disk, cm^{-1}): 3425 (s), 2923(s), 1668 (s), 1436 (m), 705 (s).

$[Cu_2(L1\text{-}CH_3)_2(CH_3OH)_2](ClO_4)_2.H_2O\cdot{}^1/_2CH_3OH$ (3.14). $Cu(ClO_4)_2 \cdot 6H_2O$ (0.043 g, 0.12 mmol) was dissolved in methanol (5 mL) to give a pale blue solution. This solution was heated for a few mins before being added dropwise to a solution of **L1** (0.063 g, 0.23 mmol) dissolved in hot methanol (15 mL). The light blue solution was heated for 45 mins and left to evaporate at room temperature. After a week, the solution afforded **3.14** as turquoise blue crystals (0.037 g, 67%). Mp 280-285 °C; Anal. found: C, 36.17; H, 3.04; N 9.49; $C_{28}H_{30}N_6O_{17}Cl_2Cu_2$ requires: C, 36.53; H, 3.29; N 9.13%. Selected IR bands (KBr disk, cm^{-1}): 3421 (s), 1635 (s), 1436 (m), 1370 (m), 1086 (s, Cl-O stretch). *m/z* (ES-MS) 918.7 ($\{[^{63}Cu_2(\mathbf{L1\text{-}CH_3})(H_2O)(\mathbf{L1\text{-}CH_3})H](^{35}ClO_4)_2\}^+$, 30%) 920.9 ($\{[^{63}Cu^{65}Cu(\mathbf{L1\text{-}CH_3})(H_2O)(\mathbf{L1\text{-}CH_3})H](^{35}ClO_4)_2\}^+$, $\{[^{63}Cu_2(\mathbf{L1\text{-}CH_3})(H_2O)(\mathbf{L1\text{-}CH_3})H](^{35}ClO_4)\ (^{37}ClO_4)\}^+$, 18%).

$[Cu_6(NO_3)_2(L3\text{-}CH_3)_6(H_2O)_6](NO_3)_4\cdot 2CH_3OH$ (3.15). $Cu(NO_3)_2\cdot 2H_2O$ (0.020 g, 0.087 mmol) was dissolved in methanol (2 mL), heated for a few mins, before being added dropwise to a solution of **L3** (0.044 g, 0.17 mmol) dissolved in hot methanol (15 mL). The mixture was heated for another 45 mins, capped and left to evaporate at room temperature. After a month, the green-blue solution afforded **3.15** as blue needle-shaped crystals (0.025 g, 75%). Mp 220-222°C; Found: C, 34.81; H, 2.53; N, 15.01; $C_{72}H_{60}N_{24}O_{42}Cu_6$ requires C, 37.36; H, 2.62; N 14.53%; Selected IR bands (KBr disk, cm^{-1}): 3432 (s), 1652 (w), 1575 (w), 1383(s, N-O stretch).

$[Cu_2(L3\text{-}CH_3)_2(ClO_4)_2(H_2O)_2]_2$ (3.16). $Cu(ClO_4)_2\cdot 6H_2O$ (0.14 g, 0.39 mmol) was dissolved in methanol (2 mL). The solution added dropwise to a solution of **L3** (0.20 g, 0.78 mmol) in hot methanol (15 mL). A light green solution was obtained, the mixture heated for another 45 min, and left to evaporate at room temperature. After a month, the greenish solution afforded **3.16** as blue needle-shaped crystals (0.12 g, 66%). Mp 225-230°C; Anal. found: C, 30.38; H, 3.07; N, 8.84. $C_{24}H_{20}N_6O_{16}Cl_2Cu_2\cdot 5H_2O$ requires C, 30.78; H, 3.24; N, 8.98%; Selected IR bands (KBr disk, cm^{-1}): 3501(s), 2932 (m), 1652 (w), 1558 (w), 1121 (m, Cl-O stretch).

$\{[Cd(L1\text{-}CH_3)(H_2O)(\mu_2\text{-}H_2O)](NO_3)\cdot ¼H_2O\}_n$ (3.17). A solution of $Cd(NO_3)_2\cdot 4H_2O$ (0.027 g, 0.088 mmol)·in methanol (10 mL) was added dropwise to a solution of **L1** (0.048 g, 0.18 mmol) in methanol (15 mL). The mixture was heated for 45 mins and left to evaporate at room temperature. After two months, the solution afforded **3.17** as colourless crystals (0.032 g, 80%). Mp 230-235ºC. Anal. found: C, 32.72; H, 3.16; N 12.56. $CdC_{13}H_{14.5}N_4O_{8.25}$ requires C, 33.13; H, 3.11; N 11.89%; Selected IR bands (KBr disk, cm^{-1}): 3075 (m), 2922 (s), 1657 (m), 1535 (s), 1409 (m), 1377 (s, N-O stretch).

$\{[Cu_3(L2\text{-}CH_3)_3(L2)_2(H_2O)_2(CH_3OH)](ClO_4)_3\}_n$ (3.18). $Cu(ClO_4)_2\cdot 6H_2O$ (0.034 g, 0.12 mmol) was dissolved in methanol (5 mL) to give a pale blue solution. This solution was heated for a few mins before being added dropwise to a solution of **L1** (0.063 g, 0.23 mmol) which also dissolved in hot methanol (15 mL). The addition of copper perchlorate solution has given to a light blue solution. The mixture was heated for 45 mins and left to evaporate at room temperature. After a week, the blue solution afforded **3.18** as turquoise blue crystals (0.095 g, 45%). Mp 280 – 285°C; Anal. found: C, 42.27; H, 3.09; N 10.51. $[Cu_3C_{68.5}H_{68}N_{15}O_{33.5}Cl_3]$ requires C, 42.53; H, 3.55; N

10.86%. Selected IR bands (KBr disk, cm^{-1}): 3421 (s), 1635 (s), 1436 (m), 1370 (m), 1086 (s, Cl-O stretch).

{[Cd(L2-CH_3)(CH_3OH)(H_2O)](NO_3)·2CH_3OH}$_n$ (3.19). A solution of $Cd(NO_3)_2·4H_2O$ (0.071 g, 0.23 mmol) in hot methanol (5 mL) was added to a solution of **L2** (0.13 g, 0.46 mmol) also in hot methanol (15 mL). This mixture was heated for 45 mins and left to evaporate at room temperature. After two months, the solution afforded **3.19** as colourless, needle-shaped crystals (0.030 g, 36%). Mp 240-245°C; Anal. found: C, 34.22; H, 2.67; N 12.96. $CdC_{13}H_{12}N_4O_7$ requires C, 34.80; H, 2.70; N 12.49%. Selected IR bands (KBr disk, cm^{-1}): 3361 (s), 1711 (s), 1642 (s), 1467 (m), 1383 (s, N-O stretch).

{[Cd_2(L2-CH_3)$_2$(SO_4)(H_2O)$_2$]·5½H_2O }$_n$ (3.20). A solution of $CdSO_4·H_2O$ (0.005 g, 0.022 mmol) in water (5 mL) was added dropwise to a solution of **L2** (0.013 g, 0.047 mmol) in methanol (10 mL) to give a clear solution. The mixture was heated for 45 mins and left to evaporate at room temperature. After about one month, the solution afforded **3.20** as colourless block-shaped crystals (0.004 g, 19%). Mp 210 – 212 ºC. Anal. found: C, 31.68; H, 3.92; N 8.96. $C_{26}H_{35.5}Cd_2N_6O_{17.5}S$·requires C, 32.22; H, 3.70; N 8.67%. Selected IR bands (KBr disk, cm^{-1}): 3287 (m), 1641 (s), 1535 (s), 1386 (m), 1044, 683 (m, S-O stretch).

{[Cd_3(L2-CH_3)$_3$(NO_3)(L2)(CH_3OH)](NO_3)$_2$·12½H_2O}$_n$ (3.21). A mixture of $Cd(NO_3)_2·4H_2O$ (0.064 g, 0.21 mmol) ·and **L2** (0.028 g, 0.10 mmol) was dissolved in DMF (1 mL), capped and heated at 110°C for 24 h. The resulting solution was slowly cooled down to room temperature, transferred to other vial containing methanol (0.5 mL), capped, and left to stand for several weeks. After a month, the solution afforded **3.21** as colourless crystals (0.005 g, 8%). Mp 292-296ºC. Found: C, 35.41; H, 3.34; N 11.11. $C_{54}H_{51}Cd_3N_{15}O_{24}·10½H_2O$ requires C, 35.45; H, 4.03; N 11.49%; selected IR bands (KBr disk, cm^{-1}): 3234 (m), 1650 (w), 1606 (m), 1558 (m), 1426 (m), 1371 (s, N-O stretch).

{[Cu(L2(-H)-CH_3)]·½H_2O}$_n$ (3.22). A mixture of $Cu(CH_3COO_3)_2$ (0.018 g, 0.097 mmol)·and **L2** (0.012 g, 0.045 mmol) was dissolved in DMF (1 mL), capped and heated at 110°C for 24h. The resulting solution was slowly cooled to room temperature before transferred to other vial containing methanol (0.5 mL) and left to stand. After a month, the solution afforded **3.22** as

bright blue crystals (0.012 g, 82%). Mp 250-252ºC. Anal. found: C, 47.70; H, 3.23; N 12.91. $CuC_{13}H_9N_3O_3 \cdot ½H_2O$ requires C, 47.63; H, 3.08; N 12.82%. Selected IR bands (KBr disk, cm^{-1}): 3323 (m), 3036 (s), 2924 (m), 1632 (m), 1601 (s).

$[CdBr_2(L5)_2] \cdot 6½H_2O$ (4.14). $CdBr_2$ (0.0047 g, 0.017 mmol) was dissolved in water (5 mL) to give a clear solution. This solution was heated for a few mins before being added dropwise to a solution of **L5** (0.012 g, 0.035 mmol), dissolved in methanol (15 mL). A fine precipitate was observed before the mixture was heated for 45 mins and left to evaporate at room temperature. After a week, the solution afforded $[CdBr_2(\mathbf{L5})_2] \cdot 6½H_2O$ as colourless crystals (0.013 g, 69%). Mp 220-225 ºC. Anal. found: C, 41.74; H, 3.42; N 12.85. $CdC_{38}H_{47}N_{10}O_{10.5}Br_2$ requires C, 42.10; H, 4.38; N 12.92%. Selected IR bands (KBr disk, cm^{-1}): 3323 (m), 1659 (s), 1525 (s), 1424 (m), 1221 (s), 1002(m).

$[Zn(L5)_4(H_2O)_2](L5)_2(ClO_4)_2 \cdot 8H_2O$ (4.15). $Zn(ClO_4)_2 \cdot 6H_2O$ (0.0077 g, 0.021 mmol) was dissolved in methanol (5 mL) to give a clear solution. This solution was heated for a few mins before being added dropwise to a solution of **L5** (0.0143 g, 0.041 mmol), also dissolved in methanol (15 mL). The resulting clear solution was heated for 45 mins and left to evaporate at room temperature. After three weeks, the solution afforded $[Zn(\mathbf{L5})_4(H_2O)_2](\mathbf{L5})_2(ClO_4)_2 \cdot 8H_2O$ as colourless block crystals (0.007 g, 54%). Mp 200-202ºC. Anal. found: C, 55.13; H, 4.92; N 16.83. $ZnC_{114}H_{118}N_{30}O_{28}Cl_2$ requires C, 54.92; H, 4.78; N 16.86%; Selected IR bands (KBr disk, cm^{-1}): 3252 (m), 1672 (m), 1654 (s), 1529 (s), 1429 (s), 1074 (s, Cl-O stretch).

$[Pd(bipy)(L5)](PF_6)_2$ (4.16). $[PdCl_2(2,2'\text{-bipy})]$ (0.114 g, 0.34 mmol) and $AgNO_3$ (0.112 g, 0.67 mmol) were dissolved in water (5 mL). A drop of concentrated HNO_3 was added and the mixture was heated at 100°C for 2 hrs. The resulting solid was removed by filtration and the filtrate was added to a stirred solution of **L5** (0.116 g, 0.34 mmol) in methanol (25 mL). After stirring for 5 mins, ammonium hexafluorophosphate (0.217 g, 1.32 mmol) was added and the reaction was left to stir overnight. The precipitate obtained was collected, washed with water and dried under vacuum to give $[Pd(bipy)(\mathbf{L5})](PF_6)_2$ as a fine white solid (0.22 g, 77%). Mp 225-228°C. Anal. found: C, 40.38; H, 4.53; N 11.64. $PdC_{29}H_{24}N_7O_2P_2F_{12}$ requires C, 39.74; H, 4.70; N 11.20%; ^1H (300 MHz; DMSO-d_6) δ = 4.36 (2H, m, pyCH_2NH), 5.32 (2H, m, pyCH_2NH), 7.25 (2H, m, bipyH5), 7.65 (2H, m, bipyH4), 7.83 (2H, m, bipyH6), 8.27 (2H, m, pyH5'), 8.44 (2H, m,

pyH4'), 8.71 (2H, m, pyH3, pyH5), 9.74 (1H, d, *J*=9.74 Hz, pyH4), 9.28 (4H, m, bipyH6, pyH6'), 9.76 (2H, 2d, pyH2') and 9.89 (1H, 2d, NH). Selected IR bands (KBr disk, cm^{-1}): 3385, 1663, 1537, 1444 and 830 cm^{-1}. *m/z* (ES-MS) 755.3 ({Pd(bipy)(**L5**)](PF_6)}$^+$, MH^+, 10%).

[Pd(en)(L5)]$(PF_6)_2$·H_2O·2CH_3OH (4.17). [$PdCl_2$(en)] (0.171 g, 0.72 mmol) and $AgNO_3$ (0.245 g, 0.40 mmol) were dissolved in water (5 mL). A drop of concentrated HNO_3 was added and the mixture was heated at 100°C for 2 hrs. The resulting solid was filtered off and the filtrate added to a stirred solution of **L5** (0.25 g, 0.72 mmol) in methanol (25 mL). After stirring for 5 mins, ammonium hexafluorophosphate (0.47 g, 2.8 mmol) was added and the reaction was left to stir overnight. The precipitate obtained was collected, washed with water and dried under vacuum to give [Pd(en)(**L5**)]$(PF_6)_2$·H_2O·2CH_3OH as a grey solid (0.20 g, 46%). Mp 215-218°C. Anal.found: C, 31.26; H, 2.87; N 10.37. $PdC_{24}H_{34}N_7O_5P_2F_{12}$ requires C, 31.18; H, 3.99; N 11.07%; ^{1}H (300 MHz; DMSO-d_6) δ = 4.77 (4H, m, py*CH*$_2$NH), 5.26 (4H, m, $CH_2CH_2NH_2$), 7.64 (2H, 2d, *J* = 7.98, 5.57 Hz, pyH3', pyH5'), 8.08 (1H, m, pyH4'), 8.30 (2H, m, pyH3, pyH5), 8.86 (2H, m, pyH4), 8.89 (2H, m, pyH2', pyH6') and 9.76 (1H, m, NH). Selected IR bands (KBr disk, cm^{-1}): 3389, 1671, 1541, 1440 and 831 cm^{-1}. *m/z* (ES-MS) 513.2 ({[Pd(en)(**L5**)]$(PF_6)^+$}, MH^+, 10%).

[Pd(bipy)(L6)]$_{2n}$$(PF_6)_{2n}$ (4.18a and 4.18b). [$PdCl_2$(2,2'-bipy)] (0.110 g, 0.33 mmol) and $AgNO_3$ (0.113 g, 0.67 mmol) were dissolved in water (5 mL). A drop of concentrated HNO_3 was added and the mixture was heated at 100°C for 2 hrs. The resulting solid was filtered off while the filtrate obtained was added to the stirred solution of ligand **L6** (0.114 g, 0.33 mmol) in methanol (25 mL). After stirring for 5 mins, ammonium hexafluorophospate (0.217 g, 1.32 mmol) was added and the reaction was left to stir overnight. The precipitate obtained was collected, washed with water and dried under vacuum to give [Pd(bipy)(**L6**)]$_{2n}$$(PF_6)_{2n}$ as a grey powder (0.10 g, 33%). Mp 219-220 °C. Anal. found: C, 38.24; H, 2.90; N 10.32. [Pd(bipy)(**L6**)]$_{2n}$$(PF_6)_{2n}$ requires C, 38.74; H, 2.74; N 10.91%; ^{1}H [2+2] (300 MHz; DMSO-d_6) δ = 4.77 (2H, 2d, *J* = 6.92, 0.40 Hz, , py*CH*$_2$NH), 7.51 (2H, m, bipyH5), 8.15 (2H, m, bipyH4), 8.30 (2H, m, bipyH6), 8.40 (2H, m, pyH5'), 8.67 (2H, m, pyH4'), 8.77 (2H, m, pyH3, pyH5), 8.88 (1H, m, pyH4), 9.03 (4H, m, bipyH6, pyH6), 9.123 (2H, d, *J* = 6.45 Hz,, pyH2) and 9.94 (1H, m, NH). ^{1}H [1+1] (300 MHz; DMSO-d_6) δ = 4.66 (2H, 2d, py*CH*$_2$NH), 8.09 (2H, m, bipyH5), 8.19 (2H, m, bipyH4), 8.35 (2H, m, bipyH6), 8.35 (2H, m, pyH5'), 8.49 (2H, m, pyH4'), 8.79 (2H, m, pyH3, pyH5), 8.91 (1H, m,

pyH4), 8.92 (4H, m, bipyH6, pyH6), 9.15 (2H, m, pyH2) and 9.73 (1H, m, NH).Selected IR bands (KBr disk, cm^{-1}): 3097, 1642, 1531, 1448, 989, 835 and 710 cm^{-1}.

[{Pd(en)}$_2$(L6)$_2$](PF$_6$)$_4$ (4.19). [$PdCl_2$(en)] (0.239 g, 0.102 mmol) and $AgNO_3$ (0.342 g, 0.203 mmol) were dissolved in water (5 mL). A drop of concentrated HNO_3 was added and the mixture was heated at 100°C for 2 hrs. The resulting solid was filtered and the the filtrate was added to a stirred solution of ligand **L6** (0.350 g, 0.101 mmol) in methanol (25 mL). After stirring for 5 mins, ammonium hexafluorophospate (0.70 g, 2.9 mmol) was added and the reaction was left to stir for two days. The precipitate obtained was collected, washed with water, and dried under vacuum to give [{Pd(en)}$_2$(**L6**)$_2$](PF$_6$)$_4$ as a cream powder (0.46 g, 26%). Mp 216-218. °C. Anal. found: C, 30.87; H, 3.37; N 11.45. [{Pd(en)}$_2$(**L6**)$_2$](PF$_6$)$_4$ requires C, 31.01; H, 3.44; N 11.51%; (300 MHz; DMSO-d$_6$) δ = 4.66 (4H, m, py*CH*$_2$NH), 5.51 (4H, m, $CH_2CH_2NH_2$), 7.53 (2H, m, pyH3', pyH5'), 8.22 (1H, m, pyH4'), 8.23 (2H, m, pyH3, pyH5), 8.69 (2H, d, pyH4) and 9.74 (2H, d, *J*=9.74 Hz, pyH2', pyH6'). *m/z* (ES-MS) 511.9 ({[Pd(en)(**L6**)], MH^+,50%), ({[Pd_2(en)$_2$(**L6**)$_2$](PF$_6$)}$^{3+}$ 1172.6, MH^+,40%), ({[Pd_2(en)$_2$(**L6**)$_2$](PF$_6$)$_2$}$^{2+}$, MH^+,18%) 1316.8. Selected IR bands (KBr disk, cm^{-1}): 3189, 1663, 1528, 1441, 988, 837 and 703 cm^{-1}.

[{Pd(PPh$_3$)$_2$}(L6)$_2$](PF$_6$)$_4$·2CH$_3$OH (4.20). [Pd(OTf)$_2$(PPh$_3$)$_2$] was formed by reacting [$PdCl_2$(PPh$_3$)$_2$] (0.36 g, 0.52 mmol) with silver triflate (0.27 g, 1.0 mmol) in dichloromethane-acetonitrile (9:1). The resulting precipitate of silver chloride was filtered and the solvent removed *in vacuo* to give colourless oil. This residue was dissolved in dichloromethane (10 mL) and combined with **L6** (0.38 g, 1.04 mmol) and ammonium hexafluorophosphate (0.34 g, 0.205 mmol). This mixture was stirred for three days, and the solvent removed to give a yellow oily residue. This residue was redissolved in chloroform (5 mL) and the product precipitated by addition of diethyl ether (5 mL). The resulting pale yellow solid was filtered under vacuum, collected and recrystallised from methanol to give a fine cream solid (0.38 g, 55%). Mp 180-181°C. Found: C, 49.61; H, 3.75; N 6.15. [{Pd(PPh$_3$)$_2$}(**L6**)$_2$](PF$_6$)$_4$·2CH$_3$OH requires C, 51.73; H, 3.95; N 5.39%; ^{1}H (300 MHz; CD_3CN) δ = 4.49 (2H, d, py*CH*$_2$NH), 7.17 (2H, m, pyH3, pyH5), 7.4-7.60 (12H, m, PPh_3), 8.153 (1H, m, pyH4),7.93 (2H, m, pyH5'), 8.15 (2H, m, pyH3'), 8.27 (2H, m, pyH6'), 8.48 (2H, m, pyH2') and 9.14 (1H, s, NH). Selected IR bands (KBr disk, cm^{-1}): 3212, 1665, 1525 1435 and 831 cm^{-1}. *m/z* (ES-MS) 1122.4 ({[Pd(PPh$_3$)(**L6**)](PF$_6$)]}$^+$, MH^+, 5%).

{[Cd(L5)$_2$(H$_2$O)$_2$](NO$_3$)$_2$·H$_2$O}$_n$ (4.21). Cd(NO$_3$)$_2$·4H$_2$O (0.0056 g, 0.018 mmol) was dissolved in methanol (5 mL) to give a clear solution. This solution was heated for a few mins before being added dropwise to a solution of **L5** (0.0125 g, 0.036 mmol) also dissolved in hot methanol (15 mL). This gave a clear solution, which was heated for 45 mins, and left to evaporate at room temperature. After two weeks, the solution afforded {[Cd(**L5**)$_2$(H$_2$O)$_2$](NO$_3$)$_2$.H$_2$O}$_n$ as colourless crystals (0.013 g, 73%). Mp 249-250 ºC. Anal. found: C, 46.46; H, 4.03; N 17.00. CdC$_{38}$H$_{40}$N$_{12}$O$_{13}$ requires C, 46.32; H, 4.10; N 17.06%. Selected IR bands (KBr disk, cm^{-1}): 3264 (s), 1667 (s), 1542 (m), 1050 (s), 1346 (s, N-O stretch).

{[Cd(L5)$_2$(H$_2$O)$_2$](ClO$_4$)$_2$}$_n$ (4.22). Cd(ClO$_4$)$_2$·6H$_2$O (0.0073 g, 0.017 mmol) was dissolved in methanol (5 mL) to give a clear solution. This solution was heated for a few mins before being added dropwise to a solution of **L5** (0.012 g, 0.034 mmol) also dissolved in hot methanol (15 mL). The resulting clear solution was heated for 45 mins and left to evaporate at room temperature. After three weeks, the solution afforded {[Cd(**L5**)$_2$(H$_2$O)$_2$](ClO$_4$)}$_n$ as colourless block-shaped crystals (0.014 g, 78%). Mp 210-211 ºC. Anal. found: C, 44.06; H, 3.72; N 13.78. CdC$_{38}$H$_{38}$N$_{10}$Cl$_2$O$_{14}$ requires C, 43.79; H, 3.68; N 13.44%. Selected IR bands (KBr disk, cm^{-1}): 3324 (m), 1658 (s), 1535 (s), 1433 (m), 1001 (s), 1070 (s, Cl-O stretch).

{[Co(L5)$_2$(H$_2$O)$_2$](NO$_3$)$_2$·3H$_2$O}$_n$ (4.23). A solution of Co(NO$_3$)$_2$·6H$_2$O (0.0059 g, 0.020 mmol) was dissolved in methanol (5 mL) to give a pale pink solution. This solution was heated for a few mins before being added dropwise to a solution of **L5** (0.0141 g, 0.041 mmol), also dissolved in hot methanol (15 mL). The resulting dark pink solution was heated for 45 mins and left to evaporate at room temperature. After two months, the solution afforded {[Co(**L5**)$_2$(H$_2$O)$_2$](NO$_3$)$_2$·3H$_2$O}$_n$ as pink plate-shaped crystals (0.006 g, 33%). Mp 210-212 ºC. Anal. found: C, 49.95; H, 4.36; N 18.17. CoC$_{38}$H$_{38}$N$_{12}$O$_{12}$ requires C, 49.94; H, 4.20; N 18.40%. Selected IR bands (KBr disk, cm^{-1}): 3267 (s), 1666 (s), 1544 (m), 1384 (vs, N-O stretch).

{[Cu$_3$(L5-2H)$_2$(CH$_3$COO)$_2$(H$_2$O)$_2$(CH$_3$OH)$_2$]·5(CH$_3$OH)}$_n$ (4.24). Cu(CH$_3$COO)$_2$·H$_2$O (0.0040 g, 0.020 mmol) was dissolved in methanol (5 mL) to give a blue solution, heated for a few mins before being added dropwise to a solution of **L5** (0.0138 g, 0.040 mmol) dissolved in hot methanol (15 mL). The resulting deep blue solution was heated for 45 mins and left to evaporate at room temperature. After a month, the blue solution afforded {[Cu$_3$(L5-2H)$_2$(CH$_3$COO)$_2$(H$_2$O)$_2$(CH$_3$OH)$_2$]·5(CH$_3$OH)}$_n$ as blue crystals (0.006 g, 59%). Mp 230-232

ºC. Anal. found: C, 49.05; H, 4.31; N 13.56. $C_{49}H_{68}Cu_3N_{10}O_{17}$ requires C, 46.71; H, 5.45; N 11.12%. Selected IR bands (KBr disk, cm^{-1}): 3422 (w), 1576 (s), 1430 (m).

{[Cd(L6)$_2$(H$_2$O)$_2$](NO$_3$)$_2$·6H$_2$O}$_n$ (4.25). $Cd(NO_3)_2.4H_2O$ (0.0050 g, 0.016 mmol) was dissolved in methanol (5 mL). This solution was heated for a few mins before being was added dropwise to a solution of **L6** (0.0113 g, 0.0325 mmol) dissolved in methanol (15 mL). The resulting colourless solution was heated for 45 mins and left to evaporate at room temperature. After a month, the solution afforded $\{[Cd(\mathbf{L6})_2(H_2O)_2](NO_3)_2{\cdot}6H_2O\}_n\}_n$ as colourless block-shaped crystals (0.008 g, 51%). Mp 240-241ºC. Found: C, 53.86; H, 4.42; N 17.95. $CdC_{38}H_{50}N_{12}O_{18}$ requires C, 42.44; H, 4.70; N 15.63%. Selected IR bands (KBr disk, cm^{-1}): 3298 (s), 1658 (s), 1603 (m), 1526 (s), 1415 (s), (NO_3); 1311 (m, N-O stretch).

{[Zn(L6)$_2$(H$_2$O)$_2$](NO$_3$)$_2$·4H$_2$O}$_n$ (4.26). $Zn(NO_3)_2{\cdot}4H_2O$ (0.0054 g, 0.018 mmol) was dissolved in methanol (5 mL) to give a colourless solution which, after being heated for a few mins was added dropwise to a solution of **L6** (0.0125 g, 0.036 mmol) dissolved in methanol (15 mL). The addition gave a colourless solution that was heated for 45 mins and left to evaporate at room temperature. After a month, the solution afforded $\{[Zn(\mathbf{L6})_2(H_2O)_2](NO_3)_2{\cdot}4H_2O\}_n$ as colourless crystals (0.008 g, 45%). Mp 200-210 ºC. Anal. found: C, 45.72; H, 4.59; N 17.11. $ZnC_{38}H_{46}N_{12}O_{16}$ requires C, 45.99; H, 4.68; N 16.94%. Selected IR bands (KBr disk, cm^{-1}): 3252 (s), 1653 (m), 1619 (m), 1537 (m), 1393 (m), 1315 (s, N-O stretch).

{[CdBr$_2$(L6)(CH$_3$OH)]·CH$_3$OH}$_n$ (4.27). $CdBr_2$ (0.0057 g, 0.021 mmol) was dissolved·in water (5 mL), heated for a few mins, before being added dropwise to a solution of **L6** (0.0145 g, 0.0417 mmol) dissolved in methanol (15 mL). The resulting cloudy solution was heated for 45 mins to re-dissolve the precipitate and left to evaporate at room temperature. After three weeks, the solution afforded $\{[CdBr_2(\mathbf{L6})(CH_3OH)]{\cdot}CH_3OH\}_n$ as colourless crystals (0.005 g, 36%). Mp 280-282ºC. Found: C, 33.43; H, 3.16; N 10.05. $CdC_{19}H_{23}N_5O_5Br_2$ requires C, 33.87; H, 3.45; N 10.40%. Selected IR bands (KBr disk, cm^{-1}): 3316 (s), 1677 (s), 1528 (m), 1440 (m), 1304 (m), 1176 (m).

{[Cd(L6)$_2$(H$_2$O)$_2$](ClO$_4$)$_2$·3½H$_2$O·CH$_3$OH}$_n$ (4.28). $Cd(ClO_4)_2.6H_2O$ (0.0092 g, 0.022 mmol) was dissolved in methanol (5 mL), the solution heated for a few mins, before being added dropwise to a solution of **L6** (0.0153 g, 0.044 mmol) also dissolved in methanol (15 mL). The colourless solution that formed was heated for 45 mins and left to evaporate at room temperature.

After a month, the solution afforded $\{[Cd(\mathbf{L6})_2(H_2O)_2](ClO_4)_2\cdot 3½H_2O\cdot CH_3OH\}_n$ as colourless block-shaped crystals (0.009 g, 38%). Mp 270-275 ºC. Anal. found: C, 41.19; H, 3.50; N 10.90. $CdC_{39}H_{49}N_{10}O_{18.5}Cl_2$ requires C, 41.18; H, 4.32; N 12.32%. Selected IR bands (KBr disk, cm^{-1}): 3317 (s), 1612 (s), 1537 (s), 1426 (m), 1100 (s), 1061 (s, Cl-O stretch).

$[Cd_{1.5}(ClO_4)_3(L5)(H_2O)_3]$ and **$[Cd_2(SO_4)_2(L5)(H_2O)_5]$ (4.29).** Cadmium(II) salts, CdX_2 (where, X = Br, Cl, ClO_4, NO_3, or $X_2 = SO_4$; all 0.05 mmol) were combined together in a single vial. The cadmium salt mixtures were dissolved in H_2O (5 mL) by heating at 80°C for 20 minutes. A ligand (**L5**) solution (0.1 mmol) was formed by dissolving the ligand in methanol (5 mL). The ligand solution was added into complexes solution and the reaction mixture heated for another 20 minutes to give a colourless solution. This solution was capped, and left to evaporate at room temperature. After 24h, a cream solid precipitated out from the solution. Mp 230-235 °C. Anal. found: C, 26.43%; H, 2.61% N: 8.29%. $[Cd_{1.5}(ClO_4)_3(\mathbf{L5})(H_2O)_3]$ requires C, 26.44% H, 3.39% N, 8.12%; $[Cd_2(SO_4)_2(\mathbf{L5})(H_2O)_5]$ requires C, 21.68% H, 2.50% N, 6.66%. Selected IR bands (UATR, cm^{-1}): 3349(s), 1666(s), 1526(s), 1437(s), 1091(m), 1057(m), 706(s) and 659 (m).

$[Cd_{2.5}(ClO_4)_5(L6)(H_2O)]$ and **$[Cd_{3.5}(SO_4)_{3.5}(L6)(H_2O)_2]$ (4.30).** Cadmium(II) salts, CdX_2 (where, X = Br, Cl, ClO_4, NO_3, or $X_2 = SO_4$; all 0.05 mmol) were combined together in a single vial. The cadmium salt mixtures were dissolved in H_2O (5 mL) by heating at 80°C for 20 minutes. A ligand (**L5**) solution (0.1 mmol) was formed by dissolving the ligand in methanol (5 mL). The ligand solution was added into complexes solution and the reaction mixture heated for another 20 minutes to give a colourless solution. This solution was capped, and left to evaporate at room temperature. After 24h, a cream solid precipitated out from the solution. Mp 225-230 °C. Anal. found: C, 20.17%; H, 2.08% N, 6.49%. $[Cd_{2.5}(ClO_4)_5(\mathbf{L6})(H_2O)]$ requires C, 19.95% H, 1.68% N, 6.12%; $[Cd_{3.5}(SO_4)_{3.5}(\mathbf{L6})(H_2O)_2]$ requires C, 20.50% H, 1.91% N, 6.29%. Selected IR bands (UATR, cm^{-1}): 3355 (s), 1642 (s), 1531(s), 1427(m), 1089(m), 1067(m), 783(s) and 656(m).

$\{[Cd_{1.5}(L8)_2(H_2O)_4](NO_3)_3\cdot CH_3OH\}_n$ (4.31). $Cd(NO_3)_2\cdot 4H_2O$ (0.0064 g, 0.021 mmol) was dissolved in methanol (5 mL), heated for a few mins, before being added dropwise to a solution of **L8** (0.0223 g, 0.0414 mmol) which was dissolved in 1:1 methanol-acetonitrile (15 mL). The resulting colourless solution was heated for 45 mins and left to evaporate at room temperature. After two months, the solution afforded $\{[Cd_{1.5}(\mathbf{L8})_2(H_2O)_4](NO_3)_3\cdot CH_3OH\}_n$ as colourless

crystals (0.008 g, 36%). Mp 240-245ºC. Found: C, 42.02; H, 3.99; N 16.65. $Cd_{1.5}C_{57}H_{64}N_{19}O_{22}$ requires C, 42.20; H, 3.39; N 16.56%. Selected IR bands (KBr disk, cm^{-1}): 3294 (s), 1654 (s), 1541 (s), 1315 (s, N-O stretch), 1002 (s), 744 (m).

{[Cd(SO$_4$)(L10)(H$_2$O)$_2$]·2H$_2$O·2CH$_3$OH}$_n$ (4.32). $Cd(SO_4)\cdot H_2O$ (0.0023 g, 0.010 mmol) was dissolved in methanol (5 mL), heated for a few mins, before being added dropwise to a solution of **L10** (0.0114 g, 0.021 mmol) which was also dissolved in methanol (15 mL). The addition gave a colourless solution that was heated for 45 mins and left to evaporate at room temperature. After two months, the solution afforded $\{[Cd(SO_4)(\mathbf{L10})(H_2O)_2]\cdot 2H_2O\cdot 2CH_3OH\}_n$ as colourless block-shaped crystals (0.003 g, 32%). Mp 250-252ºC. Anal. found: C, 42.51; H, 4.12; N 13.94. $CdC_{31}H_{44}N_8O_{14}S$ requires C, 41.49; H, 4.95; N 12.49%. Selected IR bands (UATR, cm^{-1}): 3236 (s), 1647 (s), 1535 (m), 1432 (w), 1468 (m), 1305 (m), 1022, 670 (s, S-O stretch).

{[CdBr$_2$(L11)$_4$]·4H$_2$O}$_n$ (4.33). $CdBr_2$ (0.0026 g, 0.010 mmol) was dissolved in water (5 mL), heated for a few mins, before being added dropwise to a solution of **L11** (0.0120 g, 0.020 mmol) dissolved in methanol (15 mL). The resulting slightly cloudy solution was heated for 45 mins to re-dissolve the precipitate and left to evaporate at room temperature. After two months, the solution afforded $\{[CdBr_2(\mathbf{L11})_4]\cdot 4H_2O\}_n$ as colourless crystals (0.009 g, 24%). Mp 230-235ºC. Anal. found: C, 51.01; H, 4.56; N 14.00. $CdC_{128}H_{136}N_{32}O_{20}Br_2$ requires C, 51.32; H, 4.86; N 14.97%. Selected IR bands (UATR, cm^{-1}): 3281 (s), 1647 (s), 1529 (m), 1001 (w), 650 (s).

[Ag$_2$(L13)$_2$](NO$_3$)$_2$·2H$_2$O·2CH$_3$OH (5.10). $AgNO_3$ (0.046 g, 0.27 mmol) was dissolved in methanol (5 mL), heated for a few mins, before being added dropwise to a solution of **L13** (0.068 g, 0.135 mmol) which was dissolved in hot methanol-acetonitrile (15 mL). The resulting slightly brown colour solution was heated for 45 mins and left to evaporate at room temperature. After one month, the solution afforded $[Ag_2(\mathbf{L13})_2](NO_3)_2\cdot 2CH_3OH\cdot 2H_2O$ as rod-like crystals (0.020 g, 21%). Mp 180-181ºC. Anal. found: C, 46.96; H, 3.20; N 15.48. $Ag_2C_{60}H_{62}N_{16}O_{14}$ requires C, 48.65; H, 4.36; N 15.13%; ^{1}H NMR (600 MHz, DMSO-d$_6$) δ 6.48 (2H, d, CH), 7.35 (4H, dd, pyH5'), 7.72 (4H, m, pyH3'), 7.85 (4H, m, pyH4'), 8.22 (3H, m, pyH3, pyH4, pyH5), 8.48 (4H, m, pyH6'), 8.50 (4H, m, pyH6') and 10.01 (2H, m, NH). *m/z* (ES-MS, DMSO/methanol) 608.1 ($[^{107}Ag(\mathbf{L13})]^+$, 100%), 610.1 ($[^{109}Ag(\mathbf{L13})]^+$, 95%), 713.9 ($[^{107}Ag_2(\mathbf{L13}\text{-H})]^+$, 9%), 715.9 ($[^{107}Ag^{109}Ag(\mathbf{L13}\text{-H})]^+$, 18%), 717.9 ($[^{109}Ag_2(\mathbf{L13}\text{-H})]^+$, 8%), 1214.6 ($[^{107}Ag_2(\mathbf{L13})(\mathbf{L13}\text{-H})]^+$, 3%), 1216.8 ($[^{107}Ag^{109}Ag(\mathbf{L13})(\mathbf{L13}\text{-H})]^+$, 5%), 1218.8 ($[^{109}Ag_2(\mathbf{L13})(\mathbf{L13}\text{-H})]^+$, 3%). Selected

IR bands (UATR, cm^{-1}): 3256 (w), 1654 (m), 1598 (m), 1527(m), 1155 (m), 1282 (s, N-O stretch).

[Pd_2(L13)Cl_4] (5.11). Palladium chloride (0.079 g, 0.46 mmol) was dissolved in a 2 M hydrochloric acid. This solution was added dropwise to a solution of ligand **L13** (0.11 g, 0.23 mmol) in methanol. A yellow precipitate formed that was stirred overnight, collected by filtration, washed with distilled water, and dried to give **[Pd_2(L13)Cl_4]** (0.08 g, 40%). Mp 278-280 °C. Anal. found: C, 40.00; H, 2.75; N 11.14. $Pd_2C_{30}H_{24}N_5O_2Cl_4$ requires C, 40.68; H, 2.71; N 11.45. Selected FTIR bands (UATR, cm^{-1}): 3270 (w), 1663(s), 1522(m), 1437(w), 761(s) and 355 (s) cm^{-1}.

[{$CdCl_2$(CH_3OH)(L14)$CdCl_2$}$_2$] (5.13). A solution of $CdCl_2$ (0.037 g, 0.20 mmol) was dissolved in methanol (5 mL), heated for a few mins, before being added dropwise to a solution of **L14** (0.051 g, 0.10 mmol) in methanol-acetonitrile (15 mL). The colourless solution was heated for 45 mins and left to evaporate at room temperature. After three weeks, the solution afforded [($CdCl_2$)$_2$(**L14**)]·CH_3OH·H_2O as colourless crystals (0.015 g, 16%). Mp 230-235 ºC. Anal. found: C, 40.83; H, 3.08; N 9.09. $Cd_2C_{31}H_{27}N_6O_4Cl_4$ requires C, 40.72; H, 2.98; N 9.19%. Selected IR bands (UATR, cm^{-1}): 3345 (m), 3227 (m), 1671 (s), 1602 (s), 1514 (m), 1441 (m), 1339 (m) 1282 (s), 1018 (s) and 792 (m).

[($CdBr_2$)$_2$(L15)(CH_3OH)$_2$] (5.15). A solution of $CdBr_2$ (0.0195 g, 0.072 mmol)·was dissolved in water (5 mL), heated for a few mins, before being added dropwise to a solution of **L15** (0.0180 g, 0.036 mmol) in methanol-acetonitrile (15 mL). The colourless solution was heated for 45 mins and left to evaporate at room temperature. After a week, the solution afforded [($CdBr_2$)$_2$(**L15**)(CH_3OH)$_2$] as colourless crystals (0.012 g, 75%). Mp 270-275 ºC. Anal. found: C, 34.04; H, 2.90; N 7.42. $Cd_2C_{32}H_{32}N_6O_4Br_4$ requires C, 34.65; H, 2.91; N 7.58%. Selected IR bands (UATR, cm^{-1}): 3268(s), 1637 (s), 1600 (m), 1523 (m), 1478 (s), 1347 (m), 1000 (m) and 759 (m).

[Pd_2(L15)Cl_4] (5.16). Palladium chloride (0.080 g, 0.46 mmol) was dissolved in a 2 M hydrochloric acid. This solution was added dropwise to a solution of ligand **L15** (0.12 g, 0.23 mmol) in methanol. A yellow precipitate formed that was stirred overnight, collected by filtration, washed with ethanol, and dried to give [Pd_2(**L15**)Cl_4] (0.05 g, 25%). Mp 285-290 °C. Anal. found: C, 42.21; H, 2.86; N 9.50. $Pd_2C_{28}H_{26}N_8O_4Cl_4$ requires C, 42.13; H, 2.83; N 9.83%.

^{1}H (300 MHz; DMSO-d_6) = 6.30 (1H, m, CH), 7.54 (1H, m, pyH5'), 7.84 (1H, m, pyH4'), 8.13 (1H, m, pyH3'), 8.32 (2H, m, ph-H3,H5), 8.83 (2H, 2d, pyH6'), and 10.33 (1H, m, NH).Selected FTIR bands (UATR, cm^{-1}): 3251, 2922, 1669, 1520, 1445, 863, 762 and 350 cm^{-1}. *m/z* (ES-MS) 823.1 ([(Pd_2Cl_3)(**L15**)]$^{+}$, 33%).

APPENDICES

Appendix 1: ^{1}H NMR Spectra of L8, L9 and L10.

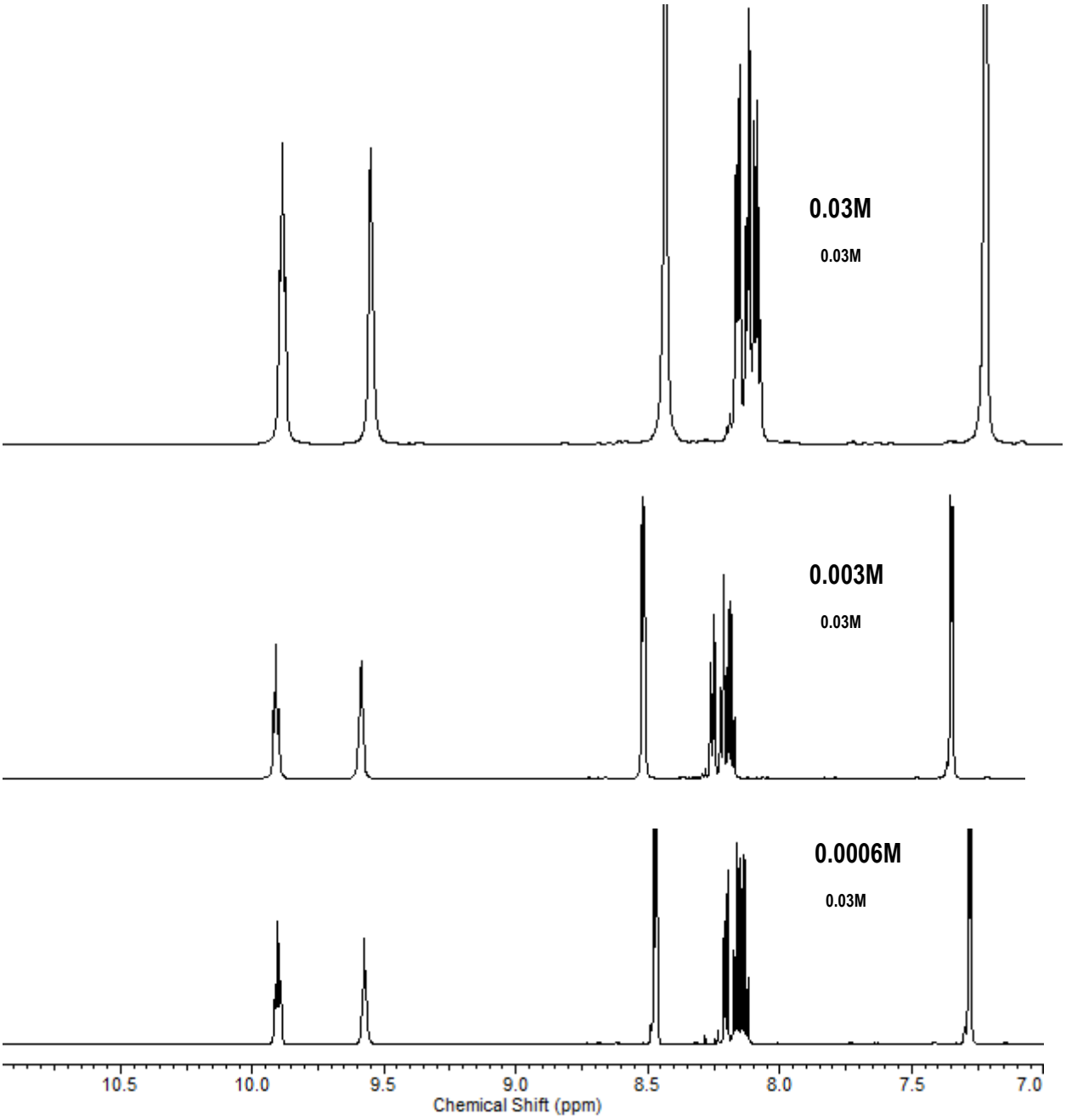

Figure A1.1. The aromatic regions of the ^{1}H NMR spectra of **L8** DMSO-d_6 recorded at different concentrations.

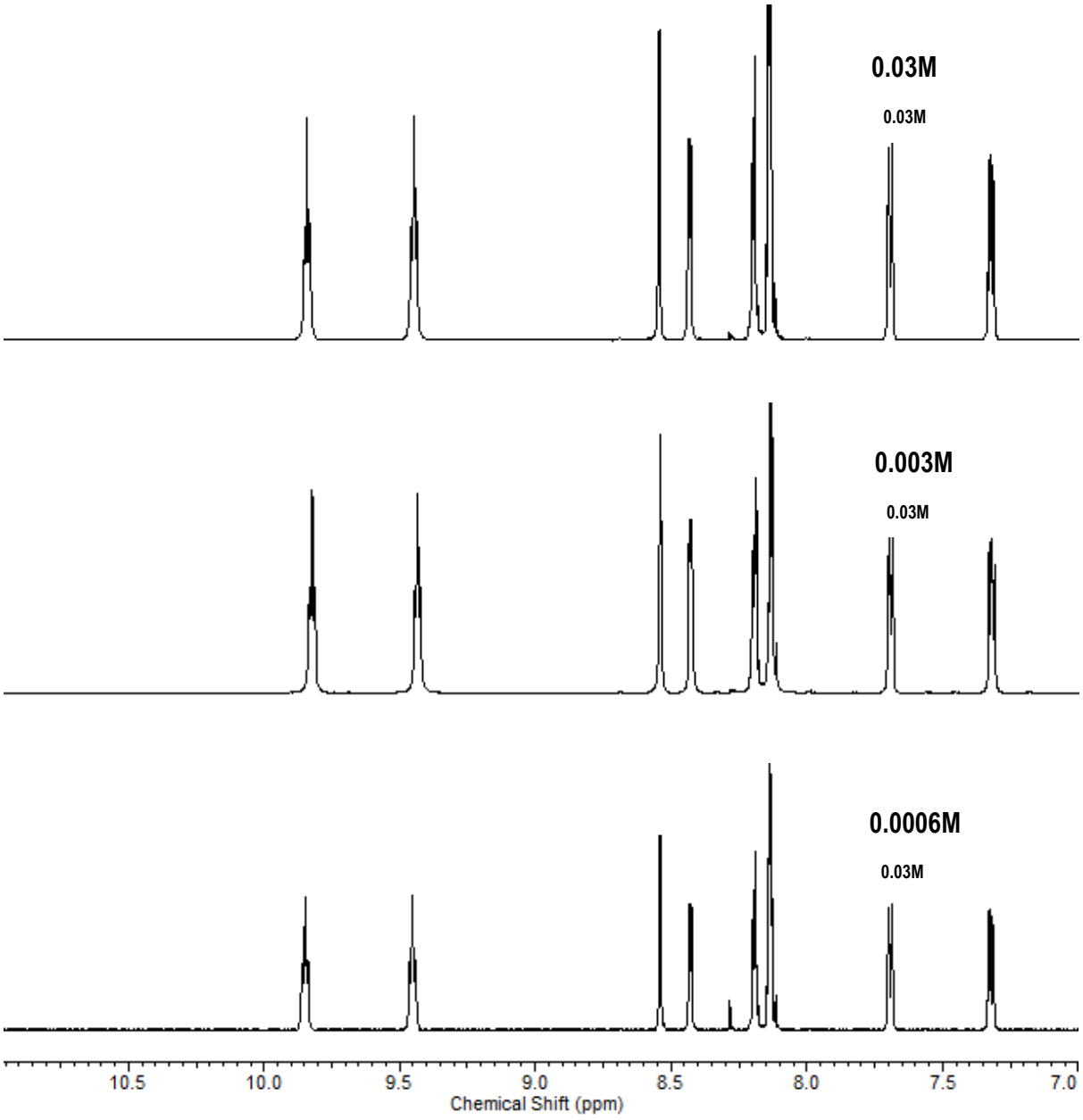

Figure A1.2. The aromatic regions of the ^{1}H NMR spectra of **L9** in DMSO-d_6 recorded at different concentrations.

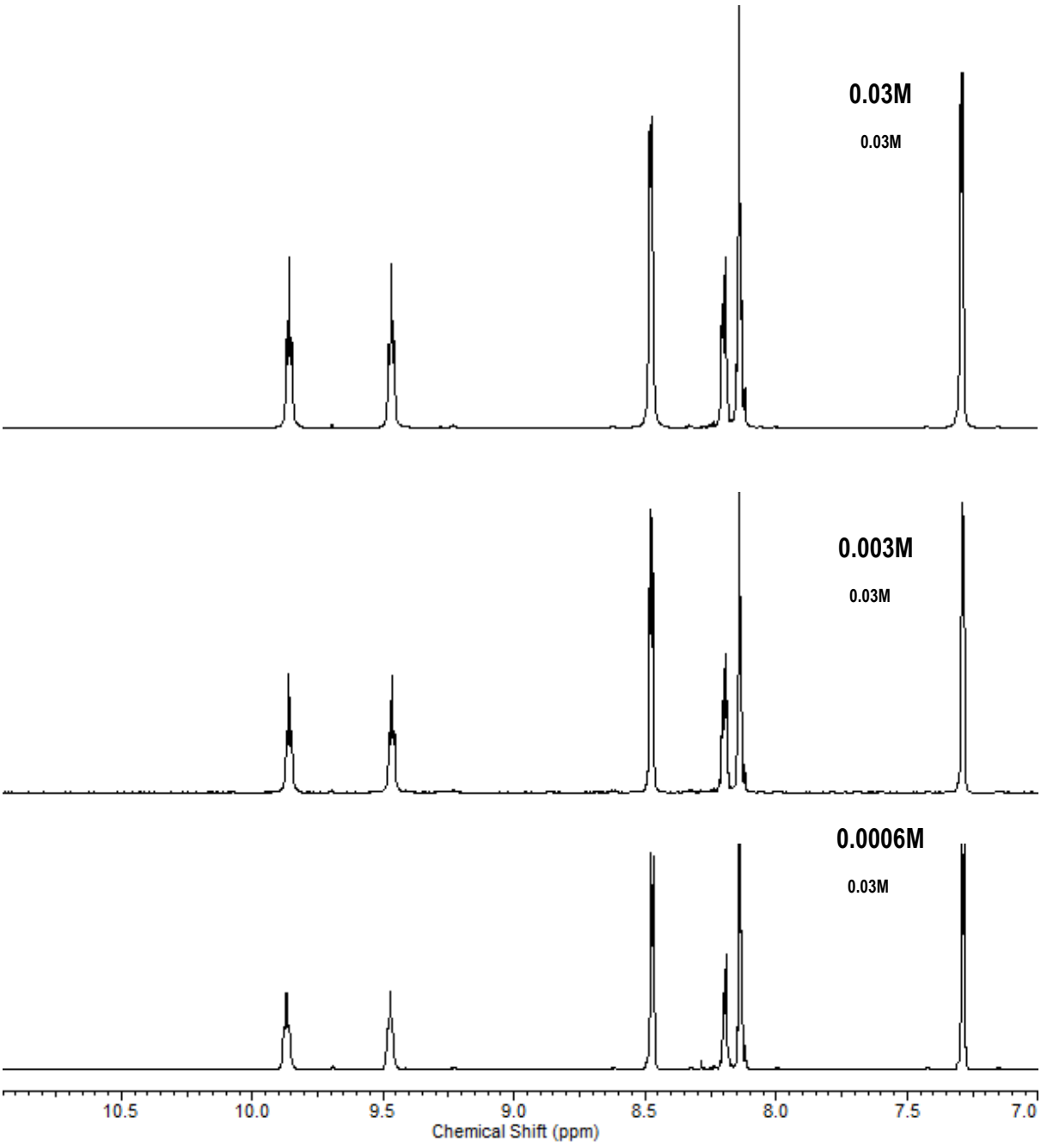

Figure A1.3. The aromatic regions of the ^{1}H NMR spectra of **L10** DMSO-d_6 recorded at different concentrations.

Appendix 2 : Crystallography

Tables A1-A8 list the crystal data and X-ray experimental details for the thirty four fully refined crystal structures described in this thesis. Selected bond lengths and angles for the structures reported in the thesis are outlined and listed under appropriate figures throughout the text, while other completed data, such as atom coordinates, anisotropic displacement parameters and hydrogen atom coordinates are not included in the printed version of the thesis.

Data on structures **L8**, **L13**, **3.11**, **3.15**, **3.17**, **3.18**, **3.21**, **3.22**, **4.21**, **4.22**, **4.23** and **4.28** were collected on the MX1 and MX2 beamlines at the Australian Synchrotron, Victoria, Australia. Crystals were mounted on a nylon loop and data collected using phi scans at 150 K (see: Blu-Ice: McPhillips, T. M., McPhillips, S. E., Chiu, H. J., Cohen, A. E., Deacon, A. M., Ellis, P. J., Garman, E., Gonzalez, A., Sauter, N. K., Phizackerley, R. P., Soltis, S. M., Kuhn, P. Blu-Ice and the Distributed Control System: software for data acquisition and instrument control at macromolecular crystallography beamlines. (2002) J. Synchrotron Rad. 9, 401-406).

Specific details of the structure refinements

Structure 3.14: The structure possesses crystallographically imposed twofold symmetry with two molecules of the discrete metallo-macrocyclic complex in the asymmetric unit. The hydrogen atoms of the non-coordinated water solvate molecule could not be located in the difference map. An anti-bumping restraint was used to maintain an appropriate C–O bond length for the non-coordinated methanol molecule in the structure.

Structure 3.15: Six restraints are used in the refinement of compound 10 to maintain chemically sensible bond lengths for the hydrogen atoms of the coordinated water molecules.

Structure 3.16: There is additional electron density (2.66 eA−3) adjacent to a coordinated water molecule (027a). This could not be adequately modelled as another solvent moiety.

***Structure 3.19*.** Three DFIX restraintswere used in the refinement to maintain chemically sensible bond lengths for the hydroxyl hydrogen atom of the coordinated methanol molecule, one of the hydrogen atoms of the coordinated water ligand, and for the C–O bond of a non-coordinated methanol solvate.

***Structure 3.20*.** There is disorder of the pendant pyridyl ring in the ligand moiety and this is modelled over two major positions. The refinement still indicates that there is some further minor disorder. Six restraints were used to maintain chemically sensible bond lengths for the coordinated water molecule and the second component of the disordered pendant pyridine ring. The structure has large solvent accessible voids. These contained a number of diffuse electron density peaks that could not be adequately identified and refined as solvent. The SQUEEZE routine of PLATON**22** was applied to the collected data, which resulted in significant reductions in *R*1 and w*R*2 and an improvement in the GOF. *R*1, w*R*2 and GOF before SQUEEZE routine: 15.5%, 48.8% and 1.24; after SQUEEZE routine: 11.0%, 28.9% and 1.18. The contents of the solvent region calculated from the result of SQUEEZE routine (2 3 4H2O per asymmetric unit) are represented in the unit cell contents in crystal data.

***Structure 3.21*.** The methyl carbon (C43) of a coordinated methanol molecule has comparatively large thermal ellipsoids indicating minor disorder and consequently alerts for the coordinated oxygen atom (O42). Ten restraints were used in the refinement of the structure for C43 (ISOR) and to maintain chemically sensible bond lengths for a disordered nitrate anion. The structure also contains disordered solvent molecules in the large channels that run along the *a*-axis. The SQUEEZE routine of PLATON**22** was applied to the collected data, which resulted in significant reductions in *R*1 and w*R*2 and an improvement in the GOF. *R*1, w*R*2 and GOF before SQUEEZE routine: 6.8%, 20.8% and 1.06; after SQUEEZE routine: 6.0%, 16.8% and 1.05. The contents of the solvent region calculated from the result of SQUEEZE routine ($2H_2O$ per asymmetric unit) are represented in the unit cell contents in crystal data.

TABLE A1. Crystal data and experimental data for **$(L2)_3 \cdot 9H_2O$**, **L7**, **$L8 \cdot 4H_2O \cdot 2CH_3OH$** and **L11**.

Compound	**$(L2)_3 \cdot 9H_2O$**	**L7**	**$L8 \cdot 4H_2O \cdot 2CH_3OH$**	**L11**
Empirical formula	$C_{42}H_{57}N_9O_{18}$	$C_{28}H_{26}N_8O_4$	$C_{30}H_{42}N_8O_{10}$	$C_{32}H_{32}N_8O_4$
Formula weight	975.97	538.57	674.72	592.66
Crystal system	Triclinic	Monoclinic	Triclinic	Triclinic
Space group	*P*-1	*C*2/c	*P*-1	*P*-1
a (Å)	9.0408(13)	13.669(6)	7.5200(15)	9.0155(10)
b (Å)	13.781(2)	17.763(7)	8.8860(18)	12.1413(9)
c (Å)	19.538(3)	11.013(4)	12.696(3)	13.7390(16)
α (º)	90.043(11)	90	86.06(3)	81.057(8)
β (º)	94.355(11)	108.857(16)	82.85(3)	81.067(9)
γ (º)	94.307(12)	90	73.69(3)	78.114(8)
Volume ($Å^3$)	2420.4(6)	2530.5(17)	807.4(3)	1441.9(3)
Z	2	4	1	2
Density (calculated) (Mg/m^3)	1.339	1.414	1.388	1.365
Absorption coefficient (mm^{-1})	0.106	0.099	0.106	0.094
F(000)	1032	1128	358	624
Crystal size (mm^3)	0.26x0.14x0.02	0.35x0.06x0.02	0.15x0.05x0.04	0.30x0.13x0.09
Theta range for data (º)	2.96 – 27.00	1.95 – 25.95	2.84 – 24.17	2.91 – 29.86
Reflections collected	19905	15729	8609	27261
Observed reflections [I>2s(I)]	10346	2386	2304	7549
Data/restraints/parameters	10346/0/625	2386/0/81	2304/0/231	7549/0/397
Goodness-of-fit on F^2	0.675	1.082	1.067	0.819
R_1 [I>2s(I)]	0.0445	0.0579	0.0655	0.0604
wR_2 (all data)	0.0914	0.1697	0.1810	0.2629
Largest diff. peak and hole ($e.Å^{-3}$)	0.196 and -0.219	0.528 and -0.400	0.417 and 0.326	0.194 and -0.213

TABLE A2. Crystal data and experimental data for **L12**, **L13**, **L15** and **3.11**

Compound	**L12**	**L13**	**L15**	**3.11**
Empirical formula	$C_{32}H_{32}N_8O_4$	$C_{29}H_{23}N_7O_2$	$C_{30}H_{24}N_6O_2$	$C_{28}H_{30}Cl_2N_6O_8Zn$
Formula weight	592.66	501.54	500.55	714.85
Crystal system	Triclinic	Monoclinic	Triclinic	Monoclinic
Space group	*P*-1	$P2_1/c$	*P*-1	*P2/c*
a (Å)	13.0319(15)	11.012(2)	8.4621(4)	13.348(3)
b (Å)	15.1859(13)	14.741(3)	8.8809(5)	6.1610(12)
c (Å)	16.7954(16)	15.305(3)	9.7782(5)	22.924(7)
α (º)	111.971(8)	90	68.479(5)	90
β (º)	103.352(9)	105.71(3)	72.112(5)	124.00(2)
γ (º)	101.168(8)	90	69.326(5)	90
Volume ($Å^3$)	2965.8(5)	2391.6(8)	626.13(6)	1562.9(7)
Z	4	4	1	2
Density (calculated) (Mg/m^3)	1.327	1.393	1.328	1.519
Absorption coefficient (mm^{-1})	0.091	0.092	0.087	1.015
F(000)	1248	1048	262	736
Crystal size (mm^3)	0.35x0.08x0.04	0.24x0.15x0.06	0.41x0.26x0.09	0.25x0.16x0.08
Theta range for data (º)	2.47 – 28.24	1.92 – 25.00	2.29 – 29.63	1.84 – 25.05
Reflections collected	34643	24545	12303	13978
Observed reflections [I>2s(I)]	12267	3914	6245	2657
Data/restraints/parameters	12267/0/793	3996/0/328	6245/3/343	2657/0/210
Goodness-of-fit on F^2	1.044	0.962	0.902	1.119
R_1 [I>2s(I)]	0.0336	0.0442	0.0341	0.0827
wR_2 (all data)	0.2629	0.1214	0.0780	0.2382
Largest diff. peak and hole ($e.Å^{-3}$)	1.369 and -0.775	0.392 and -0.349	0.233 and -0.198	1.032 and -1.593

TABLE A3. Crystal data and experimental data for **3.12**, **3.13**, **3.14**, **3.15** and **3.16**.

Compound	**3.12**	**3.13**	**3.14**	**3.15**	**3.16**
Empirical formula	$C_{26}H_{20}Cu_2N_8O_{12}$	$C_{26.5}H_{31}Cl_2Cu_2N_6O_{11}$	$C_{28.5}H_{32}Cl_2Cu_2N_6O_{17.5}$	$C_{37}H_{34}Cu_3N_{12}O_{22}$	$C_{48}H_{38}Cl_4Cu_4N_{12}O_{32}$
Formula weight	763.58	807.55	936.58	1189.38	1690.86
Crystal system	Orthorhombic	Monoclinic	Monoclinic	Monoclinic	Monoclinic
Space group	*Pbcn*	$P2_1$	*C*2	$P2_1/c$	$P2_1/c$
a (Å)	16.775(2)	8.1844(5)	29.080(15)	16.799(3)	14.659(3)
b (Å)	11.972(2)	15.7522(9)	7.3944(3)	19.571(4)	13.711(2)
c (Å)	14.055(2)	12.9435(8)	17.888(3)	13.054(3)	15.440(3)
α (º)	90	90	90	90	90
β (º)	90	100.672(3)	108.212(7)	99.06(3)	112.636(7)
γ (º)	90	90	90	90	90
Volume ($Å^3$)	2822.8(6)	1639.8 (2)	3653(3)	4238.2(15)	2864.2(9)
Z	4	2	4	4	2
Density (calculated) (Mg/m^3)	1.797	1.635	1.711	1.864	1.961
Absorption coefficient (mm^{-1})	1.59	1.526	1.403	1.598	1.765
F(000)	1544	824	1908	2412	1700
Crystal size (mm^3)	0.35x0.25x0.09	0.36x0.28x0.16	0.40x0.12x0.05	0.17x0.05x0.04	0.43x0.19x0.13
Theta range for data (º)	2.90 – 29.28	2.84 – 27.00	1.20 – 25.00	1.23 – 26.00	2.79 – 29.65
Reflections collected	58721	41273	19477	52118	57356
Observed reflections [I>2s(I)]	3782	10387	5524	8308	6259
Data/restraints/parameters	3085/0/217	6845/3/439	5528/2/509	8308/6/692	6259/0/451
Goodness-of-fit on F^2	1.052	1.059	1.028	1.04	1.046
R_1 [I>2s(I)]	0.0369	0.0256	0.0611	0.0493	0.0497
wR_2 (all data)	0.1062	0.0605	0.1652	0.1326	0.1379
Largest diff. peak and hole ($e.Å^{-3}$)	0.550 and -0.498	0.352 and -0.341	1.551 and -1.216	1.210 and -1.143	2.663 and -0.812
Absolute structure parameter		-0.012(6)	0.27(2)		

TABLE A4. Crystal data and experimental data for **3.17**, **3.18**, **3.19**, **3.20** and **3.21**.

Compound	**3.17**	**3.18**	**3.19**	**3.20**	**3.21**
Empirical formula	$C_{13}H_{16}CdN_4O_9$	$C_{68.50}H_{68}Cl_3Cu_3N_{15}O_{33.50}$	$C_{16}H_{24}CdN_4O_{10}$	$C_{13}H_{17.5}CdN_3O_{8.75}S_{0.50}$	$C_{54}H_{48}Cd_3N_{15}O_{22.50}$
Formula weight	484.7	1934.35	544.79	484.23	1604.27
Crystal system	Triclinic	Monoclinic	Triclinic	Monoclinic	Monoclinic
Space group	*P*-1	*C2/c*	*P*-1	*C2/c*	$P2_1/n$
a (Å)	6.1440(12)	49.155(10)	8.109(6)	11.5605(11)	10.403(2)
b (Å)	10.443(2)	10.849(2)	11.029(9)	19.9973(12)	33.827(7)
c (Å)	15.363(3)	33.877(7)	13.128(10)	19.0547(13)	19.688(4)
α (º)	108.94(3)	90	104.427(12)	90	90
β (º)	91.62(3)	112.48(3)	104.395(3)	103.352(9)	92.82(3)
γ (º)	103.19(3)	90	104.536(11)	90	90
Volume ($Å^3$)	902.1(3)	16693(6)	1038.3(14)	4286.0(6)	6920(2)
Z	2	8	2	8	4
Density (calculated) (Mg/m^3)	1.784	1.539	1.743	1.347	1.54
Absorption coefficient (mm^{-1})	1.266	0.948	1.114	1.093	0.995
F(000)	484	7920	552	1720	3204
Crystal size (mm^3)	0.37x0.12x0.03	0.40x0.25x0.06	0.40x0.20x0.20	0.32x0.28x0.16	0.12x0.04x0.02
Theta range for data (º)	2.82 – 29.30	0.90 – 24.20	3.04 – 27.49	2.54 to 29.86°	1.59 to 26.00
Reflections collected	16419	12557	16110	17934	93958
Observed reflections [I>2s(I)]	4401	10953	4645	5550	13532
Data/restraints/parameters	2705/0/240	12557/6/922	4645/3/294	5550/2/253	13532/10/872
Goodness-of-fit on F^2	0.999	2.146	1.044	1.183	1.054
R_1 [I>2s(I)]	0.0275	0.1438	0.0346	0.1095	0.0597
wR2 (all data)	0.0677	0.4275	0.0912	0.2890	0.1679
Largest diff. peak and hole ($e.Å^{-3}$)	0.981 and -1.030	2.020 and -2.042	2.229 and -1.119	2.449 and -1.173	1.826 and -1.330

TABLE A5. Crystal data and experimental data for **3.22**, **4.14**, **4.15** and **4.17**.

Compound	**3.22**	**4.14**	**4.15**	**4.17**
Empirical formula	$C_{13}H_9CuN_3O_3$	$C_{19}H_{17}BrCd_{0.50}N_5O_2$	$C_{57}H_{61}ClN_{15}O_{15}Zn_{0.50}$	$C_{22}H_{26}F_{12}N_7O_6P_2Pd$
Formula weight	318.77	483.49	1264.34	880.84
Crystal system	Orthorhombic	Triclinic	Triclinic	Monoclinic
Space group	*Pbca*	*P*-1	*P*-1	$P2_1/n$
a (Å)	15.507(3)	7.7108(3)	8.9545(2)	13.7360(10)
b (Å)	7.0840(14)	10.2810(6)	12.8509(2)	10.8580(9)
c (Å)	20.918(4)	12.0894(5)	25.8713(5)	21.6696(19)
α (º)	90	72.779(4)	87.219(2)	90
β (º)	90	87.177(3)	88.478(2)	91.173(3)
γ (º)	90	87.287(4)	85.686(2)	90
Volume ($Å^3$)	2297.9(8)	913.77(7)	2964.38(10)	3231.2(5)
Z	8	2	2	4
Density (calculated) (Mg/m^3)	1.843	1.757	1.416	1.811
Absorption coefficient (mm^{-1})	1.912	2.841	0.343	0.792
F(000)	1288	482	1320	1756
Crystal size (mm^3)	0.11x0.09x0.06	0.36x0.32x0.08	0.47x0.43x0.19	0.35x0.20x0.05
Theta range for data (º)	3.27 – 24.99	2.65 – 26.36	2.19 – 29.85	2.97 – 25.71
Reflections collected	23066	11389	72970	20758
Observed reflections [I>2s(I)]	1979	3579	15687	5134
Data/restraints/parameters	2006/0/126	3579/0/252	15687/2/867	5134/1/431
Goodness-of-fit on F^2	1.105	1.092	1.071	1.064
R_1 [I>2s(I)]	0.0352	0.128	0.0404	0.0489
wR_2 (all data)	0.1003	0.1158	0.1142	0.1199
Largest diff. peak and hole ($e.Å^{-3}$)	3.466 and -2.858	4.605 and -5.872	0.653 and -0.604	1.646 and -1.092

TABLE A6. Crystal data and experimental data for **4.21**, **4.22**, **4.23**, **4.24** and **4.25**.

Compound	**4.21**	**4.22**	**4.23**	**4.24**	**4.25**
Empirical formula	$C_{38}H_{38}CdN_{12}O_{12}$	$C_{19}H_{19}Cd_{0.50}ClN_5O_7$	$C_{38}H_{38}CoN_{12}O_{12}$	$C_{24.50}H_{34}Cu_{1.50}N_5O_{8.50}$	$C_{38}H_{46}CdN_{12}O_{16}$
Formula weight	967.2	521.04	913.73	629.88	1004.20
Crystal system	Triclinic	Triclinic	Triclinic	Triclinic	Triclinic
Space group	*P*-1	*P*-1	*P*-1	*P*-1	*P*-1
a (Å)	8.9470(18)	9.0650(18)	8.8360(18)	10.100(6)	12.229(2)
b (Å)	10.135(2)	10.668(2)	10.054(2)	11.810(5)	26.630(5)
c (Å)	11.063(2)	11.303(2)	11.053(2)	13.770(7)	15.307(3)
α (º)	78.48(3)	73.28(3)	78.13(3)	68.910(16)	90
β (º)	87.06(3)	85.69(3)	86.95(3)	87.73(2)	109.185(11)
γ (º)	87.84(3)	81.53(3)	86.25(3)	80.34(2)	90
Volume ($Å^3$)	981.3(3)	1034.8(3)	958.1(3)	1510.4(13)	4708.0(15)
Z	1	2	1	2	4
Density (calculated) (Mg/m^3)	1.637	1.672	1.584	1.385	1.414
Absorption coefficient (mm^{-1})	0.639	0.739	0.532	1.119	0.538
F(000)	494	530	473	655	2052
Crystal size (mm^3)	0.15x0.10x0.06	0.28x0.14x0.08	0.15x0.10x0.04	0.45x0.30x0.10	0.15x0.15x0.16
Theta range for data (º)	1.88 – 24.20	1.88 – 27.09	1.88 – 24.19	2.99 – 27.32	1.60 - 20.78
Reflections collected	11022	14972	10916	6636	4839
Observed reflections [I>2s(I)]	2852	4043	2788	5372	4137
Data/restraints/parameters	2852/0/292	4043/0/330	2788/2/292	9749/5/721	4839/7/581
Goodness-of-fit on F^2	1.067	1.083	1.085	1.06	1.137
R_1 [I>2s(I)]	0.0414	0.0783	0.0433	0.0726	0.1158
wR_2 (all data)	0.1059	0.2107	0.1250	0.2045	0.2515
Largest diff. peak and hole ($e.Å^{-3}$)	0.512 and -1.416	3.211 and -2.828	0.321 and -0.991	1.615 and -0.723	1.258 and -1.594

TABLE A7. Crystal data and experimental data for **4.26**, **4.27**, **4.28** and **4.31**.

Compound	**4.26**	**4.27**	**4.28**	**4.31**
Empirical formula	$C_{38}H_{42}ZnN_{12}O_{14}$	$C_{20.50}H_{227}Br_2CdN_5O_{4.50}$	$C_{19.50}H_{21}Cd_{0.50}ClN_5O_{7.50}$	$C_{56.50}H_{54}Cd_{1.5}N_{10}O_{27.50}$
Formula weight	948.14	685.68	537.06	1607.79
Crystal system	Triclinic	Monoclinic	Monoclinic	Triclinic
Space group	*P-1*	C2/c	C2/c	*P*-1
a (Å)	12.3568(3)	33.097(6)	26.652(5)	9.2577(10)
b (Å)	25.4241(6)	7.8360(7)	7.6050(15)	19.914(2)
c (Å)	15.5652(5)	23.771(5)	22.795(5)	20.577(2)
α (º)	90	90	90	81.080(9)
β (º)	108.468(3)	123.54(3)	109.29(3)	87.128(9)
γ (º)	90	90	90	77.041(9)
Volume ($Å^3$)	4638.1(2)	5139(1)	4360.9(15)	3651.7(6)
Z	4	8	8	2
Density (calculated) (Mg/m^3)	1.358	1.773	1.636	1.462
Absorption coefficient (mm^{-1})	0.604	3.997	0.706	0.532
F(000)	1952	2696	2192	1636
Crystal size (mm^3)	0.16x0.15x0.15	0.26x0.15x0.10	0.25x0.19x0.14	0.18x0.16x0.10
Theta range for data (º)	2.36 - 29.95	2.50 – 29.87	1.62 – 27.09	2.46 – 29.94
Reflections collected	11993	23968	30425	18323
Observed reflections [I>2s(I)]	6513	6714	4703	5581
Data/restraints/parameters	11993/0/581	6714/2/306	4703/4/287	18323/5/941
Goodness-of-fit on F^2	1.474	1.080	1.052	0.843
R_1 [I>2s(I)]	0.1632	0.0690	0.0711	0.0948
wR_2 (all data)	0.2056	0.1806	0.1834	0.2302
Largest diff. peak and hole ($e.Å^{-3}$)	7.211 and -1.861	1.781 and -1.012	1.536 and -1.081	3.273 and -1.611

TABLE A8. Crystal data and experimental data for **4.32**, **4.33**, **5.10**, **5.13** and **5.15**.

Compound	**4.32**	**4.33**	**5.10**	**5.13**	**5.15**
Empirical formula	$C_{30}H_{42}CdN_8O_{15}S$	$C_{33}H_{36}BrCd_{0.50}N_8O_5$	$C_{60}H_{58}Ag_2N_{16}O_{14}$	$C_{31}H_{28}Cd_2Cl_4N_6O_3$	$C_{32}H_{32}Br_4Cd_2N_6O_4$
Formula weight	899.18	760.81	1442.96	899.19	1109.08
Crystal system	Triclinic	Triclinic	Orthorhombic	Triclinic	Monoclinic
Space group	*P*-1	*P*-1	*Pbca*	*P*-1	$P2_1/c$
a (Å)	9.9059(4)	9.4207(5)	10.0396(3)	10.0062(6)	9.4783(2)
b (Å)	12.3979(5)	11.4609(7)	23.0612(8)	13.7799(9)	13.8293(3)
c (Å)	16.1984(6)	16.1643(9)	25.4876(7)	13.9357(8)	14.3145(3)
α (º)	85.918(3)	103.151(5)	90	64.558(6)	90
β (º)	88.741(3)	103.088(5)	90	81.854(5)	107.028(3)
γ (º)	73.194(4)	97.360(5)	90	82.060(5)	90
Volume ($Å^3$)	1899.56(13)	1625.38(16)	5901.0(3)	1711.23(18)	1794.06(7)
Z	2	2	4	2	2
Density (calculated) (Mg/m^3)	1.572	1.555	1.624	1.745	2.053
Absorption coefficient (mm^{-1})	0.708	1.638	0.747	1.597	1.685
F(000)	924	778	2944	888	1068
Crystal size (mm^3)	0.10x0.16x0.08	0.20x0.08x0.04	0.15x0.10x0.07	0.12x0.14x0.06	0.43x0.04x0.03
Theta range for data (º)	2.49 – 30.19	2.57 – 29.94	2.35 – 29.66	2.48 – 29.81	2.69– 29.92
Reflections collected	10023	8454	29891	8293	4736
Observed reflections [I>2s(I)]	7470	5156	7666	5989	3676
Data/restraints/parameters	10023/1/511	8454/0/432	7666/2/425	8293/0/416	4736/0/218
Goodness-of-fit on F^2	1.06	1.33	0.877	1.074	0.932
R_1 [I>2s(I)]	0.0964	0.0485	0.0394	0.0630	0.0226
wR_2 (all data)	0.2404	0.1369	0.0722	0.1851	0.0479
Largest diff. peak and hole ($e.Å^{-3}$)	4.593 and -3.468	1.049 and -0.727	1.181 and -0.683	3.664 and -2.101	0.569 and -0.594

Appendix 3: Crystallographic Information Files (CIFs)

The Crystallographic Information Files (CIFs) for each structures discussed in this thesis are enclosed in the CD. The CIFs file for each compounds are named as follow:

Compounds	CIFs File
L7	Makx1
3.12	Makx3
3.14	Makx4
L8	Makx7
3.18	Makx8
4.21	Makx9
4.23	Makx10
4.24	Makx12
3.19	Makx13
L2	Makx16
3.13	Makx18
4.25	Makx19
3.16	Makx23
3.15	Makx25
3.21	Makx29
4.22	Makx31
4.28	Makx32
4.17	Makx33

3.11	Makx41
L13	Makx42
3.22	Makx45
3.17	Makx46
4.26	Makx47
4.15	Makx48
5.10	Makxcs
L15	Makx51
5.15	Makx55
4.31	Makx57
5.13	Makx59
3.20	Makx60
4.27	Makx61
4.14	Makx62
4.33	Makx63
L11	Makx65
L12	Makx67
4.32	Makx68

Appendix 4: Publications

The following is a list of publications that have resulted from the research work described in this thesis.

1. Maisara Abdul-Kadir, Lyall R. Hanton, Christopher J. Sumby, Self-assembled metallo-macrocycle based coordination polymers with unsymmetrical amide ligands, *Dalton Trans.* **2011**, *40*, 12374 – 12380.

2. Maisara Abdul-Kadir, Lyall R. Hanton, Christopher J. Sumby, Building blocks for coordination polymers: Self-assembled cleft-like and planar-discrete metallo-macrocyclic complexes, *Dalton Trans.* **2012**, *41*, 4497 – 4505.

3. Maisara Abdul-Kadir, Philip R. Clements, Lyall R. Hanton, Courtney A. Hollis, Christopher J. Sumby, Pre-organisation or a hydrogen bonding mismatch: silver(I) diamide ligand coordination polymers versus discrete metallo-macrocyclic assemblies, *Supramol. Chem.* **2012**, *24*, 1 – 15.

REFERENCES

References

(1) J. M. Lehn, *Angew. Chem., Int. Ed.* **1988**, *27*, 89.

(2) J. M. Lehn, *Science* **2002**, *295*, 2400.

(3) S. T. Nguyen; D. L. Gin; J. T. Hupp; X. Zhang, *Proc. Nat. Acad. Sci.* **2001**, *98*, 11849.

(4) F. Hibbert; J. Emsley, *Adv. Phys. Org. Chem.* **1990**, *26*, 255.

(5) C. Janiak, *J. Chem. Soc., Dalton Trans.* **2000**, 3885.

(6) C. A. Hunter; J. K. M. Sanders, *J. Am. Chem. Soc.* **1990**, *112*, 5525.

(7) J. M. Lehn, *Chem. Soc. Rev.* **2007**, *36*, 36151.

(8) A. J. Wilson, *Annu. Rep. Prog. Chem., Sect. B., Org. Chem.* **2008**, *104*, 164.

(9) G. V. Oshovsky; D. N. Reinhoudt; W. Verboom, *Angew. Chem., Int. Ed.* **2007**, *46*, 2366.

(10) A. Dorazco-Gonzalez; H. Hopfl; F. Medrano; A. K. Yatsimirsky, *J. Org. Chem.* **2010**, *75*, 2259.

(11) K. Bowman-James, *Acc. Chem. Res.* **2005**, *38*, 671.

(12) P. A. Gale, *Coord. Chem. Rev.* **2006**, *250*, 2917.

(13) P. D. Beer; P. A. Gale, *Angew.Chem., Int. Ed.* **2001**, *40*, 486.

(14) S. O. Kang; R. A. Begum; K. Bowman-James, *Angew. Chem., Int. Ed.* **2006**, *45*, 7882.

(15) J. F. Stoddart, *Nat. Chem.* **2009**, *1*, 14.

(16) S. Kubik; C. Reyheller; S. Stuewe, *J. Inclusion Phenom. Macrocyclic Chem.* **2005**, *52*, 137.

(17) C. R. Bondy; P. A. Gale; S. J. Loeb, *J. Am. Chem. Soc.* **2004**, *126*, 5030.

(18) P. A. Gale, *Chem.Commun.* **2011**, 82.

(19) R. Custelcean; B. A. Moyer; B. P. Hay, *Chem. Commun.* **2005**, 5971.

(20) R. Custelcean; D. Jiang; B. P. Hay; W. Luo; B. Gu, *Cryst. Growth Des.* **2008**, *8*, 1909.

(21) C. R. Bondy; S. J. Loeb, *Coord. Chem. Rev.* **2003**, *240*, 77.

(22) S. J. Coles; P. A. Gale; M. B. Hursthouse; M. E. Light; C. N. Warriner, *Supramol. Chem.* **2004**, *16*, 469

(23) C. H. Park; H. E. Simmons, *J. Am .Chem. Soc.* **1968**, *90*, 2431.

(24) E. Graf; J. M. Lehn, *J. Am .Chem. Soc.* **1976**, *98*, 6403.

(25) J. L. Sessler; M. J. Cry; V. Lynch; E. McGhee; J. A. Ibers, *J. Am .Chem. Soc.* **1990**, *112*, 2810.

(26) W. E. Allen; P. A. Gale; C.T. Brown; V. M. Lynch; J. L. Sessler, *J. Am. Chem. Soc.*, **1996**, *118*, 12471.

(27) P. A. Gale; J. L.Sessler; l. V. Kral, *Chem. Commun.* **1998**, 1.

(28) P. A. Gale; J. L. Sessler; I. V. Kral; V. Lynch, *J. Am. Chem. Soc.* **1996**, *118*, 5140.

(29) C. J. Woods; S. Camiolo; M. E. Light; S. J. Coles; M. B. Hursthouse; M. A. King; P. A. Gale; J. W. Essex, *J. Am. Chem. Soc.* **2002**, *124*, 8864.

(30) P. A. Gale; P. A. Anzenbacher; J. L. Sessler, *Coord. Chem. Rev.* **2001**, *222*, 57.

(31) C. A. Ilioudis; J. W. Steed, *Supramol. Chem.* **2001**, *1*, 165.

(32) G. Gokel, Crown Ethers and Crystands, The Royal Society of Chemistry, Cambridge, England, **1991**.

(33) J. L. Sessler; G. D. Pantos; P. A. Gale; M. E. Light, *Org. Lett.* **2006**, *8*, 1593.

(34) M. Chmielewski; J. Jurczak, *Tetrahedron Lett.* **2004**, *45*, 6007.

(35) S. O. Kang; J. M. Llinares; D. Powell; D. Vandervelde; K. Bowman-James, *J. Am .Chem. Soc.* **2003**, *125*, 10152.

(36) J. A. Wisner; P. D. Beer; M. G. B. Drew, *Angew. Chem. Int. Ed. Engl.* **2001**, *40*, 3606.

(37) L. M. Hancock; P. D. Beer, *Chem. Eur. J.* **2009**, *15*, 42.

(38) E. C. Constable, *Chem. & Ind.* **1994**, *56*, 59.

(39) A. Rajbanshi; B. A. Moyer; R. Custelcean, *Cryst. Growth Des.* **2011**, *11*, 2702.

(40) B. J. Holliday; C. A. Mirkin, *Angew. Chem., Int. Ed.* **2001**, *40*, 2022.

(41) D. W. Johnson; K. N. Raymond, *Supramol. Chem.* **2001**, *13*, 639.

(42) P. J. Steel, *Acc. Chem. Res.* **2005**, *38*, 243.

(43) P. J. Steel; C. M. Fitchett, *Coord. Chem. Rev.* **2008**, *252*, 990.

(44) S. R. Siedel; P. J. Stang, *Acc. Chem. Res.* **2002**, *35*, 972.

(45) S. Leininger; B. Olengyuk; P. J. Stang, *Chem. Rev.* **2000**, *100*, 853.

(46) G. F. Swiegers; T. J. Malefetse *Chem. Rev.* **2000**, *100*, 3483.

(47) B. Moulton; M. J. Zawarotko, *Chem. Rev.* **2001**, *101*, 1629.

(48) M. Fujita; K. Umemoto; M. Yoshizawa; N. Fujita; T. Kusukawa; K. Biradha, *Chem. Commun.* **2001**, 509.

(49) G. F. Swiegers; T. J. Malefetse, *Coord. Chem. Rev.* **2002**, *225*, 91.

(50) M. Fujita; J. Yazaki; K. Ogura, *J. Am. Chem. Soc.* **1990**, *112*, 5645.

(51) C. M. Fitchett; P. J. Steel, *New J. Chem.* **2000**, *24*, 945.

(52) G. Hennrich; E. V. Anslyn, *Chem. Eur. J.* **2002**, *8*, 2218.

(53) T. M. Garret; U. Koert; J. M. Lehn; A. Rigault; D. Meyer; J. Fischer, *J. Chem. Soc., Chem. Commun.* **1990**, 557.

(54) P. N. W. Baxter; J. M. Lehn; J. Fischer; M. T. Youinou, *Angew. Chem., Int. Ed. Engl.* **1994**, *33*, 2284.

(55) T. K. Maji; M. Ohba; S. Kitagawa, *Inorg. Chem.* **2005**, *44*, 9225.

(56) P. J. Stang; B. Olenyuk, *Acc. Chem. Res.* **1997**, *30*, 502.

(57) P. J. Stang; D. H. Cao, *J. Am. Chem. Soc.* **1994**, *116*, 4981.

(58) C. M. Drain; J. M. Lehn, *J. Chem. Soc., Chem. Commun.* **1994**, 2313.

(59) R. M. Nelson; J. T. Hupp; D. I. Yoon, *J. Am .Chem. Soc.* **1995**, *117*, 9085.

(60) S. B. Lee; S. G. Hwang; D. S. Chung; H. S. Yun; J. I. Hong, *Tetrahedron Lett.* **1998**, *39*, 873.

(61) S. Ghosh; D. R. Turner; S. R. Batten; P. S. Mukherjee, *Dalton Trans.* **2007**, 1869.

(62) R. D. Schenebeck; L. Randaccio; E. Zangrando; B. Lippert, *Angew. Chem., Int. Ed.* **1998**, *37*, 119.

(63) X. Chi; A. J. Guerin; R. A. Haycock; C. A. Hunter; L. D. Sarson, *J. Chem. Soc., Chem. Commun.* **1995**, 2563.

(64) S. Roche; C. Haslam; H. Adams; S. L. Heath; J. A. Thomas, *Chem. Commun.* **1998**, 1681.

(65) S. C. Johannessen; R. G. Brisbois; J. P. Fischer; P. A. Grieco; A. E. Counterman; D. E. Clemmer, *J. Am. Chem. Soc.* **2001**, *123*, 3818.

(66) S. R. Seidel; P. J. Stang, *Acc. Chem. Res.* **2002**, *35*, 972.

(67) L. J. Barbour; G. W. Orr; J. L. Atwood, *Nature* **1998**, *393*, 671.

(68) N. L. S. Yue; D. J. Eisler; M. C. Jennings; R. J. Puddephatt, *Inorg. Chem.* **2004**, *43*, 7671.

(69) D. K. Chan; K. Biradha; M. Fujita, *Chem. Commun.* **2001**, 1652.

(70) C. Piguet; G. Bernardinelli; G. Hopfgartner, *Chem. Rev.* **1997**, *97*, 2005.

(71) L. P. Harding; J. C. Jeffery; T. R. Johanessen; C. R. Rice; Z. Zeng, *Dalton Trans.* **2004**, *654*, 2396.

(72) B. Wu; X. J. Yang; C. Janiak; P. G. Lassahn, *Chem. Commun.* **2003**, 902.

(73) R. Kramer; J. M. Lehn; A. DeCian; J. Fischer, *Angew. Chem., Int. Ed. Engl.* **1993**, *32*, 764.

(74) K. Kavallieratos; S. R.de Gala; D. J. Austin; R. H. Crabtree, *J. Am. Chem. Soc.* **1997**, *119*, 2325.

(75) S. Kubik; R. Kirchner; D. Nolting; J. Seidel, *J. Am. Chem. Soc.* **2002**, *124*, 12752.

(76) A. Ojida; I. Takashima; T. Kohira; H. Nonaka; I. Hamachi, *J. Am. Chem.Soc.* **2008**, *130*, 12095.

(77) Y. Kim; F. P. Gabbai, *J. Am. Chem.Soc.* **2009**, *131*, 3363.

(78) R. Custelcean; B. A. Moyer, *Eur. J. Inorg. Chem.* **2007**, *10*, 1321

(79) P. Byrne; G. O. Lloyd; N. Clarke; J. W. Steed, *Angew. Chem., Int. Ed. Engl.* **2008**, *47*, 5761

(80) R. Vilar, *Eur. J. Inorg. Chem.* **2008**, 357.

(81) X. D. Chen; T. C. W. Mak, *Dalton Trans.* **2005**, 3646.

(82) J. N. Moorthy; R. Natarajan; G. Savitha; A. Suchopar; R. M. Richards, *J. Mol. Struct.* **2006**, *796*, 216.

(83) N. R. Champness; M. Schroder, *Curr. Opin. Solid State Mater. Sci.* **1998**, *3*, 419.

(84) D. K. Kumar; A. Das; P. Dastidar, *Inorg. Chem.* **2007**, *46*, 7351.

(85) D. K. Kumar; A. Das; P. Dastidar, *Cryst. Growth Des.* **2007**, *7*, 2096.

(86) P. D. Beer, *Acc. Chem. Res.* **1998**, *31*, 71.

(87) P. D. Beer, *Chem. Commun.* **1999**, 689.

(88) S. Watanabe; O. Onogawa; Y. Komatsu; K. Yoshida, *J. Am .Chem. Soc.* **1998**, *120*, 229.

(89) D. Curiel; E. J. Hayes; P. D. Beer, *Top. Fluoresc. Spectrosc.* **2005**, *9*, 59.

(90) I. E. D. Vega; P. A. Gale; M. E. Light; S. J. Loeb, *Chem. Commun.* **2005**, 4913.

(91) S. L. Tobey; B. D. Jones; E. V. Anslyn, *J. Am. Chem. Soc.* **2003**, *125*, 4026.

(92) S. R. Batten; N. R. Champness; X. M. Chen; J. Garcia-Martinez; S. Kitagawa; L. Ohrstrom; M. O'Keeffe; M. P. Suh; J. Reedijk, *CrystEngComm.* **2012**, *14*, 3001.

(93) A. Y. Robin; K. M. Fromm, *Coord. Chem. Rev.* **2006**, *250*, 2127.

(94) G. Ferey, *Chem. Mater.* **2001**, *13*, 3084.

(95) V. Kiritsis; A. Michealides; S. Skoulika; S. Golhen; L. Quahab, *Inorg. Chem.* **1998**, *37*, 3407.

(96) J. Kim; B. L. Chen; T. M. Reineke; H. L. Li; M. Eddaoudi; D. B. Moler; M. O'Keeffe; O. M. Yaghi, *J. Am .Chem. Soc.* **2001**, *123*, 8239.

(97) T. K. Venkatachalam; E. Sudbeck; F. M. Uckun, *J. Mol. Struct.* **2005**, *751*, 41.

(98) S. Y. Yang; L. S. Long; Y. B. Jiang; R. B. Huang; L. S. Zheng, *Chem. Mater.* **2002**, *14*, 3229.

(99) L. M. Duan; J. Q. Xu; F. T. Xie; Y. B. Liu; H. Ding, *Inorg. Chem. Commun.* **2004**, *7*, 216.

(100) L. A. Borkowski; C. L. Cahill, *Inorg. Chem. Commun.* **2004**, 725.

(101) D. V. Soldatov; J. A. Ripmeester, *Stud. Surf. Sci. Catal.* **2002**, *141*, 353.

(102) W. L. Leong; J. J. Vittal, *Chem. Rev.* **2011**, *111*, 688.

(103) B. F. Hoskins; R. Robson, *J. Am. Chem. Soc.* **1990**, *112*, 1546.

(104) K. S. Min; M. P. Suh, *J. Am. Chem. Soc.* **2000**, *122*, 6834.

(105) Z. Qin; M. C. Jennings; R. J. Puddephatt, *Inorg. Chem.* **2003**, *42*, 1956.

(106) Z. Qin; M. C. Jennings; R. J. Puddephatt, *Chem. Commun.* **2001**, 2676.

(107) N. L. S. Yue; M. C. Jennings; R. J. Puddephatt, *Eur. J. Inorg. Chem.* **2007**, 1690.

(108) Z. Qin; M. C. Jennings; R. J. Puddephatt, *Inorg. Chem.* **2002**, *41*, 3967.

(109) S. L. Jain; P. Bhattacharyya; H. L. Milton; A. M. Z. Slawin; J. A. Crayston; J. D. Woollins, *Dalton Trans.* **2004**, 8593.

(110) K. Yamada; S. Yagishita; H. Tanaka; K. Tohyama; K. Adachi; S. Kaizaki; H. Kumagai; K. Inoue; R. Kitaura; H-C. Chang; S. Kitagawa; S. Kawata, *Chem. Eur. J.* **2004**, *10*, 2647.

(111) B. F. Hoskins; R. B. Robson, *J. Am. Chem. Soc.* **1989**, *111*, 5962.

(112) D. Venkataraman; G. B. Gardner; S. Lee; S. Moore, *Nature* **1995**, *374*, 792.

(113) O. M. Yaghi; G. M. Li; H. L. Li, *Nature* **1995**, *378*, 703.

(114) M. P. Suh; H. J. Park; T. K. Prasad; D. W. Lim, *Chem. Rev.* **2012**, *112*, 782.

(115) L. C. R. Jesse; O. M. Yaghi, *Angew. Chem., Int. Ed.* **2005**, *44*, 4670.

(116) M. J. Rosseinky, *Micropor. Mesopo. Mater.* **2004**, *73*, 15.

(117) C. J. Kerpert; M. J. Rosseinky, *Chem. Commun.* **1999**, 375.

(118) J. J. Vittal, *Coord. Chem. Rev.* **2007**, *251*, 1781.

(119) C. Serre; C. M. Draznieks; S. Surble; N. Audebrand; Y. Filinchuk; G. Ferey, *Science* **2007**, *315*, 1828.

(120) R. Matsuda; R. Kitaura; S. Kitagawa; Y. Kubota; T. C. Kobayashi; S. Horike; M. Takata, *J. Am .Chem. Soc.* **2004**, *126*, 14063.

(121) P. Kanoo; R. Sambhu; T. K. Maji, *Inorg. Chem.* **2011**, *50*, 400.

(122) S. Kitagawa; M. Kondo, *Bull. Chem. Soc. Jpn.* **1998**, *71*, 1739.

(123) T. K. Maji; S. Kitagawa, *Pure. Appl. Chem.* **2007**, *79*, 2155.

(124) K. Uemura; S. Kitagawa, *J. Solid State Chem.* **2005**, *178*, 2420.

(125) D. Bradshaw; J. B. Claridge; E. J. Cussen; T. J. Prior; M. Rosseinsky, *Acc. Chem. Res.* **2005**, *38*, 273.

(126) R. Custelcean, *Curr. Opin. Solid State Mater. Sci.* **2009**, *13*, 68.

(127) N. N. Adarsh; P. Dastidar, *Chem. Soc. Rev.* **2012**, *41*, 3039.

(128) S. Banarjee; N. N. Adarsh; P. Dastidar, *Eur. J. Inorg. Chem.* **2010**, *40*, 3770.

(129) D. Kumar; D. A. Jose; A. Das; P. Dastidar, *Inorg. Chem.* **2005**, *44*, 6933.

(130) K. Uemura; S. Kitagawa; M. Kondo; K. Fukui; R. Kitaura; H-C. Chang; T. Mizutani, *Chem. Eur. J.* **2002**, *8*, 3586.

(131) S. A. Dalrymple; G. K. H. Shimizu, *Chem. Eur. J.* **2002**, *8*, 3010

(132) P. A. Gale; J. L. Sessler; W. E. Allen; N. A. Tvermoes; V. Lynch, *Chem. Commun.* **1997**, 665 .

(133) R. Custelcean; T. J. Haverlock; B. A. Moyer, *Inorg. Chem.* **2006**, *45*, 6446

(134) S. R. Collinson; T. Gelbrich; M. B. Hursthouse; J. H. R.Tucker, *Chem. Commun.* **2001**, *6*, 555.

(135) I. Huc; M. J. Krische; D. P. Funeriu; J. M. Lehn, *Eur. J. Inorg. Chem.* **1999**, 1415.

(136) J. D. Epperson; L. J. Ming; G. R. Barker; G. R. Newkome, *J. Am. Chem. Soc.* **2001**, *123*, 8583.

(137) D. A. Conlon; N. Yasuda, *Adv. Synth. Catal.* **2001**, *1*, 343.

(138) B. M. Trost; I. Hachiya, *J. Am. Chem. Soc.* **1998**, *120*, 1104.

(139) M. Matsuzaki; H. Okabe; S. Tanaka, *Japan Kokai.* **1982**, *77*, 33676.

(140) S. Biniecki; W. Mordzejewska; G. Rogala-Zawadzka, *Acta Pol. Pharm.* **1985**, *42*, 1.

(141) M. P. Hughes; B. D. Smith, *J. Org. Chem.* **1997**, *62*, 4492.

(142) S. J. Brooks; L. S. Evans; P. A. Gale; M. B. Hursthouse; M. E. Light, *Chem. Commun.* **2005**, *6*, 734.

(143) K. Kavallieratos; C. M. Bertao; R. H. Crabtree, *J. Org. Chem.* **1999**, *64*, 1675.

(144) K. Kavallieratos; S. R. de Gala; D. J. Austin; R. H. Crabtree, *J. Am. Chem. Soc.* **1997**, *119*, 2325.

(145) P. V. Santacroce; J. T. Davis; M. E. Light; P. A. Gale; J. C. Iglesias-Sanchez; P. Prados; R. Quesada, *J. Am .Chem. Soc.* **2007**, *129*, 1886.

(146) P. A. Gale; J. Garric; M. E. Light; B. A. Mcnally; B. D. Smith, *Chem. Commun.* **2007**, 1736.

(147) C. A. Hunter; L. D. Sarson, *Angew. Chem., Int. Ed. Engl.* **1994**, *33*, 2313.

(148) M. G. Fisher; P. A. Gale; M. E. Light, *New J. Chem.* **2007**, *31*, 1583.

(149) M. Kinsella; P. G. Duggan; J. Muldoon; K. S. Eccles; S. E. Lawrence; C. M. Lennon, *Eur. J. Inorg. Chem.* **2011**, *6*, 1125.

(150) S. J. Zuend; E. N. Jacobsen, *J. Am. Chem. Soc.* **2009**, *131*, 15358.

(151) Z. G. Zhang; P. R. Schreiner, *Chem. Soc. Rev.* **2009**, *38*, 1187.

(152) P. R. Schreiner; A. Wittkopp, *Org. Lett.* **2002**, *4*, 217.

(153) P. R. Schreiner; A. Wittkopp, *Chem. Eur. J.* **2003**, *9*, 407.

(154) J. March, *Advanced Organic Chemistry, John Wiley & Sons, 4th Ed.*, **1992**.

(155) J. Zablicky, *The Chemistry of Amides, Wiley, New York*, **1970**.

(156) J. Lin; J. Y. Zhang; Y. Xu; X. K. Ke; Z. Guo, *Acta Crystallogr. Sect. C.* **2001**, *57*, 192.

(157) H. Kurosaki; R. K. Sharma; S. Aoki; T. Inoue; Y. Okamoto; Y. Sugiura; M. Doi; T. Ishida; M. Otsuka; M. Goto, *J. Chem. Soc., Dalton Trans.* **2001**, 441.

(158) M. J.Chmielewski; J. Jurczak, *Chem.Eur. J.* **2005**, *11*, 6080.

(159) M. T. Huggins; P. Barber; J.Hunt, *Chem. Commun.* **2009**, 5254.

(160) L. V. Simov; D. G. Drueckhammer, *J. Org. Chem.* **2007**, *72*, 1742.

(161) C. J. Sumby; L. R. Hanton, *Tetrahedron* **2009**, *65*, 4681.

(162) N. W. Alcock; G. Clarkson; P. B. Glover; G. A. Lawrance; P. Moore; M. Napitupulu, *Dalton Trans.* **2005**, 518.

(163) M. Napitupulu; B. L. Griggs; S. X. Luo; P. Turner; M. Maeder; G. A. Lawrance, *J. Heterocyclic Chem.* **2006**, *46*, 243

(164) F. A. Chavez; M. M. Olmstead; P. K. Mascharak, *Inorg. Chem.* **1996**, *35*, 1410.

(165) D. S. Marlin; M. M. Olmstead; P. K. Mascharak, *Inorg. Chem.* **2001**, *40*, 7003.

(166) M. Napitupulu; G. A. Lawrance; G. J. Clarkson; P. Moore, *Aust. J. Chem.* **2006**, *59*, 796.

(167) Z. Qin; M. C. Jennings; R. J. Puddephatt, *Chem. Commun.* **2002**, 354.

(168) L. Rajput; S. Singha; K. Biradha, *Cryst. Growth Des.* **2007**, *7*, 2788.

(169) T. Weilandt; R. W. Troff; H. Saxell; K. Rissanen; C. A. Schalley, *Inorg. Chem.* **2008**, *47*, 7588.

(170) J. Pansanel; A. Jouaiti; S. Ferlay; M. W. Hosseini; J. M. Planeix; N. Kyritsakas, *New J. Chem.* **2006**, *30*, 71.

(171) F. Luo; J. Zheng; S. R. Batten, *Chem. Commun.* **2007**, 3744.

(172) S. S. Sun; A. J. Lees; P. Y. Zavalij, *Inorg. Chem.* **2003**, 3445.

(173) C. Schumuck; W. Machon, *Chem. Eur. J.* **2005**, *11*, 1109.

(174) P. Teo; T. S. A. Hor, *Coord. Chem. Rev.* **2010**, 3456.

(175) M. Biswas; G. Pilet; M. S. El Fallah; J. Ribas; S. Mitra, *Inorg. Chim. Acta.* **2008**, *361*, 387.

(176) C. Pena; J. G. Sabin; I. Alfonso; F. Rebolledo; V. Gotor, *Tetrahedron* **2008**, *64*, 7709.

(177) L. Rajput; K. Biradha, *Polyhedron.* **2008**, *27*, 1248.

(178) P. J. Steel; C. J. Sumby, *Dalton Trans.* **2003**, 4505.

(179) B. M. Trost; M. J. Krische; R. Radinov; G. Zanoni, *J. Am. Chem. Soc.* **1996**, *118*, 6297.

(180) C. J. Sumby, *Coord. Chem. Rev.* **2011**, *255*, 1937.

(181) Y. Hamuro; S. J. Geib; A. D. Hamilton, *Angew Chem., Int. Ed. Engl.* **1994**, *105*, 465.

(182) G. T. Crisp; Y. L. Jiang, *Tetrahedron* **1999**, *55*, 549.

(183) O. Q. Munro; S. D. Joubert; C. D. Grimmer, *Chem Eur. J.* **2006**, *12*, 7987.

(184) M. Renz; C. Hemmert; B. Meunier, *Eur. J. Inorg. Chem.* **1998**, *30*, 1271.

(185) B. David; C. Jin; S. Plummer; E. S. F. Berman; D. Striplin, *Inorg. Chem.* **2004**, *43*, 1735.

(186) F. F. Blicke; C. E. Maxwell, *J. Am. Chem. Soc.* **1939**, *61*, 1780.

(187) B. Antonioli; J. K. Clegg; D. J. Bray; K. Gloe; K. Gloe; O. Kataeva; L. F. Lindoy; J. C. McMurtrie; P.J. Steel; C. J. Sumby; M. Wenzela, *Dalton Trans.* **2006**, 4783.

(188) C. M. Chamchoumis; P. G. Potvin, *J. Chem. Soc., Dalton Trans.* **1999**, 1373.

(189) B. Antonioli; J. K. Clegg; D.J. Bray; K. Gloe; K. Gloe; H. Hesske; L. F. Lindoy, *CrystEngComm.* **2006**, *8*, 748.

(190) C. L. Chen; B. S. Kang; C.Y. Su, *Aust. J. Chem.* **2006**, *2*, 3.

(191) F. A. A. Paz; J. Klinowski; S. M. F. Vilela; J. P. C. Tome ; J. A. S. Cavaleiro ; J. Rocha, *Chem. Soc. Rev.* **2012**, *41*, 1088.

(192) L. Brammer, *Chem. Soc. Rev.* **2004**, *33*, 476.

(193) S. Kitagawa; R. Kitaura; S. I. Noro, *Angew. Chem., Int. Ed.* **2004**, *43*, 2334.

(194) A. U. Czaja; N. Trukhan; U. Muller, *Chem. Soc. Rev.* **2009**, *38*, 1284.

(195) J. M. Lehn; A. Rigault; J. Siegel; J. Harrowfield; B. Chievrier; D. Moras, *Proc. Natl. Acad. Sci. USA* **1987**, *84*, 2565.

(196) L. J. Murray; M. Dinca; J. R. Long, *Chem. Soc. Rev.* **2009**, *38*, 1294.

(197) L. Ma; C. Abney; W. Lin, *Chem. Soc. Rev.* **2009**, *38*, 1248.

(198) C. Janiak; J. K. Vieth, *New J. Chem.* **2010**, 2366.

(199) J. J. I. V. Perry; J. A. Perman; M. J. Zaworotko, *Chem. Soc. Rev.* **2009**, *38*, 1400.

(200) H. Li; M. Eddaoudi; M. O'Keeffe; O. M. Yaghi, *Nature* **1999**, *402*, 276

(201) X. Lin; A. J. Blake; C. Wilson; X. Z. Sun; N. R. Champness; M. W. George; P. Hubberstey; R. Mokaya; M. Schroder, *J. Am. Chem. Soc.* **2006**, *128*, 10745.

(202) S. Xiang; J. Huang; L. Li; J. Zhang; L. Jiang; X. Kuang; C. Y. Su, *Inorg. Chem.* **2011**, *50*, 1743.

(203) J. F. Eubank; L. Wojtas; T. Bousquet; V. C. Kravtsov; M. Eddaoudi, *J. Am. Chem. Soc.* **2011**, *133*, 17532.

(204) M. C. Das; H. Xu; S. Xiang; Z. Zhang; H. D. Arman; G. Qian; B. Chen, *Chem. Eur. J.* **2011**, *17*, 7817.

(205) K. Koh; A. G. Wong-Foy; A. Matzger, *Angew. Chem., Int. Ed.* **2008**, *47*, 677.

(206) K. Koh; A. G. Wong-Foy; A. J. Matzger, *J. Am. Chem. Soc.* **2010**, *132*, 15005.

(207) H. Chun; D. N. Dybtsev; H. Kim; K. Kim, *Chem. Eur. J.* **2005**, *11*, 3521.

(208) A. G. Wong-Foy; O. Lebel; A. J. Matzger, *J. Am. Chem. Soc.* **2007**, *129*, 15740.

(209) Z. Y. Guo; G. H. Li; L. Zhou; S. Q. Su; Y. Q. Lei; S. Dang; H. J. Zhang, *Inorg. Chem.* **2009**, *48*, 8069.

(210) See for example; A. Pichon; A. Lazuen-Garay; S. L. James, *CrystEngComm.* **2006**, *8*, 211.

(211) See for example; Y. Liu; V. C. Kravtsov; D. A. Beauchamp; J. F. Eubank; M. Eddaoudi, *J. Am. Chem. Soc.* **2005**, *127*, 7266.

(212) A. Pichon; A. Lazuen-Garay; S. L. James, *CrystEngComm.* **2006**, *8*, 211.

(213) Y. Liu; V. Kravtsov; D. A. Beauchamp; J. F. Eubank; M. Eddaoudi, *J. Am. Chem. Soc.* **2005**, *127*, 7266.

(214) N. N. Adarsh; D. K. Kumar; P. Dastidar, *CrystEngComm.* **2009**, *11*, 796.

(215) N. N. Adarsh; D. K. Kumar; E. Suresh; P. Dastidar, *Inorg. Chim. Acta* **2010**, *363*, 1367.

(216) S. Hasegawa; S. Horike; R. Matsuda; S. Furukawa; K. Mochizuki; Y. Kinoshita; S. Kitagawa, *J. Am. Chem. Soc.* **2007**, *129*, 2607.

(217) P. Kapoor; A. P. S. Pannu; M. Sharma; G. Hundal; R. Kapoor; M. S. Hundal, *J. Coord. Chem.* **2011**, *64*, 256.

(218) M. Dasgupta; S. Nag; G. Das; M. Nethaji; S. Bhattacharya, *Polyhedron.* **2008**, *27*, 139.

(219) K. Gudasi; R. Vadavi; R. Shenoy; M. Patil; S. A. Patil; M. Nethaji, *Inorg. Chim. Acta.* **2005**, *358*, 3799.

(220) Y.Perez; A. L. Johnson; P. R. Raithby, *Polyhedron.* **2011**, 284.

(221) J. F. Kou; M. Su; Y. H. Zhang; Z. D. Huang; S. W. Ng ; G. A. Yang, *Z. Naturforsch. B.* **2010**, *65*, 1467.

(222) J. Montes-Ayala; S. E. Castillo-Blum; E. O. Rodriguez-Hernandez; S. Bernes; N. Barba-Behrens, *J. Inorg. Biochem.* **2005**, *99*, 1676.

(223) Y. Zhang; H. C. Liang; L. N. Zakharov; S. K. Das; M. M. Hetu ; A. L. Rheingold, *Inorg. Chim. Acta.* **2007**, *460*, 1691.

(224) Y. S. Song; B. Yan, *J. Coord.Chem.* **2005**, *58*, 817.

(225) J. K. Clegg; S. S. Iremonger; M. J. Hayter; P. D. Southon; R. B. Macquart; M. B. Duriska; P. Jensen; P. Turner; K. A. Jolliffe; C.J. Kepert; G. V. Meehan; L. F. Lindoy *Angew. Chem., Int. Ed.*, **2010**, *49*, 1075.

(226) J. K. Clegg; M. J. Hayter; K. A. Jolliffe; L. F. Lindoy; J. C. McMurtrie; G. V. Meehan; S. M. Neville; S. Parsons; P. A. Tasker; P. Turner; F. J. White, *Dalton Trans.* **2010**, 2804.

(227) J. K. Clegg; L. F. Lindoy; J. C. McMurtrie; D. Schilter, *Dalton Trans.* **2005**, 857.

(228) J. K. Clegg; K. Gloe; M. J. Hayter; O. Kataeva; L. F. Lindoy; B. Moubaraki; J. C. McMurtrie; K. S. Murray; D. Schilter, *Dalton Trans.* **2006**, 3977.

(229) B. Antonioli; D. J. Bray; J. K. Clegg; K. Gloe; O. Kataeva; L. F. Lindoy; J. C. Mc Murtrie; P. J. Steel; C. J. Sumby; M. Wenzel, *J. Chem. Soc., Dalton Trans.* **2006**, 4783.

(230) C. M. Biagini; V. A. Chiesi; C. Guastini; M. Nardelli, *Gazz. Chim. Ital.* **1972**, *100*, 1026.

(231) D. Hu; W. Huang; S. Gou; S. Chantrapromma; H. K. Fun; Y. Xu, *Synth. React.Inorg. Met.* **2002**, *32*, 127.

(232) F. Vogtle; W. M. Mueller; E. Buhleir; W. Wehner, *Chem. Ber.* **1979**, *112*, 899.

(233) M. Hardouin–Lerouge; P. Hudhomme; M. Salle, *Chem. Soc. Rev.* **2011**, *40*, 30.

(234) C.L. Chen; J. Y. Zhang; C. Y. Su, *Eur. J. Inorg. Chem.* **2007**, 2997.

(235) D. A. McMorran; P. J. Steel *Chem. Commun.* **2002**, 2120.

(236) M. Barboiu; E. Petit; G. Vaughan *Chem. Eur. J.* **2004**, *10*, 2263.

(237) G. H. Ning; L. Y. Yao; L. X. Liu; T. Z. Xie; Y. Z. Li; Y. Qin; Y. J. Pan; S. Y. Yu, *Inorg. Chem.* **2010**, *49*, 7783.

(238) G. H. Ning; T. Z. Xie; Y. J. Pan; Y. Z. Li; S. Y. Yu, *Dalton Trans.* **2010**, 3203.

(239) E. Zangrando; M. Casanova; E. Alessio, *Chem. Rev.* **2008**, *108*, 4979.

(240) L. X. Liu; H. P. Huang; X. Li; Q. F. Sun; C. R. Sun; Y. Z. Li; S. Y. Yu, *Dalton Trans.* **2008**, 1544.

(241) M. Maekawa; H. Konoka; T. Minematsu; T. Kuroda-Sowa; M. Munakata; S. Kitagawa *Chem. Commun.* **2007**, 5179.

(242) M. Maekawa; S. Kitagawa; T. Kuroda-Sowa; M. Munakata, *Chem. Commun.* **2006**, 2161.

(243) M. J. Hardie; R. Ahmad; C. J. Sumby, *New J. Chem.* **2005**, *29*, 1231.

(244) M. J. Hardie, *Chem. Soc. Rev.* **2010**, *39*, 516.

(245) C. Carruthers; T. K. Ronson; C. J. Sumby; A. Westcott; L. P. Harding; T. J. Prior; P. Riskallah; M. J. Hardie, *Chem. Eur. J.* **2008**, *14*, 10286.

(246) C. J. Sumby; M. J. Carr; A. Franken; J. D. Kennedy; C. A. Kilner; M. J. Hardie, *New J. Chem.* **2006**, *30*, 1390.

(247) A. W. Addison; T. N. Rao; J. Reedijk; J. V. Rrijn; G. C. Verschoor, *J. Chem. Soc., Dalton Trans.* **1984**, 1349.

(248) B. P. Hay; V. S. Bryantsev, *Chem. Commun.* **2008**, 2417.

(249) T. J. Mooibroek; C. A. Black; P. Gamez; J. Reedijk, *Cryst. Growth Des.* **2008**, *8*, 1082.

(250) J. Jin; M. J.Jia; J. J. Zhao; J. H. Yu; J. Q. Xu, *J. Clust. Sci.* **2011**, *22*, 715.

(251) J. M. Lehn, *Supramolecular Chemistry: Concepts and Perspectives; Wiley-VCH: New York* **1995**.

(252) A. Bianchi; K. Bowman-James; Garcia-Espana, *Supramolecular Chemistry of Anions, Wiley-VCH: New York* **1997**.

(253) P. A. Gale, *Coord. Chem. Rev.* **2003**, *191*, 240.

(254) C. Caltagirone; P. A. Gale, *Chem. Soc. Rev.* **2009**, *38*, 520.

(255) P. A. Gale; T. Gunnlaugsson, *Chem. Soc.Rev.* **2010**, *39*, 3595.

(256) P. A. Gale, *Coord. Chem. Rev.* **2000**, *199*, 181.

(257) P. A. Gale, *Chem. Soc. Rev.* **2010**, *39*, 3746.

(258) F. P. Schmidtchen; M. Berger, *Chem. Rev.* **1997**, *97*, 1609.

(259) F. P. Schmidtchen, *Top. Curr. Chem.* **2005**, *255*, 1.

(260) F. P. Schmidtchen, *Coord. Chem. Rev.* **2006**, *250*, 2918.

(261) P. A. Gale, *Acc.Chem. Res.* **2006**, *39*, 465.

(262) E. A. Katayev; Y. A. Ustynyuk; J. L. Sessler, *Coord. Chem. Rev.* **2006**, *250*, 3004.

(263) A. P. de Silva; H. Q. N.Gunaratne; T. Gunnlaugsson; A. J. M. Huxley; C. P. McCoy; J. T. Rademacher; T. E. Rice, *Chem. Rev.* **1997**, *97*, 1515.

(264) J. F. Callan; A. P. de Silva; D. C. Magri, *Tetrahedron* **2005**, *61*, 8551.

(265) M. Manez; F. Sancenon *Chem. Rev.* **2003**, *103*, 4419.

(266) T. Gunnlaugsson; M. Glynn; G. M. Tocci; P. E. Kruger; F. M. Pfeffer, *Coord. Chem. Rev.* **2006**, *250*, 3094.

(267) P. Buhlmann; E. Pretsch; E. Bakker, *Chem. Rev.* **1998**, *98*, 1593.

(268) F. Davis; S. D. Collyer; S. P.J. Higson, *Top. Curr. Chem.* **2005**, *255*, 97.

(269) Y. Sasson; R. Neumann, In Handbook of Phase Transfer Catalysis, Chapman & Hall: London, **1997**, 510.

(270) M. D. Lankshear; P. D. Beer, *Coord. Chem. Rev.* **2006**, *250*, 3142.

(271) N. Gimeno; R. Vilar, *Coord. Chem. Rev.* **2006**, *250*, 3161.

(272) P. A. Gale; S. Camiolo; C. P. Chapman; M. E. Light; M. B. Hursthouse, *Tetrahedron Lett.* **2001**, *42*, 5095.

(273) P. A. Gale; S. Camiolo; G. J.Tizzard; C. P. Chapman; M. E. Light; S. J. Coles; M. B. Hursthouse, *J. Org. Chem.* **2001**, *66*, 7849.

(274) K. Navakhun; P. A. Gale; S. Camiolo; M. E. Light; M. B. Hursthouse, *Chem. Commun.* **2002**, 2084.

(275) I. E. D. Vega; P. A. Gale; M. B. Hursthouse; M. E. Light, *Org. Biomol. Chem.* **2004**, *2*, 2935.

(276) P. A. Gale, *Chem. Commun.* **2005**, 3761.

(277) I. E. D. Vega; S. Camiolo; P. A. Gale; M. B. Hursthouse; M. E. Light, *Chem. Commun.* **2003**, 1686.

(278) S. Valiyaveetil; J. F. J. Engbersen; W. Verboom; D. N. Reinhoudt, *Angew.Chem., Int. Ed. Engl.* **1993**, *32*, 900.

(279) P. D. Beer; C. Hazlewood; D. Hesek; J. Hodacova; S. E. Stokes, *J. Am .Chem. Soc., Dalton Trans.* **1993**, 1327.

(280) P. A. Gale; S. E. Garcia-Garrido; J. Garric, *Chem. Soc. Rev.* **2008**, *37*, 151.

(281) V. Amendola; M. Bonizzoni; D. Esteban-Gomez; L. Fabbrizzi; M. Licchelli; F. Sancenn; A. Taglietti, *Coord. Chem. Rev.* **2006**, *250*, 1451.

(282) B. D. Smith; T. N. Lambert, *Chem. Commun.* **2003**, 2261.

(283) C. R. Bondy; P. A. Gale; S. J. Loeb, *Chem. Commun.* **2001**, 729.

(284) C. R. Bondy; P. A. Gale; S. J. Loeb, *Supramol. Chem.* **2002**, *2*, 93.

(285) K. J. Wallace; R. Daari; W. J. Belcher; L. O. Abouderbala; M. G. Boutelle; J. W. Steed, *J. Organomet. Chem.* **2003**, *666*, 63.

(286) P. A. Gale, Amide- and Urea-Based Anion Receptors in Encyclopedia of Supramolecular Chemistry, J.L. Atwood, J.W. Steed (Eds.), Marcel Dekker, New York, **2004**, 31.

(287) J. L. Sessler; P. A. Gale; J. W. Genge, *Chem. Eur. J.* **1998**, *4*, 1095.

(288) R. Custelcean; P. V. Bonnesen; B. D. Roach, *Chem. Commun.* **2012**, doi: 10.1039/C2CC33062H.

(289) J. L. Sessler; N. A. Tvermoes; J. Davis; Jr., P. A.; K. Jursıkova; W. Sato; D. Seidel; V. Lynch; C. B. Black; A. Try; B. Andrioletti; G. Hemmi; T. D. Mody; D. J. Magda; l. V. Kral, *Pure Appl. Chem.* **1999**, *71*, 2009.

(290) J. L. Sessler; J. M. Davis, *Acc. Chem. Res.* **2001**, *34*, 989.

(291) G. Cafeo; F. H. Kohnke; G. L. La Torre; M. F. Parisi; R. Pistone Nascone; A. J. P. White; D. J. Williams, *Chem. Eur. J.* **2002**, *8*, 3148.

(292) J. L. Sessler; S. Camiolo; P. A. Gale, *Coord. Chem. Rev.* **2003**, *240*, 17.

(293) J. L. Sessler; J. M. Davis; I. V. Kral; T. Kimbrough; V. Lynch, *Org. Biomol. Chem.* **2003**, *1*, 4113.

(294) R. Nishiyabu; P. Anzenbacher Jr., *J. Am. Chem. Soc.* **2005**, *127*, 8270.

(295) J. L. Sessler; D. An; W. S, C.; V. Lynch; M. Marquez, *Chem. Eur. J.* **2005**, *11*, 2001.

(296) J. R. Blas; J. M. Lopez-Bes; M. Marquez; J. L. Sessler; F. J. Luque; M. Orozco, *Chem. Eur. J.* **2007**, *13*, 1108.

(297) P. K. Lo; M. S. Wong, *Sensors* **2008**, *8*, 5313.

(298) M. S. Wong; W. H. Chan; J. Li; X. Dan, *Tetrahedron Lett.* **2000**, *41*, 9293.

(299) M. S. Wong; X. L. Zhang; D. Z. Chen; W. H. Cheung, *Chem. Commun.* **2003**, 138.

(300) H. B. Liu; Y. Xu; B. L. Li; G. Yin; Z. Xu, *Chem. Phys. Lett.* **2001**, *345*, 395.

(301) Y. L.Cho; D. M. Rudkevich; J. Rebek Jr., *J. Am .Chem. Soc.* **2000**, *122*, 9868.

(302) X. H. Sun; W. Y. Li; P. F. Xia; H. B. Luo; Y. L. Wei; M. S. Wong; Y. K. Cheng; S. M. Shuan, *J. Org. Chem.* **2007**, *72*, 2419.

(303) K. M. Mullen; P. D. Beer, *Chem. Soc. Rev.* **2009**, *38*, 1701.

(304) L. Y. Yao; L. Qin; T. Z. Xie; Y. Z. Li; S. Y. Yu, *Inorg. Chem.* **2011**, *50*, 6055.

(305) M. H. Filby; J. W. Steed, *Coord. Chem. Rev.* **2006**, *250*, 3200.

(306) B. Hasenknopf; J. M. Lehn; B. O. Kniesel; G. Baum; D. Fenske, *Angew Chem., Int. Ed. Engl.* **1996**, *108*, 1838.

(307) M. Fujita; K. Umemoto; M. Yoshizawa; N. Fujita; T. Kusukawa; K. Biradha, *Chem. Commun.* **2001**, 509.

(308) D. A. McMorran; P. J. Steel, *Angew. Chem., Int. Ed. Engl.* **1998**, *37*, 3295

(309) J. S. Flemming; K. L. V. Mann; C. A. Carraz; E. Psillakis; J. C. Jeffery; J. A. McCleverty; M. D. Ward, *Angew Chem., Int. Ed. Engl.* **1998**, *37*, 1279.

(310) P. D. Beer; P. A. Gale, *Angew Chem., Int. Ed. Engl.* **2001**, *40*, 486.

(311) C. S. Campos-Fernandez; R. Clerac; K. R. Dunbar, *Angew Chem., Int. Ed. Engl.* **1999**, *23*, 3477.

(312) R. Vilar, *Angew Chem., Int. Ed. Engl.* **2003**, *42*, 1460.

(313) S. R. Seidel; P. J. Stang, *Acc. Chem. Res.* **2002**, *35*, 972.

(314) D. J. Mercer; S. J. Loeb, *Chem. Soc. Rev.* **2010**, *39*, 3612.

(315) M. Aleskovic; N. Basaric; K. Mlinaric-Majerski; K. Molcanov; B. Kojic-Prodic; M. K. Kesharwani; B. Ganguly, *Tetrahedron* **2010**, *66*, 1689.

(316) P. Diaz; J. A. Tovilla; P. Ballester; J. Benet-Buchholz; R. Vilar, *Dalton Trans.* **2007**, 3516.

(317) C. Lin; V. Simov; D. G. Drueckhammer, *J. Org. Chem.* **2007**, *72*, 1742.

(318) F. M. Pfeffer; K. F. Lim; K. J. Sedgwick, *Org. Biomol. Chem.* **2007**, *5*, 1795.

(319) M. T. Huggins; T. Butler; P. Barber; J. Hunt, *Chem. Commun.* **2009**, 5254.

(320) T. Zielinski; J. Jurczak, *Tetrahedron* **2005**, *61*, 4081.

(321) N. N. Adarsh; D. K. Kumar; P. Dastidar, *CrystEngComm.* **2008**, *10*, 1565.

(322) R. Custelcean; P. Remy; P. V. Bonnesen; D. E.Jiang; B. A. Moyer, *Angew Chem.* **2008**, *42*, 1866.

(323) S. Muthu; J. H. K. Yip; J. J. Vittal, *J. Chem. Soc., Dalton Trans.* **2002**, 4561.

(324) M. L. Tong; Y. M. Wu; X. M. Chen; H. C. Chang; S. Kitagawa *Inorg. Chem.* **2002**, *41*, 4846.

(325) S. Banerjee; N. N. Adarsh; P. Dastidar, *CrystEngComm.* **2009**, *11*, 746.

(326) V. Amendola; M. Boiocchi; B. Colasson; L. Fabbrizzi, *Inorg. Chem.* **2006**, *45*, 6138.

(327) S. K. Chandran; R. Thakuria; A. Nangia, *CrystEngComm.* **2008**, *10*, 1891.

(328) R. Custelcean; B. A. Moyer; V. S. Bryantsev; B. P. Hay, *Cryst. Growth Des.* **2006**, *6*, 555.

(329) D. R. Turner; B. Smith; A. E. Goeta; I. R. Evans; D. A. Tocher; J. A. K. Howard; J. W. Steed, *CrystEngComm.* **2004**, *6*, 633.

(330) D. R. Turner; B. Smith; E. C. Spencer; A. E. Goeta; I. R. Evans; D. A. Tocher; J. A. K. Howard; J. W. Steed, *New J. Chem.* **2005**, *29*, 90.

(331) D. R. Turner; E. C. Spencer; J. A. K. Howard; D. A. Tocher; J. W. Steed, *Chem. Commun.* **2004**, 1352.

(332) D. R. Turner; M. J. Paterson; J. W. Steed, *Chem. Commun.* **2008**, 1935.

(333) L. Applegarth; A. E. Goeta; J. W. Steed, *Chem. Commun.* **2005**, 2405.

(334) D. K. Kumar; A. Das; P. Dastidar, *New J. Chem.* **2006**, *30*, 1267.

(335) D. K. Kumar; A. Das; P. Dastidar, *Cryst. Growth Des.* **2006**, 1903.

(336) D. K. Kumar; A. Das; P. Dastidar, *CrystEngCommun.* **2007**, *9*, 548.

(337) B. Wu; X. Huang; Y. Xia; X. J. Yang; C. Janiak, *CrystEngComm.* **2007**, *9*, 676.

(338) M. Sarkar; K. Biradha, *Chem. Commun.* **2005**, 2229.

(339) M. Sarkar; K. Biradha, *Cryst. Growth Des.* **2006**, *6*, 1742.

(340) C. J. Sumby; L. R. Hanton, *unpublished results*.

(341) H. Yuan; L. Thomas; L. K. Woo, *Inorg. Chem.* **1996**, *35*, 2808.

(342) M. W. Cooke; D. Chartrand; G. S. Hanan, *Coord. Chem. Rev.* **2008**, *252*, 903.

(343) P. G. Jones; L. Gray, *Acta Crystallogr. Sect. C.* **2002**, *58*, 280.

(344) C. J. Sumby; J. Fisher; T. J. Prior; M. J. Hardie, *Chem. Eur. J.* **2006**, *12*, 2945.

(345) V. V. Krishnan, *J. Magn. Reson.* **1997**, *124*, 468

(346) T. Haino; M. Kobayashi; M. Chikaraishi; Y. Fukazawa, *Chem.Commun. 18*, **2005**, 2321

(347) A. G. Orpen; L. Brammer; F. H. Allen; O. Kennard; D. G. Watson; R. Taylor, *J. Chem. Soc., Dalton Trans*. **1989**, 1.

(348) G. R. Desiraju, *Acc. Chem. Res.* **2002**, *35*, 565.

(349) C. J. Sumby, *unpublished results*.

(350) N. N. Adarsh; P. Dastidar, *Cryst. Growth Des.* **2011**, *11*, 328.

(351) O. M. Yaghi; H. Li; T. L. Groy, *Inorg. Chem.* **1997**, *36*, 4292.

(352) O. M. Yaghi; H. Li, *J. Am. Chem. Soc.* **1995**, *117*, 10401.

(353) S. Noro; R. Kitaura; M. Kondo; S. Kitagawa; T. Ishii; H. Matsuzaka; M. Yamashita, *J. Am. Chem. Soc.* **2002**, *124*, 2568.

(354) B. F. Abrahams; K. D. Lu; B. Moubaraki; K. S. Murray; R. Robson, *J. Chem. Soc., Dalton Trans.* **2000**, 1793.

(355) D. Braga; S. L. Giaffreda; F. Grepioni; M. Polito, *CrystEngComm.* **2004**, *6*, 458.

(356) K. Uemura; Y. Kumamoto; S. Kitagawa, *Chem. Eur. J.* **2008**, *14*, 9565.

(357) N. N. Adarsh; P. Dastidar, *Cryst. Growth Des.* **2010**, *10*, 483.

(358) R. Custelcean; A. Bock; B. A. Moyer, *J. Am. Chem. Soc.* **2010**, *132*, 7177.

(359) R. Custelcean; V. Sellin; B. A. Moyer, *Chem. Commun.* **2007**, 1541.

(360) L. F. Lindoy; P. K. Glasson; G. V. Meehan, *Coord. Chem. Rev.* **2008**, *8* 258.

(361) V. Balzani; A. Juris; M. Venturi; S. Campagna; S. Serroni, *Chem. Rev.* **1996**, *96*, 759.

(362) K. Ha, *Acta Crystallogr. Sec. E. 68*, 501.

(363) C. J. Sumby; P. J. Steel, *Polyhedron* **2007**, *26*, 5370.

(364) C. J. Sumby; P. J. Steel, *Inorg. Chim. Acta.* **2007**, *360*, 2100.

(365) C. J. Jones, *Chem. Rev.* **2000**, *100*, 3483.

(366) C. B. Aakeroy; N. R. Champness; C. Janiak, *CrystEngComm.* **2010**, *12*, 22.

(367) J. P. Zhang; X. C. Huang; X. M. Chen, *Chem. Soc. Rev.* **2009**, *38*, 2385.

(368) R. Robson, *Dalton Trans.* **2008**, 5113.

(369) S. Kitagawa; S. I. Noro; T. Nakamura, *Chem. Commun.* **2006**, 701.

(370) T. F. Liu; J. Lu; R. Cao, *CrystEngComm.* **2010**, *12*, 660.

(371) C. Kaes; A. Katz; M. W. Hosseini, *Chem. Rev.* **2000**, *100*, 3553.

(372) P. J. Steel, *Molecules* **2004**, *9*, 440.

(373) B. Antonioli; J. K. Clegg; D. J. Bray; K. Gloe; K. Gloe; O. Kataeva; L. F. Lindoy; P.J. Steel; C. J. Sumby; M. Wenzel; A. Jagger; K. A. Jolliffe, *Polyhedron.* **2008**, *27*, 2889.

(374) A. K. Paul; H. M. Torshizi; T. S. Srivastava; S. J. Chavan; M. P. Chitnis, *J. Inorg. Biochem.* **1993**, *50*, 9.

(375) I. Puscasu; C. Mock; M. Rauterkus; A. Rondigs; G. Tallen; S. Gangopadhyay; J. E. A. Wolff; B. Krebs, *Z. Anorg.Allg. Chem.* **2001**, *627*, 1292.

(376) M. J. Rauterkus; S. Fakih; C. Mock; I. Puscasu; B. Krebs, *Inorg. Chim. Acta.* **2003**, *350*, 355.

(377) S. Fakih; W. C. Tung; D. Eierhoff; C. Mock; B. Krebs, *Z. Anorg. Allg. Chem.* **2005**, *631*, 1397.

(378) A. J. Canty; N. J. Minchin, *Aust. J. Chem.* **1986**, *39*, 1063.

(379) J. Chang; S. Plummer; E. S. F. Berman; D. Striplin; D. Blauch, *Inorg. Chem.* **2004**, *43*, 1735.

(380) C. Najera; J. G. Molto; S. Karlstrom, *Adv. Synth. Catal.* **2004**, *346*, 1798.

(381) J. J. Wilson; J. F. Lopes; S. J. Lipard, *Inorg. Chem.* **2010**, *49*, 5303.

(382) M. Trilla; R. Pleixats; M. W.C. Man; C. Bied; J. J. E. Moreau, *Tetrahedron* **2006**, *47*, 2399.

(383) M. Trilla; R. Pleixats; M. W.C.Man; C. Bied; J. J. E. Moreau, *Adv. Synth. Catal.* **2008**, *350*, 577.

(384) O. Adidou; C. G. Henry; M. Safi; M. Soufiaoui; E. Framery, *Tetrahedron* **2008**, *49*, 7217.

(385) C. R. Goldsmith; R. T. Jonas; A. P.Cole; T. D. P. Stack, *Inorg. Chem.* **2002**, *41*, 4642.

(386) M. Abdul-Kadir; P. R. Clements; L. R. Hanton; C .A. Hollis; C. J. Sumby, *Supramol. Chem.* **2012**, accepted 10 May 2012.

(387) C. Tsiamis; A. G. Hatzidimitiou; L. Tzavellas, *Inorg. Chem.* **1998**, *37*, 2903.

(388) P. J. Steel; E. C. Constable, *J. Chem. Soc., Dalton Trans.* **1990**, 1389.

(389) A. Romerosa; J. Suarez-Varela; M. A.Hidalgo; J. Avila-Roso; E. Colacio, *Inorg. Chem.* **1997**, *36*, 3784.

(390) G. M. Sheldrick, *Acta Cryst.* **1990**, *A46*, 467.

(391) G. M. Sheldrick, *SHELXL-97* **1997**.

(392) L. J. Barbour, *Supramol. Chem.* **2001**, *1*, 189.

(393) Persistence of Vision Raytracer Pty. Ltd, P.-R., Williamstown, Australia, 2003-2008.

(394) G. M. Sheldrick, University of Göttingen, Gottingen, Germany, 1997.

(395) B. J. McCormick; E. N. Janes Jr.; R. I. Kaplan, *Inorg. Synt.* **1972**, *13*, 216.

(396) L. Malatesta; M. Angoletta, *J. Chem. Soc.* **1957**, *10*, 1186.